FINAL CONTRACT REPORT
GEOTHERMAL ENERGY IN ARIZONA

by

Claudia Stone and James C. Witcher

Arizona Geological Survey
Open-File Report 83-12

September, 1982

Arizona Geological Survey
416 W. Congress, Suite #100, Tucson, Arizona 85701

Prepared for U.S. Department of Energy Division of Geothermal Energy under Contract No. DE.FC07-79ID12009

This report is preliminary and has not been edited
or reviewed for conformity with Arizona Geological Survey standards

DISCLAIMER

This report was prepared as an account of work sponsored by the United States Government. Neither the United States nor the United States Department of Energy, nor any of their employees, makes any warranty, express or implied, or assumes any legal liability or responsibility for the accuracy, completeness, or usefulness of any information, apparatus, product, or process disclosed, or represents that its use would not infringe privately owned rights. Reference herein to any specific commercial product, process, or service by trade name, mark, manufacturer, or otherwise, does not necessarily constitute or imply its endorsement, recommendation, or favoring by the United States Government or any agency thereof. The views and opinions of authors expressed herein do not necessarily state or reflect those of the United States Government or any agency thereof.

ACKNOWLEDGMENTS

The search for low- to moderate-temperature geothermal resources in Arizona got underway in May, 1977, under the direction of W. Richard Hahman, Sr. Dick's enthusiasm for geothermal energy was a beacon that helped inform all about this alternate energy source and converted many cynics into believers. Dick managed the geothermal program for four years, during which time he managed among many accomplishments, to scoop the geothermal community by producing the first state geothermal resource map (1978). To Dick, we dedicate this volume.

Nile Jones and Alice Campbell were part of the staff at various stages of the program. Both are talented, hard-working professionals, always ready for a heated but friendly geologic debate.

Drafting expertise came from Dan Dwyer, Kevin Ashley, and Bette Holt (who stayed to the end). Mike Ciroachi provided drafting and technical assistance. Numerous secretaries, typists, and graduate assistants cheerfully carried a large load in getting the work done.

Finally, we wish to acknowledge our friends at Los Alamos National Laboratory: Francis West, Jim Aldrich, and especially Bill Laughlin, for their timely and thoughtful help in overseeing the project.

Funding for this work came chiefly from the U. S. Department of Energy, Division of Geothermal Energy (Contract Nos. EG-77-S-02-4362 and DE-FC07-79ID12009), and for two concurrent years from the U. S. Department of Interior, Bureau of Reclamation (Contract No. EW-78-A 02-4760-S).

TABLE OF CONTENTS

CHAPTER I

Introduction..... 1
Well and Spring Location System.....10
Climate.....12
Use of Geothermal Energy.....16
Environmental Concerns.....21
Geothermal Exploration, Drilling, and Leasing Activities in Arizona...23
Geothermal Legislation, regulations, and Taxes.....29

CHAPTER II

Introduction.....33
Colorado Plateau.....35
Northeastern Arizona.....46
Flagstaff Region.....52
East-central Arizona.....63
Mexican Highland Section.....82
Willcox Area.....88
San Manuel Area.....108
San Bernardino Valley.....118
Gila Valley from Safford to Indian Hot Springs.....126
Buena Vista Area.....138
Bowie Area.....152
Cactus Flat -- Artesia Area.....162
San Simon Area.....184
Clifton and Gillard Hot Springs.....197
Sonoran Desert Section.....216
Tucson Basin.....223
Avra Valley.....248
Coolidge Area.....264
Castle Hot Springs Area.....276

Northern Hassayampa Plain.....283
Papago Farms.....299
Southern Palomas Plain.....316
Yuma.....326
Mohave Section.....342
CHAPTER III
Residual Temperature Map.....357
Thermal Springs in Arizona.....368
CHAPTER IV
Exploration Methods.....380
APPENDICES
Conversion Factors and Tables.....397

INDEX TO ILLUSTRATIONS

Figure		Page
	Chapter I	
1.1	Histogram showing distribution of 246 thermal and nonthermal Arizona spring temperatures, minus mean annual air temperatures	8
1.2	Histograms showing distribution of nonthermal spring temperatures, minus mean annual air temperatures in the (a) Colorado Plateau and (b) Basin and Range province	8
1.3	Well and spring location system used in this report	11
1.4	Map showing mean annual air temperatures (MAT) in Arizona. Contour interval is 5°C	14
1.5	Temperature ranges for some industrial processes and agricultural applications (from Anderson and Lund, 1979)	18
1.6	Map showing Arizona KGRAs, areas currently using geothermal energy, and areas of planned development	28
	Chapter II	
2.1	Physiographic provinces and subprovinces of Arizona	34
2.2	Major structural features of northeastern Arizona (from Conley, 1975)	36
2.3	Major structural features of north-central and northwestern Arizona (from Lucchitta, 1974)	36
2.4	Geologic map showing generalized limits of Permian (shaded) and Mesozoic (nonshaded) outcrops in northeastern Arizona	37
2.5	Principal structures in the Flagstaff region	39
2.6	Major anticlines and uplifts of northeastern Arizona (from Davis and Kiven, 1975)	40
2.7	Major silicic centers in the San Francisco volcanic field	42

2.8 Principal strata comprising the major multiple-aquifer systems for three areas in northeastern Arizona (from Sass, Stone, and Bills, 1982..... 43

2.9 Location of principal multiple-aquifer systems in north-central and northeastern Arizona (from Brown, 1976)..... 44

2.10 Topographic map of northeastern Arizona..... 46

2.11 Locations of thermal wells in northeastern Arizona. Inset A shows thermal-well cluster and heat-flow values (from Shearer and Reiter, 1979) near Sanders. Inset B shows thermal-well cluster near the Petrified Forest..... 49

2.12 Map showing possible change (dotted line) in Bodell and Chapman, 1982, thermal boundary (solid line). Solid circles are published heat flow (taken from Bodell and Chapman, 1982); solid triangles are apparent heat flow (taken from Sass and others, 1982)..... 50

2.13 Physiographic map of the Flagstaff region..... 52

2.14 Stratigraphy of the Flagstaff region..... 55

2.15 Residual Bouguer gravity of the Flagstaff region and silicic volcanic centers..... 58

2.16 Residual aeromagnetic map of the Flagstaff region and silicic volcanic centers..... 59

2.17 Physiographic map of east-central Arizona..... 64

2.18 Land status of east-central Arizona..... 65

2.19 Present (solid line) and projected final configuration (dashed line) of Mount Baldy volcano (from Merrill and Pewe, 1977)... 68

2.20 Map of east-central Arizona showing approximate boundary of high TDS water (diagonal line pattern) and surface-water divide (dotted line)..... 68

2.21 Silica geothermometers for east-central Arizona. Values exceeding 90°C, the mean plus one standard deviation, are indicated by open circles with dots..... 70

2.22 Temperature-depth graphs of wells measured in east-central Arizona. Well locations are given in Table 2.1..... 72

2.23 Temperature-depth graphs of wells measured in east-central Arizona. Well locations are given in Table 2.1..... 73

2.24 Temperature-depth graphs of wells measured in east-central Arizona. Well locations are given in Table 2.1..... 74

2.25 Geothermal gradients ($^{o}C/km$) for east-central Arizona. Measured gradients indicated by closed triangles and larger numbers. Calculated gradients indicated by closed circles and smaller numbers. Thermal wells shown by open circles with dots..... 75

2.26 Heat flow (MW/m^2) for east-central Arizona. Open circles with dots represent wells that are also thermal..... 76

2.27 Intersection of lineaments (based on the alignment of young volcanic fields) in the region of the White Mountain volcanic field, east-central Arizona..... 77

2.28 Complete residual Bouguer gravity, east-central Arizona (from Lysonski and others, 1980). Contour interval is 5 milligals. 78

2.29 Principal pre-Tertiary tectonic features of the Mexican Highlands subprovince..... 84

2.30 Location map of Willcox area..... 88

2.31 Generalized geology of the Willcox area..... 91

2.32 Temperature gradients versus depth of water for wells in the Willcox basin..... 96

2.33 Location map of thermal wells in the Willcox area..... 98

2.34 Stratigraphic cross sections of the Willcox basin..... 99

2.35 Location map of stratigraphic cross sections shown in Figure 2.34..... 100

2.36 Location of anomalous thermal wells in the Willcox basin..... 102

2.37 Piper diagram of thermal well chemistry, Willcox area..... 104

2.38 Physiographic map of northern San Pedro River valley and San Manuel area..... 108

2.39 Water table of shallow unconfined ground water in the San Manuel area..... 111

2.40 Thermal wells in the San Manuel area..... 113

2.41 Generalized stratigraphy of thermal wells in the San Manuel area..... 114

2.42 Piper diagram showing chemistry of thermal wells in the San Manuel area..... 116

2.43 Physiographic map of San Bernardino Valley..... 118

2.44 Location of the Pedregosa basin..... 120

2.45 Generalized geologic map of the San Bernardino Valley..... 121

2.46 Physiographic map of Gila Valley from Safford north to Indian Hot Springs and of San Simon Valley from Safford south to Willow Spring Wash..... 126

2.47 Basin-fill stratigraphy in the Safford basin..... 129

2.48 Major lineaments, faults, and spring alignments in the Safford area..... 133

2.49 Schlumberger resistivity sounding..... 134

2.50 Map showing extent of evaporite deposits in basin fill of the Safford area..... 136

2.51 Physiographic map of the Buena Vista area..... 138

2.52 Subsurface geology of the Buena Vista area..... 143

2.53 General geology of the Buena Vista area..... 144

2.54 Selected thermal wells in the Buena Vista area..... 146

2.55 Map of fluoride distribution in the Buena Vista area..... 147

2.56 Temperature-depth profile of a deep well east of Buena Vista (from Reiter and Shearer, 1979)..... 149

2.57 Physiographic map of the Bowie area..... 152

2.58 Map of water table in the Bowie area, 1975..... 156

2.59 Map of selected thermal wells in the Bowie area..... 158

2.60 Distribution of Na-K-Ca geothermometer temperatures in the Bowie area..... 160

2.61 Physiographic map of the Cactus-Flat-Artesia area..... 162

2.62 Generalized geology of the Cactus-Flat-Artesia area..... 165

2.63 Maps showing locations of thermal wells in the Cactus-Flat-Artesia area..... 169

2.64 Lithium compared to the ratio of chloride plus sulfate, versus carbonate species..... 172

2.65 Temperature versus depth for artesian wells in the Cactus-Flat-Artesia area..... 173

2.66 Distribution of mercury in soil, Cactus-Flat-Artesia area.... 174

2.67 Locations of shallow heat-flow holes and elevation of the ground-water table (in feet above mean sea level), Cactus-Flat-Artesia..... 176

2.68 Temperature-depth profiles of heat flow holes..... 177

2.69 Heat flow at the Artesia geothermal anomaly..... 178

2.70 Comparison of structure, Bouguer gravity, and soil mercury anomalies, and heat flow in the Cactus-Flat-Artesia area..... 181

2.71 Map of the San Simon area..... 184

2.72 Structure contour map of the base of the blue clay unit..... 189

2.73 Structure contour map of the top of the blue clay unit..... 190

2.74 Water-table elevations of artesian wells during 1915 in the San Simon area..... 191

2.75 Plot of well depths versus surface discharge temperatures.... 192

2.76 Map of wells with temperatures greater than 35°C in the San Simon area..... 193

2.77 Map of the Clifton and Gillard Hot Springs region..... 197

2.78 Generalized geologic and structure map of the Clifton and Gillard Hot Springs area..... 199

2.79 Map showing generalized topography of the Clifton and Gillard Hot Springs area and postulated regional ground-water flow paths..... 204

2.80 Boron versus chloride in Clifton Hot Springs..... 207

2.81 Measured temperatures and silica temperatures compared to chloride in Clifton Hot Springs..... 208

2.82 Proposed model of a fracture-controlled thermal spring system showing mixing and cooling relationships.....208

2.83 Temperature-depth profile of the Clifton 1 heat-flow hole.....213

2.84 Location map of the Tucson basin, Arizona.....224

2.85 Water table elevations in the Tucson basin, 1956.....229

2.86 Map of heat-flow measurements in the Tucson area.....231

2.87 Temperature of ground water at the water table in the Tucson basin.....232

2.88 Temperature since last mud circulation in the Humble (Exxon) 2 State 1 well in the Tucson basin.....234

2.89 Map of wells and springs in the Tucson basin with temperatures greater than 30°C.....235

2.90 Piper diagram showing water chemistry of thermal waters (greater than 30°C) in the Tucson basin.....240

2.91 Piper diagram showing water chemistry of nonthermal water (less than 30°C) in the Tucson basin.....241

2.92 Pumping level changes in Tucson Electric Power wells 5 and 6, 1960 to 1980.....243

2.93 Generalized lithology of Tucson Electric Power Company well 6....244

2.94 Location map of Avra Valley, Arizona.....248

2.95 Generalized geologic map of Avra Valley, Arizona.....250

2.96 Map of Avra Valley showing ground-water flow paths, thermal wells, area of anomalous mercury in soil, and averaged geothermometers..256

2.97 Map of Avra Valley showing mercury concentrations in soil, area of anomalous mercury, and residual Bouguer gravity.....257

2.98 Map of Avra Valley showing area of anomalous mercury, measured temperatures (°C) and thermal gradients (°C/km).....258

2.99 Map of Avra Valley showing area of anomalous mercury, measured temperatures at 100 m depth (°C), and heat flow (mW/m^2).....259

2.100 Location map of thermal wells (greater than 35°C) and selected deep geothermal, oil, and gas exploration tests, Coolidge.....264

2.101 Location map of the Coolidge area.....267

2.102 Piper diagram showing chemistry of thermal water in the Coolidge area.....272

2.103 Temperature logs of the Geothermal Kinetics-Amax Exploration Pima Farms 1 geothermal test well.....273

2.104 Physiographic map of Castle Hot Springs area.....276

2.105 Generalized geologic map, Castle Hot Springs area.....278

2.106 Locations of sampled wells and springs, Castle Hot Springs area..281

2.107 Physiographic map of the northern Hassayampa plain.....284

2.108 Locations of samples collected for mercury-soil survey.....286

2.109 Piper diagram showing chemically distinct waters in the northern Hassayampa area.....287

2.110 Temperature-depth profiles for wells measured on the northern Hassayampa plain.....291

2.111 Isothermal cross sections, northern Hassayampa plain.....292

2.112 Aeromagnetic map of the northern Hassayampa plain.....294

2.113 Residual Bouguer gravity map of the northern Hassayampa plain....296

2.114 Location map of Papago Indian Reservation and Papago Farms.....300

2.115 Generalized geologic map of Papago Farms area and major surface drainage.....302

2.116 Well locations for San Simon Wash area and Papago Farms.....304

2.117 Graphs of chemical constituents and temperature showing three distinct groups of ground water for samples listed in Table 2.22.305

2.118 Boron (mg/L) versus temperature (^{o}C) for Papago Farms ground water.....311

2.119 Temperature (^{o}C) versus depth (m) for three Papago Farms wells...311

2.120 Second order residual Bouguer gravity map of Papago Farms and surrounding area (from Greenes, 1980).....312

2.121 Proposed fault zones and fault intersection at Papago Farms.....313

2.122 Location map of Palomas Plain.....317

2.123 General geology of the Palomas Plain area.....318

2.124 Averages of silica and Na-K-Ca geothermometers for the southern Palomas Plain.....320

2.125 Discharge temperatures (greater than 35°C) for wells, southern Palomas Plain.....322

2.126 Thermal and nonthermal wells, southern Palomas Plain.....333

2.127 Map showing physiographic provinces of southwestern Arizona and Yuma area of investigation.....336

2.128 Physiographic map of the Yuma area.....337

2.129 Generalized geologic map of the Yuma area.....338

2.130 Map showing deep basins, bedrock highs, and approximate depth to crystalline rock.....343

2.131 Complete residual Bouguer gravity anomaly map of Yuma area.....346

2.132 Upward-continued composite aeromagnetic map of the Yuma area.....346

2.133 Heat flow in the Yuma area.....347

2.134 Map showing warm-water anomalies of Olmsted and others, 1973 and geothermal gradient anomaly of Stone, 1981.....348

2.135 Map of Mohave section, Basin and Range province, northwest corner of Arizona.....352

2.136 Generalized geology of the Mohave section of the Basin and Range province, northwestern Arizona.....355

2.137 Thermal wells and springs in the Mohave section, Basin and Range province, northwestern Arizona.....360

Chapter III

3.1 Areas for which measured temperature logs are available.....368

3.2 Residual temperature map of Arizona.....369

3.3 Temperature-depth profile showing excessive ground-water disturbance.....370

3.4 Temperature-depth profile showing slight hydrologic disturbance due to ground water moving up the borehole.....370

3.5 Temperature-depth profile showing slight hydrologic disturbance due to ground water moving down the borehole.....370

3.6 Map showing major Arizona lineaments and discontinuities.....375

3.7 Map showing historical earthquake epicenters (1890-1980) and preliminary seismic source regions.....376

3.8 Pipe model for forced convection thermal spring system.....380

3.9 Diagram showing thermal disturbance from a regional ground-water flow system in a basin 100 km long, with a hydraulic conductivity of 200 millidarcies, and a hydraulic gradient of 0.1 percent.....381

3.10 Diagram showing the effects of topography on regional ground-water flow patterns.....381

3.11 Diagram showing the influence of geology and regional ground-water flow patterns.....382

3.12 Locations of Arizona thermal springs.....384

3.13 Residual aeromagnetic map of Arizona showing major lineaments....386

3.14 Relationship of thermal springs to Quaternary volcanism, faulting, and historical earthquakes.....387

INDEX TO TABLES

Table		Page
	Chapter I	
1.1	Classification of geothermal energy based on resource temperature	5
1.2	Classification of geothermal energy based on reservoir fluid phase	5
1.3	Classification of geothermal energy based on heat source	5
1.4	Criteria for defining thermal springs and wells in Arizona	7
1.5	Climatic data for selected Arizona cities	15
1.6	Shallow (less than 400 m) temperature gradient/heat flow holes drilled in Arizona	25
1.7	Status of geothermal leasing on state and federal land - 1981	27
	Chapter II	
2.1	Location information for wells measured in east-central Arizona	71
2.2	List of thermal wells in the Willcox area	97
2.3	Chemistry of thermal water in the Willcox area	103
2.4	Geothermometers of thermal water in the Willcox area	104
2.5	Thermal wells in the San Manuel area	112
2.6	Chemistry of thermal waters in the Gila Valley	132
2.7	Chemistry of selected wells in the Buena Vista area	146
2.8	Selected thermal wells in the Bowie area	157
2.9	Chemistry of selected wells in the Bowie area	159

2.10 Thermal wells in the Cactus-Flat-Artesia area..... 170

2.11 Chemistry of thermal wells in the Cactus-Flat-Artesia area.... 171

2.12 Wells with temperatures greater than 35°C, San Simon area..... 194

2.13 Selected chemistry of Clifton Hot Springs..... 205

2.14 Selected chemistry of Gillard Hot Springs..... 211

2.15 Chemistry of Eagle Creek thermal springs..... 211

2.16 Wells and springs with temperatures greater than 30°C in the Tucson basin..... 236

2.17 Selected chemical analyses of thermal water in the Tucson basin..... 237

2.18 Temperatures, depths, and geothermometers for wells in Avra Valley..... 261

2.19 Thermal wells in the Coolidge area..... 266

2.20 Geothermometers..... 289

2.21 Measured geothermal gradients, northern Hassayampa plain, Arizona..... 290

2.22 Chemical analyses of ground water, Papago Farms and surrounding areas (Chemical constituents in milligrams per liter).... 306

2.23 Averaged values for three groups of ground water, Papago Indian Reservation..... 307

2.24 Ratios of selected chemical constituents, chemical geothermometers, total dissolved solids, temperatures, well depths, and geothermal gradients calculated by method 1 (see text) for 26 wells at the Papago Farms and surrounding areas..... 308

2.25 Geothermometers and measured temperatures for selected wells, Papago Farms and surrounding areas..... 309

2.26 Temperatures, depths, and geothermometers for wells in the southern Palomas Plain..... 321

Chapter III

3.1 Names of areas shown in Figure 3.1 for which measured temperature logs are available..... 368

3.2 Thermal springs of Arizona..... 385

CHAPTER 1

INTRODUCTION

PURPOSE. The purpose of this book is to bring together in a single volume current knowledge and basic data on geothermal energy resources in the State of Arizona. We hope that our preliminary investigations, data compilations, and models will provide investigators with a sound scientific basis for future exploration and development work. For readers primarily interested in understanding geothermal energy, what it is, and its sources and occurrences in Arizona, we hope this volume provides helpful insights into all aspects of this most fascinating alternate energy source.

Following the introductory chapter, this report is divided into major sections as follow. Ch. 2, specific area investigations; Ch. 3, thermal aspects of Arizona; Ch. 4, exploration methods. References follow each section. Basic data not in this report can be found in the original open-file reports, as referenced.

EARLY INVESTIGATIONS. Some of the earliest references to mineral waters in the United States date from the late 1860s when Moorman published his comprehensive volumes "Mineral waters of the United States and Canada" (1867) and "Mineral springs of North America" (1871). The earliest known work devoted solely to thermal water (mineral water need not be thermal) was U. S. Geological Survey Bulletin 701, "Geothermal data on the U. S." by Darton (1920). About that same time the first papers were published on Arizona hot springs. Everit (1925) wrote about Clifton Hot Springs; Buehrer (1927) wrote about Castle Hot Springs; and Knechtel (1935), about

Indian Hot Springs. In 1937 Stearns, Stearns, and Waring compiled "Thermal springs in the United States," which was revised and expanded nearly 30 years later (Waring, 1965).

Between the mid-1930s and the mid-1960s, only a few heat-flow and geothermal studies were published in the United States. Basic heat-flow research was carried out the latter part of this period, but it was not done specifically to aid geothermal exploration. After about 1965 geothermal research, exploration, and development began to accelerate, with a corresponding increase in the number of publications devoted to geothermal energy. The biggest boost to geothermal exploration and development followed the 1973 OPEC oil embargo.

Publications related to thermal waters of Arizona did not appear until the late 1960s and after. Haigler (1969) listed 32 selected thermal springs and wells in Arizona in a volume devoted to the mineral and water resources of the state. Wright (1971) was the first to examine in some detail the thermal waters of southern Arizona. He concluded that occurrences of thermal springs and wells are related to structural elements of the Basin and Range province. Other early papers were written by Harshbarger (1972); Norton and Gerlach (1975); Norton, Gerlach, DeCook, and Sumner (1975); Dellechaie (1975); and Swanberg, Morgan, Stoyer, and Witcher (1977).

DEFINITIONS. *Geothermal energy* is natural heat from the interior of the earth. Because it exists everywhere, it is one of the most abundant energy resources available to man. If one drills deep enough into the earth at any location, to depths presently exceeding man's current economic and technological ability, an inexhaustible quantity of heat is available.

This heat flows outward to the earth's surface, but in the process it becomes so diffuse that the heat is not recognized as an energy resource by most people. The major sources of diffuse earth heat are the radioactive decay of a number of elements in the upper crust, chiefly uranium (U), thorium (Th), and potassium (K), and the outward transfer of heat from the interior of the earth. Current technology cannot yet reach and (or) utilize either deep heat or diffuse heat.

There are numerous regions around the world, however, where geologic conditions have created unusually large and concentrated areas of accessible heat at or near the earth's surface. These shallow deposits are called *geothermal anomalies*. When heat from a geothermal anomaly can be economically extracted and used, it becomes a *geothermal resource*, more formally defined by the U. S. Geological Survey as "...the thermal energy that could be extracted at costs competitive with other forms of energy at a foreseeable time, under reasonable assumptions of technological improvement and economic favorability" (see Muffler and Guffanti, 1979, p. 4). Areas of concentrated heat are associated with abnormally high heat flow, which is caused by magma intrusions in the shallow crust (<10 km), active volcanoes, very thin crust, hot water rising along deep faults, or burial beneath very thick sequences of insulating sediments (>5 km). These phenomena are discussed in more detail in Chapter 3. In nearly all instances, circulating ground water heated at depth brings this usable heat to the surface or to shallow depths (<4 km) where it can be reached by man. This is the process of *hydrothermal convection*. In some areas of the world, geysers, boiling springs, and fumaroles vividly reveal the existence of a geothermal anomaly. Yellowstone National Park in Wyoming is a notable

example of surface thermal features marking a geothermal anomaly. In other places, hot springs and hot wells only hint at what may exist at some depth beneath the land surface. Still other geothermal anomalies are "blind," their existence totally unexpected until tapped by deep exploratory drilling usually in search of natural gas or petroleum.

In order to discuss geothermal resources more readily, three distinct *classifications of geothermal energy* have evolved and are in common usage today. The first and most conventional classification is based on temperature of the resource (Table 1.1). The second (Table 1.2) is based on the fluid phase extracted from the reservoir, a classification especially useful to geothermal engineers. Table 1.3 classifies geothermal systems according to the heat source that produces the anomaly. Terminology from all three classifications can be applied to a single resource. For example, The Geysers geothermal field in northern California is a high-temperature, vapor-dominated system with a magmatic heat source.

Among the different types of geothermal resources that exist, vapor-dominated reservoirs are more desirable to develop for electrical generation than hydrothermal reservoirs. This is because steam carries more energy per unit of mass. In vapor-dominated reservoirs steam is piped directly from the wellhead to the generator and is the working fluid that drives the turbines to produce electricity. A vapor-dominated resource can be the most economical way to generate electricity, but these systems, which typically produce 240°C "dry steam" (little or no water), are rare. Hydrothermal systems are more common, but they usually require more innovative technology for electrical generation. The hot water can be used to heat another fluid that drives the turbines, or it can be allowed to

TABLE 1.1. Classification of geothermal energy based on resource temperature

Low temperature	<90°C
Moderate temperature	90 to 150°C
High temperature	>150°C

TABLE 1.2. Classification of geothermal energy based on reservoir fluid phase

Vapor-dominated system
- steam only

Hydrothermal system
- steam and hot water mixed
- hot water only

Hot dry rock
- no fluid

Geopressured
- hot water

TABLE 1.3. Classification of geothermal energy based on heat source

- Very thin crust
- Recent volcanic activity (<1 m.y. old)
- Recent intrusion of magma into the shallow crust (<10 km)
- High concentrations of radioactive elements buried beneath very thick sediments
- Very deep circulation of ground water

flash to steam, which is then used to drive the turbines. In some hydrothermal systems, temperatures up to 360°C have been found.

Hydrothermal systems make up all of the low- to moderate-temperature resources used for direct-heat applications. In fact, hot-water geothermal resources are now known to make up the majority of geothermal occurrences worldwide, but development lags significantly behind the development of high-temperature resources. Most identified geothermal resources in Arizona are characterized by low- to moderate-temperature water, either stored in the earth in blind reservoirs or discharging at the surface as thermal springs. It is presumed that further exploration will discover many other resources.

The object of all geothermal-energy exploration and assessment is to locate and define geothermal resources near a user, at economically favorable drilling depths. Thus, identification of thermal springs and wells is very useful because they occur where geothermal waters are flowing upward into near-surface aquifers, and the geothermal potential is probably most favorable. The determination of what temperature distinguishes a thermal spring from a nonthermal spring, however, is difficult and somewhat arbitrary. The definition varies in different parts of the country and even varies in different parts of Arizona. Basically the definition is linked to the local mean annual air temperature (MAT) where the spring occurs. In Alaska, for example, where the MAT can be lower than 0°C, a spring issuing 20 to 25°C water would be considered a thermal spring. The same water in southern Arizona, where the MAT can be as high as 20°C, would be considered nonthermal.

Witcher (1981) showed that the mean spring discharge temperature for 246 Arizona springs exceeds the local MAT by 6.55°C ± 8.34°C (Fig. 1.1). Based on these statistics, he defined a *hot spring* as one with a discharge temperature that exceeds the local MAT by 15°C or more.

To further refine the definition of a thermal spring, Witcher separated nonthermal spring temperatures for the Colorado Plateau (CP) from those of the Basin and Range province (B&R) (Fig. 1.2). Using additional statistics he determined that the definition of a *warm spring* on the CP would include those with temperatures exceeding the local MAT by 6°C; in the B&R, the term *warm spring* would include those with temperatures greater than 10°C above the local MAT (Table 1.4).

TABLE 1.4 Criteria for defining thermal springs and wells in Arizona

Province	Warm Spring	Hot Spring	Thermal Well
Basin and Range	10.0-14.9°C>MAT	15°C>MAT	10°C>MAT; TG>45°C/km
Colorado Plateau	6.0-14.9°C>MAT	15°C>MAT	10°C>MAT; TG>30°C/km

Defining a thermal well, on the other hand, has an important constraint imposed on it by the *geothermal gradient*, the rate at which temperature normally increases with depth in the earth. This quantity can be measured in test holes and wells. The definition of a thermal well must include both the temperature of the well water and the geothermal gradient. Studies show that in Arizona normal gradients range between 20 and 45°C/km, with a mean value of 32.7 ± 12.6°C/km. We define a *thermal well* as one with a surface discharge temperature exceeding the MAT by 10°C or more and a geothermal gradient greater than 45°C/km, for wells in the Basin and Range province, and a gradient greater than 30°C/km, the continental

Figure 1.1. Histogram showing distribution of 246 thermal and nonthermal Arizona spring temperatures, minus mean annual air temperatures

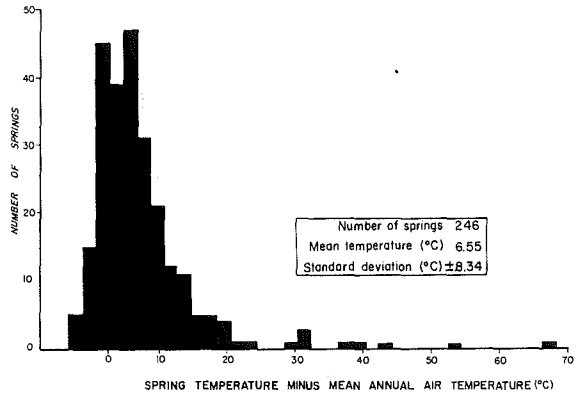

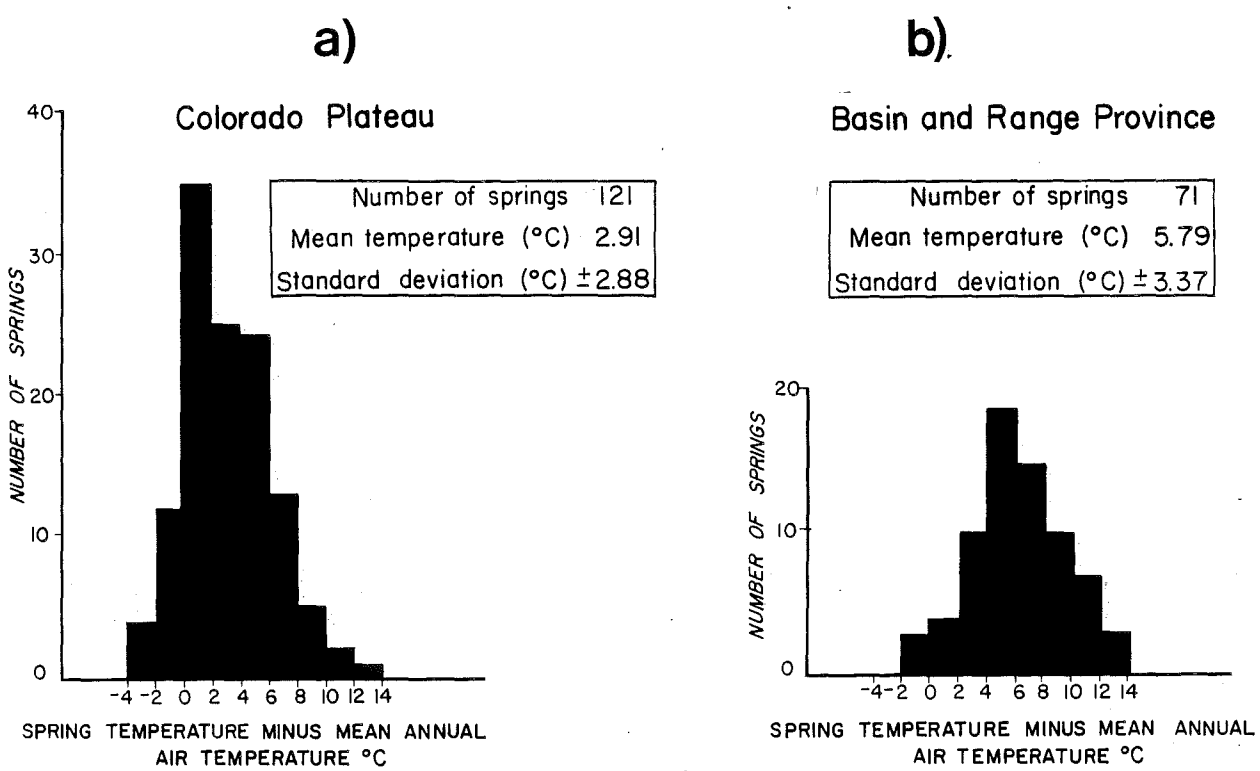

Figure 1.2. Histograms showing distribution of nonthermal spring temperatures, minus mean annual air temperatures in the (a) Colorado Plateau and (b) Basin and Range province

average, for wells on the Colorado Plateau. When actual geothermal gradients cannot be measured, an average gradient can be calculated using the following equation: $\frac{T\ (^{o}C)-MAT\ (^{o}C)}{DEPTH\ (M)} \times 1000$ where T (^{o}C) is the bottom-hole temperature. For this calculation, it is assumed that the well temperature represents the bottom-hole temperature, which is not always the case. Nonetheless the calculation gives a conservative minimum average gradient for a well. The reader is cautioned not to use gradients to predict temperatures below the depth of the well due to possible disturbances at depth, such as deeper water flows and changes in rock thermal conductivity.

It should be emphasized here that a very deep well that is producing warm water is discharging geothermal water, even if the geothermal gradient for that well is within normal range (20 to 45°C/km), so long as heat can be economically extracted from the fluid for a direct-use application.

INTRODUCTION

Muffler, L. J. P., and Guffanti, M., 1979, Introduction, in Muffler, L. P. J., ed., Assessment of Geothermal Resources of the United States -- 1978: U. S. Geological Survey Circular 790, p. 1-7.

Witcher, J. C., 1981, Thermal springs of Arizona: Fieldnotes, v. 11, no. 2, Bureau of Geology and Mineral Technology, Tucson, AZ, p. 1-4.

WELL AND SPRING LOCATION SYSTEM

In this report, thermal wells and springs are identified according to their location within a township and range grid. Arizona is divided into quadrants by the Gila and Salt River Base Line and Meridian (Fig. 1.3). Quadrants are designated A, B, C, and D for northeast, northwest, southwest, and southeast, respectively. Townships and ranges are numbered outward from the intersection of the Base Line and Meridian.

Township, range, section, and location within the section are designated by the following scheme. The first letter refers to the quadrant of the state. The following three numbers are the township, range, and section. Letters following the section number indicate the quarter section, quarter/quarter section, and quarter/quarter/quarter section. Again, letters a, b, c, and d refer to the northeast, northwest, southwest, and southeast quarters of each subdivision. Thus, D-4-5-19caa is a well or spring in the northeast quarter, of the northeast quarter, of the southwest quarter of section 19, Township 4 South, Range 5 East, in the southeast quadrant of Arizona. In the Navajo Survey, locations are referred to the Navajo Base Line and Meridian, and the first letter is N.

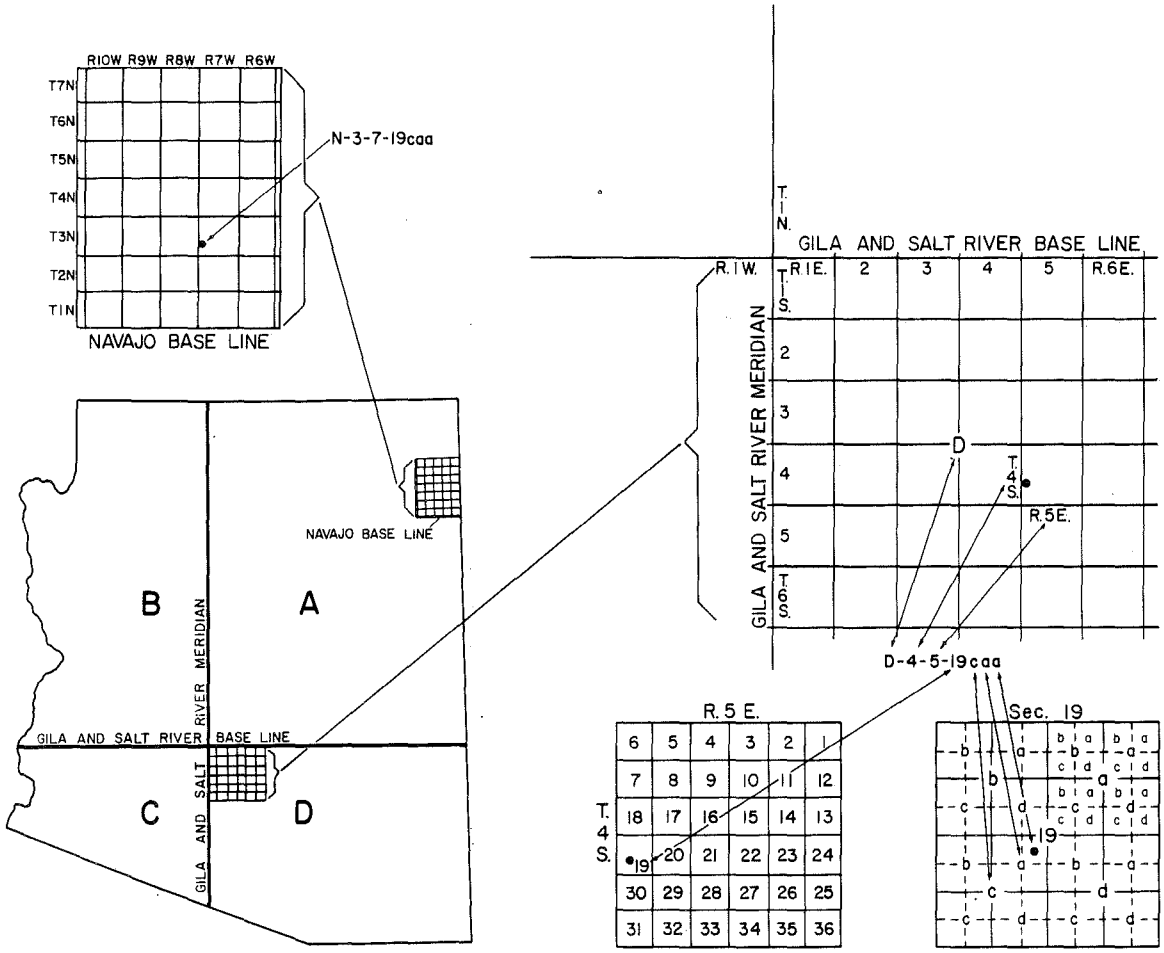

Figure 1.3. Well and spring location system used in this report

CLIMATE

Climate is an important factor in determining whether a particular geothermal project will be efficient and economic. For example, design of a geothermal space-cooling system must accurately account for the length of the hot season and for the usual and maximum amounts of geothermal energy required for operation. Climatic data such as mean temperature, annual and monthly degree cooling days, and maximum recorded temperature are necessary information to evaluate, plan, and manage a successful geothermal cooling system.

Climate is determined largely by geographic location. Because Arizona lies inland hundreds of miles from the ocean, in an area where prevailing wind circulation does not normally carry large quantities of moisture, scant cloud cover and low humidity are the general rule. As a result, night temperatures are as much as 30°C cooler than day temperatures.

Significant differences in elevation and latitude cause highly variable local climates throughout the state. Elevations range between 45 and 3,800 m above mean sea level, and latitude changes nearly 6 degrees north-south across the state. Temperatures generally decrease 8°C per 1,000 m increase in elevation (Sellers and Hill, 1974). Figure 1.4 shows that mean annual temperatures range between 15 and 22°C in southern and western Arizona where most geothermal resource potential exists.

Precipitation, like mean temperature, varies mainly according to elevation. Below 1,800 m annual rainfall in Arizona is less than 38 cm;

above 2,400 m precipitation may exceed 75 cm. Summer thundershowers, July through September, produce locally heavy but scattered rainfall. Probably the most important precipitation comes from widespread rain at lower elevations and significant snow at higher elevations during winter months, brought inland by cyclonic storm systems originating in the Pacific Ocean. Snow melt feeds Arizona rivers, which originate in the higher mountains. At lower elevations, runoff is low due to high evaporation, resulting from high mean temperatures and low humidity.

Table 1.5 gives important climatic data for selected cities in Arizona. Note that areas with high cooling degree days have the greatest potential for geothermal cooling. The reverse is evident for space heating.

CLIMATE

National Oceanographic and Atmospheric Administration, 1973, Monthly normals of temperature, precipitation, and heating and cooling degree days, 1941-70, Climatography of the United States, No. 81 -- Arizona: U. S. Department of Commerce, National Climatic Center, Asheville, NC, 10 p.

Sellers, W. D., and Hill, R. H., eds., 1974, Arizona climate 1931-1972: University of Arizona Press, Tucson, AZ, 616 p.

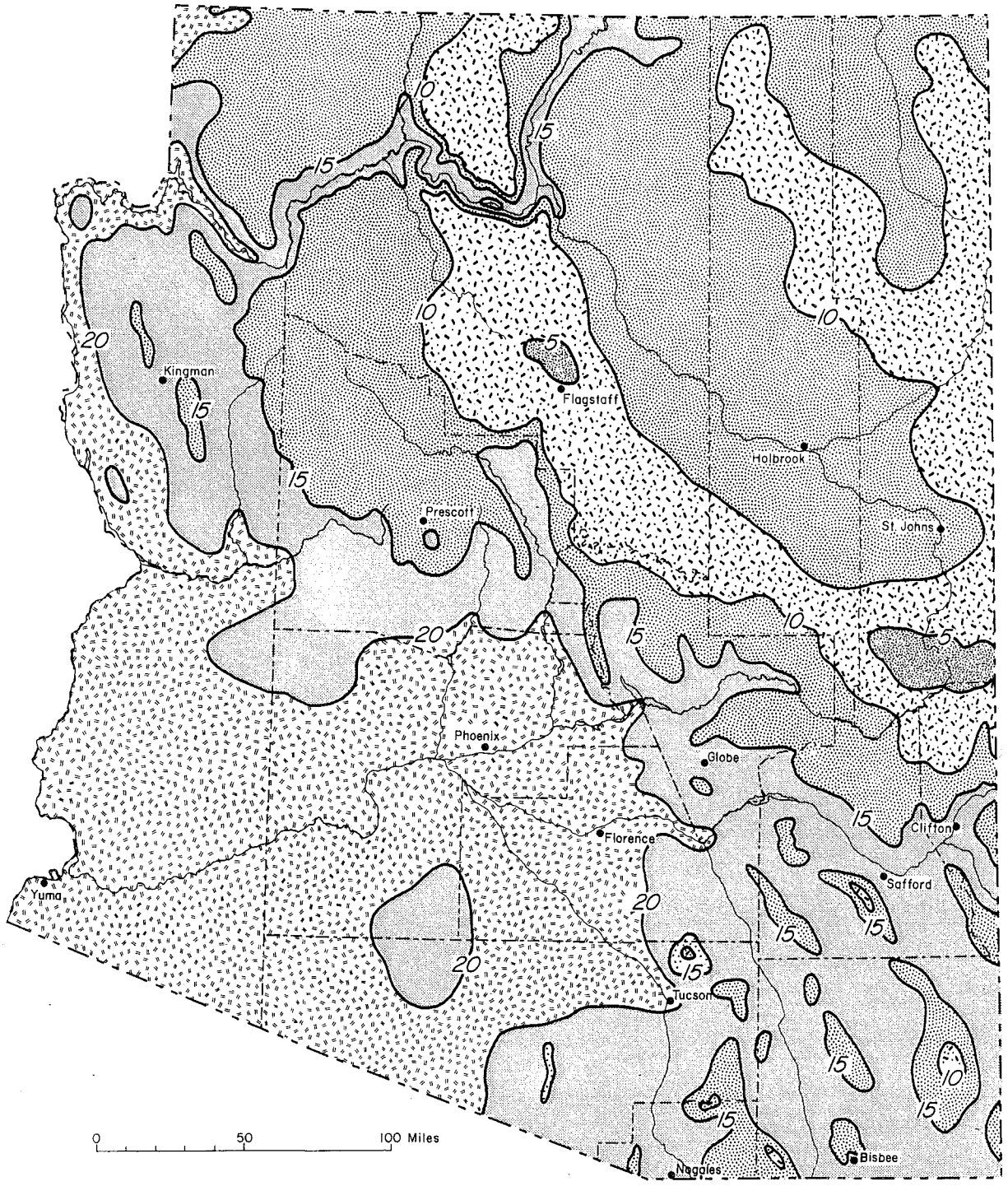

Figure 1.4. Map showing mean annual air temperatures (MAT) in Arizona. Contour interval is 5°C.

TABLE 1.5. CLIMATIC DATA FOR SELECTED ARIZONA CITIES

WEATHER STATION	ELEVATION FEET	ELEVATION METERS	MEAN ANNUAL TEMP °F	MEAN ANNUAL TEMP °C	ANNUAL DEGREE HEATING DAYS [3]	ANNUAL DEGREE COOLING DAYS [3]	RECORD TEMPERATURE[1] LOW °F	LOW (°C)	LOW YEAR	HIGH °F	HIGH (°C)	HIGH YEAR	PRECIPITATION INCHES	PRECIPITATION CENTIMETERS
CASA GRANDE[2]	1405	428.2	70.1	21.2	1629	3515	15	-9.4	1954	120	48.9	1936	8.11	20.60
FLAGSTAFF[2] WSO AIRPORT	7006	2135.4	45.3	7.4	7320	140	-22	-30	1971	96	35.6	1970	19.31	49.05
GILA BEND	737	224.6	72	22.2	1348	3943	10	-12.2	1963	123	50.6	1936	5.76	14.63
KINGMAN[1]	3360	1024.1	61.6	16.4	2906	1633	6	-14.4	1937	111	43.9	1967	9.39	23.85
PHOENIX[2] WSO AIRPORT	1117	340.5	70.3	21.3	1552	3508	17	-8.3	1950	118	47.8	1958	7.05	17.91
SAFFORD[2]	2900	883.9	64.3	17.9	2542	2316	9	-12.8	1964	116	46.7	1971	8.43	21.41
SPRINGERVILLE[2]	7060	2151.9	48.5	9.0	6170	181	-21	-29.4	1971	100	37.8	1953	11.33	28.77
TUCSON[2] WSO AIRPORT	2584	787.6	68.2	20.1	1707	2896	16	-8.9	1949	111	43.9	1970	11.05	28.07
WILLCOX[2]	4190	1277.1	59.1	15.1	3485	1356	-1	-18.3	1960	109	42.8	1970	11.19	28.42
AIRPORT[2]	194	59.1	73.7	23.2	1005	4195	24	-4.4	1971	123	50.6	1950	2.67	6.78

DATA FROM: [1] Sellers and Hill, 1974, Arizona Climate (1973-1972).

[2] NOAA, 1973, Monthly Normals of Temperature, Precipitation, and Heating and Cooling Degree Days

[3] Annual degree days are the sum of monthly degree days which are calculated using a 65°F(18.3°C) base temperature.
Monthly heating degree days = (days in month) ($65^{o}F-T_h$) where T_h is mean monthly temperature below 65°F.
Monthly cooling degree days = (days in month) ($Tc-65^{o}F$) where Tc is mean monthly temperature over 65°F.

USE OF GEOTHERMAL ENERGY

ELECTRIC POWER GENERATION. The use of geothermal energy to generate electric power is expanding rapidly. Production in the United States has grown from 11 megawatts electrical (MWe) in 1960 to 70 MWe in 1970, to 932 MWe in 1981. More than 3,000 MWe have been projected for 1990 (Kestin and others, 1980; Roberts and Kruger, 1981). (One MWe supplies the electrical needs of nearly 1,000 people.)

In 1979 geothermal power plants worldwide produced 1,450 MWe. Additional plants are either planned or under construction.

DIRECT-HEAT APPLICATIONS. It is now recognized that the most abundant geothermal energy is in the form of low- to moderate-temperature resources, with the result that the most widespread potential use for geothermal energy is in direct-heat (nonelectric) applications. Such utilization has potential for a wide variety of processes that presently use hot water from conventional boilers. Direct-heat geothermal energy has several inherently favorable qualities (Anderson and Lund, 1979):

(1) It has generally good energy efficiency because the thermal water is used directly without conversion to an intermediate energy form.

(2) Low- to intermediate-temperature water is available in large quantities that are readily accessible in Arizona (Witcher and others, 1982).

(3) It uses "off-the-shelf" technology. Engineering designs and materials used in direct-heat applications generally are well known

and require little to no modifications.

(4) It has shorter development time and is less capital intensive than all forms of electrical development.

(5) It requires less expensive well development than geothermal electrical power production. In many cases wells can be drilled with conventional water-well drilling equipment.

(6) Geothermal water can be piped more than 30 km without detrimental heat loss, although costs are greater for long distances.

Direct-heat geothermal technology, reliability, and environmental acceptability have been demonstrated in a number of places worldwide. In 1979, over 7,000 megawatts thermal (MWt) of geothermal energy were utilized for space heating and cooling, in agriculture and aquaculture production, and for industrial processes (Anderson and Lund, 1979). In Iceland, more than half the homes and buildings rely on geothermal space heating. The 100-room Rotorua International Hotel in New Zealand is air conditioned by a geothermal absorption refrigeration system. In Arizona, where demand for cooling is high, geothermal resources have significant potential for space cooling. Large multistory buildings, apartment complexes, shopping malls, and commercial districts have the best economic potential for geothermal space heating and cooling.

Agriculture and aquaculture generally use the lowest temperature geothermal resources. These applications have excellent potential in Arizona where the use of lower quality geothermal water could conserve potable ground water without reducing agricultural productivity.
Furthermore, after the heat has been extracted, geothermal water with sufficiently good quality can be added to drinking water and irrigation

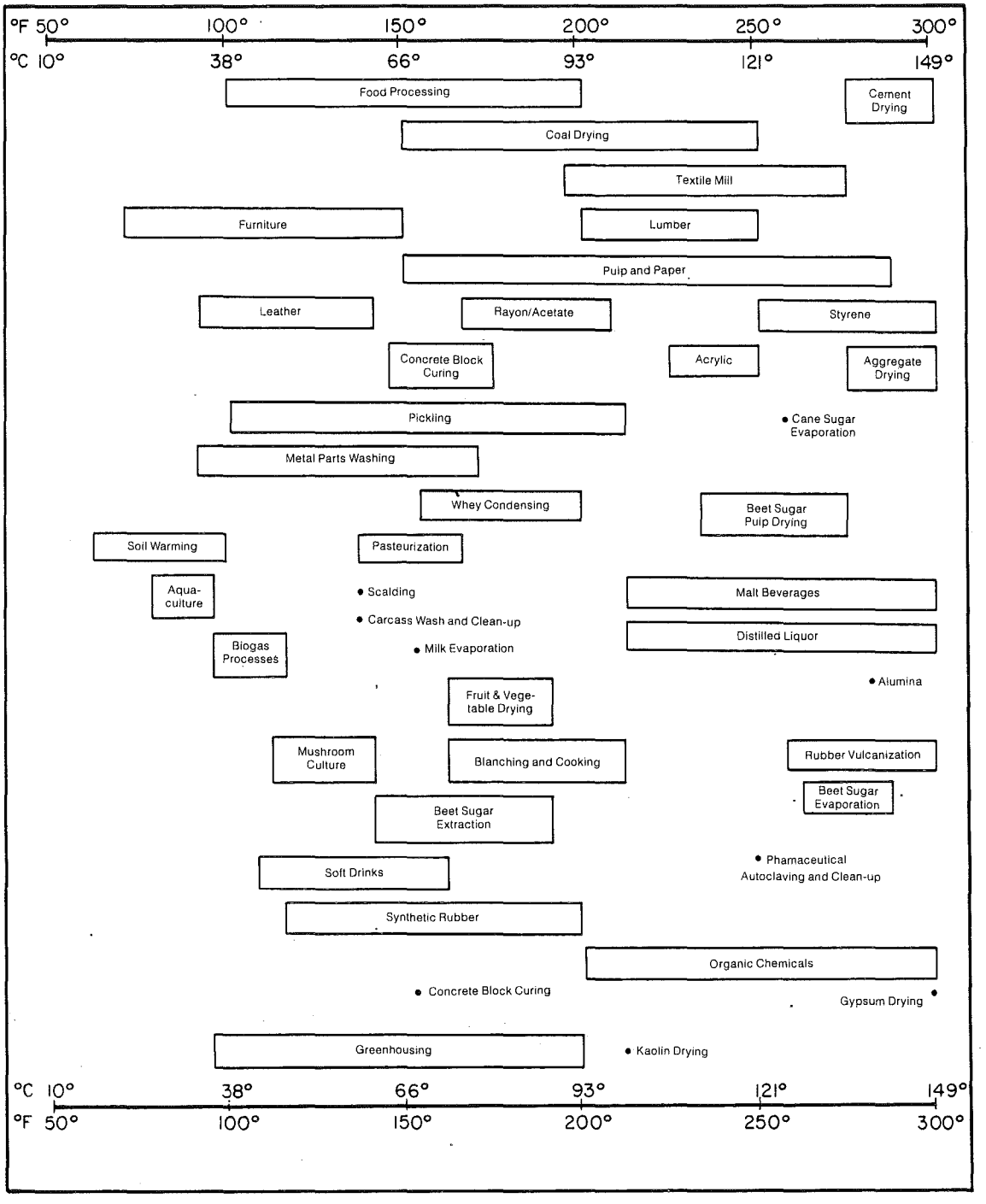

Figure 1.5. Temperature ranges for some industrial processes and agricultural applications (from Anderson and Lund, 1979)

supplies without harmful effects. This practice also would conserve water supplies. In the future, phycoculture, growing algae for food or fuel, may be a viable use of saline geothermal water, further conserving potable ground water.

Industrial processes typically require intermediate-temperature resources in the form of either steam or superheated hot water. Basic processes that could substitute geothermal energy are preheating, cooling, refrigerating, evaporating, distilling, drying, separating, peeling, blanching, and washing. Low-temperature resources may have future importance in the mining industry for the extraction and refinement of metals (Goldstone, 1982, personal commun.). Figure 1.5 shows a few important direct-use geothermal applications that have potential in Arizona.

Since every geothermal resource has a different temperature, water quality, water-production rate, and depth, each direct-use project must be designed accordingly and be co-located near a suitable resource. Corrosion and scaling problems, generally associated with high-temperature resources, are often surmounted by proper selection of materials and appropriate engineering design.

Geothermal energy is not free, but a major benefit of geothermal development is long-term price stability of energy, independent of escalating fossil-fuel prices. Finally, "cascading" systems, whereby several successive operations extract additional heat from the same geothermal water, enhance the economics of geothermal development and again conserve valuable water.

USES OF GEOTHERMAL ENERGY

Anderson, D. N., and Lund, J. W., 1980, Direct utilization of geothermal energy - A layman's guide: Geothermal Resources Council Special Report No. 8, Davis, CA, 97 p.

_____, 1979, Direct utilization of geothermal energy - A technical handbook: Geothermal Resources Council Special Report No. 7, Davis, CA, 250 p.

Armstead, C. H. 1978, Geothermal energy: Halstead Press, New York, NY, 357 p.

Kestin, J., DiPippo, R., Khalifa, H. E., and Ryley, D. J., 1980, Sourcebook on the production of electricity from geothermal energy: Brown University, Providence, RI, 997 p.

Wahl, E. F., 1977, Geothermal energy utilization: John Wiley and Sons, New York, NY, 302 p.

Wehlage, E. F., 1976, The basics of geothermal engineering: Geothermal Information Services, West Covina, CA, 211 p.

See also open-file reports by the Arizona Geothermal Commercialization Team, in Chapter 5.

ENVIRONMENTAL CONCERNS

It is widely known that geothermal resources produce relatively clean energy. Although knowledge of environmental impacts related to geothermal energy development is incomplete, geothermal does offer signficant environmental advantages over other energy sources. (1) Geothermal energy is utilized in the immediate vicinity of the resource, both for electric power generation and direct-heat projects. Thus, environmental impacts are localized and certainly are not as severe as those resulting from mining coal or uranium. Large refineries and extensive transportation systems, except major power grids, are not required. (2) Geothermal development generally does not place large demands on scarce potable water supplies. Some geothermal power plants using steam as the working fluid do not require an external water source for cooling purposes

Environmental impacts depend on the type of geothermal resource; quality of and chemical constituents in the geothermal fluid; overall geology, hydrology, vegetation, and topography of the development site; and engineering design of the facility. In general, high-temperature resources have the greatest impact; low-temperature resources have minimal impact.

The chief environmental issues concerning exploration and development of geothermal resources are land-use conflicts; disturbance of fish, wildlife, natural vegatation, and their habitats; air and ground-water quality; effect on natural hot spring activity; lowering of the water table; noise; land subsidence; induced seismicity; landslides; socioeconomic factors; and

disturbance of archaeological and cultural resources. Careful planning to avoid environmental problems, coupled with appropriate mitigation measures for unavoidable problems, can generally result in minimal impact at a reasonable cost.

GEOTHERMAL EXPLORATION, DRILLING, AND LEASING ACTIVITIES IN ARIZONA

EARLY EXPLORATION. Exploration for geothermal energy was meager in Arizona until the late 1970s. This early lack of interest can best be attributed to the philosophy still widely held by many people that electrical power production, which requires vapor dominated or high-temperature hydrothermal systems, is the only significant use for geothermal energy. Thus it followed that only high-temperature geothermal resources were worth expensive exploration programs. Unfortunately Arizona has few surface thermal features. The hot springs that exist in Arizona compare poorly to the natural geysers, fumaroles, and boiling springs found in neighboring states such as Nevada and California.

Three geothermal drilling projects did take place during the early 1970s. In 1973 following considerable exploration, Geothermal Kinetics, Inc. drilled two geothermal wells in section 1, T. 2 S., R. 6 E. The wells were drilled to depths of 2,800 m (Power Ranch #1) and 3,200 m (Power Ranch #2). Reported bottom-hole temperatures conflict, but in all cases the geothermal gradients did not exceed $50^{o}C/km$.

One year later Geothermal Kinetics, Inc. and Amax Exploration, Inc. drilled Pima Farms #1 in section 8, T. 7 S., R. 8 E. This geothermal test was 2,440 m deep, had a maximum output temperature of $82^{o}C$, and a maximum bottom-hole temperature of $120^{o}C$ after pumping (Dellechaie, 1975). These temperatures again indicate geothermal gradients less than $50^{o}C/km$.

Dellechaie (1975) stated that a normal gradient heat source could be inferred for this well on the basis of pump-test, geochemical, and temperature information.

The fourth geothermal well, State #1, was drilled by Nix Drilling Company of Globe, Arizona in section 16, T. 5 S., R. 24 E. Drilling started in April, 1974, and ceased in November, 1977, when the drilling permit was not renewed by the Arizona State Land Department. Temperatures and depths have not been reported.

RECENT ACTIVITY. The major companies involved in geothermal leasing and exploration in Arizona (in 1982) include Hunt Oil, Chevron USA, Union Geothermal, Phillips Petroleum Co., Atlantic Richfield, Trans-Pacific Geothermal, O'Brien Resources, Amax, and Geothermal Kinetics Systems. Deep drilling for high-temperature resources suitable for electrical production, however, has been limited to the three unsuccessful "wildcat" geothermal tests drilled in early 1970s discussed above. For the past five years exploration has consisted of shallow (less than 400 m) temperature gradient/heat flow holes, and geophysical, geochemical, and geological surveys. Table 1.6 lists areas, number of wells, and operators of the temperature gradient holes.

Exploration for potential hot-dry-rock geothermal energy has been conducted at two sites in western Arizona by the Los Alamos National Laboratory. These areas are the Aquarius Mountains and the Castle Dome Mountains. A third hot-dry-rock geothermal project is in the exploration and planning stages in the Springerville-Alpine area of the White Mountains, east-central Arizona, by a private developer. The Aquarius Mountains and the White Mountains hot-dry-rock areas are described in Chapter 2.

TABLE 1.6. Shallow (<400 m) temperature gradient and heat flow holes drilled in Arizona

Area	Number of Wells	Year	Operator
Ajo	7	1981	Phillips Petroleum Company, Salt Lake City, UT
Alpine-Springerville	5	1979	U.S. Bureau of Reclamation, Boulder City, NV; Arizona Bureau of Geology and Mineral Technology, Tucson, AZ
Clifton	1	1979	U.S. Bureau of Reclamation, Boulder City, NV; Arizona Bureau of Geology and Mineral Technology,Tucson, AZ
State Wide	49	1979	U.S. Geological Survey, Menlo Park, CA
Clifton	6	1980	Phillips Petroleum Co, Salt Lake City, UT
Hyder Valley	37	1981	Phillips Petroleum Co., Salt Lake City, UT
Safford	1	1974	Nix Drilling Company, Reed Nix, Globe, AZ
Safford	8	1981	U.S. Department of Energy, Idaho Falls, ID; Arizona Bureau of Geology and Mineral Technology, Tucson, AZ

To date (1982), no high-temperature (greater than 150°C) geothermal resources have been confirmed in Arizona.

Geothermal leases and lease applications pending approval total over 242,000 acres on state and federal lands (Table 1.7). All leases that are pending approval occur on federal land.

Arizona has two federal Known Geothermal Resource Areas (KGRAs), both near Clifton: the Gillard KGRA, 2,420 acres, and Clifton KGRA, 780 acres (Fig. 1.6).

Currently the only direct-use geothermal energy projects in Arizona are mineral baths at Safford and Mesa, and soil heating in the Hyder Valley (Fig. 1.6). An aquaculture project is in the initial stages of development near Safford. Planning and feasibility studies are under way for space heating (1) a hotel-motel complex in Tucson by a Tucson land developer, (2) the Swift Trail Facility near Safford by the Federal Prison system, and (3) Williams Air Force Base near Chandler by the U. S. Air Force (Fig. 1.6).

TABLE 1.7. Status of geothermal leases on state and federal land, 1981

Area	State		Federal	
	Approved	Pending	Approved	Pending
San Bernardino Valley	30,596 Acres	-0-	-0-	16,591 Acres
Clifton	-0-	-0-	6,304 Acres	11,864 Acres
Flagstaff	-0-	-0-	-0-	118,556 Acres
Aquarius Mts. East of Kingman	-0-	-0-	-0-	30,638 Acres
Burro Creek Near Bagdad	-0-	-0-	-0-	12,360 Acres
Hassayampa Plain	-0-	-0-	15,033 Acres	564 Acres
Total (Statewide)	30,596 Acres	-0-	21,337 Acres	190,573 Acres

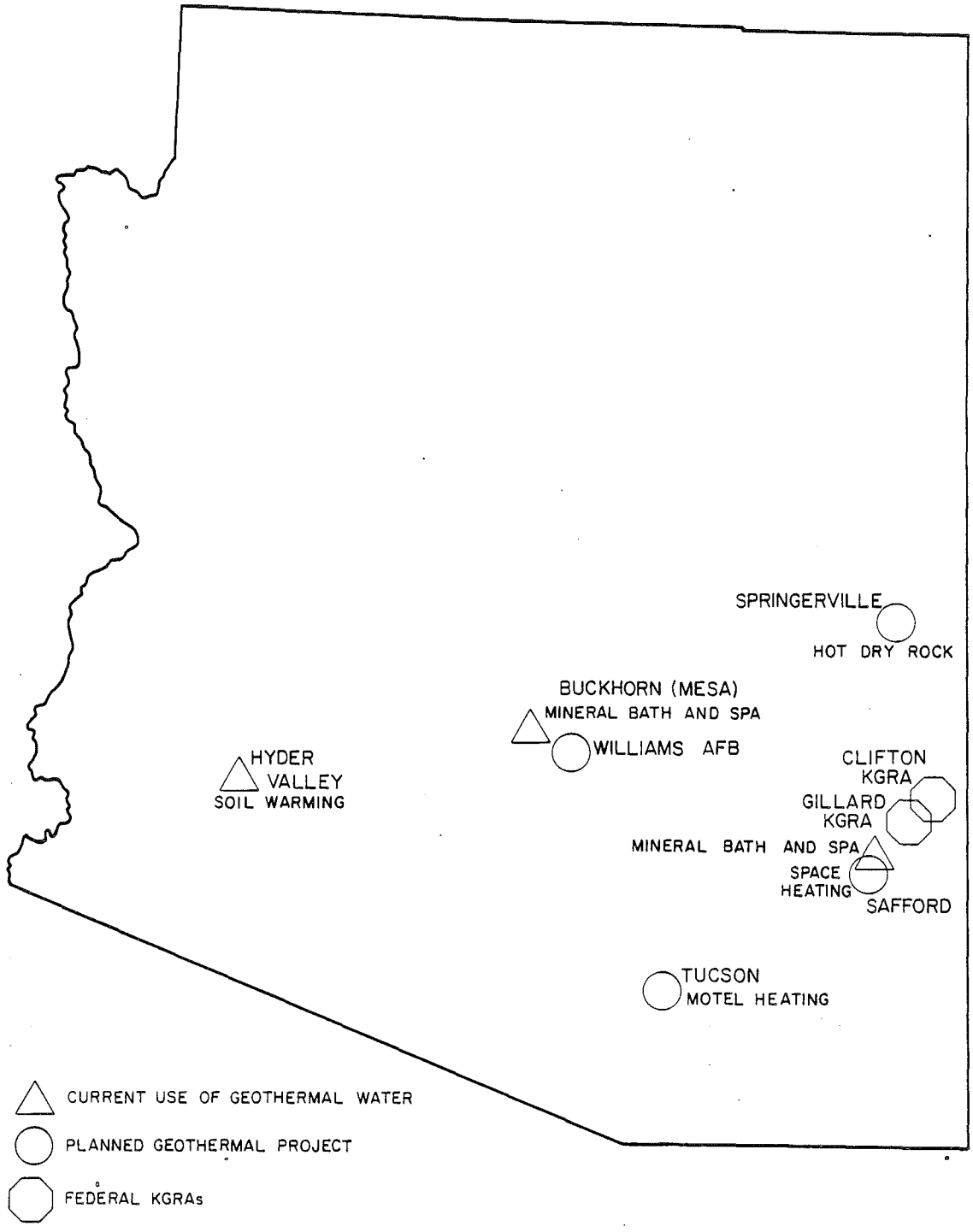

Figure 1.6. Map showing Arizona KGRAs, areas currently using geothermal energy, and areas of planned development

GEOTHERMAL LEGISLATION, REGULATIONS, AND TAXES

A successful geothermal development must acquire legal rights to a resource and comply with federal, state, and local laws, ordinances, and regulations covering exploration, development, and use.

FEDERAL. The Geothermal Steam Act of 1970[1] provides for leasing on federal land and licensing of geothermal power plants. Leases and licenses are issued by the Bureau of Land Management (BLM). Exploration and operations are conducted within the rules of the Geothermal Resources Operations Orders (GROOs), issued under the Geothermal Steam Act of 1970. After federal leases are issued, operations are supervised by the U. S. Geological Survey, Conservation Division Area Geothermal Supervisor within the framework of the GROO's and the Geothermal Steam Act.

Provisions for federal taxation applicable to geothermal energy are made in the Energy Tax Act of 1978[2]. The Act covers intangible drilling costs, depletion allowance, and tax credits for all forms of geothermal energy whether steam, hot water, or hot dry rock. Additional legislation is pending.

STATE. In Arizona, the Geothermal Resources of 1972[3] legislation, which was revised in 1977, provides for leasing and development of geothermal resources on state land. Under this legislation, the Arizona

---

[1] Public Law 90-581, 91st Congress, 5.368, Dec. 24, 1970.
[2] Public Law 95-618, 403 (b), Amending IRC 613A (b).
[3] Geothermal Resources (1972); Amended HB 2257 (1977) A.R.S. 27-651 through A.R.S. 27-686.

State Land Department issues leases and land permits for exploration and development of geothermal energy; the Arizona Oil and Gas Conservation Commission supervises all drilling and reinjection operations. Arizona geothermal legislation broadly defines geothermal resources in a manner similar to the federal Geothermal Steam Act of 1970 and also provides for taxation of geothermal endeavors.

Geothermal development is exempt from ground water laws under current state geothermal legislation. However, the language and qualifications in the Ground Water Management Act of 1980 leave exemption as a matter of interpretation in Active Management Areas, which were designated by the provisions of the Act (Goldstone, 1982, personal commun.). Other potential institutional problems also exist. First, State legislation does allow exploration deductions and a depletion allowance, but no definite rules exist for calculating royalty rates. Since direct utilization does not have an easily defined market value, the royalty rate could be tied to the value of energy replaced. However, the price of electricity, coal, and gas varies considerably and the value of direct-use geothermal could be tied to the most expensive conventional energy available in a given location (Goldstone, 1982, personal commun.). Secondly, current Arizona tax structure offers advantages to solar energy as an alternate energy source, but it does not offer the same advantages to geothermal development. State tax incentives exclude cooling devices that utilize geothermal energy in conjunction with other energy sources. These problems have not been addressed to date.

GEOTHERMAL LEGISLATION, REGULATIONS, AND TAXES

Anderson, D. W., and Lund, J. W., 1979, Direct utilization of geothermal energy - A technical handbook: Geothermal Resources Council Special Report No. 7, Davis, CA, 250 p.

Arizona Oil and Gas Conservation Commission, 1972, Rules and regulations on geothermal energy: OGCC, Phoenix, AZ, 39 p.

Godwin, L. H., Haigler, L. B., Rioux, R. L., White, D. E., Muffler, L. J. P., and Wayland, R. G., 1971, Classification of public lands valuable for geothermal steam and associated geothermal resources: U. S. Geological Survey Circular 647, 18 p.

Malysa, L., 1979, Arizona Geothermal Institutional Handbook: Arizona Bureau of Geology and Mineral Technology Open-File Report 80-7, Tucson, AZ, 70 p.

U. S. Geological Survey, 1976, Geothermal resources operations orders (GROOs): U.S. Geological Survey, Conservation Division, Menlo Park, CA, 30 p.

CHAPTER 2

INTRODUCTION

Arizona is the sixth largest state in the United States, with a total land area of 295,000 km^2. The state includes large parts of two major physiographic provinces, the Colorado Plateau to the north and the Basin and Range province chiefly to the south and west (Fig. 2.1). Dividing these two provinces is the Transition Zone, a mountainous region crossing the state approximately southeast-northwest. Some investigators considered the Transition Zone a third physiographic province (i.e. Ransome, 1904; Wilson and Moore, 1959; Wilson, 1962). Other workers did not (i.e. Fenneman, 1931; Bromfield and Shride, 1956; Heindl and Lance, 1960; Hayes, 1969).

The Basin and Range province was a region of major crustal extension in the not-so-distant geologic past. As such, it is today the area in Arizona containing the greatest abundance of geothermal resources. Therefore, exploration was directed principally toward this part of the state.

In this chapter we present a summary of each area for which a geothermal resource assessment was made. The areas are arranged into sections according to the physiographic province (and in southern and western Arizona, subprovince) in which they occur. Each section is preceded by a brief description of the geology, structure, and geohydrology of that province (and subprovince). More detailed discussions of these features are given in individual area reports.

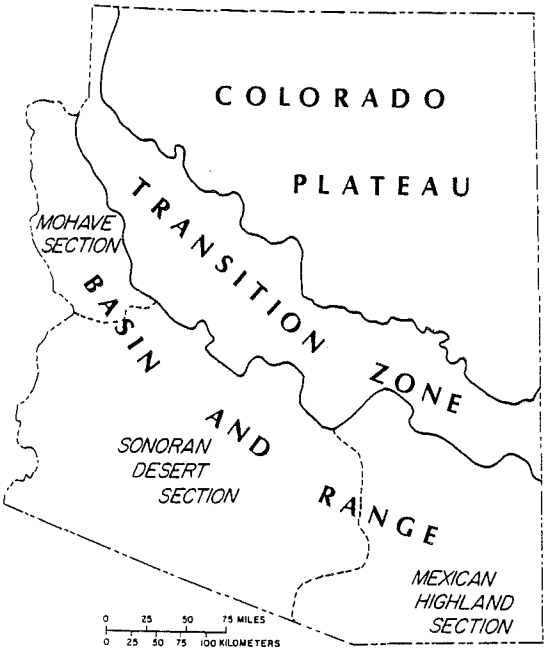

Figure 2.1. Physiographic provinces and subprovinces of Arizona

INTRODUCTION REFERENCES

Bromfield, C. S., and Shride, A. F., 1956, Mineral resources of the San Carlos Indian Reservation, Arizona: U. S. Geological Survey Bulletin 1027-N, p. 613-691.

Fenneman, N. M., 1931, Physiography of western United States: McGraw-Hill Book Company, New York, 534 p.

Hayes, P. T., 1969, Geology and topography: Mineral and water resources of Arizona: Arizona Bureau of Mines Bulletin 180, p. 35-58.

Heindl, L. A., and Lance, J. F., 1960, Topographic, physiographic, and structural subdivisions of Arizona: Arizona Geological Society Digest, v. 3, p. 12-18.

Ransome, F. L., 1904, Description of the Globe quadrangle, Arizona: U. S. Geological Survey Folio 111, 17 p.

Wilson, E. D., 1962, A resume of the geology of Arizona: Arizona Bureau of Mines Bulletin 171, 140 p.

Wilson, E. D., and Moore, R. T., 1959, Structure of Basin and Range province in Arizona: Arizona Geological Society Guidebook II Southern Arizona, p. 89-106.

COLORADO PLATEAU

PHYSIOGRAPHY. In Arizona the Colorado Plateau province is an elevated area of comparatively flat-lying, relatively undeformed sedimentary rocks that are slightly tilted to the northeast. Broad regional uplifts have been eroded into large-scale mesas that form a vast steplike topography, dissected by canyons. Major regional features are the Defiance uplift along the Arizona-New Mexico border, Black Mesa basin nearly in the center of northeastern Arizona, the Mogollon Slope in the southeast, and six major structural blocks that comprise the southwestern margin of the Colorado Plateau in Arizona (Figs. 2.2 and 2.3). Much of the Colorado Plateau exceeds 1,800 m in elevation, and some areas attain altitudes greater than 2,700 m. Mean annual air temperature is 10 to 13°C.

GEOLOGY. Precambrian rocks are exposed on the plateau only in the Grand Canyon and in two small outcrops on the Defiance uplift. They have been encountered in drill holes at depths varying from 700 to 2,300 m. Plutonic, metamorphic, and sedimentary Precambrian rocks have been identified.

Lower Paleozoic strata are generally thin and discontinuous, and are absent in much of the eastern plateau. Upper Paleozoic rocks are more abundant, with the Permian System being thicker than all other Paleozoic units combined. Permian rocks form most of the surface outcrops south and west of the Little Colorado River. Mesozoic strata are the principal surface exposures north and east of the river (Fig. 2.4).

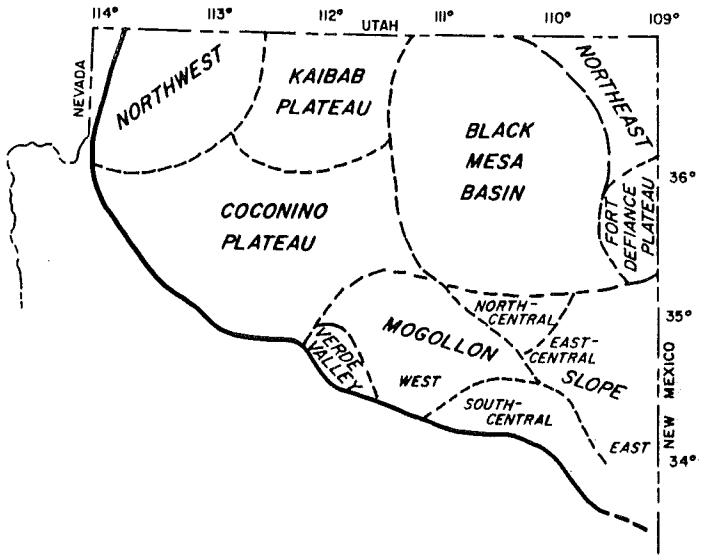

Figure 2.2. Major structural features of northeastern Arizona (from Conley, 1975)

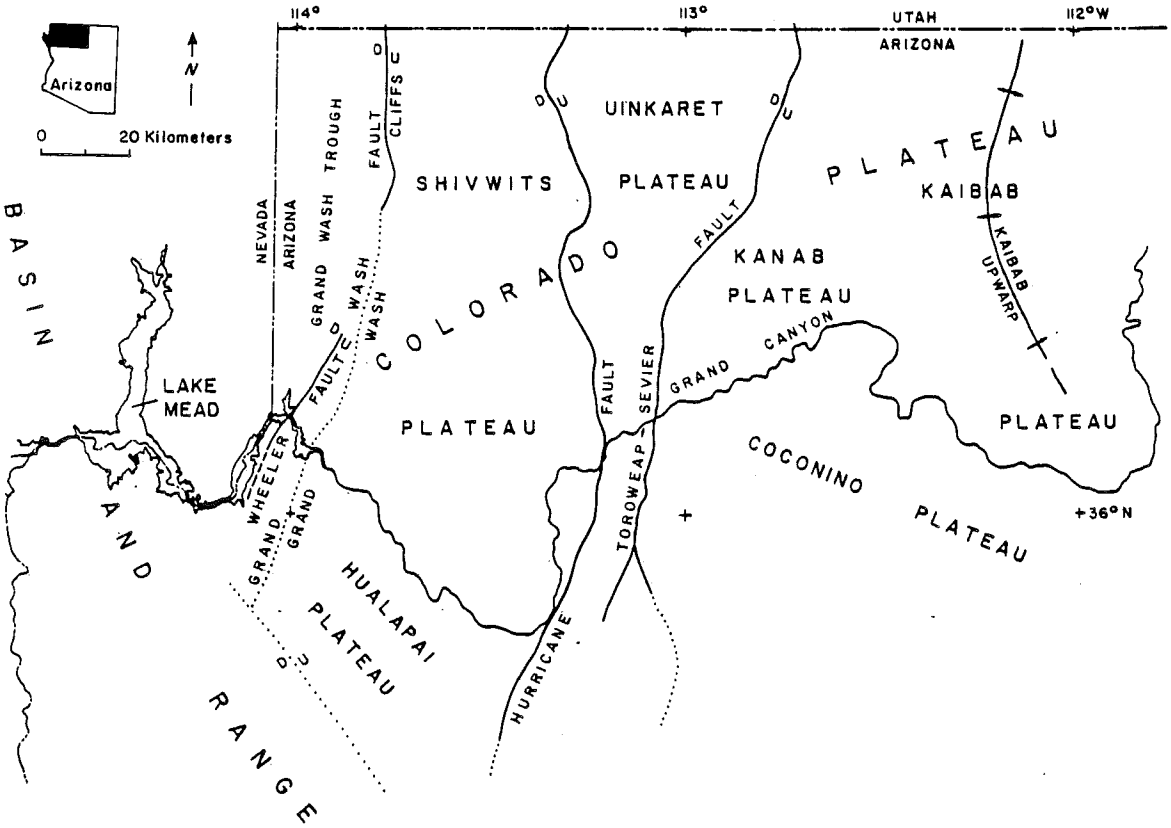

Figure 2.3. Major structural features of north-central and northwestern Arizona (from Lucchitta, 1974)

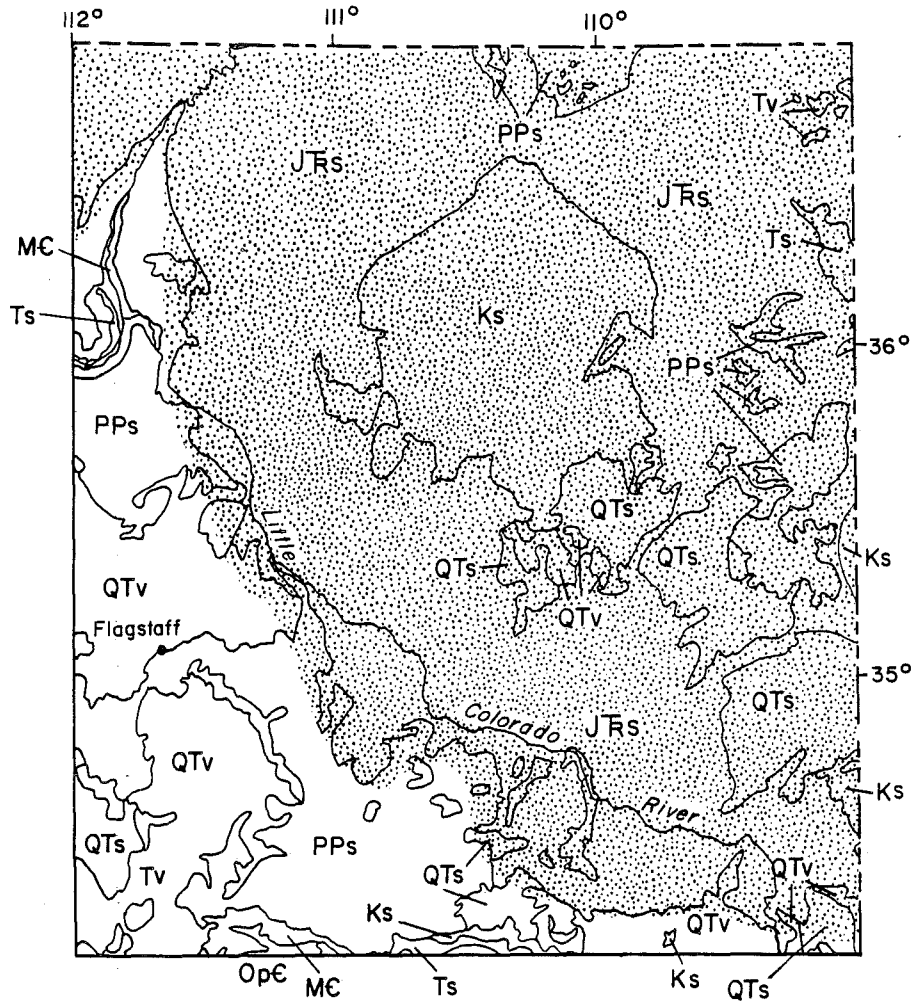

Figure 2.4. Geologic map showing generalized limits of Permian (nonshaded) and Mesozoic (shaded) outcrops in northeastern Arizona

The north-trending Defiance uplift limits Black Mesa basin on the east. The uplift is about 120 km long and rises to about 2,150 m. The Paleozoic section thins to about 400 m on the Defiance uplift, where Permian strata rest unconformably on pink Precambrian granite. All of

Arizona's oil, gas, and helium production is on or near the Defiance region.

Black Mesa, which is situated in the central part of Black Mesa basin, is an erosional remnant and topographic high that stands 150 to 300 m above the surrounding terrane. Formerly extensive Cretaceous rocks were locally preserved at Black Mesa due to down warping of Black Mesa basin. Cretaceous rocks also crop out farther south in the eastern part of the Mogollon Slope. Minor exposures of middle Tertiary to early Quaternary clastic sediments are present locally in river and stream channels on the Mogollon Slope and in the Hopi Buttes area, on the southern margin of Black Mesa basin.

The Mogollon Slope covers about 25,900 km^2 within the area bounded by the southern Navajo Indian Reservation on the north to the Mogollon Rim on the south and Flagstaff on the west to the Arizona-New Mexico border. The region slopes south to north about 6.5 m per 1,000 m and accounts for the southward wedge out of Triassic and Jurassic rocks beneath Cretaceous strata (Peirce and others, 1970).

The Mogollon Slope is lithologically varied both in outcrop and in the subsurface. Stratigraphy in this region contains Precambrian crystalline rocks, sedimentary rocks of Paleozoic, Mesozoic, and Cenozoic age, and Cenozoic volcanic rocks.

The plateau of northwestern Arizona is composed of structural blocks that dip gently (2 to 4 degrees) northeast. The blocks are bounded by major north-trending normal faults having lengths of tens to hundreds of kilometers and displacements of hundreds to thousands of meters (Lucchitta, 1974). Many of these fault zones such as the Toroweap, Grand Wash, and

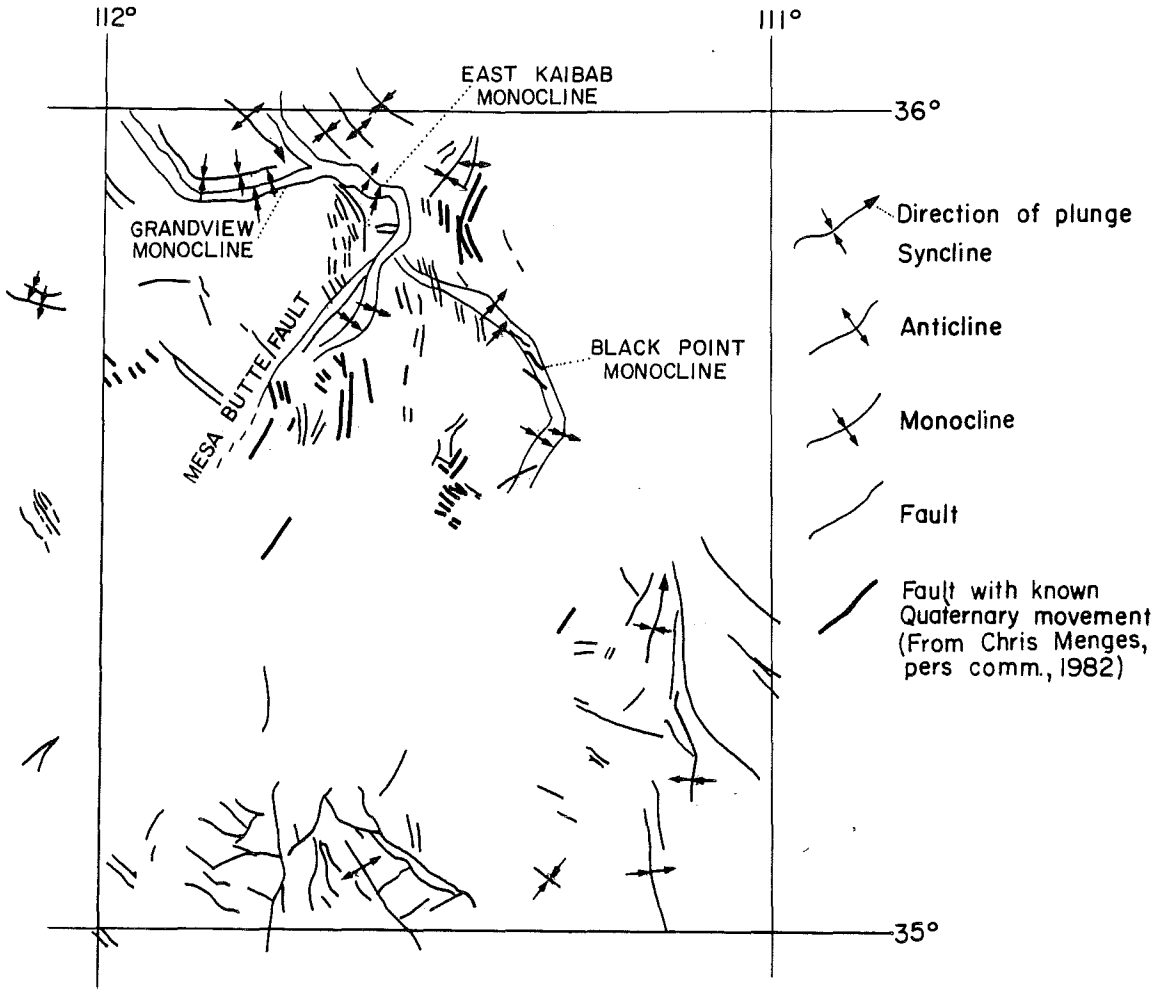

Figure 2.5. Principal structures in the Flagstaff region

Hurricane faults have been active during Quaternary time. The most common rocks exposed at the surface are the Permian Kaibab Limestone, Triassic Moenkopi Formation, and Cenozoic basaltic lavas.

Deformation in the Flagstaff region is dominated by arcuate northwest-trending monoclines, consistently flexed downward to the east (Fig. 2.5) (Shoemaker and others, 1974; Huntoon, 1974; Lucchitta, 1974). The monoclines (the East Kaibab, Grandview, and Black Point) are transected by a system of northeast-trending lineaments and faults. The prominant Mesa

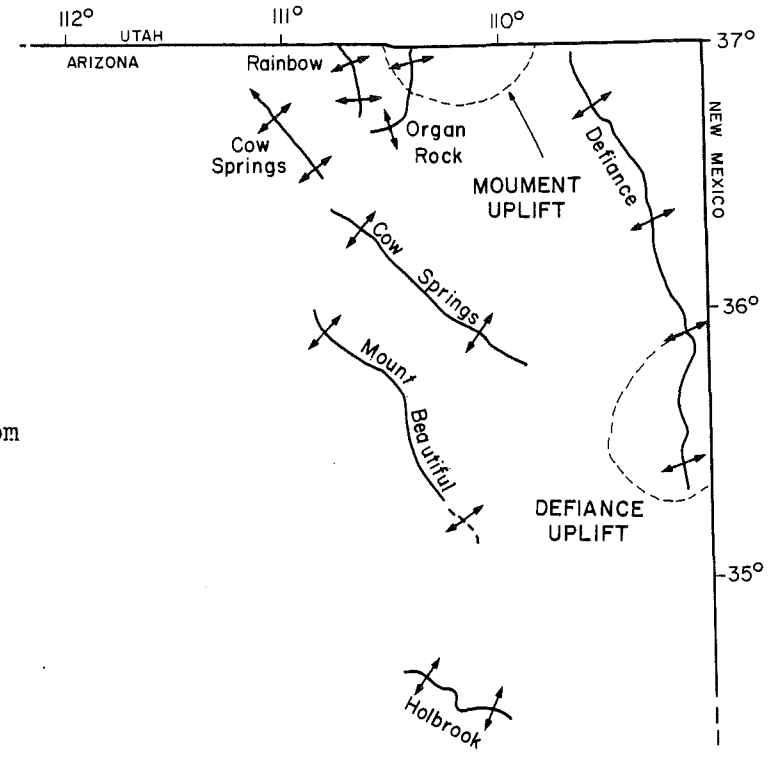

Figure 2.6. Major anticlines and uplifts of northeastern Arizona (from Davis and Kiven, 1975)

Butte fault system splays into the East Kaibab-Grandview monocline and separates this latter structure from the Black Point monocline. A linear, 300-km long aeromagnetic high anomaly coincides with the trace of the Mesa Butte fault system, which suggests a major crustal inhomogeneity. Quaternary deformation has occured on the Mesa Butte fault and related fault splays and grabens. Faults with Quaternary movement are shown in Figure 2.5.

The principal faults of the plateau occur west of Longitude 111°, while eastward of that line, deformation is reflected by mostly northwest-trending anticlines (Organ Rock, Boundary Butte, Holbrook) and major uplifts (Defiance and Monument) (Fig. 2.6).

Four young volcanic fields are located along the south and southwest margins of the Colorado Plateau. Extrusions of predominantly basaltic

Tertiary-Quaternary lavas cover large areas in both the White Mountain and San Francisco volcanic fields. In both fields, cinder cones are abundant toward the plateau interior where lavas are younger (<1 m.y.). In the San Francisco volcanic field, intermediate to silicic lavas (<3 m.y. old) were erupted contemporaneously with the basaltic lavas, and formed stubby flows, domes, and dome complexes. The silicic centers form two distinct northeast-trending, en echelon chains (Fig. 2.7). A third but less extensive volcanic field, the Quaternary Uinkaret field, lies mostly north of the Grand Canyon but at one location basaltic lavas cascaded into the canyon at Vulcan's throne. The fourth volcanic field, Hopi Buttes, erupted on the southern flank of Black Mesa basin during the Pliocene. Maar craters and volcanic plugs characterize much of this field today.

GEOHYDROLOGY. Ground water in northeastern Arizona occurs in three principal multiple-aquifer systems in Mesozoic and Paleozoic strata (Kister, 1973) (Fig. 2.8). The D (Dakota) multiple-aquifer system consists of the Cretaceous Dakota Sandstone and the Jurassic Morrison Formation and Cow Springs Sandstone. The N (Navajo) multiple-aquifer system comprises principally the Navajo Sandstone of Jurassic and Triassic(?) age and the upper part of the Triassic Wingate Sandstone. The C (Coconino) multiple-aquifer system consists of the Shinarump Member of the Triassic Chinle Formation and the Permian Coconino and De Chelly Sandstones. Water from the D aquifer contains from 1,000 to 3,000 mg/L TDS; water from the N aquifer contains less than 1,000 mg/L TDS; and water from the C aquifer contains from about 200 to 25,000 mg/L TDS. These water-bearing units are separated by thick relatively impermeable layers of siltstone and mudstone.

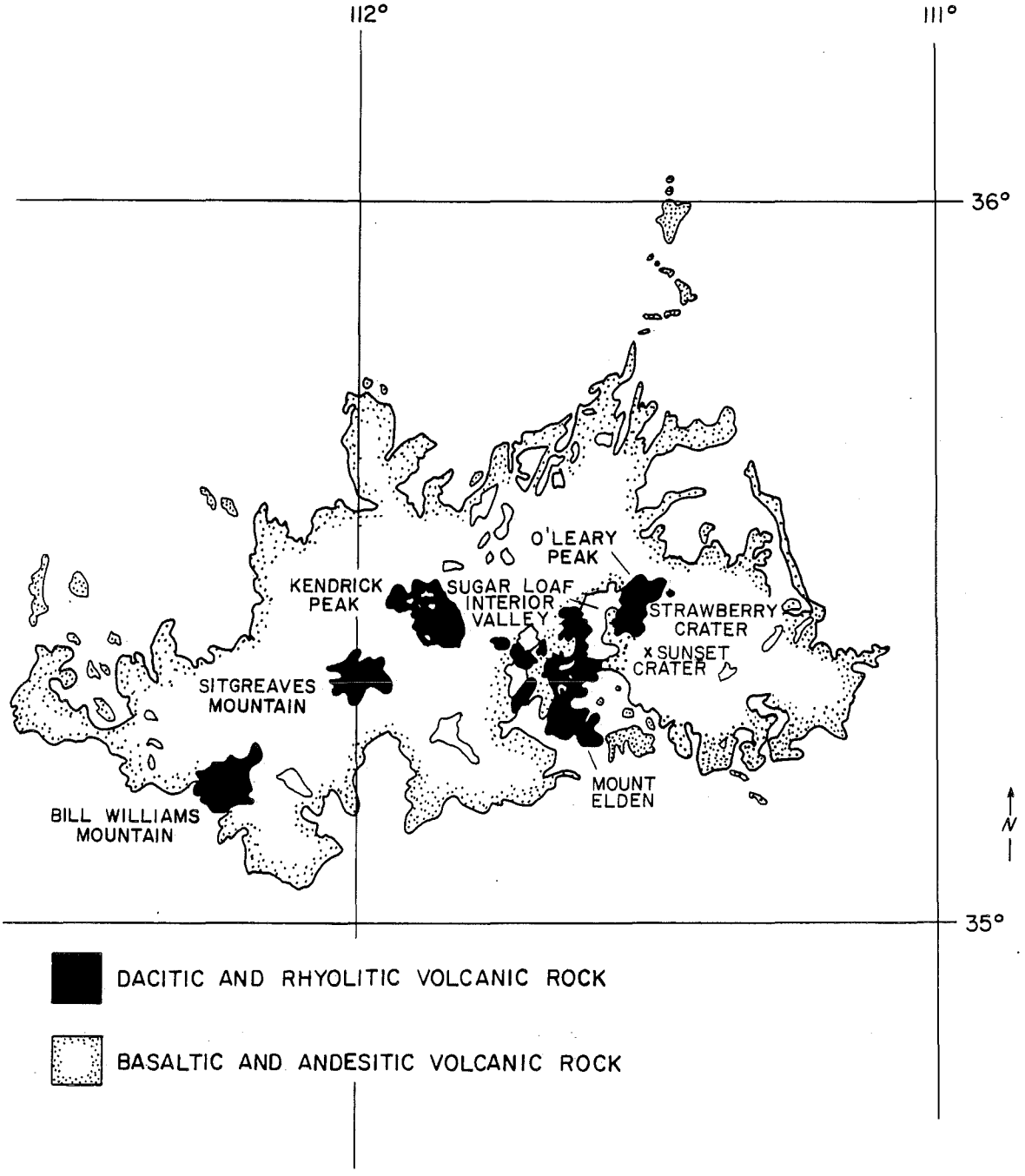

Figure 2.7. Major silicic centers in the San Francisco volcanic field

ERA	SYSTEM		BLACK MESA	SAN FRANCISCO VOLCANIC FIELD	SOUTH-CENTRAL COLORADO PLATEAU	GEOHYDROLOGIC CHARACTERISTICS
WELL LOCATIONS			(A-29-19) 8ad	(A-19-6) 17da	(A-10-30) 27ac	
CENOZOIC	TERT-QUAT			Volcanics		Water-bearing
MESOZOIC	CRETACEOUS		Wepo Fm			
			Toreva Fm			Water-bearing
			Mancos Sh			Aquiclude
			Dakota Ss			
	JURASSIC		Morrison Fm			D Multi-Aquifer
			Cow Springs Ss			
			Entrada Ss			
			Carmel Fm			Aquitard
	~ JTR ~		Navajo Ss			
	TRIASSIC		Kayenta Fm			N Multi-Aquifer
			Moenave Fm			
			Wingate Fm			
			Chinle Fm			Water-bearing
			Moenkopi Fm		Moenkopi Fm	Aquitard
PALEOZOIC	PERMIAN			Kaibab Ls	Kaibab Ls	C Multi-Aquifer
			De Chelly Ss	Coconino Ss	Coconino Ss	
			Supai Fm	Supai Fm	Supai Ss	
	~ PENN-PERM ~		Naco Fm	Naco Fm		Water-bearing ?
	PENN		Redwall Ls	Redwall Ls		Limestone Aquifer
	DEVONIAN		Ouray Fm	Martin Fm		
			Elbert Fm			?
			Aneth Fm			
	CAMBRIAN		Bright Angel Sh			Aquitard
			Tapeats Ss			Water-bearing
PRECAMBRIAN	PRECAMBRIAN		Granite	Granite	Granite	Aquiclude ?

Figure 2.8. Principal strata comprising the major multiple-aquifer systems for three areas in northeastern Arizona (from Sass, Stone, and Bills, 1982)

The D and N aquifers are chiefly in the north-central and northeast parts of Arizona (Fig. 2.9). To the south, these aquifers cease to yield water and eventually the formations thin to extinction as a result of erosion. The C multiple-aquifer system becomes the principal aquifer in the southern portions of northeastern Arizona.

These major aquifer systems are generally continuous, occasionally confined, and possibly interconnected. However, aquifer characteristics are not uniform throughout the plateau. Regionally, the aquifers are controlled by lithology and bedding, and locally by faults and joints. Three major hydrologic basins and parts of four others exist beneath northeastern Arizona, and ground water locally moves between these basins. Shallow perched aquifers under water-table conditions locally yield water to wells. West of the Kaibab Plateau ground-water movement is controlled chiefly by the northward-plunging Coconino and Virgin troughs and by the Hurricane, Sevier, and Grand Wash faults (Ligner and others, 1969).

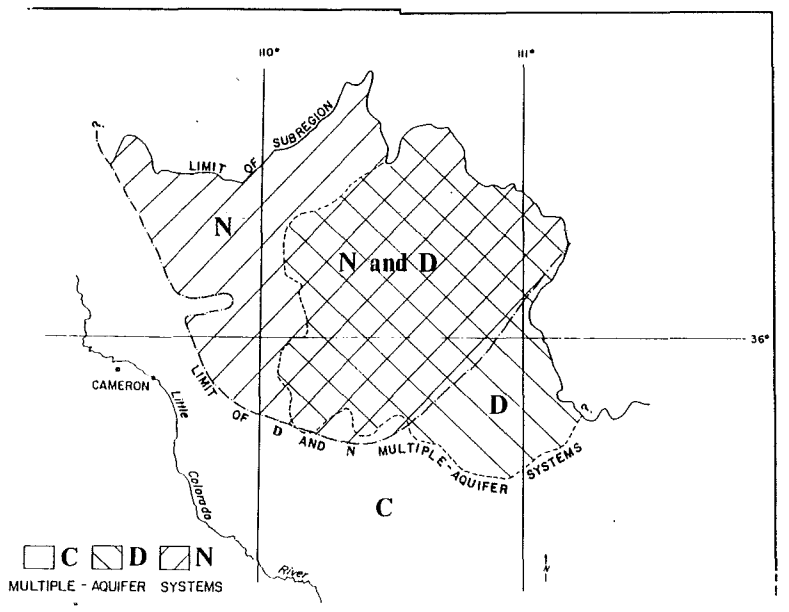

Figure 2.9. Location of principal multiple-aquifer systems in north-central and northeastern Arizona (from Brown, 1976)

COLORADO PLATEAU REFERENCES

Brown, S. G., 1976, Preliminary maps showing ground-water resources in the lower Colorado River region, Arizona, Nevada, New Mexico, and Utah: U. S. Geological Survey Hydrologic Investigations Atlas HA-542, scale 1:1,000,000.

Conley, J. N., 1975, Explanatory text and well-data tabulation to accompany well-location map nine, Colorado Plateau province, Arizona: Arizona Oil and Gas Conservation Commission, 45 p.

Davis, G. H., and Kiven, C. W., 1975, Structure map of folds in Phanerozoic rocks, Colorado Plateau tectonic province of Arizona: Office of Arid Lands Studies and the Department of Geosciences, University of Arizona.

Huntoon, P. W., 1974, Synopsis of the Laramide and post-Laramide structural geology of the eastern Grand Canyon, Arizona: *in* Karlstrom, N. V., Swann, G. A., and Eastwood, R. L. (eds.) Geology of northern Arizona: Geological Society of America Rocky Mountain Section Meeting, Flagstaff, p. 317-335.

Ligner, J. J., White, N. D., Kister, L. R., and Moss, M. E., 1969, Water resources: *in* Mineral and water resources of Arizona, Arizona Bureau of Mines Bulletin 180, p. 471-569.

Lucchitta, I., 1974, Structural evolution of northwest Arizona and its relation to adjacent Basin and Range province structures: *in* Karlstrom, N. V., Swann, G. A., and Eastwood, R. L. (eds.) Geology of northern Arizona: Geological Society of America Rocky Mountain Section Meeting, Flagstaff, p. 336-354.

Peirce, H. W., Keith, S. B., and Wilt, J. C., 1970, Coal, oil, natural gas, helium, and uranium in Arizona: Arizona Bureau of Mines Bulletin 182, 289 p.

Sass, J. H., Stone, C., and Bills, D. J., 1982, Shallow subsurface temperstures and some estimates of heat flow from the Colorado Plateau of northeastern Arizona: U. S. Geological Survey Open-File Report 82-994, 112 p.

Shoemaker, E. M., Squires, R. L., and Abrams, M. J., 1974, The Bright Angel and Mesa Butte fault systems of northern Arizona: *in* Karlstrom, N. V., Swann, G. A., and Eastwood, R. L. (eds.), Geology of northern Arizona: Geological Society of America Rocks Mountain Section Meeting, Flagstaff, p. 355-391.

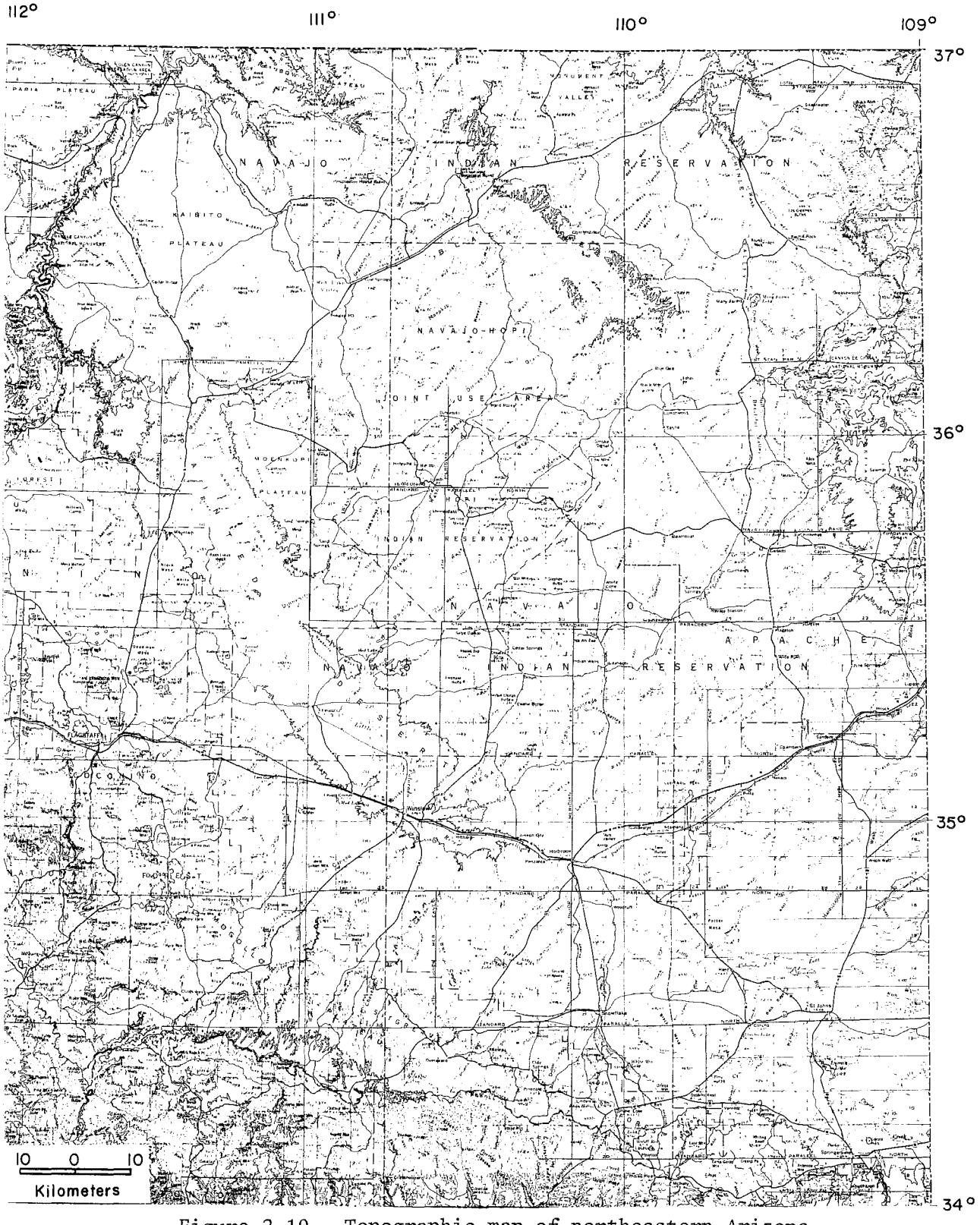

Figure 2.10. Topographic map of northeastern Arizona

NORTHEASTERN ARIZONA

INTRODUCTION. Northeastern Arizona (Fig. 2.10) is a vast semiarid land of high elevation that lies completely within the Colorado Plateau province. Most of the land belongs to the Navajo and Hopi Indian Tribes or is managed by the U.S. Forest Service.

Little exploration for geothermal resources has been conducted in this part of the state chiefly because the regional geology and structure do not appear conducive to occurrences of geothermal energy. Possible exceptions are the San Francisco and White Mountain volcanic fields to the southwest and south, which are discussed in separate reports. In addition, population centers in northeastern Arizona are small and widely spaced, severely limiting possible direct-use geothermal applications.

This summary covers parts of Apache, Navajo, and Coconino Counties. However, because the more western parts of this region have fewer available data, our findings may be a reflection of data density rather than actual conditions.

THERMAL WELLS. In northeastern Arizona, 91 wells have reported temperatures greater than $10^{\circ}C$ above the MAT, but depths are unknown for 33 of these. Of the remaining 58 wells, 35 are thermal by our definition, which in the case of the Colorado Plateau are temperatures approximately $20^{\circ}C$ or greater and gradients $30^{\circ}C/km$ or greater.

The thermal wells occur either as single point anomalies separated by large distances, or in three distinct groups: the Four-Corners area,

south-southwest of Sanders, and west of the Petrified Forest (Fig. 2.11). Over this very large region, nearly half of the thermal wells cluster near Sanders and the Petrified Forest. These and most other wells in Apache County either penetrate or bottom in the formations comprising the C multiple-aquifer system. In the Four Corners area and in northern Navajo County, the thermal wells intersect or bottom principally in the formations of the D or N multiple-aquifer systems.

HEAT FLOW. Average heat flow on the Colorado Plateau generally is lower than it is in the Basin and Range province. Bodell and Chapman (1982) presented data from Utah that confirmed low heat flow in the plateau interior (about 60 mWm^{-2}) They used two high heat flows near Sanders, Arizona (109 and 160 mWm^{-2}) from Reiter and Shearer (1979) to define the southern thermal boundary of the Colorado Plateau interior in Arizona. Sass and others (1982) presented two high apparent heat flows (94 and 110 mWm^{-2}) 30 to 50 km northwest of Sanders and suggested that a slight northward adjustment in the Bodell and Chapman thermal boundary between the plateau interior and periphery would easily accommodate the new data (Fig. 2.12).

All four of these heat-flow values (Reiter and Shearer, 1979; Sass and others, 1982), however, are considerably higher even than the 80 to 90 mWm^{-2} average peripheral value determined by Bodell and Chapman (1982). They are possibly indicative of thermal enhancement of this area. In addition, the high heat flows of Shearer and Reiter (1979) are located in the same area southwest of Sanders that has the high density of thermal wells. Two heat-flow measurements have been published for the Four Corners

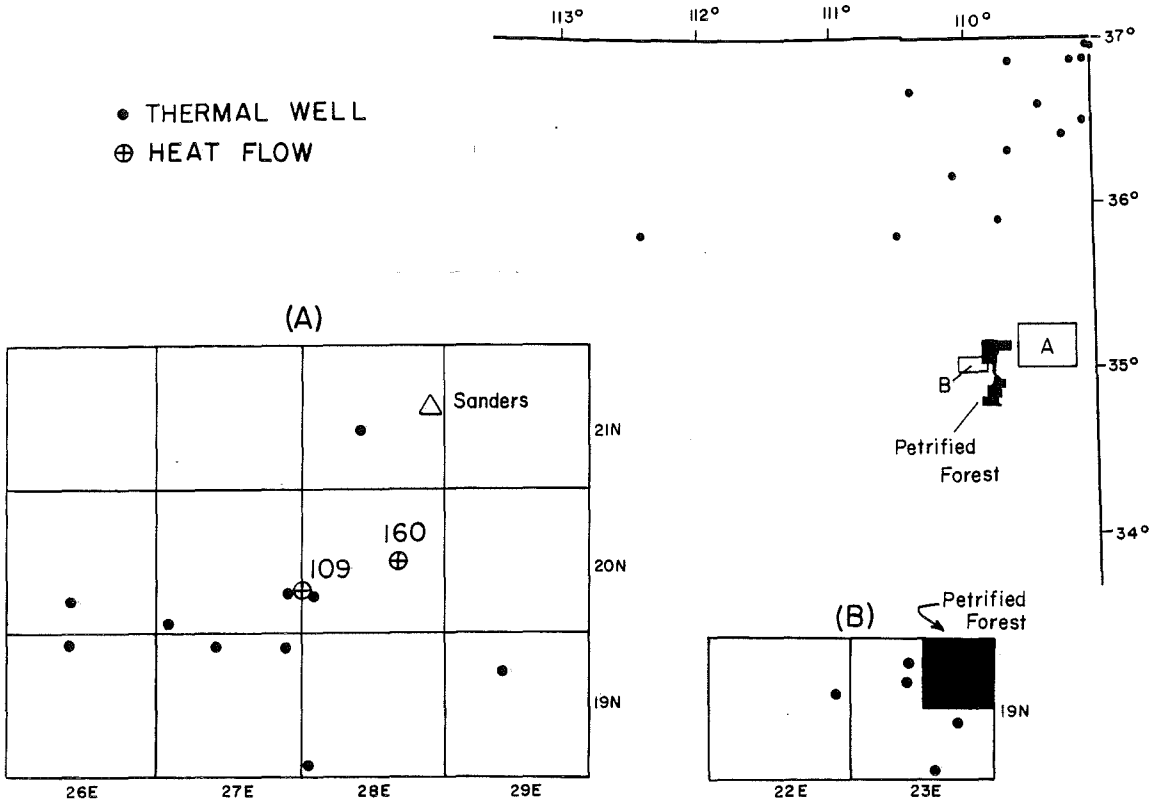

Figure 2.11. Locations of thermal wells in northeastern Arizona. Inset A shows thermal-well cluster and heat-flow values (from Shearer and Reiter, 1979) near Sanders. Inset B shows thermal-well cluster near the Petrified Forest.

area (Reiter and others, 1979), but these values (47 and 65 mWm^{-2}) are about normal for the plateau interior.

Reiter and Shearer (1979) suggested that the high heat flow of the eastern Mogollon Slope, which includes the Sanders area, is from the same sources that caused extensive Quaternary basaltic volcanism in east-central Arizona and west-central New Mexico. Bodell and Chapman (1982) presented alternative evidence that the high heat flow of the plateau periphery is a result of lithosphere thinning and upward mass flux in the mantle, transient processes that are slowly migrating into the plateau interior. They

suggested that high elevation, voluminous volcanic activity, and normal faulting, which are also associated with the plateau periphery, likewise result from these processes.

CONCLUSIONS. Based on the thermal data presented here, plus the Residual Temperature Map (this volume), we suggest that northeastern Arizona is an area of slight thermal enhancement. The Sanders area in particular warrants additional geothermal exploration.

It is questionable whether the Four Corners area is thermally enhanced. Heat flow values there are normal for the plateau interior, but several of the deep oil and gas tests are thermal. Additional exploration is warranted in this area also, to resolve the question.

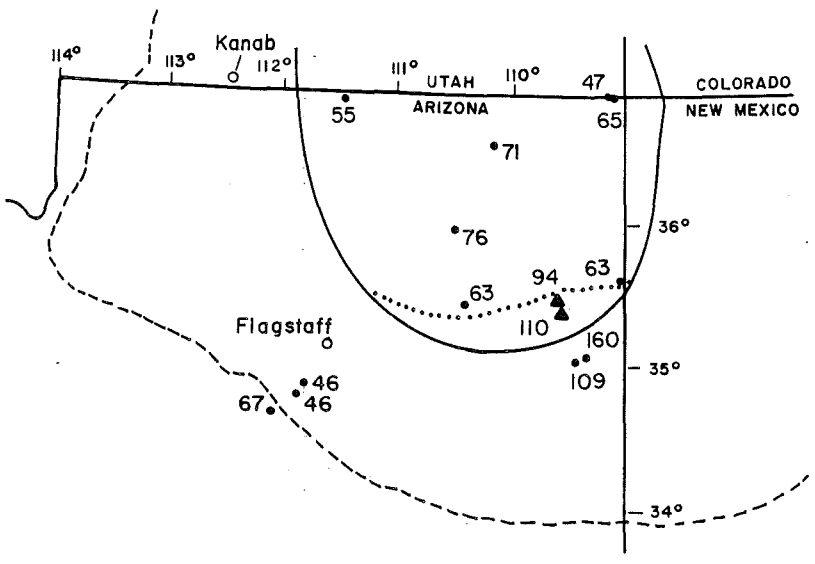

Figure 2.12. Map showing possible change (dotted line) in Bodell and Chapman, 1982, thermal boundary (solid line). Solid circles are published heat flow (taken from Bodell and Chapman, 1982); solid triangles are apparent heat flow (taken from Sass, Stone, and Bills, 1982).

NORTHEASTERN ARIZONA REFERENCES

Bodell, J. M., and Chapman, D. S., 1982, Heat flow in the north-central Colorado Plateau: Journal of Geophysical Research, v. 87, p. 2869-2884.

Kister, L. R., 1973, Quality of the ground water in the lower Colorado River region, Arizona, Nevada, New Mexico, and Utah: U.S. Geological Survey Hydrologic Investigations Atlas HA-478.

Lysonski, J. C., Aiken, C. L. V., and Sumner, J. S., 1980, The complete residual Bouguer gravity anomaly map of Arizona: Tucson, University of Arizona, 1:1,000,000 scale.

Reiter, M., and Shearer, C., 1979, Terrestical heat flow in eastern Arizona: A first report: Journal of Geophysical Research v. 84, p. 6115-6120.

Sass, J. H., Stone, C., and Bills, D. J., 1982, Shallow subsurface temperatures and some estimates of heat flow from the Colorado Plateau of northeastern Arizona: U. S. Geological Survey Open-File Report 82-994, 112 p.

Sauck, W. A., 1972, Compilation and preliminary interpretation of the Arizona aeromagnetic map: Ph.D. dissertation, Tucson, University of Arizona, 147 p.

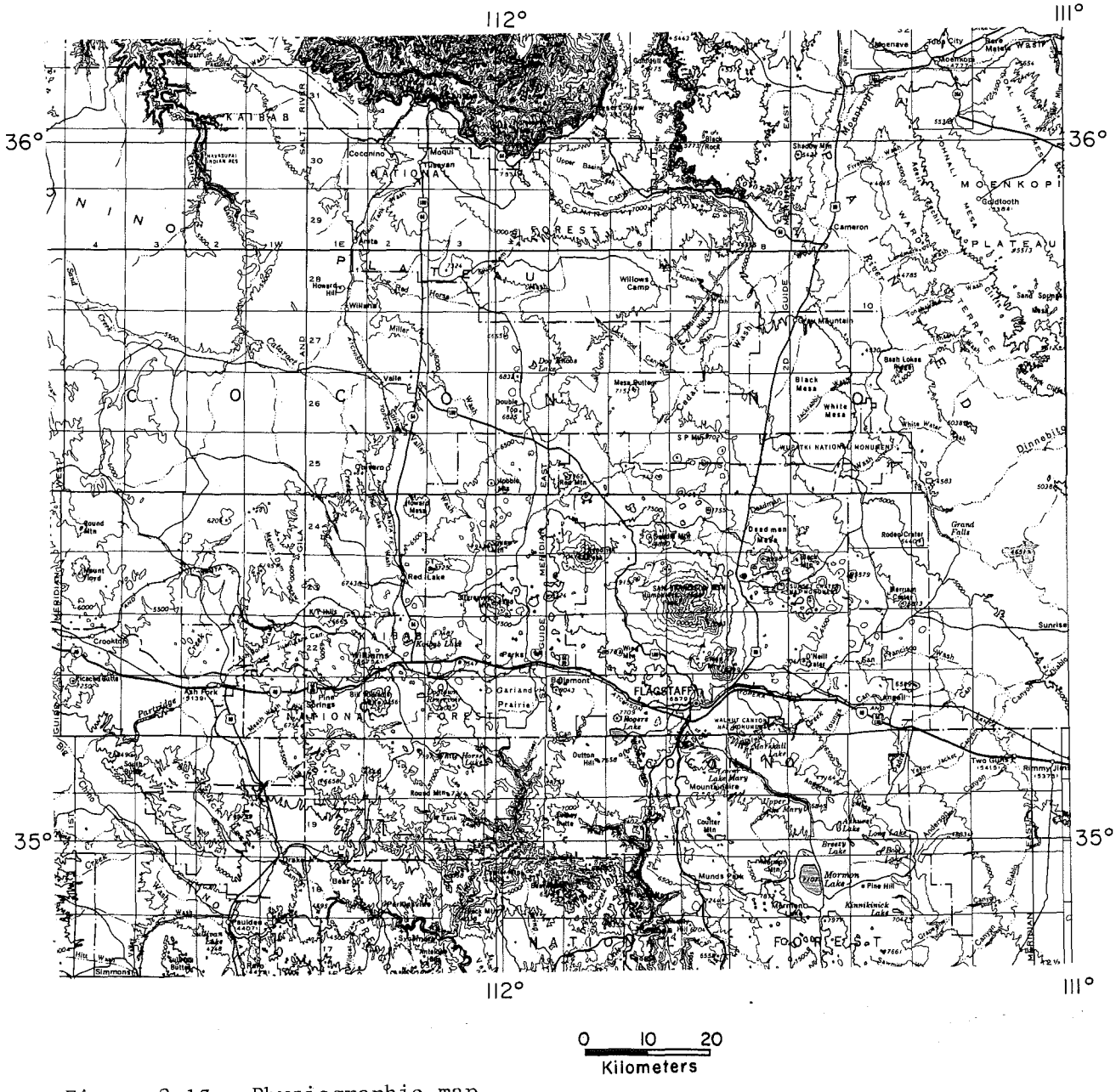

Figure 2.13. Physiographic map of the Flagstaff region

LOCATION DIAGRAM

FLAGSTAFF REGION

INTRODUCTION. A striking 3,800 m Quaternary strato-volcano, the San Francisco Mountain, overlooks the Flagstaff region and is the dominant feature in the San Francisco volcanic field (Fig. 2.13). Since the Pliocene, volcanism in this field has produced a large volume of volcanic rocks, ranging in composition from olivine basalt to rhyolite. The last basaltic eruption about A.D. 1067 formed Sunset Crater (Colton, 1945). Thermal water has not yet been identified in this region, but a significant geothermal resource may exist at depth judging from the number, size, and youth of silicic volcanic centers. Geophysical anomalies suggest unusual geothermal heat beneath the silicic centers.

Potential for discovery of geothermal resources in the Flagstaff area has been recognized by the geothermal-energy industry. At present (1982), more than 118,000 acres of federal land in the region have geothermal lease applications pending approval.

GEOLOGY. The Flagstaff region encompasses the San Francisco volcanic field on the southwest margin of the Colorado Plateau. The region is bounded by the Grand Canyon on the north, the Mogollon Rim on the south, the Little Colorado River on the east, and the Aubrey Cliffs and Chino Valley on the west (Fig. 2.13).

Figure 2.14 is a stratigraphic section of rocks underlying the Flagstaff region. San Francisco volcanic field lavas unconformably overlie both the Triassic Moenkopi Formation and the Permian Kaibab

Limestone. Paleozoic stratigraphy is well exposed in the Grand Canyon and in the Oak Creek Canyon. Precambrian basement consists mainly of granitic plutonic rocks and schist. Precambrian Grand Canyon Series sedimentary rocks may also exist locally beneath the Paleozoic rocks.

Volcanic rocks in the San Francisco volcanic field comprise a compositional spectrum that ranges from alkali olivine basalt to rhyolite. The silicic and basaltic rocks are closely associated in both time and location. Robinson (1913) suggested that the silicic rocks (andesite and rhyolite) make up about half the total volume of rock extruded in the field. Moore and others (1974) stated that this ratio is excessive based on a simple differentiation model of fractional crystallization of a single volume of magma. In addition, no evidence for systematic evolution of magma with time has been found in the volcanic stratigraphy of the field. Repeated partial melting in the mantle could explain observed relations (Moore and others, 1974), and could result in periodic replenishment of the magma supply. The new magma could be extruded as basalt or it could be added to a holding chamber where it is differentiated to silicic magma prior to eruption. Mafic xenoliths from the San Francisco field volcanic rocks were interpreted by Stoeser (1974) (1) as representing layered intrusive bodies that cooled at depths of 15 to 42 km in the crust and (2) as having an alkali olivine basalt parentage.

The San Francisco volcanic field began to evolve about 6 m.y. ago with widespread basaltic eruptions. In the western half of the field, silicic volcanism began 5.7 m.y. ago and formed Bill Williams Mountain, the first in a northeast-striking belt of silicic domes, which also includes Kendrick

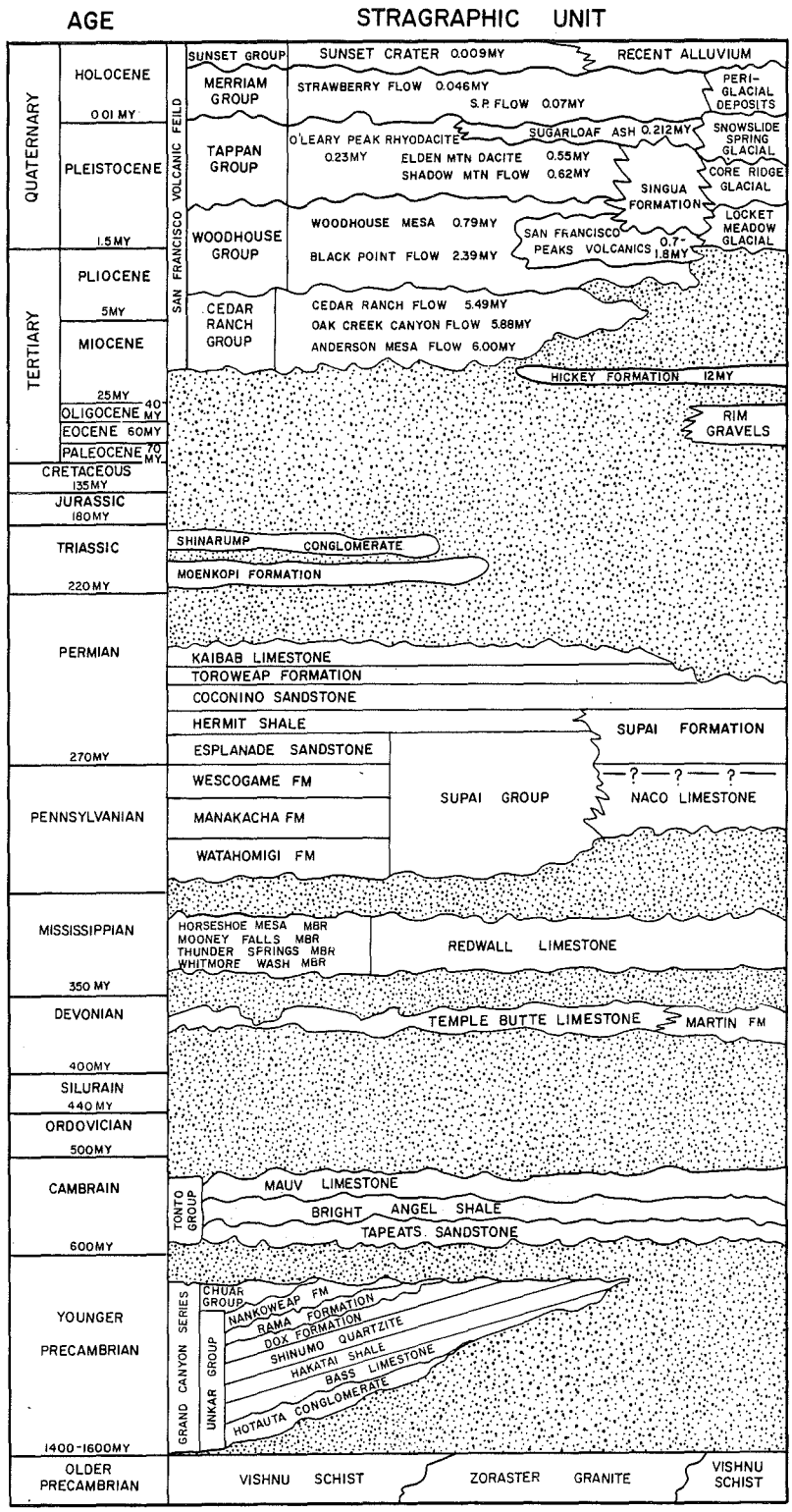

Figure 2.14. Stratigraphy of the Flagstaff region

Peak and Sitgreaves Mountain. Between 2 and 3 m.y. ago silicic volcanism was largely confined to Kendrick Peak and Sitgreaves Mountains (See Fig. 2.7), areas having the most extensive volcanism in this zone. Radiometric ages show progressively younger silicic eruptions from southwest to northeast along this belt (Wolfe and others, 1977).

Rhyolitic eruptions between 2.0 and 0.7 m.y. ago were concentrated in the central part of the field from Kendrick Peak eastward through San Francisco Mountain. Between 0.4 and 0.7 m.y. ago, the San Francisco strato-volcano was the main center of andesitic to rhyolitic volcanic activity. Silicic volcanism, between 0.25 m.y. to 0.05 m.y., was concentrated in a northeast-trending belt from the Interior Valley of San Francisco Mountain to Strawberry Crater, a zone that includes Sugarloaf and O'Leary Peak. Phenocrysts and basement xenoliths and fragments indicate magmatic processes in the shallow crust such as those associated with magma chambers (Wolfe and others, 1977).

STRUCTURAL SETTING. Localization of silicic volcanism along the Bill Williams-Kendrick Peak belt is coincident with the Mesa Butte fault system (Shoemaker and others, 1974). Southeast of the Mesa Butte fault system, the northwest-trending Black Point monocline curves into another northeast-trending fault system, which localized the Sugarloaf-O'Leary-Strawberry Crater silicic belt.

GEOHYDROLOGY. At present no thermal water (>30°C) is known in the Flagstaff region. The geohydrology provides a possible explanation for the absence of thermal water from wells less than 1 km depth. In the eastern part of the San Francisco volcanic field, the static water table

is contained in upper Paleozoic sediments at depths exceeding 300 m (Appel and Bills, 1981). Because this area has relatively high precipitation, significant recharge seepage over a deep static water table carries heat downward to cause lower temperatures and temperature gradients. Lateral ground-water flow toward the Mogollon Rim and the Grand Canyon then carries heat away from the Flagstaff area. Thus, water flow masks any heat that may be flowing upward from depth. Measured temperature-gradient data support this explanation (See Fig. 3.2). In other areas water is found at shallower depths, chiefly in perched ground-water bodies over impermeable volcanic strata, over the Moenkopi Formation, and over impermeable zones in the Kaibab and Supai Formations. Hydrothermal convection is unlikely in the perched water. Thermal water, if present, probably occurs at depths greater than 1 to 2 km.

GEOPHYSICS. Available geophysical information implies the presence of shallow (>5 km) plutonism in the areas or belts having silicic volcanism (Wolfe and others, 1977). Bouguer gravity data (Fig. 2.15) shows two closed gravity lows coinciding with the Sitgreaves and Kendrick Peak silicic centers. A weak gravity low is coincident with the Sugarloaf Peak and Strawberry Crater belt of silicic volcanism. Possibly of greater significance, a magnetic low is aligned along the Sugarloaf Peak-Strawberry belt (Fig. 2.16). The magnetic anomaly indicates either rocks of relatively low magnetic susceptibility, or high temperature, or both.

High temperatures beneath San Francisco Mountain can be inferred from teleseismic data. During three months of 1979, a U.S. Geological Survey

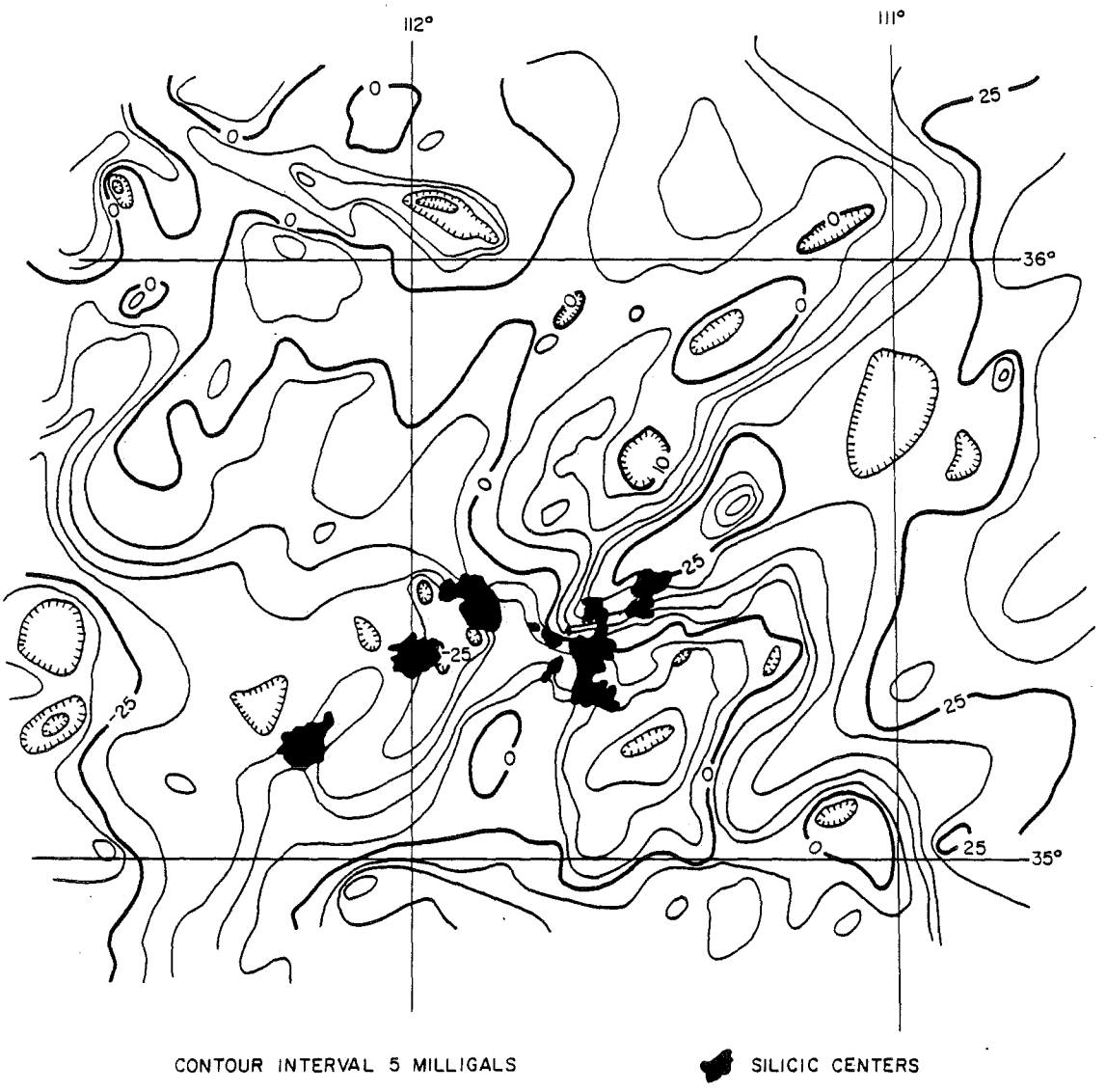

Figure 2.15. Residual Bouguer gravity of the Flagstaff region and silicic volcanic centers

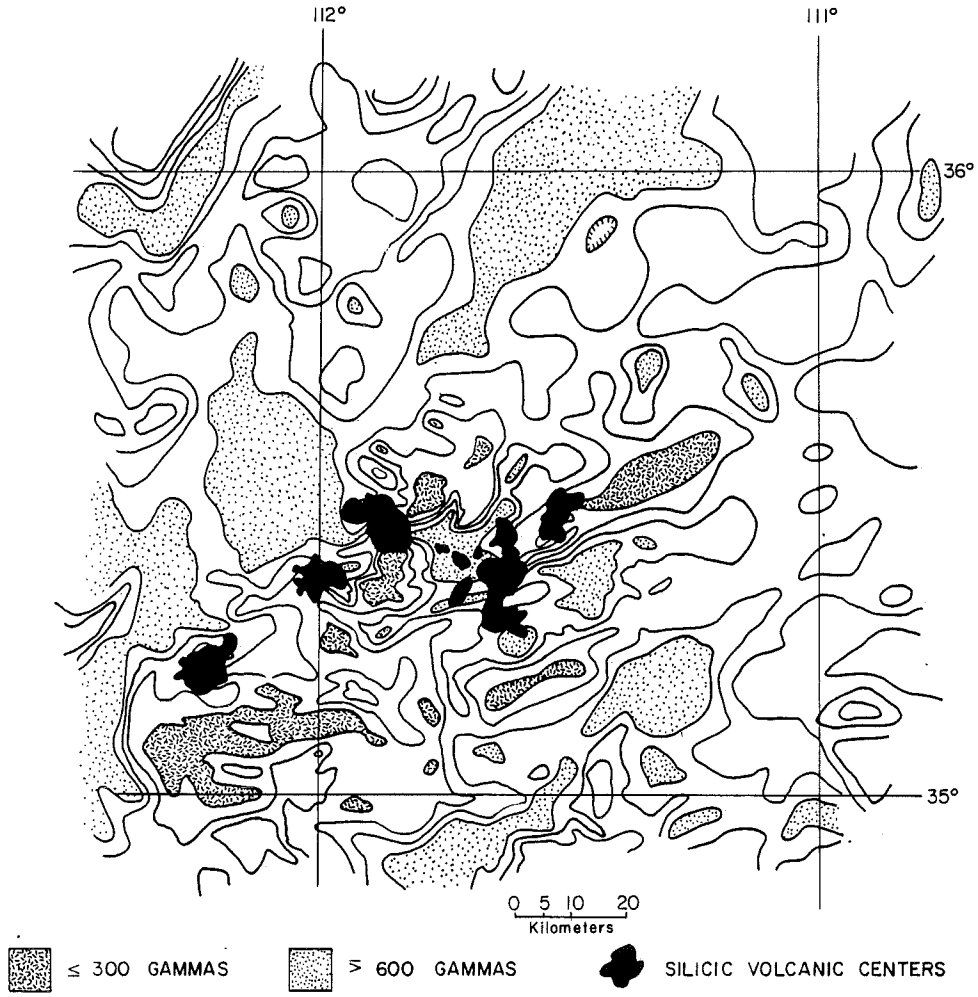

Figure 2.16. Residual aeromagnetic map of the Flagstaff region and silicic volcanic centers

seismograph array centered on San Francisco Mountain detected P-wave, residual travel-time delays of up to 13 percent, at depths between 20 and 45 km in the crust (Stauber, 1980). Diameter of the anomalous velocity zone is between 10 and 25 km; the top is unconstrained at depths shallower than 20 km because of uncertainty in the velocity structure of the San Francisco volcanic pile. Magma may cause the P-wave delay; however, other inhomogeneities in the crust are not ruled out (Stauber, 1980).

CONCLUSION. Exploration for high temperature geothermal resources suitable for electrical power production is probably warranted considering the youthful age of silicic volcanism. The Sitgreaves Mountain-Kendrick Peak and the Sugarloaf-Strawberry Crater silicic belts are favorable exploration targets. While very young basaltic volcanism has occurred, its significance as an indicator of geothermal potential is less favorable. Basalt generally does not form voluminous shallow magma bodies in the crust as does silicic magma. Rather basalt travels up from the mantle and is extruded as thin flows on the surface or is intruded as small dikes, sills, and plugs, which cool to ambient temperature in a matter of months or years. Silicic magmas, on the other hand, collect in shallow magma chambers having volumes exceeding several hundred cubic kilometers and require up to several hundred thousands years to cool (Norton and Knight, 1977). The possibility of continuous replenishment of magma that is not expressed by volcanism could be of greater importance to geothermal potential in the Flagstaff region than the type and youth of volcanism.

FLAGSTAFF REFERENCES

Appel, C. L. and Bills, D. J., 1981, Maps showing ground-water conditions in the San Francisco Peaks area, Coconino County, Arizona - 1979: U. S. Geological Survey Water Resources Investigations Open-File Report 81-914.

Colton, H. S., 1945, A revision of the date of the eruption of Sunset Crater: Southwestern Journal of Anthropology, vol. 1, p. 345-355.

Luedke, R. G. and Smith, R. L., 1978, Map showing distribution, composition, and age of late Cenozoic volcanic centers in Arizona and New Mexico: U. S. Geological Survey Miscellaneous Investigations Series Map I-1091-A, 1:1,000,000 scale.

Lysonski, J. C., Sumner, J. S., Aiken, C. L. V., and Schmidt, J. S., 1980, Complete residual Bouguer gravity map of Arizona: Arizona Bureau of Geology and Mineral Technology, University of Arizona, Tucson, scale 1:500,000.

Moore, R. B., Wolfe, E. W., and Ulrich, G. E., 1974, Geology of the eastern and northern parts of the San Francisco volcanic field, Arizona: *in* Karlstrom, T. N. V., Swann, G. A., and Eastwood, R. L., eds., Geology of Northern Arizona with notes on archaeology and paleoclimate, Part II, Area Studies and Field Guides--Guidebook for Geological Society of America Rocky Mountain Section meeting, p. 465-494.

Norton, D. and Knight, J., 1977, Transport phenomena in hydrothermal systems--cooling plutons: American Journal of Science, vol. 277, p. 937-981.

Pèwè, T. L., and Updike, R. G., 1976, San Francisco Peaks--A guidebook to the geology: Museum of Northern Arizona, Flagstaff, 80 p.

Robinson, H. H., 1913, The San Franciscan volcanic field, Arizona: U. S. Geological Survey Professional Paper 76, 213 p.

Sauck, W. A., and Sumner, J. S., 1970, Residual aeromagnetic map of Arizona: University of Arizona, Department of Geosciences, 1:1,000,000.

Shoemaker, E. M., Squires, R. L., and Abrams, M. J., 1974, The Bright Angel and Mesa Butte fault systems of northern Arizona: *in* Karlstrom, T. N. V., Swann, G. A., and Eastwood, R. L., eds., Geology of Northern Arizona with notes on archaeology and paleoclimate, Part I Regional Studies--Guidebook for Geological Society of America Rocky Mountain Section meeting, p. 355-391.

Stauber, D. A., 1980, Short-period teleseismic P residual study of San Francisco volcanic field, Arizona (abs.): EOS, American Geophysical Union, vol. 60, no. 46, p. 1025.

Stoeser, D. B., 1974, Xenoliths of the San Francisco volcanic field, northern Arizona: *in* Karlstrom, T. N. V., Swann, G. A., and Eastwood, R. L., eds., Geology of Northern Arizona with notes on archaeology and paleoclimate, Part II, Area Studies and Field Guides--Guidebook for Geological Society of America Rocky Mountain Section meeting, p. 530-546.

Wolfe, E. W., Ulrich, G. E., and Moore, R. E., 1977, San Francisco Peaks, Arizona: *in* Hot Dry Rock Geothermal Energy: Status of exploration and assessment, report no. 1 of the Hot Dry Rock Assessment Panel, Energy Research and Development Administration, Division of Geothermal Energy, Report ERDA 77-74, p. 126-133.

EAST-CENTRAL ARIZONA

INTRODUCTION. Preliminary geological and geophysical evidence strongly suggest the existence of one (and possibly two) geothermal anomalies in east-central Arizona (Fig. 2.17). The evidence consists chiefly of the following information. Lavas in the White Mountain volcanic field, although chiefly of basaltic composition, have K-Ar dates as young as 0.75 ± 0.13 m.y. (Aldrich and Laughlin, 1981), and probably some flows are younger. Regional lineaments, defined by the alignment of young volcanic fields, intersect in the White Mountains. Warm springs and moderate to high geothermometers were noted to occur near the town of St. Johns. A geothermal evaluation of this area confirmed the presence of a geothermal anomaly (Stone, 1980), although the magnitude of the anomaly appears to be less than what was first suspected.

Most of the land between Alpine and Springerville is within the Apache National Forest. To the west the land belongs to the White Mountain Apache Indian Tribe. North of Springerville most land is held in state trust or is privately owned (Fig. 2.18).

PHYSIOGRAPHY. East-central Arizona lies along the southern edge of the Colorado Plateau in the region called the Mogollon Slope (see Fig. 2.2). Voluminous basaltic lava flows and, to the north where lavas are younger, numerous cinder cones of the White Mountain volcanic field cover much of the land surface. Beneath the lavas, pre-Cretaceous strata dip gently northeastward. Elevations average 1,800 to 2,700 m but exceed

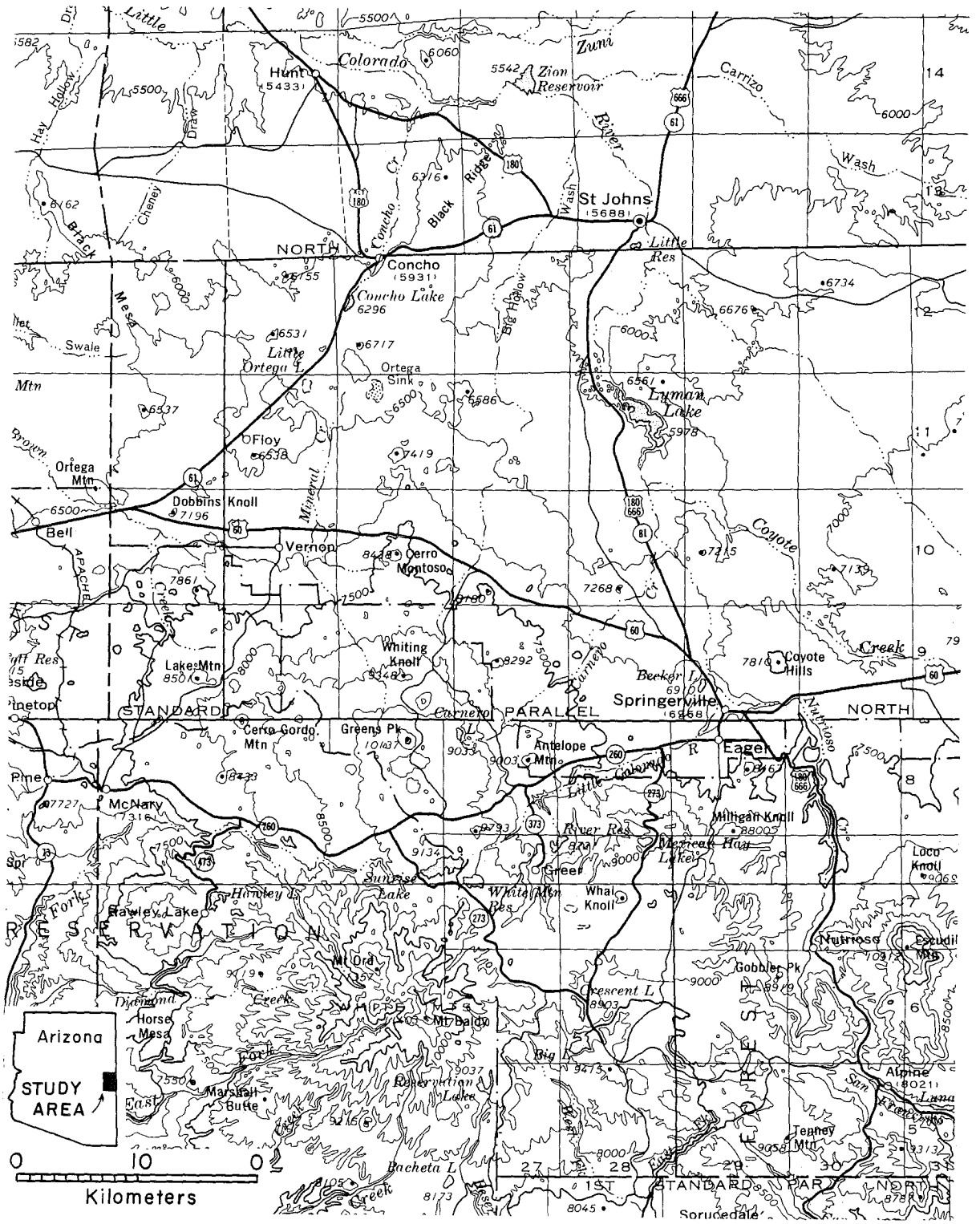

Figure 2.17. Physiographic map of east-central Arizona

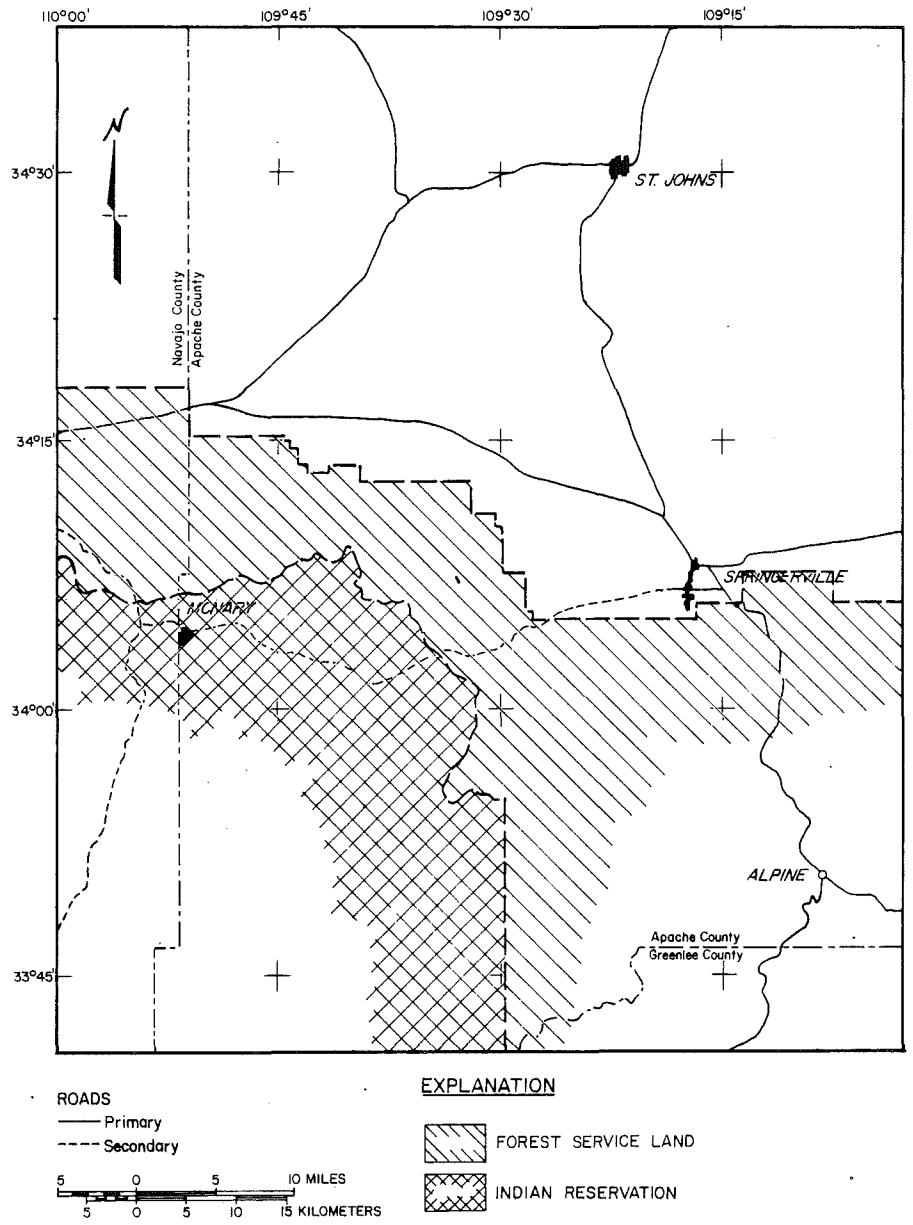

Figure 2.18. Land status of east-central Arizona

3,350 m on Mount Baldy, the partial remnant of a formerly large volcanic edifice (Fig. 2.19).

GEOLOGY. Drilling logs confirm that depth to Precambrian granitic basement in east-central Arizona varies from about 700 to 1,400 m. Paleozoic strata, which overlie the basement and which crop out at the surface to the west, are buried in this area beneath the White Mountain lavas. These Paleozoic units are the Kaibab Limestone, Coconino Sandstone, and Supai Formation, all of Permian age. Some unknown distance south of Springerville, these units thin to extinction, but an absence of deep drill holes leaves unanswered the question of where exactly this happens. Mid-Tertiary volcaniclastic rocks are exposed in discontinuous patches south of Springerville almost to Morenci. To the north, the Triassic Moenkopi and Chinle Formations overlie the Paleozoic strata in the subsurface and are eventually exposed at the surface (about 10 km north of Springerville) where they are no longer covered by volcanic rocks. Younger sedimentary rocks were mostly removed from this region by erosion.

Active volcanism began in the White Mountain volcanic field in the middle Tertiary, with the eruption of volcanic and volcaniclastic rocks of basaltic to trachyandesitic composition. Minor rhyolite flows occurred south and east of the Mount Baldy area. A second episode of volcanism, which produced the Mount Baldy volcanics, began in late Miocene. These rocks are composed principally of latite, quartz latite, and alkali trachyte, and have an aggregate thickness of less than 500 m. Field evidence and K-Ar dates suggest that the transition from intermediate to basaltic volcanism in the White Mountains occurred about early Pliocene (Merrill and Péwé, 1977). During the third and latest pulse of volcanic

activity, three units of basaltic lavas were erupted, with some late-stage differentiation (Aubele and Crumpler, 1979, unpub. report). K-Ar dates on these youngest basaltic rocks range from about 6.03 to 0.75 m.y. (Aldrich and Laughlin, 1981). Chemical trends of the three major episodes of volcanism (Merrill and Pewe, 1977) clearly show that the lavas were not generated by continuous differentiation from a single source.

Travertine deposits are present in many places in east-central Arizona, with one of several concentrations being located between and to the east of St. Johns and Lyman Lake. Akers (1964) noted that some spring orifices at the center of travertine deposits in this area are very well preserved, which suggests that the deposits are very young. Some warm springs along the Little Colorado River south of St. Johns are still actively depositing travertine (Akers, 1964).

GEOHYDROLOGY. The principal ground-water reservoir in east-central Arizona is the C multiple-aquifer (Brown, 1976). The potentiometric surface in the C aquifer shallows to the north. Thus depth to water ranges from about 200 m below the land surface to the south, to a meter or so above land surface where springs and seeps discharge in the St. Johns area and feed tributaries to the Little Colorado River. West of Concho (Fig. 2.20) ground water generally contains less than 300 mg/L TDS. East of Concho water quality is poor, and dissolved solids concentrations may be as great as 2,500 mg/L.

South of the approximate surface-water divide (Fig. 2.20), surface water flows south and southwest to the Blue, White, and Black Rivers, and eventually into the Salt and Gila River. North of that boundary, water flows north to the Little Colorado River.

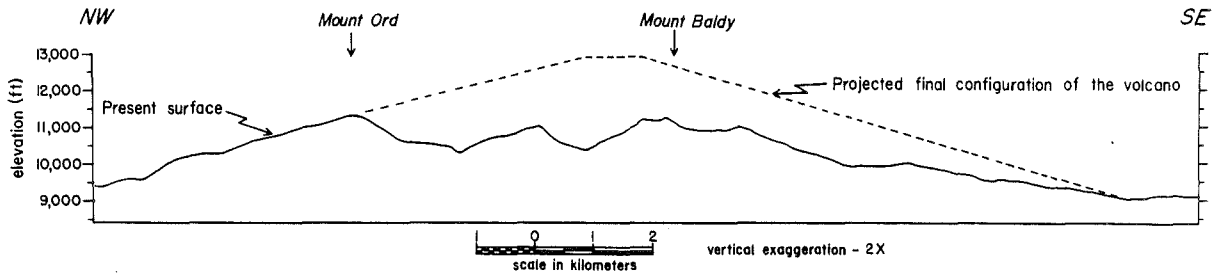

Figure 2.19. Present (solid line) and projected final configuration (dashed line) of Mount Baldy volcano (from Merrill and Pewe, 1977)

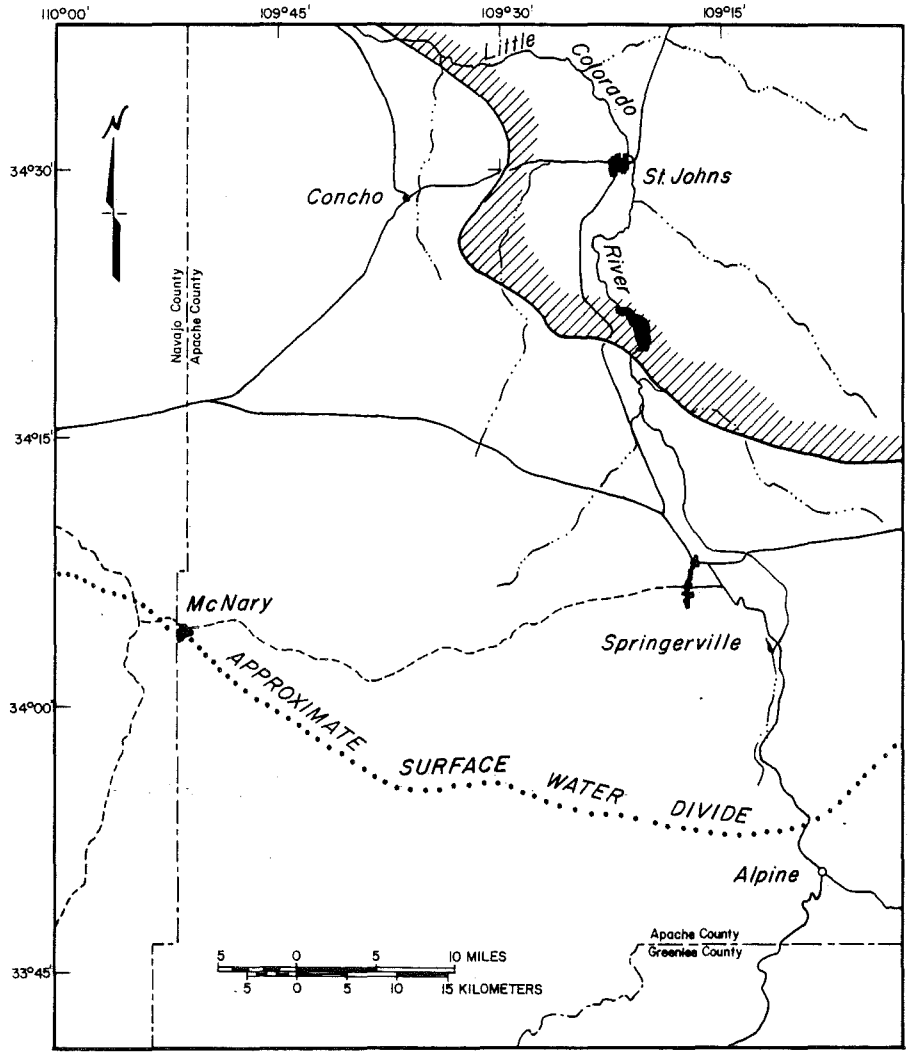

Figure 2.20. Map of east-central Arizona showing approximate boundary of high TDS water (diagonal line pattern) and surface-water divide (dotted line)

GEOTHERMOMETERS. Swanberg and others (1977) determined that the average silica temperature for the Colorado Plateau, based on 420 samples, is 49.8°C. Based on 54 chemical analyses from east-central Arizona we established a mean silica temperature of 67.8 ± 22.1°C for this area. Figure 2.21 shows that anomalous silica geothermometers for this area (those exceeding the mean value plus one standard deviation, ≥ 90°C) occur in a corridor from north of Springerville to south of Alpine. The geothermometers predict temperatures of about 100 to 110°C for this zone.

There is no apparent correlation between the silica and the Na-K-Ca geothermometers. Waters from springs and wells between and west of Lyman Lake and St. Johns (where TDS is as high as 2,500 mg/L) predict subsurface temperatures of 170 to 190°C, values that are significantly higher than both measured temperatures (≈13 to 18°C) and silica temperatures (≈40 to 70°C). Active deposition of travertine enables us to postulate that the high Na-K-Ca geothermometers are a result of calcium depletion in the water rather than of thermal conditions. South of Lyman Lake, Na-K-Ca geothermometers predict temperatures that are much lower (≈20 to 45°C) than the mean silica temperature.

THERMAL REGIME. Temperatures were measured in 18 wells having depths between 75 and 420 m (Table 2.1), but nearly all show disturbance due to ground-water movement (Figs. 2.22, 2.23 and 2.24). Only three measured wells are thermal. Two of these are located between Alpine and Springerville where the silica temperatures are anomalously high (Fig. 2.25). The third well is north of St. Johns. Three wells for which gradients were calculated rather than measured are thermal also. Two of these wells are north of St. Johns; the other is west of Springerville.

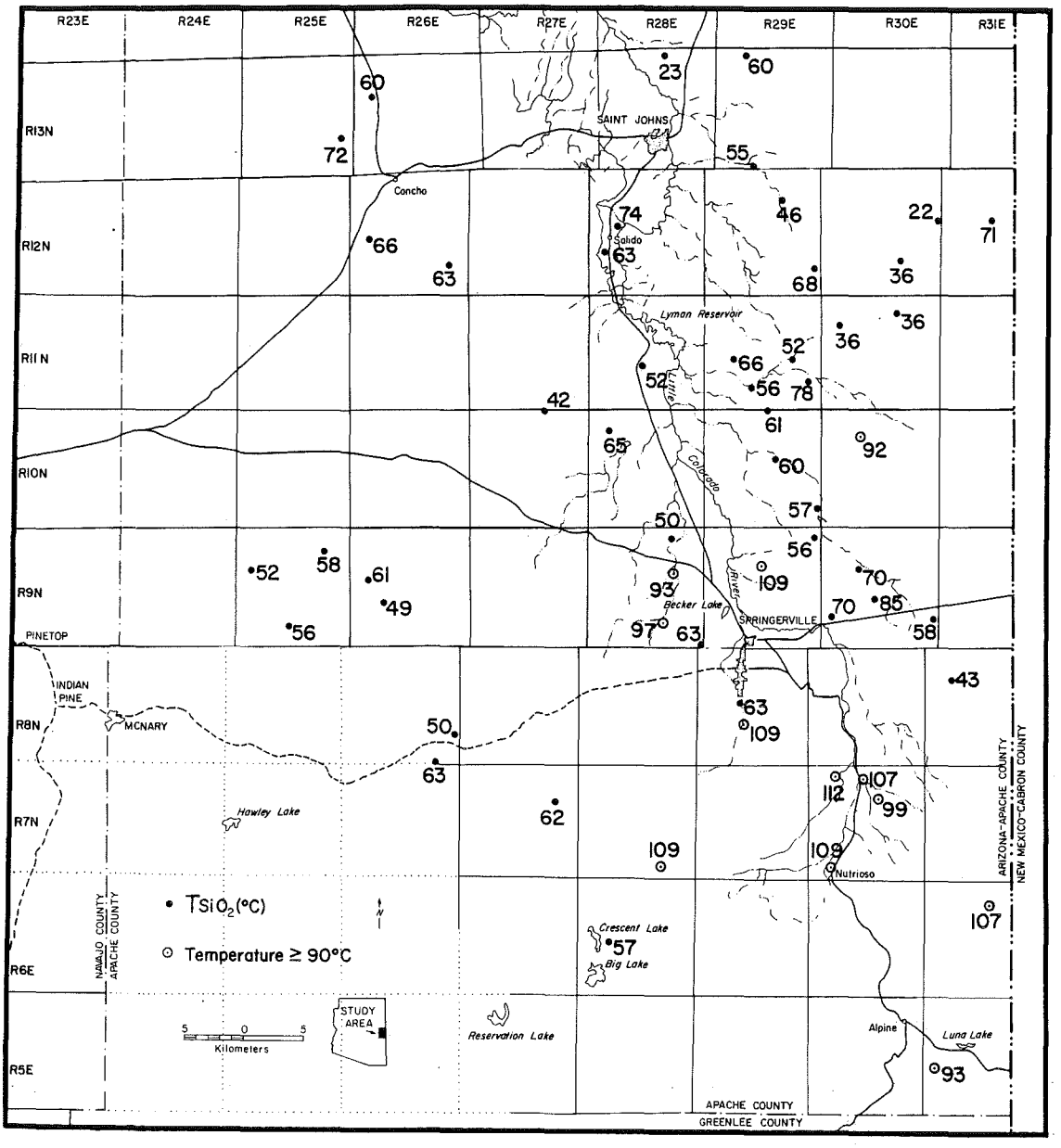

Figure 2.21. Silica geothermometers for east-central Arizona. Values exceeding 90°C, the mean plus one standard deviation, are indicated by open circles with dots.

TABLE 2.1. Location information for wells measured in east-central Arizona

NO.	LOCATION	BHT (^{o}C)	D (m)	TG (^{o}C/Km)	Apparent Heat Flow (mWm^{-2})
PWF3	A-13-29-6acc	20.9	230	23.3	86
PWF1	A-13-29-5abd	20.8	160	33.0	149
PWF2	A-13-28-3abb	18.7	80	38.9	116
CN24	A-13-25-24cad	17.4	160	12.3	-
TGE2	A-11-29-23aba	19.7	225	24.7	79
TGE3	A-11-29-34cdc	27.4	400	21.5	63
TGE1	A-11-29-28daa	27.0	420	29.1	76
TGE8	A-11-29-20baa	26.4	400	27.7	-
CN8	A-13-26-8bcc	18.0	200	11.8	-
SLP1	A-11-24-22dbc	19.8	230	30.6	-
NARY	A-8-24-20cbc	12.2	110	23.6	-
NUTR	A-7-30-16ca	15.0	80	51.1	101
PT1	A-8-23-5acd	13.9	125	25.8	-
SJ107	A-7-30-7daa	27.3	350	43.9	87
SJ112	A-7-28-27bca	13.6	155	34.5	56
SJ113	A-6-27-12cdc	8.2	105	25.3	42
SJ114	A-6-28-13aaa	16.7	220	35.4	51
SJ116	A-6-30-23cac	32.9	355	71.6	115

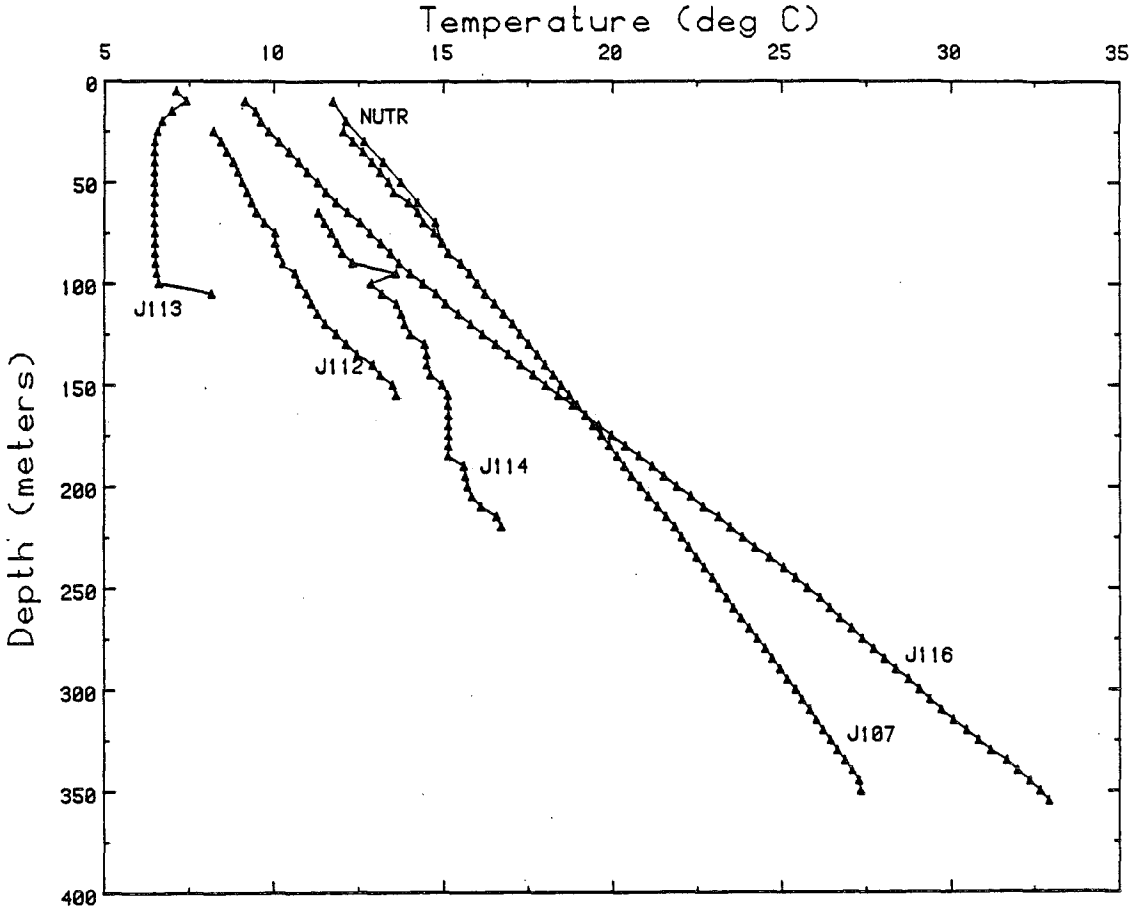

Figure 2.22. Temperature-depth graphs of wells measured in east-central Arizona. Well locations are given in Table 2.1.

The three lowest gradients are in wells on the west side of the study area where silica temperatures are normal.

Apparent heat flows were calculated for 12 holes (Table 2.1 and Fig. 2.26) (Sass and others, 1982; Stone, 1980). These values clearly show that east-central Arizona is outside the 65 mWm^{-2} heat-flow contour used by Bodell and Chapman (1982) to separate the cool plateau interior ($\approx$60 ± 9 mWm^{-2}) from the warmer plateau periphery ($\approx$80 to 90 ± 20 mWm^{-2}). The three low apparent heat flows southwest of Springerville were measured

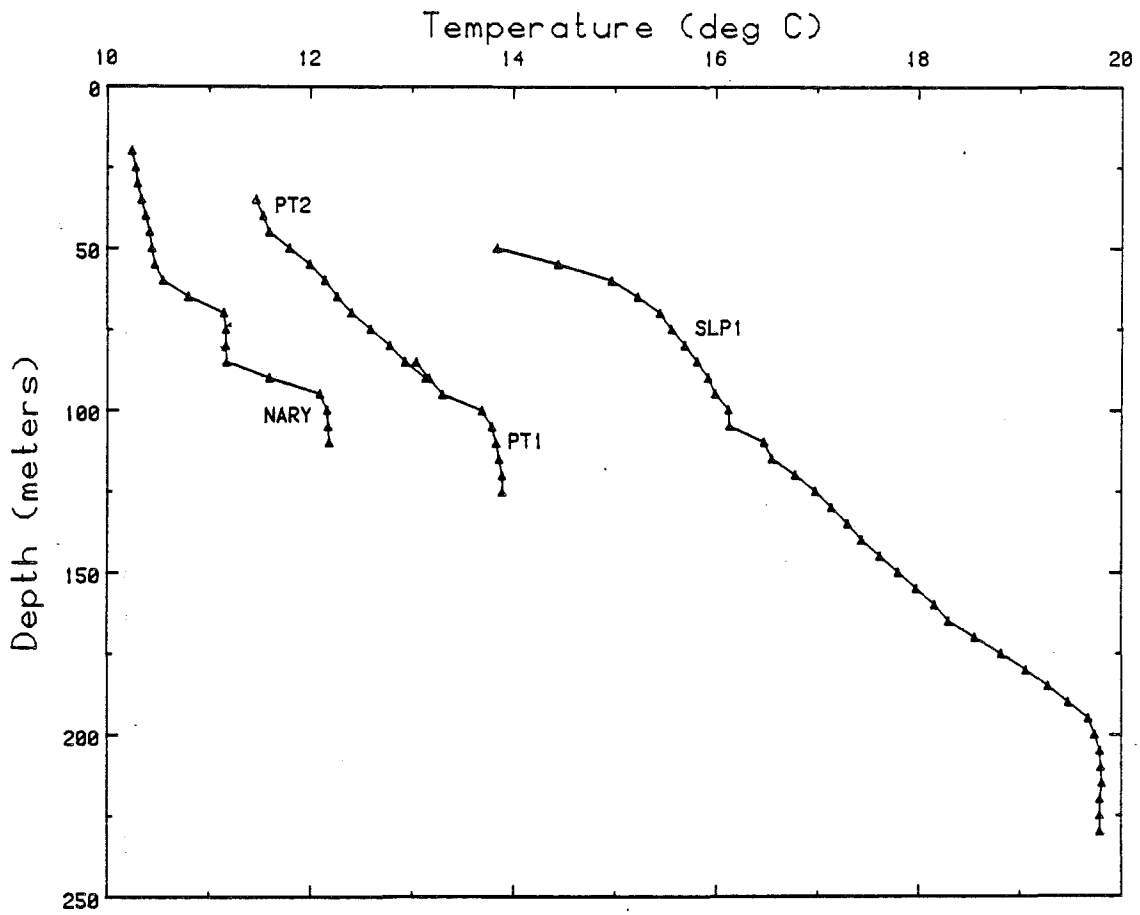

Figure 2.23. Temperature-depth graphs of wells measured in east-central Arizona. Well locations are given in Table 2.1.

in basaltic rocks that are highly disturbed by ground-water flow. The remaining heat flows are on the high and low ends of normal for the Colorado Plateau periphery (Bodell and Chapman, 1982). The areas north of St. Johns and between Springerville and Alpine have heat flows that may be slightly higher than normal.

GEOPHYSICS. Regional geophysical anomalies are indicative of geothermal potential in this area. Regional lineaments based on the alignment of young volcanic fields intersect in the White Mountains (Fig. 2.27). A

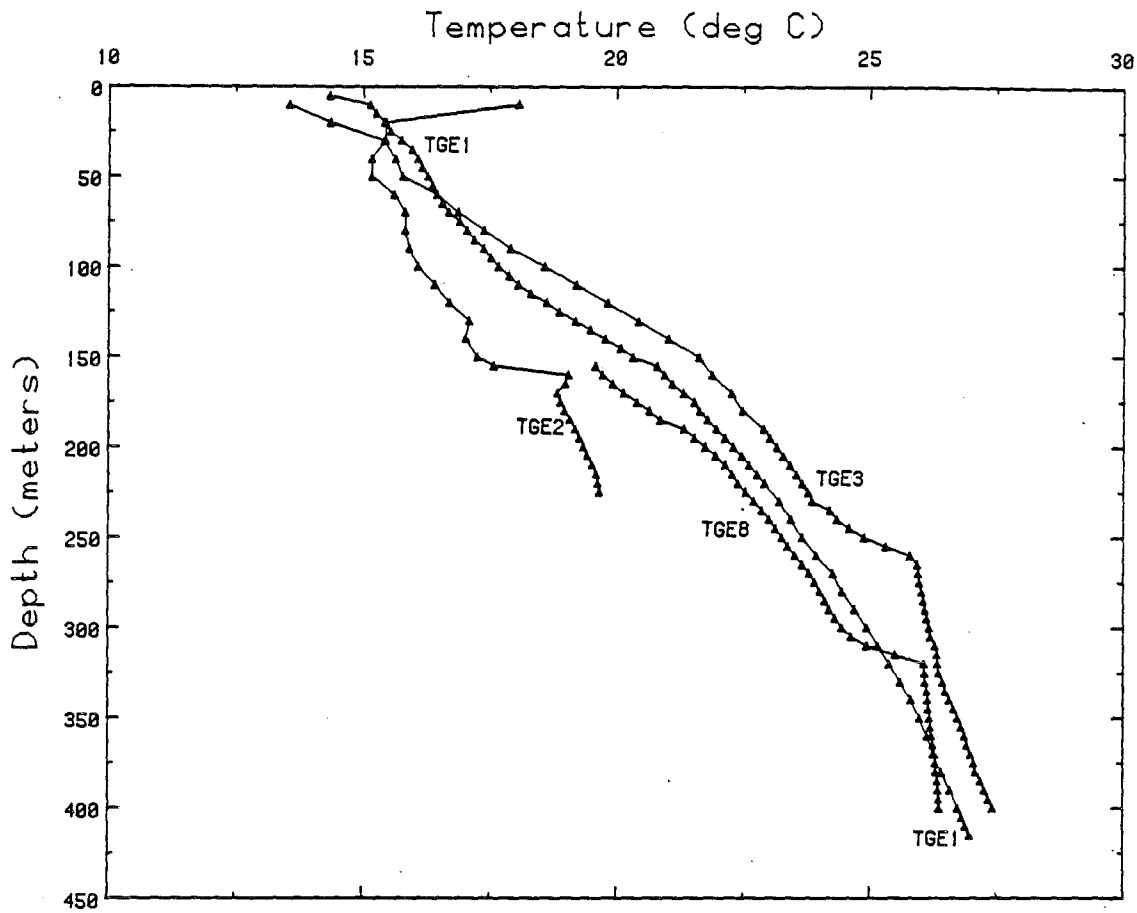

Figure 2.24. Temperature-depth graphs of wells measured in east-central Arizona. Well locations are given in Table 2.1.

large residual Bouguer gravity low, >-30 milligals, occurs around and west of Alpine (Fig. 2.28) (Lysonski and others, 1980), and could indicate elevated temperatures in the crust (Aiken, 1976). The possibility of elevated crustal temperatures is supported by the apparent presence of a good electrical conductor at about 12 km depth (Young, 1979, unpub. report) in the same area. In addition, Byerly and Stolt (1977) identified a narrow zone crossing central Arizona where depth to the base of the magnetic crust shallows to about 10 km or less. The base of the magnetic crust is an isothermal surface at approximately the Curie temperature, about 525°C.

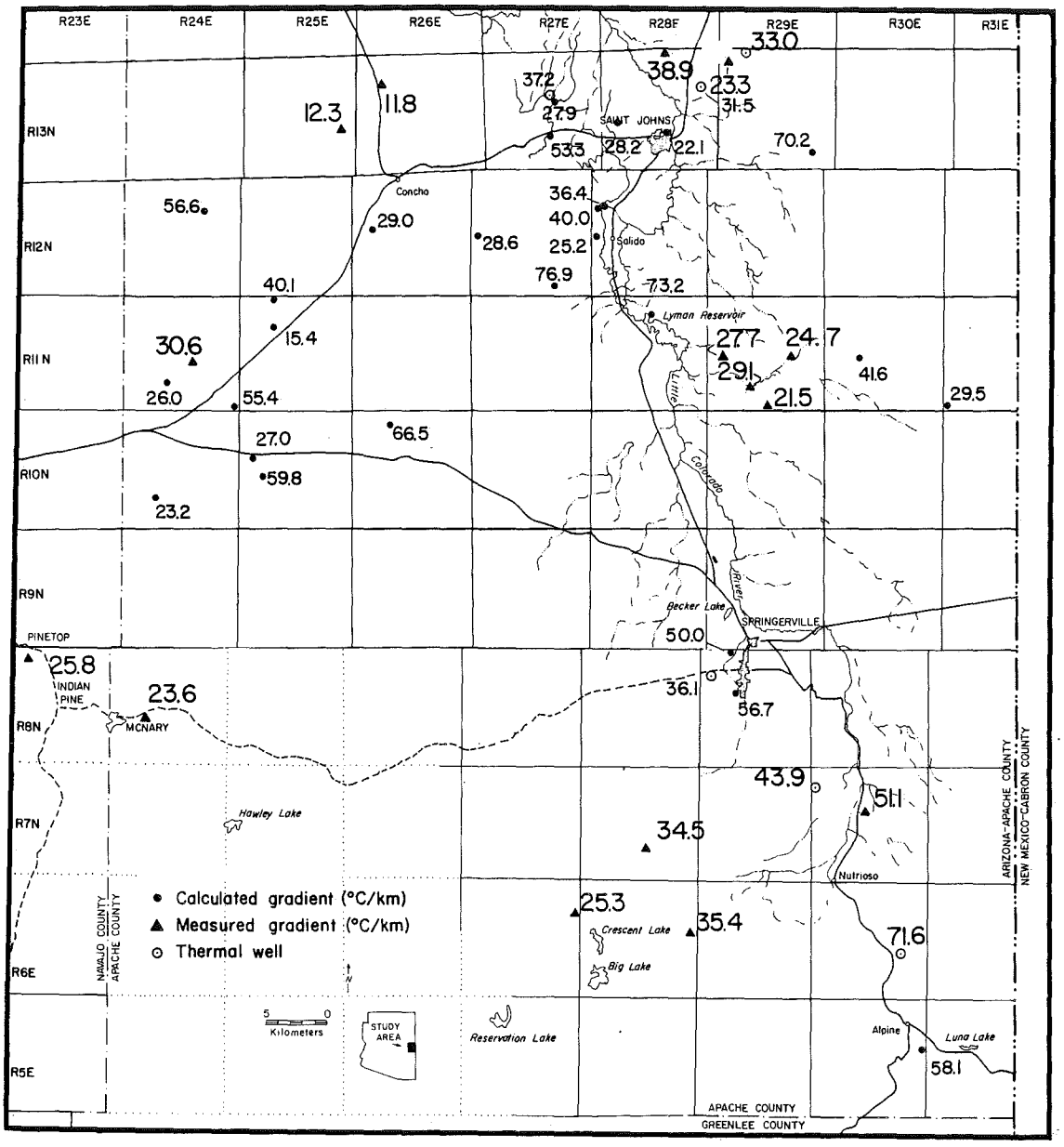

Figure 2.25. Geothermal gradients (^{o}C/km) for east-central Arizona. Measured gradients indicated by closed triangles and larger numbers. Calculated gradients indicated by closed circles and smaller numbers. Thermal wells shown by open circles with dots.

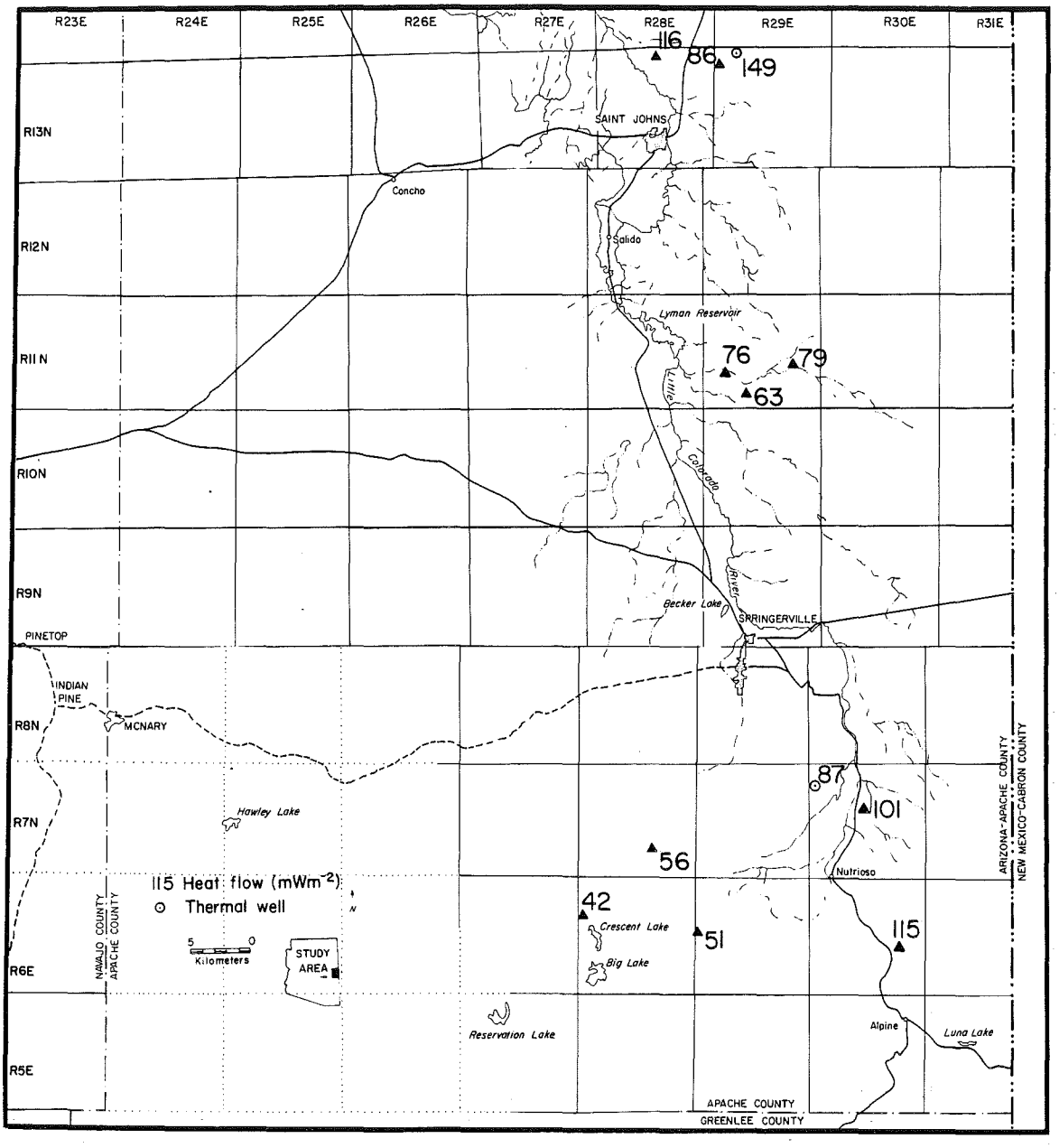

Figure 2.26. Heat flow (mW/m^2) for east-central Arizona. Open circles with dots represent wells that are also thermal.

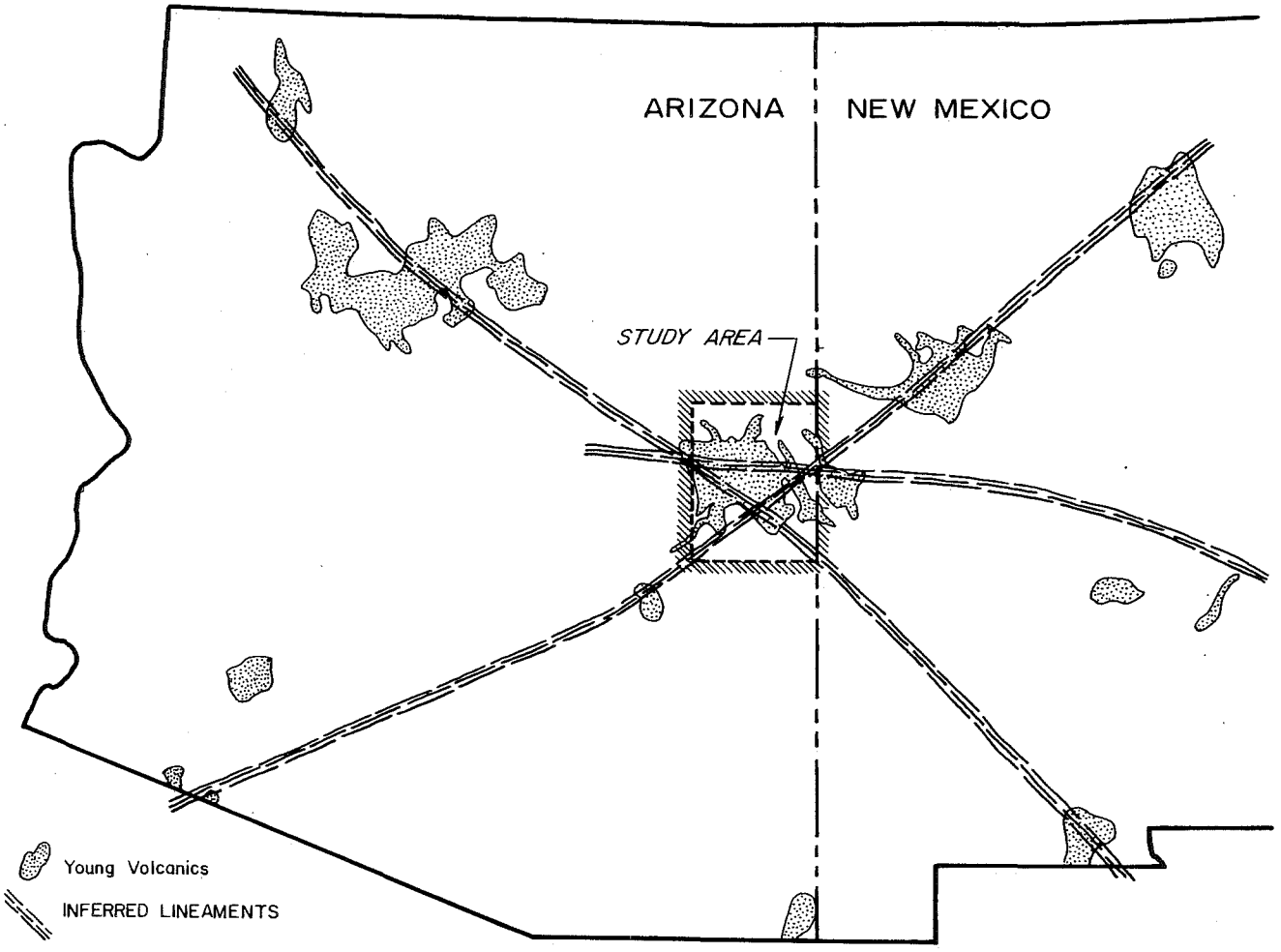

Figure 2.27. Intersection of lineaments (based on the alignment of young volcanic fields) in the region of the White Mountain volcanic field, east-central Arizona

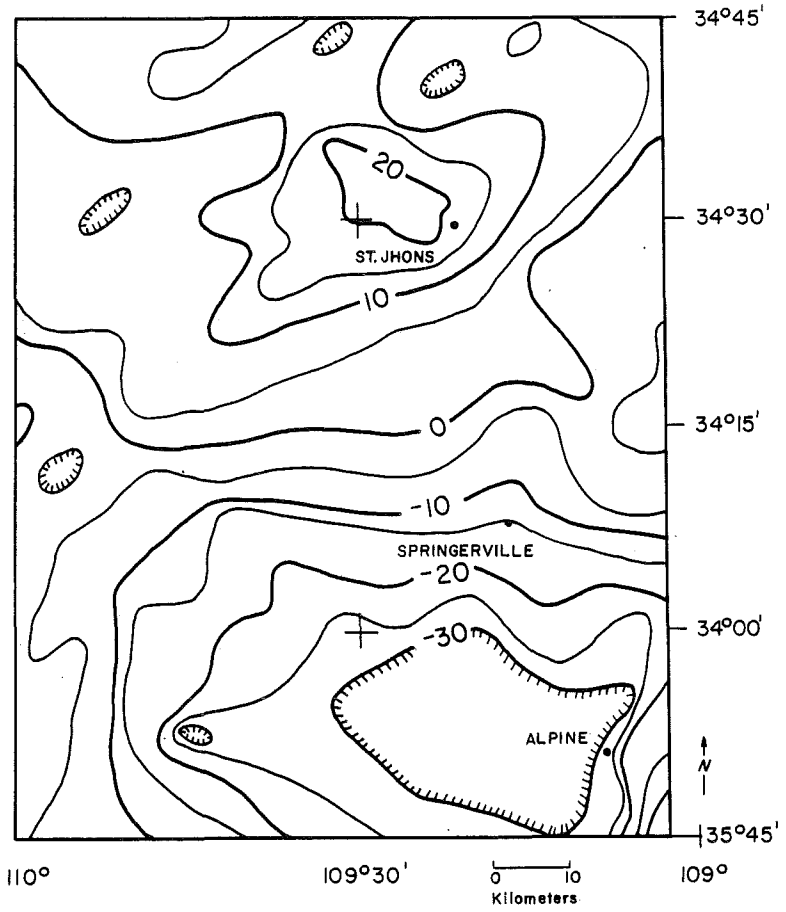

Figure 2.28. Complete residual Bouguer gravity, east-central Arizona (from Lysonski and others, 1980). Contour interval is 5 milligals.

CONCLUSIONS. Significant evidence points to two possible geothermal resource areas in east-central Arizona. Volcanic activity has occurred in the more southerly part of this area in three pulses, the latest being less than 750,000 years old and probably younger. Rock chemical analyses show that the magmas were not generated by continuous differentiation from a single source. Thus three episodes of partial melting in the mantle have occurred over a very long period of time, beginning about 32 m.y. ago. The tectonism responsible for this periodic volcanic activity would also be responsible for the geophysical anomalies cited.

Bodell and Chapman (1982) postulated a model of Cenozoic lithospheric thinning under the plateau to explain the anomalous heat flow found in the Colorado Plateau periphery. They noted that lateral warming and weakening of the Colorado Plateau lithosphere, starting at the Basin and Range boundary some 20 m.y. ago and working toward the interior, would place the heat-flow transition between interior and periphery in the northwest plateau about where it is found today. Lithospheric thinning was accompanied by substantial uplift, followed by more modest uplift due to warming and expansion, and eventually followed by enhancement of surface heat flow. Bodell and Chapman estimated that the lag between uplift and enhanced heat flow is about 15 to 20 m.y. ago. We suggest that the volcanism and enhanced heat flow in east-central Arizona are also a result of Cenozoic lithospheric thinning.

Two areas of slightly above-normal heat flow in east-central Arizona are probable geothermal anomalies and should be investigated in detail to identify their magnitude and areal extent. The heat source for these potential resource areas is probably not magmatic as might be expected at

first glance. Basaltic lavas originate in the upper mantle at depths of about 60 km. The magma is very hot ($\approx 1,300^{\circ}C$) and fluid, and ascends to the surface rapidly through narrow fissures and vents. Thus, there is little conductive transfer of heat to the surrounding country rock that would cause partial melting in the crust and create a shallow magmatic heat source. Instead the heat source for the potential geothermal anomalies identified in east-central Arizona is most likely enhanced surface heat flow caused by Cenozoic lithospheric thinning under the plateau.

EAST-CENTRAL ARIZONA REFERENCES

Aiken, C. L. V., 1976, The analysis of the gravity anomalies of Arizona: Ph.D. dissertation, Tucson, University of Arizona, 127 p.

Akers, J. P., 1964, Geology and ground water in the central part of Apache County, Arizona: U. S. Geological Survey Water Supply Paper 1771, 107 p.

Aldrich, M. J., and Laughlin, A. W., 1981, Age and location of volcanic centers ≤ 3.0 m.y. old in Arizona, New Mexico and the Trans-Pecos area of West Texas: Los Alamos National Laboratory, LA-9812-MAP, Revised.

OFR 83-12

Aubele, J. C., and Crumpler, L. S., 1979, Springerville-White Mountains volcanic field: Report on activities and research results for academic year 1978-1979: Unpublished report submitted to the Bureau of Geology and Mineral Technology, Tucson, 41 p.

Bodell, J. M., and Chapman, D. S., 1982, Heat flow in the north-central Colorado Plateau: Journal of Geophysical Research, v. 87, p. 2869-2884.

Brown, S. G., 1976, Preliminary maps showing ground-water resources in the lower Colorado River region, Arizona, Nevada, New Mexico, and Utah: U.S. Geological Survey Hydrologic Investigations Atlas HA-542, scale 1:1,000,000.

Byerly, P. E., and Stolt, R. H., 1977, An attempt to define the Curie point isotherm in northern and central Arizona: Geophysics, v. 42, p. 1394-1400.

Lysonski, J. S., Sumner, J. S., Aiken, C. L. V., and Schmidt, J. S., 1980, The complete residual Bouguer gravity anomaly map of Arizona: Bureau of Geology and Mineral Technology, Tucson, scale 1:1,000,000.

Merrill, R. K., and Pewe, T. L., 1977, Late Cenozoic geology of the White Mountains, Arizona: Bureau of Geology and Mineral Technology, Tucson, Special Paper No. 1, 65 p.

Sass, J. H., Stone, C., and Bills, D. J., 1982, Shallow subsurface temperatures from the Colorado Plateau of northeastern Arizona: U.S. Geological Survey Open-File Report ~~(in prep)~~. 82-994

Stone C., 1980, Springerville geothermal project--geology, geochemistry, geophysics--final report: BGMT Open-File Report ~~81~~ 80-A, 23 p.

Swanberg, C. A., Morgan, P., Stoyer, C. H., and Witcher, J. C., 1977, An appraisal study of the geothermal resources of Arizona and adjacent areas in New Mexico and Utah and their value for desalination and other uses: New Mexico Energy Institute Report 006, Las Cruces, 76 p.

Young, C. T., 1980 79, ~~Results of~~ Geoelectric studies: ~~Bureau of Geology and Mineral Technology Open-File Report 80-4,~~ 68 p. near Springerville, AZ, in TRANSACTIONS: GEOTHERMAL RESOURCES COUNCIL, DAVIS, CALIF., v. 3, p. 805-808

MEXICAN HIGHLAND SECTION

INTRODUCTION. The Mexican Highland section of the Basin and Range province of Fenneman (1931) and Hayes (1969) covers all of southeastern Arizona and extends eastward into New Mexico and southward into northeastern Sonora, Mexico. In Arizona, the Mexican Highland is bound on the west by the Sonoran Desert section at about 111° West longitude. A transition zone between 35° and 36° North latitude separates the Mexican Highland section from the Colorado Plateau. This transition zone has closer affinity to the Mexican Highland than to the Colorado Plateau because it has been the site of voluminous Tertiary volcanism and is traversed by numerous faults.

PHYSIOGRAPHY. Topography in the Mexican Highland section is similar to the Great Basin of Nevada and Utah. However, major geologic differences exist. For example, Paleozoic strata (<2.5 km thick) in the Mexican Highland were deposited on relatively stable continental crust until late Paleozoic time, in contrast to the Great Basin Paleozoic rocks, which were deposited in a geosyncline and are greater than 3 km thick.

Mountain ranges in the Mexican Highland trend north and northwest; they are between 25 and 100 km long and 7 to 25 km wide. These mountains attain altitudes of 1,500 to 3,300 m, some 700 to 1,800 m higher than the adjacent valleys. Valleys in southeastern Arizona are 15 to 25 km wide. All except the Willcox basin are drained by intermittent and perennial through-flowing streams. Intermittent runoff in the Willcox basin and surrounding mountains drains into the Willcox Playa.

GEOLOGY. Late Tertiary horst and graben structures of the Mexican Highland were created by rifting in a highly anisotropic crust. This anisotropicity is characterized by west-northwest and north-northwest striking outcrop patterns and by major structures that are frequently transverse to Basin and Range landforms (Titley, 1976). The northwest-trending grain is superimposed upon an older northeast-trending structural fabric (Silver, 1978; Swan, 1982).

The two main pre-Tertiary tectonic features in this region are the Pedregosa Basin and the Mogollon Highland (Fig. 2.29). During late Paleozoic, subsidence in the southernmost portion of the Mexican Highland region formed the Pedregosa Basin, into which thick (up to 1.5 km) mostly marine carbonate sediments were deposited (Peirce, 1976). In early Cretaceous, this zone, the Pedregosa Basin Region, was faulted to create the Bisbee Group depositional basin (Titley, 1976).

During the Mesozoic, the Mogollon Highland evolved north of the Pedregosa Basin region. Elements of the Mogollon Highland include the Burro uplift (Elston, 1958), the Florence uplift, and the Graham uplift (Turner, 1962). Mesozoic and Cenozoic erosion has removed most of the Paleozoic strata originally deposited on the Mogollon Highland so that Late Cretaceous and Tertiary sediments unconformably overlie Precambrian rocks or lower Paleozoic strata.

Thick piles (>1.5 km) of mid-Tertiary volcanic flows and thick sequences (>2.0 km) of deformed and indurated mid-Tertiary clastic sediments are observed in several areas in the Mexican Highland. The most prominant outcrops of these rocks are in the Chiricahua Mountains, in the Gila and Peloncillo Mountains, in the San Francisco-Blue River areas, in

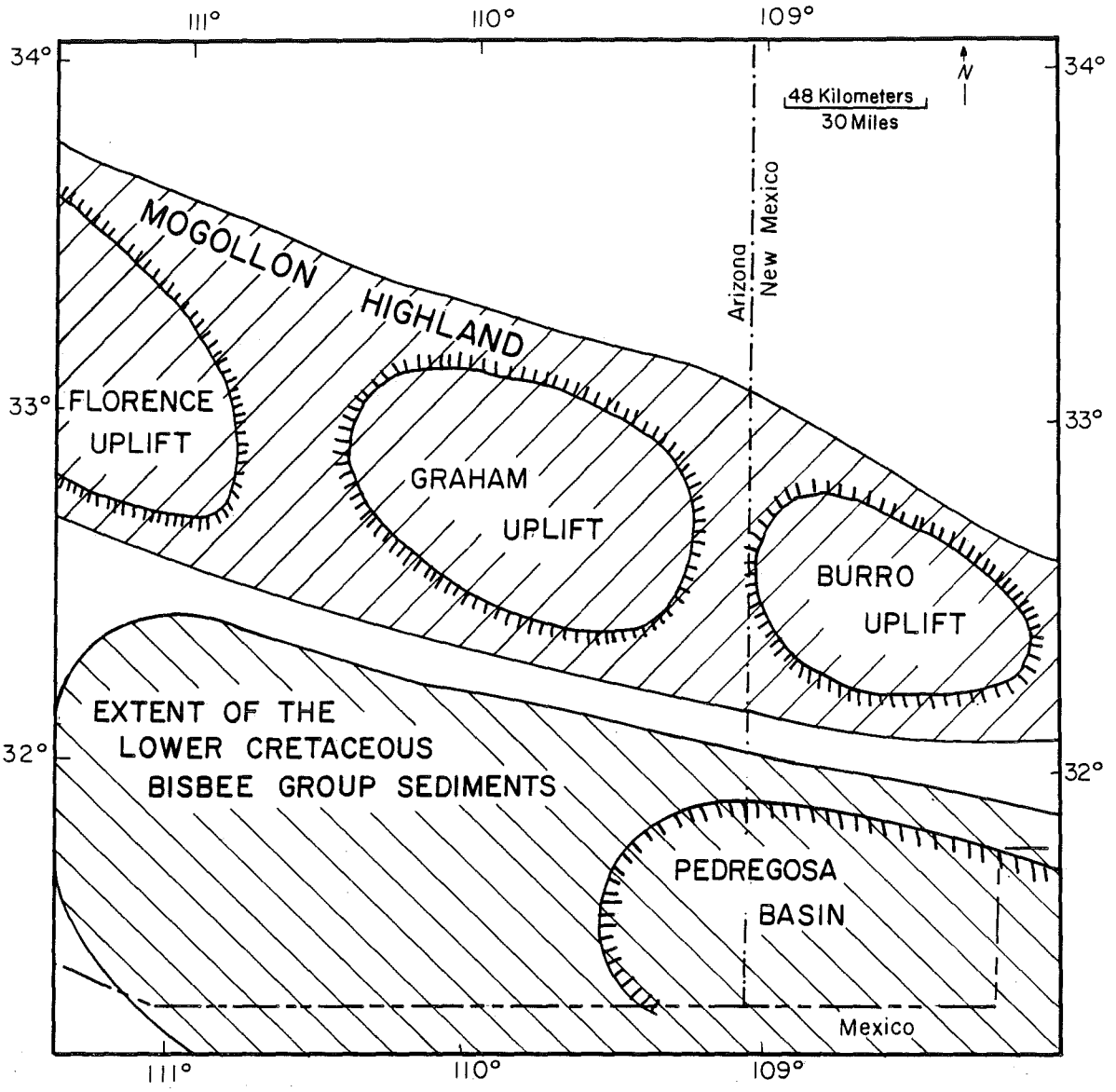

Figure 2.29. Principal pre-Tertiary tectonic features of the Mexican Highland subprovince

the Galliuro-Winchester Mountains, in the Tucson area, and in the Tumacacori-Patagonia-Nogales area. The only identified, large-scale cauldron subsidence and resurgence feature is the Oligocene Turkey Creek cauldron in the Chiricahua Mountains (Marjaniemi, 1968).

Two mid-Tertiary metamorphic core complexes, the Santa Teresa-Pineleno complex and the Rincon-Tanque Verde-Santa Catalina-Tortolita complex (Davis and Coney, 1979) are the highest areas both structurally and topographically in the Mexican Highland section. These apparent mid-Tertiary thermal-tectonic uplifts are separated from adjacent unmetamorphosed rocks by low angle faults that frequently display extensive brecciation.

Late Tertiary Basin and Range tectonism broke the area into a zig-zag pattern of mountains and basins. Sediments filling the basins (post mid-Miocene) generally show four divisions or facies: (1) a basal moderately indurated clay, sand, and gravel unit, (2) an overlying evaporite, clay, and silt unit, (3) an upper nonindurated silt, sand, and gravel unit, and (4) a marginal silt, sand, and gravel unit, which intertongues with the other units along basin margins. Maximum thickness and distribution of these units vary within the basins.

The Mexican Highland section is the most tectonically active portion of the Basin and Range province in Arizona. Except for the Yuma area and the Lake Mead area, this section has greater seismicity than either the Mohave or the Sonoran Desert sections (DuBois and others, 1982). Several scattered zones of Pleistocene fault scarps are observed mostly along basin margins (Menges and others, 1982). Most of these scarps are found in a north-trending belt near the Arizona-New Mexico border, in the Duncan-Clifton area, in the Safford-San Simon basin, and in the San Bernardino Valley. Pleistocene fault scarps are also observed adjacent to the Santa Rita Mountains, the Huachuca Mountains, and the Swisshelm Mountains (Menges and others, 1982).

Quaternary basaltic lavas were extruded in the San Bernardino Valley and in the San Carlos area (Luedke and Smith, 1978).

Although conductive heat flow is not dramatically different in the Mexican Highland section when compared to the Mohave or Sonoran sections, higher elevation, greater seismicity, more Quaternary fault scarps, and younger volcanism suggest higher temperatures in the crust and mantle beneath this region. In any case, large relief in topography and high precipitation in the mountains, seismic activity, and young faults are favorable for deep forced-convection geothermal systems.

REFERENCES MEXICAN HIGHLAND SECTION

Davis, G. H. and Coney, P. J., 1979, Geologic development of the cordilleran metamorphic core complexes: Geology, Vol. 7, p. 120-124.

DuBois, S. M., Sbar, M. L., and Nowak, T. A., 1982, Historical seismicity in Arizona: U. S. Nuclear Regulatory Commission Report NUREG/CR-2577, 199 p.

Elston, W. E., 1958, Burro uplift, northeastern limit of sedimentary basin of southwestern New Mexico and southeastern Arizona: American Association of Petroleum Geologists Bulletin, Vol. 42, p. 2513-2517.

Fenneman, N. M., 1931, Physiography of Western United States: McGraw-Hill, New York, 534 p.

Hayes, P. T., 1969, Geology and topography: *in* Mineral and Water Resources of Arizona, Arizona Bureau of Mines Bulletin 180, p. 35-58.

Luedke, R. G. and Smith, R. L., 1978, Map showing distribution, composition and age of late Cenozoic volcanic centers in Arizona and New Mexico, 1:1,000,000 scale: U. S. Geological Survey Miscellaneous Investigation Series Map I-1091-A.

Marjaniemi, D. K., 1968, Tertiary volcanism in the northern Chiricahua Mountains, Cochise County, Arizona: in Southern Arizona, Guidebook III, Arizona Geological Society, p. 209-214.

Menges, C. M., Peartree, P. A., and Calvo, S., 1982, Quaternary faulting in southeast Arizona and adjacent Sonora, Mexico (abs): Abstracts, 78th annual meeting Cordilleran Section, The Geological Society of America, April 19-21, 1982, Anaheim, California, p. 215.

Peirce, H. W., 1976, Elements of Paleozoic tectonics in Arizona: Arizona Geological Society Tectonic Digest, Vol. X, p. 37-57.

Silver, L. T., 1978, Precambrian formations and Precambrian history in Cochise County, southeastern Arizona: *in* Callender, J. F., Wilt, J. C., and Clemons, R. E., eds., Land of Cochise, New Mexico Geological Society Guidebook, 29th Field Conference, p. 157-163.

Swan, M. M., 1982, Influence of pre-Cretaceous structure upon late Cretaceous-Tertiary magmatism in southern Arizona and New Mexico (abs): Abstracts, 78th annual meeting Cordilleran Section, The Geological Society of America, April 19-21, 1982, Anaheim, California, 238 p.

Titley, S. R., 1976, Evidence for a Mesozoic linear tectonic pattern in southeastern Arizona: *in* Tectonic Digest, Arizona Geological Society Digest, Vol.10, p. 71-101.

Turner, G. L., 1962, The Deming axis, southeastern Arizona, New Mexico and Trans-Pecos, Texas: *in* Mogollon Rim, New Mexico Geological Society Guidebook, 13th Field Conference, 1962, p. 59-71.

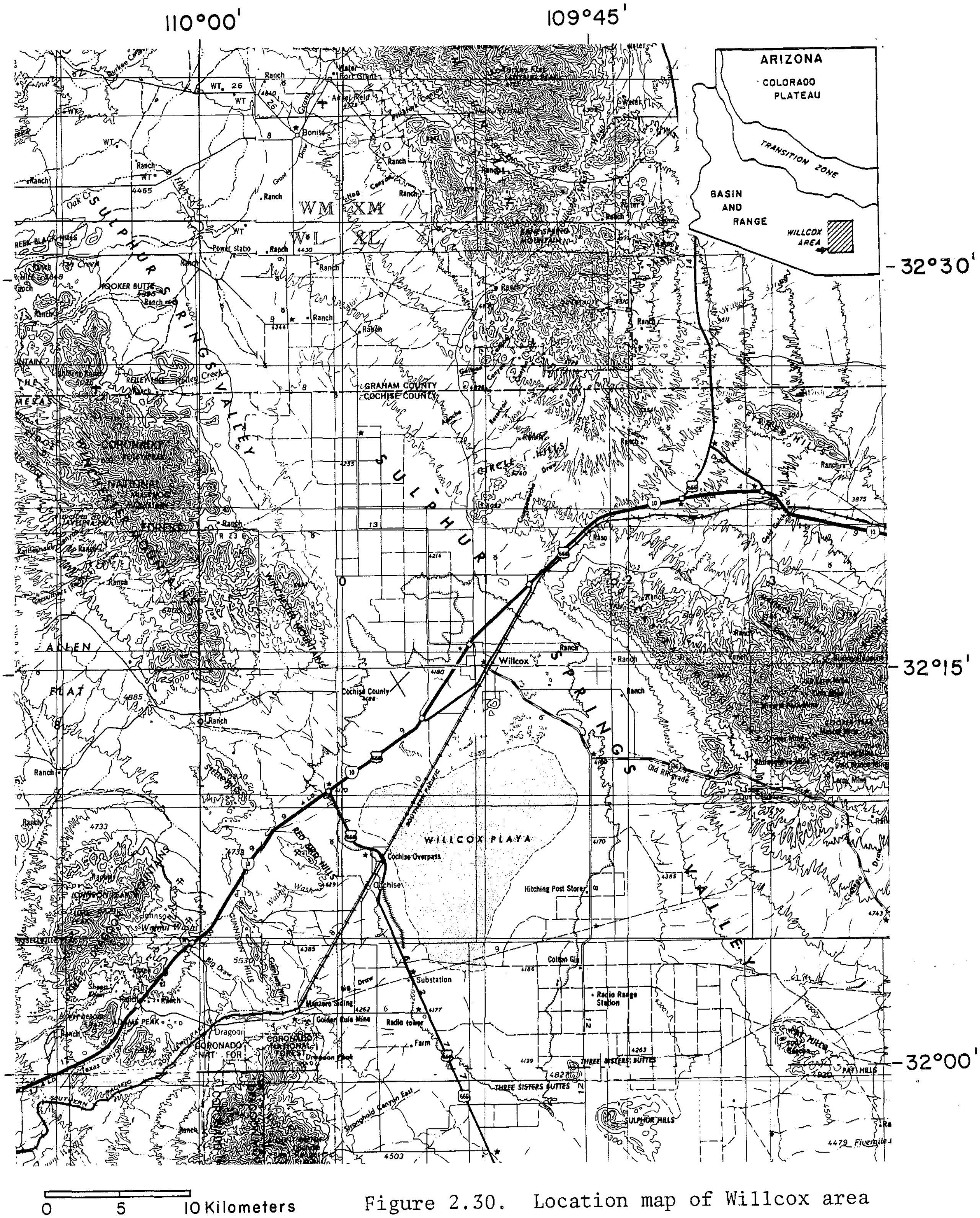

Figure 2.30. Location map of Willcox area

WILLCOX AREA

INTRODUCTION. Willcox lies on the east edge of the Willcox playa in the northern Sulphur Springs Valley of southeastern, Arizona (Fig. 2.30). Springs, which have ceased to flow near low hills south of the playa, give the valley its name. While sulphurous springs are sometimes hot and may indicate significant geothermal potential, the springs south of Willcox were apparently not thermal. However, several wells drilled for irrigation and domestic water supplies have encountered thermal water (>30°C) and they indicate potential low-temperature geothermal resources.

Because the Willcox area has a large agricultural economic base and has relatively cool nights in the winter, significant opportunities may exist for direct use of geothermal heat. In general, the area has a favorable land status for geothermal development. A probable exception is a military reservation on the playa; however, practical considerations such as flooding may also make the playa unsuitable for geothermal development.

PHYSIOGRAPHY. The Willcox area overlies a sediment-filled structural basin that forms the Sulphur Springs Valley. Surface drainage in the Willcox basin is mostly internal; runoff from precipitation in the surrounding Dos Cabezas, Chiricahua, Pinaleno, Galiuro, and Dragoon Mountains flows toward the playa in the basin center. Topography in the basin is relatively flat and slopes gently upward toward the mountains.

GEOLOGY. The Willcox basin is separated into two terranes by a major west-northwest zone of faults and complex structures, the Dos Cabezas discontinuity of Titley (1976). This zone is characterized by left-lateral strike-slip faults, reverse faults, thrusts faults, and normal faults, which have had repeated movement since Precambrian (Fig. 2.31). North of this zone, Tertiary sedimentary and volcanic rocks unconformably overlie Precambrian metamorphic and plutonic rocks. This northern terrane apparently lost its cover of Paleozoic and Mesozoic rocks during erosion that post-dated and accompanied uplift of the pre-late-Cretaceous Burro uplift, a west-northwest striking structural high that extends eastward into New Mexico (Elston, 1958). The Burro uplift is an element of the Mogollon Highland (Turner, 1962; Coney, 1978). South of the Dos Cabezas discontinuity, Tertiary rocks unconformably overlie Precambrian, Paleozoic, and Mesozoic rocks.

Drewes (1976) postulated that much of the region south of the Dos Cabezas discontinuity is underlain by a regionally extensive allochthon that was thrust northward and northeastward. Jones (1963), Keith and Barrett (1976), and Davis (1979) presented geologic arguments that support basement cored uplift, which was accompanied by local thrusting and high angle reverse faults during the Laramide orogeny.

Precambrian rocks consist of Pinal Schist and granite. Lower and middle Paleozoic strata, which occur south of the Dos Cabezas discontinuity, consist of a basal sandstone overlain by a sequence of interbedded sandstones, shales, and carbonate rocks. Carbonate rocks are the predominant lithology. These rocks are overlain by deposits (>1 km thick)

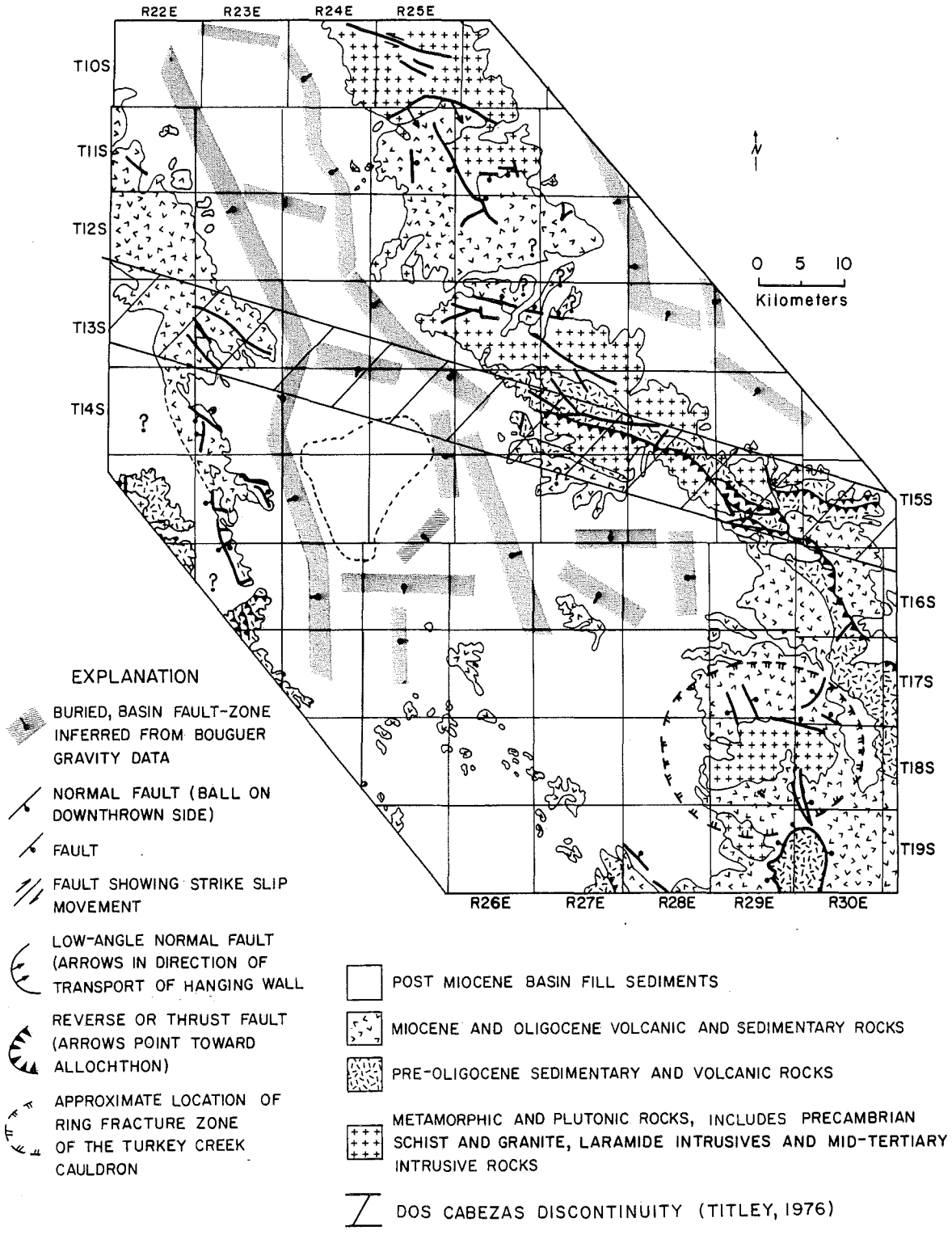

Figure 2.31. Generalized geology of the Willcox area

of late Paleozoic, mostly carbonate strata, which have increased clastic content and are separated by numerous disconformities. Paleozoic carbonate strata of this region have the potential to act as a geothermal reservoir. The Wadell-Duncan #1 Murray oil and gas test (D-22-27-5b) in the Douglas basin south of Willcox encountered an artesian flow (379 L/min) of 54°C water originating from below 692 m in Mississippian limestone (Coates and Cushman, 1955).

Mesozoic stratigraphy includes small outcrops of Triassic to Jurassic volcanic and sedimentary rocks on the southwest slope of the Dos Cabezas Mountains and in the little Dragoon Mountains (Hayes and Drewes, 1978). Lower Cretaceous Bisbee Group sediments unconformably overlie the older Mesozoic rocks. Geothermal reservoir potential of Mesozoic rocks is unknown.

The Laramide orogeny (≈75 to 50 m.y.) was accompanied by plutonism and volcanism. Erickson (1968) described a large intrusive breccia in the Dos Cabezas Mountains that intruded both the deformed Bisbee Group and the west-northwest striking Apache Pass fault zone, an element of the Dos Cabezas discontinuity. The breccia forms the two peaks that give the Dos Cabezas range its name.

A renewed phase of volcanism and plutonism began in the area during the mid-Tertiary, after an apparent lull during the Eocene. In the Chiricahua Mountains, mid-Tertiary volcanism culminated in the eruption of several extensive, welded ash-flow tuffs. These flows, comprising the Rhyolite Canyon Formation (25 m.y.), originated from the resurgent Turkey

Creek caldera centered in the Chiricahua Mountains (Marjaniemi, 1968; Shafiqullah and others, 1978; Latta, 1982) (Fig. 2.31).

In the Galiuro Mountains, Winchester Mountains, and Little Dragoon Mountains a sequence of mid-Tertiary volcanic rocks is divided into two parts (Creasey and Krieger, 1978). The lower section consists of andesite to rhyodacite, which is capped locally by a "turkey track" andesite flow (Creasey and Krieger, 1978). A disconformity with up to 300 m of relief separates the 29 to 26 m.y. old andesite to rhyodacite unit from the younger, overlying ash-flow tuff unit (Creasey and Krieger, 1978). The ash-flow tuff unit has intercalated andesite flows and conglomerate strata, whose clasts were derived from Precambrian, Paleozoic, and underlying andesite-rhyodacite flows (Creasey and Krieger, 1978).

In the southern Pinaleno Mountains, the granite of Gillespie Mountain (≈36 m.y.) was intruded into Precambrian rock; however, it is now in low-angle fault contact with overlying and younger Miocene volcanic rocks (Swan, 1976; Thorman, 1981). The Miocene volcanic rocks were interpreted by Thorman (1981) as remnants of a complex eruptive center (27 to 23 m.y.), which began with andesitic flows and culminated in felsic flows, tuffs, and a dome.

In the southern Pinaleno Mountains, a normal low-angle oblique-slip fault having a breccia-gouge zone up to 10 m thick, separates monoclinally deformed Miocene volcanic rocks from the Oligocene Gillespie Mountain stock and Precambrian rocks. Quartz latite dikes (23 m.y.) are cut by this fault. Similarly, a low-angle fault in the Eagle Pass area on the north-west end of the Pinaleno Mountains cuts 24 to 25 m.y. old dikes (Blacet and

Miller, 1978; Shafiqullah and others, 1980) and displaces steeply dipping Tertiary gravels into fault contact with Precambrian rocks.

Fractured and deformed pre-mid-Miocene volcanic and sedimentary rocks may underlie the northern Willcox basin at depth. Their presence is indicated by deformed Tertiary sediments mapped northeast of Willcox by Cooper (1960). These rocks and an associated low-angle fault zone may act as a geothermal reservoir where they are present and hydrologically connected to deeply circulating water flow.

The Willcox basin began to develop during middle to late Miocene (15 to 10 m.y.) as the crust cooled after a mid-Tertiary thermal disturbance and low-angle faulting was replaced by high-angle normal faulting (Scarborough and Peirce, 1978). This crustal rifting broke the area into a zig-zag pattern of horsts (mountains) and grabens (basins). High-angle dip-slip normal faults forming the grabens may provide fracture permeability for hydrothermal systems. Modeling of Bouguer gravity data shows the Willcox basin is a composite of several grabens and may be filled with over 1.5 km of clastic sediments (Aiken, 1978).

Sediments filling the Willcox basin are poorly understood. Brown and Schumann (1969) broke the stratigraphy into two major subdivisions: consolidated alluvium and unconsolidated alluvium. The consolidated alluvium as described by Brown and Schumann (1969) in locations near the Circle I Hills is not "basin-fill" sediment. The deformed nature of these sediments indicates they are probably pre-late Miocene.

The unconsolidated sediments of Brown and Schumann (1969) were divided into two facies. The lake-bed facies (clay and silt) is underlain and

overlain by an alluvial facies (sand and conglomerate). The clay and silt beds (lake-bed facies) provided a very important geologic setting for the occurrence of low-temperature geothermal resources. These fine-grained sediments are characterized by low thermal conductivities, which can cause high temperature gradients (35 to 45°C/km) even with normal crustal heat flow. Because clay and silt are relatively impermeable, they act as aquacludes and confine water in underlying sand and conglomerate aquifers, which prevents significant convective heat loss.

GEOHYDROLOGY. Prior to large-scale withdrawal of ground water from the Willcox basin, ground water flowed from recharge areas on the basin margins toward the playa where discharge occurred through evapotranspiration (Brown and Schuman, 1969). Today, ground water movement is toward water-table depressions resulting from extensive ground-water pumping for irrigation. These ground-water depressions are found in T. 12 and 13 S., R. 24 E. and in T. 15 and 16 S., R. 25 and 26 E. (Fig. 2.31).

THERMAL REGIME. No Quaternary volcanic rocks have been identified in the Willcox basin. A magmatic heat source probably does not exist in the basin.

Conductive heat flow studies show a mean heat flow of 79.5 mWm ^{2} for southern Arizona (Shearer and Reiter, 1981). While no conductive heat flow measurements have been published for the Willcox basin, it is reasonable to assume a similar value as background heat flow for the basin.

Because silt and clay-rich sediments that fill the basin have thermal conductivities less than 2.0 W/mk, temperature gradients between 35 and 45°C/km are normal, provided there is no ground-water flow.

Figure 2.32 compares calculated temperature gradients in the Willcox basin with respective well depths. Wells deeper than 230 m have gradients mostly between 20 and 45°C/km. Variations in gradients from wells below 230 m is probably due to differences in depth of water entry into the wells and possibly rock thermal conductivity differences.

In wells less than 230 m deep, calculated temperature gradients range from 25 to over 300°C/km. The systematically higher gradients from shallower holes result from ground-water movement and to a lesser extent, lower conductivity sediments.

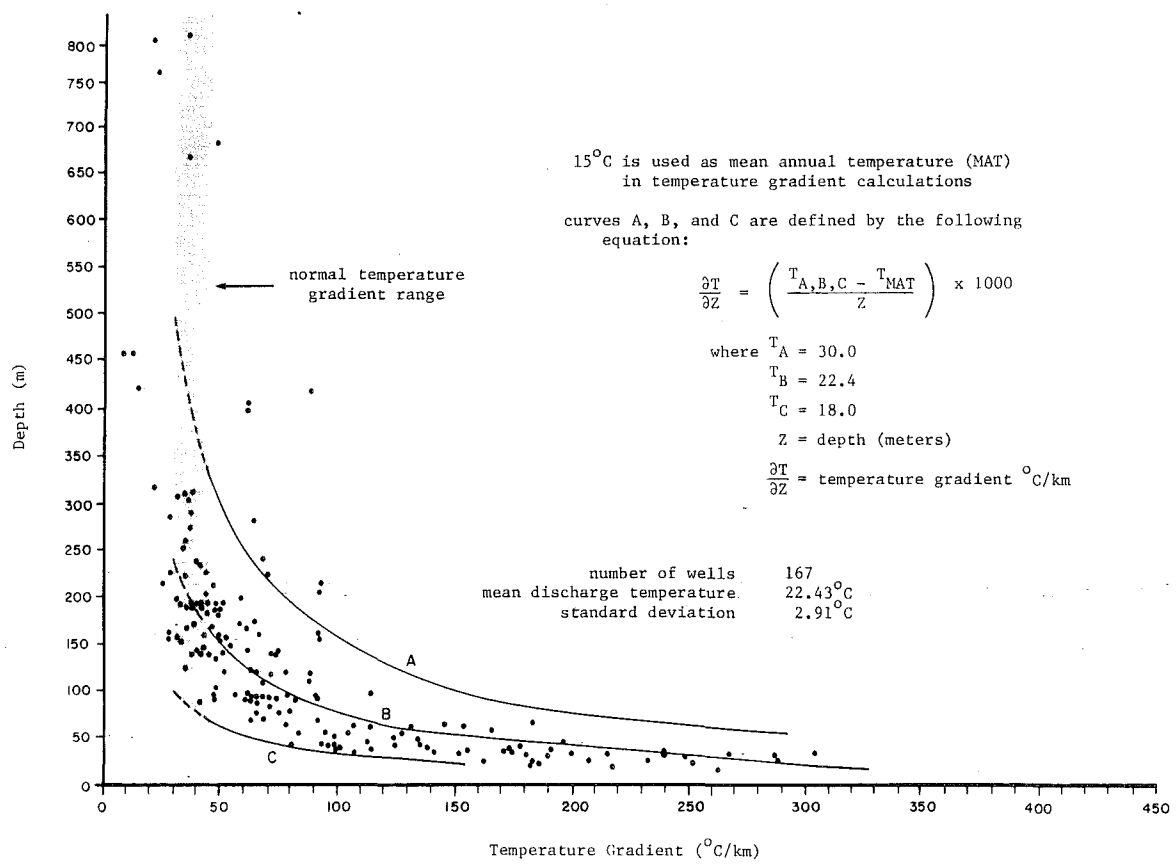

Figure 2.32. Temperature gradients versus depth of water for wells in the Willcox basin

THERMAL WELLS. Thermal wells (Table 2.2 and Figure 2.33) are widely scattered throughout the basin. Such a distribution suggests either several discrete resources or a single extensive thermal aquifer at depth. Temperatures range between 30 and 54°C for wells from 200 to 1,000 m deep.

Figure 2.34 shows cross sections of subsurface stratigraphy constructed from drillers' logs; locations of the cross sections are shown in Figure 2.35. Zones of thermal water were noted in some of these wells by the drillers. Thermal water occurs below clay and silt beds in moderately indurated conglomerate and sand at depth greater than 500 m. Aquifers containing thermal water are confined to semi-confined, as indicated by the artesian flow from several of the thermal wells. Beneath clay and silt depositional centers, at depth greater than 700 m, thermal water may have temperatures greater than 50°C. However, these areas are untested at the present time. Other thermal wells, which are not shown in the stratigraphic cross sections, encounter warm water at depth less than 500 m. Some of these wells are unusually warm and have estimated temperature

TABLE 2.2. List of thermal wells in the Willcox area

Well	Location	Depth (meters)	Temperature	Data Source
1	D-12-24-20 BAA	832	44.0	4
2	D-12-24-20 CAA	664.5	37.0	4
3	D-12-24-31 CB	445	54.4	3,4
4	D-13-24-2 BAA(2)	257	31.7	2,3
5	D-13-24-5 BA	670	47.8	3
6	D-13-24-11 ABB	412	40.6	3,5
7	D-13-25-5	762	31.1	1
8	D-13-25-31 CAB(2)	243	31.7	1,2
9	D-14-25-4 BAC	824	31.1	2,6
10	D-14-25-6 AAD	235	36.7	6
11	D-14-25-6 CBD	214	35.0	1,2
12	D-15-26-19 BBC	1005	43.0	1,6

DATA SOURCES:

1. Brown and others (1963)
2. U.S. Geological Survey
3. Dutt and McCreary (1970)
4. Arizona Bureau of Geology and Mineral Technology
5. Arizona State Land Department
6. Peirce and Scurlock (1972)

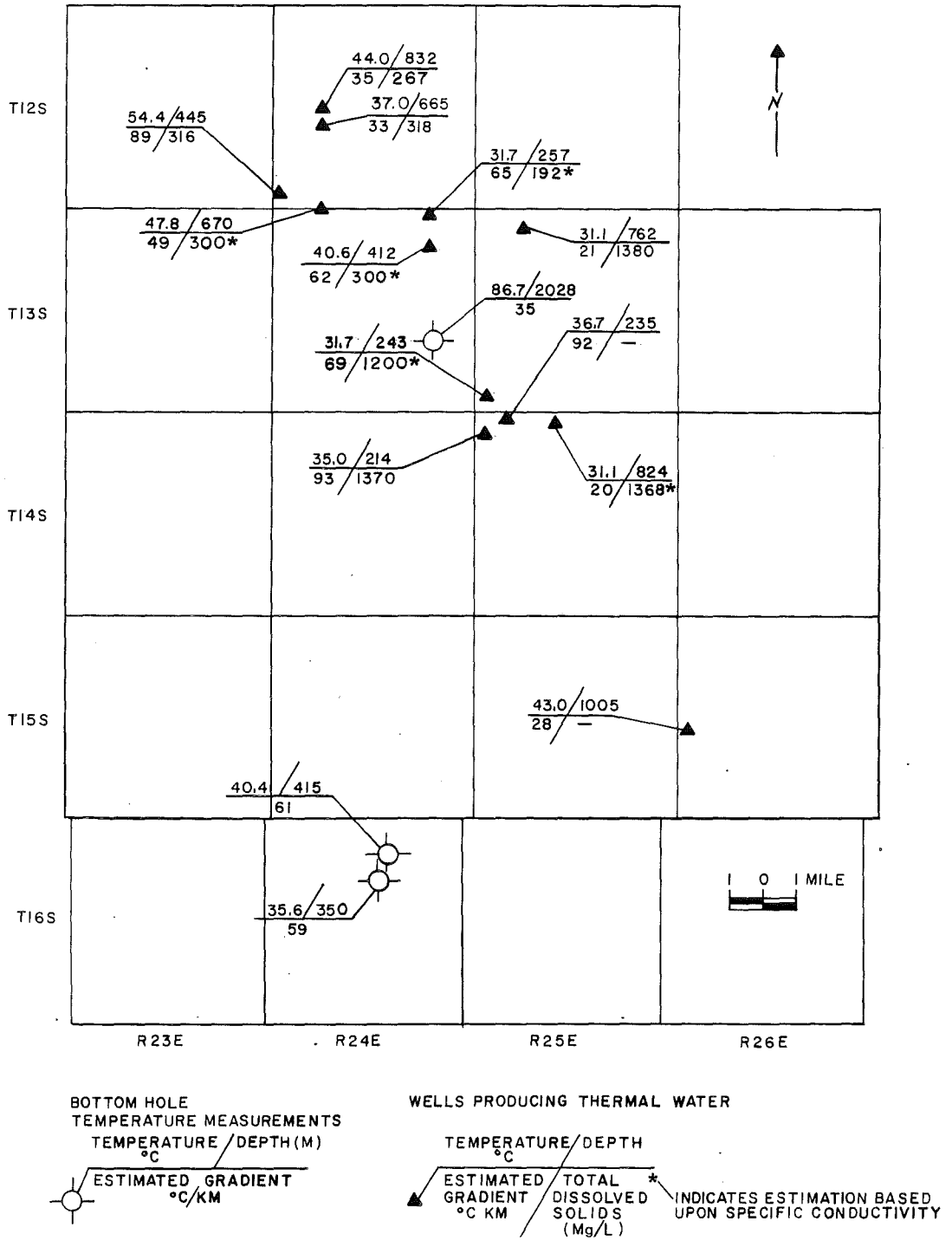

Figure 2.33. Location map of thermal wells in the Willcox area

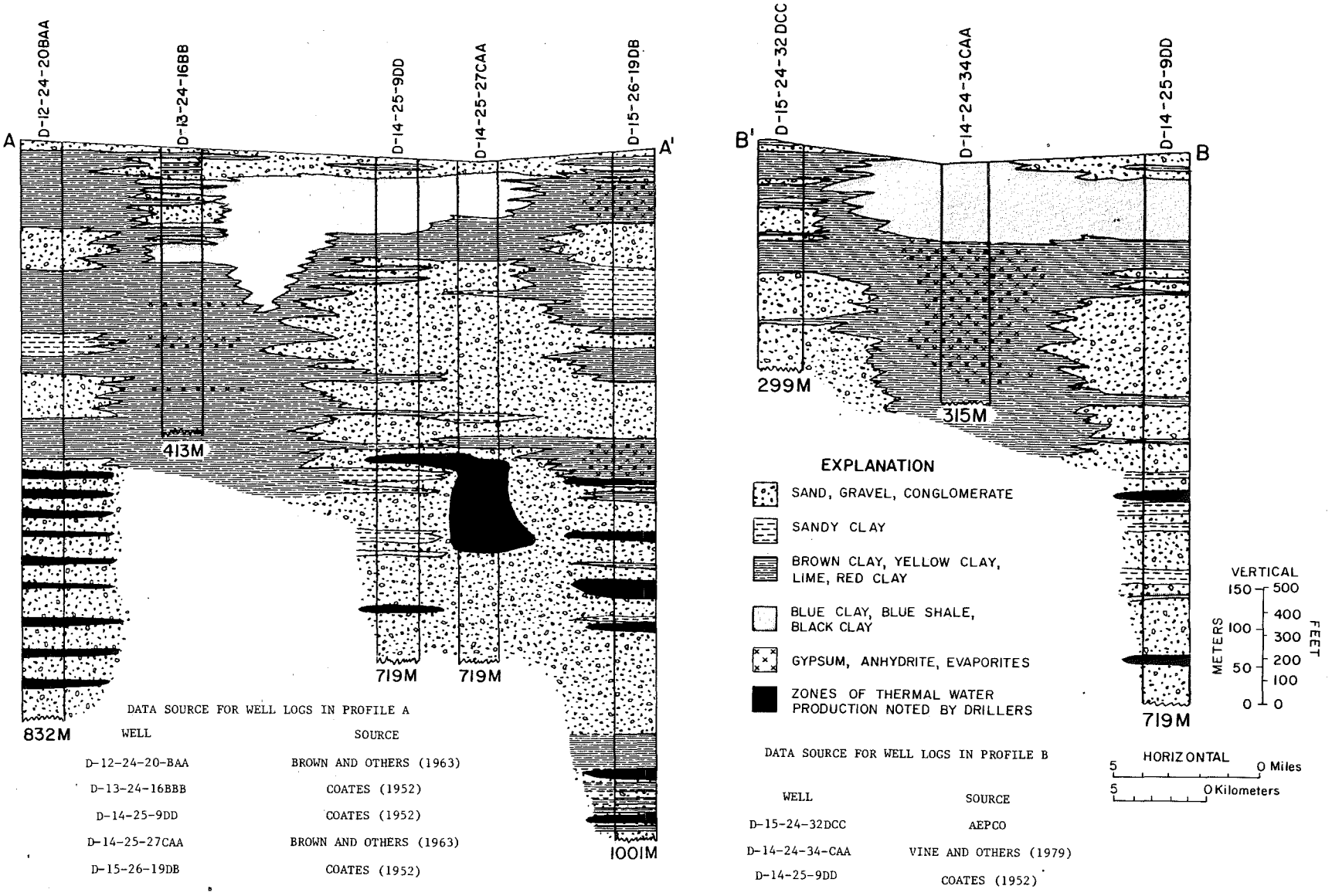

Figure 2.34. Stratigraphic cross sections of the Willcox basin

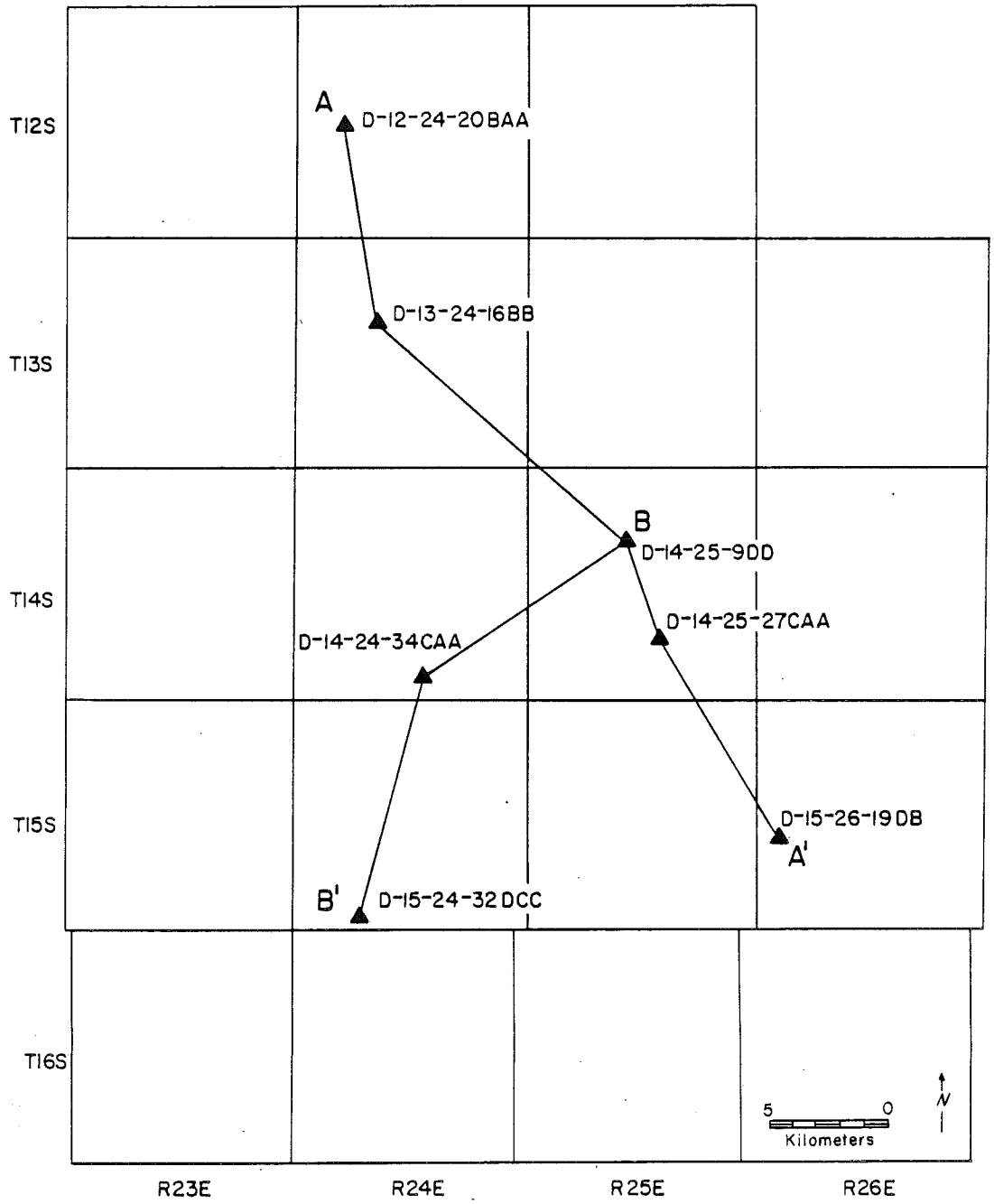

Figure 2.35. Location map of stratigraphic cross sections shown in Figure 2.34

gradients exceeding 60°C/km. The anomalous thermal wells occur in three different areas and may intersect or overlie hydrothermal convection systems (Fig. 2.36). A normal conductive heat flow regime is indicated by thermal wells outside the anomalous areas because these wells have estimated gradients between 20 and 45°C/km.

Chemical quality of thermal water in the Willcox basin ranges between approximately 200 and 1,500 mg/L TDS (Table 2.3). In general, the higher temperature waters from deeper wells have lower TDS. Compositions range from sodium sulfate-bicarbonate water to sodium bicarbonate-chloride water (Fig. 2.37). Fluoride contents of thermal water is high and ranges from 2.6 to over 20 mg/L. Magnesium concentrations are very low in all the thermal waters.

Silica and Na-K-Ca geothermometers were computed for wells with the more complete chemical information (Table 2.4). Analyzed silica concentrations were corrected for nontemperature dependent ionization. Thermal waters from these wells are all saturated with respect to quartz.

The Na-K-Ca geothermometers for wells 1, 2, and 3 are within 5 to 12°C of temperatures predicted by the chalcedony geothermometers. The geothermometers predict subsurface reservoir temperatures averaging between 58 to 65°C. Surface discharge temperatures range from 37 to 54.4°C. Differences between the geothermometers and measured temperatures in wells 1 and 2 are puzzling because these wells are in an apparent conductive thermal regime as indicated by a normal estimated gradient (20 to 45°C/km). Well 3, which occurs over a probable hydrothermal convection system (anomaly 1), as indicated by a high estimated gradient, shows an average

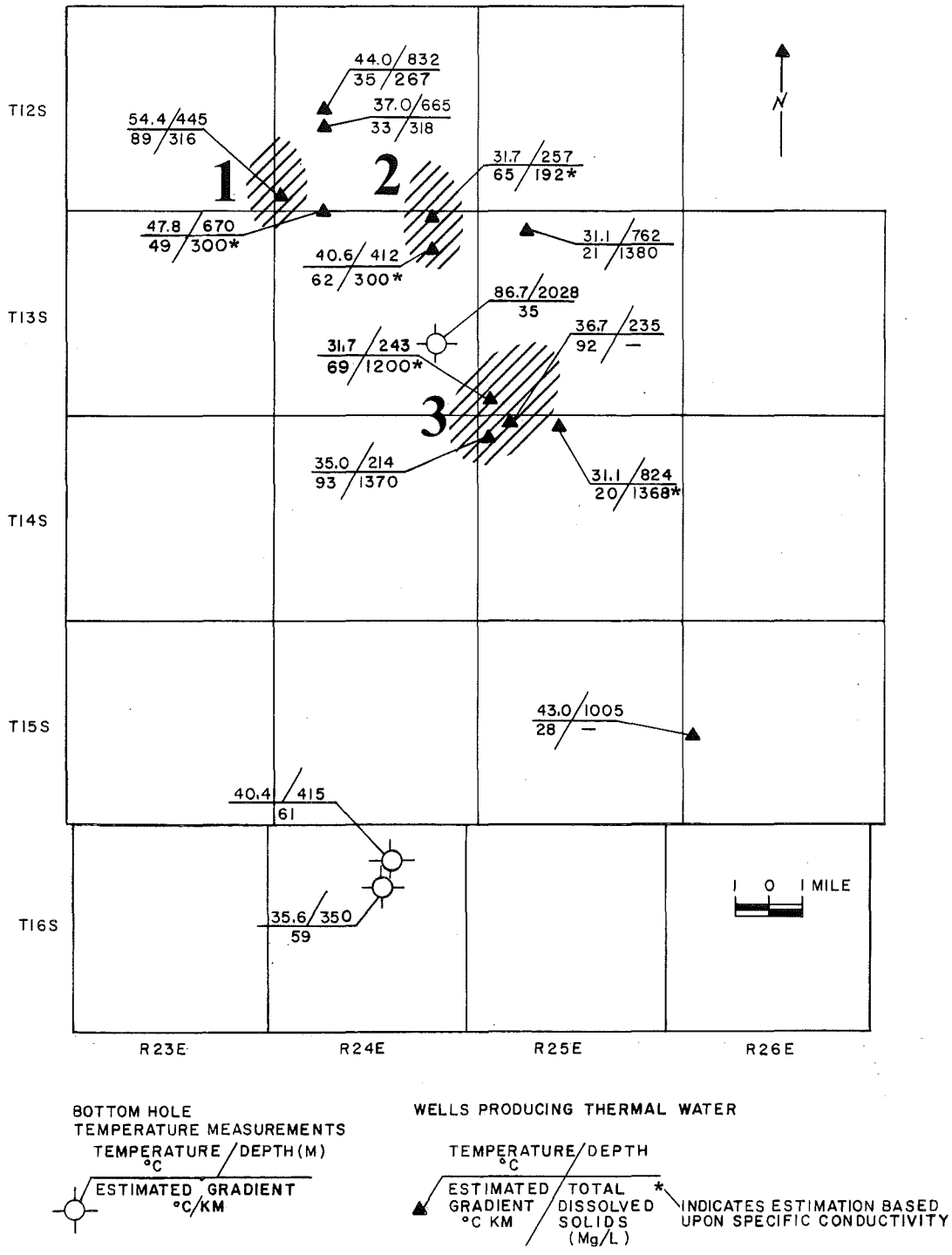

Figure 2.36. Location of anomalous thermal wells in the Willcox basin

TABLE 2.3. Chemistry of thermal water in the Willcox area

Number	Sample	Location	Temperature	TDS	pH	Na	Na+K	K	Ca	Mg	Cl	SO_4	HCO_3+CO_3	SiO_2	Li	B	F	Date	Data Source
1	6037	D-12-24-20 BAA	44.0	267	9.3	97		0.66	2.0	0.38	24	22	88	73.8	0.032	0.15	3.2	8/81	4
2	6038	D-12-24-20 CAA	37.0	318	9.1	79		0.68	1.9	0.40	27	30	68.3	70.8	0.042	0.14	3.1	8/81	4
3	100	D-12-24-31 CB	54.4	316	9.1	47		0.7	<1	<0.1	16	30	136	65.0	0.06	<0.10	20.3	7/79	4
4	8095	D-13-24-2 BAA	31.7	320*	8.8	80		1.5	8	0	10	60	115	---	0.002	0.04	5.0	7/66	2,3
5	8100	D-13-24-5 BA	47.8	500*	9.3	138		2.0	2.0	0	2	110	127	---	0.001	0.09	18.0	7/66	3
6	8115	D-13-24-11 ABB	40.6	500*	9.4	106		1.0	0	0	24	60	98	---	0.002	0.62	10.0	7/66	3
7	----	D-13-25-5	31.1	1380	---		502		7.0	2.8	360	262	302	46	-----	----	12.0	6/50	1
8	8609	D-13-25-31 CAB(2)	31.7	2000*	8.7	428		5.5	3	0	344	200	298	17	0.219	0.44	2.6	5/67	3
9	4817	D-14-25-4 BAC	31.1	2280*	---	---		---	6.9	2.7	---	---	302	46	-----	----	----	----	2
11	----	D-14-25-6 CBD	35.0	1370	---		516		80	3.7	430	238	336	---	-----	----	9.9	5/42	1

Results in Milligrams per liter (mg/L)

Temperatures in Degrees Celsius

* TDS is calculated from specific conductivity using a0.6 conversion factor

Data Sources:
1. Brown and others (1963)
2. U.S. Geological Survey
3. Dutt and McCreary (1970)
4. Arizona Bureau of Geology and Mineral Technology

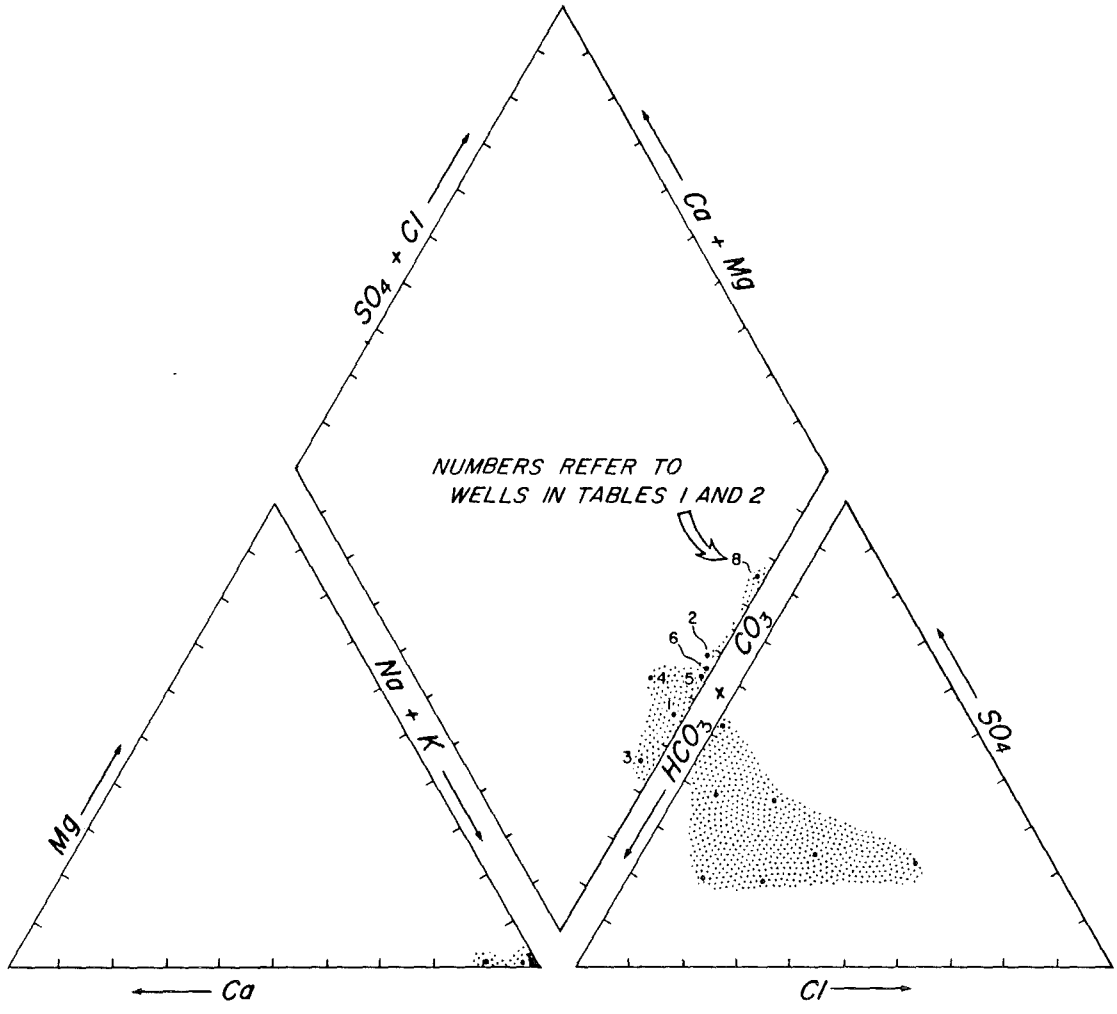

Figure 2.37. Piper diagram of thermal well chemistry, Willcox area

TABLE 2.4. Geothermometers of thermal water in the Willcox area

Well	Measured Temperature (°C)	pH Corrected Silica (mg/L)	Estimated Gradient (°C/km)	Silica Geothermometer (°C) Quartz	Chalcedony	Cristobalite	Na-K-Ca Geothermometer (°C)
1	44.0	34.8	35	86	55	26	60
2	37.0	49.8	33	102	72	51	60
3	54.4	39.0	89	91	60	41	69
8	31.7	15.2	69	54	21	5	104

geothermometer temperature of 65°C. Well 8 has a Na-K-Ca geothermometer of 104°C, but this is most likely a result of nontemperature-dependent solution of evaporite minerals in the basin fill. Well 8 is a sodium-chloride rich water with higher dissolved solids than wells 1, 2, and 3.

CONCLUSION. A large and extensive low-temperature geothermal resource occurs in the Willcox basin at 500 to 700 m depths. The thermal water is confined to semi-confined and is contained in moderately cemented gravel below silt and clay beds. Artesian flow at the surface may occur in some areas. Excellent water quality is indicated except for locally high fluoride concentrations and near the playa where TDS may exceed 2,000 mg/L.

Three areas adjacent to and north of Willcox have anomalous temperature gradients and potential for thermal water with temperatures over 50°C. Geothermometry predicts 60 to 65°C reservoir temperatures.

The basin is untested for normal-gradient type resources at depths greater than 1 km. Although thermal water at a temperature of about 100°C may exist at 2.5 km depths, economics and risk factors may preclude deep exploration and development in the Willcox area.

REFERENCES WILLCOX AREA

Aiken, C. L. V., 1978, Gravity and aeromagnetic anomalies of southeastern Arizona: *in* Callender, J. E., Wilt, J. C., and Clemons, R. E., eds., Land of Cochise, New Mexico Geological Society Guidebook, 29th Field Conference, p. 301-313.

Blacet, P. M. and Miller, S. T., 1978, Reconnaissance geologic map of the Jackson Mountain quadrangle, Graham County, Arizona: U. S. Geological Survey Miscellaneous Field Studies Map MF-939.

Brown, S. G., Schumann, H. H., Kister, L. R., and Johnson, P. W., 1963, Basic ground-water data of the Willcox basin, Graham and Cochise Counties, Arizona: Arizona State Land Department Water-Resources Report 14, 93 p.

Brown, S. G. and Schumann, H. H., 1969, Geohydrology and water utilization in the Willcox basin, Graham County and Cochise County, Arizona: U. S. Geological Survey Water Supply Paper 1859-F, 32 p.

Coates, D. R. and Cushman, R. L., 1955, Geology and ground-water resources of the Douglas basin, Arizona: U. S. Geological Survey Water Supply Paper 1354, 56 p.

Coney, P. J., 1978, The plate tectonic setting of southeastern Arizona: *in* Callender, J. K., Wilt, J. C., and Clemons, R. E., eds., Land of Cochise, New Mexico Geological Society Guidebook, 29th Field Conference, p. 285-290.

Cooper, J. R., 1960, Reconnaissance map of Willcox, Fisher Hills, Cochise and Graham Counties, Arizona: U. S. Geological Survey Miscellaneous Field Studies Map MF-231.

Creasey, S. C. and Krieger, M. H., 1978, Galiuro volcanics, Pinal, Graham, and Cochise Counties, Arizona: U. S. Geological Survey Journal of Research,Vol. 6, no. 1, p. 115-131.

Davis, G. H., 1979, Laramide folding and faulting in southeastern Arizona: American Journal of Science, Vol. 279, p. 534-569.

Drewes, H., 1976, Laramide Tectonics from Paradise to Hells Gate, southeastern Arizona: *in* Wilt, J. C., and Jenney, J. P., eds., Tectonic Digest, Arizona Geological Society Digest, Vol. 10, p. 151-168.

Elston, W. E., 1958, Burro uplift, northeastern limit of sedimentary basin of southwestern New Mexico and southeastern Arizona: American Association of Petroleum Geologists Bulletin, Vol. 42, p. 2513-2517.

Erickson, R. C., 1968, Geology and geochronology of the Dos Cabezas Mountains, Cochise County, Arizona: *in* Southern Arizona, Guidebook III, Arizona Geological Society, p. 192-198.

Hayes, P. T. and Drewes, H., 1978, Mesozoic depositional history of southeastern Arizona: *in* Callender, J. F., Wilt, J. C., and Clemons, R. E., eds., Land of Cochise, New Mexico Geological Society Guidebook, 29th Field Conference, p. 201-208.

Jones, R. W., 1963, Structural evolution of part of southeast Arizona: *in* Backbone of the Americas-Tectonic History from Pole to Pole, American Association Petroleum Geologists Memoir 2, p. 140-151.

Keith, S. B. and Barrett, L. F., 1976, Tectonics of the central Dragoon Mountains, a new look: *in* Wilt, J. C. and Jenney, J. P., eds., Tectonic Digest, Arizona Geological Society Digest, Vol. 10, p. 169-204.

Latta, J. S., IV, 1982, Welded ash-flow tuffs of Rhyolite Canyon-geological and geochemical relations to the Turkey Creek Caldera, Chiricahua Mountains (abs.): 10th Annual Geoscience Daze, Department of Geosciences, University of Arizona, Tucson, p. 15.

Marjaniemi, D. K., 1968, Tertiary volcanism in the northern Chiricahua Mountains, Cochise County, Arizona: in Southern Arizona, Guidebook III, Arizona Geological Society, p. 209-214.

Scarborough, R. B. and Peirce, H. W., 1978, Late Cenozoic basins of Arizona: *in* Callender, J. F., Wilt, J. C., and Clemons, R. E., eds., Land of Cochise, New Mexico Geological Society Guidebook, 29th Field Conference, p. 253-259.

Shafiqullah, M., Damon, P. E., Lynch, D. J., Kuck, P. H., and Rehig, W. A., 1978, Mid-Tertiary magmatism in southeastern Arizona: *in* Callender, J. F., Wilt, J. C., and Clemons, R. E., eds., Land of Cochise, New Mexico Geological Society Guidebook, 29th Field Conference, p. 231-241.

Shafiqullah, M., Damon, P. E., Lynch, D. J., Reynolds, S. J., Rehrig, W. A., and Raymond, R. H., 1980, K-Ar geochronology and geologic history of southwestern Arizona and adjacent areas: *in* Jenney, J. P. and Stone, C., eds., Studies in Western Arizona, Arizona Geological Society Digest, Vol. 12, p. 201-260.

Shearer, C. and Reiter, M., 1981, Terrestrial heat flow in Arizona: Journal of Geophysical Research, Vol. 86, no. B7, p. 6249-6260.

Swan, M. M., 1976, The Stockton Pass fault - an element of the Texas Lineament: unpub. M.S. Thesis, University of Arizona, 119 p.

Thorman, C. H., 1981, Geology of the Pineleno Mountains, Arizona a preliminary report: *in* Stone, C. and Jenney, J. P., eds., Arizona Geological Society Digest, Vol. 13, p. 5-11.

Titley, S. R., 1976, Evidence for a Mesozoic linear tectonic pattern in southeastern Arizona: *in* Tectonic Digest, Arizona Geological Society Digest, Vol. 10,p. 71-191.

Turner, G. L., 1962, The Deming axis, southeastern Arizona, New Mexico and Trans-Pecos, Texas: *in* Mogollon Rim, New Mexico Geological Society Guidebook, 13th Field Conference, 1962, p. 59-71.

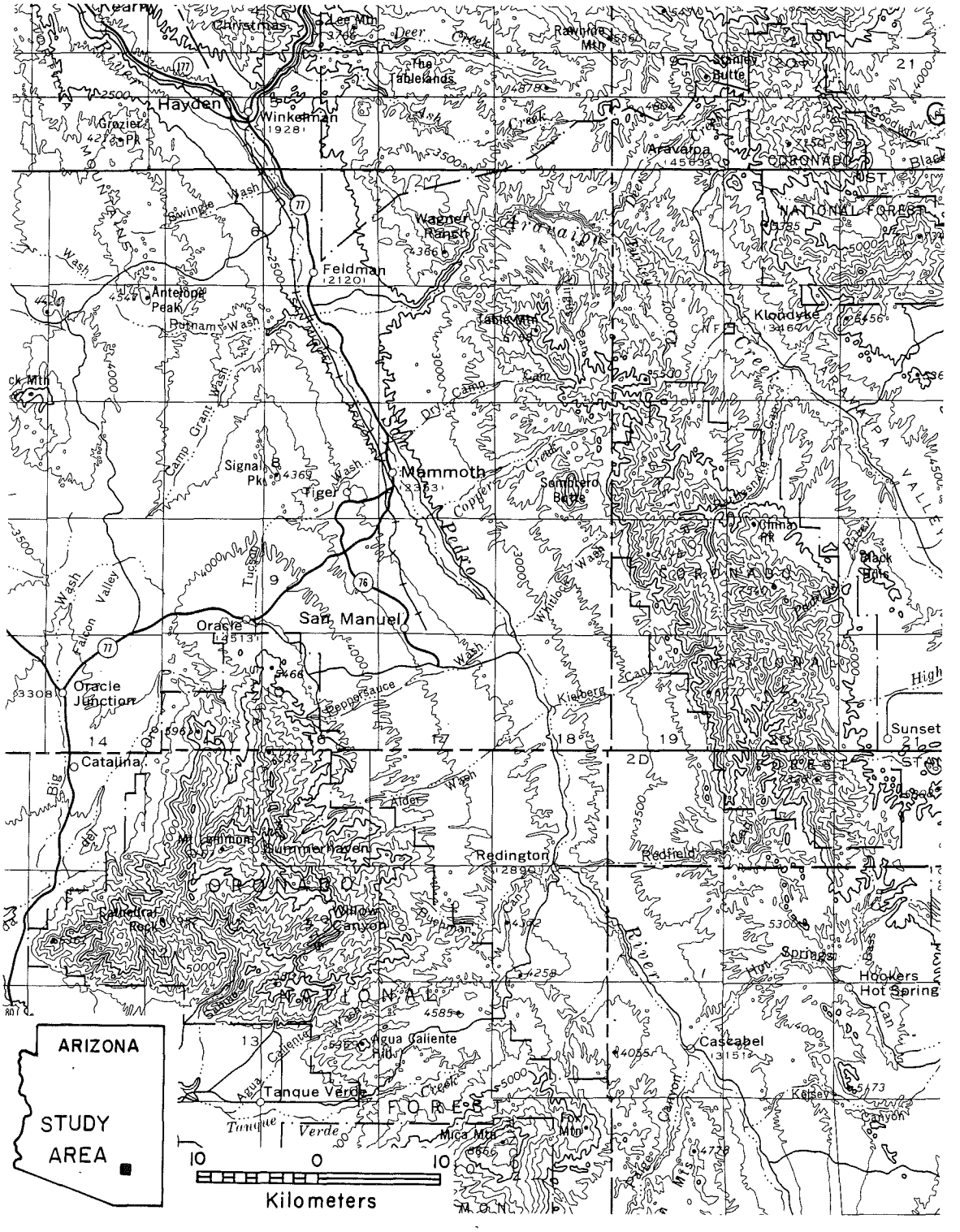

Figure 2.38. Physiographic map of northern San Pedro River valley and San Manuel area

SAN MANUEL AREA

INTRODUCTION. The San Manuel area (Fig. 2.38) is a potential geothermal target because of the presence of thermal water and the possibility of directly using these fluids in a copper-extraction process. Copper ore is mined from the large underground San Manuel mine a few miles west of Mammoth, and a smelter operates at San Manuel. Roeske and Werrel (1973) reported that 38°C water was pumped from the San Manuel mine. In addition, thermal water (31 to 42°C) discharges from several artesian wells in the lower San Pedro River Valley near the communities of Mammoth and San Manuel. Cattle ranching and farming are also important occupations in the valley, and they too are potential users of geothermal energy.

PHYSIOGRAPHY. The San Manuel area is traversed by the intermittently flowing San Pedro River, which flows along the axis of a 24 to 32 km wide valley bound by the Galiuro Mountains on the east and the Santa Catalina Mountains to the west. The valley floor consists of a relatively narrow flood plain (<2 km wide) and a series of gently to moderately sloping terraces that are dissected by drainage originating in the mountains.

GEOLOGY. Pre-Cenozoic structure in the San Pedro Valley is dominated by northwest- to west-northwest-striking faults. Precambrian diabasic and felsic dikes are intruded in Oracle Granite, along structure, in both northwest and northeast directions; however, the largest diabase dikes strike northwest. The principal pre-Cenozoic structure in this area is the northwest-striking Mogul fault, which shows normal, oblique-slip movement.

This fault, which separates the area into two major terranes, has had repeated movement since the Mesozoic, the latest of which displaced Tertiary gravel into fault contact with Precambrian, Paleozic, and Mesozoic rocks (Creasey, 1967). On the southerly, down-thrown side of the fault, Cretaceous(?) clastic sediments show angular unconformable deposition on Mississippian limestone (Creasey, 1967). These Mesozoic and Paleozoic sediments are juxtaposed against a terrane dominated by Precambrian Oracle Granite. The Mogul fault may be a structural element of a major crustal discontinuity (Titley, 1976). Rocks south and north of the Mogul fault are intruded by Laramide plutons and dikes. Mineralization at the San Manuel mine is related to this plutonism.

North of the Mogul fault, Cenozoic volcanic flows and clastic sediments are in either normal low-angle fault contact or unconformable contact with Precambrian rocks and Laramide plutonic or volcanic rocks. West of Mammoth, andesite flows (28 m.y.B.P.) of the basal Cloudburst Formation are in low-angle fault contact with Laramide and Precambrian rocks (Weibel, 1981). Moving up section, the Cloudburst Formation is disconformably overlain by the post-22-m.y. old, monoclinally deformed San Manuel Formation, which in turn is angularly unconformably overlain by the basin-filling Quiburis Formation (Weibel, 1981). The Sacaton Formation, which are ancestral San Pedro River gravels, disconformably overlies the Quiburis Formation.

In the Galiuro Mountains, a sequence of mid-Tertiary volcanic rocks, correlative in time to the volcanic flows and gravels of the Cloudburst Formation, is divided into two parts separated by a major disconformity (Creasey and Krieger, 1978). The lower unit consists of andesite to

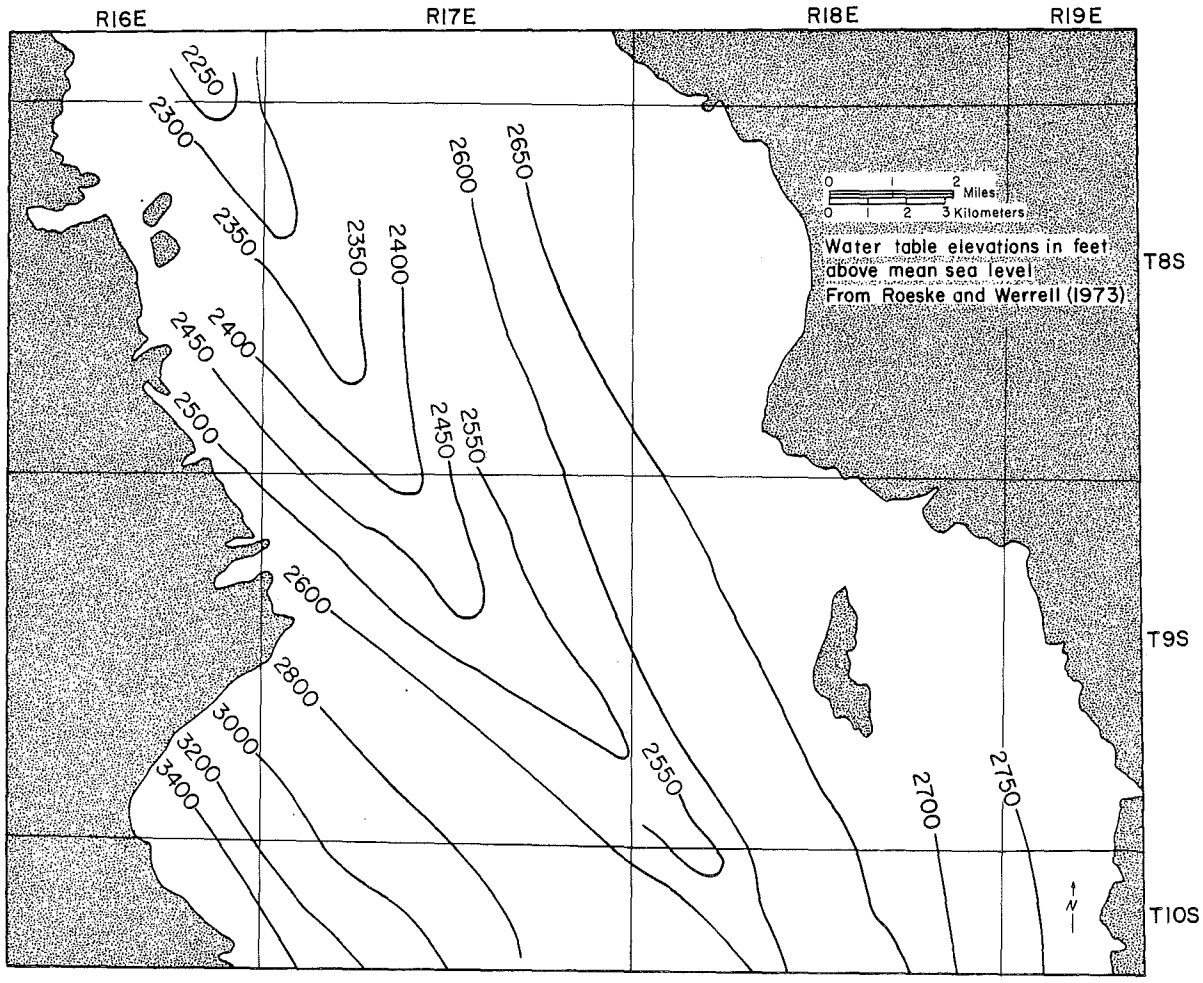

Figure 2.39. Water table of shallow unconfined ground water in the San Manuel area

rhyodacite locally intercalated with tuff. An erosional unconformity with up to 300 m of relief separates the 29 to 26 m.y. old andesite-to-rhyodacite unit from an overlying ash-flow tuff unit and a lenticular rhyolite-obsidian unit (Creasey and Krieger, 1978). The ash-flow tuff unit has intercalated andesite flows and conglomerate strata whose clasts were derived from Precambrian, Paleozoic, and underlying andesite-rhyodacite flows (Creasey and Kreiger, 1978).

GEOHYDROLOGY. Shallow ground-water flow in the lower San Pedro Valley is from the mountains toward the San Pedro River and then northward along the valley axis (Roeske and Werrel, 1973) (Fig. 2.39). Shallow ground water occurs under unconfined conditions. Confined thermal water is encountered at depths between 165 and 420 m in clastic sediments of uncertain age and stratotectonic position. Artesian wells in the area flow up to 1,890 L/min (Roeske and Werrel, 1973). The piezometric surface of the confined water is undetermined, but probably varies in different parts of the basin due to the probability that several discrete aquifers exist in the basin.

THERMAL WELLS. Thermal water, 31 to 42°C, flows from wells that range from 17 to 453 m depth (Table 2.5; Fig. 2.40). These thermal wells occur east of Mammoth and San Manuel in a zone trending northwest. This distribution may reflect the thermal regime or it may be a result of the thermal wells coincidentally being located in an area with the greatest ground-water development. More extensive drilling may expand the known resource areas in this basin. Thermal wells near the river, which are greater than 200 m deep, flow at the surface. Drillers' logs show that clay and

TABLE 2.5. Thermal wells in the San Manuel area

Well	Location	Temperature	Depth	TDS	Flow Rate
1	D-8-17-32daa	42°C	453 m	434 mg/l	76 L/min
2	D-9-16-2 bab	38	396	440	4391
3	D-9-17-10dcb	32	26	744	15
4	D-9-17-14cdb	31	17	590	--
5	D-9-17-14cdd	31	--	234	114
6	D-9-17-24ddc	31	265	352	1514
7	D-9-19-32cab	"hot"	373	--	26.5
8	D-10-18-3bab	41	84	454	45

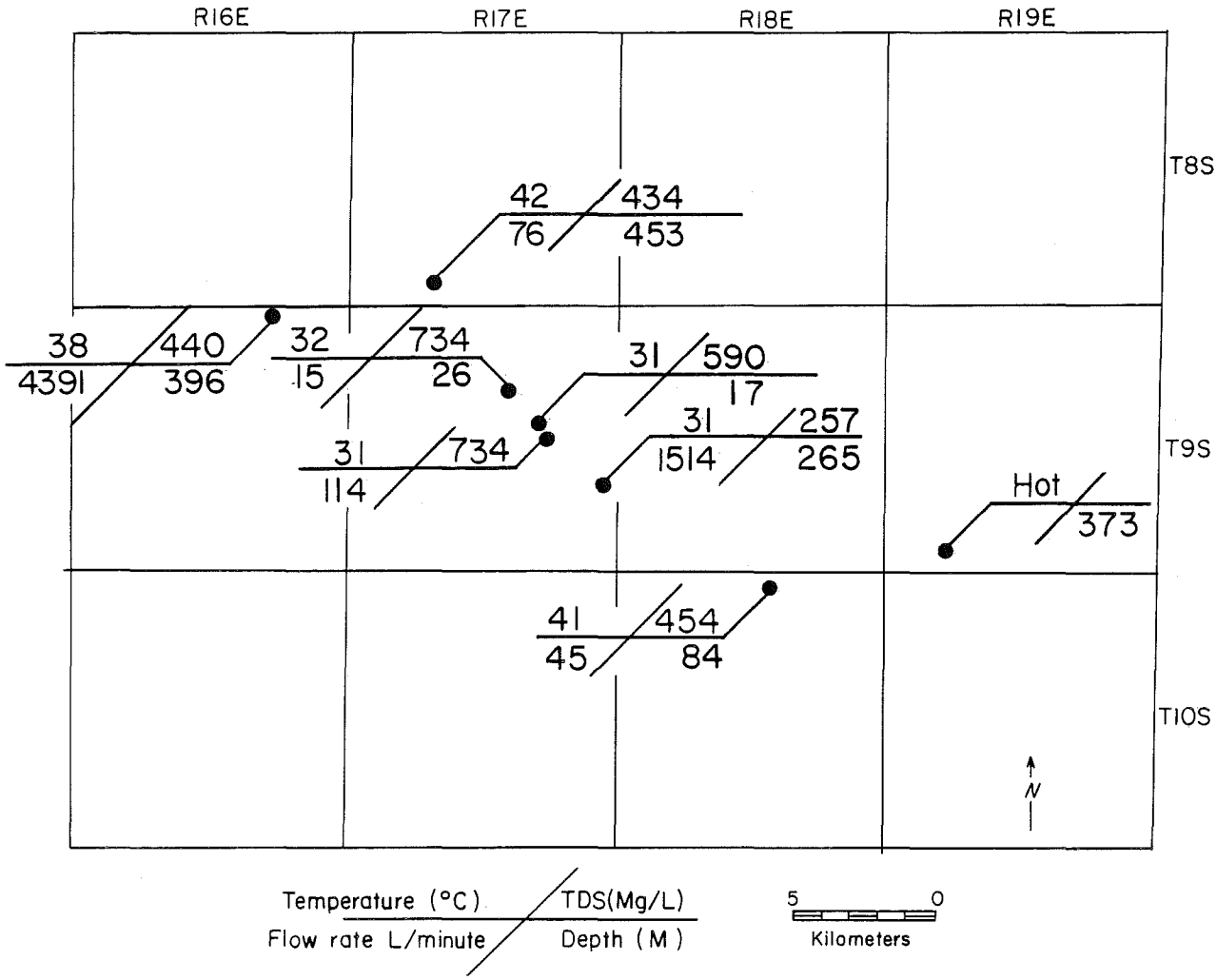

Figure 2.40. Thermal wells in the San Manuel area

gypsiferous sediments overlie sand and gravel that act as the thermal aquifer (Fig. 2.41). Estimated gradients in thermal wells exceed 50°C/km. Exceedingly high estimated gradients in the shallowest wells suggest that thermal water encountered in those wells originates from leakage from deep confined aquifers. Fault zones in basin-fill sediments may provide vertical passage for thermal-water leakage.

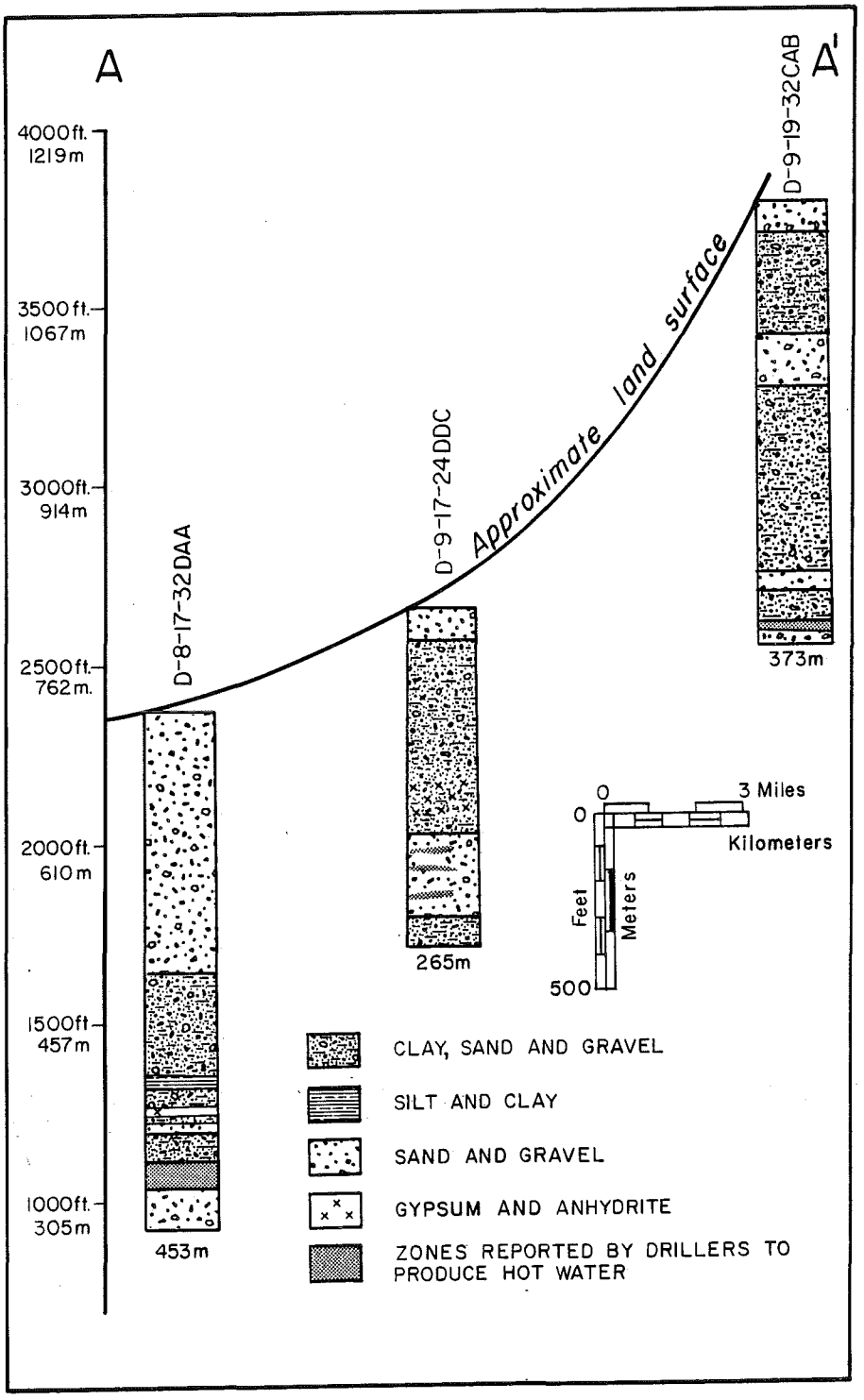

Figure 2.41. Generalized stratigraphy of thermal wells in the San Manuel area

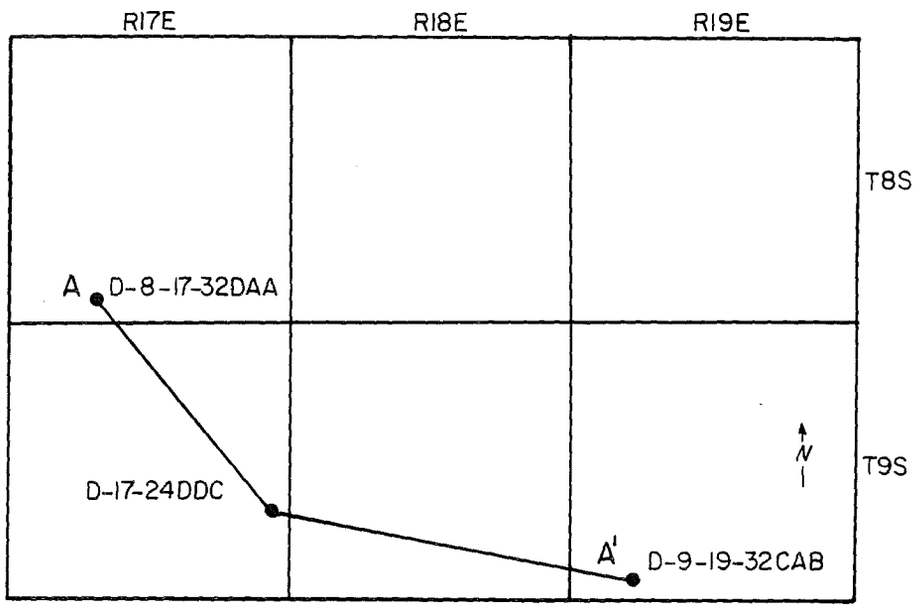

Location of wells shown in Figure 2.41, facing page

Well D-9-16-2bab is actually a mine shaft. Thermal water encountered in this shaft may result from eastward flowing water that is forced upward along the San Manuel fault. Either the fault or fractured Oracle Granite and Cloudburst Formation act as the aquifer in this area.

Chemistry of the mine water indicates a source outside of the basin. The mine water is calcium bicarbonate, while thermal water found in the basin is sodium sulfate to sodium bicarbonate (Fig. 2.42). Sulfate is obtained from solution of gypsum contained in the basin-fill sediments. Sodium may come from ion exchange of calcium with clay minerals in the basin fill.

The Na-K-Ca geothermometer is not applicable because of probable ion exchange and the presence of gypsiferous sediments in the basin fill. Chalcedony geothermometers indicate temperatures less than 60°C for the San Manuel area.

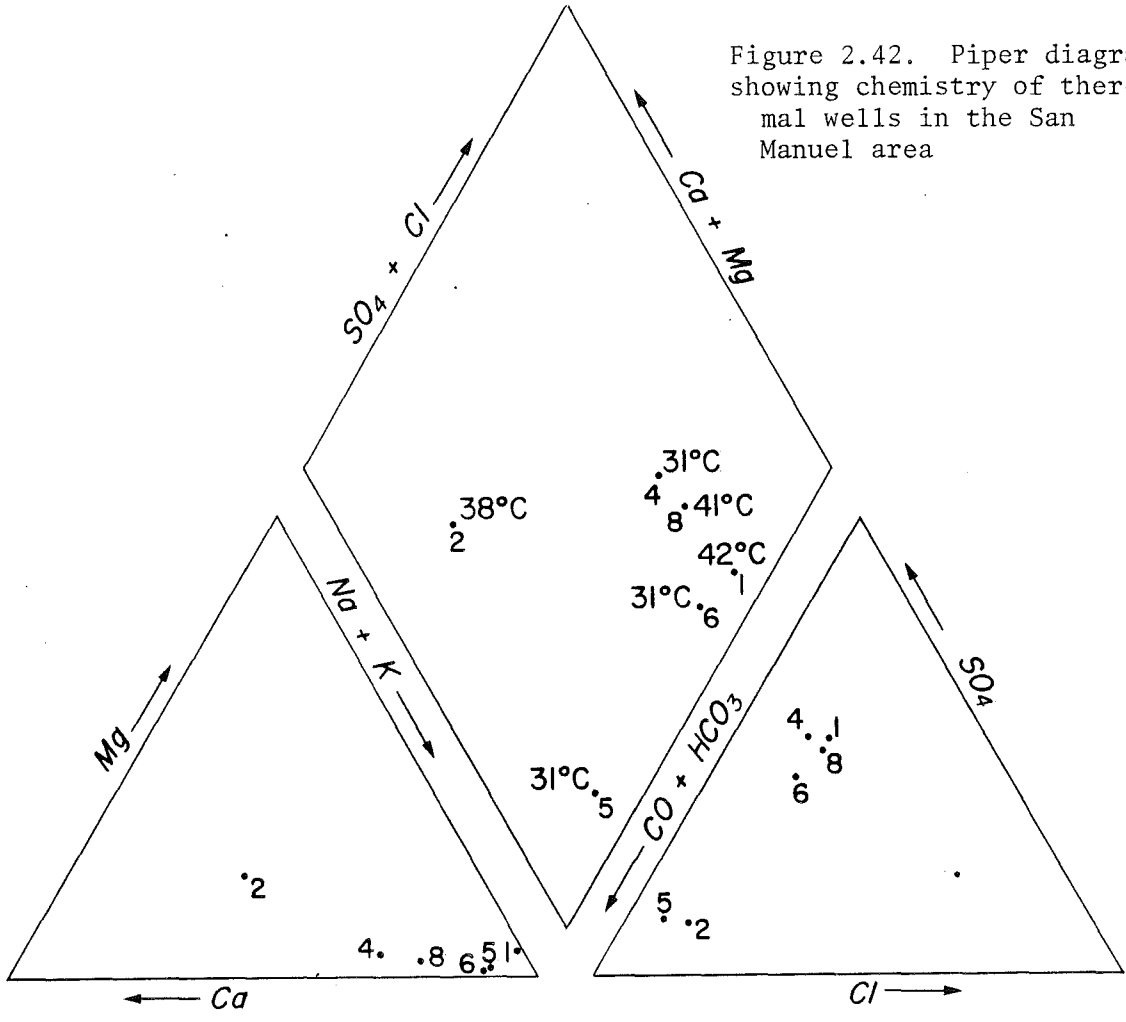

Figure 2.42. Piper diagram showing chemistry of thermal wells in the San Manuel area

CONCLUSION. Confined aquifers contained in basin-fill sediments at depths greater than 200 m apparently contain thermal water in the San Manual area. Temperatures exceeding 60°C are not indicated from known wells in the area, or from the chalcedony geothermometers. However, more extensive resource evaluation might locate numerous additional sites within this basin, which may or may not contain higher temperature thermal waters. Improved copper extraction at San Manuel mine or the smelter is one possible application for these thermal waters.

SAN MANUEL AREA REFERENCES

Creasey, S. C., 1967, General geology of the Mammoth Quadrangle, Pinal County, Arizona: U. S. Geological Survey Bulletin 1218, 94 p.

Creasey, S. C. and Krieger, M. H., 1978, Galiuro volcanics, Pinal, Graham, and Cochise Counties, Arizona: U. S. Geological Survey Journal of Research, Vol. 6, No. 1, p. 115-131.

Roeske, R. H. and Werrell, W. L., 1973, Hydrologic conditions in the San Pedro River Valley, Arizona, 1971: Arizona Water Commission Bulletin 4, 76 p.

Titley, S. R., 1976, Evidence for a Mesozoic linear tectonic pattern in southeastern Arizona: *in* Wilt, J. C., and Jenney, J. P., eds., Tectonic Digest, Arizona Geological Society Digest 10, p. 71-101.

Weibel, W. L., 1981, Depositional history and geology of the Cloudburst Formation near Mammoth Arizona: Unpub. M. S. thesis, University of Arizona, 81 p.

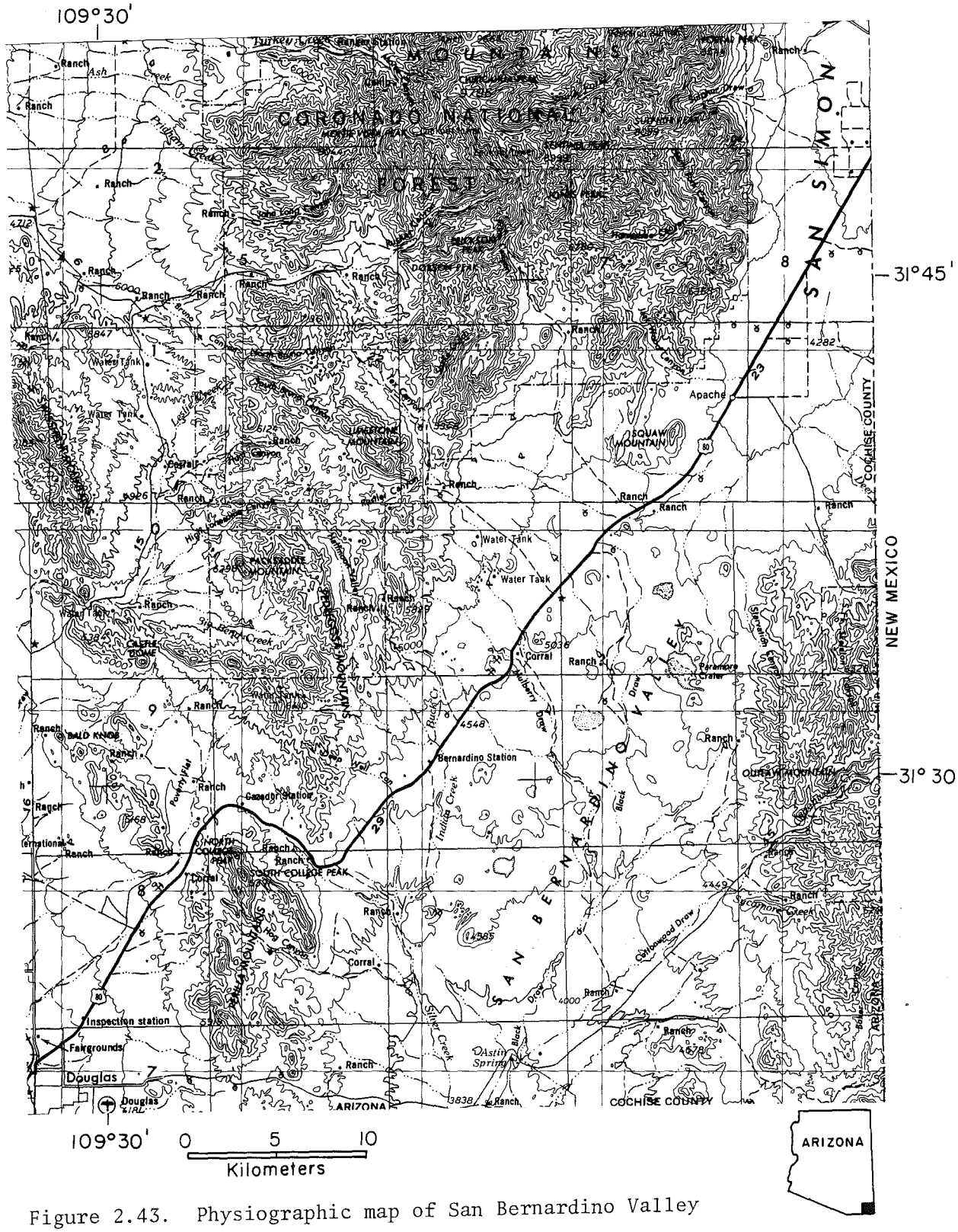

Figure 2.43. Physiographic map of San Bernardino Valley

SAN BERNARDINO VALLEY

INTRODUCTION. San Bernardino Valley (Fig. 2.43) has been a geothermal exploration target for the emerging geothermal industry. As of January 1982, lease applications on 16,591 acres of federal land were pending approval, and 30,596 acres of state land were leased. In addition to leasing, at least one temperature gradient hole has been drilled by a major company. No thermal waters have been observed in the valley north of the international border with Mexico. However, Pleistocene volcanism, resulting in extensive volcanic deposits in the valley, has made this area a geothermal target.

PHYSIOGRAPHY. The San Bernardino Valley lies in the extreme southeast corner of Arizona in an apparent physiographic subprovince of the Mexican Highland section. This subprovince encompasses that part of Sonora and Chihuahua, Mexico north of the Sierra Madre province, and the San Bernardino, Animas, and Playas Valleys in New Mexico and Arizona. It contrasts with the surrounding Mexican Highland section by having generally north-south oriented basins and ranges as opposed to the surrounding northwest physiographic grain.

GEOLOGY. Precambrian basement in the valley probably consists of rocks equivalent to the Pinal Schist of Ransome (1903). Some xenolithic bombs in Hans Cloos Crater resemble Pinal Schist according to Lynch (1972, 1978). Sedimentation in the northwest-oriented Pedregosa Basin (Fig. 2.44), an element of the Mexican geosyncline, deposited thick

sequences of Paleozoic and Early Cretaceous sediments. Over 2,500 m of mainly carbonate Paleozoic rocks, of which 1,500 m are Permian, may be preserved in the subsurface. These carbonate strata could act as geothermal reservoirs in fault zones where brecciation, silicification, and solution have created permeability.

Thrust faults are mapped in the Pedregosa Mountains and in the hills on the southeast margin of the valley. Their extent and relation to subsurface structure is uncertain. Thrust faults in the Pedregosa Mountains (Fig. 2.45) coincide with a west-northwest crustal discontinuity defined by the southern terminous of the symmetrical San Simon graben (interpreted from Bouguer gravity data) and with a zone of Quaternary basalt vents in the southern Chiricahua Mountains. Offset of physiographic features is easily seen on maps of this region. The northern boundary of the assymetric, north-striking graben that forms the San Bernardino Valley also coincides with the discontinuity.

A mid-Teritiary volcanotectonic feature called the Geronimo Trail cauldron is hypothesized to underlie the Peloncillo and Guadalupe

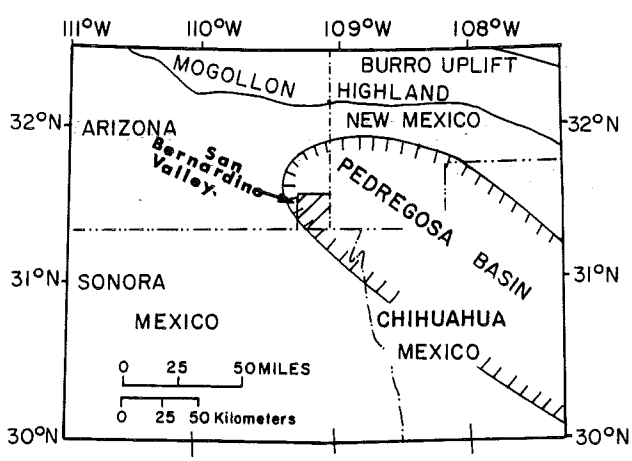

Figure 2.44. Location of the Pedregosa basin

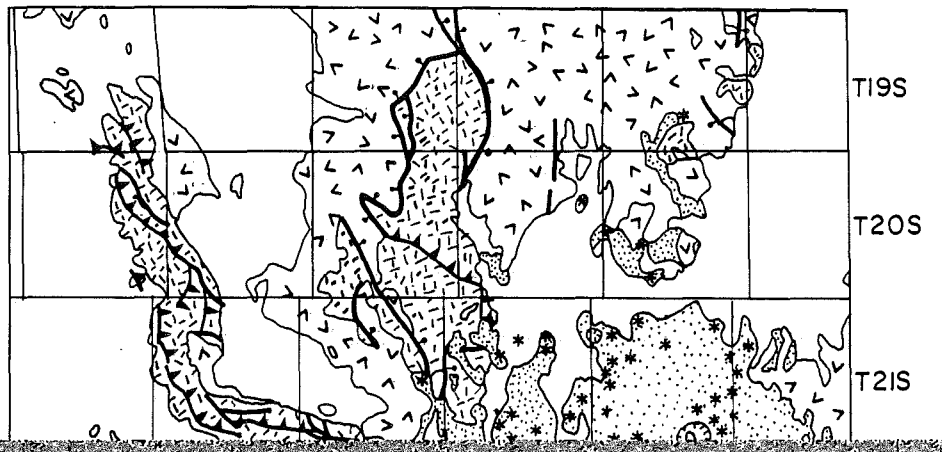
T19S
T20S
T21S

More than 130 pyroclastic cones, with associated flows of limited extent, coalesce to form an alkalic olivine basalt field covering 850 km^2. Water wells that are as deep as 250 m penetrate up to seven flows in the center of the valley. Lynch (1978) reported that mineral equilibrium studies by Evans and Nash (1978) showed that the San Bernardino basalts probably originated in the mantle at depths up to 67 km, that the basalts are not contaminated by crustal material and that they have probably traveled directly from the mantle to the surface. Silicic lavas are not associated with the basaltic lavas, giving additional support to the hypothesized absence of a crustal magma chamber. While lavas in the San Bernardino volcanic field range in age from 3.3. to 0.3 m.y., the volcanism probably has not contributed large quantities of heat to the crust. Rather, most of the igneous heat probably has been dissipated at the surface.

Evidence of steam and hot water associated with basaltic eruptions is found in at least five tuff rings, two of which are large maar craters, Paramore Crater and Hans Cloos Crater. These craters were formed by steam explosions, possibly the result of magma contacting large quantities of water contained in the "water courses" of fault zones. No residual heat from these steam explosions is known to exist today.

Tectonically, the San Bernardino area is one of the more active in Arizona. Just south of the international border, a large (magnitude greater than 7.0) earthquake disrupted the Pitaicachi fault on May 3, 1887 and formed the east side of the San Bernardino Valley in Sonora, Mexico (Sumner, 1976; DuBois and Smith 1981). Pleistocene faulting has been

observed in the adjacent Animas Valley in New Mexico and along White Water Draw below the Swisshelm Mountains, west of the valley. Lava flow remnants, which form distinctive mesas on the west side of the San Bernardino Valley, contain intercalated gravels, which are presently isolated from possible source areas by post-3-m.y. faulting (Lynch, 1972, 1978). Geomorphic anomalies, trenched alluvial fan apexes, straight mountain-front facets along the east side of the Chiricahua Mountains, and unusual drainage patterns such as Cienuguita Creek in Sonora, also suggest active tectonism (Lynch, 1972, 1978). Pyroclastic cone alignment in N. 23° E. and N. 65° W. trends and the north-striking Pitaicachi fault indicate west-northwest extension (Menges and Lynch, 1982, in prep.). Microseismicity along the Pitaicachi fault indicates focal depths of 15 km, and is also due to west-northwest extensional strain in the crust (Natali and Sbar,1982).

CONCLUSIONS. The San Bernardino Valley has potential for low to intermediate temperature resources. High temperature resource potential is speculative even though high Na-K-Ca geothermometers (229°C) were calculated using nonthermal waters (Swanberg and others, 1977; Swanberg, 1978). Further geochemical evaluation is required to assess these geothermometer temperatures. Swanberg (1981) showed two thermal springs in the San Bernardino Valley south of the international border. Geothermometers for these waters are in the low to intermediate temperature range. High regional heat flow probably acts as the heat source for these springs rather than an igneous heat source. The San Bernardino Valley area has the following characteristics, all of which are indicative of geothermal

resources: (1) extensive basaltic volcanism; (2) active extensional tectonics; (3) alignment of pyroclastic cones and young faults that differ from the regional grain (Lynch, 1978; Seager and Morgan, 1979).

REFERENCES SAN BERNARDINO VALLEY

Deal, E. G., Elston, W. E., Erb, E. D., Peterson, S. L., Reiter, D. E., Damon, P. E., and Shafiqullah, M., 1978, Cenozoic volcanic geology of the Basin and Range province in Hidalgo County, southwestern Nex Mexico: *in* Callender, J. E., Wilt, J. C., and Clemons, R. E., eds., Land of Cochise, New Mexico Geological Society Guidebook, 29th Field Conference, p. 219-229.

DuBois, S. M. and Smith, A. W., 1980, the 1887 earthquake in San Bernardino valley, Sonora: Arizona Bureau of Geology and Mineral Technology Special Paper no 3, 112 p.

Evans, S. H. and Nash, W. P., 1978, Quaternary mafic lavas and ultramafic xenouths from southeastern Arizona (abs): Geological Society of America Abstracts with Programs, Vol. 10, 216 p.

Lynch, D. J., 1978, The San Bernardino volcanic field of southeastern Arizona: *in* Callender, J. F., Wilt, J. C., and Clemons, R. E., eds., Land of Cochise, New Mexico Geological Society, 29th Field Conference Guidebook, p. 261-268.

Lynch, D. J., 1973, Reconnaissance geology of the Bernardino volcanic field, Cochise County, Arizona: unpub. M.S. Thesis, University of Arizona, 101 p.

Menges, C. and Lynch, D. J., 1982, Significance of late Cenozoic fault and volcanic field orientation data in the Basin and Range province of southern Arizona and northern Sonora; unpub. manuscript, 36 p.

Natali, S. G. and Sbar, M. L., 1982, Seismicity in the epicentral region of the 1887 northeastern Sonoran earthquake, Mexico: Bulletin of Seismological Society of America, v. 72, no. 1, p. 181-196.

Ransome, F. L., 1903, Geology of the Globe Copper District, Arizona: U. S. Geological Survey Professional Paper 12, 168 p.

Seager, W. R. and Morgan, P., 1979, Rio Grande Rift in southern New Mexico, West Texas, and northern Chihuahua: *in* Riecker, R. E., Ed., Rio Grande Rift: Tectonics and Magmatism: American Geophysical Union, p. 87-106.

Swanberg, C. A., 1978, Chemistry, origin and potential of geothermal resources in southwestern New Mexico and southeastern Arizona: *in* Callender, J. F., Wilt, J. C., and Clemons, R. E., eds., Land of Cochise, New Mexico Geological Society, 29th Field Conference Guidebook, p. 349-351.

Swanberg, C. A., Morgan, P., Stoyer, C. H., and Witcher, J. C., 1977, An appraisal study of the geothermal resources of Arizona and adjacent areas in New Mexico and Utah and their value for desalination and other uses: New Mexico Energy Institute Report 6, New Mexico State University, 76 p.

Swanberg, C. A., Marvin, P. R., Luis Salazar, S., Gutierrez, Carlos Garcia, 1981, Hot springs, geochemistry, and regional heat flow of northern central Mexico: Geothermal Resources Council Transactions, Vol. 5, p. 141-144.

Sumner, J. R., 1977, The Sonoran earthquake of 1887: Bulletin Seismological Society of America, Vol. 67, p. 1219-1223.

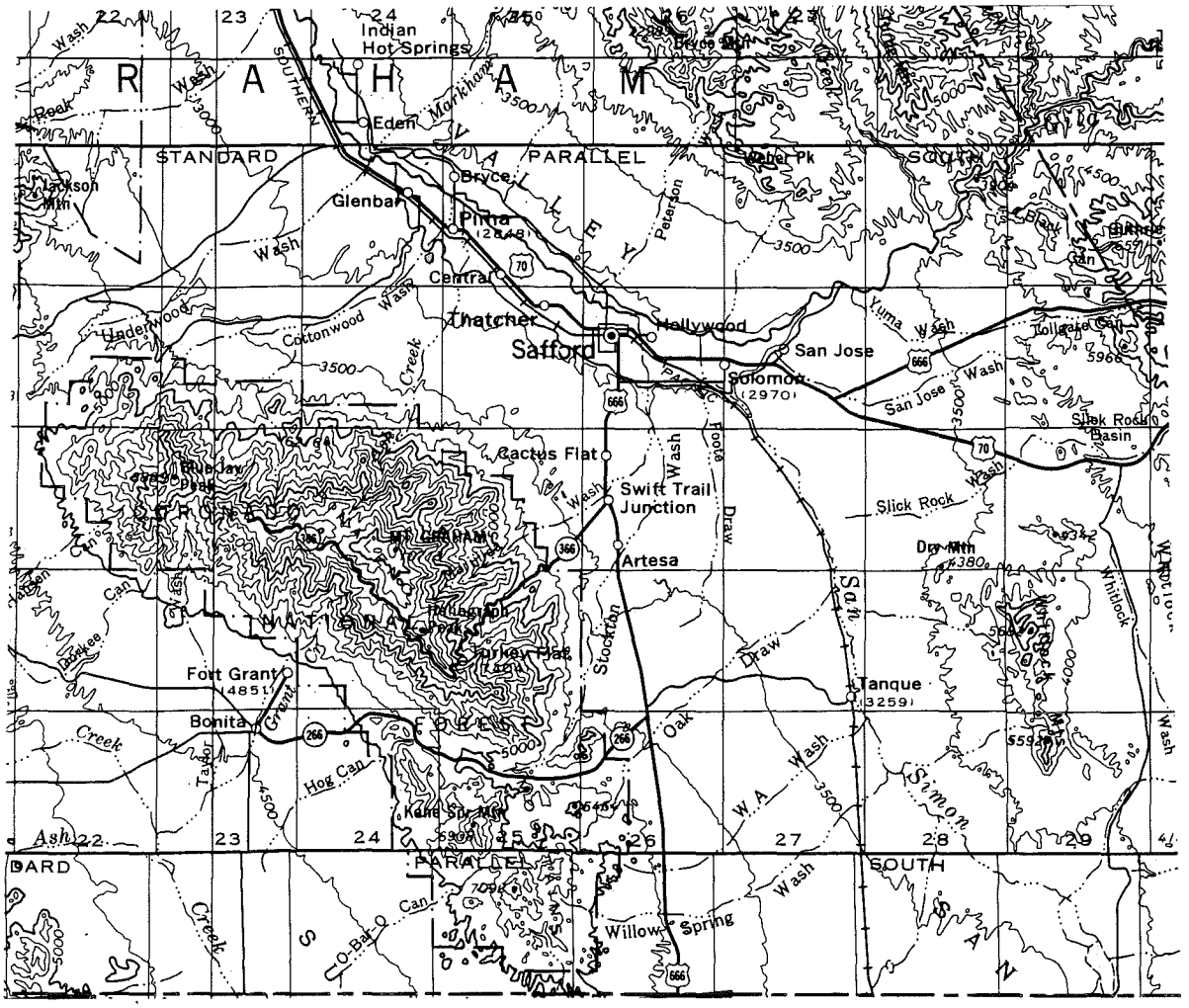

Figure 2.46. Physiographic map of Gila Valley from Safford north to Indian Hot Springs and of San Simon Valley from Safford south to Willow Spring Wash

GILA VALLEY FROM SAFFORD TO INDIAN HOT SPRINGS

INTRODUCTION. Indian Hot Springs, 26 km northwest of Safford is notable because it has been the site of a spa and resort at various times during the past 50 years (Fig. 2.46). Several deep (>500 m) wells have been drilled in the Gila Valley which have artesian flows of hot water (>40°C). The 1929 Underwriters Syndicate 1 Mack oil and gas test or "Mary Mack well" is the hottest of these wells, with a reported discharge temperature of 59°C (Knechtel, 1938). This well, near the town of Pima, is no longer flowing; we believe water pressure broke through the deteriorated casing after the well was temporarily shut in several years ago. The Smithville Canal well, near the town of Thatcher, produces 46°C water and was formerly used by the Mount Graham Mineral Bath before this spa was destroyed by flooding of the Gila River in the winter of 1977-78. Today, this well flows freely into the Gila River.

PHYSIOGRAPHY. The Gila River has entrenched into the sediments that fill the northwestern Safford-San Simon Basin, and has formed a northwest-trending flat-bottomed valley or flood plain 5 to 8 km wide (Fig. 2.46). Elevation of the flood plain ranges from about 884 m at Safford to 823 m at Fort Thomas, 5 km northwest of Indian Hot Springs. Paired terraces 20 to 30 m high flank the Gila River flood plain. Above the terraces, a 10 to 20 km wide piedmont slopes gently upward toward the Pinaleno Mountains on the south and the Gila Mountains on the north. Relief of the Pinaleno Mountains above the piedmont exceeds 2,200 m, while the Gila

Mountains rise 1,000 m above the valley floor. Normal precipitation in the Gila Valley is less than 25 cm/yr, but exceeds 75 cm/yr in the Pinaleno Mountains. The fertile flood plan is irrigated for crops of cotton, alfalfa, corn, and other grains. Many farms in the valley raise hogs for slaughter. Above the flood plain on the piedmont surface, cattle ranches are the major land use.

GEOLOGY. The Gila Valley between Indian Hot Springs and Safford overlies a segment of the northwestern Safford-San Simon basin, a deep sediment-filled, Basin and Range, composite graben bounded by major horsts that form the Pinaleno Mountains to the south and the Gila Mountains to the north.

The Pinaleno Mountains expose a mid-Tertiary metamorphic core complex of mostly gneiss and mylonitic gneiss (Davis and Coney, 1979; Thorman, 1981). On the opposite side of the basin, mid-Tertiary basaltic to latitic volcanic flows unconformably overlie Laramide andesitic to rhyolitic flows, breccias, and stocks.

Sediments filling the Safford-San Simon basin were broken into two major units by Harbour (1966). The upper basin fill unit, consisting of predominately coarse-grained clastic sediments, is separated from lower basin fill by a time-stratigraphic horizon that marks a change in sedimentation processes and by a Pliocene to Quaternary faunal transition (Harbour, 1966).

Near Indian Hot Springs, the lower basin fill consists of four facies. At Safford, it is formed by three facies (Fig. 2.47). The basal strata of the lower basin fill is the conglomerate facies, a sequence of interbedded clay, sand, and conglomerate. Near Indian Hot Springs, a red facies

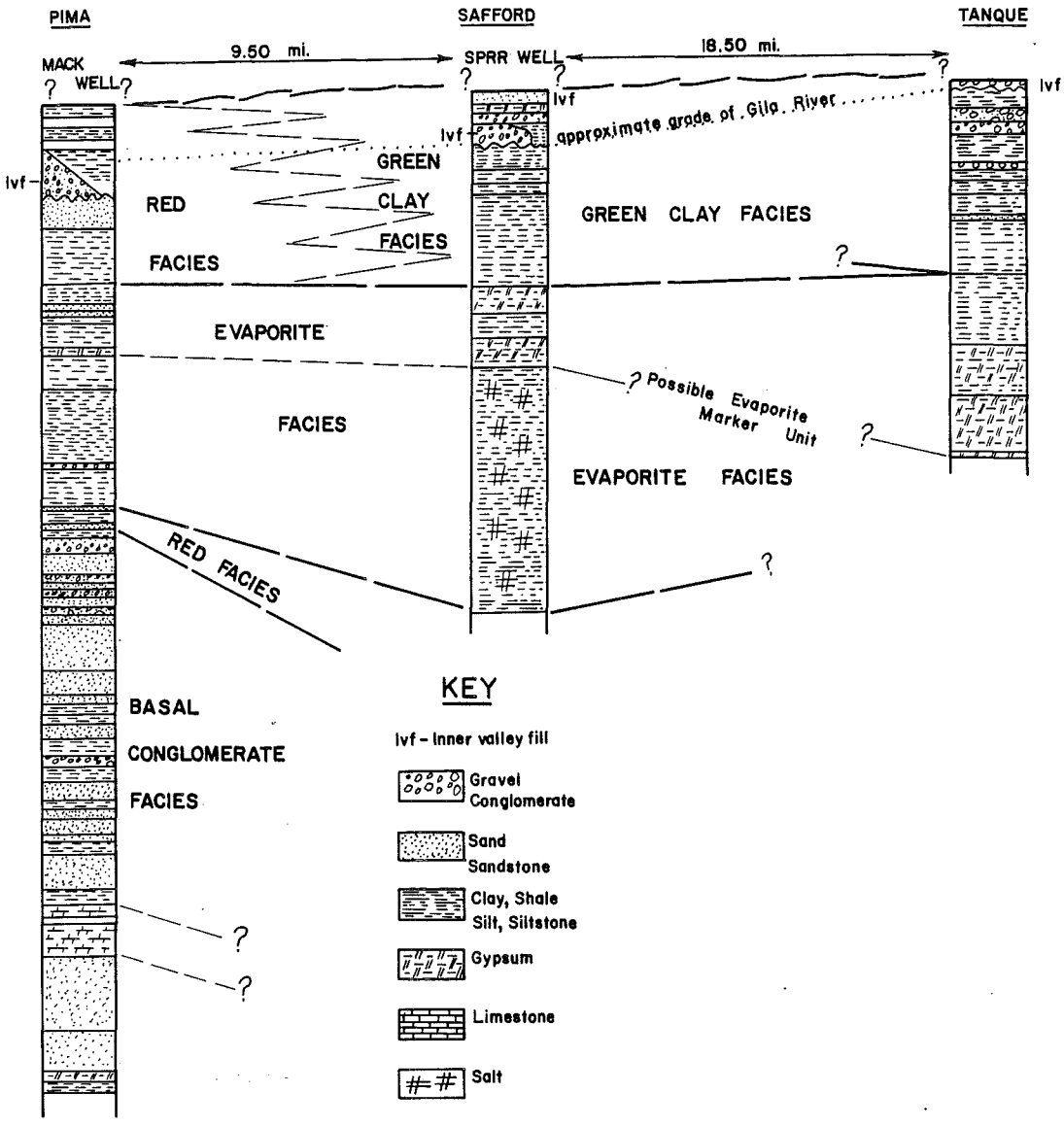

Figure 2.47. Basin-fill stratigraphy in the Safford basin (after Muller and others, 1973)

consisting of red to brown sand and silt intertongues with a clay-silt facies. Both overlie the basal conglomerate except on basin margins where the red facies and the clay-silt facies pinch out into the conglomerate. At Safford, the clay and silt are interbedded with an evaporite facies. This evaporite sequence consists of gypsiferous clay, gypsum, anhydrite, and minor halite beds.

The conglomerate facies is important because it is permeable and it acts as a thermal artesian aquifer. Clay and silt, capping the conglomerate, have low thermal conductivity, which results in high temperature gradients (40 to 50°C/km). Also, the basal conglomerate facies probably is hydrologically connected with upper basin-fill sands and gravels at recharge zones along the basin margin. Such geohydrologic conditions may account for the artesian pressure in the basal conglomerate.

Bouguer gravity data indicate that the thickness of basin fill between Safford and Indian Hot Springs may exceed 2 km. The Underwriters Syndicate 1 Mack well near Pima failed to reach bedrock at 1,148 m depth. This hole bottomed in coarse sediments of the basal conglomerate facies of Harbour (1966).

GEOHYDROLOGY. Ground water occurs under two distinct conditions in the Gila Valley. The shallowest ground water is nonthermal and it forms the water table in the alluvial flood plain sediments in the valley. Deep artesian water is encountered below the clay and silt. This water is thermal and has a variable piezometric surface in any one location due to the presence of several confined aquifers with different hydraulic head. The Mary Mack well near Pima encountered five such stacked aquifers (Knechtel, 1938).

THERMAL SPRINGS AND WELLS. Indian Hot Springs, discharge 45 to 48°C water from basin fill on the first major terrace north of the Gila River. Travertine (calcium carbonate) cements terrace gravels near many spring orifices. Total flow rate of five springs is approximately 1,000 L/min (Mariner and others, 1977). Minor amounts of gas, mainly nitrogen, evolve at the spring orifices (Mariner and others, 1977). Thermal springs that evolve nitrogen gas are generally associated with low temperature geothermal systems (Ellis and Mahon, 1977).

Indian Hot Springs have a sodium chloride composition, with TDS between 2,510 and 3,004 mg/L (Table 2.6). This thermal water has sulfate content up to 15 milliequivalent percent total anions, which suggests the water has had contact with gypsum or gypsiferous sediments. Fluoride content of Indian Hot Springs ranges from 2.8 to 4.8 mg/L.

An artesian well drilled to 183 m at the springs in 1933 was reported to discharge 48.3°C water at a rate of 156 gpm (Knechtel, 1938). An estimated temperature gradient of about 165°C/km indicates this well intersected a zone of upward-flowing water. This same zone probably contributes to spring flow.

Direct evidence for structural control for Indian Hot Springs is lacking due to the cover of colluvium and travertine cemented terrace gravels. However, a known fault zone is inferred to allow vertical passage of thermal water to the springs. Projection of the north-northwest striking Pleistocene faults west of the Cactus Flat-Artesia area into Indian Hot Springs is possible because the Gila River changes course in conformance with such a fault zone. Also, Muller (1973) reported high salinity in shallow wells downstream from the inferred fault trace and "dog leg" in the river course.

An additional fault, oriented west-northwest, may also cross Indian Hot Springs. This fault zone is inferred from an alignment of springs (Fig. 2.48). At Big Spring, section 25, T. 6 S., R. 25 E., deformed and laminated clay (clay-silt facies) is angularly overlain by terrace gravel in arroyo walls. Mud intrusions are seen in the shears and faults. This deformation may be evidence of a major fault zone that controls the apparent spring alignment.

Deep artesian wells in the valley discharge sodium chloride water (Table 2.6) with cation and anion ratios similar to Indian Hot Springs. Deepest of the wells, the Mary Mack, produced 2,250 gpm of sodium chloride water, with a TDS of 3,530 mg/L (Knechtel, 1938). Thermal water in this hole came from five water-producing zones below 495 m depth.

The Smithville Canal well, drilled in 1957 to 659 m depth (Files, USGS, Tucson), produces sodium chloride water with TDS of 7,950 mg/L. Lithology in this well comprises mudstone to 312 m depth; gypsum, gypsi-

TABLE 2.6. Chemistry of thermal waters in the Gila Valley

Number	Sample	Location	Temperature	TDS	pH	Na	Na+K	K	Ca	Mg	Cl	SO_4	HCO_3+CO_3	SiO_2	Li	B	F	Remarks
1	57	D-6-25-36CBBB	46	4431	6.8	1390		13.1	64	7.6	4011	672	64	55	2.3	0.6	6.7	W
2	53W80	D-5-24-17ADDCA	46	2967	7.5	670		13	39	7.2	1430	365	69	45	1.41	1.64	2.8	S
3	54W80	D-5-24-17ADDDB	45	2929	7.5	540		14	38	7.1	1414	348	98	48	1.42	0.94	5.2	S
4	55W80	D-5-24-17ADDBB	47		7.5	610		14	38	8.0	1257	325	120	49	1.25	1.64	4.0	S
5	1817	D-5-24-17AD	47.8	2570	-	879			78	9.6	1195	348	105	-	-	2.0	3.9	S
6	1818	D-5-24-17AD	40	2970	-	1027			83	11	1400	395	106	-	-	0.8	4.8	S
7	1822	D-5-24-17AD	47.8	2970	-	1023			81	14	1400	402	101	-	-	-	3.4	S
8	1823	D-5-24-17AD	47.8	2960	-	1026			80	12	1400	393	100	-	-	0.8	4.6	S
9	2600	D-6-24-13AB	58.9	3530	-	1220			74	8.7	1660	416	101	-	-	7.0	6.0	W
10	2683	D-7-24-17BD	30.0	2740	-	739			226	33	1250	426	116	-	-	8.0	1.4	W
11	AZ10	D-5-24-17A	47	2672	7.9	837		13.6	80	9.0	1196	323	107	44	1.30	0.58	3.4	S
12	AZ11	D-5-24-17A	46.5	3004	7.9	1023		12.9	93	10.3	1382	361	101	44	-	0.70	3.8	S
13	AZ14	D-6-25-36C	43.5	8292	7.9	3027		10.9	135	7.9	4517	787	81	56	2.77	1.65	7.2	W
14	AZ21	D-5-24-17AD	33	3048	7.5	921		12.9	81	8.0	1412	338	109	57	-	0.84	3.9	S
15	AZ155	D-7-25-7CCC	29.5	9288	8.1	3072		14.5	133	28	3956	1455	46	27.5	4.05	2.33	6.27	W
16	AZ156	D-7-24-14DD	25.5	1804	8.3	709		2.7	9.2	0.7	688	452	107	27.0	-	1.62	7.8	W

W = well; S = spring

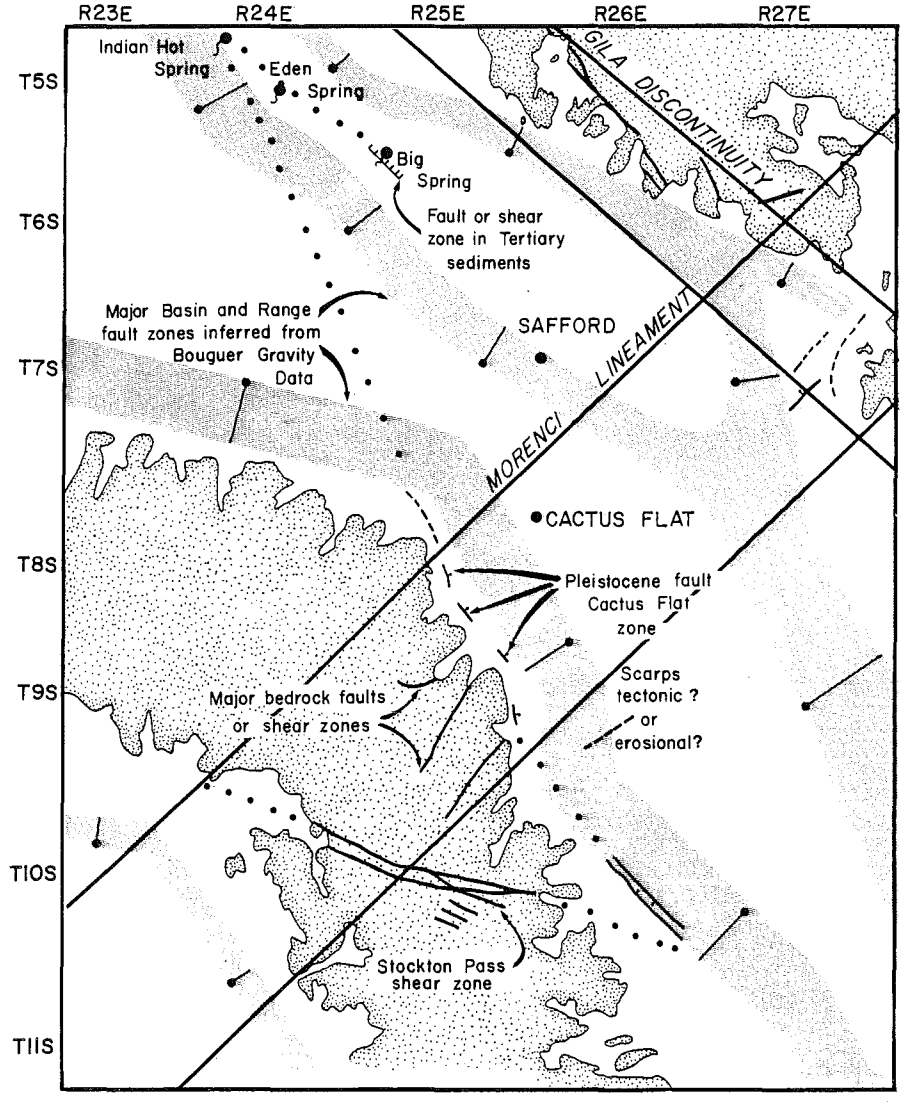

Figure 2.48. Major lineaments, faults, and spring alignments in the Safford area

ferous silt, and clay between 312 and 488 m; and "volcanic" sand below 488 m (Files, USGS, Tucson).

Use of the Na-K-Ca geothermometer is not valid given the qualifying assumptions required for its use because these waters apparently have dissolved highly soluble evaporite minerals and are probably in tempera-

ture-chemical disequilibrium. Silica concentrations in Indian Hot Springs are in equilibrium with α-cristobalite, while water from the Smithville Canal well is supersaturated with respect to all solid silica species except opal. The α-cristobalite geothermometer for this water ranges between 56 and 64°C.

CONCLUSIONS. An extensive low-temperature (40 to 70°C) geothermal resource is indicated in the Gila Valley northwest of Safford at Indian Hot Springs and in the area of the deep thermal wells. Water produced by the springs and the wells is apparently from the same source(s) because they have similar chemistry and temperatures. Thermal wells north of Safford produce thermal water from below 480 m depth. However, close to Safford the reservoir is either at a depth greater than 500 m or is non-existent. An abandoned Southern Pacific well at Safford bottomed in gypsiferous clay at 555 m. Another nearby dry well, D-7-26-26aba, reached a total depth of 689 m in salty clay. A Schlumberger resistivity sounding south of Safford and centered over the north boundary of section 2, T. 8 S.,

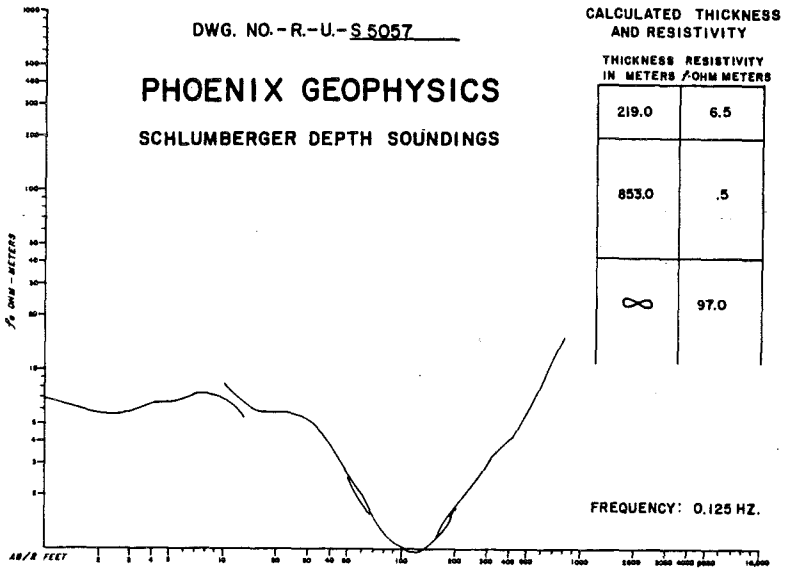

Figure 2.49. Schlumberger resistivity sounding

R. 26 E., was modeled as a three-layered earth (Phoenix Geophysics, 1979) (Fig. 2.49). This model shows a 1,072 m thickness of low resistivity (<6.5 ohm-meters) clay, silt, and evaporites or sand and gravel containing hot salty water. Below 1,072 m the resistance is higher, possibly indicative of highly cemented sand and gravel deposits or volcanic rocks.

Figure 2.50 is a map derived from dipole-dipole resistivity profiling which shows the approximate extent of gypsiferous clay and salty clay. Wells drilled in the evaporite (low resistivity) zone are likely to encounter water with TDS exceeding 3,000 mg/L. Localized aquifers in these zones may contain brine.

REFERENCES GILA VALLEY FROM SAFFORD TO INDIAN HOT SPRINGS

Davis, G. H. and Coney, P. J., 1979, Geologic development of the Cordilleran metamorphic core complexes: Geology, Vol. 7, p. 120-124.

Ellis, A. J. and Mahon, W. A. J., 1977, Chemistry and Geothermal Systems: Academic Press, New York, 392 p.

Harbour, J., 1966, Stratigraphy and sedimentology of the upper Safford basin sediments: unpub. Ph.D. Thesis, University of Arizona, 242 p.

Knechtel, M. M., 1938, Geology and ground-water resources of the valley of the Gila River and San Simon Creek, Graham County, Arizona: U. S. Geological Survey Water-Supply Paper 796, p. 222.

Mariner, R. H., Presser, D. D., and Evans, W. C., 1977, Chemical, isotopic, and gas compositions of selected thermal springs in Arizona, New Mexico, and Utah: U. S. Geological Survey Open File Report 77-654, 42 p.

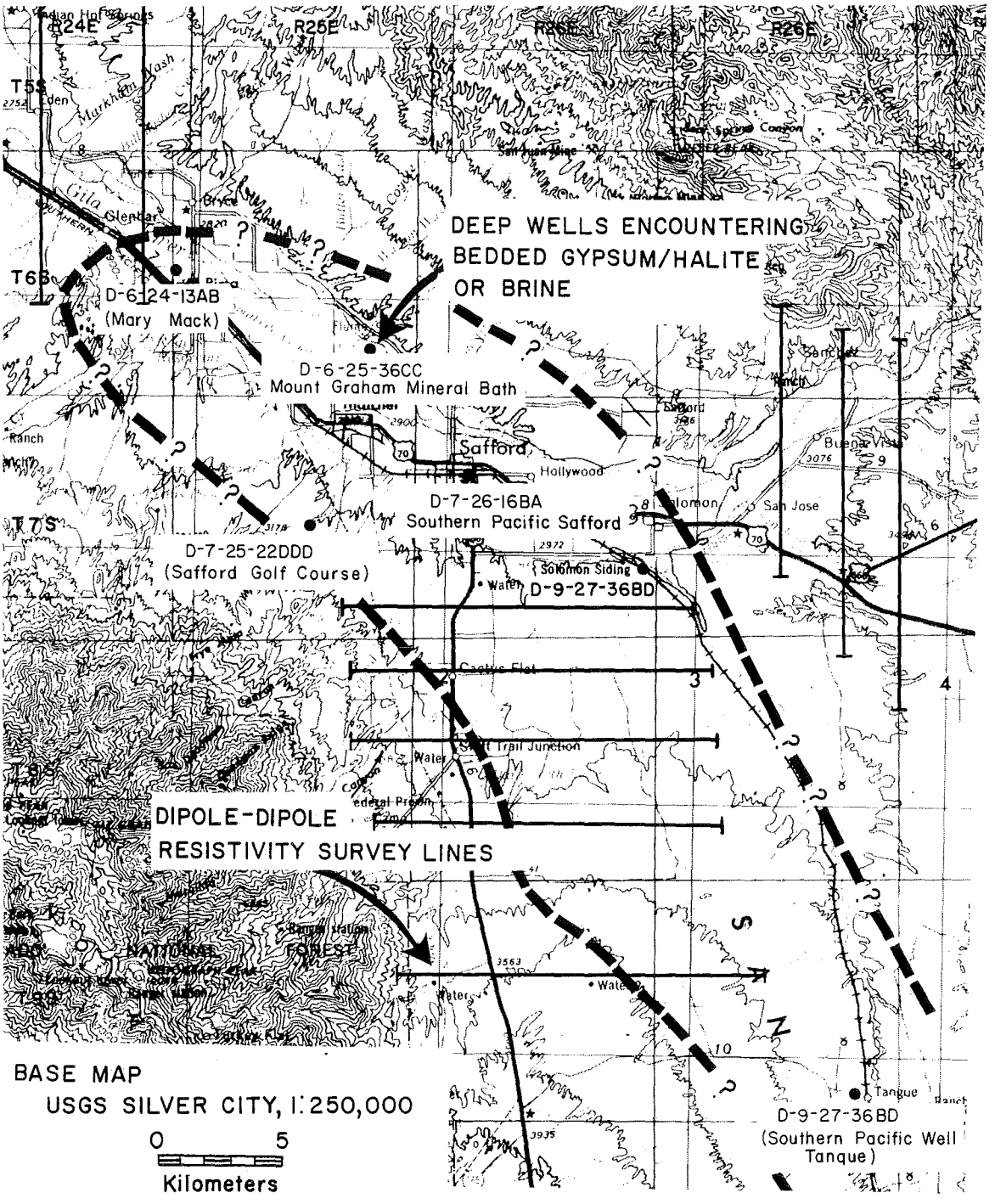

Figure 2.50. Map showing extent of evaporite deposits in basin fill or the Safford area

Muller, A. B., Battaile, J. F., Bond, L. A., and Lamson, P. W., 1973, An analysis of the water quality problems of the Safford Valley, Arizona: Technical Report No. 15, Department of Hydrology and Water Resources, University of Arizona, 126 p.

Phoenix Geophysics, Inc., 1979, Report on the reconnaissance resistivity and VLF-EM surveys of the Safford Valley area, Graham county, Arizona: Arizona Bureau of Geology and Mineral Technology Open File Report 81-23.

Thorman, C. H., 1981, Geology of the Pinaleno Mountains, Arizona a preliminary report: *in* Stone, C. and Jenney, J. P., eds., Arizona Geological Society Digest, Vol. 13, p. 5-11.

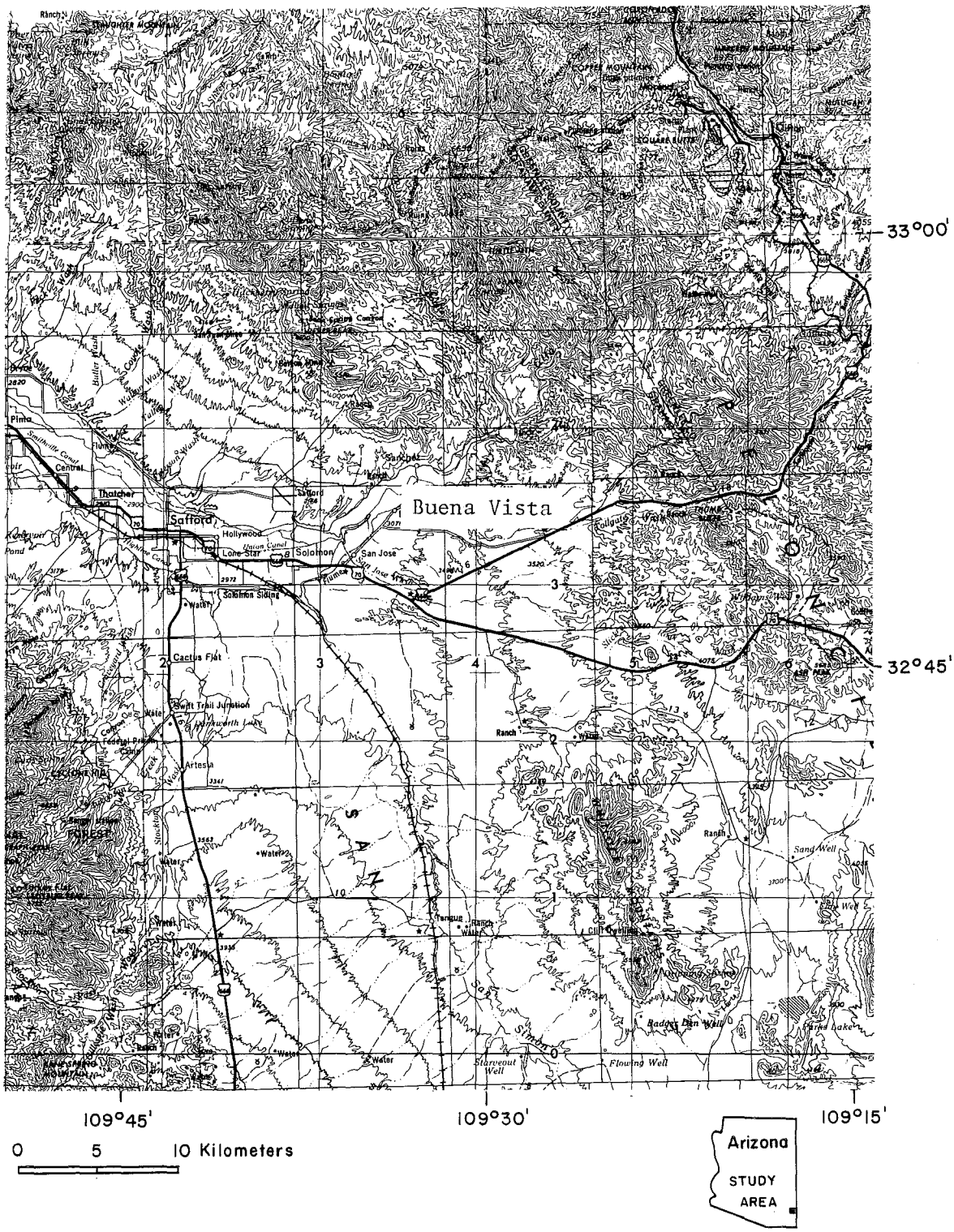

Figure 2.51. Physiographic map of the Buena Vista area

BUENA VISTA AREA

INTRODUCTION. Eight irrigation wells, less than 213 m deep discharge unusually warm water (30 to 49°C) in the Buena Vista area. The hottest of these wells, when it is not pumped, discharges an artesian flow of 49°C water. A state-of-Arizona correctional facility is located about 1.5 km south of this thermal well.

Agriculture is the main industry in the area; however, deposits of copper are known in the Gila Mountains north of the area and they may be economic to mine in the future. Direct-heat geothermal energy may be used in all these endeavors.

PHYSIOGRAPHY. The Buena Vista area, southeastern Arizona, is located on the northeast margin of the Safford-San Simon Basin on the Gila River plain at an elevation of 914 m. West of this area, the flood plain widens and curves northwest to form a flat-bottomed valley 5 to 8 km across (Fig. 2.51). Eastward, the flood plain narrows into the northeast trending Gila Box, a canyon formed by the Gila River between the Gila and Peloncillo Mountains. The Gila River flood plain is bound by steep terrace escarpments between 20 and 30 m high, while beyond the escarpments the surface of the Safford-San Simon basin slopes upward toward surrounding mountains: the Gila Mountains on the north, the Pinaleno Mountains to the southwest, and eastward, the Peloncillo Mountains. The Gila and Peloncillo Mountains range from 1,524 to 2,133 m in elevation, while the Pinaleno Mountains rise to about

3,261 m. Annual precipitation is less than 25 cm/yr at Buena Vista; however, precipitation in nearby mountains exceeds 38 cm/yr.

GEOLOGY. Bouguer gravity data and drill logs show the Buena Vista area overlies a sediment-covered structural bench that separates the Safford-San Simon basin to the southwest from the Gila Mountains on the northeast side of the basin (Witcher, 1981). These features are major structures that were formed by high-angle normal faults associated with the Basin and Range disturbance (15 to 8 m.y. ago) of Scarborough and Peirce (1978). The triangular structural bench underlying this area is bounded by major Basin and Range fault zones on its northern, southwestern, and eastern margins. Approximately 213 m of basin-filling sediments overlie basement rocks that comprise the bench (Witcher, 1981).

Major regional lineaments intersect in this area. The Morenci lineament (Chapin and others, 1978) crosses from the northeast and intersects the northwest striking Gila discontinuity of Titley (1976). Regionally, these lineaments are directionally coincident with anisotropic structure developed in Precambrian rocks (Titley, 1976; Silver, 1978; Swan, 1982). The west-northwest grain is dominant and it is superimposed on the older northeast grain (Swan, 1982; Silver, 1978). The Gila discontinuity or west-northwest grain is evident in the Gila Mountain escarpment and in the alignment of Laramide copper deposits in the Gila and Peloncillo Mountains (Titley, 1976). Northeast-oriented fracturing and shearing is pervasive in much of the Laramide volcanic terrane, especially near copper mineralization (Dunn, 1978; Robinson and Cook, 1966).

Laramide volcanic rocks (53 to 58 m.y.) in the Gila Mountains consist of andesite and felsic tuff that are intruded by small silicic to

intermediate Laramide stocks (Dunn, 1978; Robinson and Cook, 1966; Livingston and others, 1968). Drill holes up to 1,220 m deep have failed to reach the base of these rocks. Part of the andesite may be a hypabyssal intrusion based upon an apparent gradational contact with diorite intrusions and lack of flow or bedding structure (Dunn, 1978). Xenoliths of quartzite are observed in the andesite and they may be Precambrian Pinal Schist or Cambrian-Ordovician Coronado Sandstone. Because this area lies on the northern part of the Mesozoic Mogollon Highland or Burro uplift, Paleozoic rocks are probably thin or mostly absent beneath the Laramide volcanic-intrusive sequence.

Reddish-brown amygdaloidal basaltic andesite ranging from 30 to 27 m.y. old (K-Ar) unconformably overlies the Laramide volcanic rocks (Strangway and others, 1976). Flows are one to two meters thick and flow breccias are common. A large latite dome complex in the Bryce Mountain and Weber Peak area overlies the basal mid-Tertiary basaltic andesite. In many areas the latite is extensively brecciated. The youngest mid-Tertiary volcanic rocks in the Gila Mountains consist of dark gray and massive basaltic andesite flows two to five meters thick. Contemporaneous with younger basaltic volcanism another center of silicic volcanism erupted in Tolgate Canyon of the northern Peloncillo Mountains east of Buena Vista. Overall, the mid-Tertiary volcanic sequence in the Gila and Peloncillo Mountains dips gently northeast. It ranges between 600 and 1,200 m thick.

Clastic basin-fill sediments overlie mid-Tertiary and Laramide volcanic rocks that form the structural bench beneath Buena Vista. Well D-6-27-35cbb penetrated gravels containing "red" granite clasts (Morenci Granite?) to a depth of 211 m; between 211 and 275 m, volcanic and

volcanoclastic sediments overlie epidotized andesite containing copper mineralization (Files, USGS, Tucson). Figure 2.52 shows the lithology of the basin fill as it is interpreted from drillers' logs of thermal wells (Witcher, 1981). Gravel and sand with clay lenses provide an aquifer for thermal water produced by these wells. Clay, silt, and sandy clay with gravel lenses confine the underlying aquifer. At Sanchez Monument the base of the clay and silt is 105 m deep while near the Gila River, northeast of the Monument the clay and silt pinch out. At that point the base is less than 45 m deep. Pleistocene to Recent flood plain deposits, less than 30 m thick overlie the clay and silt deposits. The clay and silt probably grade into the green clay facies of Harbour (1966) in the Safford-San Simon basin to the west.

South and east of Buena Vista several scarps are observed in Quaternary alluvial deposits (Fig. 2.53). At least one of these scarps is a possible fault scarp based upon the absence of terrace gravel above or below it and the presence of similar soil stratigraphy on both sides of it. However, terraces cut by the ancestral Gila River are probable explanations for most of these scarps. Several large benches north of Buena Vista, which are capped by fluvial gravels containing well-rounded clasts of Morenci Granite, are terraces cut by the ancestral Gila River.

GEOHYDROLOGY. Flood plain deposits of the Gila River contain shallow unconfined ground water. Other ground water found in the area is confined and is under artesian pressure. The artesian water is found beneath fine grained basin-fill deposits in sand and gravel. Thermal water encountered by local wells occurs in the confined aquifers. At least three of the thermal wells flow freely during winter months (Witcher, 1981).

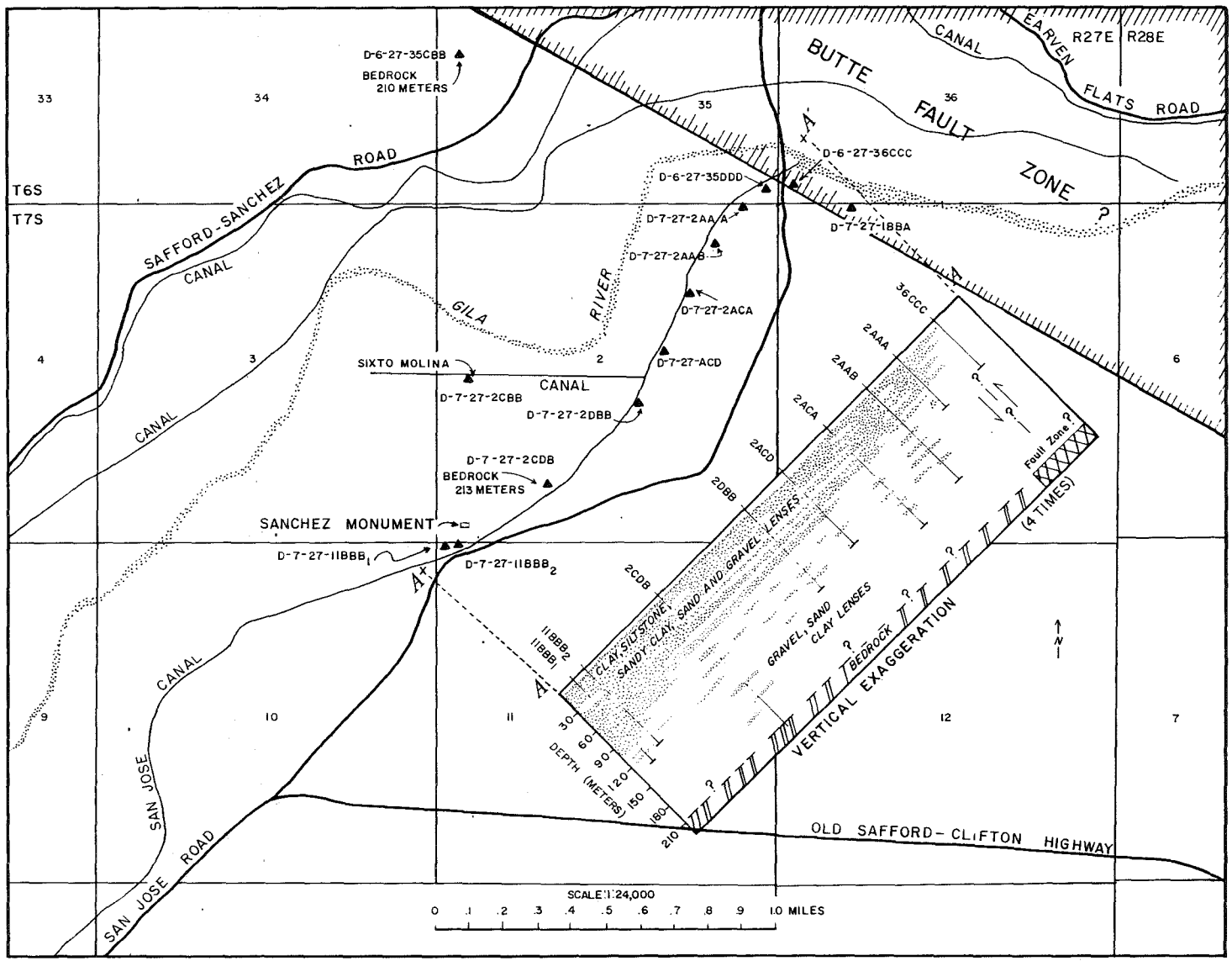

Figure 2.52. Subsurface geology of the Buena Vista area

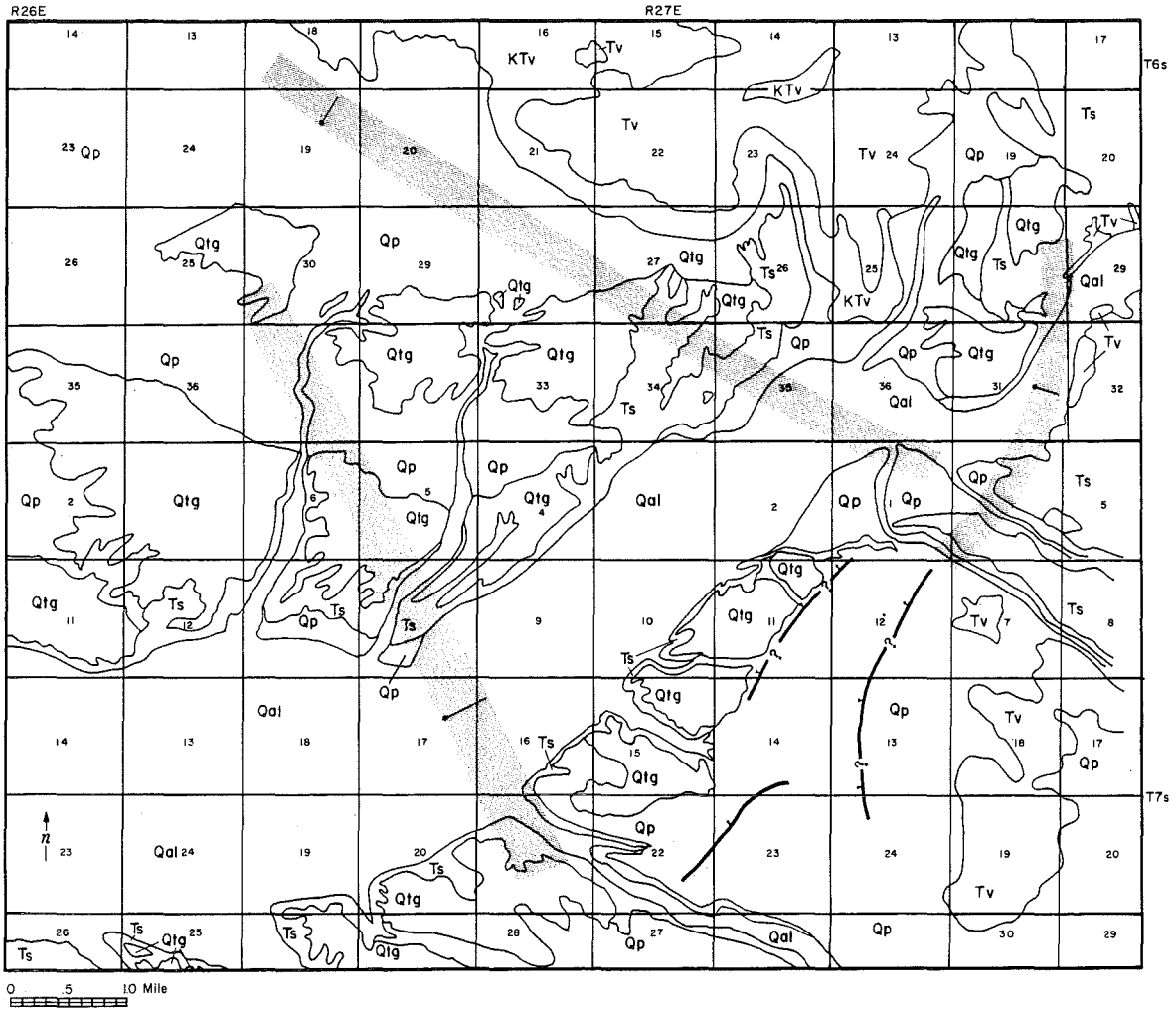

EXPLANATION

Qal	RECENT GILA RIVER DEPOSITS AND ARROYO DEPOSITS
Qp	PLEISTOCENE TO RECENT PEDIMENT, ALLUVIAL FAN AND SLOPE DEPOSITS
Qtg	MID TO LATE PLEISTOCENE ANCESTRAL GILA RIVER TERRANCE DEPOSITS
Ts	MID MIOCENE TO EARLY PLEISTOCENE BASIN FILL SEDIMENTS
Tv	TERTIARY BASALTIC VOLCANIC ROCKS
KTv	LATE CRETACEOUS-PALEOCENE (LARAMIDE) INTERMEDIATE VOLCANIC AND INTRUSIVE ROCKS

SCARP IN Qp SEDIMENTS AS DELINEATED FROM BLACK AND WHITE AERIAL PHOTOGRAPHS. TECTONIC ORIGIN IS ONLY RIVER TERRACING.

INFERRED BURIED "BASIN AND RANGE" FAULT ZONE BASED UPON LITHOLOGIC DISCONTINUITY AND BOUGUER GRAVITY DATA. LOCATIONS ONLY APPROXIMATE. BALL ON DOWN THROWN DIRECTION.

Figure 2.53. General geology of the Buena Vista area

THERMAL WELLS. Thermal waters (30 to 49°C) (Fig. 2.54) in the Buena Vista area have a chemistry distinct from local nonthermal water. The thermal water has calcium concentrations less than 20 mg/L, magnesium concentrations less than 8 mg/L, and high fluoride concentrations (>4.0 mg/L) (Witcher, 1981). Fluoride concentrations up to 14.0 mg/L are reported in the thermal water (Table 2.7). Nonthermal water has high calcium (>20 mg/L), high magnesium (>8.0 mg/L) and low fluoride (<4.0 mg/L). The thermal water has sodium chloride-sulfate chemistry with total dissolved solids less than 1,200 mg/L.

Figure 2.55 is a map of fluoride distribution for water from thermal and nonthermal wells. Fluoride concentration decreases northward and westward from the area that has the highest temperature wells. The fluoride anomaly is open on the east, mostly due to low data density, but additional high fluoride thermal water is likely to be found eastward in sections 11 and 12, T. 7 S., R. 27 E.

Quartz and Na-K-Ca geothermometers were calculated for the highest temperature (49°C) well (D-7-27-11bbb). The quartz and the Na-K-Ca geothermometers are 112 and 114°C, respectively.

Wells encountering thermal water are all less than 215 m deep. Three wells have artesian flow that exceeds 100 gpm. Pumped flow rates reported by the U.S. Geological Survey range between 900 and 1,600 gpm (Files, USGS, Tucson).

THERMAL REGIME. Background heat flow for the area is about 80 mWm^{-2}, which is the approximate average value obtained in heat-flow studies of several deep (>300 m) mineral exploration drill holes in the Gila Mountains (Reiter and Shearer, 1979). Reiter and Shearer (1979) also reported

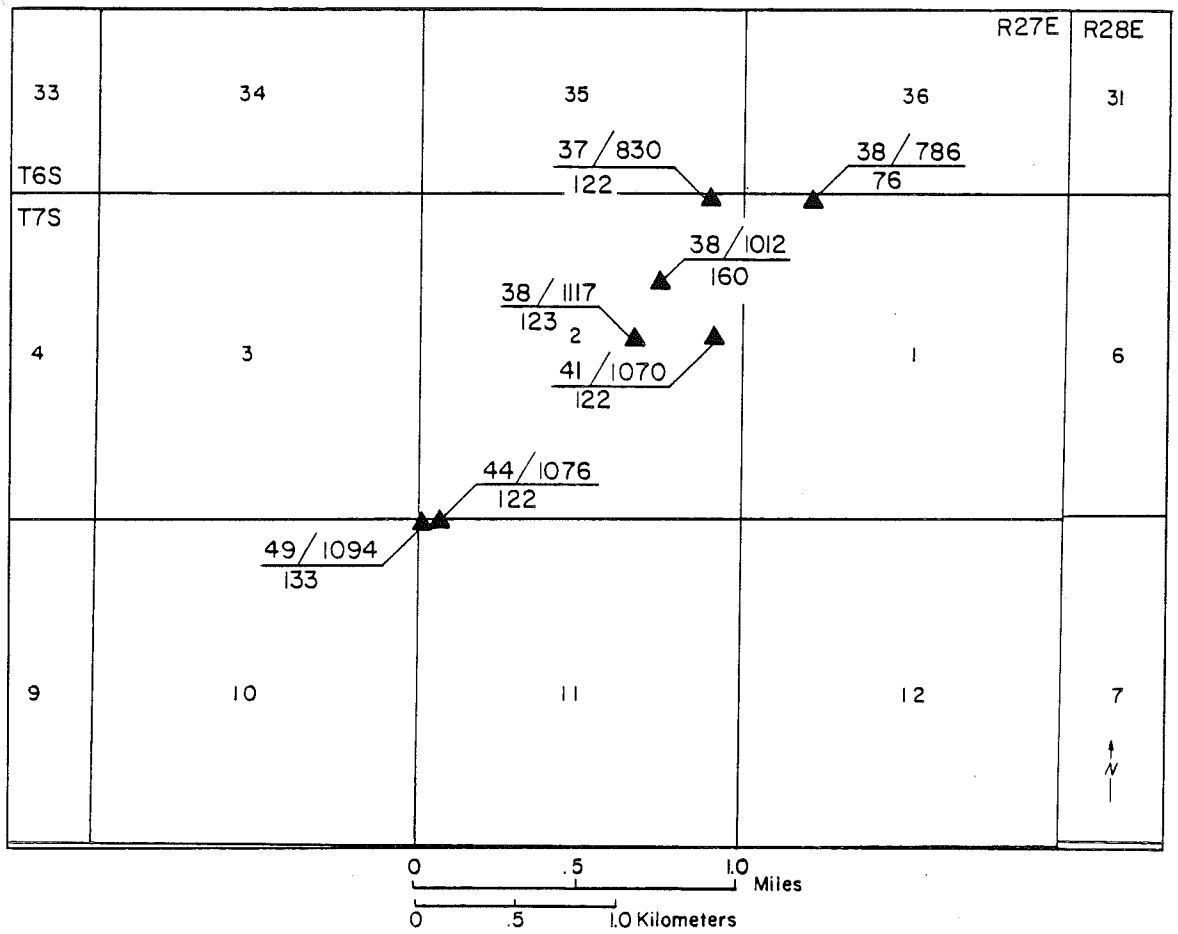

Figure 2.54. Selected thermal wells in the Buena Vista area

TABLE 2.7. Chemistry of selected wells in the Buena Vista area

Sample	Location	Temperature	TDS	pH	Na	K	Na+K	Ca	Mg	Cl	SO_4	HCO_3+CO_3	SiO_2	Li	B	F
3548	D-7-27-10AAD	—	792	7.7	163	—		69	15	218	70	244	—	—	—	1.0
58	D-7-27-11BBB	49	1094	7.5	333	3.9		1	0.1	212	272	205	62	0.4	<.1	10.2
59	D-7-27-2ACB	38	1117	7.3	360	3.5		1	0.4	249	265	195	61	0.4	<.1	8.6
74	D-6-27-35DDDD	27	894	7.4	284	2.9		1	0.4	232	120	202	52	0.3	0.3	6.9
17W80	D-7-27-2AADC	36	826	8.6	52	4.5		19.6	2.6	189	24	122	28	0.2	<.01	4.8
18W80	D-7-27-11BBBB	46	1011	7.9	60	1.0		4.5	0.1	201	190	124	31	0.1	<.01	4.1
19W80	D-7-27-2ADBB	40	961	7.6	61	0.8		12.4	0.4	210	111	134	27	0.1	<.01	7.0
30W80	D-7-27-2ADDCB	39	1055	8.3	321	3.8		0.6	0.2	195	180	186	63	0.4	—	13
8307	D-7-27-7	46.1	—	8.6	368	4.7		7	2	256	270	239	65	0.2	0.46	9.0
927	D-7-27-2CC	35.6	1029	—	369			9.5	6.6	230	275	259	—	—	—	11
AZ15	D-7-27-11BBB	43.5	1076	8.5	331	4.3		7.4	1.3	203	296	246	67	0.36	0.43	10.6
AZ16	D-7-27-2ACA	37.5	1012	8.4	358	3.9		6.2	1.0	168	227	259	67	—	0.46	10.2
—	D-7-27-2ADD	41.0	—	—	360	4.3		4.3	0.9	240	250	255	65	—	0.49	14.0

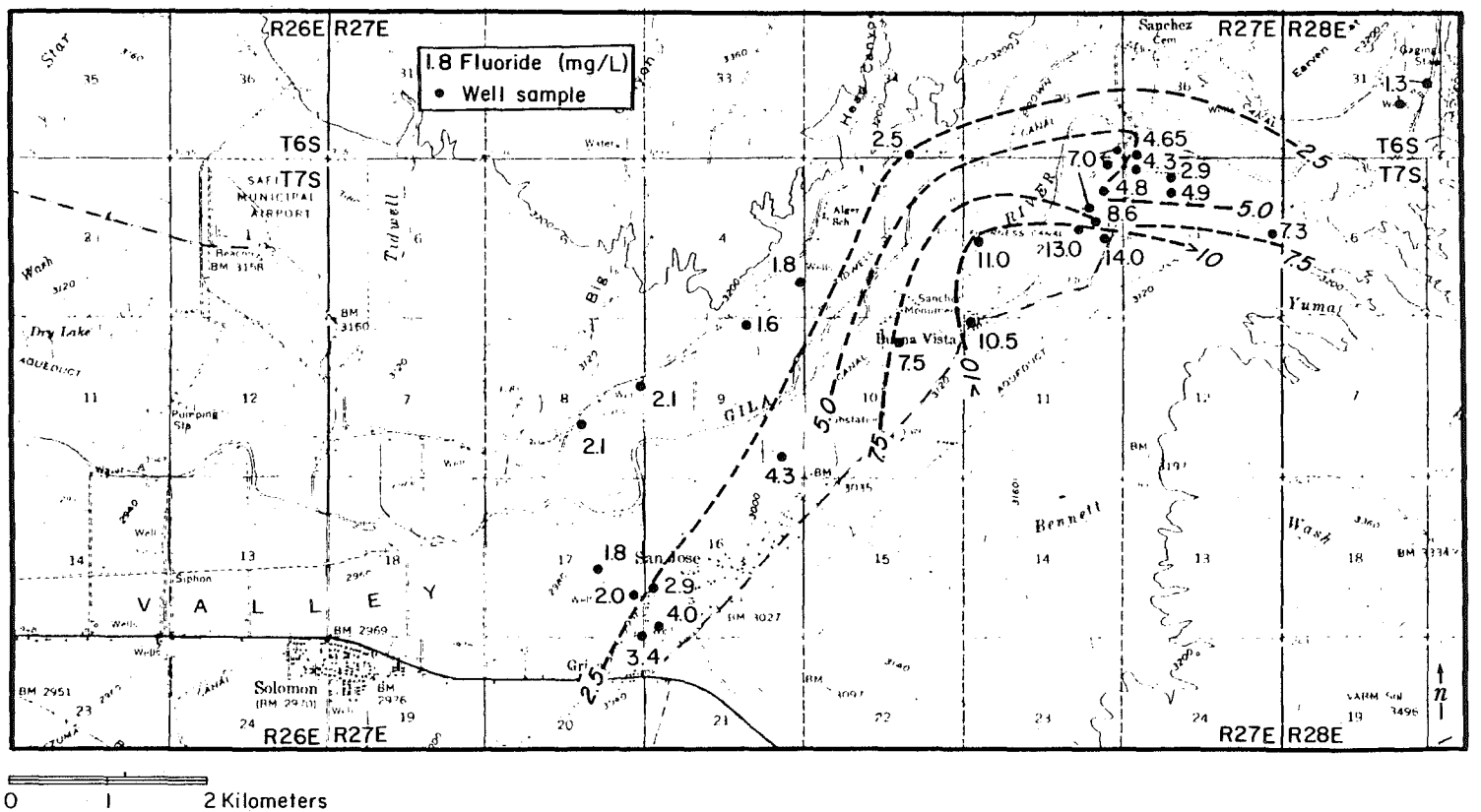

Figure 2.55. Map of fluoride distribution in the Buena Vista area

results of measurements in a deep well 5 km east of Buena Vista. A heat flow of 209 mWm^{-2} was measured for the 300 to 500 m interval; 50 mWm^{-2} was determined for the 950 to 1,050 m interval. A temperature versus depth profile of this well (Fig. 2.56) shows a temperature inversion below 500 m, which is consistent with the heat flow data. Apparently, this hole encountered a horizontal flow of thermal water (70°C) at about 600 m in Laramide volcanic rocks. A hydrothermal convection system near the well is indicated by this temperature log (Reiter and Shearer, 1979; Ziago and Blackwell, 1981). These data imply that the thermal anomaly at Buena Vista is more extensive and hotter than is apparent from measured temperatures and known locations of thermal irrigation wells.

CONCLUSION. A shallow geothermal resource 30 to 50°C is found in a basin-fill reservoir of sand and gravel to 215 m depth beneath Buena Vista. Top of the reservoir is formed by a confining clay and silt unit whose base ranges from 105 m depth at Sanchez Monument to less than 46 m depth northeast of the Monument near the Gila River. Apparently this thermal water originates from upward leakage along fractures and structure in an underlying bedrock structural bench. A deep heat-flow measurement 5 km east of Buena Vista confirms the presence of at least one hydrothermal convection system in Laramide bedrock. Laramide volcanic and intrusive rocks beneath this area are probably highly fractured like the Laramide rocks in the Gila Mountains and may act as a deep geothermal reservoir. This conclusion is inescapable considering that the area lies astride the intersection of the Morenci lineament and the Gila discontinuity.

The known shallow, low-temperature resource at Buena Vista has potential direct-heat applications in agriculture, aquaculture, and space

heating. Heat-flow studies and deep drill tests are necessary to adequately assess the deep geothermal resource potential. Geothermometry information suggests that temperatures may range up to 115°C in an inferred deep reservoir contained in mid-Tertiary and Laramide volcanic rocks.

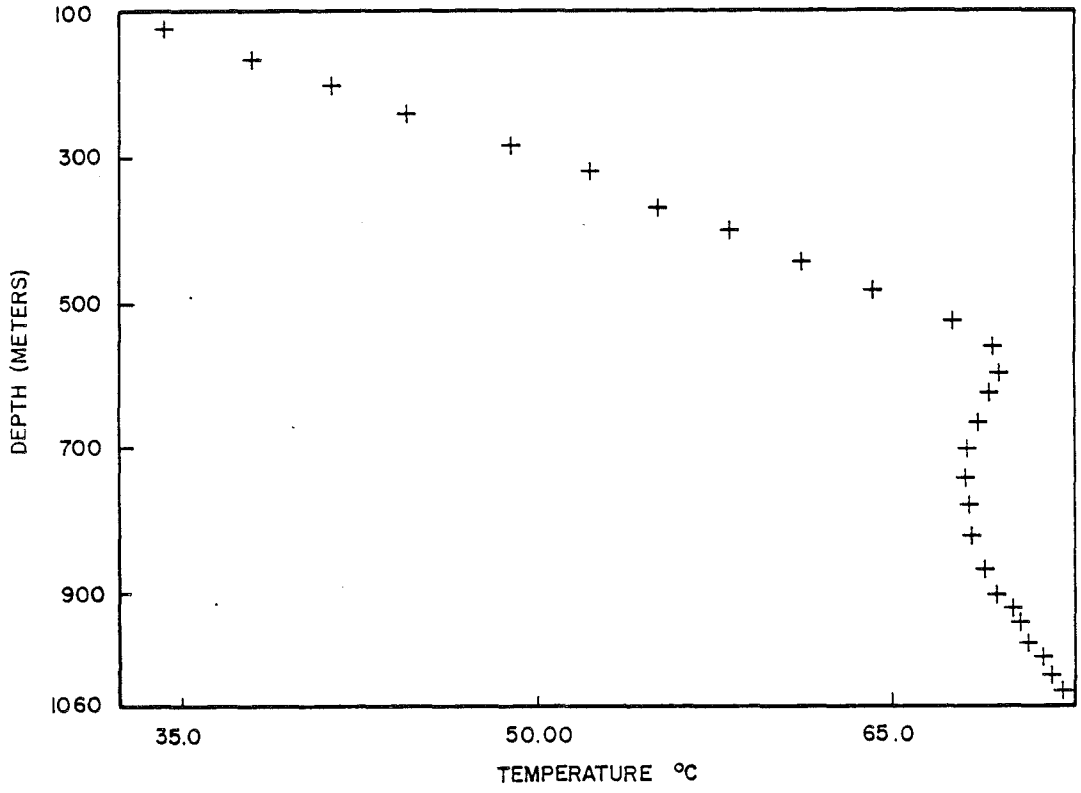

Figure 2.56. Temperature-depth profile of a deep well east of Buena Vista (from Reiter and Shearer, 1979)

REFERENCES BUENA VISTA AREA

Dunn, P. G., 1978, Regional structure of the Safford District, Arizona: Arizona Geological Society Digest, Vol. II, p. 9-16.

Chapin, C. E., Chamberlin, R. M., Osburn, G. R., Sanford, A. R., and White, D. W., 1978, Exploration framework of the Socorro geothermal area, New Mexicao: *in* Field guide to selected cauldrons and mining districts of the Datil-Mogollon volcanic field, New Mexico, New Mexico Geological Society Special Publication 7, p. 115-129.

Harbour, J., 1966, Stratigraphy and sedimentology of the upper Safford basin sediments: unpub. Ph.D. Thesis, University of Arizona, 242 p.

Livington, D. E., Maucer, R. L., and Damon, P. E., 1968, Geochronology of the emplacement, enrichment, and preservation of Arizona porphyry copper deposits: Economic Geology, Vol. 63, p. 30-36.

Reiter, M. and Shearer, C., 1979, Terrestrial heat flow in eastern Arizona, A first report: Journal of Geophysical Research, Vol. 84, no. B11, p. 6115-6120.

Robinson, R. F. and Cook, A., 1966, The Safford Copper Deposit, Lone Star mining district, Graham County, Arizona: *in* Titley, S. R. and Hicks, C. L., eds., Geology of the Porphyry Copper Deposits, southwestern North America, University of Arizona Press, p. 251-266.

Scarborough, R. B. and Peirce, H. W., 1978, Late Cenozoic basins of Arizona: *in* Callender, J. F., Wilt, J. C., and Clemons, R. E., eds., Land of Cochise, New Mexico Geological Society Guidebook, 29th Field Conference, p. 253-259.

Silver, L. T., 1978, Precambrian formations and Precambrian history in Cochise County, southeastern Arizona: *in* Callendar, J. F., Wilt, J. C., and Clemons, R. E., eds., Land of Cochise, New Mexico Geological Society Guidebook, 29th Field Conference, p. 157-163.

Strangway, D. W., Simpson, J., and York, D., 1976, Paleomagnetic studies of volcanic rocks from the Mogollon Plateau area of Arizona and New Mexico: *in* Cenozoic volcanism in southwestern New Mexico, New Mexico Geological Society Special Publication 5, p. 119-124.

Swan, M. M., 1982, Influence of pre-Cretaceous structure upon late Cretaceous-Tertiary magmatism in southern Arizona and New Mexico (abs): Abstracts, 78th annual meeting Cordilleran Section, The Geological Society of America, April 19-21, 1982, Anaheim, California, p. 238.

Titley, S. R., 1976, Evidence for a Mesozoic linear tectonic pattern in southeastern Arizona: *in* Tectonic Digest, Arizona Geological Society Digest, Vol.10, p. 71-101.

Witcher, J. C., 1981, Geothermal resource potential of the Safford-San Simon basin, Arizona: Arizona Bureau of Geology and Mineral Technology Open File Report 81-26, 135 p.

Ziagos, J. P., and Blackwell, D. D., 1981, A model for the effect of horizontal fluid flow in a thin aquifer on temperature depth profile: Geothermal Resources Council Transactions, Vol. 5, p. 221-223.

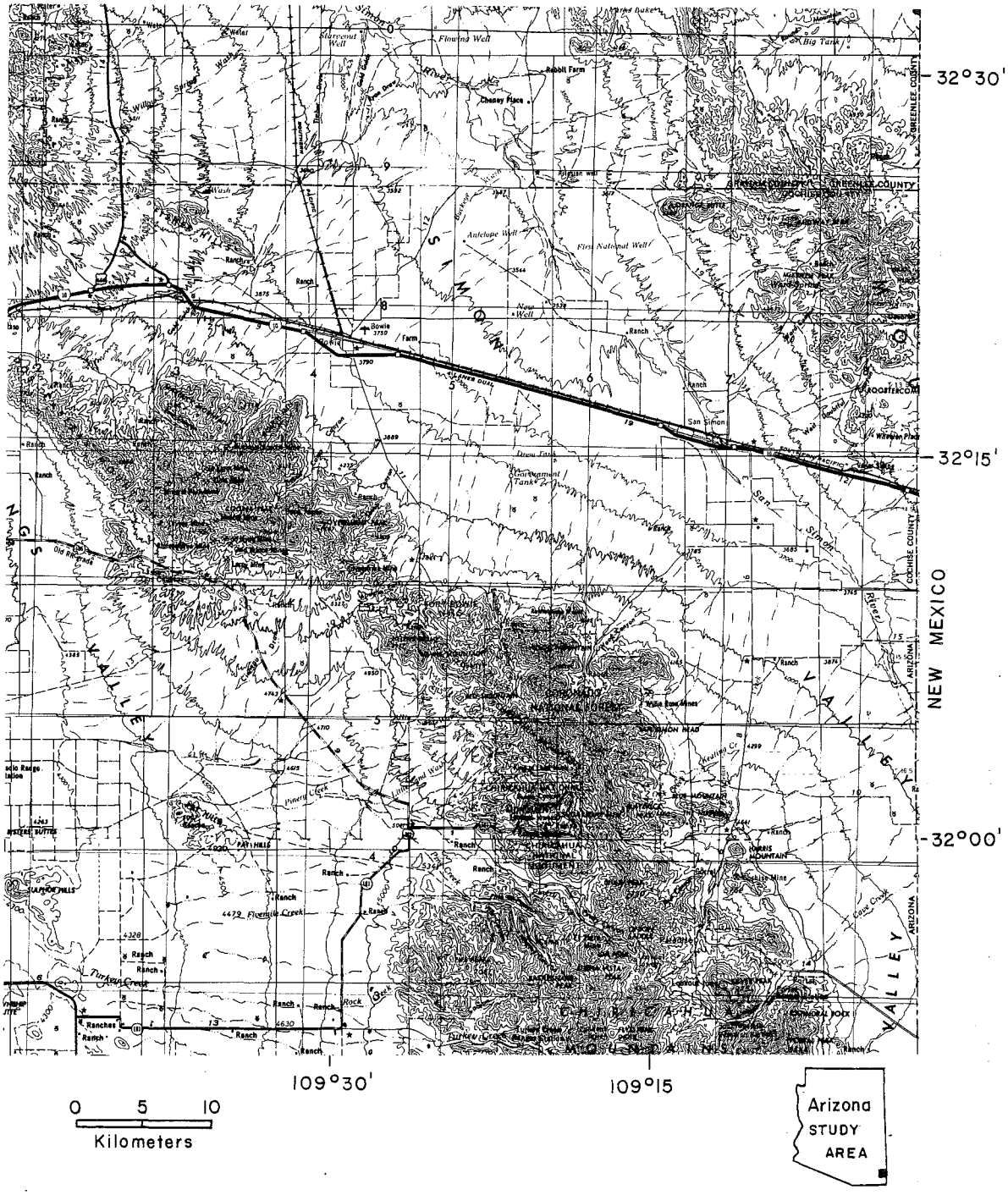

Figure 2.57. Physiographic map of the Bowie area

BOWIE AREA

INTRODUCTION. Thermal water (30 to 37°C) has been pumped from irrigation wells for many years in the Bowie area. Current use of this thermal water is for watering crops of cotton, alfalfa, corn, and pecans. Extraction of heat contained in the thermal water may have important use in the future in aquaculture, greenhousing, and space heating.

PHYSIOGRAPHY. Bowie is a small farming and railroad community on Interstate 10 in southeastern Arizona. Agricultural development in the vicinity is situated on a broad and gentle east-sloping piedmont of the San Simon Valley at about 1,128 m elevation. This area lies within the Mexican Highland section of the Basin and Range province. The Dos Cabezas Mountains border the area on the southwest while the Fisher Hills and Pinaleno Mountains rise above the San Simon Valley on the west. Across the San Simon Valley to the east are the Peloncillo and Whitlock Mountains. Annual precipitation at Bowie is less than 25 cm/yr. (See Figure 2.57.)

GEOLOGY. Bowie overlies a graben structure that forms a western portion of the larger Safford-San Simon structural basin. Gravity modeling by Eaton (1972) defined a north-trending graben about 8 km wide and 16 km long. This graben is separated from the San Simon graben on the east by a sediment buried horst block. The Bowie graben is filled with up to approximately 760 m of clastic sediments (Eaton, 1972). Tertiary volcanic rocks between 300 and 600 m thick may underlie the sediments in the graben. These volcanic rocks may be correlative with outcrops of mid-Tertiary

intermediate and silicic flows in the Fisher Hills and southern Pinaleno Mountains west of Bowie. A structurally and lithologically complex assemblage of plutonic, metamorphic, and sedimentary rocks probably comprise the basement below the volcanic rocks in the graben, an inference based upon the geology of the nearby Dos Cabezas Mountains.

Two terranes typify the Dos Cabezas Mountains (Sabins, 1957). The southern terrane on the southwest side of the mountains is an allochthon thrust north over a northern autochthonous terrane. Mapped thrust and reverse faults dividing these terranes coincide with a major west-northwest trending zone of complex faulting, which demarcates the Dos Cabezas discontinuity of Titley (1976). Early Cretaceous Glance Conglomerate, basal unit of the Bisbee Group, unconformably overlies Pennsylvanian Horquilla Limestone west of the discontinuity (Sabins, 1957). East of the discontinuity, the Glance Conglomerate is thinner and it overlies the early Paleozoic El Paso Formation and Coronado Sandstone. The apparent thinning of the Paleozoic sequence and the Glance Conglomerate may indicate a southwest margin of the Mesozoic Burro uplift of Elston (1958). If so, mid-Tertiary volcanic rock and basin fill deposits in the Bowie area may rest unconformably on Precambrian crystalline rocks or thin remnants of Paleozoic and Mesozoic rocks. Geochronologic and petrologic studies in the Dos Cabezas by Erickson (1968) show that the Precambrian plutonic rocks and Pinal Schist are intruded by several Laramide and mid-Tertiary stocks.

Drillers' logs published in White (1963) and White and Smith (1965) describe the stratigraphy of the upper portion of the basin fill in the Bowie graben. A blue-clay strata, probably correlative with the blue-clay unit at San Simon to the east, separates an upper sand, gravel, and clay

unit from a lower mostly coarse-grained unit. Three kilometers northeast of Bowie the blue clay is 120 m thick, but it thins to less than 15 m thick south of Interstate 10.

Recent tectonic deformation is inferred to have occurred in the Bowie area. While no Quaternary fault scarps have been identified, studies by Eaton (1972) point toward Recent uplift of the buried horst block east of the Bowie graben. First order leveling data show horst uplift between 1902 and 1952 relative to bedrock on either side of the Safford-San Simon basin. Topographic profiles crossing the uplifted area are convex, while in other areas of the Safford-San Simon basin the profiles are concave (Eaton, 1972). Holzer (1980) has mapped earth fissures that may have resulted in part from subsidence created by ground-water removal. Additional leveling studies show up to 1.25 m of subsidence over the graben since 1972. However, Holzer (1980) pointed out that aerial photographs taken over the Bowie area in 1935 show many polygonal earth fissures but no significant ground-water withdrawal occurred before 1935. The 1935 fissures may have originated during the 1887 Sonoran earthquake. DuBois and Smith (1981) reported that many areas of southeastern Arizona experienced earth fissuring during that event.

GEOHYDROLOGY. Extensive ground-water pumping has created a water-table depression roughly centered at Bowie. The depression is bounded by closespaced water-table elevation contours west, south, and east of Bowie (Fig. 2.58) (Wilson and White, 1976), and roughly corresponds with the Bowie graben margins deduced from Bouguer gravity data. These contours may indicate faults, which in clastic sediments are sometimes characterized by

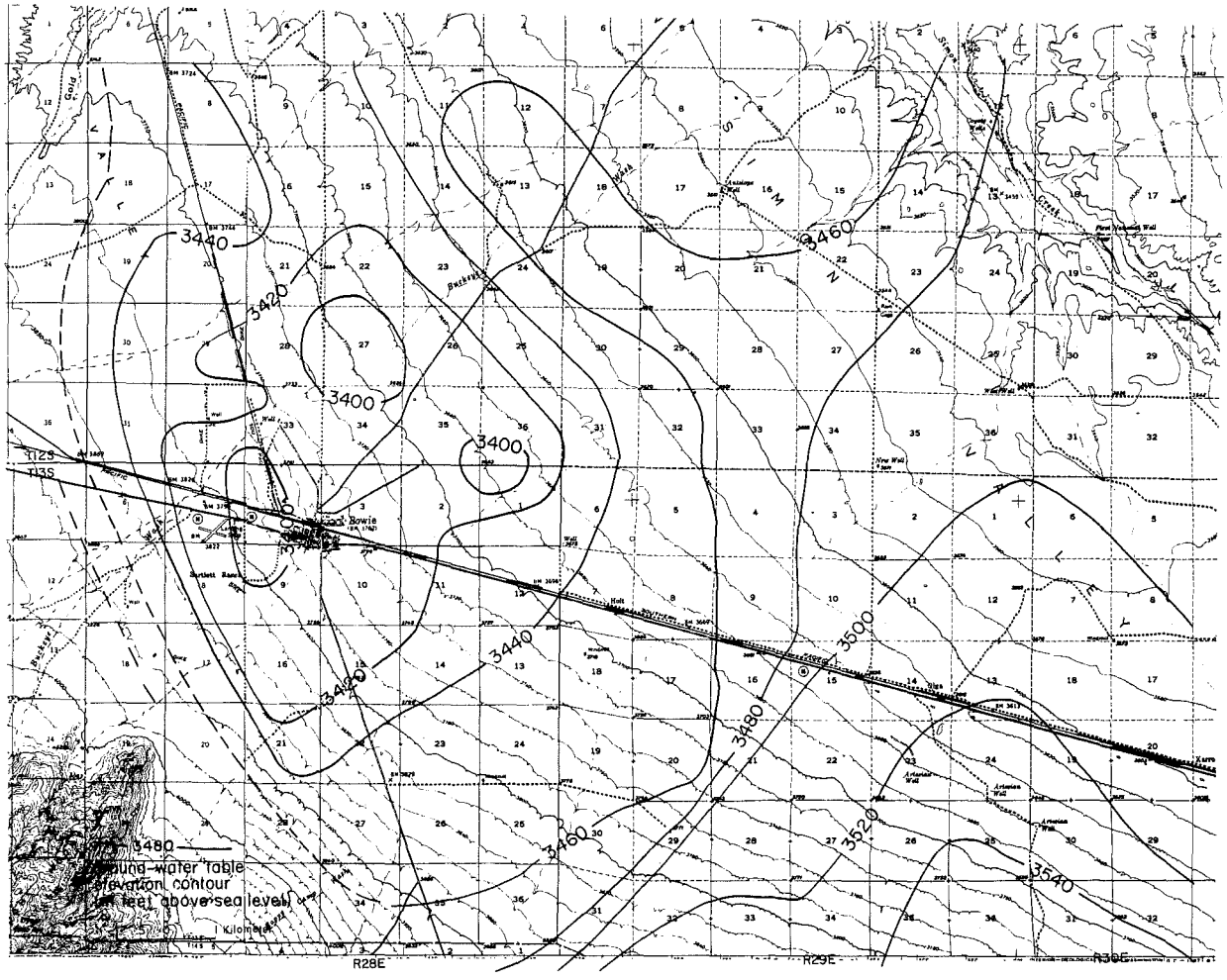

Figure 2.58. Map of water table in the Bowie area, 1975

vertical sheets of relatively impermeable gouge that can impede water flow and cause ground-water falls.

Ground water below the blue-clay unit is confined and frequently has artesian pressure. Thermal wells in the Bowie area pump water from aquifers below the blue clay.

THERMAL WATER. At least 20 irrigation wells between 183 and 610 m deep pump 30 to 37°C water (Table 2.8; Fig. 2.59). Chemical quality of the thermal water is good; total dissolved solids range between 250 and 500 mg/L

TABLE 2.8. Selected thermal wells in the Bowie area

Well	Temperature °C	Flow Rate L/min	TDS mg/l	Depth m
D-12-28-10CCC	36	--	686	305
D-12-28-26CCD	37	--	496	305
D-12-28-34CCB	36	--	--	457
D-13-28-3C	37	--	--	244
D-13-28-4DDB	37	--	231	253
D-13-28-10BCC	37	6435	247	305
D-13-28-15BDC	35	2990	253	309
D-13-28-15DCC	35	8707	264	145

(Table 2.9). Fluoride concentrations are generally less than 3.0 mg/L, although a few wells produce water with fluoride over 7.0 mg/L.

Thermal waters at Bowie have either sodium bicarbonate or sodium chloride-sulfate chemistry. No distinguishable trend in chemical type or measured temperature has been observed. The variability in composition is most likely due to contact of these waters with different kinds of rock in shallow (<600 m) aquifers (Witcher, 1981). Thermal water with the highest chloride and sulfate concentrations is pumped from aquifers that are overlain by at least 50 m of blue clay.

Geothermometers of these waters are highly variable. Sodium bicarbonate thermal water, with the lowest calcium (<5 mg/L) and magnesium (<0.4 mg/L) have the highest Na-K-Ca geothermometers (120 to 124°C). In other thermal waters, which trend toward sodium-chloride-sulfate chemistry, the Na-K-Ca temperatures are below 95°C. The conductive quartz geothermometer for the sodium bicarbonate water with the high Na-K-Ca geothermometers are about 100°C. Quartz geothermometers for other wells are less than 85°C.

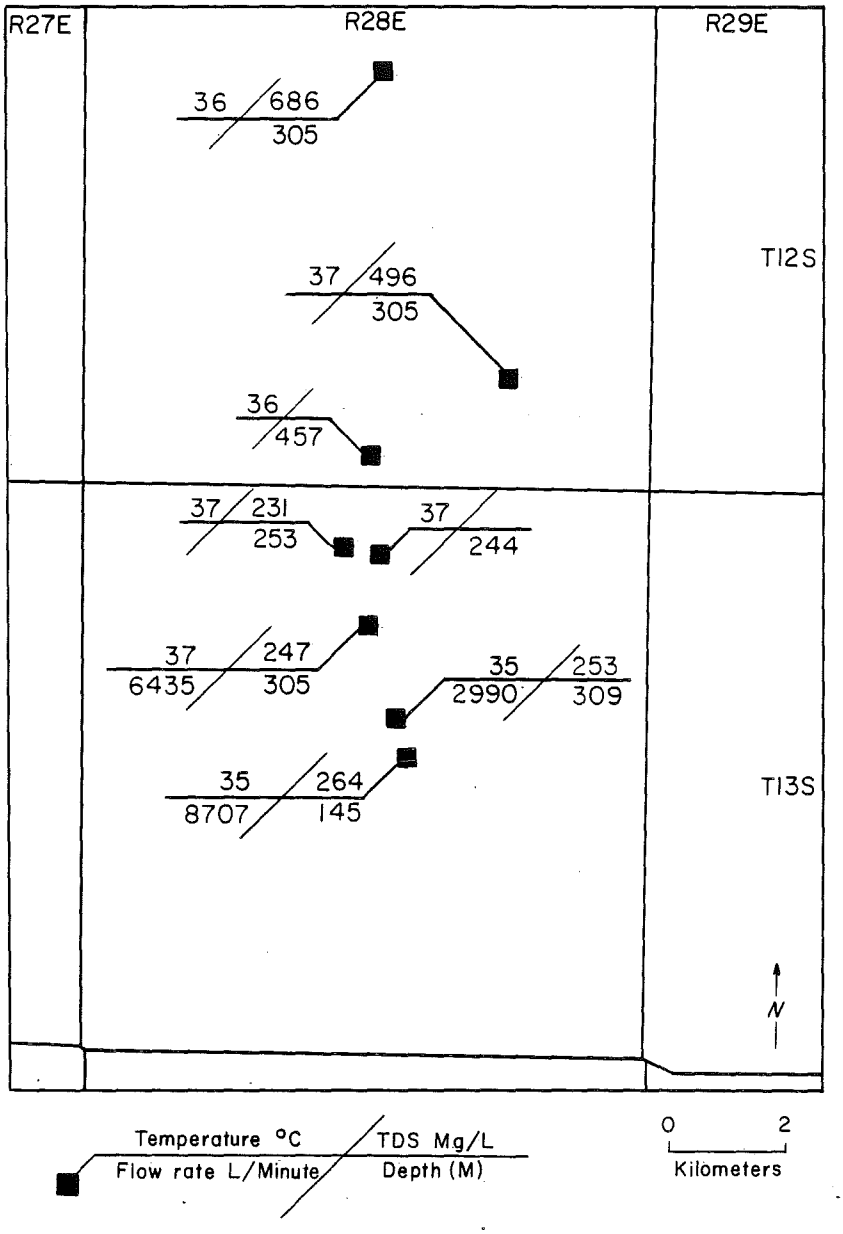

Figure 2.59. Map of selected thermal wells in the Bowie area

Wells with the highest Na-K-Ca geothermometers (Fig. 2.60) occur on the southwest margin of the Bowie graben near the intersection of structures inferred from gravity and ground-water falls.

CONCLUSIONS. Wells producing low calcium and magnesium, sodium bicarbonate water, with high Na-K-Ca geothermometers (>120°C) coincide with an

apparent structural intersection inferred from Bouguer gravity and water table information. One of these wells D-13-28-15dcc, which has the highest Na-K-Ca geothermometer (124°C), is the most thermally anomalous well from a consideration of both measured discharge temperature and depth. This well 145 m deep has a discharge temperature of 35°C and an estimated average temperature gradient of 124°C/km. Other thermal wells, which are north of the anomalous wells, have average gradients between 30 and 80°C/km with a mean gradient of 49°C/km. Thermal water in these wells may result from a normal geothermal gradient, which is relatively high (50°C/km) due to the low thermal conductivity of the basin-fill sediments. The area with high geothermometers and average gradients may overlie a hydrothermal convection system (Witcher, 1981).

TABLE 2.9. Chemistry of selected wells in the Bowie area

Number	Sample	Location	Temperature	TDS	pH	Na	K	Na+K	Ca	Mg	Cl	SO_4	HCO_3+CO_3	SiO_2	Li	B	F	Remarks
1	90	D-12-28-34CCC	37	645	7.9	185	6.9		19	1.5	163	140	80	25	0.3	3.7	2.2	W
2	91	D-12-28-27CCC	25	248	8.0	62	1.9		11	1.3	34	115	74	25	0.1	3.7	1.1	W
3	92	D-12-28-27BBB	26	334	7.9	70	2.1		19	2.2	68	65	94	26	0.1	4.1	0.9	W
4	93	D-12-28-10CCC	35	686	8.0	2.5	3.4		16	0.4	183	115	88	33	0.4	3.7	2.4	W
5	20W80	D-13-28-10BCCC	37	247	7.7	156	8.9		12.8	1.8	31	36	191	-	0.5	<.1	<.1	W
6	21W80	D-13-28-15DCCCB	35	264	7.7	142	4.3		2.6	0.2	31	26	207	44	0.3	<.1	<.1	W
7	22W80	D-13-28-15ADDD	34	492	7.6	166	4.5		3.2	0.3	97	80	177	48	0.4	<.1	2.6	W
8	23W80	D-13-28-15BDCDC	35	253	7.4	164	4.1		2.6	0.2	30	23	195	49	0.4	<.1	0.9	W
9	24W80	D-13-28- 9BCCC	33	488	7.5	29	3.3		16.6	1.4	86	8	86	37	0.1	<.1	8.0	W
10	25W80	D-12-28-26CCDDC	37	496	8.1	28	2.2		14.6	2.4	92	28	93	31	<.1	<.1	7.5	W
11	26W80	D-12-28-34BCBBB	37	649	7.3	72	5.9		16.1	1.7	157	112	72	26	0.2	<.1	7.1	W
12	27W80	D-12-28-27ABBCC	34	376	7.0	25	2.6		22.0	3.4	44	24	108	33	0.1	<.1	6.8	W
13	28W80	D-13-29-25CDDD	37	299	8.4	50	3.1		35.8	8.8	21	4	115	35	<.1	<.1	3.1	W
14	29W80	D-13-29-25CDDD	36	303	8.5	82	5.3		7.7	0.4	22	8	108	36	0.3	<.1	2.2	W
15	8290	D-13-29-27ACC	33.3	1020	8.0	113	1		14	2	24	76	210	23	0.08	0.02	2.8	W
16	-	D-13-28-4DDB	37.2	231	-	57			16	3.2	24	34	126	32	-	-	0.8	W
17	-	D-13-28-9BCC	31.7	402	7.8	69			52	12	63	57	216	40	-	-	0.8	W
18	-	D-13-29-24DCC	41.7	315	-	124			3.0	1.1	12	47	195	-	-	-	4.0	W
19	AZ30	D-12-28-34BC	31	268	8.0	55	2.0		22.2	1.9	31.5	61	99	31	-	0.02	0.30	W
20	AZ31	D-12-28-34BA	29	424	7.7	77.4	2.7		41.9	6.4	66	79	171	35	-	0.10	0.82	W
21	AZ32	D-12-28-34AA	36	392	8.7	113	2.7		7.6	0.2	63	113	89	31	0.17	0.04	1.02	W
22	AZ33	D-13-28-10CB	36	256	8.1	49.4	2.7		23.2	2.1	27	57	117	26	-	0.02	0.11	W
23	AZ34	D-12-28-10CC	35.5	704	8.1	204	3.5		26	0.4	173	121	117	30	-	0.14	2.17	W
24	AZ35	D-11-29-36BB	30.5	2016	7.9	518	6.2		81.1	12.0	175	1026	184	41	-	1.18	4.65	W
25	AZ36	D-13-30-3DB	23	584	7.9	145	2.0		27.4	8.4	20.5	134	325	61	-	0.22	5.10	W
26	AZ37	D-13-30-15	27.5	372	9.3	136	0.8		1.2	0.1	1.8	56.7	212	25	-	0.18	16.8	W

Active tectonism, which may occur in the area could create and sustain open fractures that allow deep circulation of water. A deep geothermal reservoir is inferred to exist in faulted basement of the Bowie graben south of Interstate 10. Temperatures will probably not exceed 125°C and the thermal water is likely to have a sodium bicarbonate chemistry with low total dissolved solids (<1,000 mg/L).

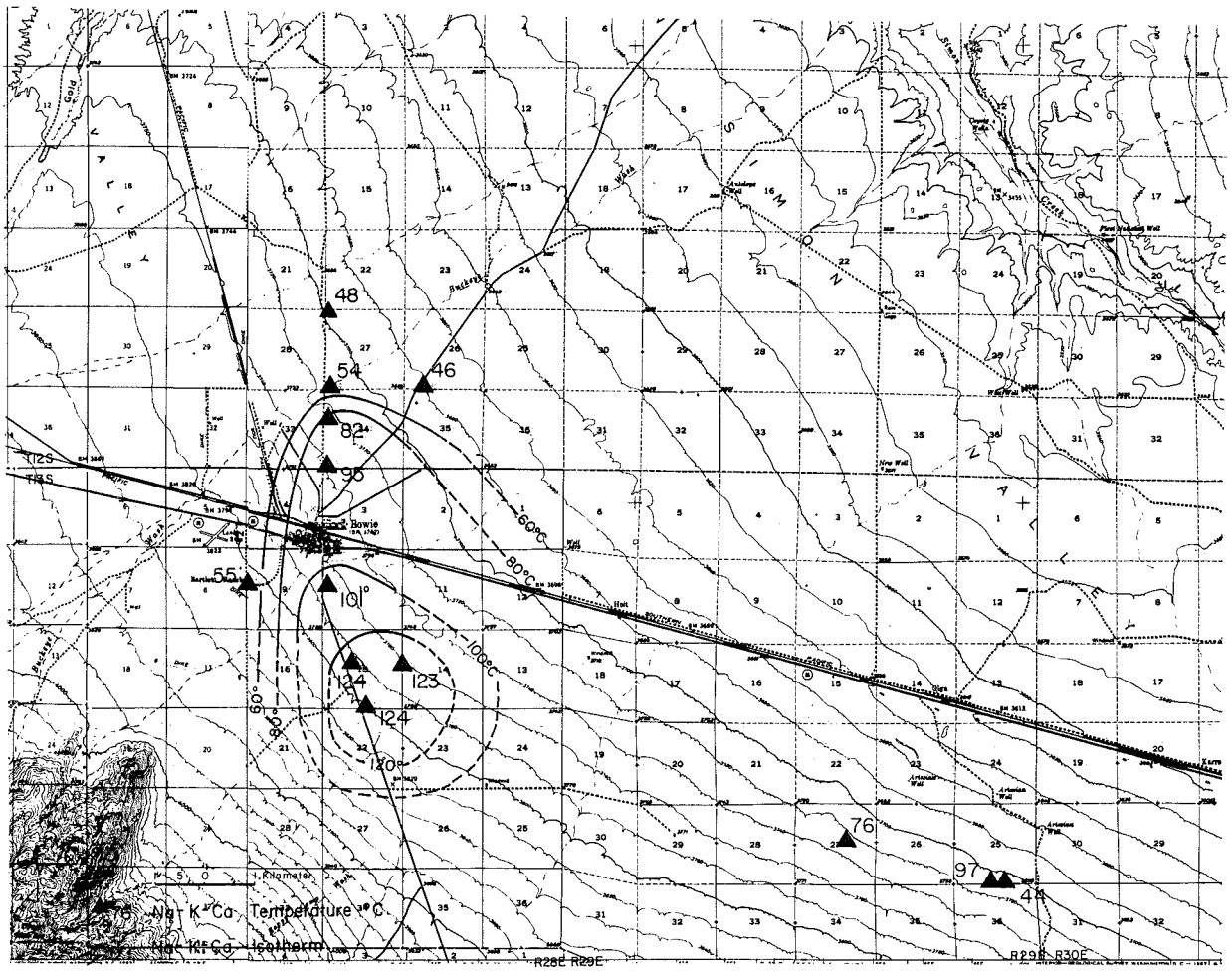

Figure 2.60. Distribution of Na-K-Ca geothermometer temperatures in the Bowie area

REFERENCES BOWIE AREA

DuBois, S. M. and Smith, A. W., 1980, the 1887 earthquake in San Bernardino valley, Sonora: Arizona Bureau of Geology and Mineral Technology Special Paper no. 3, 112 p.

Eaton, G. P., 1972, Deformation of Quaternary deposits in two intermontane basins of southern Arizona, U. S. A.: 24th IGC, section 3, p. 607-616.

Elston, W. E., 1958, Burro uplift, northeastern limit of sedimentary basin of southwestern New Mexico and southeastern Arizona: American Association of Petroleum Geologists Bulletin, Vol. 42, p. 2513-2517.

Erickson, R. C., 1968, Geology and geochronology of the Dos Cabezas Mountains, Cochise County, Arizona: *in* Southern Arizona, Guidebook III, Arizona Geological Society, p. 192-198.

Holzer, T. L., 1980, Reconnaissance maps of earth fissures and land subsidence, Bowie and Willcox areas Arizona: U. S. Geological Survey Miscellaneous Field Studies Map MF-1156.

Sabins, F. F., 1957, Geology of the Cochise Head and western part of Vanar Quadrangles, Arizona: Geological Society of American Bulletin, Vol. 68, p. 1315-1342.

Titley, S. R., 1976, Evidence for a Mesozoic linear tectonic pattern in southeastern Arizona: *in* Tectonic Digest, Arizona Geological Society Digest, Vol.10, p. 71-101.

White, N. D., 1963, Analysis and evaluation of available hydrologic data for the San Simon basin, Cochise and Graham Counties, Arizona: U. S. Geological Survey Water Supply Paper 1619-DD, 33 p.

White, D. D. and Smith, C. R., 1965, Basic hydrologic data for San Simon basin, Cochise and Graham Counties, Arizona, and Hidalgo County, New Mexico: Arizona State Land Department Water Resources Report 21, 42 p.

Wilson, R. P. and White, N. D., 1975, Maps showing ground-water conditions in the San Simon area, Cochise and Graham Counties, Arizona and in Hidalgo County, New Mexico-1975: U. S. Geological Survey Water Resources Investigations Open File Report 76-89.

Witcher, J. C., 1981, Geothermal resource potential of the Safford-San Simon basin, Arizona: Arizona Bureau of Geology and Mineral Technology Open File Report 81-26, 135 p.

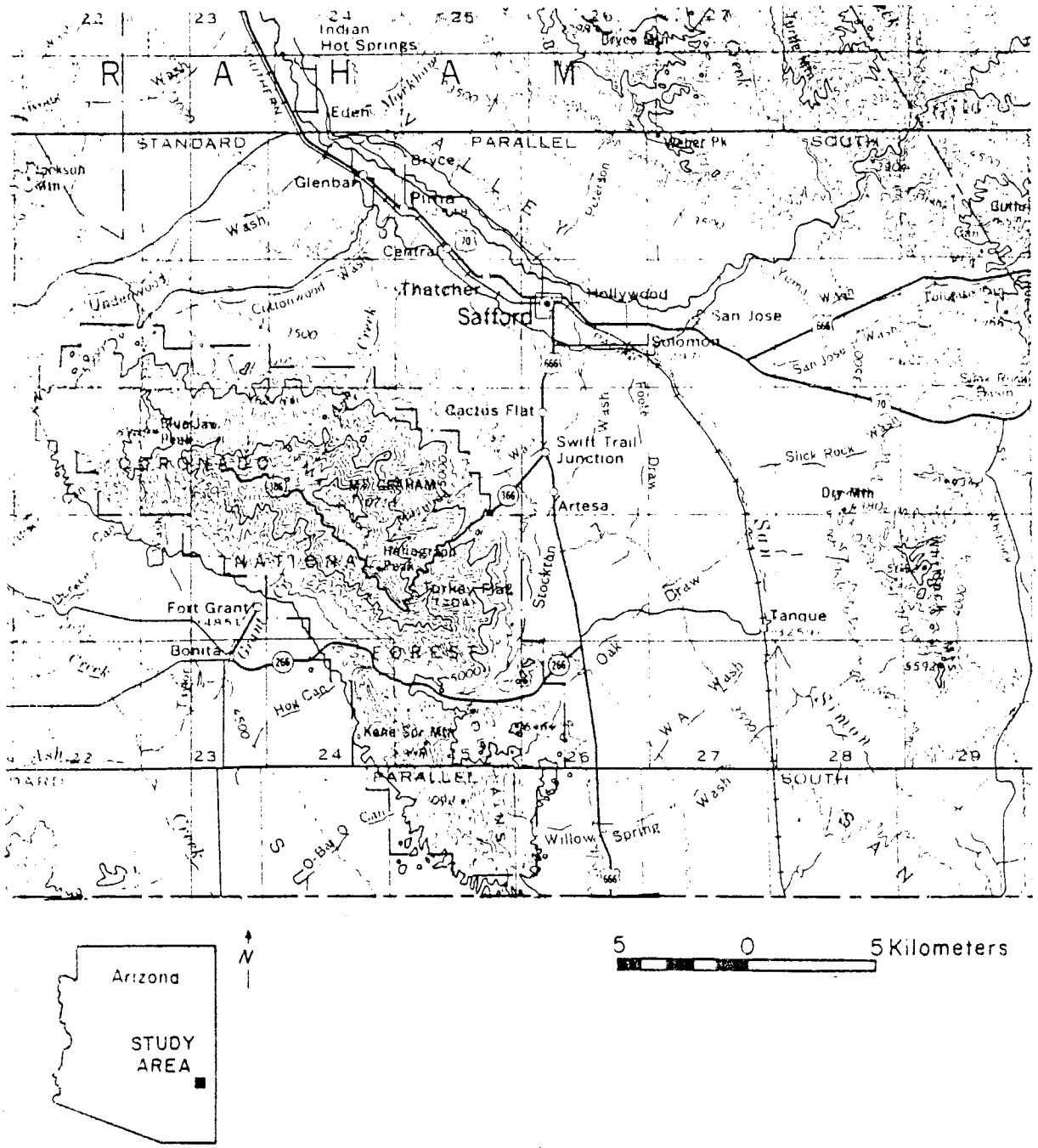

Figure 2.61. Physiographic map of the Cactus Flat-Artesia area

CACTUS FLAT-ARTESIA AREA

INTRODUCTION. Thermal water up to 46°C is discharged from artesian wells in the Cactus Flat-Artesia area, 8 to 15 km south of Safford along U. S. Highway 666 (Fig. 2.61). Currently three commercial mineral baths use this geothermal water for balneological purposes. Three more thermal wells provide water to a lake at Roper State Park, and several artesian wells discharge into Dankworth Lake. Another current use of thermal water in the area is catfish aquaculture. The feasibility of using geothermal water for space heating and hot-water supply at the Swift Trail Federal Prison Facility has been studied and the results discussed in a preliminary report funded by the U. S. Department of Energy. Apparently, the scope of retrofit required to convert the prison to geothermal energy makes this project only marginally cost beneficial, given the current fossil-fuel-cost projections used for planning and comparison studies by Federal agencies (Oregon Institute of Technology, 1981).

In addition to thermal artesian wells in the Cactus Flat-Artesia area, a probable hydrothermal system was discovered 18 km south of Safford adjacent to U. S. Highway 666 (Witcher, 1982). This "blind" system, which underlies a soil mercury anomaly, is characterized by anomalous estimated heat flow values of >200 mWm^{-2} (Witcher, 1982).

PHYSIOGRAPHY. The Cactus Flat-Artesia area is situated in the Safford-San Simon basin at the base of the Pinaleno Mountains (Fig. 2.61). Stockton, Marijilda, and Graveyard Washes, which discharge from deeply eroded,

linear canyons in the Pinaleno Mountains, have dissected the area into a succession of mesas, fans, and arroyos. All drainage flows north and eastward toward the Gila River north of Safford. The impressive Pinaleno Mountains rise abruptly above the basin to form a range nearly 3,350 m in elevation, where more than 76.2 cm/yr of precipitation falls. The Cactus Flat-Artesia area, which lies in the Pinaleno Mountains rain shadow at 914 to 1,067 m above sea level, only receives about 20 to 25.4 cm of precipitation annually.

GEOLOGY. Fig. 2.62 is a generalized geologic map of the Cactus Flat-Artesia area. The Pinaleno Mountains are an exposed mid-Tertiary metamorphic core complex (Davis and Coney, 1979). This rugged mountain range is dissected by several linear canyons, which are eroded into the gneiss and mylonitic gneiss. The canyons coincide with major northeast-trending fault zones displaying left-lateral strike-slip movement (Thorman, 1981). Mylonitic foliation in the gneiss dips gently north to northeast near the base of the Pinaleno Mountains and it dies out rapidly into the range (Thorman, 1981). Metamorphic complexes such as the Pinaleno Mountains generally have a distinctive structural morphology (Coney and Davis, 1979): low angle fault zone (decollement) of chloritized mylonite and mylonite breccia overlies mylonitized metamorphic rocks and gneiss. Deformed, but unmetamorphosed rock overlie the low angle fault. While a low angle fault is not observed in the Pinaleno Mountains adjacent to the Cactus Flat-Artesia area, outcrops of mylonitic gneiss at the base of the mountains suggest that a decollement is preserved in the basin basement beneath this area. A mid-Tertiary age for cataclasis of the gneiss is unconfirmed (Thorman, 1981), but low-angle Miocene faults are observed at

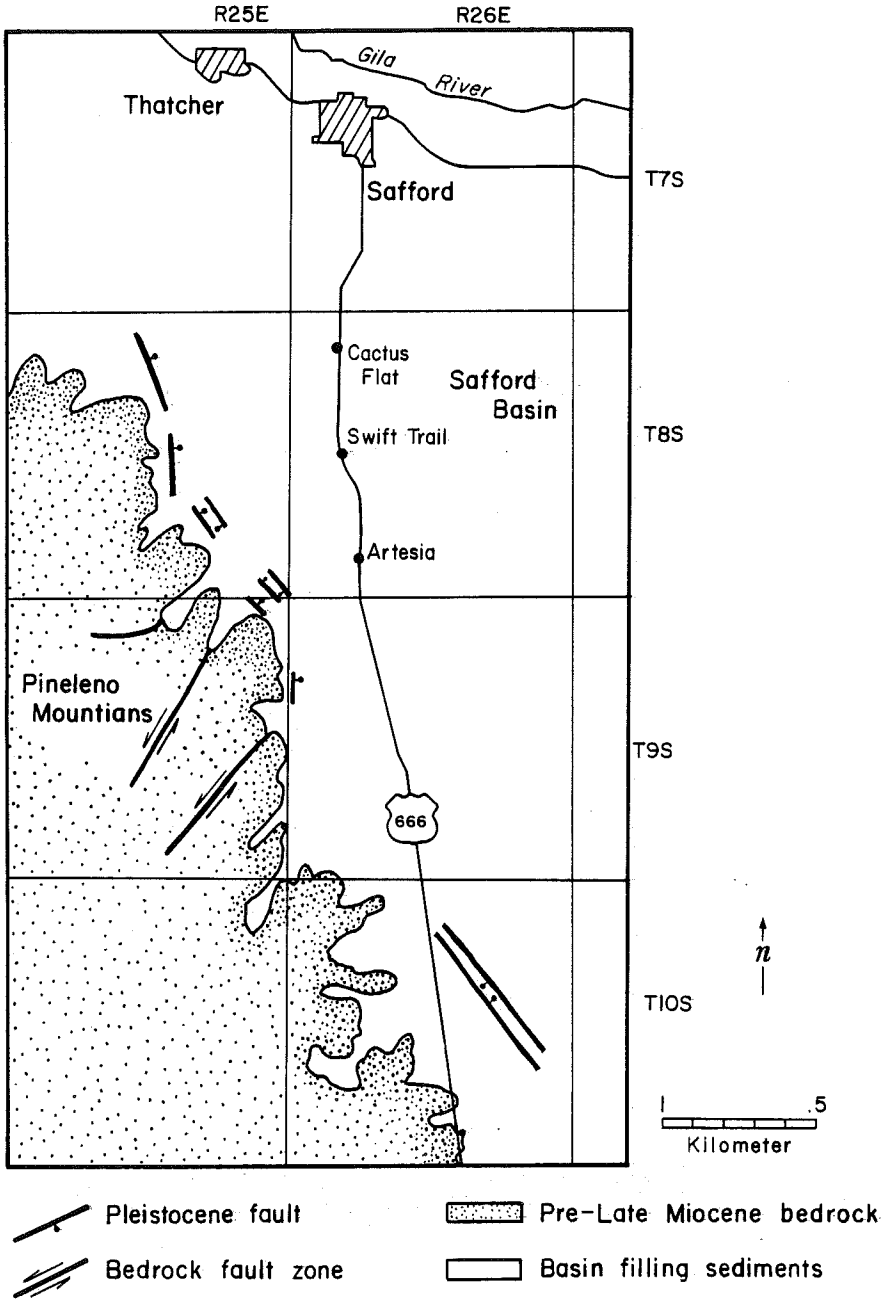

Figure 2.62. Generalized geology of the Cactus Flat-Artesia area

Eagle Pass (Blacet and Miller, 1978) and near Gillespie Mountain (Thorman, 1981) on the northwest and southeast ends, respectively, of the Pinaleno Mountains.

A complete Bouguer gravity map of the area (Wynn, 1981) shows very closely spaced isogals between 0.2 and 4 km east of and parallel to the Pinaleno Mountains front. A large-displacement high-angle Basin and Range fault zone is interpreted from these gravity data. The fault zone forms the western boundary of the Safford-San Simon Basin, which may contain up to 3 km (Oppenheimer and Sumner, 1981) of post mid-Miocene basin-filling sediments. Pleistocene movement along the fault zone has been inferred from multiple and composite fault scarps displacing Pleistocene geomorphic surfaces up to 30 m (Morrison and others, 1981). Menges and others (1982) estimated that faulting recurs on an interval about every 100,000 years.

Basin-fill stratigraphy is divided into two major units in this area, upper and lower basin fill. These units are separated by a time-stratigraphic horizon showing a change in sedimentation processes and by a Pliocene to Quaternary faunal transition (Harbour, 1966).

Lower basin fill consists of three facies: (1) a conglomerate facies (2) a clay-silt facies, and (3) an evaporite facies. The evaporite facies consists of gypsiferous clay, gypsum, anhydrite and halite beds and it intertongues with the clay-silt facies, which also overlies the evaporites into the basin axis, north and east of the Cactus Flat-Artesia area (Harbour, 1966). The lacustrine and fluvial overbank clay-silt facies is extensive and occurs to within 2 or 3 km of the Pinaleno Mountains front. Nonindurated to moderately indurated sand and gravel form the conglomerate facies, which occurs along the basin margins. This conglomerate is

postulated to underlie the clay-silt and evaporite facies in the basin interior and it is known to be interbedded with the clay-silt facies at depth along U. S. Highway 666. The conglomerate facies hosts stacked, thermal artesian aquifers in the Safford basin, which are confined by the clay-silt beds.

Upper basin fill consists of nonindurated gruslike sand with gravel lenses. This unit overlies a narrow gneiss pediment and the clay-silt and conglomerate facies of the lower basin fill. The upper basin fill no doubt has an important hydrologic connection with the conglomerate facies next to the mountain front. A thin less-than-20-m-thick, cobble-to-boulder conglomerate caps the upper basin fill to form the mid-Pleistocene to Recent geomorphic surfaces.

Because the Pinaleno Mountains are a mid-Tertiary metamorphic core complex, basement structures (pre-late Miocene) favorable for geothermal resources are inferred to exist below the basin fill (post mid-Miocene). Monoclinally dipping Cretaceous to pre-late-Miocene sediments and volcanic flows deformed by listric normal faults, which merge into a decollement, are inferred beneath the basin fill adjacent the Pinaleno Mountains. Highly fractured zones near the inferred low angle faults may act as deep geothermal reservoirs.

GEOHYDROLOGY. Ground water in the Cactus Flat-Artesia area is found in sand and gravel confined between clay-silt strata. Deep wells in the area flow at the surface and are thermal (>30°C, gradient >45°C/km). The water-table is quite variable due to the presence of several vertically stacked artesian aquifers with differing artesian pressures. Artesian pressure generally increases with depth and it is higher when only a few

wells are producing from a single aquifer in a given area. Well interference is common in this area due to arealy large cones of depression, which are typical of confined aquifers (Feth, 1952). Recharge in this area is mostly from meteoroic water seeping into coarse-grained basin fill near the mountain front, chiefly along washes which discharge runoff from the Pinaleno Mountains. The recharge water flows downward and laterally toward the basin axis.

THERMAL WATER. At least 18 flowing artesian wells discharge thermal water between 35 and 45°C (Fig. 2.63). In addition, 20 other wells reportedly discharge thermal water ($\geq$30°C). These wells range from 110 to 488 m deep (Table 2.10).

Nonthermal (<30°C) ground water in the area has sodium bicarbonate to sodium sulfate-bicarbonate chemistry with TDS less than 1,000 mg/L. Thermal waters (>30°C) have sodium sulfate to sodium chloride-sulfate chemistry with TDS between 1,000 and 9,000 mg/L (Table 2.11). Witcher (1981) showed the chloride-sulfate versus bicarbonate ratio has a logarithmic relationship to lithium concentration, which suggests that thermal and nonthermal water chemistry evolves from contact with differing lithology through equilibria and ion exchange processes (Fig. 2.64). The clay-silt facies provides a source for sulfate, chloride, and lithium. Silica concentrations are highest in nonthermal sodium bicarbonate water.

Silica and Na-K-Ca geothermometers are not applicable to thermal waters in the Cactus Flat-Artesia area given the assumptions governing their use (Fournier, White, and Truesdell, 1974).

THERMAL REGIME. Surface discharge temperatures of artesian wells were plotted against their respective depths (Fig. 2.65). These wells

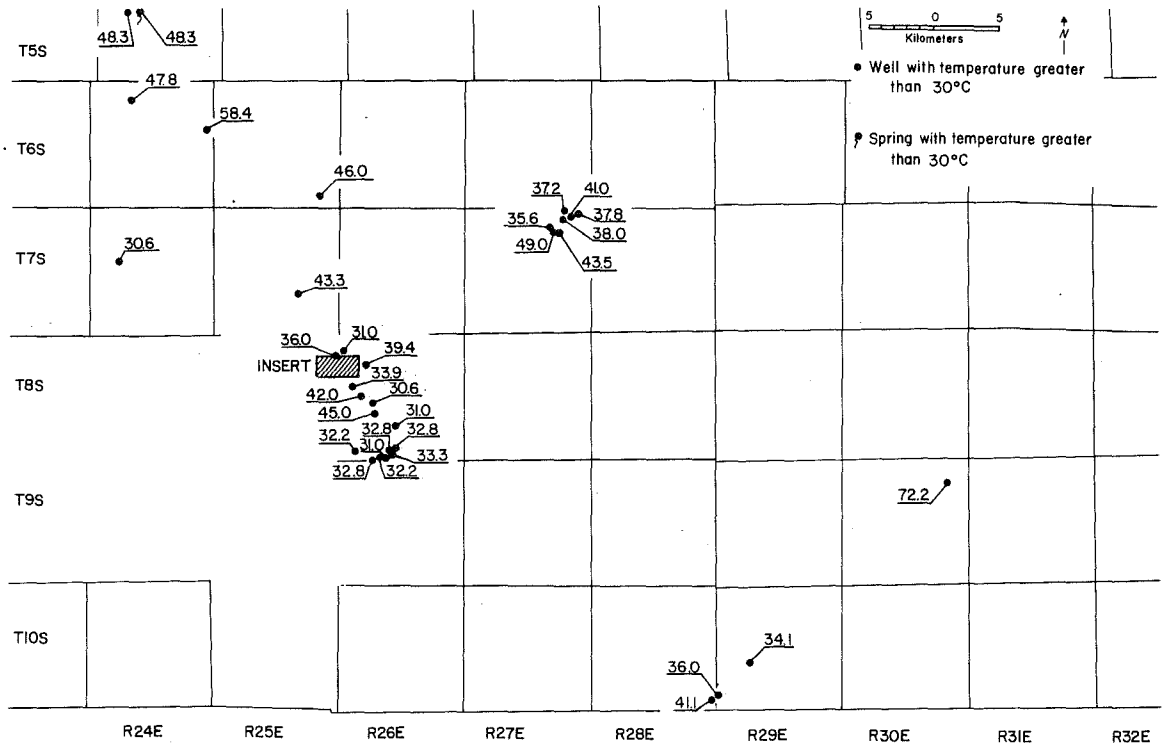

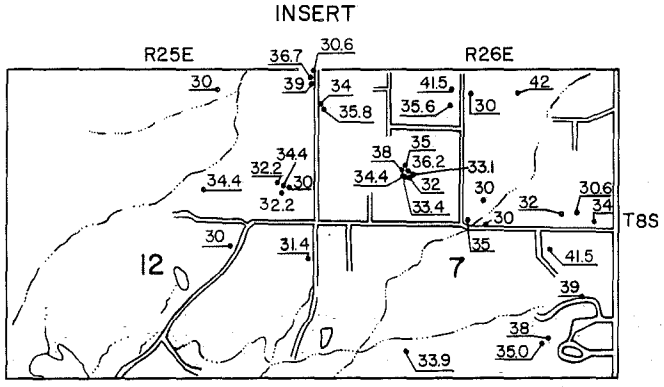

Figure 2.63. Maps showing locations of thermal wells in the Cactus-Flat-Artesia area. Map at left is enlargement of shaded area show in map above.

exclusive of those in sections 32 and 33, T. 8 S., R. 26 E., show a linear increase in temperature with depth (4.5°C per 100 m). At least five separate, vertically stacked aquifers, confined by clay and silt, provide water to these wells (Witcher, 1979).

From studies of several deep (>300 m) mineral exploration holes 18 km north of Safford, Reiter and Shearer (1979) reported an average heat flow

TABLE 2.10. Thermal wells in the Cactus-Flat-Artesia area

Location	Temperature °C	Total Dissolved Solids mg/l	Depth m
D-8-25- 1 DDD	36	-	213
D-8-25-12AA	37	-	320
D-8-25-12AAA	39	2447	366
D-8-26-7BA	36	-	344
D-8-26-7BAA	42	-	463
D-8-26-7BB	36	-	320
D-8-26-7AC	35	-	329
D-8-26-7ABA	42	-	467
D-8-26-7DDA	39	1345	421
D-8-26-8BDC	39	2866	195
D-8-26-7BD	35	-	366
D-8-26-7CA	37	-	244
D-8-26-7BDB	38	-	476
D-8-26-7DA	42	-	488
D-8-26-7DDB	38	-	387
D-8-26-7DDB	35	-	381
D-8-26-20DBC	45	1358	390
D-8-26-18DDA	42	-	463

of about 80 mWm^{-2} for that area, which is a typical value for the southern Basin and Range province. Because basin fill in the Cactus Flat-Artesia area has thermal conductivities generally less than 1.88 ($Wm^{-1}K^{-1}$)(Witcher, 1982), a 45°C/km gradient is normal for a conductive heat flow of 80 mWm^{-2}.

Unusually warm wells occur in sections 32 and 33, T. 8 S., R. 26 E. These wells have estimated gradients exceeding 100°C/km (Fig. 2.65) and chemistry that is indistinct from that of other waters in the Cactus Flat-Artesia area. No artesian well data are available south of this anomaly.

Location	Temperature	TDS	pH	Na	Na+K	K	Ca	Mg	Cl	SO_4	HCO_3+CO_3	SiO_2	Li	B	F
D-8-25-12AAA	39	2447	8.6	881		7.7	50	0.9	941	535	32	17.6	-	-	-
D-8-26-7DDA	39	1345	8.8	470		3.5	15	0.2	503	335	33	18.5			
D-8-26-8BDCC	39	2866	8.5	1152		10.6	31	4.3	1066	607	90	14.1			
D-8-26-20DBCC	45	1358	8.4	579		5.8	17	0.6	510	290	79	18.4			
D-8-26-6CBB	31	1767	7.5	644		2.7	1	0.5	538	330	223	17	0.8	2.5	8.6
D-8-26-7BBB	34	1402	7.7	444		3.0	9	0.4	457	313	42	18	1.3	0.7	10.2
D-8-25-12AAA	39	2803	7.1	810		5.3	26	0.8	965	542	31	20	2.1	0.3	7.8
D-8-25-1DDD	36	1774	7.4	605		3.1	19	0.6	655	392	42	20	1.7	0.6	11.0
D-8-26-7ADC	32	1315	7.7	474		2.6	2	0.5	483	309	129	15	1.0	0.6	8.3
D-8-26-7DDA	39	1367	7.5	449		2.4	15	0.2	505	300	38	22	1.3	0.1	12.5
D-8-26-7DDB	35	1325	7.6	448		2.2	13	0.2	424	325	40	22	1.5	0.1	12.0
D-8-26-7DDB	38	1634	7.5	539		2.8	22	0.2	580	377	38	23	1.6	0.3	11.5
D-8-26-33CCCC	31	685	7.9	171		4.3	75	2.8	82	345	110	33	0.3	4.8	5.2
D-8-26-32DCC	28	523	8.3	161		1.6	3.4	0.6	111	265	113	28	0.3	5.1	9.8
D-8-26-19DCCB	27	231	7.3	21		2.1	8	3.9	16	5	132	50	0.1	0.4	1.1
D-8-26-19CDDA	27	243	7.5	23		2.2	7	4.1	19	6	116	47	0.1	0.2	1.2
D-8-26-19CDDB	27	429	8.0	48		3.1	14	2.7	108	58	104	36	0.3	0.5	1.0
D-8-26-19CDDBC	29	679	8.0	60		2.8	10	2.0	201	95	96	34	0.5	<0.1	1.8
D-8-26-33CCD	34	690	8.0	61		3.6	13	1.8	156	120	118	26	0.3	0.7	0.5
D-8-26-32DC	33.3	456					9.5	3.9	101	88	164	-	-	-	10
D-8-26-7DD	42	1152	8.5	524		3.9	21	0.4	204	282	83	24	-	0.90	13.6
D-8-26-7AB	45	2256	8.1	1054		6.6	69	2.6	447	605	48	20	-	1.29	9.0
D-8-26-20CD	44	1248	8.4	498		4.3	16	0.7	197	267	99	26	1.38	0.55	14.2
D-8-26-7DA	41.5	1992	8.5	678		3.9	22	0.5	818	369	43	28	-	1.04	9.6
D-8-25-1ZAAA	39	2660	8.5	783		5.5	65	1.1	1024	497	34	28	2.40	1.18	8.4
D-8-26-7AC	37	1160	8.8	384		2.3	18	0.2	418	294	54	31.7	-	0.8	11.7
D-8-26-7BA	34.5	1116	9.0	379		2.3	7.2	0.2	399	247	82	28	-	0.94	13.95
D-8-26-7BB	33.5	900	8.9	306		1.6	9.2	0.1	294	195	60	29	-	0.60	14.55
D-9-26-5BA	33	504	8.5	161.9		1.2	4.6	0.1	109	106	146	28	-	0.28	10.35
D-9-26-5BA	33	740	8.2	249		2.3	17.2	1.0	151	172	218	29	-	0.30	14.55
D-8-26-8CA	39.4	3000	7.9	1025		6.2	42.1	5.7	1125	585	117	22	2.32	1.78	9.45
D-8-26-9BC	29.4	9048	7.6	3283		14.1	67.9	20.7	4097	1688	165	30	5.16	8.40	1.17
D-8-26-9BC	38.9	1464	7.9	442.8		6.2	37.7	11.4	365	410	172	20	0.93	2.06	5.40,
D-8-26-20DC	39.4	816	8.8	303.5		1.2	7.2	0.1	260	203	95	28	-	0.84	14.54

TABLE 2.11. Chemistry of thermal wells in the Cactus Flat-Artesia area

SOIL MERCURY. Soil mercury anomalies are frequently associated with high temperature hydrothermal systems. Matlick and Buseck (1975) and Capuano and Bamford (1978) have used soil mercury sampling with success over known high temperature systems to define structure, which controls fluid flow. Mercury gas diffuses upward over these structures and systems where it can be measured in near-surface soil.

A soil mercury survey was conducted south of the area having anomalous wells in order to delineate the extent of the anomaly, to identify potential structural control on this apparently hidden convective system, and to

test the applicability of a soil mercury survey on a probable low to intermediate temperature geothermal system in a southern Basin and Range geologic setting.

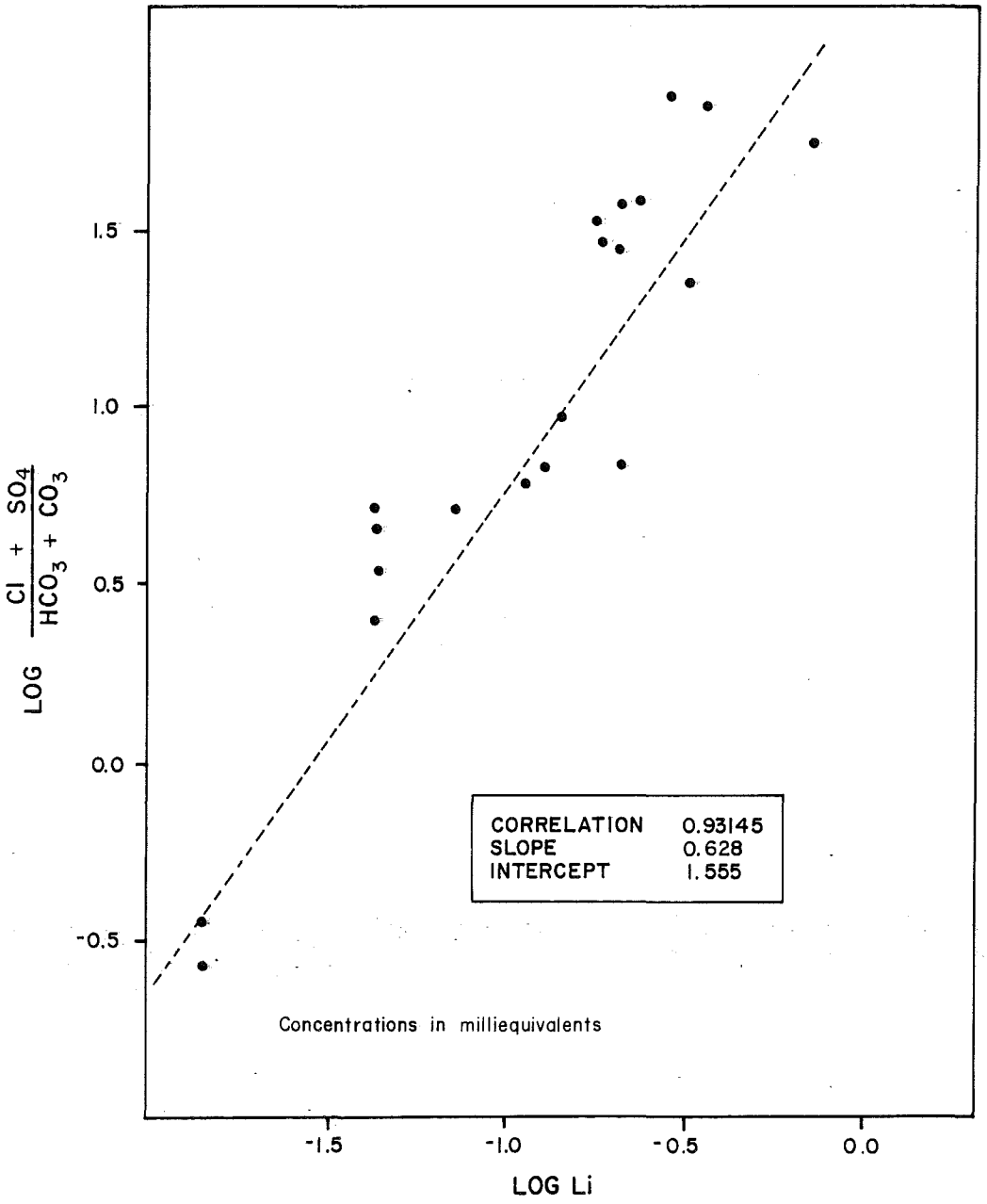

Figure 2.64. Lithium compared to the ratio of chloride plus sulfate, versus carbonate species

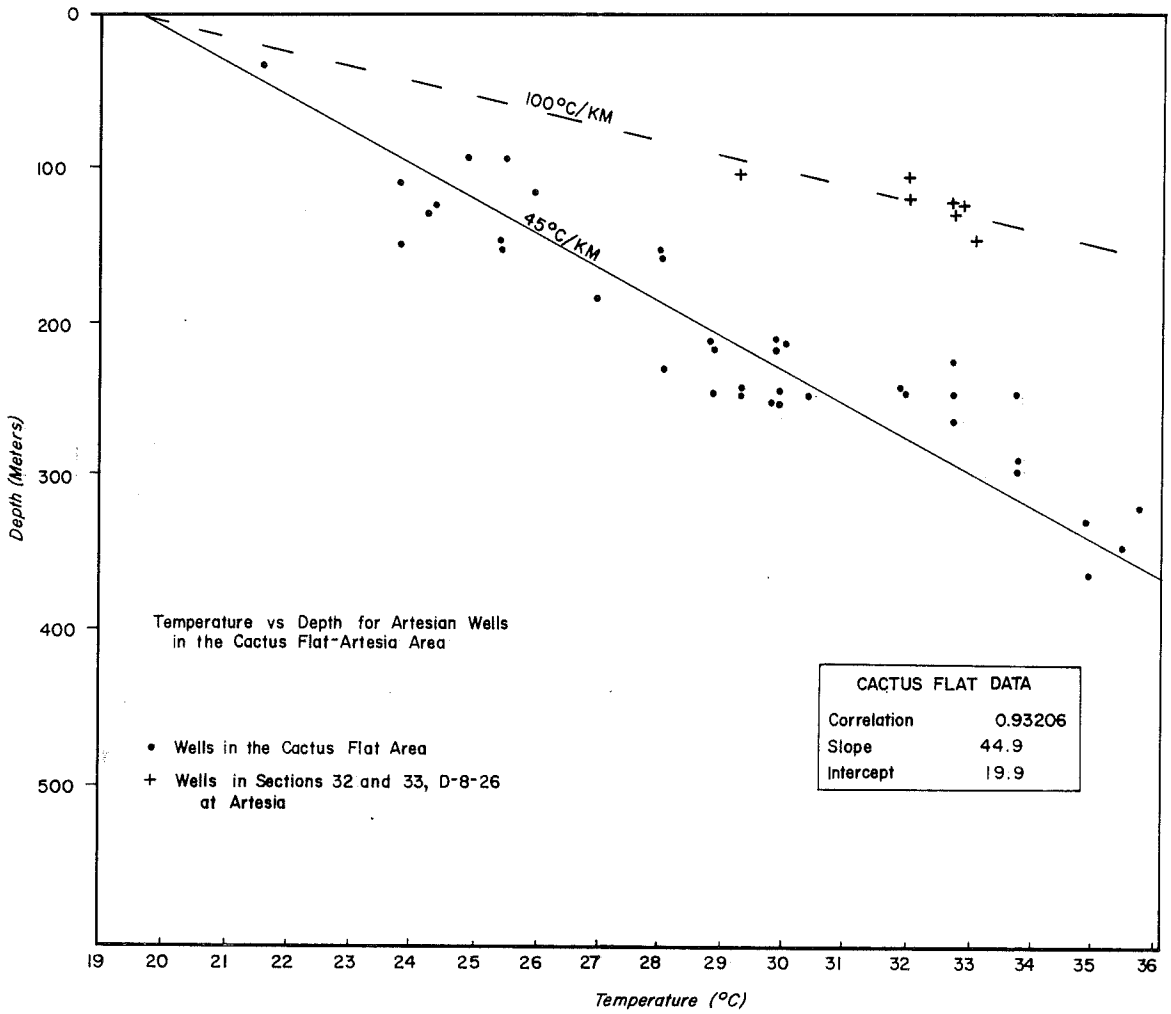

Figure 2.65. Temperature versus depth for artesian wells in the Cactus Flat-Artesia area

Background mercury concentration in the Artesia area was 225 ± 99 parts per billion (ppb), which is high but may in some way reflect the geologic setting. Above normal mercury contents were arbitrarily defined as values exceeding 303 ppb, which is the mean plus one standard deviation. No correlation existed among mercury concentration and different stratigraphic-geomorphic surfaces in the area.

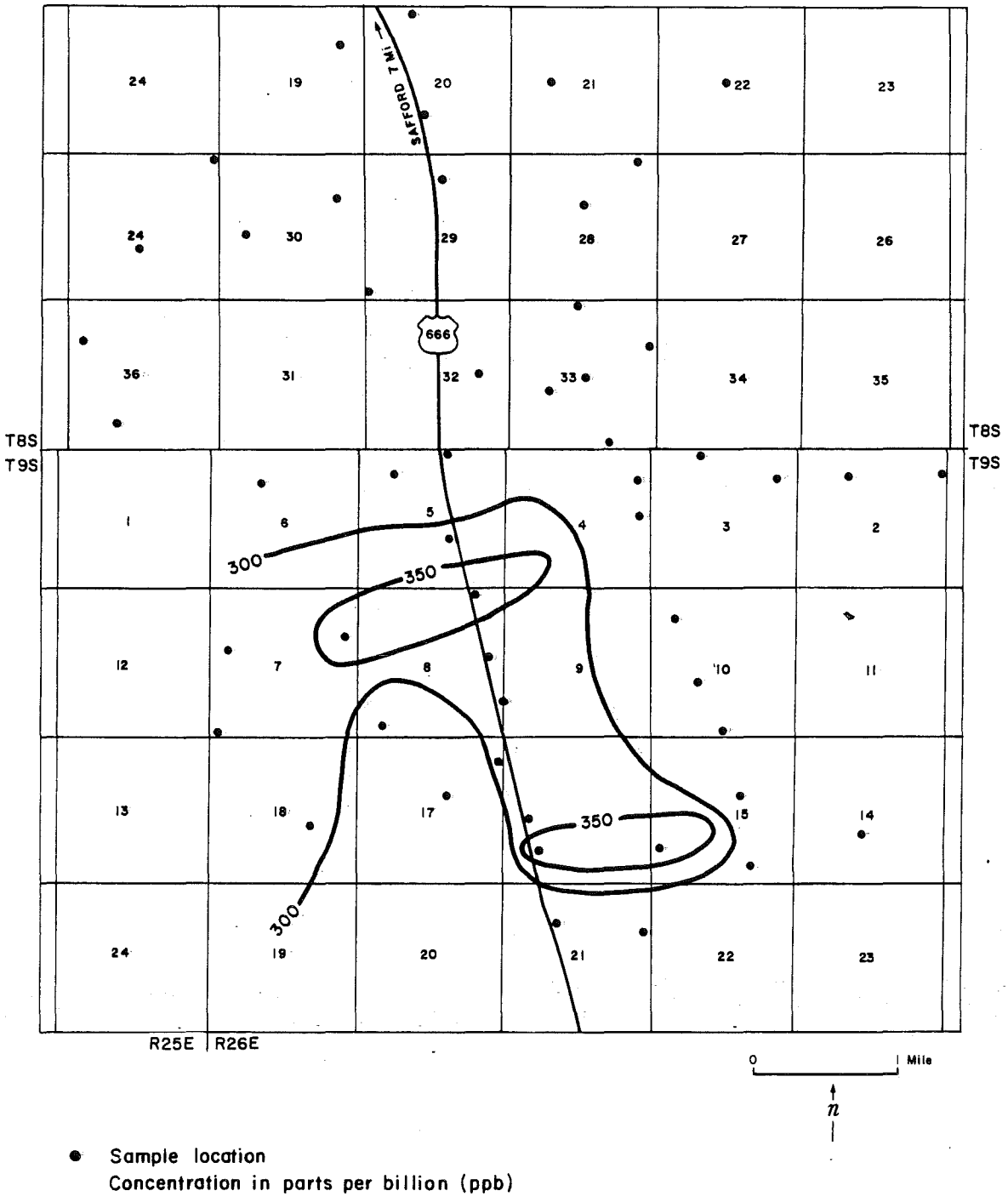

Figure 2.66. Distribution of mercury in soil, Cactus-Flat-Artesia area

High concentrations of mercury occur south of Artesia and adjacent to sections 32 and 33, T. 8 S., R. 26 E., both of which have anomalous-temperature wells (Fig. 2.66). A northwest trending zone of high soil mercury (>303 ppb) encloses two east-northeast trending closures with mercury exceeding 350 ppb.

HEAT FLOW STUDY. A heat flow study was conducted to confirm the presence of a hidden geothermal system that was inferred from the soil mercury anomalies and the anomalous-temperature wells at Artesia (Witcher, 1982). Eight shallow (<61 m deep) holes (Fig. 2.67) were drilled and cased with one-inch PVC pipe plugged at the bottom and filled with water. Bulk thermal conductivity measurements were made on formation samples collected at 3 m intervals. Porosity was estimated.

Fig. 2.68 shows temperature versus depth profiles of these wells. All holes except HF1 and HF10 show a nearly conductive (linear) gradient. The temperature profile of HF1 is concave downward and may indicate upward seepage of water, possibly from a leaky artesian aquifer at about 60 m depth. HF10 encountered the only significant quantity of water during drilling, which accounts for the observed thermal disturbance.

All temperature logs show a slight gradient decrease below about 30 to 45 m depth. This decrease indicates a small thermal conductivity change attributable to the hole penetrating water saturated sediments at the water table. Fig. 2.67 is a static water table map derived from the temperature gradient decreases. Ground-water flow is from south to north and all wells except HF1 and HF10 apparently encounter mostly low permeability sediments as indicated by a lack of noticable water during drilling and the nearly conductive (linear) gradients.

Bulk thermal conductivity measurements of drill cuttings were corrected for porosity, using values determined by Davidson (1973) for shallow basin fill in the Tucson basin. Estimated heat flows ranged from

Figure 2.67. Locations of shallow heat-flow holes and elevation of the ground-water table (in feet above mean sea level), Cactus-Flat-Artesia

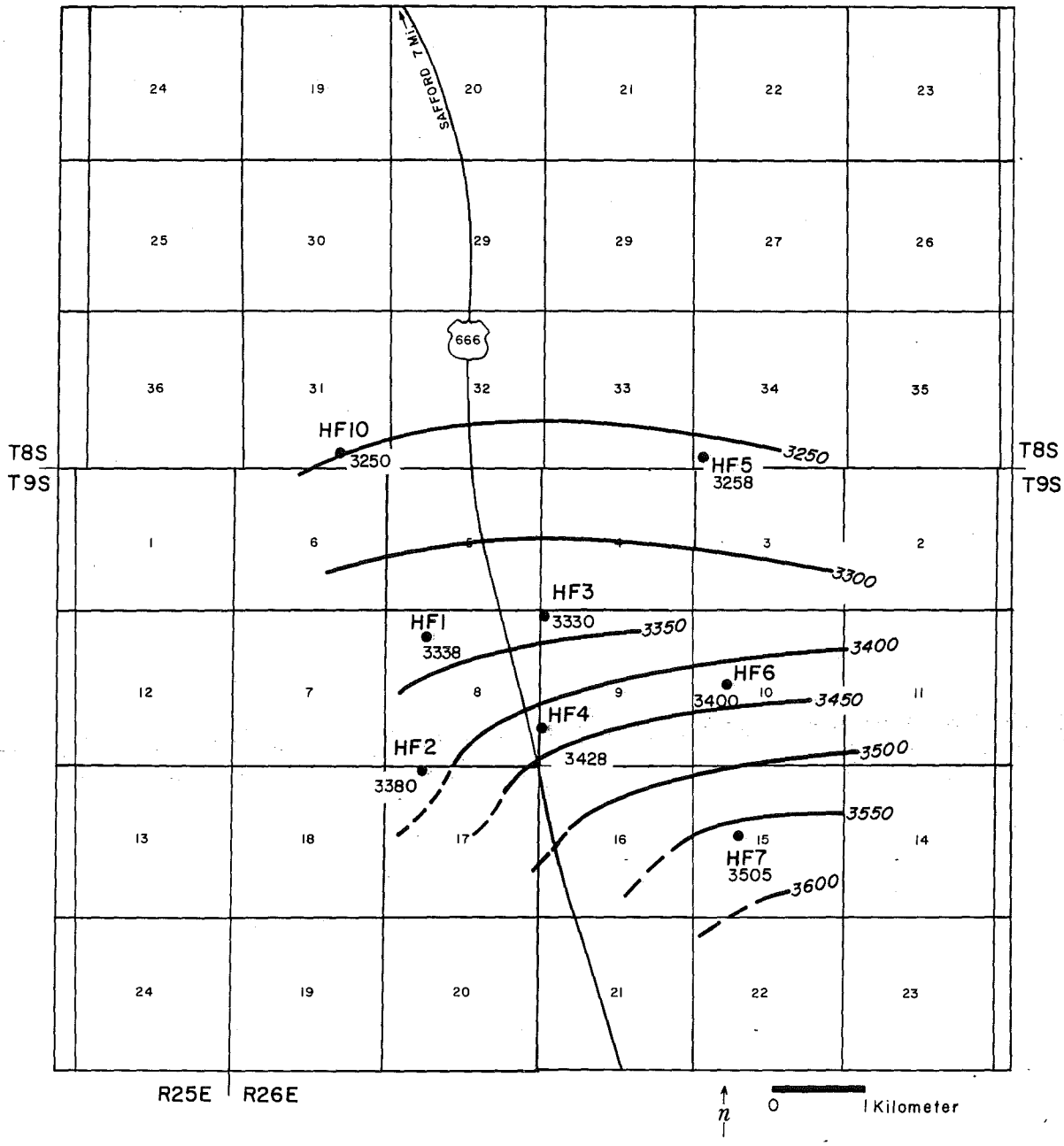

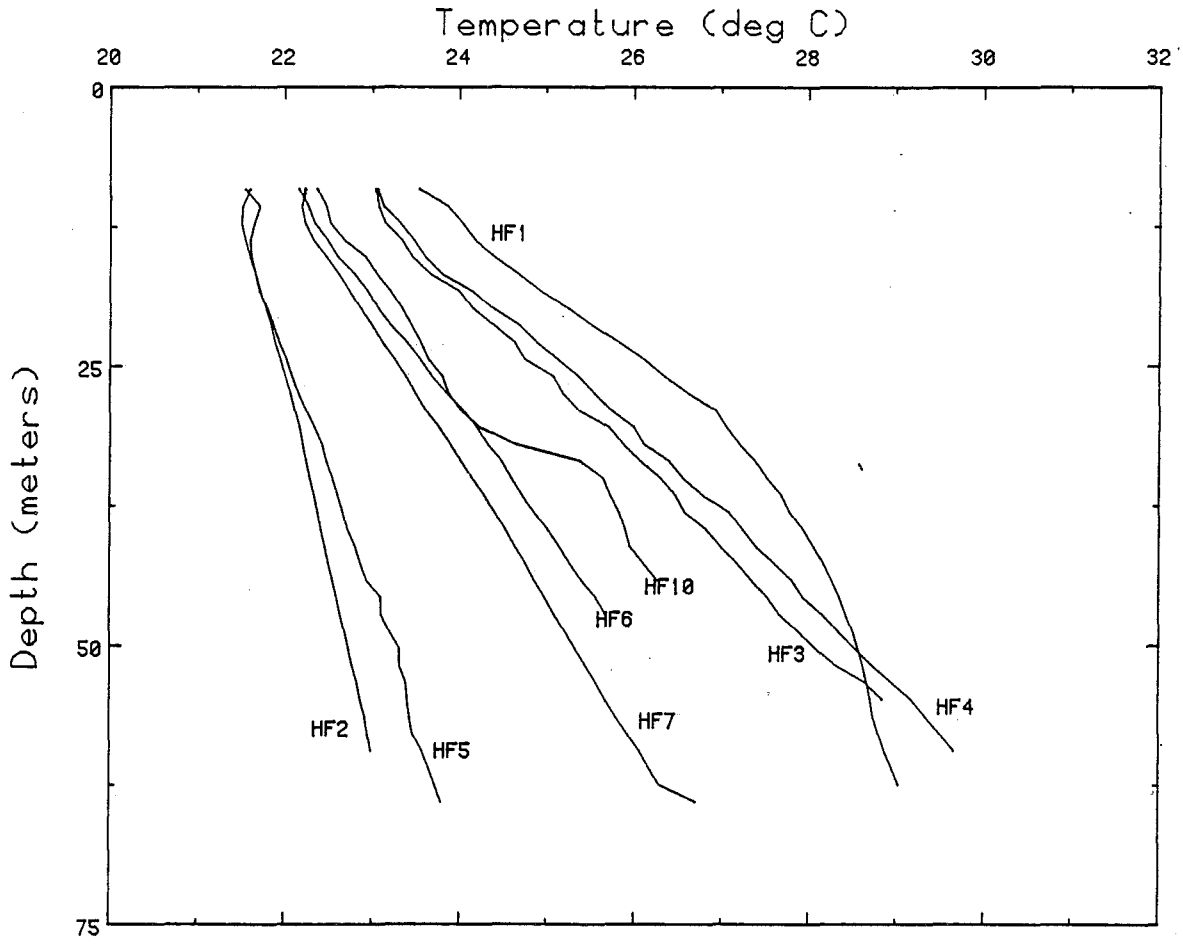

Figure 2.68. Temperature-depth profiles of heat flow holes

56 mWm^{-2} in HF1 to 220 mWm^{-2} in HF3. Fig. 2.69 shows the distribution of heat flow in the area. Contours in the figure show temperature distribution at 44.2 m depth.

A north-northwest-trending heat flow high (>167 mWm^{-2}) overlies the high soil mercury anomaly (>303 ppb) of the same trend. Highest heat flow estimates (220 mWm^{-2}) coincide with a 350 ppb soil mercury closure having an east-northeast trend.

CONCLUSIONS. South of Artesia, a hidden hydrothermal convection system is indicated by anomalous heat flow (>167 mWm^{-2}) over a 3 km^2 area

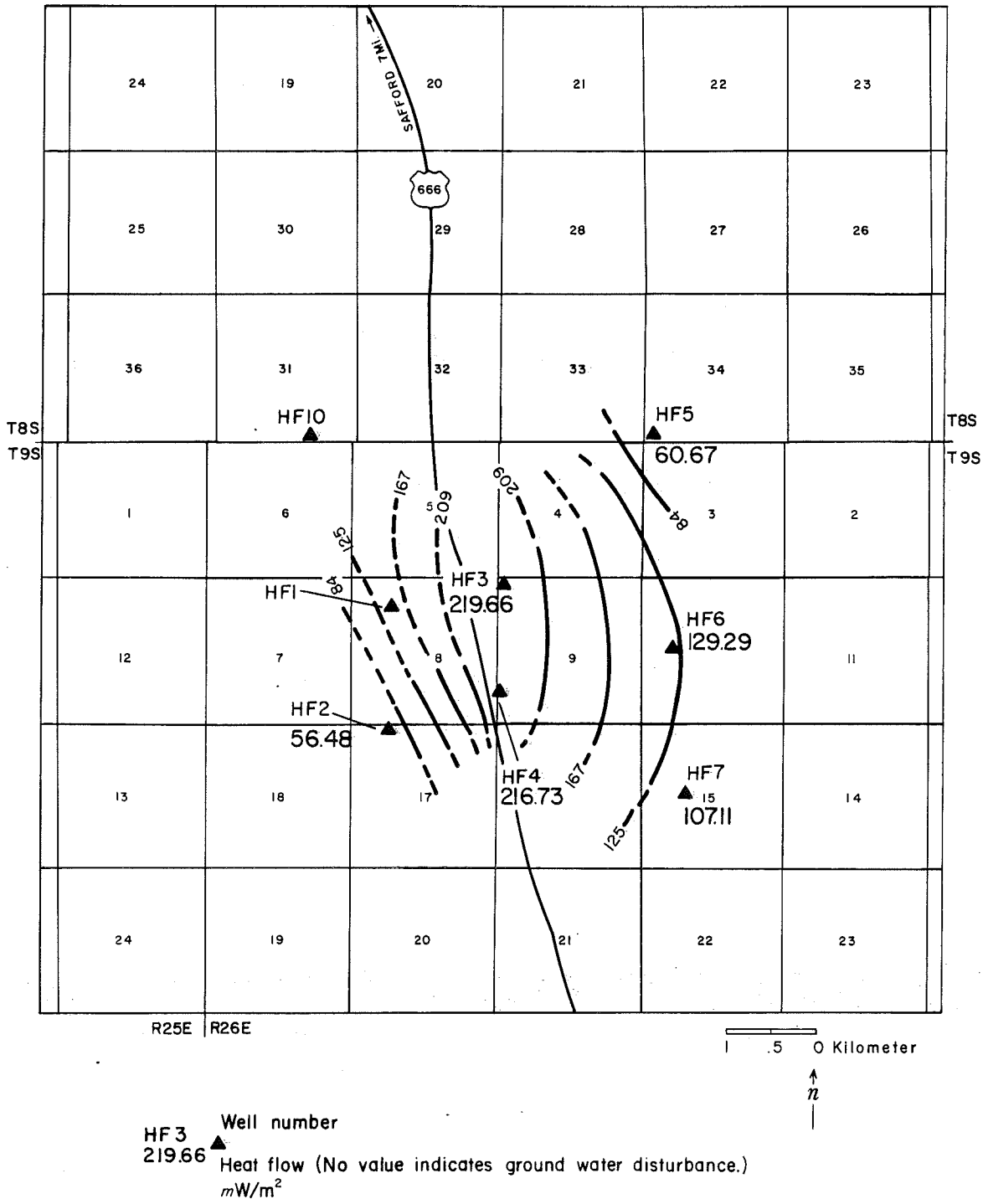

Figure 2.69. Heat flow at the Artesia geothermal anomaly

(Witcher, 1982). This area has a high soil mercury anomaly (>303 ppb) and temperature gradients exceeding 120°C/km. All these anomalies overlie a major Basin and Range fault zone interpreted from Bouguer gravity data (Fig. 2.70). The thermal anomaly overlies the structural intersection of northeast trending faults in the Pinaleno Mountains with the Basin and Range fault zone. Recurrent Pleistocene faulting on the Basin and Range fault zone may sustain fracture permeability at depth, while high precipitation and runoff over the northeast-trending mountain fault zones may provide recharge with sufficient hydraulic head to drive convection (Witcher, 1982).

Projection of temperature gradients to depths greater than 60 m, the depth of the heat flow holes, is speculative because the top of the hydrothermal system is not known. Temperatures typically do not continue to increase dramatically with depth within a hydrothermal convective system because flowing water is a very efficient heat transporting medium. However, tentative temperature estimates of the top of the geothermal system were made on the assumption the clay-silt basin-fill strata confine the top of this system. A reconnaissance dipole-dipole resistivity profile across the area was modeled to show between 450 and 950 m of relatively impermeable silt and clay ($\leq$10 ohm-m) sediments (Witcher, 1981). Projection of a 120°C/km gradient to 500 m gives a 78°C temperature when using a mean surface temperature of 18°C. The most accessible potential reservoir is in the conglomerate facies below the clay and silt. Another potential reservoir, which is highly speculative, may lie in a complex basement structural setting. A low angle fault (decollement), overlain by

highly deformed and fractured pre-Basin and Range tectonism (pre-late Miocene) rocks, may act as the reservoir.

A shallow (<500 m) normal-gradient (45°C/km) resource is ubiquitous in this area. Warm water (30 to 45°C) is found in at least five vertically stacked artesian aquifers. Recharge is apparently from meteoric water entering the ground water system near the mountain front. The relatively high carbon-dioxide content of this water attacks silicate minerals to form sodium-bicarbonate water. As this ground water flows deeper and laterally through sand and gravel zones confined by clay and silt, evaporite and carbonate minerals in the clay dissolve to transform the sodium bicarbonate water into sodium sulfate-chloride water. Ion exchange between ground water and clay minerals probably occurs, also. As a result, deeper thermal water encountered east of U. S. Highway 666 may have TDS exceeding 5,000 mg/L and a large percentage of sulfate and chloride.

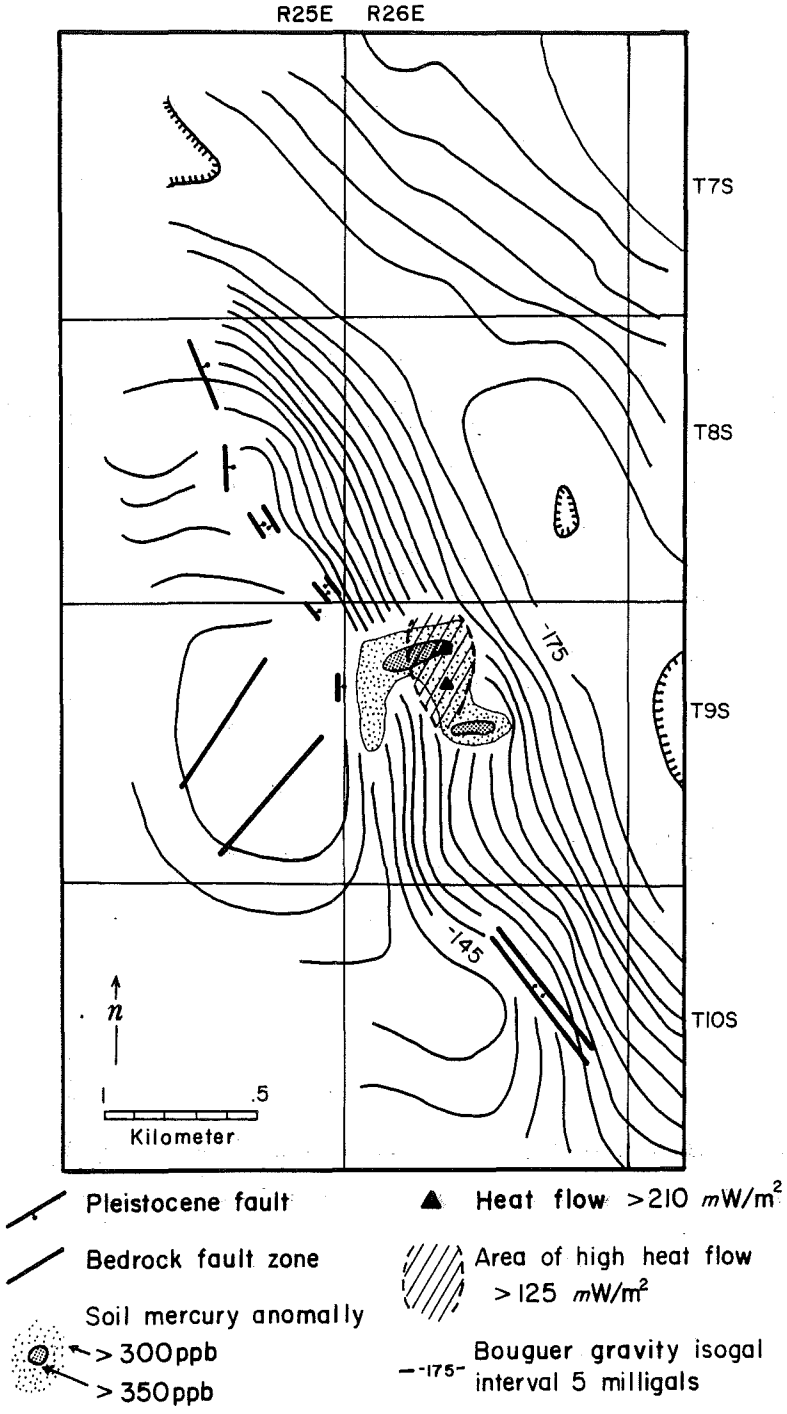

Figure 2.70. Comparison of structure, Bouguer gravity, and soil mercury anomalies, and heat flow in the Cactus Flat-Artesia area

REFERENCES CACTUS FLAT-ARTESIA AREA

Blacet, P. M. and Miller, S. T., 1978, Reconnaissance geologic map of the Jackson Mountain quadrangle, Graham County, Arizona: U. S. Geological Survey Miscellaneous Field Studies Map MF-939.

Capuano, R. M. and Bamford, R. W., 1978, Initial investigation of soil mercury geochemistry as an aid to drill site selection in geothermal systems: Earth Science Laboratory Report ESL-13, University of Utah Research Institute, Salt Lake City, Utah, prepared under U. S. DOE Contract EG-78-C-07-1701, 32 p.

Davidson, E. S., 1973, Geohydrology and water resources of the Tucson basin, Arizona: U. S. Geological Survey Water Supply Paper 1939-E, 81 p.

Davis, G. H., and Coney, P. J., 1979, Geologic development of the Cordilleran metamorphic core complexes: Geology, Vol. 7, p. 120-124.

Feth, J. H., 1952, Safford basin, Graham County: *in* groundwater in the Gila River basin and adjacent areas, Arizona-A summary by Halpenny and others, 1952: U. S. Geological Survey Open File Report, p. 45-58.

Fournier, R. O. and White, D. E., and Truesdell, A. H., 1974, Geochemical indicators of subsurface temperature-part 1, basic assumptions: U. S. Geological Survey Journal of Research, Vol. 2, no. 3, p. 259-262.

Harbour, J., 1966, Stratigraphy and sedimentology of the upper Safford basin sediments: unpub. Ph.D. Thesis, University of Arizona, 242 p.

Matlick, J. S. III and Buseck, P. R., 1976, Exploration for geothermal areas using mercury: a new geochemical technique: in Proceedings 2nd U. N. Symposium on Development and Use of Geothermal Resources, U. S. Government Printing Office, Vol. 1, p. 785-792.

Menges, C. M., Peartree, P. A., and Calvo, S., 1982, Quaternary faulting in southeast Arizona and adjacent Sonora, Mexico (abs): Abstracts, 78th annual meeting Cordilleran Section, The Geological Society of America, April 19-21, 1982, Anaheim, California, p. 215.

Morrison, R. B., Menges, C. M., and Lepley, L. K., 1981, Neotectonic maps of Arizona: *in* Stone C. and Jenney, J. P., eds., Arizona Geological Society Digest, Vol. 13, p. 179-183.

Oregon Institute of Technology, 1981, Feasibility study for geothermal water space heating for the Safford Federal Prison Camp, Safford, Arizona: prepared by Johannessen and Girand Consulting Engineers, Inc., Tucson, Arizona, for Oregon Institute of Technology, Klamath Falls, Oregon, 50 p.

Oppenheimer, J. M. and Sumner, J. S., 1981, Gravity modeling of the basins in the Basin and Range province Arizona: *in* Stone, C. and Jenney, J. P., eds., Arizona Geological Society Digest, Vol. 13, p. 111-115 with 1:1,000,000 scale, depth to bedrock map.

Reiter, M. and Shearer, C., 1979, Terrestrial heat flow in eastern Arizona, a first report: Journal of Geophysical Research, Vol. 84, no. B11, p. 6115-6120.

Thorman, C. H., 1981, Geology of the Pinaleno Mountains, Arizona a preliminary report: *in* Stone C. and Jenney, J. P., eds., Arizona Geological Society Digest, Vol. 13, p. 5-11.

Witcher, J. C., 1979, A preliminary report on the geothermal energy potential of the Safford basin southeastern Arizona: *in* Geothermal site evaluation in Arizona, Semi-annual progress report for period July 1978-January 1979, D.O.E. contract EG-77-S-02-4362, p. 42-72.

Witcher, J. C., 1981, Geothermal resource potential of the Safford-San Simon basin, Arizona: Arizona Bureau of Geology and Mineral Technology Open File Report 81-26, 135 p.

Witcher, J. C., 1982, Exploration for geothermal energy in Arizona Basin and Range - a summary of results and interpretation of heat flow and geochemistry studies in Safford basin, Arizona: Arizona Bureau of Geology and Mineral Technology Open File Report 82-5, 51 p.

Wynn, J. C., 1981, Complete Bouguer gravity anomaly map of the Silver City $1^{\circ} \times 2^{\circ}$ quadrangle, New Mexico-Arizona: U. S. Geological Survey Miscellaneous Investigations Map I-1310-A.

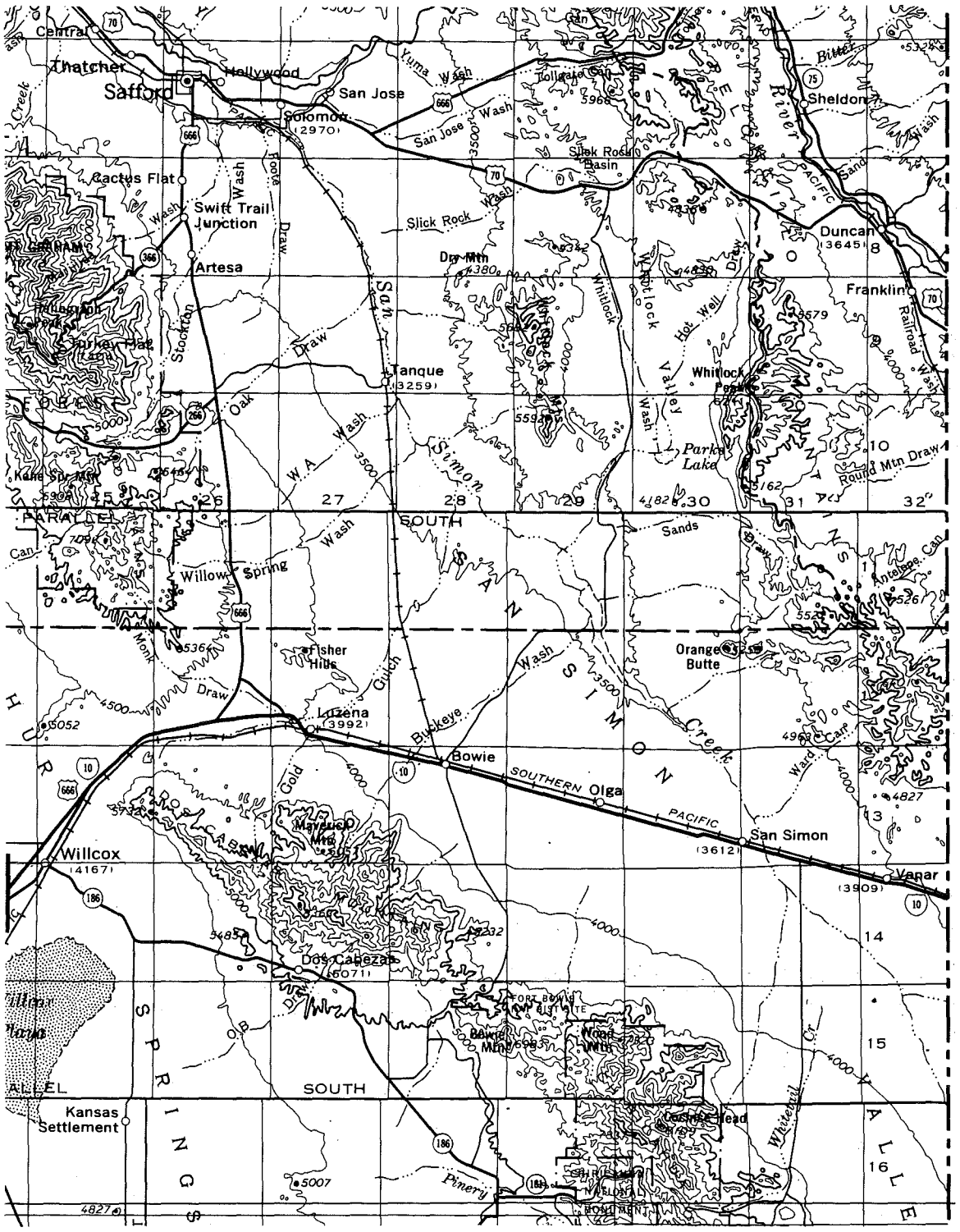

Figure 2.71. Map of the San Simon area

SAN SIMON VALLEY

INTRODUCTION. During the early 1900s numerous artesian wells were drilled for irrigation and water supply in the San Simon Valley. Many of these were flowing artesian wells discharging thermal water. Today, flowing wells are found only north of San Simon near the Whitlock Mountains because the water table or artesian pressure has dropped as a result of ground-water development. However, several pumped wells discharge thermal water near San Simon.

PHYSIOGRAPHY. The San Simon area lies astride Interstate 10 in the southern portion of the Safford-San Simon basin and it includes the small farming and railroad community of San Simon (Fig. 2.71). The Safford-San Simon basin is the largest continuous basin in the Mexican Highland section. The basin forms a valley that is drained by the north-flowing San Simon River. The San Simon Valley is bound by the Peloncillo Mountains on the northeast and the Dos Cabezas and Chiricahua Mountains on the southwest. Topography of the valley is subdued and mostly flat; elevation of the valley floor at San Simon ranges from 1,067 to 1,220 m. San Simon has a mean annual temperature of 17°C and it receives about 23 cm/yr of precipitation annually. The Dos Cabezas and Chiricahua Mountains rise to 2,440 m elevation, while the Peloncillo Mountains do not exceed 2,010 m elevation. Precipitation in the Dos Cabezas and Chiricahua Mountains exceeds 38 to 50 cm/yr annually.

GEOLOGY. Crystalline basement rocks in the San Simon area are likely to have a strong west-northwest to northwest structural grain. The Dos Cabezas discontinuity of Titley (1976) traverses the Dos Cabezas and northern Chiricahua Mountains as a complex structural zone characterized by numerous faults that have been subjected to repeated movements since Precambrian time (Sabins, 1957). Movements on individual faults have included strike-slip, normal, and reverse or thrust displacements. The Dos Cabezas discontinuity divides this region into a northern area where Mesozoic and Tertiary rocks generally overlie crystalline basement, and a southern area where Mesozoic and Tertiary rocks mostly overlie Paleozoic rocks (Titley, 1976). In the Stockton Pass area in the Pinaleno Mountains northwest of San Simon, Swan (1976) mapped another major west-northwest to northwest trending structural zone. Swan's studies of the Stockton Pass fault zone indicate repeated movement since Precambrian time. Continuation of this structural zone beneath the San Simon area is likely. Beneath San Simon, crystalline basement rocks may underlie a discontinuous cover of Mesozoic and possibly lower Paleozoic rocks. Laramide and mid-Tertiary volcanic rocks may overlie these older rocks at great depths. In the Whitlock, Peloncillo, and Chiricahua Mountains mid-Tertiary volcanic rocks range in composition from basalt to rhyolite. Basaltic and andesitic rocks are the dominant lithology in the Whitlock and much of the Peloncillo Mountains. Silicic volcanic rocks are voluminous in the southern Peloncillo and Chiricahua Mountains and they are associated with mid-Tertiary cauldrons (Deal and others, 1978; Marjaniemi, 1968). Richter and others (1981) mapped discontinuous (less than 20 m thick) outcrops of 16 m.y. old basalt, which caps older mid-Tertiary volcanic rocks in the Peloncillo

Mountains. Chemistry of these rocks resembles alkali basalts, which are commonly associated with extensional tectonism (Richter and others, 1981).

The present day Safford-San Simon basin is a product of extensional tectonism. Scarborough and Peirce (1978) named this event the Basin and Range disturbance. The main phase of Basin and Range deformation occurred between 15 and 8 m.y. B.P. This deformation, characterized by complex high-angle normal faulting, broke the crust into a zig-zag pattern of interconnected grabens, which form the Safford-San Simon basin. Today over two kilometers of mostly undeformed sediment fill the basin. White (1963) used an informal two-fold classification for basin-filling sediments in the San Simon area: younger alluvial fill and older alluvial fill.

The younger alluvial fill is restricted to sediment deposited by present day washes or to gravel-capped terraces. Older alluvial fill is subdivided into four groups or facies; (1) lower unit, (2) blue clay unit, (3) upper unit and (4) marginal zone. The lower unit is continuous throughout the basin and is probably correlative with the basal conglomerate facies of Harbour (1966) in the Safford area. Sand, gravel, and clay comprise the lower unit. The blue clay unit overlies the lower unit and attains a maximum thickness of 183 m. Correlation of the blue clay unit with Harbour's (1966) green clay facies at Safford is reasonable because both have similiar lithology and formation top elevations. The upper unit sediments overlie the blue clay unit and consist of 20 to 60 m of silt, sand, and gravel. These sediments correlate with the upper basin-fill unit of Harbour (1966). The marginal unit is coarse clastic sediments occurring beyond the blue clay pinchout. Marginal unit sediments include both the upper and lower unit sediments.

The blue clay unit forms a cap over confined aquifers contained in the lower unit. Relatively high temperature gradients (40 to 50°C/km) occur in this unit mainly as a result of its low thermal conductivity. As a consequence the blue clay unit provides a favorable setting for thermal artesian aquifers.

The blue clay is easily distinguishable from other basin-fill sediments; as a consequence, drillers' logs are highly useful to map its extent and thickness.

Figure 2.72 is a structure contour map at the base of the blue clay, showing the shape and extent of the deposition basin for the clay. Close-spaced contours indicate the basin margin. Another structure map on top of the blue clay (Fig. 2.73) exhibits nearly the same geometry. The exception is that the lowest elevation at the top of this stratum is adjacent to the southwest margin, whereas at the base, the lowest elevation is in the basin center. A significant evaporite occurrence was found above the clay stratum in the well with the lowest clay-top elevation. This evaporite indicates desiccation of the lake that deposited the clay.

Structural and tectonic inferences are tentatively drawn from the structure contour maps of the blue clay. Steep or close-spaced contours may correlate with faults that formed the basin. In addition, faulting contemporaneous with desiccation of the Tertiary lake in the basin may have displaced the last remnants of this lake against the southwest margin of the basin where evaporites overlie clay. As an anology, sag ponds or small lakes sometimes occur adjacent to large Holocene faults.

GEOHYDROLOGY. Figure 2. 74 is a piezometric surface map of the confined aquifer beneath the San Simon area. Close-spaced contours on this surface

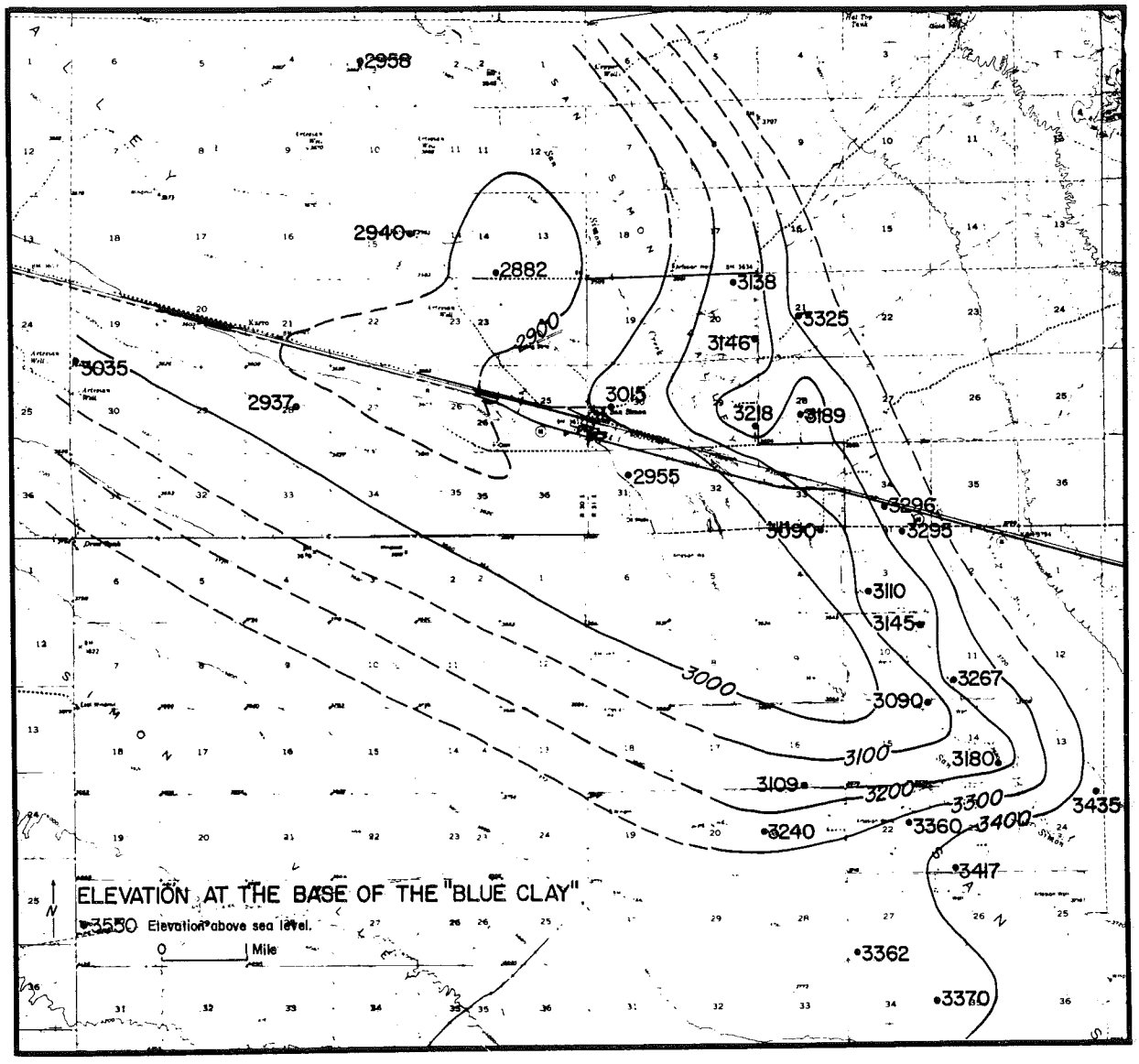

Figure 2.72. Structure contour map of the base of the blue clay unit

indicate rapidly changing hydraulic pressure. These steep hydraulic gradients, commonly called ground-water falls, can be caused by fault zones or by facies changes in basin fill, where coarse permeable sediments change laterally into relatively less permeable fine-grained sediments. The ground-water falls also coincide with one area where average estimated tem-

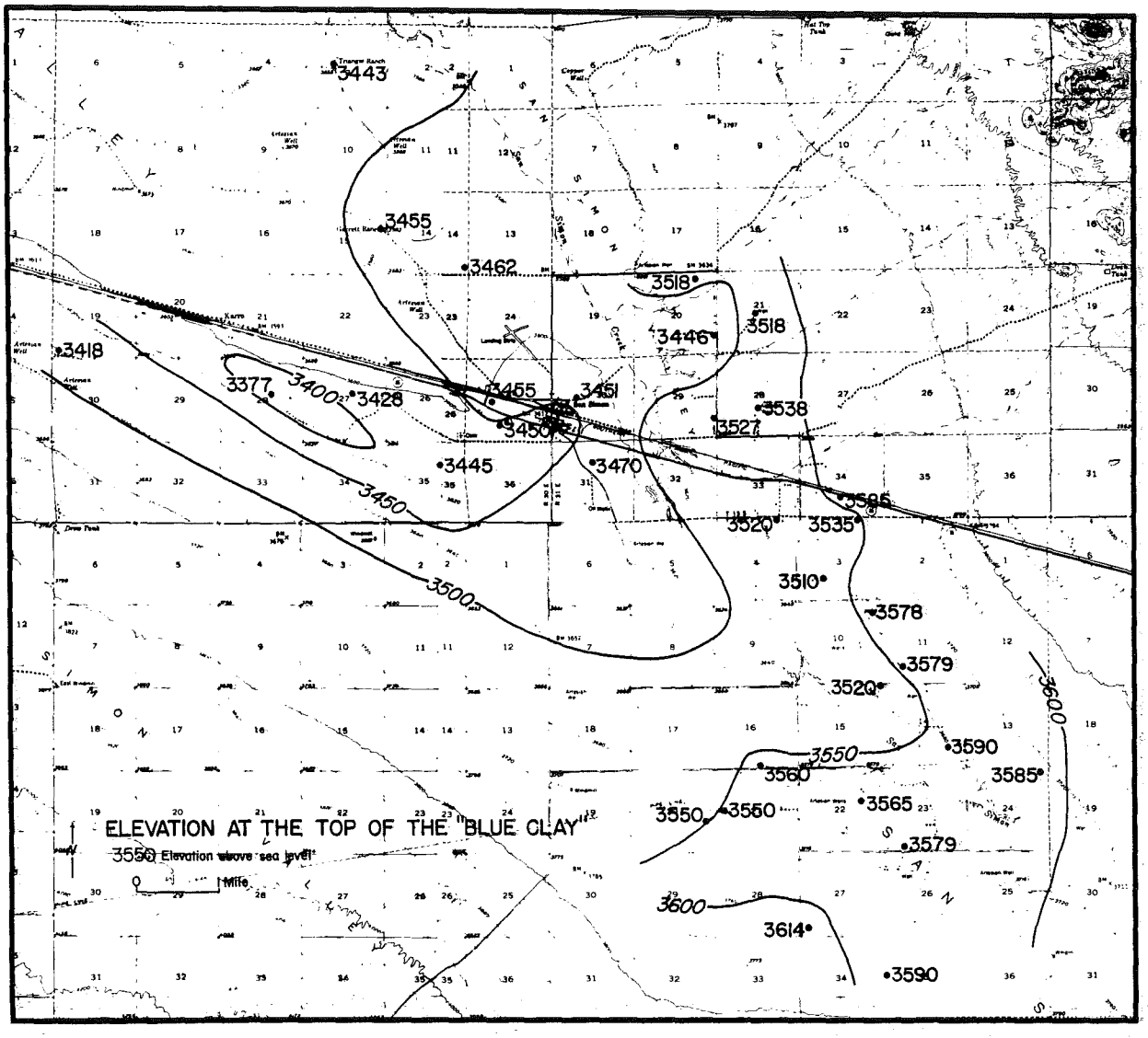

Figure 2.73. Structure contour map of the top of the blue clay unit perature gradients of artesian wells are less than 40°C/km. Gradients in other areas generally exceed 45°C/km. Because the relatively impermeable blue clay unit thickens rapidly at the ground-water falls, ground-water flow is apparently impeded by the clay or a fault zone and the low temperature gradients may indicate that ground-water flow is forced downward beneath the clay. Downward flowing water transports heat downward and can cause lower temperature gradients.

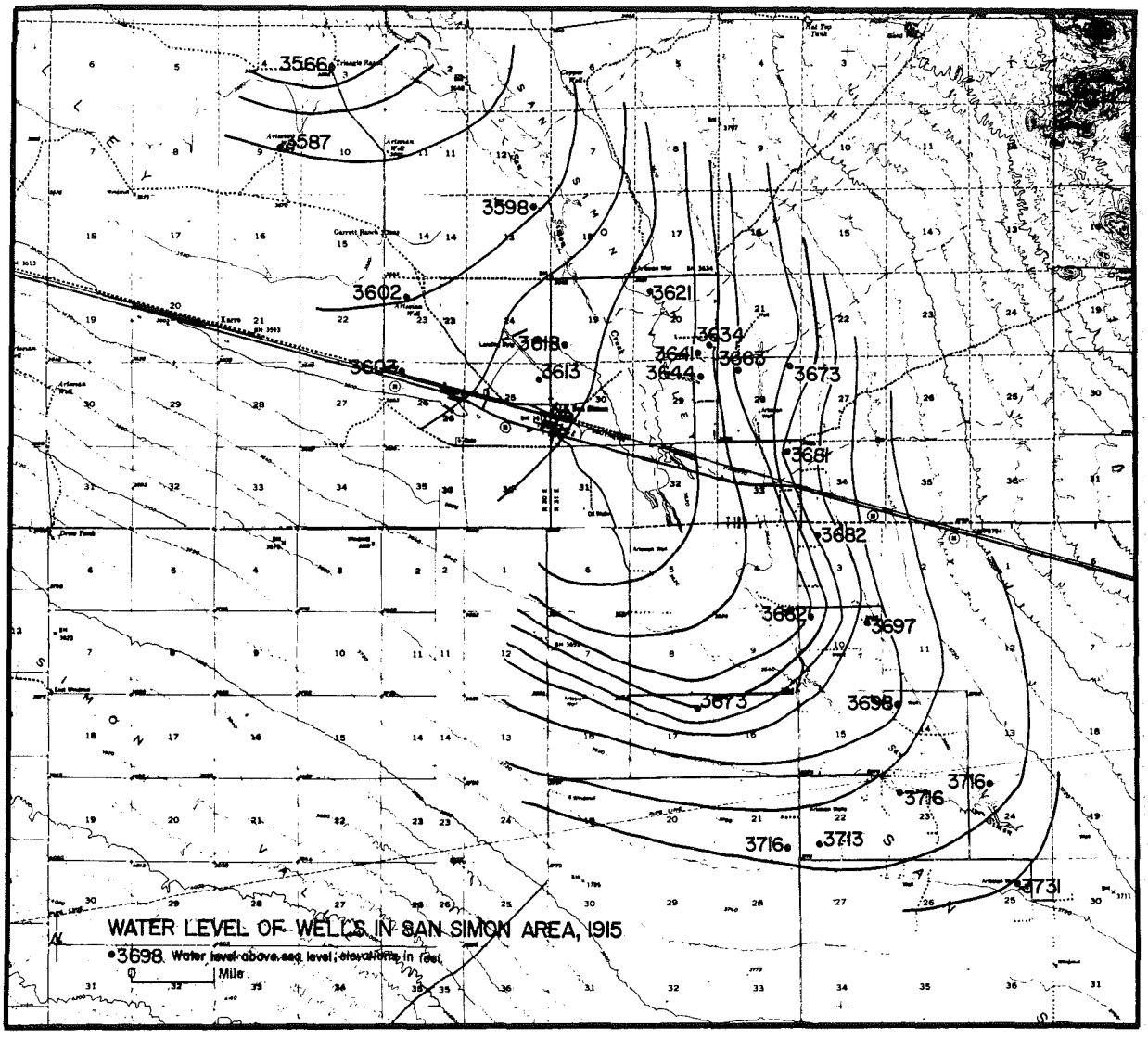

Figure 2.74. Water-table elevations of artesian wells during 1915 in the San Simon area

THERMAL REGIME. Schwennessen (1917) published temperature and depth data for artesian wells in the San Simon area before significant ground-water withdrawal had occurred. Schwennessen's data were used to define the thermal regime of this area prior to water-table lowering. Figure 2.75 is a plot of well depth versus surface discharge temperature. Wells with flow rates less than 37.8 L/min and an artesian head less than 3 m above

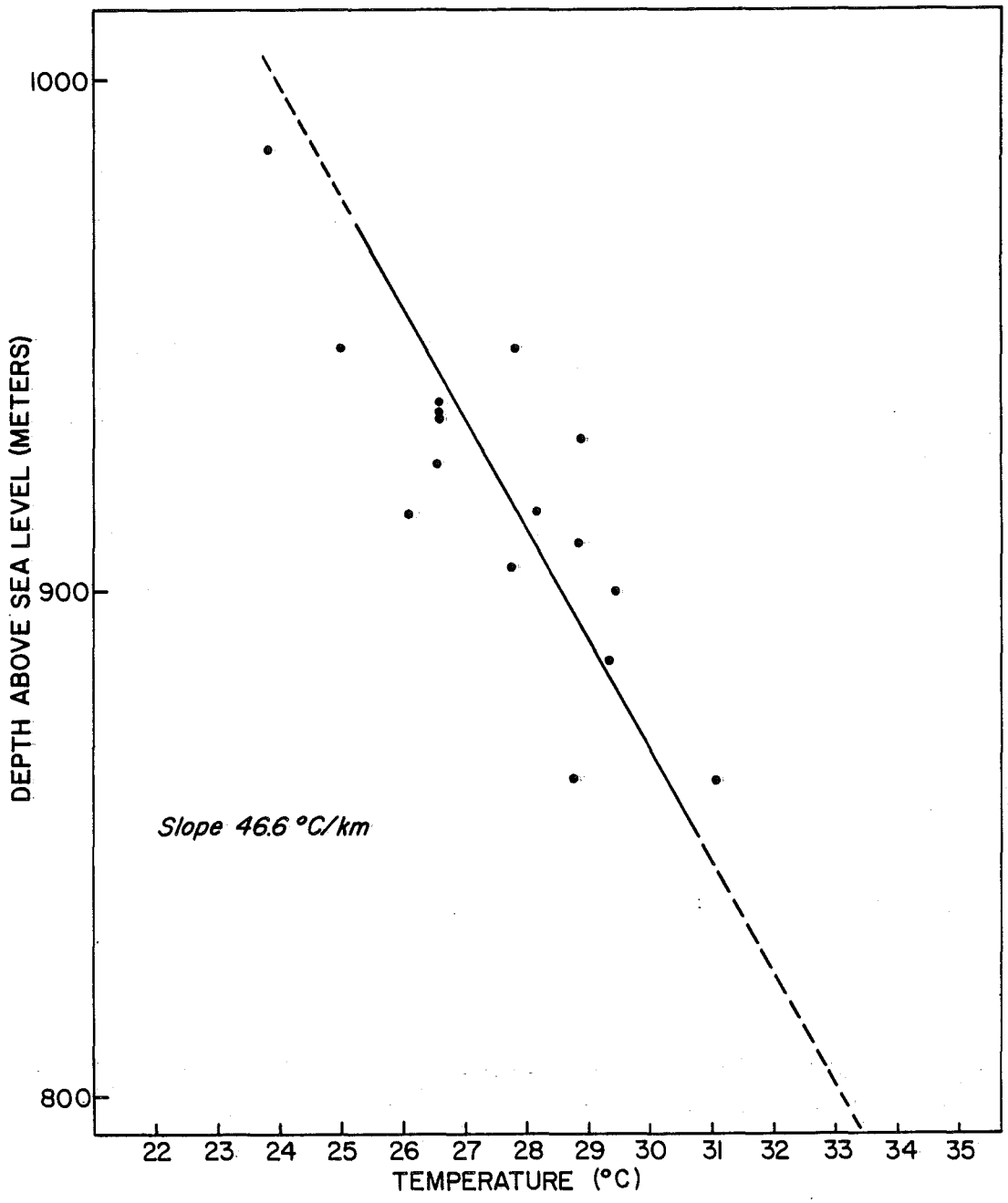

Figure 2.75. Plot of well depths versus surface discharge temperatures

the surface were not used. A nearly linear relationship exists between well depths and measured discharge temperatures. The slope (temperature gradient) of this data is 46.6°C/km, and the surface intercept temperature

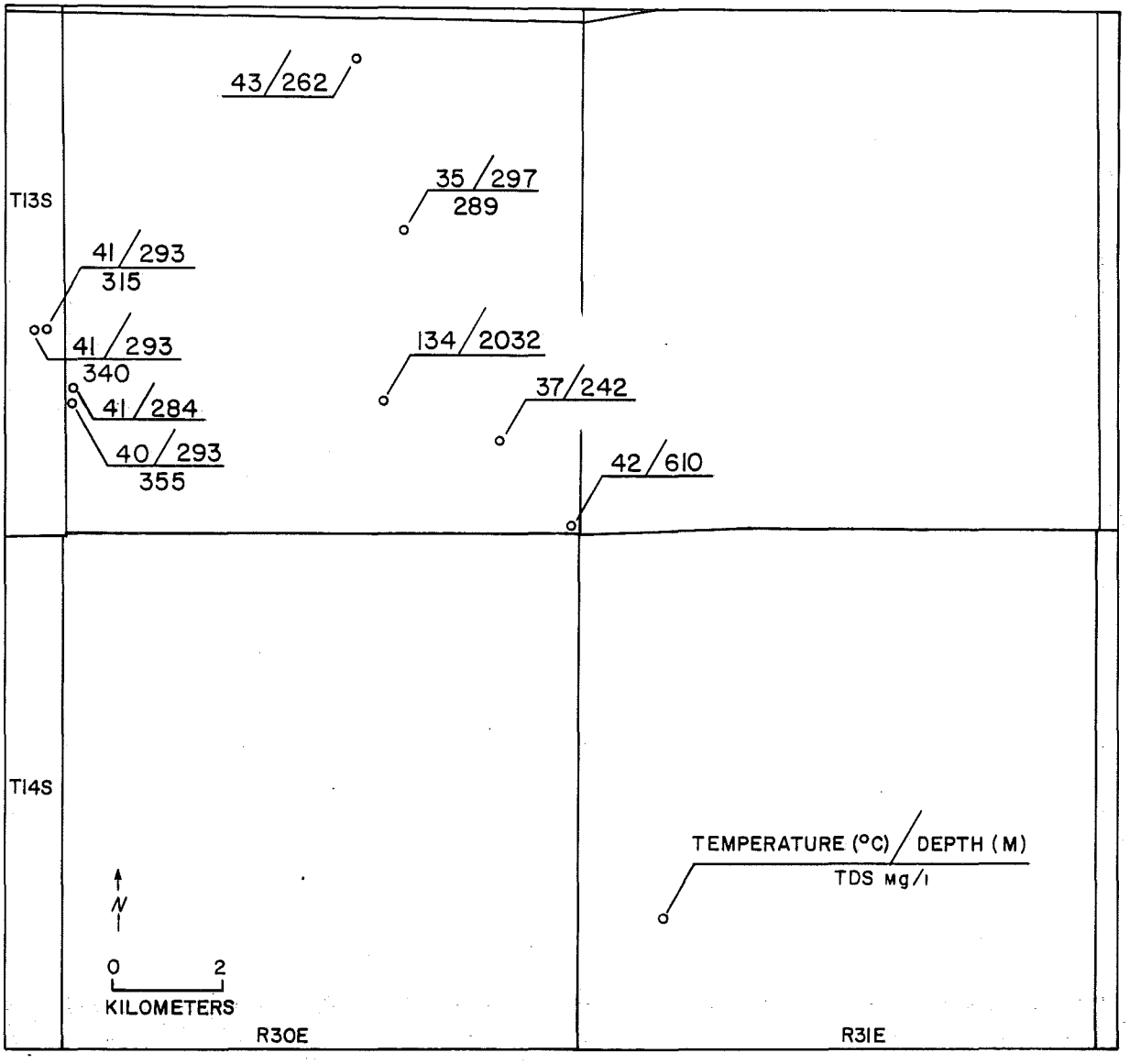

Figure 2.76. Map of wells with temperatures greater than 35°C in the San Simon area

is 18.5°C, which is close to the mean annual air temperature (17°C). Thus, it appears that temperatures in the artesian aquifers increase systematically with depth (about 4.7°C per 100 m).

THERMAL WELLS. Thermal water (>30°C) has been reported to discharge from more than 20 wells in the San Simon area (Figure 2.76; Table 2.12).

TABLE 2.12. Wells with temperatures greater than 35°C, San Simon area

Location	Temperature °C	Total Dissolved Solids, mg/l	Depth m
D-13-29-24CD	41	340	293
D-13-29-24DCC	41	315	293
D-13-30-03B	43	--	262
D-1330-15DAA	35	289	297
D-13-30-27AD	134	--	2,032
D-13-30-25CCD	37	--	242
D-13-29-25CDD	36	--	305
D-13-30-30B	41	--	284
D-13-30-30BCB	40	355	293
D-13-30-36DDD	42	--	610

These thermal wells occur in three clusters: (1) at the southern end of the Whitlock Mountains, (2) adjacent to the San Simon River and, (3) south of Interstate 10, half way between Bowie and San Simon.

In the Whitlock Mountain area, the Pinal Oil Company Whitlock #1 State (D-10-28-36aac) was unsuccessfully drilled for oil in 1927 and 1928; however, this hole did encounter a strong artesian flow of thermal water (41°C) from a conglomerate aquifer between 440 and 587 m depth. Today artesian flow of thermal water from this well continues (Witcher, 1981).

Another nearby oil and gas test, the Bear Springs Oil #1 Allen (D-10-28-25dd), formerly discharged "lukewarm" water (Knechtel, 1938). This well, drilled to 474 m, has since been destroyed (Witcher, 1981).

Thermal water from the Whitlock #1 State well has sodium chloride-sulfate composition with total dissolved solids of 962 mg/L.

Reportedly, thermal water from wells adjacent to the San Simon River have temperatures between 30°C and 43°C and depths between 200 and 610 m. Thermal water in these wells is mostly sodium bicarbonate, although a few

wells produce water trending toward sodium chloride-sulfate composition.

Thermal water between San Simon and Bowie is produced from wells 242 to 305 m deep at pumped flow rates up to 5,300 L/min. Chemical composition of these waters is sodium bicarbonate with TDS approximately 300 mg/L.

CONCLUSION. An extensive geothermal resource (35 to 45°C) is indicated in the San Simon area between 450 and 600 m depth. Thermal water is confined below a clay and silt strata (blue clay) in an aquifer of interbedded coarse and fine grained clastic sediments. In general, temperatures increase systematically with depth (4.7^{o}C per 100 m) in conformance with the normal geothermal gradient in the area. Thermal water with sodium bicarbonate chemistry and TDS less than 500 mg/L is observed in areas adjacent to Interstate 10. In areas nearest the Whitlock Mountains, dissolved solids content is greater than 900 mg/L and the thermal water trends toward sodium chloride-sulfate composition.

Geothermal potential at depths greater than 1 km is possible. In 1938, a deep oil and gas test, the Funk Benevolent 1 Fee, (D-13-30-27ad) was completed to 2,032 m depth. In a 1940 memorandum, E. D. Wilson of the Arizona Bureau of Mines gave an account of a visit to this well where he was told that 134°C water was encountered in the bottom 100 m. A slightly anomalous average temperature gradient (60°C/km) is necessary to explain this temperature (134°C at 2 km depth). A hydrothermal convection system may exist at this location. A zone of steep west-northwest trending structural contours in the blue clay crosses the Funk Benevolent 1 Fee location and this may indicate a fault zone, which can provide vertical permeability at depth for hydrothermal convection. However, with available information the existence of a resource greater than 100°C at depths greater than 1 km is speculative.

REFERENCES SAN SIMON VALLEY

Deal, E. G., Elston, W. E., Erb, E. D., Peterson, S. L., Reiter, D. E., Damon, P. E., and Shafiqullah, M., 1978, Cenozoic volcanic geology of the Basin and Range province in Hidalgo County, southwestern New Mexico: *in* Callender, J. E., Wilt, J. C., and Clemons, R. E., eds., Land of Cochise, New Mexico, Geological Society Guidebook, 29th Field Cofnerence, pp. 219-229.

Harbour, J., 1966, Stratigraphy and sedimentology of the upper Safford basin sediments: unpub. Ph.D. Thesis, University of Arizona, 242 p.

Knechtel, M. M., 1938, Geology and ground-water resources of the valley of the Gila River and San Simon Creek, Graham County, Arizona: U. S. Geological Survey Water-Supply Paper 796, p. 222.

Marjaniemi, D. K., 1968, Tertiary volcanism in the northern Chiricahua Mountains, Cochise County, Arizona: in Southern Arizona, Guidebook III, Arizona Geological Society, p. 209-214.

Richter, D. H., Shafiqullah, M., and Lawrence, V. A., 1981, Geologic map of the Whitlock Mountains and vicinity, Graham County, Arizona: U. S. Geological Survey Miscellaneous Investigations Series Map I-1302, 1:48,000 scale.

Sabins, F. F., 1957, Geology of the Cochise Head and western part of Vanar Quadrangles, Arizona: Geological Society of American Bulletin, Vol. 68, p. 1315-1342.

Scarborough, R. B. and Peirce, H. W., 1978, Late Cenozoic basins of Arizona: *in* Callender, J. F., Wilt, J. C., and Clemons, R. E., eds., Land of Cochise, New Mexico Geological Society Guidebook, 29th Field Conference, p. 253-259.

Schwennesen, A. T., 1917, Groundwater in San Simon valley, Arizona and New Mexico: U. S. Geological Survey Water-Supply Paper 425, p. 1-35.

Swan, M. M., 1976, The Stockton Pass fault: An element of the Texas Lineament: unpub. M.S. Thesis, University of Arizona, 119 p.

Titley, S. R., 1976, Evidence for a Mesozoic linear tectonic pattern in southeastern Arizona: *in* Tectonic Digest, Arizona Geological Society Digest, Vol.10, p. 71-101.

Witcher, J. C., 1981, Geothermal resource potential of the Safford-San Simon basin, Arizona: Arizona Bureau of Geology and Mineral Technology Open File Report 81-26, 131 p.

White, N. D., 1963, Analysis and evaluation of available hydrologic data for the San Simon basin, Cochise and Graham Counties, Arizona: U. S. Geological Survey Water-Supply Paper 1619-DD, 33 p.

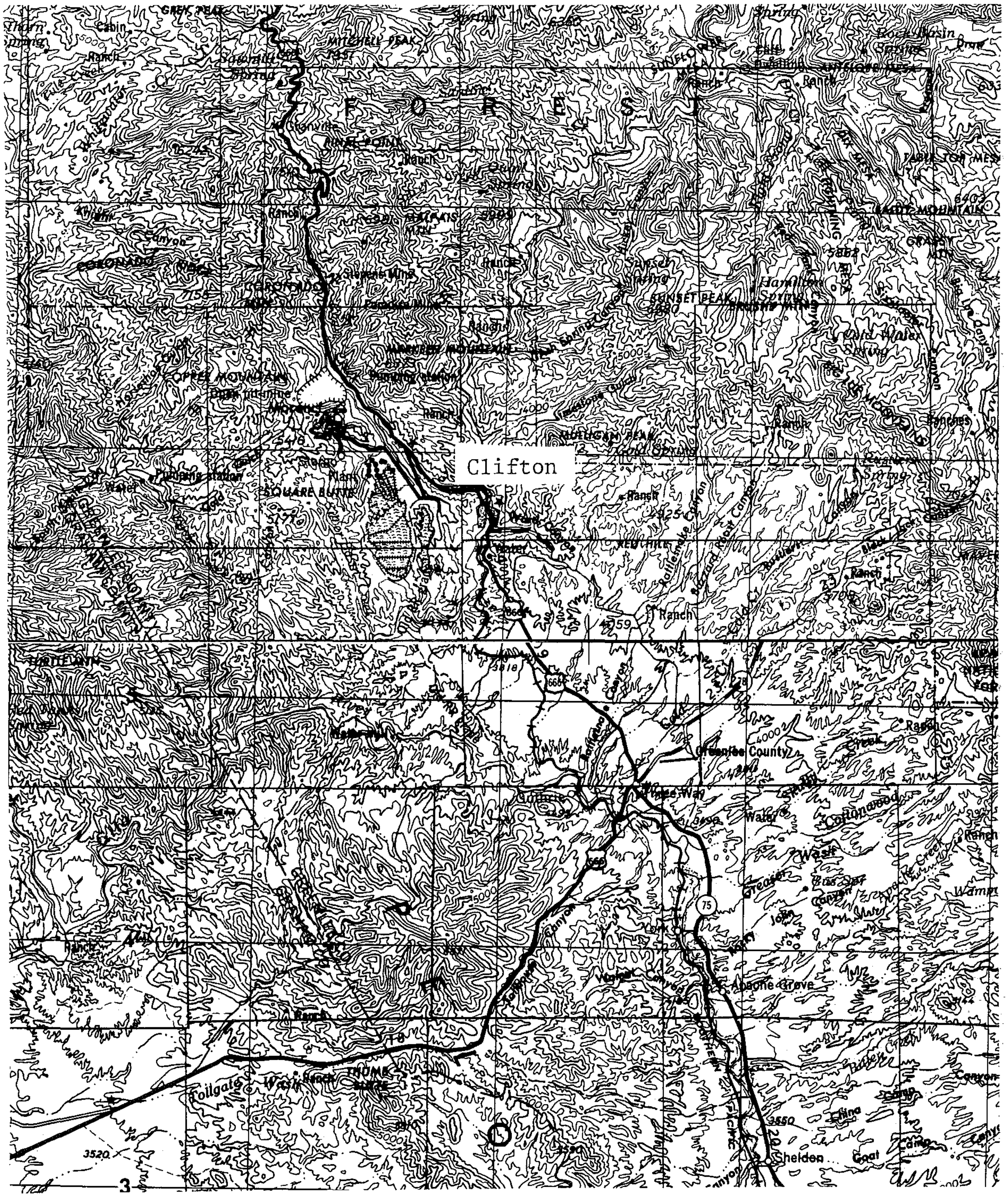

Figure 2.77. Map of the Clifton and Gillard Hot Springs region

CLIFTON AND GILLARD HOT SPRINGS

INTRODUCTION. Arizona's highest temperature thermal springs, Gillard Hot Springs, 84°C, and Clifton Hot Springs, 30 to 72°C, occur in the Clifton-Morenci region. Land adjacent to these springs has been designated by the U.S. Geological Survey as Known Geothermal Resource Areas (KRGRAs). The Gillard KGRA (2,920 acres) and the Clifton KGRA (780 acres) are Arizona's only federal KGRAs. At present only the Clifton KGRA is leased. Figure 2.77 is a map of the Clifton-Morenci region showing thermal springs, KGRAs, and major political and topographic features.

PHYSIOGRAPHY. Situated in a transition zone between the Colorado Plateau to the north and the Basin and Range province to the south, the Clifton-Morenci region is characterized by rugged canyons cut by the San Francisco River, Gila River, Eagle Creek, Blue River, and Chase Creek. Elevations range from 900 to 2,500 m above mean sea level.

GEOLOGY. Paleozoic rocks, resulting from deposition during a period of tectonic inactivity, overlie a distinctive red Precambrian granite and the Pinal Schist at Clifton (Fig. 2.78). Within the Paleozoic section, a basal arkosic sandstone is overlain by interbedded shales and carbonate rocks, the latter becoming dominant in the upper portion of the Paleozoic section. At Clifton, sediments from all Paleozoic periods except Silurian and Permian are exposed (Lindgren, 1905). Precambrian granite, Pinal Schist, and the Coronado Sandstone are potential geothermal reservoir hosts in areas where they may be extensively fractured at depth along major

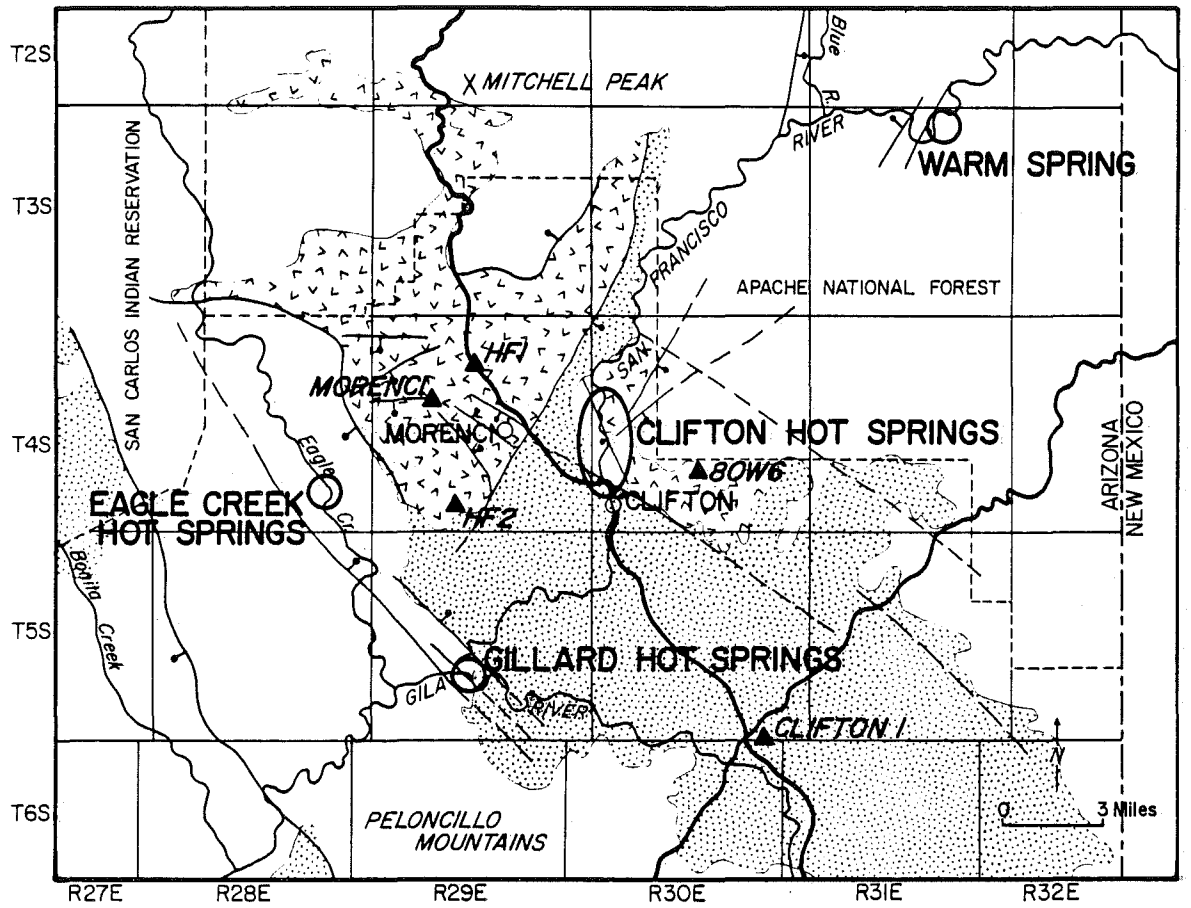

PRE-TERTIARY ROCKS; INCLUDES PRECAMBRIAN GRANITE, PALEOZOIC AND CRETACEOUS ROCKS AND PALEOCENE INTRUSIVE ROCKS

PRE-PLIOCENE AND POST PALEOCENE ROCKS THAT ARE MOSTLY MID-TERTIARY VOLCANIC ROCKS AND CLASTIC SEDIMENT

POST MIOCENE BASIN FILLING SEDIMENT CONSISTING OF LOCALLY DERIVED CLASTIC ROCKS

HOT SPRING LOCATION

HEAT FLOW MEASUREMENT

NORMAL FAULT
BALL ON DOWN-THROWN SIDE

INFERRED FAULT

Figure 2.78. Generalized geologic and structure map of the Clifton and Gillard Hot Springs area

structures. Paleozoic carbonate strata, the Second Value Dolomite, Modoc Limestone, and Horquilla Limestones are potential reservoir rocks due to secondary solution permeability and silicification-brecciation along fault zones. The El Paso Limestone and the Morenci Shale could be important impermeable cap rocks.

Jurassic and Triassic rocks are not observed in the Clifton-Morenci region. Instead, Mesozoic uplift and erosion of the Burro uplift (Elston, 1958) exposed upper Paleozoic rocks, which were later capped by Late Cretaceous shale. During latest Cretaceous and Paleocene, tectonism intensified, with forceful intrusion of stocks and laccoliths (Langton, 1973). Intense hydrothermal alteration and economic copper mineralization is associated with the Paleocene plutonism.

Compressional tectonism of probable Mesozoic age is evident in the region. Lindgren (1905) and Cunningham (1979) mapped low-angle thrust faults in Chase Creek and along the San Francisco River north of Clifton The total extent of these faults is uncertain but they could act as geothermal reservoirs where deeply buried. Another structure of Late Cretaceous to Paleocene age, with important bearing on geothermal potential, is intense N. 25° to 45° E. fracturing of Precambrian rocks. The fracturing appears most prominent near Paleocene intrusions and is easily distinguished as close-spaced lineaments on aerial photographs. The region was apparently structurally high and undergoing erosion during Eocene because clasts of Paleocene rocks are observed in thin discontinuous gravels below Oligocene volcanic rock.

Oligocene to early-Miocene volcanism buried the Clifton-Morenci region beneath 1 to 5 km of mostly andesitic to basaltic flows and breccias,

localized but structurally important dacitic to rhyolitic lavas and tuffs, and volcano-clastic sediments (Lindgren, 1905; Ratte and others, 1969; Strangway and others, 1976; Damon and others, 1968; Elston, 1968; Berry, 1976; Wahl, 1980; Rhodes, 1976; Rhodes and Smith, 1972). These mid-Tertiary volcanic rocks comprise two suites, an older andesite to dacite suite called the Datil Group (Elston, 1968) and a younger basaltic andesite and latite-rhyolite suite (Berry, 1976). Latite-rhyolite and dacite plugs, domes, and dikes are aligned in west-northwest- and northeast-trending zones. East of Clifton along the New Mexico-Arizona border, volcanic stratigraphy and seismic refraction studies show an elongated Tertiary basin trending northwest, the Blue Creek basin, which is filled with up to 5 km of early Oligocene to late Miocene volcanic rocks (Berry, 1976; Wahl, 1980; and Gish, 1980). Volcano-tectonic subsidence or Tertiary synclinal warping appear responsible for the Blue Creek basin. While a significant thickness of welded ash-flow tuff exists at Clifton, no definite Oligocene ring fracture zones or cauldrons have been identified in the immediate area.

Fractured basaltic and andesitic flows and breccias where deeply buried, may host geothermal resources, especially along faults. Dacitic to rhyolitic plugs, domes, and dikes are usually highly fractured and brecciated, allowing for potential recharge and discharge of water to and from deeply buried aquifers.

During and after the last stages of Miocene volcanism, low lying areas between volcanic centers and structural depressions filled with generally coarse clastic sediments. These shallow-dipping Miocene

sediments along Eagle Creek, San Francisco River, and Blue River north of Clifton are highly cemented and make poor aquifers.

Major, post-volcanism rifting broke the crust along steeply dipping normal faults, and formed the first-order structures observed today. This mid- to late-Miocene-Pliocene Basin and Range faulting (Scarborough and Pierce, 1978) largely ended by late Pliocene. However, an early-Pleistocene(?) geomorphic surface has been vertically displaced 20 m by the Ward Canyon fault east of Clifton (Christopher H. Menges, 1981, personal communication).

The complex Ward Canyon fault forms the northern margin of a structural basin, which is filled with mostly undeformed Pliocene to Quarternary, generally coarse clastic sediments. North of this basin the northeast and north-northwest-striking San Francisco, Limestone Gulch, and Clifton Peak faults divide a basement uplift exposing pre-Tertiary rocks into two segments: the wedge-shape Morenci uplift on the west, and the smaller Clifton uplift on the east. In general, Paleozoic rocks dip 15 to 40 degrees northwest, while Tertiary volcanic rocks dip 15 to 40 degrees northeast. A northwest-trending zone of probably early Miocene age rhyolite-latite dikes and associated domes traverses the Clifton-Morenci basement uplift 8 km north of Clifton. These dikes and domes may indicate a major structural zone of regional extent. The Gillard fault forms the southern boundary of the Pliocene structural basin.

Major, post-Miocene Basin and Range faults localize hot-spring occurrences in canyons. These faults cut across drainage and presumably ground-water flow. The Limestone Gulch and Clifton Peak faults appear to control the Clifton Hot Springs system, while the Gillard fault zone

apparently controls the Gillard Hot Springs and the Eagle Creek Hot Springs. The thermal springs in the Martinez Ranch area are controlled by northeast-trending faults, which project southward into the Limestone Gulch fault zone.

GEOHYDROLOGY. Ground-water conditions in the Clifton-Morenci region are poorly understood due to the limited ground-water development. Thus, extrapolation of ground-water conditions from one locality to another is inadvisable because geology, topography, and climate are highly variable. However, one generalization is possible. Because the Gila and San Francisco Rivers flow year around we estimate that ground-water is shallow (less than 30 m) along their courses. In addition, we have assumed the ground water is not perched and that it roughly coincides with the static water table in a continuous ground-water flow system. Due to relatively higher precipitation and lower evaporation with increasing elevation, and because it follows topography, the static water-table elevation probably rises away from the Gila and San Francisco River canyons. Figure 2.79 is a generalized map of ground-water flow in the Clifton-Morenci area based upon these assumptions.

THERMAL WELLS AND SPRINGS. Numerous, scattered thermal springs and seeps, comprising Clifton Hot Springs, discharge from alluvium along the San Francisco River in sections 19 and 30, T. 4 S., R. 30 E., in and north of Clifton. Discharge from individual springs is small (<5 gpm). Measured temperatures range between 30 and 70°C. These thermal springs are characterized by sodium-chloride chemistry with TDS between 7,000 and 14,000 mg/L (Table 2.13).

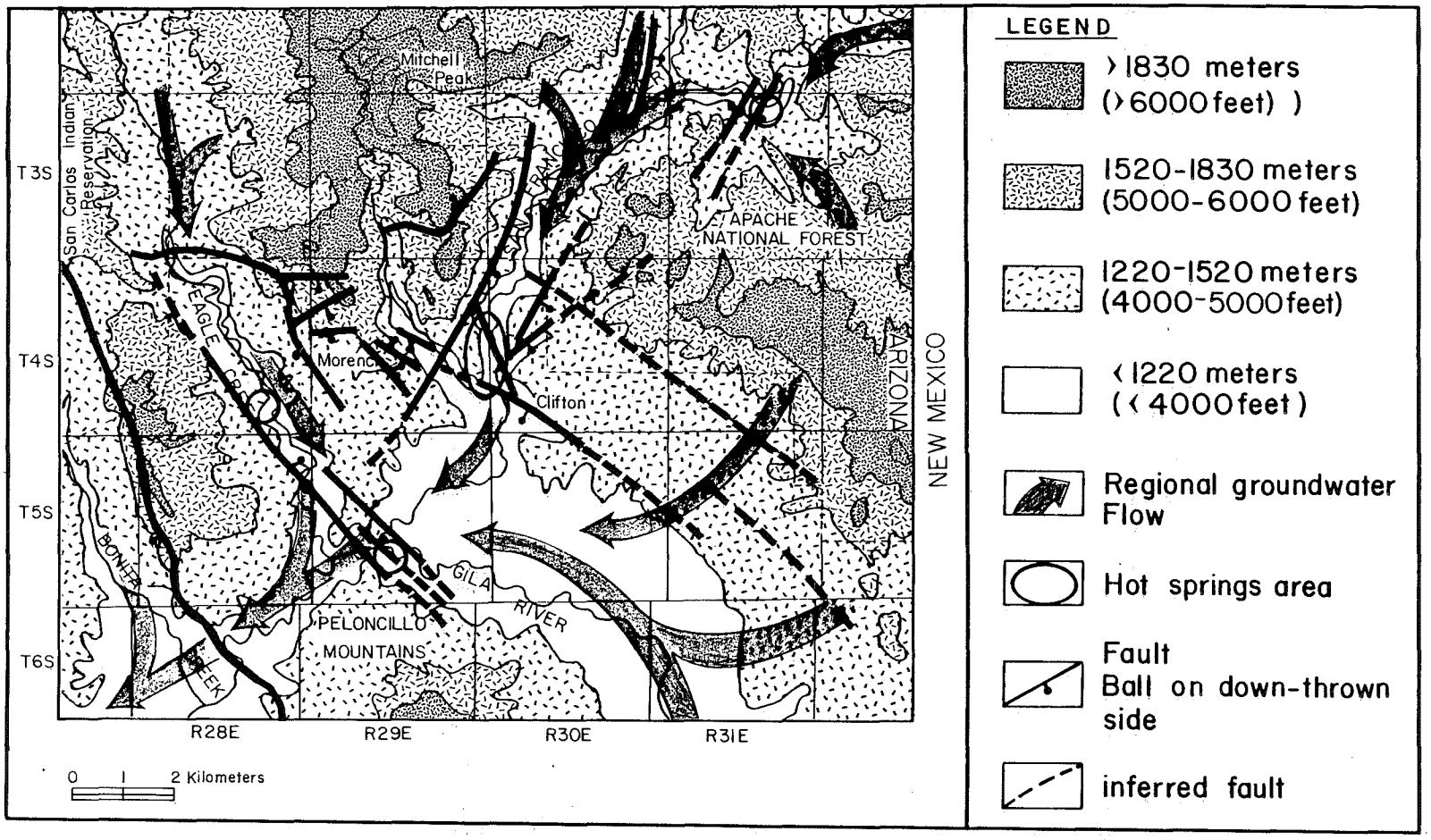

Figure 2.79. Map showing generalized topography of the Clifton and Gillard Hot Springs area and postulated regional ground-water flow paths

TABLE 2.13 SELECTED CHEMISTRY OF CLIFTON HOT SPRINGS

Location	Temperature C°	TDS	pH	Na	K	Na+K	Ca	Mg	Cl	SO_4	HCO_3+CO_3	SiO_2	Li	B	F
D-4-30-18CCA	71	13900	--	3300	220		880	22	7000	60	130	110	--	1.4	3.6
D-4-30-30CA	39	5526	7.0	1500	82		430	16	3150	72	163	55	2.6	0.64	2.3
D-4-30-18C	44	9696	6.6	2700	170		790	21	5700	62	146	94	4.1	1.4	2.7
D-4-30-18C	59	9352	7.1	2600	170		740	20	5500	68	146	95	4.0	1.2	2.8
D-4-30-30DB	48.8	8740	--			2540	767	37	5230	110	111	--	--	--	4.3
D-4-30-30DB	40	8880	--			2570	782	43	5280	138	136	--	--	--	4.1
D-4-30-30DB	37.8	8940	--			2620	754	41	5280	178	129	--	--	--	5.0
D-4-30-30DB	40.6	7490	--			2212	619	38	4470	68	152	--	--	--	3.6
D-4-30-19CA	34.8	12576	7.7	3207	210		1064	52	6460	--	92	82	--	1.48	1.8
D-4-30-18CD	48.0	14548	8.2	3586	243		926	23	7485	--	150	131	6.96	1.51	3.5
D-4-30-18C	61.0	7205	7.5	2015	175		601	13	4400	58	114	95	--	--	--
D-4-30-18C	45.0	10141	7.5	2502	239		959	23	6060	59	130	95	--	--	--
D-4-30-18CCDAC	70.0	11395	6.2	2700	195		800	21	6600	56	88	90	5.1	1.53	1.75
D-4-30-18CCDBB	70.0	10730	5.3	2650	176		748	21	6286	55	98	85	4.9	1.09	1.35
D-4-30-18CCBDD	67.0	10329	6.4	2650	180		728	21	6129	57	120	89	4.8	1.27	1.20
D-4-30-18CCBBD	67.0	9789	6.3	2450	159		707	20	5722	54	131	82	4.5	1.38	0.15
D-4-30-18CDCCC	50.0	14272	--	--	--		--	--	7213	--	--	88	5.4	1.64	0.40
D-4-30-19CADBC	32.0	--	6.9	--	--		--	--	2719	--	--	62	2.2	0.65	0.65
D-4-30-19CAAAA	33.0	10923	6.8	2350	138		735	41	7260	65	120	64	4.2	1.02	0.78
D-4-30-30DBCBA	38.0	10381	7.1	2280	103		757	33	5312	53	131	50	4.2	1.09	3.80
D-4-30-30DBDCC	31.0	2140	7.6	2140	113		701	45	5296	53	88	51	3.9	0.73	0.42

Figure 2.80 shows that the concentration of chloride versus boron varies systematically among the various Clifton Hot Springs. The observed systematic variation in these constituents suggests that individual springs are discrete and are composed of volumetrically varied mixtures of thermal and nonthermal water. In addition nonthermal spring waters in the area typically have lower chloride and boron concentrations than the thermal springs.

Different volumes of nonthermal water mixed with thermal water cause measured temperatures to vary significantly. In addition, the quartz temperatures vary between 90 and 150°C. When quartz temperatures are plotted against chloride, a linear relationship results similar to that observed between chloride and boron (Fig. 2.81). Interestingly, there is not as good a linear correlation between dissolved silica concentrations and chloride. There is also no correlation between measured spring temperatures and chloride concentrations as would be expected if mixing were the only cooling process. Apparently, these thermal waters lose significant heat to country rock by conduction.

We believe the Clifton Hot Springs discharge from a chemically and thermally inhomogenous and fracture-controlled 90-to-150°C geothermal system. Apparently, thermal water flows upward to the surface through discrete fracture systems and "water courses" (Fig. 2.82). During ascent thermal water mixes with nonthermal water. During and before mixing and before conductive heat loss, silica concentrations apparently equilibrate with quartz. The largest chloride concentrations and highest quartz geothermometers in the Clifton Hot Springs system are found in springs that intercept the least relative volume of nonthermal or previously mixed

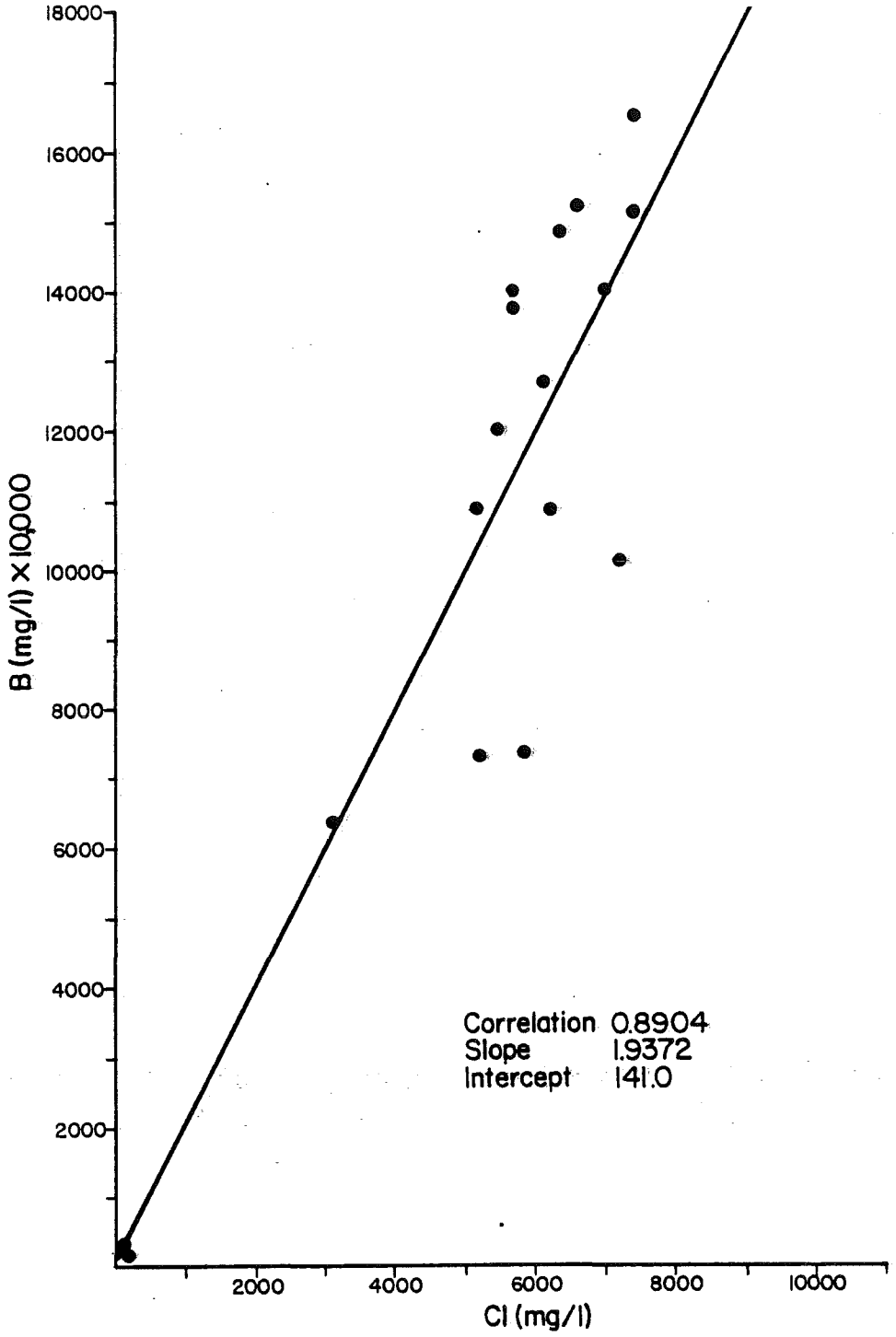

Figure 2.80. Boron versus chloride in Clifton Hot Springs

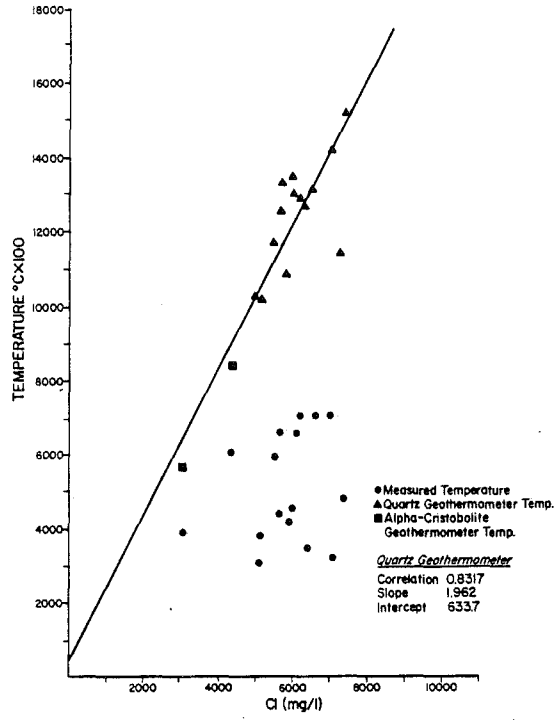

Figure 2.81. Measured temperatures and silica temperatures compared to chloride in Clifton Hot Springs

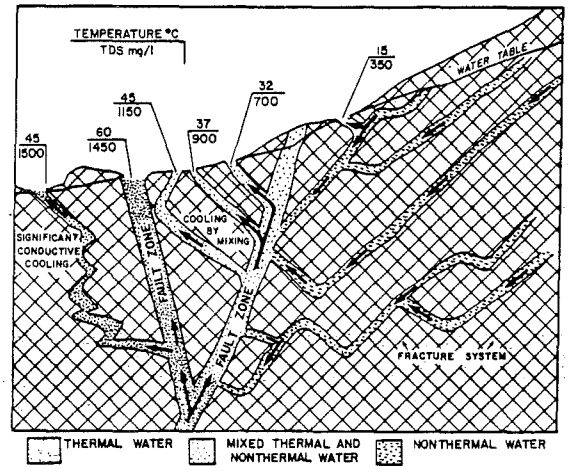

Figure 2.82. Proposed model of a fracture-controlled thermal spring system showing mixing and cooling relationships

water. These springs do not necessarily have the highest measured temperature. Measured temperatures are highest where flow rate and volume of contained fluid versus fracture surface area are largest and length of flow path is shortest. This environment would have the least conductive heat loss to country rock. In any case, the Clifton Hot Spring system does have significant conductive loss of heat to the country rock. This heat loss is evident in the large difference between measured temperatures and the equilibrated geothermometers of the mixed water. Low flow rates observed in individual springs is a possible cause of the conductive heat loss.

Temperatures greater than 150°C are predicted in the Clifton Hot Springs system by Na-K-Ca geothermometers and chloride-enthalpy diagrams (Witcher, 1981). Deep reservoir temperatures of 160°C to 180°C are inferred, but additional work is needed to confirm these estimates.

Composite flow rate of the Clifton Hot Springs system was determined as 75.6 L/s by chloride balance of the thermal springs and the San Francisco River, which receives all the spring flow. Witcher (1981) estimated natural heat loss from this system into the San Francisco River at 18 to 27 MWt.

Gillard Hot Springs discharge 80 to 84°C water along the banks of the Gila River in section 27, T. 5 S., R. 29 E. (Fig. 2.78). These springs discharge sodium chloride water with equal concentrations of sulfate and bicarbonate. TDS ranges between 1,200 and 1,500 mg/L. Chemical data for Gillard Hot Springs reveal no significant variations (Table 2.14). Both the quartz and Na-K-Ca geothermometers predict 130° to 139°C subsurface temperatures for this geothermal system.

Witcher (1981) calculated a cumulative discharge rate of 29.9 L/s for Gillard Hot Springs, using the chloride balance of the springs and the Gila River. Convective heat loss from the system into the Gila River is approximately 7.8 MWt.

Thirteen km northwest of Gillard Hot Springs, and east of the Gillard fault zone (Fig. 2.78) Eagle Creek Hot Springs in section 35, T. 4 S., R. 28 E., discharge 42°C sodium bicarbonate-chloride water. Eagle Creek thermal water has TDS of less than 1,000 mg/L (Table 2.15). Geothermometry for this water is unreliable due to low flow rates and possible precipitation of calcite and silica. At a spring temperature of 42°C silica is in equilibrium with α-cristobalite.

The Eagle Creek system may be a part of the Gillard geothermal system because both are on the same structural trend. However, it should be pointed out that significant differences in chemistry exist, making this hypothesis very tentative at present. Heindl (1967) reported that wells drilled in Eagle Creek (exact location unknown) tapped 48 to 56°C water in basaltic rock at depths of less than 100 m. The wells were reported to pump 60 L/s.

North of Clifton along the San Francisco River, near the Martinez Ranch, a thermal spring seeps from a river gravel bar. Spring temperature is 26.6°C; spring chemistry is sodium chloride, with 6,594 mg/L TDS. The chloride and lithium ratio and the Na-K-Ca geothermometry are similar to those for the Clifton Hot Springs; in addition, both occur on the northeast-trending Limestone Gulch fault zone (Witcher, 1981).

THERMAL REGIME. Six heat-flow measurements are available in the Clifton-Morenci region. Analysis of temperature-gradient and heat-flow

TABLE 2.14 SELECTED CHEMISTRY OF GILLARD HOT SPRINGS

Location	Temperature C^o	TDS	pH	Na	K	Ca	Mg	Cl	SO_4	HCO_3+CO_3	SiO_2	Li	B	F
D-5-29-27AA	82	1244	8.0	411	13.2	20	0.7	464	175	220	98	1.01	0.4	10.6
D-5-29-27AA	82	1483	7.4	450	14	22	0.8	490	180	216	95	0.87	0.41	11
D-5-29-27AA	82.8	1224	--	437		27	3.5	470	174	228	--	--	0.8	--
D-5-29-27AA	76.7	1252	--	448		26	3.1	500	178	196	--	--	0.9	--
D-5-29-27AA	82.8	1242	--	450		22	2.2	480	182	215	--	--	0.7	--
D-5-29-27AA	--	1260	--	449		28	4.7	475	183	217	--	--	3.0	10
D-5-29-27AAC	81	1400	7.3	--	--	--	--	486	--	--	90	0.49	0.12	3.5
D-5-29-27AAC	82	1347	7.1	--	--	--	--	469	--	--	88	0.47	0.08	4.1
D-5-29-27AAC	84	1410	7.1	--	--	--	--	494	--	--	87	0.49	0.08	6.5
D-5-29-27AAC	66	1435	7.7	542	13	7.9	0.8	519	162	151	89	0.50	0.09	6.0

TABLE 2.15 CHEMISTRY OF EAGLE CREEK THERMAL SPRINGS

Location	Temperature C^o	TDS	pH	Na	K	Ca	Mg	Cl	SO_4	HCO_3+CO_3	SiO_2	Li	B	F
D-4-28-35ABBA	42	626	7.0	159	7.7	25.0	1.3	121	49	209	21	.04	2.0	<.01
D-4-28-35AB	35	731	8.2	190	7.8	16.0	2.1	120	45	283	64	0.39	0.12	10.0
D-4-28-35ABBA	42	676	8.1	198	9.0	14.4	2.2	120	77	288	67	6.96	0.15	10.2
D-4-28-35ABBA	42	658	8.3	179	9.5	3.4	2.4	126	51	197	60	0.4	<.01	8.0

data shows significant thermal disturbance from ground-water flow. The Clifton-1 heat-flow hole dramatically illustrates this phenomenon. Due to lateral water movement with a downward flow component, the temperature-depth profile of this well is concave up (Fig. 2.83). The heat flow increases systematically with depth because heat is transported downward by water movement. Two other heat-flow holes, one on the Clifton uplift, the other on the Morenci uplift, apparently are not disturbed by ground-water movement. These measurements, in Precambrian granite and Cambrian quartzite, have heat flows of 94 mWm^{-2} and 97 mWm^{-2}, respectively (Witcher, 1981; Witcher and Stone, 1981). These values suggest that regional heat flow for the Clifton-Morenci area is about 96 mWm^{-2}, which is high compared to the 80 mWm^{-2} average estimated for southeastern Arizona by Shearer and Reiter (1981). Witcher (1981) suggested that the high heat flow results either from unusual radiogenic heat production in the crust or anomalous temperatures in the underlying mantle. The low magnitude of this heat anomaly is not indicative of an igneous heat source such as a cooling magma chamber. Absence of Quaternary volcanic rocks supports this conclusion. Area geothermal systems probably result from deep water circulation through a region having an enhanced thermal regime.

CONCLUSION. Geothermal studies show a complex distribution of temperatures in the shallow crust, which are favorable for geothermal resources in the Clifton-Morenci area. Thermal springs in this area probably originate from predominantly forced convection, which circulates water through fractured Precambrain granite and Paleozoic rocks that have been displaced to great depth by Cenozoic volcano-tectonic processes and faulting. Thick sequences of volcanic flows and clastic sediment cap these

aquifers. Fault zones transverse to regional ground-water flow leak this hot water to the surface. A magmatic heat source is not indicated for this area; rather, above normal mantle heat flow or radiogenic crustal heat production provides heat to hydrothermal systems in the Clifton-Morenci region. Excellent potential exists for geothermal resources between 90 and 150°C. Potential for resources over 150°C is speculative.

Future uses of these geothermal resources include copper extraction, space heating and cooling, and possibly electrical power production.

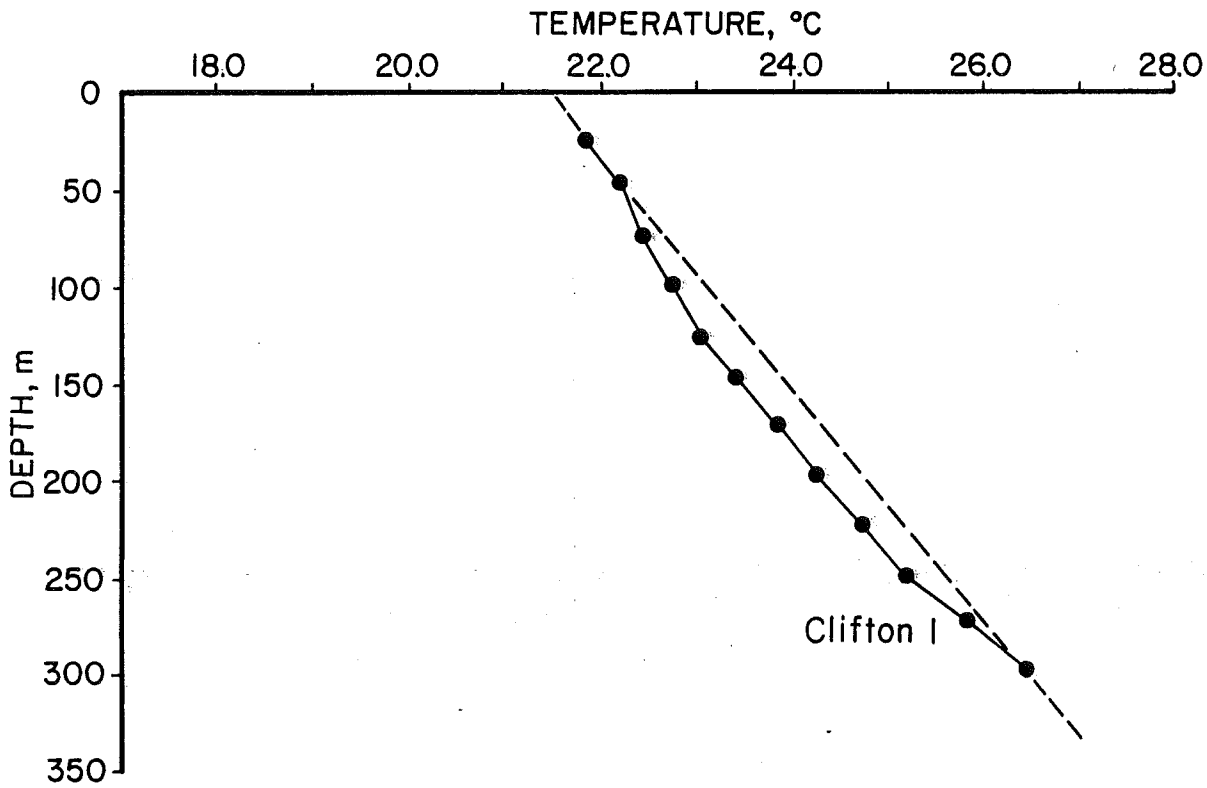

Figure 2.83. Temperature-depth profile of the Clifton 1 heat-flow hole

REFERENCES CLIFTON AND GILLARD HOT SPRINGS

Berry, R. C., 1976, Mid-Tertiary volcanic history and petrology of the White Mountains volcanic province, southeastern Arizona: unpub. Ph.D. Thesis, Princeton University, 317 p.

Cunningham, J. E., 1979, Geologic map of the Clifton, Arizona area: Arizona Bureau of Geology and Mineral Technology Open File Report 81-22, 1:24,000 scale.

Damon, P. E., and associates, 1966, Correlation and chronology of the ore deposits and volcanic rocks: Atomic Energy Commission Ann. Rept. No. 1966 COO-689-60, University of Arizona.

Elston, W. E., 1958, Burro uplift, northeastern unit of sedimentary basin of southwestern New Mexico and southeastern Arizona: American Association of Petroleum Geologists Bulletin, Vol. 42, p. 2513-2517.

Elston, W. E., 1968, Terminology and distribution of ash flows of the Mogollon-Silver City-Lordsburg Region, New Mexico: Arizona Geological Society Guidebook III, Southern Arizona, p. 231-240.

Gish, D. M., 1980, A refraction study of deep crustal structure of the Basin and Range-Colorado Plateau in eastern Arizona: unpub. M.S. Thesis, University of Arizona, 32 p.

Heindl, L. A., 1967, Groundwater in fractured volcanic rocks in southern Arizona: *in* Hydrology of fractured rocks-Dubrovnik symposium, 1965 proc. Vol. 2, International Association of Sci. Hydrol. Pub. 74, p. 503-513.

Langton, J. M., 1973, Ore genesis in the Morenci-Metcalf District: AIME transaction, Vol. 254, p. 248-257.

Lindgren, W., 1905, Description of the Clifton quadrangle: U. S. Geological Survey Geologic Atlas, Folio 129.

Menges, C. M., Peartree, P. A., and Calvo, S., 1982, Quaternary faulting in southeast Arizona and adjacent Sonora, Mexico (abs): Abstracts, 78th annual meeting Cordilleran Section, The Geological Society of America, April 19-21, 1982, Anaheim, California, p. 215.

Ratte, J. C., Landis, E. R., Gaskill, D. L., and Rabbe, R. G., 1969, Mineral Resources of the Blue Range Primitive area, Greenlee County, Arizona, and Catron County, New Mexico: U. S. Geological Survey Bulletin 1261-E, 91 p.

Reiter, M. and Shearer, C., 1979, Terrestrial heat flow in eastern Arizona, A first report: Journal of Geophysical Research, Vol. 84, no. B11, p. 6115-6120.

Rhodes, R. C., 1976, Volcanic geology of the Mogollon Range and adjacent areas, Catron and Grant Counties, New Mexico: *in* Cenozoic volcanism in southwestern New Mexico, New Mexico Geological Society Special Publication 5, p. 42-50.

Rhodes, R. C. and Smith, E. I., 1972, Geology and tectonic setting of of the Mule Creek Caldera, New Mexico, U.S.A.: Bulletin of Volcanology, Vol. 36, p. 401-411.

Scarborough, R. B. and Peirce, H. W., 1978, Late Cenozoic basins of Arizona: *in* Callender, J. F., Wilt, J. C., and Clemons, R. E., eds., Land of Cochise, New Mexico Geological Society Guidebook, 29th Field Conference, p. 253-259.

Strangway, D. W., Simpson, J.,and York, D., 1976, Paleomagnetic studies of volcanic rocks from the Mogollon Plateau area of Arizona and New Mexico: *in* Cenozoic volcanism in southwestern New Mexico, New Mexico Geological Society Special Publication, 5, p. 119-124.

Wahl, D. E., Jr., 1980, Mid-Tertiary volcanic geology in parts of Greenlee County, Arizona, Grant and Hidalgo Counties, New Mexico: unpub. Ph.D. Dissertation, Arizona State University, 147 p.

Witcher, J. C., 1981, Geothermal energy potential of the lower San Francisco River region, Arizona: Arizona Bureau of Geology and Mineral Technology Open File Report 81-7, 135 p.

Witcher, J. C. and Stone, C., 1981, Thermal regime of the Clifton-Morenci area, Arizona (abstract): Geological Society of America Abstracts with Programs, Cordilleran Section, Vol. 13, No. 2, p. 114.

SONORAN DESERT SECTION

PHYSIOGRAPHY. The Sonoran Desert section of the Basin and Range province covers most of south-central and southwestern Arizona. Relatively small mountain ranges, 5 to 10 km wide, separate alluvial plains that are 30 to 50 km wide. Mountain ranges generally rise only 1,200 m to 1,500 m above sea level, while adjacent basins lie below 900 m elevation. Due to a very arid climate, the mountain ranges are bare of vegetation, very rocky, and rugged. Basins are generally characterized as gently sloping bajadas. While through-flowing drainage exists, very little entrenchment of the bajadas by drainage is evident in the topography.

GEOLOGY. Lithology and structure in the Sonoran section are exceedingly diverse and relatively complex. Precambrian (1.7 to 1.8 b.y.) gneiss, schist, quartzite, and amphibolite are intruded by several generations of plutonic rocks ranging from Precambrian to mid-Tertiary age (Reynolds, 1980; Silver, 1978). Precambrian granodiorite plutons (1.7 to 1.6 b.y.) are intruded by anorogenic megacrystic granites (1.5 to 1.4 b.y.) (Silver, 1978). Precambrian diabase dikes intrude all other Precambrian units. A major unconformity separates Precambrian and Paleozoic rocks.

Paleozoic rocks occur in scattered outcrops that are mostly in the Plomosa, Harquahala, Little Harquahala, Rawhide, Vekol, Slate, and Silver Bell Mountains. Among these limited Paleozoic outcrops, some are structurally deformed and some are underformed. In addition, Paleozoic

rocks in some areas have undergone regional metamorphism. Paleozoic units in the Sonoran Desert section were deposited in a cratonic shelf environment. These rocks are similar in appearance and correlative to Paleozoic strata on the Colorado Plateau and on shelf depositional areas in southeastern Arizona. Quartzite of Cambriam age grades upward into predominantly carbonate rocks of Mississippian age. Pennsylvanian to Permian red silts and shales are overlain by Permian cross-bedded sandstones and cherty limestones (Reynolds, 1980; Peirce, 1976).

Early to mid-Jurassic volcanic rocks, up to 5 km thick, and coeval plutonic rocks overlie or intrude Paleozoic strata (Reynolds, 1980). The Jurassic volcanic-plutonic sequence is unconformably overlain by Jurassic to Lower Cretaceous clastic sediments (Harding, 1980; Robison, 1980). Deposition of these sediments occurred in east-to-west and southeast-to-northwest-trending grabens (Harding, 1982; Robison, 1980). These sediments are tectonically deformed and metamorphosed. Small Late Cretaceous, mostly equigranular stocks, plugs, and dikes intrude these sediments.

Late Cretaceous plutonism was accompanied by regional metamorphism ranging from greenschist to locally higher grade metamorphism (Reynolds, 1980; Haxel and others, 1980). Areas with higher grade metamorphism are frequently distinguished from other areas by migmatitic gneiss. Paleocene to Eocene tectonism was particularly intense and was accompanied in part by southwest vergent thrusting and initial development of extensive mylonitization (Keith, 1982). Peraluminous granites, apparently derived from melting of continental crust, were emplaced along a few of the thrust faults. The thrust faults separate upper plate unmetamorphosed and

unmylonitized crystalline rocks from underlying metamorphic complexes. These thrust faults provided planar dislocation surfaces in some areas for mid-Tertiary extension associated with thermal arching of the crust.

Mid-Tertiary (mostly post 26 m.y.) volcanism was voluminous in the Ajo area, Castle Dome Mountains, Vulture-Big Horn Mountains, Superstition Mountains, and the Tucson-Roskrudge Mountains. Miocene dike swarms that trend northwest to north-northwest are common (Rehrig, 1976; Rehrig and others, 1980). Deposition of Tertiary arkosic and volcanoclastic sediments preceded and accompanied the main phases of volcanism (Scarborough and Wilt, 1979). Depositional basins formed as a result of regional extension although volcano-tectonic subsidence was possibly locally important.

Normal faulting and concurrent antithetic block rotation occurred over low-angle dislocation faults during regional extension between 25 and 15 m.y. ago (Rehrig and others, 1980; Shafiqullah and others, 1980). Mylonitization of crystalline rocks accompanied this extension in some areas; however, in other areas major extension also post-dated mylonitization. In these later areas, mylonitized rocks have been deformed into chloritic breccias by brittle strain post-dating mylonitization (Reynolds, 1980). The green breccias occur up to tens of meters below the dislocation faults, which form brown aphanitic ledges with planar upper surfaces.

Flat dislocation faults and underlying metamorphic complexes were denuded by erosion subsequent to arching, and during and after low-angle fault extension. Arching formed anticlinal to synclinal structures whose axes are oriented northeast and northwest. The northeast-

oriented folds are more significant. The anticlinal morphology of the Santa Catalina, Rincon, Tanque Verde, Harquahala, and Harcuvar Mountains are prominent examples of arching of the flat-lying dislocation faults and underlying crystalline metamorphic complexes (Reynolds, 1980; Davis, 1980; Keith and others, 1980). A major Miocene synclinal warping of a dislocation fault(s) may occur in the Gila trough (Pridmore and Craig, 1982).

Basaltic volcanic flows post-dating 15 m.y. are relatively untilted, and they overlie older rocks in angular unconformity. The flows are faulted by high-angle normal faults of the Basin and Range disturbance (Shafiqullah and others, 1980; Scarborough and Peirce, 1978). Quaternary faulting is rare and it has apparently only occurred near Yuma and Gila Bend.

Basaltic flows and cones in the Sentinel Plain-Arlington volcanic field and the Pinacate volcanic field are the youngest volcanic rocks in the Sonoran Desert section. The Pinacate field is mostly in Mexico, with only a very small portion in Arizona. The Sentinel Plain-Arlington field has isotopic dates ranging from 1.7 to 6.5 m.y. (Shafiqullah and others, 1980). However, the average date for flows and cones is between 3.0 to 3.5 m.y.

The thermal regime of the Sonoran Desert section is typical of the southern Basin and Range province. Average crustal heat flow is about 79 mWm^{-2}. A few high measurements (up to 120 mWm^{-2}) probably result from deep ground-water flow or anomalous concentrations of radioactive elements (radiogenic heat) in upper crust crystalline rock rather than from heating by magmatic intrusion.

Geothermal potential in the Sonoran Desert section is closely tied to geohydrology and regional structure. Regional structures may provide permeability for deep ground-water percolation. High-angle normal faults, forming major structural basins, are one set of important structures. Low-angle faults associated with mid-Tertiary extension may provide deep fracture permeability for reservoirs (see the section on the Coolidge area). Thick sequences of Tertiary sediments may also provide suitable reservoir rocks. The coarse facies in these units are generally permeable, and the entire Tertiary sequence has low thermal conductivity (<2.0 WmK). High temperature gradients (30 to 50°C/km) occur in low thermal conductivity sediments where conductive heat flow exceeds 70mWm^{-2}.

SONORAN DESERT SECTION REFERENCES

Davis, G. H., 1980, Structural characteristics of metamorphic core complexes, southern Arizona: *in* Crittenden, M. D. Jr., Coney, P. J., and Davis, G. H., eds., Coroilleran Metamorphic Core Complexes, Geological Society of America Memoir 153, p. 35-78.

Harding, L. E., 1980, Petrology and tectonic setting of the Livingston Hills Formation, Yuma County, Arizona: *in* Jenney, J. P. and Stone, C., eds., Studies in Western Arizona, Arizona Geological Society Digest, v. 12, p. 135-145.

Harding, L. E., 1982, A progress report on the tectonic significance of the McCoy Mountains Formation, southeast California and southwestern Arizona: *in* Frost, E. G. and Martin, D. L., eds., Mesozoic-Cenozoic tectonic evolution of the Colorado River region, California, Arizona, and Nevada, Hamilton-Anderson Volume, Cordilleran Publishers, San Diego, California, p. 135.

Haxel, G., Wright, J. E., May, D. J., and Tosdal, R. M., 1980, Reconnaissance geology of the Mesozoic and lower Cenozoic rocks of the southern Papago Indian Reservation, Arizona - A preliminary report: *in* Jenney, J. P. and Stone, C., eds., Studies in Western Arizona, Arizona Geological Society Digest, v. 12, p. 17.29.

Keith, S. B., Reynolds, S. J., Damon, P. E., Shafiqullah, M., Livingston, D. E., and Pushkar, P. D., 1980, Evidence for multiple intrusion and deformation within the Santa-Catalina-Rincon-Tortolita crystalline complex, southeast Arizona: *in* Crittenden, M. D., Jr., Coney, P. J., and Davis, G. A., eds., Cordilleran Metamorphic Core Complexes, Geological Society of America Memoir 153, p. 217-268.

Keith, S. B., 1982, Evidence for late Laramide southwest vergent underthrusting in southeast California, southern Arizona, and northeast Arizona (abstract): Abstracts with Programs, 78th annual meeting Cordilleran section, Geological Society of America, p. 177.

Peirce, H. W., 1976, Elements of Paleozoic tectonics in Arizona, Arizona Geological Society, v. 10, p. 47-55.

Pridmore, C. L. and Craig, C., 1982, Upper-plate structure and sedimentation of the Baker Peaks area, Yuma County, Arizona: *in* Frost, E. G. and Martin, D. L., eds., Mesozoic-Cenozoic tectonic evolution of the Colorado river region, California, Arizona, and Nevada, Hamilton-Anderson Volume, Cordilleran Publishers, San Diego, California, p. 357-375.

Rehrig, W. A., 1976, Regional tectonic stress during the Laramide and late Tertiary intrusive periods, Basin and Range Province, Arizona, Arizona Geological Society Digest, v. 10, p. 205-228.

Rehrig, W. A., Shafiqullah, M., and Damon, P. E., 1980, Geochronology, geology, and listric normal faulting of the Vulture Mountains, Maricopa County, Arizona: *in* Jenney, J. P. and Stone, C., eds., Studies in Western Arizona, Arizona Geological Society Digest, v. 12, p. 89-110.

Reynolds, S. J., 1980, Geologic framework of west-central Arizona: *in* Jenney, J. P. and Stone, C., eds., Studies in Western Arizona, Arizona Geological Society Digest, v. 12, p. 1-16.

Robison, B. A., 1980, Description and Analysis of Mesozoic Red Beds, western Arizona and southeastern California: *in* Jenney, J. P. and Stone, C., eds., Studies in Western Arizona, Arizona Geological Society Digest, v. 12, p. 147-154.

Scarborough, R. B. and Peirce, H. W., 1978, Late Cenozoic basins of Arizona: *in* Callender, J. F., Wilt, J. C., and Clemons, R. E., eds., Land of Cochise, 29th Field Conference Guidebook, New Mexico Geological Society, p. 253-259.

Scarborough, R. B. and Wilt, J. C., 1979, A study of uranium favorability of Cenozoic sedimentary rocks, Basin and Range province, Arizona, part I, general geology and chronology of pre-late Miocene Cenozic sedimentary rocks: U. S. Geological Survey Open-File Report 79-1429, p. 101.

Shafiqullah, M., Damon, P. E., Lynch, D. J., Reynolds, S. J. Rehrig, W. A., and Raymond, R. H., 1980, K-Ar geochronology and geologic history of southwestern Arizona and adjacent areas: *in* Jenney, J. P. and Stone, C., eds., Studies in Western Arizona, Arizona Geological Society Digest, v. 12, p. 201-260.

Silver, L. T., 1978, Precambrian formations and Precambrian history in Cochise County, southeastern Arizona: *in* Callendar, J. F., Wilt, J. C., and Clemons, R. E., eds., Land of Cochise, 29th Field Conference Guidebook, New Mexico Geological Society, p. 157-163.

TUCSON BASIN

INTRODUCTION. At present time, Tucson is one of the largest municipalities in the United States that depends entirely upon a ground-water supply source (Wright and Johnson, 1976). More than 200 domestic wells located in the Tucson basin are operated by the city of Tucson, local water companies and industry. A few of these wells pump thermal water (>30°C). The hottest wells are owned by Tucson Electric Power Company, and they discharge 50 to 57°C water from depths between 762 and 959 m. A thermal spring, Agua Caliente, discharges 30 to 32°C water near Tanque Verde.

PHYSIOGRAPHY. The Tucson basin is situated in the Sonoran Desert section of the Basin and Range province. The Santa Rita Mountains, greater than 1,829 m in elevation, form the southeast basin margin, while the rugged Rincon, Tanque Verde, and the Santa Catalina Mountains, greater than 1,829 m in elevation, form the picturesque northern and eastern boundaries (Fig. 2.84). Relatively low ranges less than 1,829 m high, the Tucson and Sierrita Mountains, form the western border to the basin. The Tucson basin floor slopes northwestward from 1,067 m at the base of the Santa Rita Mountains to 607 m near Rillito. Pantano, Tanque Verde, and Rillito Washes dissect the eastern and northern portions of the basin, and empty into the through-flowing Santa Cruz River near Cortaro. The Santa Cruz River flows south to north and is confined to the western parts of the basin. Both the Santa Cruz River and tributary washes

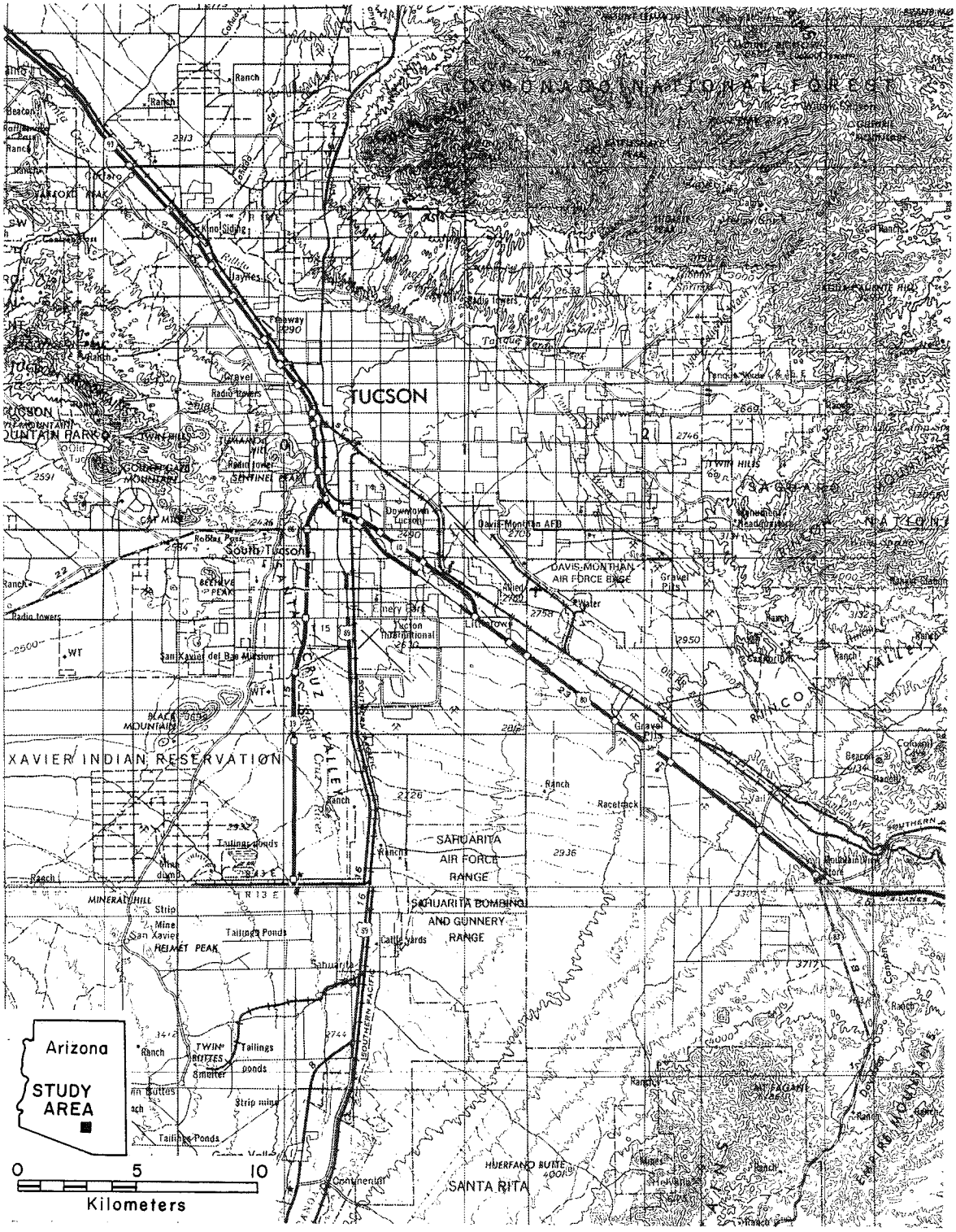

Figure 2.34. Location map of the Tucson basin, Arizona

occasionally carry water after winter and summer storms. Most of these intermittent flows of water originate in surrounding mountains where precipitation is high (>50 to 75 cm per year).

GEOLOGY. The oldest rock exposed in the Tucson basin area is the older (1.7 b.y.) Precambrian Pinal Schist, which is intruded by the Oracle Granite (1.4 b.y. old) (Silver, 1978). Scattered outcrops of younger Precambrian Apache Group sediments nonconformably overlie Pinal Schist and Oracle Granite in the Santa Catalina Mountains. All Precambrian lithologies are cut by diabase dikes and sills dated at about 1,100 m.y.B.P. (Silver, 1978).

Paleozoic rocks, which were deposited on an erosionally bevelled Precambrian terrane, occur in outcrops of limited extent in mountains adjacent to the Tucson basin. A basal arkosic sandstone, the early Paleozoic Bolsa Formation is overlain by interbedded shales and carbonate rocks; the carbonate rocks become dominant higher in the Paleozoic section (Peirce, 1976). Deposition during the Paleozoic occurred in all periods except for the Silurian.

Mesozoic time was accompanied by intense and complicated tectonism, plutonism, and sedimentation. Two periods of orogeny (mountain building) are recorded by Mesozoic rocks in the Tucson area. The first orogeny occurred during the Triassic (?) and Jurassic; and the second, called the Laramide orogeny, is Late Cretaceous to early Tertiary in age (Coney, 1978). During the Laramide, major copper deposits were emplaced in the Sierrita and Santa Rita Mountains in association with silicic and intermediate stocks. Laramide volcanic rocks crop out in portions of the southern Tucson Mountains (Bikerman and Damon, 1966).

During the Eocene, muscovite granites such as the Wilderness Granite in the Catalina Mountains were emplaced, apparently without surface volcanism (Keith and others, 1980).

Voluminous eruptions of compositionally diverse lavas accompanied mid-Tertiary (Oligocene to Miocene) tectonism in the Tucson area. In the Tucson Mountains, basaltic and siliceous flows (38.5 to 18.8 m.y. old) angularly unconformably overlie Laramide volcanic rocks (Bikerman and Damon, 1966). Contemporaneous with mid-Tertiary volcanism, thick sequences of clastic sediments, interbedded with volcanic flows, accumulated in Oligocene and early Miocene depositional basins. The tilted and indurated Pantano and Helmet Formations are examples.

Also, during the mid-Tertiary the Rincon-Santa Catalina-Tortolita metamorphic complex evolved as a result of intense thermal disturbance and regional tectonic strain (Banks, 1977; Davis and Coney, 1979). The low-angle Catalina fault zone acts as a decollement and separates underlying metamorphic rocks from overlying unmetamorphosed "cover rocks". The allochthonous "cover rocks" include Precambrian granite, Paleozoic limestones, mid-Tertiary volcanic rocks, and clastic sediments. These allochthonous rocks are frequently highly fractured and deformed, and they may be potential geothermal reservoirs in the basin.

Moderately to slightly deformed Miocene sediments on the southwest flank of the Santa Catalina Mountains contain clasts that document the erosional unroofing and probable arching of the Santa Catalina metamorphic complex (Pashley, 1966). These sediments, called the Rillito beds by Pashley (1966), are categorized into three units. The older units

contain playa deposits and few gneiss clasts, while younger units are coarse grained and contain clasts of predominantly gneiss.

During late Miocene time, listric normal faulting and volcanism waned. Listric normal faulting was replaced by high-angle normal faulting as the crust cooled and became more brittle following the mid-Tertiary volcano-tectonic thermal disturbance. Present day land forms in the Tucson area are largely the result of high angle faulting, which created horsts and grabens. Eroding horst blocks form present day mountain ranges and grabens form the basins.

High-angle normal faulting (also called Basin and Range faulting) probably began after 12.0 m.y.B.P. (Scarborough and Peirce, 1978). The uppermost volcanic strata encountered at 2,180 m depth in the Exxon (Humble) State 32-1 drill hole has been dated as 11.6 m.y. old (K-Ar) (Scarborough and Peirce, 1978). Basin-filling sediments overlie the volcanic flows.

Absence of widespread Quaternary faulting and development of erosional pediments, which were buried by basin fill prior to stream entrenchment, provide evidence of waning Basin and Range faulting in the Tucson area before drainage integration of the Gila River system. Shafiqullah and others (1980) dated the beginning of through-flowing drainage at 5.5 to 2.2 m.y.B.P. Basin and Range faulting largely ended by the time major drainage integrated to the Gulf of California.

Deep well information and Bouguer gravity modeling (Davis, 1967; Oppenheimer, 1981) show the Tucson basin is an en echelon zig-zag complex of interconnected grabens that are filled with clay, sand, and gravel. The deepest graben is south of Tucson where the Exxon State 32-1 well in

section 5, T. 16 S., R. 15 E. encountered more than 2,150 m of clastic basin-fill sediments, although the sediments immediately overlying the volcanic sequence may comprise strata correlative to the Rillito beds of Pashely (1966). Major grabens in the Tucson basin are oriented north-northeast and minor grabens are oriented northwest.

GEOHYDROLOGY. The ultimate source of ground water in the Tucson basin is from precipitation in mountains surrounding the Santa Cruz River drainage system (Davidson, 1973). This water enters the Tucson ground-water reservoir by infiltration from stream flow, underflow from adjacent basins, and by infiltration of runoff near the mountains. Recharge by direct precipitation on valley floors is believed negligible because of high evaporation potential (Davidson, 1973; Anderson, 1973). Some water is returned to ground water storage by irrigation and sewage effuent that is discharged to the Santa Cruz River.

Ground water in the Tucson basin is stored in and transmitted through unconsolidated to semi-consolidated clay-rich sand and gravel. Ground water movement is generally from south to north along the axis of the basin and from the mountains toward the basin axis (Fig. 2.85).

Prior to 1940, the geohydrologic system was in approximate equilibrium because recharge was about equal to discharge. While wells existed in the basin prior to 1940, the water pumped from these wells was probably equal to the amount formerly lost through evapotransporation along stream and arroyo courses. Since 1940, the area has experienced population growth that has resulted in accelerated ground-water usage. As a result the water table has declined at rates exceeding 2.5 m per year at several locations (Wright and Johnson, 1976). These declines show that the amount

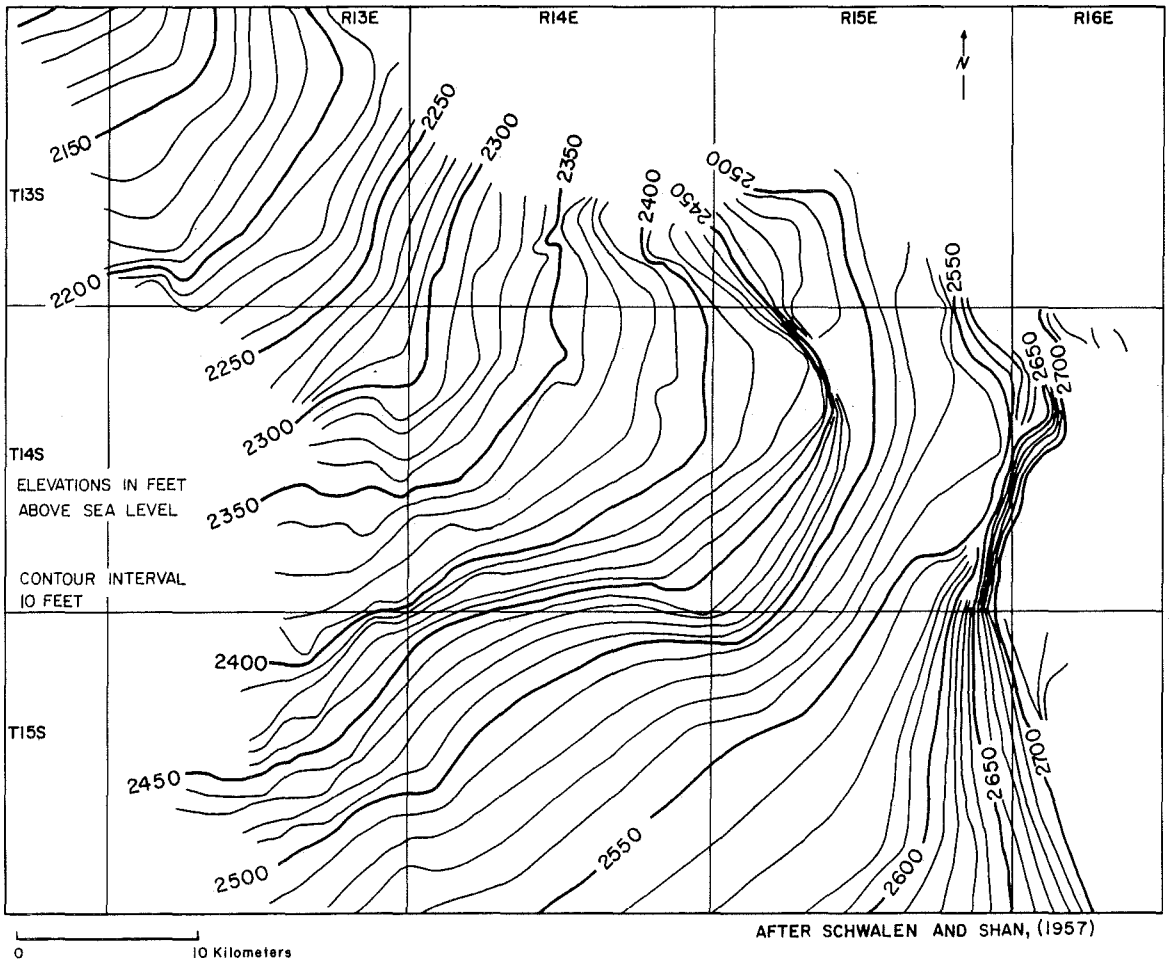

Figure 2.85. Water table elevations in the Tucson basin, 1956

of water in storage is dropping and that withdrawal is exceeding natural recharge. Continuing growth in the area coupled with present ground-water usage indicate potential for serious water-supply problems in the future. A rapidly lowering water table causes increased potential for subsidence, and higher costs because well pumps have to lift water to greater heights.

Uncertainties exist both in quantity and chemical quality of ground water deep within the basin. Several solutions are being studied and planned. They include both providing and developing additional water supplies (Central Arizona Project) and conserving present valuable ground-water supplies (Ground Water Management Act).

THERMAL REGIME. Conductive heat flow measurements have been made by Roy and others (1968), Warren and others (1969), Sass and others (1971), and Shearer and Reiter (1981) using temperature logs of mineral exploration drill holes where core is available for thermal conductivity determinations. Conductive heat flow measurements in the area surrounding the Tucson basin have a mean heat flow of 89 mWm^{-2} (Fig. 2.86). Mean heat flow for the southern Basin and Range in Arizona is about 80 mWm^{-2} (Shearer and Reiter, 1981).

Supkow (1971) compared computer simulations of subsurface temperature for several hypothetical ground-water flow regimes with measured temperatures of shallow wells in the Tucson basin. Supkow's study illustrated the applicability of temperature surveys to identify zones with downward flow or seepage (recharge of ground water).

Figure 2.87 is a generalized map of temperatures at the water table in the basin. This map was modified from the water-table temperature map presented by Supkow (1971). Areas with temperatures less than 22°C coincide with the Santa Cruz River, Rillito Wash, Tanque Verde Wash, and Pantano Wash. Supkow (1971) concluded that recharge occurs in these areas. Where water has a downward component of movement, heat is transported downward with the water in a direction opposite to upward transfer of heat by conduction. Thus, temperatures are lower in areas with downward

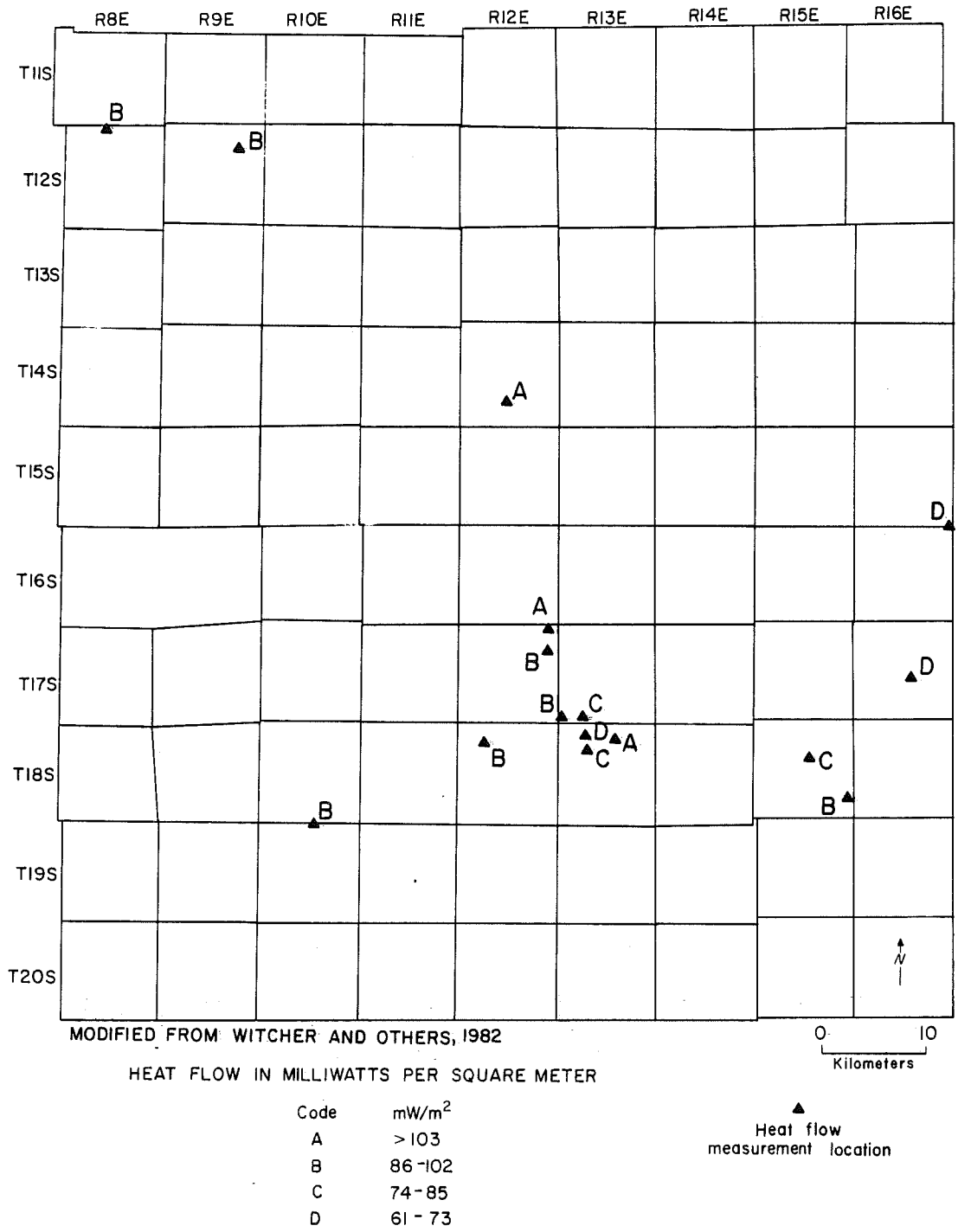

Figure 2.86. Map of heat-flow measurements in the Tucson area

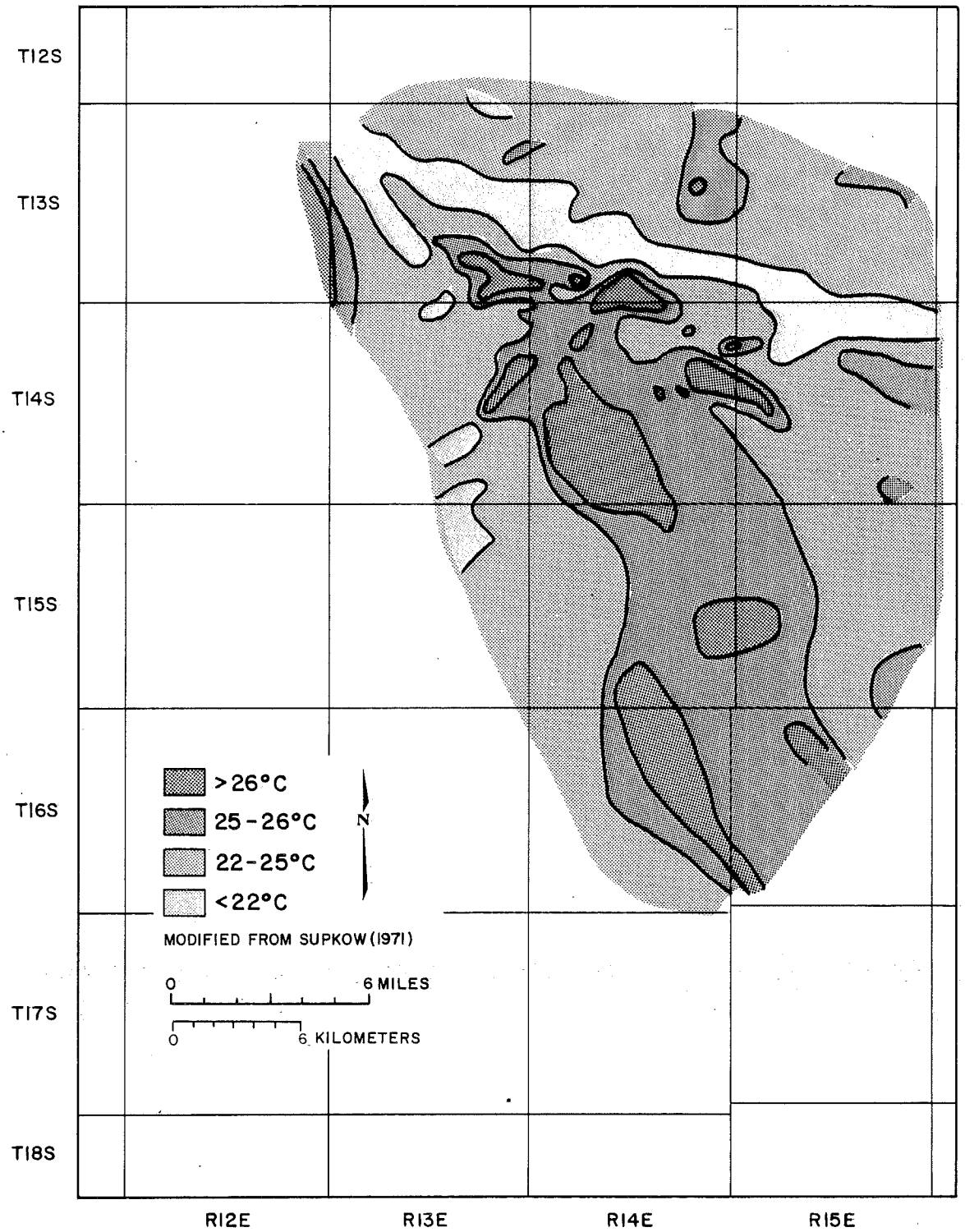

Figure 2.87. Temperature of ground water at the water table in the Tucson basin

flowing water than in areas with no water flow (conductive heat flow). The opposite temperature distribution occurs with upward moving water.

Supkow (1971) attributed areas with higher water-table temperatures to zones where permeability of shallow ground water aquifers is low. This is, in part, correct because these areas will have a large conductive component of heat flow. However, Supkow (1971) failed to account for differences in thermal conductivity, which can vary by a factor of 1.5 in basin-fill sediments and by lateral variations of conductive heat flow, which may vary locally by a factor of two or more. Local deep convection systems may heat overlying rocks to cause these heat flow variations. Also, higher water-table temperatures may result from leakage of deep thermal water into shallow ground water. We propose that areas with water-table temperatures greater than 26°C occur where rock thermal conductivity is low (<2.0 $Wm^{-1}K^{-1}$), where zones of upward flow of water occur, where an anomalous heat source exists, or where all three may occur.

The only deep (3,832 m) information on the Tucson basin is from the Humble State 32-1 stratigraphic test drilled in 1972. Bottom-hole temperatures were taken in this hole during geophysical logging at various times after mud circulation was stopped (Fig. 2.88). While depths vary, the temperature gradient (547°C/km) required to explain the bottom-hole temperature variation as a function of depth is unrealistic. The temperature increase is probably due to bore-hole temperature reequilibrating with thermal conditions that existed prior to cooling caused by mud circulation. At 3,831.3 m, the temperature of the hole was 144.4°C, 20 hours after mud circulation had stopped (Files, Arizona Oil and Gas

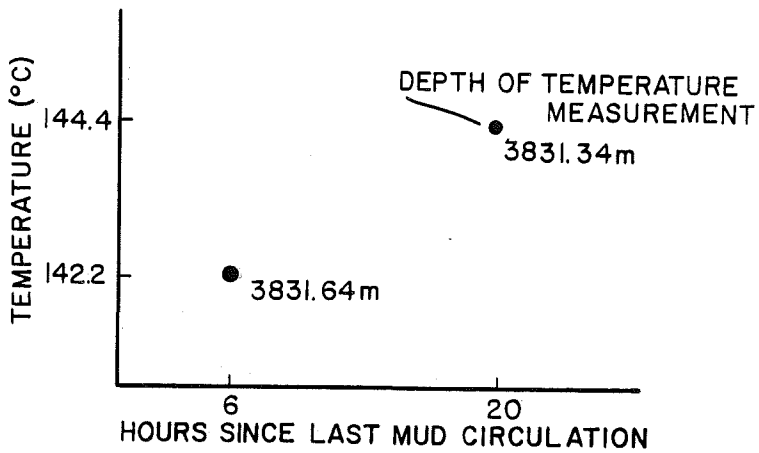

Figure 2.88. Temperature since last mud circulation in the Humble (Exxon) 32 State 1 well in the Tucson basin

Conservation Commission), giving a calculated average gradient for this hole of 32.7°C/km. This gradient is normal and agrees with gradients predicted from regional heat flow and probable thermal conductivity values.

THERMAL WATER. At least 30 wells are reported to produce thermal (>30°C) water in the Tucson basin (Fig. 2.89). A thermal spring, Agua Caliente, at the base of the Santa Catalina Mountains east of Tucson discharges 30 to 32°C water from alluvial sediments.

Thermal wells in the basin range from 64 to 959 m in depth (Table 2.16). The deeper thermal wells pump up to 6,100 L/min of 57°C water. While occurrences of water are mostly widely scattered, a notable concentration of thermal wells does exist in T. 15 S., R. 14 E., where the highest temperature thermal water known in the basin occurs.

South of Tucson in T. 16 and 17 S., R. 13, 14, and 15 E., numerous widely scattered wells have been drilled that produce thermal water (>30°C). Distribution of these wells mostly reflects deep water-well drilling by the city of Tucson.

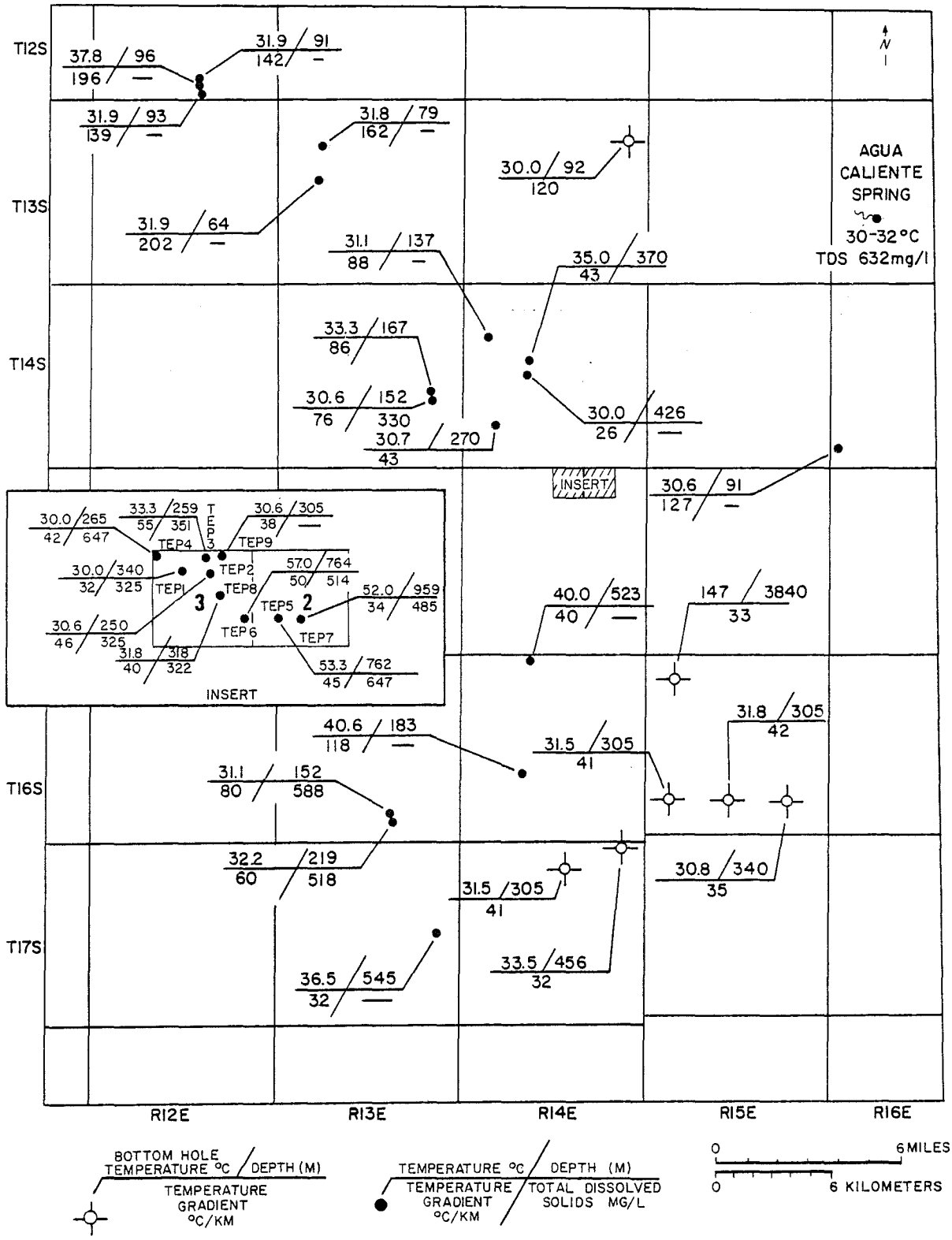

Figure 2.89. Map of wells and springs in the Tucson basin with temperatures greater than 30°C

TABLE 2.16. Wells and springs with temperatures greater than 30°C in the Tucson basin

Well	Location	Temperature	Depth	Gradient	TDS
	D-12-12-34dbb	31.9	91	142	
	D-12-12-34dbd	37.8	96	196	
	D-12-12-34dcc	31.9	93	139	
	D-13-13-8bdd	31.8	79	162	
	D-13-13-17caa	31.9	64	202	
	D-14-13-12abc	30.0T	92	120	
	D-14-13-25da$_1$	33.3	167	86	
	D-14-13-25da$_2$	30.6	152	76	330
	D-14-14-7dda	31.1	137	88	
	D-14-14-16cbb	35.0	370	43	
	D-14-14-16ccc	30.0	426	26	
	D-14-14-29cbc	30.7	270	43	
	D-14-16-31bdc	30.6	91	127	
TEP5	D-15-14-2cac	53.3	762	45	647
TEP7	D-15-14-2dbc	52.0	959	34	485
TEP9	D-15-14-3aba	30.6	305	38	
TEP3	D-15-14-3abb	33.3	259	55	351
TEP2	D-15-14-3abc	30.6	250	46	325
TEP8	D-15-14-3acd	31.8	318	40	322
TEP1	D-15-14-3bac	30.0	340	32	325
TEP4	D-15-14-3bbb	30.0	265	42	647
TEP6	D-15-14-3dad	57.0	764	50	514
	D-16-13-34aab	31.1	152	80	588
	D-16-13-34aab	32.2	219	60	518
	D-16-14-4ba	40.0	523	40	
	D-16-14-21ccb	40.6	183	118	
	D-16-15-5ca	147.0G	3840	33	
	D-16-15-26ddd	30.8T	340	35	
	D-16-15-28ddd	31.8T	305	42	
	D-16-15-30ddd	31.5T	305	41	
	D-17-13-13cdd	36.5	545	32	
	D-17-14-1baa	33.5T	456	32	
	D-17-14-3dcc	31.5T	305	41	
Agua Caliente	D-13-16-20cdd	30.4	spring	--	632

Northwest of Tucson, thermal water is pumped from two different areas near Cortaro. These wells are relatively shallow (<100 m depth) and have high estimated average temperature gradients.

Chemical quality of thermal water in the basin is generally good and is acceptable for most uses (Table 2.17). A few wells discharge high

TABLE 2.17. Selected chemical analyses of thermal water in the Tucson basin

Well No.	Location	Temperature	pH	Na	K	Ca	Mg	Cl	SO_4	HCO_3	NO_3	B	F	SiO_2
1	D-12-12-7caa	30.8	7.6	86	2.8	65	10	92	168	268	25	0.13	0.4	34
2	D-12-12-34dbb	31.9	9.2	66	0.8	4	0	60	38	63	6	0.56	1.3	11
3	D-12-12-34dbd	37.8	8.4	108	1.1	5	1	36	22	220	8	0.32	0.7	12
4	D-12-12-34dcc	31.9	8.0	55	2.6	59	9	40	26	278	7	0.12	0.5	35
5	D-13-13-17caa	31.9	7.8	105	3.3	104	12	84	200	220	7	0.07	0.4	12
6	D-14-14-29cbc	30.7	7.8	120	3.6	71	10	104	246	120	2	0.55	1.8	--
7(TEP5)	D-15-14-2cac	52.2	9.1	202	---	4	0.8	49.5	270	69	-	--	9.8	30
8(TEP7)	D-15-14-2dbc	52.0	9.1	155	---	4.3	0.4	31	182	120	1.4	--	5.7	46
9(TEP3)	D-15-14-3abb	33.3	7.9	75	---	48	3.7	10	105	165	-	--	0.7	24
10(TEP2)	D-15-14-3abc	30.6	7.8	74	---	46	5.8	10	115	154	-	--	0.6	22
11(TEP8)	D-15-14-3acd	31.8	7.8	75	---	38	3.3	11.5	133	140	-	--	1.07	32
12(TEP1)	D-15-14-3bac	30.0	7.7	68	---	40	4.6	10.5	130	140	-	--	0.73	30
13(TEP4)	D-15-14-3bbb	30.0	7.9	65	---	48	4.6	13.2	135	146	-	--	0.6	30
14(TEP6)	D-15-14-3dad	57.0	9.1	174	---	3	0.8	40.5	220	89	-	--	4.9	39
15(	D-16-13-34aab	31.1	7.5	53	4.6	87	22	61	210	145	-	0.08	--	38
16	D-16-13-34aab	32.2	7.7	52	4.5	74	21.0	54.0	180	147	-	0.11	--	41
17	D-16-14-21ccb	40.6	7.7	26	2.4	66	11	16	76	210	18	0.06	0.4	25
Agua Caliente Spring	D-13-16-20cdd	30.4	7.8	132.6	5.5	26.4	2.4	25.9	188.3	195.2	-	0.12	7.11	58

fluoride water, which is unacceptable for drinking by children. Total dissolved solids generally range between 300 and 700 mg/L and two distinct chemical groupings are observed. The highest temperature water is sodium sulfate type, while the majority of the thermal waters in the basin are calcium-sodium bicarbonate to calcium-sodium sulfate composition (Fig. 2.90). Nonthermal water in the basin has mostly a calcium-sodium bicarbonate composition (Fig. 2.91).

Basin-fill sediments (post mid-Miocene rock) act as a reservoir for known thermal-water occurrences in the basin.

IRVINGTON ROAD AND I-10 ANOMALY. The first significant indication of a possible geothermal resource in the Tucson basin was described by Schwalen and Shaw (1957), although at the time it was not recognized as a potential geothermal resource. The hot water was encountered in the Tucson Electric Power well TEP 1 (D-15-14-3bac) at the Irvington power station and was considered a nuisance and a curiosity. During drilling of this well in 1956, the water temperature changed from 27.8 to 43.3°C; drilling was stopped at 350.5 m and the hole was cemented back to 341.4 m to prevent entry of hot water into the well (Schwalen and Shaw, 1957).

Since 1956, eight additional wells have been drilled by TEP in sections 2 and 3, T. 15 S., R. 14 E. These wells range in depth between 250 and 959 m and have temperatures that range from 30°C to 57°C (Table 2.16). TEP wells 5, 6, and 7 have depths between 700 and 960 m and they pump the hottest known water in the basin (52 to 57°C) from depths below 400 m. Main production in TEP 5 is from about 564 m depth (files, USGS, Tucson).

Other TEP wells, all less than 350 m depth, pump 30 to 33°C water. Ground-water chemistry of the shallow TEP wells is distinct from the deep (>700 m) wells. The deep water has lower calcium, magnesium, and bicarbonate and higher sodium, sulfate, chloride, and fluoride concentrations than the shallow water. The composition of deep geothermal water is sodium sulfate, while the water from the shallow TEP wells is calcium-sodium sulfate (Fig. 2.90). The shallow TEP wells are chemically typical of both shallow ground water in the basin and surface water flow and runoff in local drainage (Fig. 2.90). Deep geothermal water encountered by wells TEP 5 and 6 has very high pH (>9.0) and relatively low silica concentration (<40 mg/L). Silica concentrations in the deep waters are in approximate equilibrium with quartz at measured temperatures (Silica concentration was adjusted for dissociation at high pH before silica geothermometers were estimated).

Geohydrology of the Irvington and I-10 area is complex. During drilling of the TEP 1 well in 1956, water was initially encountered at 44.8 m depth; however, after the hole was cased and perforated below 73.2 m, the static water level was 57.3 m depth. This 12.5 m drop in the static water level suggests either confined water below 73 m or a perched water table above 73 m.

The deep geothermal aquifers (>500 m depth) are apparently confined and hydrologically separate from the shallow (<200 m depth) aquifers. Evidence for confined conditions was observed during drilling of TEP 4, a shallow well, and TEP 5, a deep well. In November, 1959, TEP 4 had a static water level of 57 m depth (2,413 feet elevation). TEP 4 was perforated between 73 and 261.5 m. In January, 1960, TEP 5 was completed

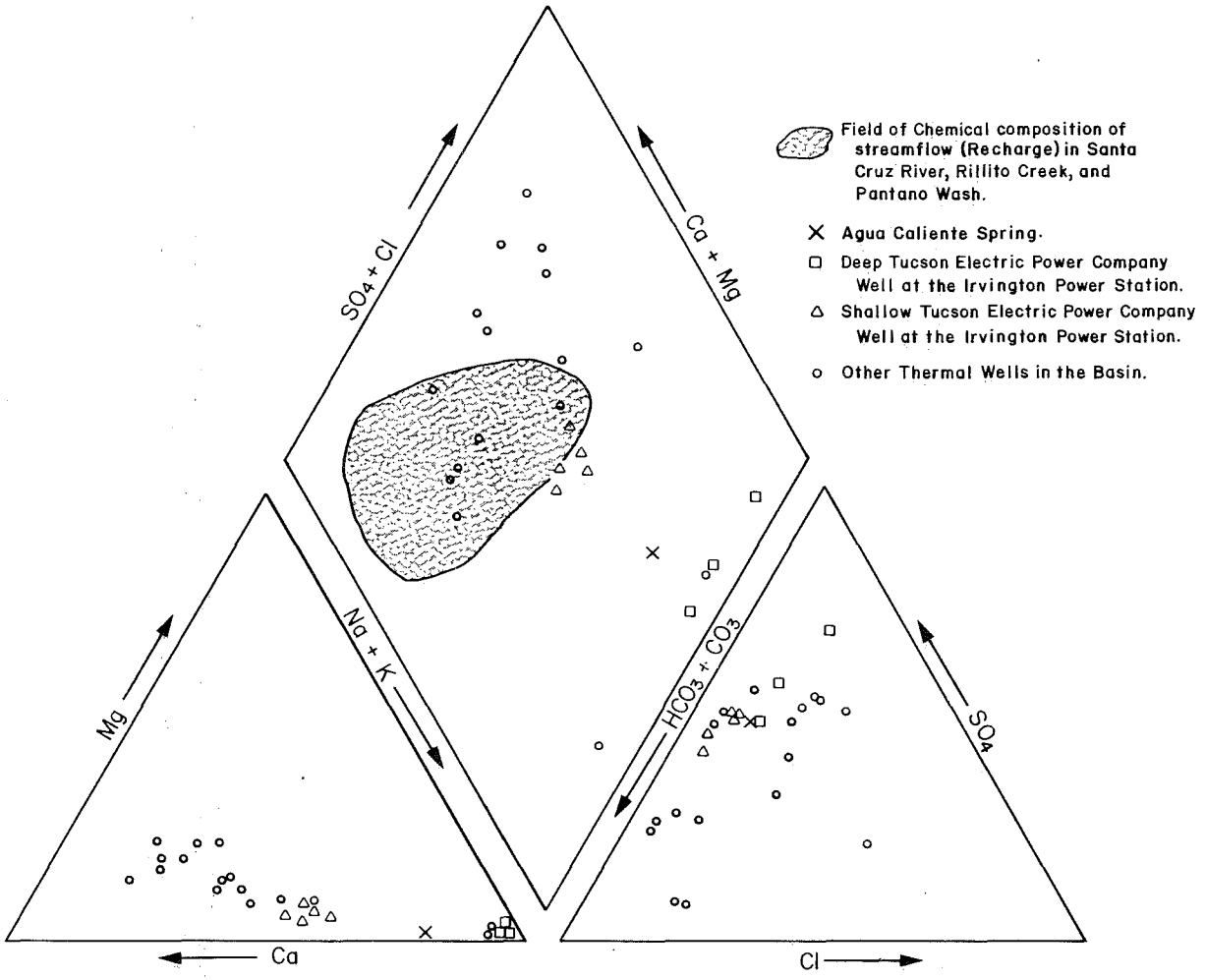

Figure 2.90. Piper diagram showing water chemistry of thermal waters (greater than 30°C) in the Tucson basin

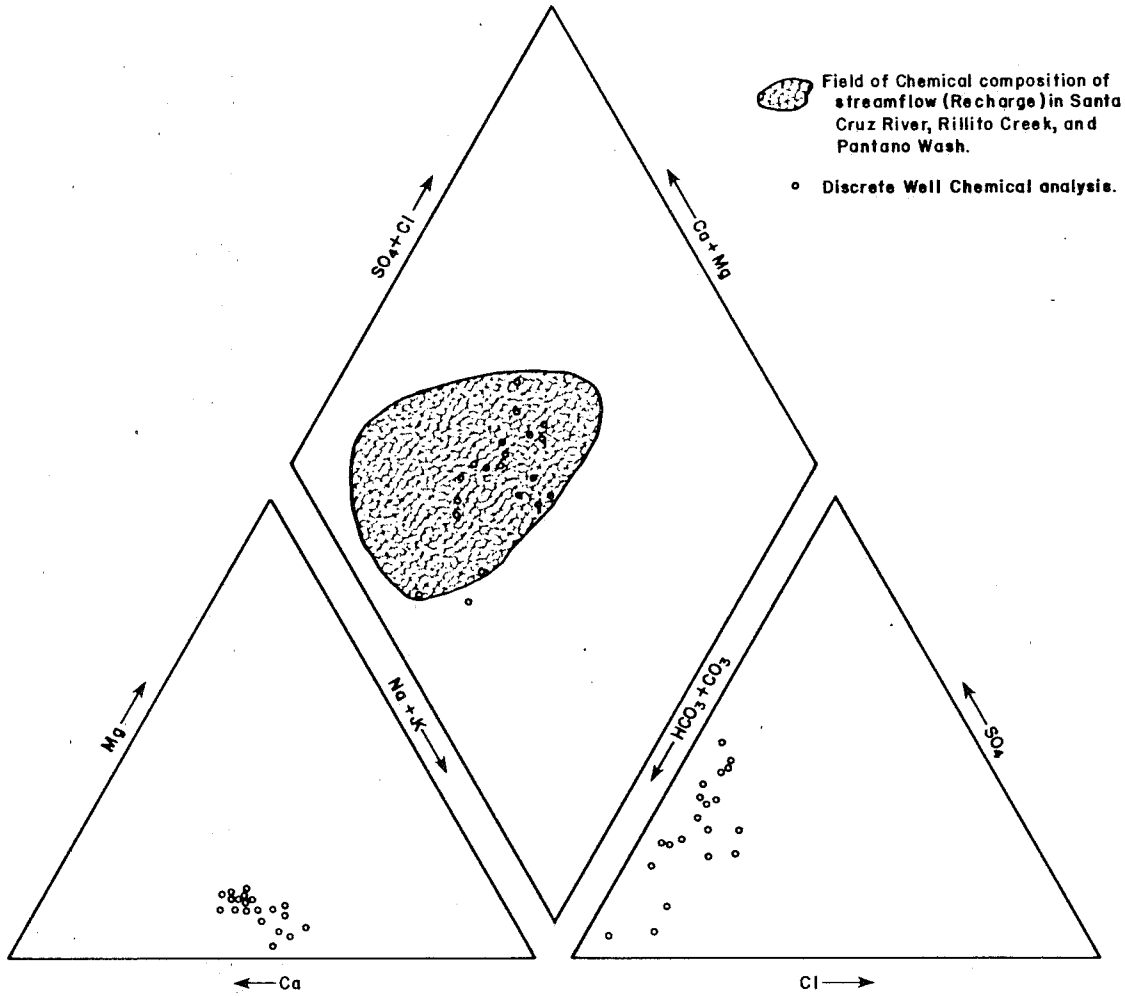

Figure 2.91. Piper diagram showing water chemistry of nonthermal water (less than 30°C) in the Tucson basin

to 762 m depth with perforated casing between 310 and 627 m. Static water level in this well was 87.5 m depth (2,378 feet elevation). A difference of 10.7 m in static water level was observed between TEP 4 and TEP 5.

Transmissivity values were determined for TEP 5 by the University of Arizona, Soils and Water Engineering Department in 1966. Drawdown transmissivity was .00765 m^2s^{-1} (63,000 gpd/ft). Prior to the test, the static level was 92.4 m; at the end of the test, the pumping level was 108.8 m. During testing of this well, which is perforated between 310 and 627 m, an approximate 6,810 L/min discharge rate was maintained. The deep thermal aquifer is very productive. However, since development of these wells by TEP, a significant drop in the pumping level has been observed. Fig. 2.92 shows the historical pumping-level drawdown. For the last twenty years the TEP 6 pumping level has dropped at a rate of .9 m/yr in contrast to the TEP 5 pumping level, which has dropped 1.4 m annually. Both wells have pumped up to 6,100 L/min (1,600 gpm) almost continuously during this time. Heavy pumping, well interference, facies changes, and possible nearby fault zones may all contribute to these drawdowns.

Thermal water encountered by TEP wells 5, 6, and 7 is contained in indurated sandstone and conglomerate below 427 m depth. These deep sediments have a more varied composition than overlying finer grained sediments. Fig. 2.93 is a lithologic log of TEP 6. Mudstone and sandy mudstone between 229 and 427 m separate thermal water from shallow ground water above 305 m depth. This confining mudstone unit apparently thickens and becomes gypsiferous to the south and southwest. Indurated

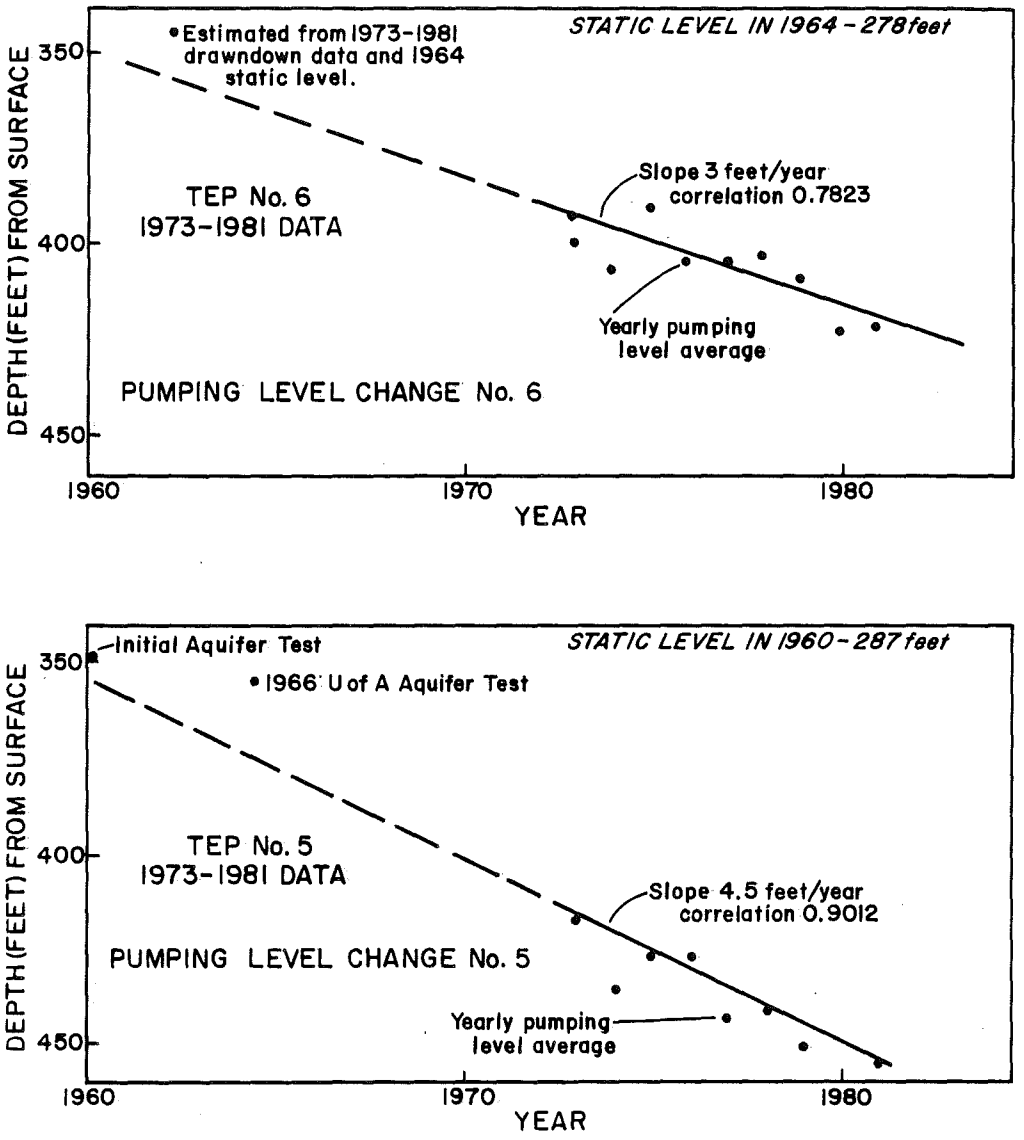

Figure 2.92. Pumping level changes in Tucson Electric Power wells 5 and 6 between 1960 and 1980

sandstone and conglomerate, which contain thermal water, may occur at greater depth in these areas below the mudstone. For example, the Humble State 32-1 hole was drilled through gypsiferous mudstone from 351 m to about 823 m depth. Below 823 m, this hole encountered sandstone

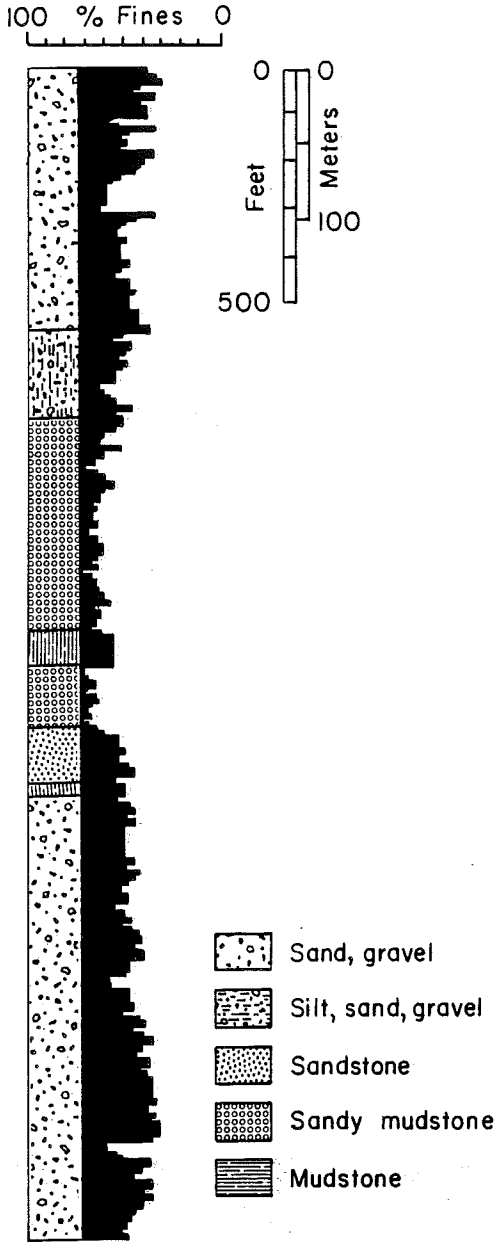

Figure 2.93. Generalized lithology of Tucson Electric Power Company well 6

and conglomerate with interbedded siltstone. The temperature of the mud increased noticeably at 1,158 m according to the geologist's log of this hole, which is on file at the Arizona Oil and Gas Conservation Commission, Phoenix. This temperature increase may have resulted from thermal water entering the drill hole.

CONCLUSIONS. A large volume of thermal water (40 to 60°C is known to occur in portions of the Tucson basin below 549 m depth. Wells producing water from this reservoir were drilled between 762 and 945 m depth in the Irvington Road-Interstate 10 area. Chemical quality of the water is good except for high fluoride concentrations. Because of Tucson's rapid growth and because its economy relies heavily upon the aerospace, agriculture, defense, education, electronics, mining, and tourist industries, significant opportunities exist for direct-heat utilization of this geothermal water. Geothermal energy could have economic impact by stabilizing and lowering energy costs to resource users.

TUCSON BASIN REFERENCES

Anderson, T. W., 1972, Electrical-analog analysis of the hydrologic system, Tucson basin, southeastern Arizona: U. S. Geological Survey Water Supply Paper 1939-C, 34 p.

Banks, N. G., 1977, Geologic setting and interpretation of a zone of middle Tertiary igneous-metamorphic complexes in south-central Arizona: U. S. Geological Survey Open File Report 77-376, 29 p.

Bikerman, M. and Damon, P. E., 1966, K/Ar chronology of the Tucson Mountains, Pima County, Arizona: Geological Society of America Bulletin, Vol. 77, no. 11 p. 1225-1234.

Coney, P. J., 1978, The plate tectonic setting of southeastern Arizona: *in* Callender, J. F., Wilt, J. C., and Clemons, R. E., eds., Land of Cochise, New Mexico Geological Society 29th Field Conference Guidebook, p. 285-290.

Davidson, E. S., 1973, Geohydrology and water resources of the Tucson basin, Arizona: U. S. Geological Survey Water Supply Paper 1939-E, 81 p.

Davis, R. W., 1967, A geophysical investigation of hydrologic boundaries in the Tucson basin, Pima County, Arizona: unpub. Ph.D. Thesis, University of Arizona, 64 p.

Davis, G. H. and Coney, P. J., 1979, Geologic development of the Cordilleran metamorphic core complexes: Geology, Vol. 7, p. 120-124.

Keith, S. B., Reynolds, S. J., Damon, P. E., Shafiqullah, M., Livingston, D. E., and Pushkar, P. D., 1980, Evidence for multiple intrusion and deformation within the Santa Catalina-Rincon-Tortolita crystalline complex, southeastern Arizona: Geological Society of America Memoir 153, p. 217-267.

Oppenheimer, J. M. and Sumner, J. S., 1981, Gravity modeling of the basin in the Basin and Range province Arizona: *in* Stone C. and Jenny, J. P., eds., Arizona Geological Society Digest, Vol. 13, p. 111-115 with 1:1,000,000 scale, depth to bedrock map.

Pashley, E. F., 1966, Structure and stratigraphy of the central, northern and eastern parts of the Tucson basin, Arizona: unpub. Ph.D. Thesis, University of Arizona, 273 p.

Peirce, H. W., 1976, Elements of Paleozoic tectonics in Arizona: Arizona Geological Society Tectonic Digest, Vol. 10, p. 37-57.

Roy, R. F., Decker, E. R., Blackwell, D. D., and Birch, F., 1968, Heat Flow in the United States: Journal of Geophysical Research, Vol. 73, no. 16, p. 5207-5221.

Sass, J. H., Lachenbruch, A. H., Munroe, R. J., Greene, G. W. and Moses, T. H., Jr., 1971, Heat flow in the western United States: Journal of Geophysical Research, Vol. 76, no. 26, p. 6376-6413.

Scarborough, R. B. and Peirce, H. W., 1978, Late Cenozoic basins of Arizona: *in* Callender, J. F., Wilt, J. C., and Clemons, R. E., eds., Land of Cochise, New Mexico Geological Society Guidebook, 29th Field Conference, p. 253-259.

Schwalen, H. C. and Shaw, R. J., 1957, Groundwater supplies of the Santa Cruz Valley of southern Arizona between Rillito Station and the international boundary: University of Arizona Agricultural Experiment Station Bulletin 288, 119 p.

Shafiqullah, M., Damon, P. E., Lynch, D. J., Reynolds, S. J., Rehrig, W. A., and Raymond, R. H., 1980, K-Ar geochronology and geologic history of southwestern Arizona and adjacent areas: *in* Jenney, J. P. and Stone, C., eds., Studies in Western Arizona, Arizona Geological Society Digest 12, p. 201-260.

Shearer, C., and Reiter, M., 1981, Terrestrial heat flow in Arizona: Journal of Geophysical Research, Vol. 86, no. B7, p. 6249-6260.

Silver, L. T., 1978, Precambrian formations and Precambrian history in Cochise County, southeastern Arizona: *in* Callendar, J. F., Wilt, J. C., and Clemons, R. E., eds., Land of Cochise, New Mexico Geological Society Guidebook, 29th Field Conference, p. 157-163.

Supkow, D. J., 1971, Subsurface heat flow as a means for determining aquifer characteristics in the Tucson basin, Pima County, Arizona: unpub. Ph.D. Thesis, University of Arizona, 182 p.

Wright, J. J. and Johnson, R. B., 1976, The significance of groundwater level declines in eastern Pima County Arizona: *in* 20th Annual Arizona Watershed Symposium, Arizona Water Commission Report 8, p. 22-29.

Warren, R. E., Sclater, J. G., Vacquier, V., and Roy, R. F., 1969, A comparison of terrestrial heat flow and transient geomagnetic fluctions in the southwestern United States: Geophysics, Vol. 34, no. 3, p. 463-478.

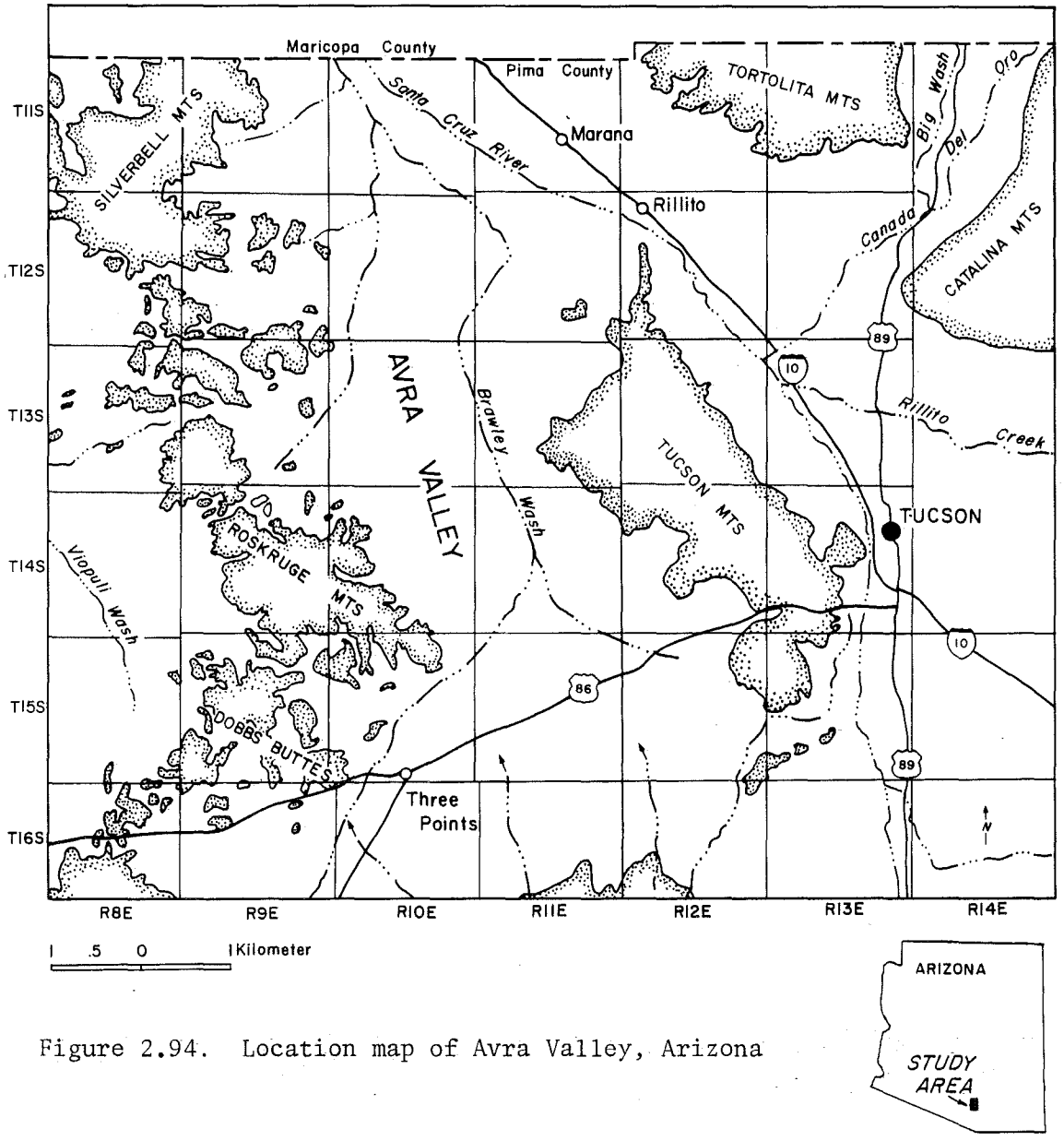

Figure 2.94. Location map of Avra Valley, Arizona

AVRA VALLEY

INTRODUCTION. Thermal wells in Avra Valley have temperatures between 32 to 53°C. The highest temperatures are generally near the Silver Bell mine at the north end of the valley. One well with 42°C water is located at the south end of the valley near Ryan Field, a small private air field. Potential for using low-temperature geothermal energy may exist at both sites.

The chief occupations in Avra Valley are farming and ranching. However, water level declines in the northern Avra Valley have been so great in recent years (4 million acre-feet between 1940 and 1978) that these activities eventually may phase out as a result of the high cost of pumping water to the surface from increasingly greater depths. Water level declines have been as great as 45 m in some parts of the basin. Ground-water withdrawals average about 100,000 acre-feet annually in Avra Valley.

The Tucson Water Department is developing a well field in the southern Avra Valley to supply water users in the Tucson metropolitan area, which lies in the next valley to the east.

PHYSIOGRAPHY. Avra Valley lies along the eastern edge of the Sonoran Desert subprovince in southeastern Arizona (Fig. 2.94). Mountains with up to 765 m of relief bound the north-northwest-trending valley along both sides. The valley floor has a very gentle slope of about 0.35 degrees or less towards the north. Elevation of the valley decreases south to north from about 760 m to 550 m.

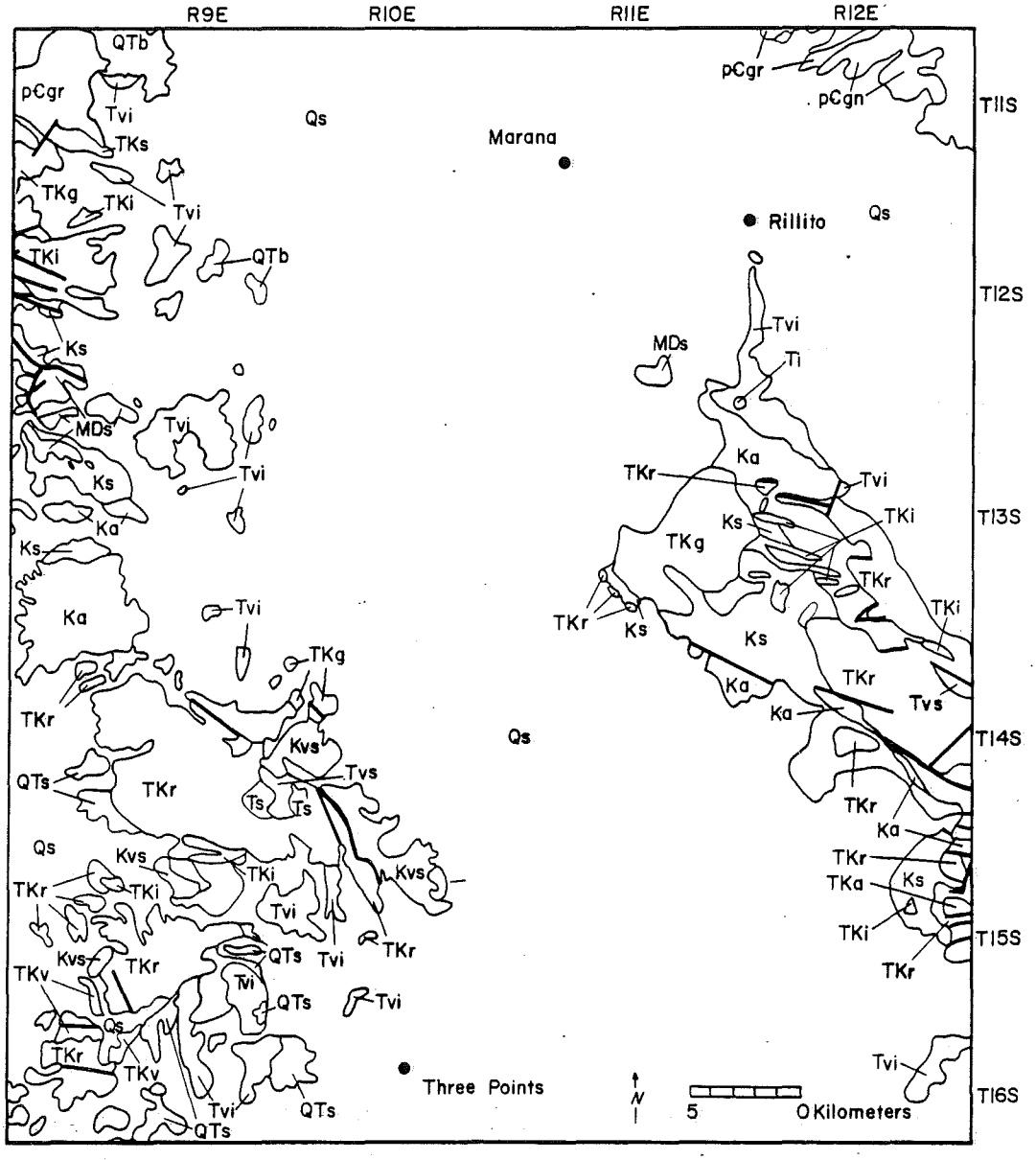

EXPLANATION

Qs	Sediments	TKs	Sediments	Kvs	Sedimentary and volcanic
QTs	Sediments	TKg	Granite	MDs	Sediments
QTb	Basalt	TKr	Rhyolite	pCgr	Granite
Ts	Sediments	TKi	Dikes, sills, and plugs	pCgn	Gneiss
Tvs	Silicic volcanics	TKv	Volcanics, undivided		
Tvi	Intermediate volcanics	Ks	Sediments		
Ti	Dikes, sills, and plugs	Ka	Andesite		

Figure 2.95. Generalized geologic map of Avra Valley, Arizona

GEOLOGY. The principal mountains bounding Avra Valley (Fig. 2.95) are the Silver Bell, Waterman, and Roskruge Mountains on the southwest side and the Tucson and Tortolita Mountains on the northeast. These ranges, except the Silver Bell and Tortolita Mountains, are composed chiefly of Late Cretaceous to mid-Tertiary volcanic rocks of andesitic to rhyolitic composition, Mesozoic sedimentary rocks, and Mesozoic to mid-Tertiary granite. The Tortolita Mountains are a metamorphic core complex composed of Precambrian to mid-Tertiary plutonic and metamorphic rocks. The Silver Bell Mountains are chiefly Mesozoic sedimentary and Laramide volcanic rocks (intermediate to silicic composition), Precambrian granitic rock, and Tertiary basalt. Small exposures of Paleozoic limestone and quartzite crop out along the southwest side of the valley between the Roskruge and Silver Bell Mountains, and just west of the Tucson Mountains on the east side of the valley.

Depth to bedrock data, based on gravity studies (Lysonski, Aiken, Sumner, 1981; Openheimer and Sumner, 1981) for the valley, show that the topography of the basin floor does not parallel the valley surface. At the narrowest part of the valley a buried bedrock "saddle" extends across the valley, dividing the graben into two smaller depressions. The northern graben is deeper, about 2,900 m (Allen, 1981). This basin is actually part of the Red Rock structural basin. The southern depression is between about 1,500 and 2,000 m deep (Oppenheimer and Sumner, 1981) and forms a subbasin at the northeastern end of the Altar Valley graben. Bedrock topography had a major controlling effect on sedimentation patterns within the basin during and after its formation.

The surficial alluvium in Avra Valley is fine-grained sand and silt, interbedded with coarse sand and gravel. These deposits are generally about 10 m thick.

Two subsurface units beneath the surficial deposits were defined by the Tucson Water Department during a drilling program in the late 1970s. The two units were informally called the younger and older alluvium by Allen (1981) who believed the upper unit is correlative with the Fort Lowell Formation of Davidson (1973), the upper and mostly unconsolidated unit in the Tucson basin.

The younger alluvium is interpreted to be fluvial, whereas the older alluvium is interpreted to be of both lacustrine and fluvial origin (Allen, 1981).

The younger alluvium is a relatively thin unit that immediately underlies the surficial deposits. The lower boundary of this unit, that is, the contact with the underlying older alluvium, was found at depths between 85 m and 146 m. Where bedrock was encountered in the Tucson Water Department drill holes, it was found directly beneath the older alluvium. In deeper portions of the basin, the older alluvium extended below the 400 m depth in holes drilled by the Tucson Water Department. Test holes drilled by other companies indicate thicknesses of greater than 1,300 m for the older alluvium in the northern part of Avra Valley.

In the north and central parts of the valley the younger alluvium is characterized by very thick interbedded layers of coarse and fine-grained sediments. These individual beds vary between 1.5 and 15 m in thickness. The fine-grained beds consist of silts and sandy silts, and probably some minor clay. The coarse-grained beds are sandy gravels and gravelly sands.

In most cases, the fine-grained material is more abundant than the coarse-grained material. In general, the younger alluvium unit coarsens upward. In the southern part of Avra Valley, the sediments of the younger alluvium exhibit more variability, which may indicate the former presence of a small Pleistocene lake within a small internal drainage depositional basin. For the most part the unit is uncemented, although some weak carbonate cementation locally occurs.

The contact between the younger and older alluvium is irregular in elevation and is apparently disconformable. The disconformity may represent a period of weathering and/or erosion of the older alluvium prior to deposition of the younger unit.

Two facies of the older alluvium have been identified, a conglomerate and a mudstone facies. The conglomerate facies is an extensive unit, so thick that it usually extends below the 400 m depth in wells drilled by the Tucson Water Department, except in areas of shallow bedrock. It consists of moderately to well-cemented, poorly sorted, angular to subangular sandy gravel to gravelly sand. In the deeper northern subbasin under Avra Valley, north of a buried bedrock saddle, the conglomerate grades laterally northwards towards the subbasin center into the mudstone facies. The mudstone is a semiconsolidated brown silt and clay mixture that contains very little sand and gravel. Some deeper sections of the mudstone are gypsiferous.

The young alluvium is apparently Pliocene to Pleistocene in age and the older alluvium is upper Miocene to mid-Pliocene in age (Allen, 1981).

GEOHYDROLOGY. The ground-water system beneath Avra Valley is recharged primarily from ground-water underflow entering the basin at Three

Points and at Rillito to the north (Fig. 2.96). At the north end of Avra Valley the ground water joins the northwest-moving ground water from the Tucson basin, and continues northwesterly toward the area of ground-water discharge from the basin between the Silver Bell Mountains and Picacho Peak. Very minor recharge is derived from infiltration of meteoric water along stream channels, principally Brawley Wash, and the contiguous mountain fronts (Osterkamp, 1973a). The basin sediments are for the most part hydraulically interconnected throughout the area to a depth of at least 400 m, and form a single water-table aquifer (Whelen, 1979, unpub. report).

Depths to water beneath Avra Valley are generally 90 to 120 m in the southern basin and 60 to 90 m at the northern end (Osterkamp, 1973b). Dissolved solids content is less than 500 mg/L (Kister, 1974).

GEOCHEMISTRY. Soil samples were collected along three traverses across Avra Valley and were analyzed for mercury content (Fig. 2.97). An approximate background value is about 75 ppb. Values greater than 75 ppb occur within a northwest-trending zone down the center of Avra Valley. A possibility exists that this mercury anomaly defines a major structural trend through the valley. Mercury is sometimes an indicator of geothermal anomalies and of structures such as normal Basin and Range faults. Another explanation for the higher mercury values along this zone, which is also the main ground-water flow path, is that the mercury has been carried there as detritus and in solution by stream flow from a known mercury deposit on the northeast side of Altar Valley, about 18 km west-southwest of Three Points. The entire length of both washes could contain anomalous concentrations of mercury, but the higher values were noted only where the

sampling survey crossed Brawley Wash. In addition, mercury is a common vapor associated with oxidizing sulfide ores, and it is a common "pathfinder element" associated with fluorspar deposits (Peters, 1978). Fluorite deposits and copper mineralization are common occurrences upstream from the presently defined anomaly, less than 10 km south of Three Points. Detritus from these deposits could also be a source of anomalous mercury in Brawley Wash.

THERMAL REGIME. At least thirteen wells in Avra Valley have both temperatures and estimated gradients sufficiently high to be thermal (Fig. 2.98). These wells cover much of the entire valley, but the higher values are mostly at the north-northwest end, near the Silver Bell mine. Gradients are in the general range of 45 to 65°C/km, except for relatively shallow wells (<100 m deep) that have gradients exceeding 100°C/km.

Temperatures were measured downhole at 5 m intervals in nine wells during a preliminary geothermal evaluation (Hahman and Allen, 1981). Five wells were isothermal. Previously measured temperature logs were available for four additional wells. Fig. 2.99 shows the temperature at 100 m depth in 12 of these wells. The higher temperatures are generally along the southwest side of the valley.

Three heat flow measurements have been made in Avra Valley: 94, 99, and 107 mWm^{-2} (Roy and others, 1968; Sass and others, 1971; Shearer, 1979) (Fig. 2.99). These values are normal to slightly above normal for the Basin and Range province. The highest value is at the southern end of the valley.

GEOTHERMOMETRY. Numerous wells have been drilled in Avra Valley for test purposes and for domestic and irrigation water supplies. Few wells,

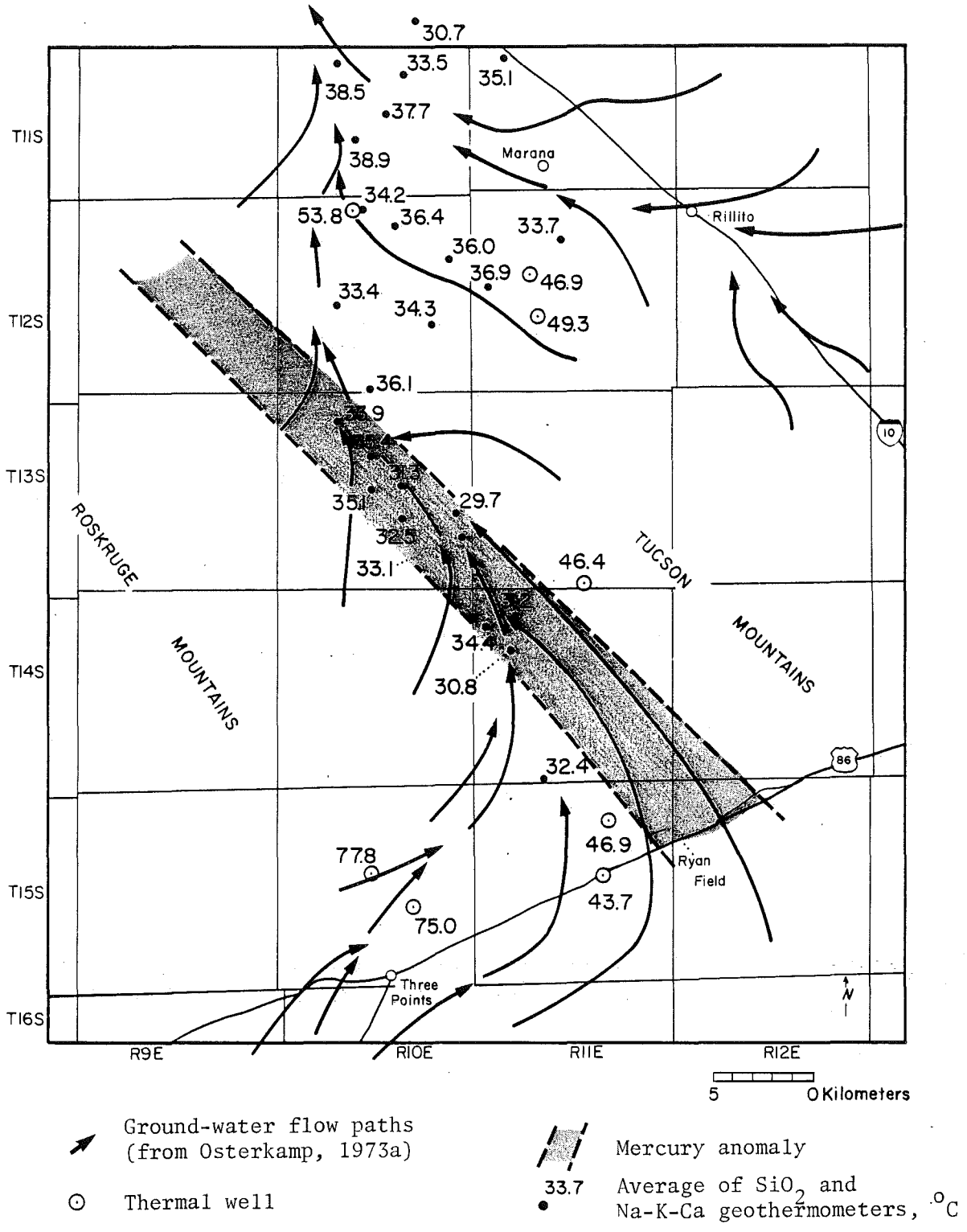

Figure 2.96. Map of Avra Valley showing ground-water flow paths, thermal wells, area of anomalous mercury in soil, and averaged geothermometers

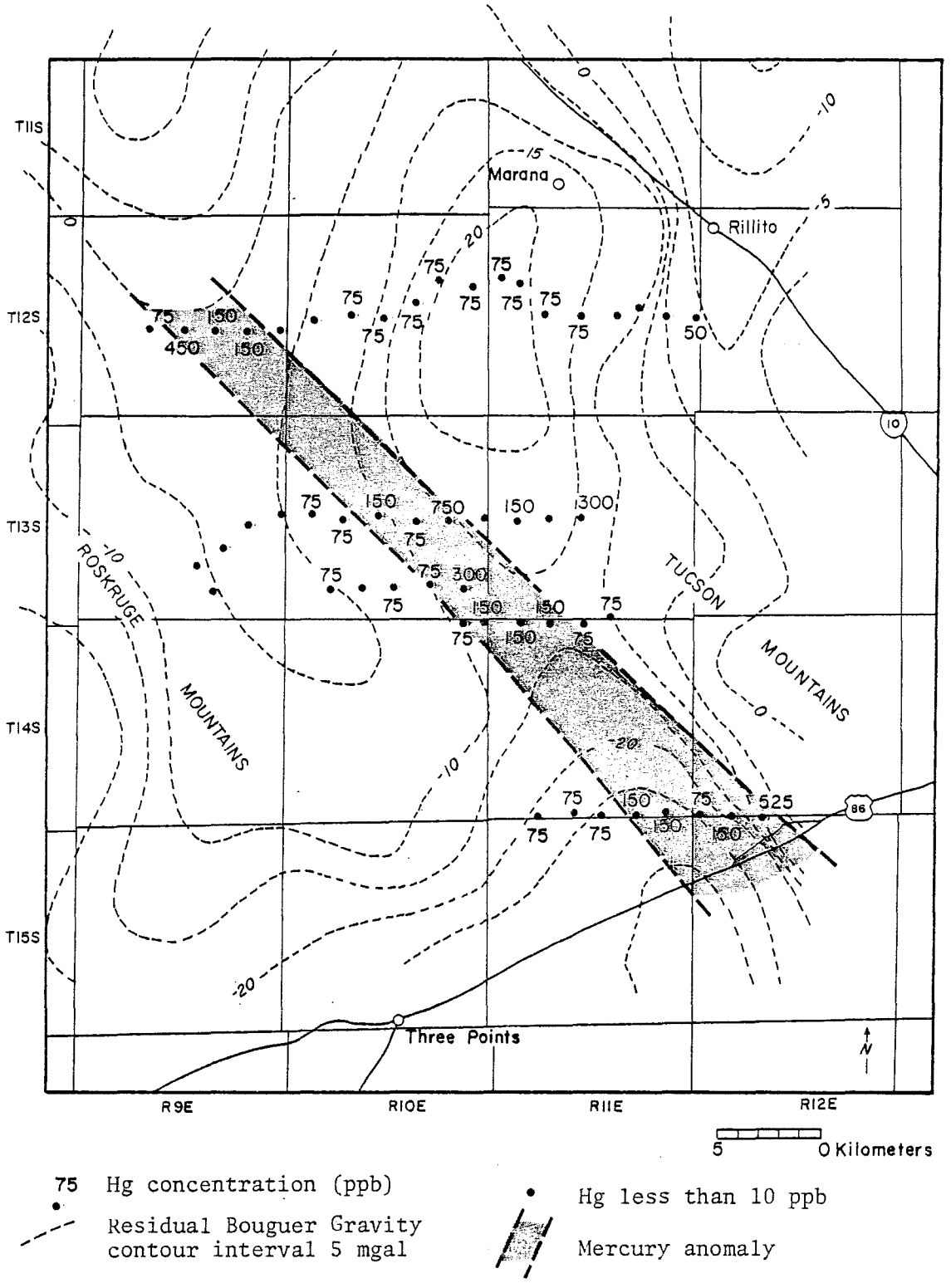

Figure 2.97. Map of Avra Valley showing mercury concentrations in soil, area of anomalous mercury, and residual Bouguer gravity

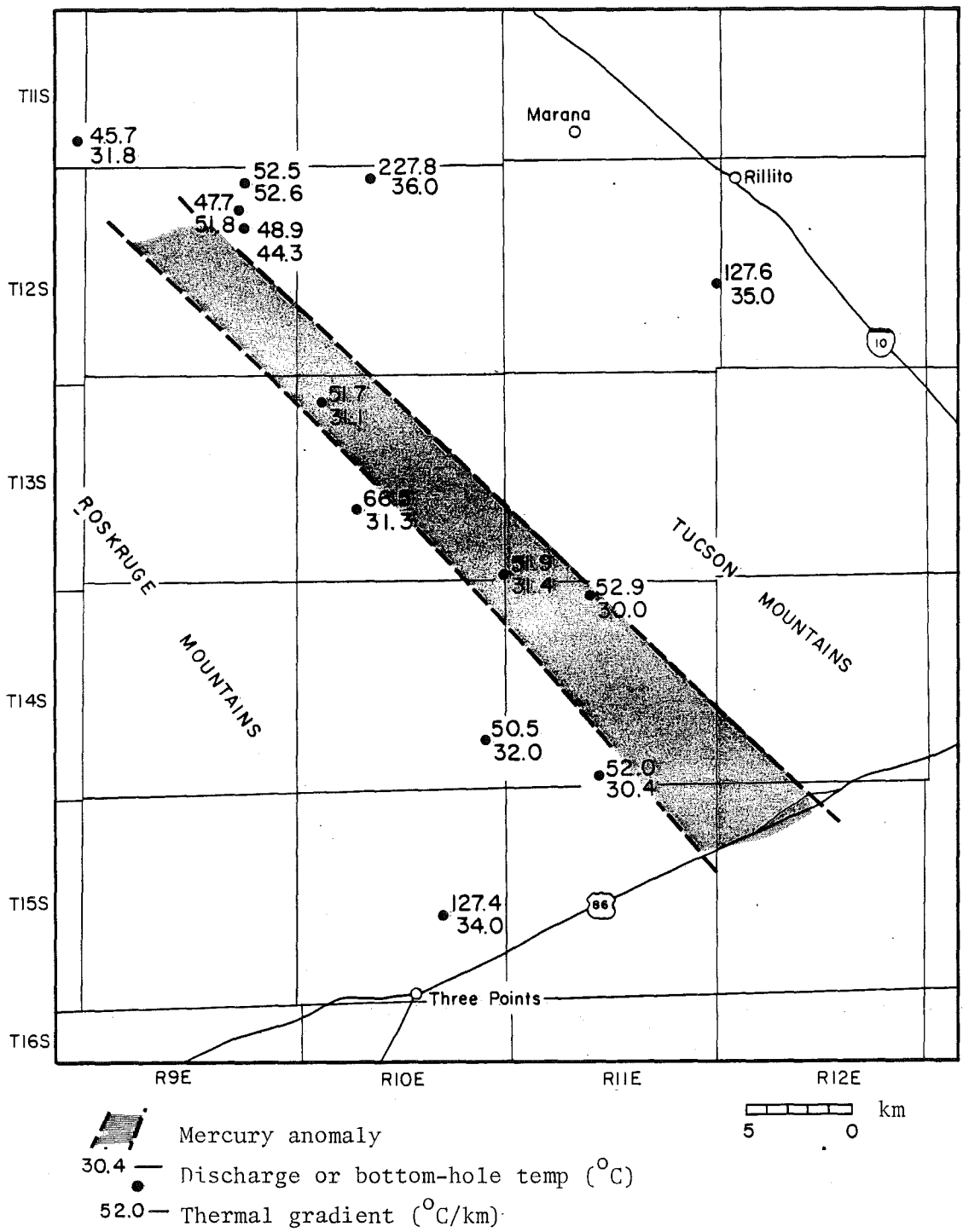

Figure 2.98. Map of Avra Valley showing area of anomalous mercury, measured well temperatures (°C) and thermal gradients (°C/km)

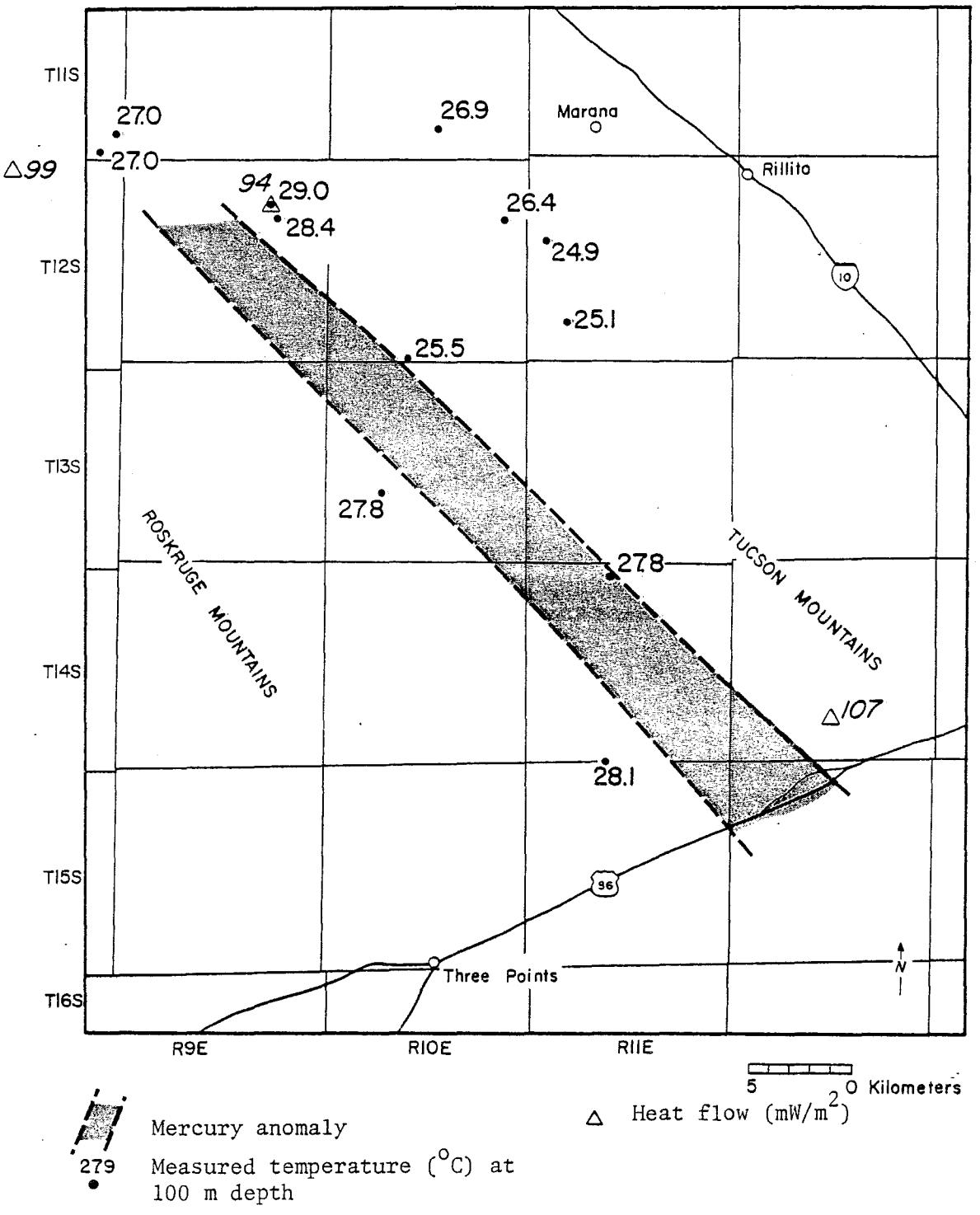

Figure 2.99. Map of Avra Valley showing area of anomalous mercury, measured temperatures at 100 m depth (°C), and heat flow (mW/m²)

however, have a full compliment of analytical data such as temperature and depth measurements, flow rates, and complete chemical analyses. Thus, in calculating geothermometers, only 33 wells have sufficient data to derive both SiO_2 and Na-K-Ca temperatures. It can be seen in Table 2.18 that 25 wells have an excellent correspondence between temperatures predicted by the Na-K-Ca geothermometer and the α-christobalite geothermometer. These geothermometers predict a mean subsurface temperature of 34.2 ± 2.5°C for ground water beneath Avra Valley. These same wells have a mean discharge temperature of 28.4 ± 2.5°C, which indicates the water may have reached temperature-dependent chemical equilibrium with their host rocks. Six wells show a correlation between the Na-K-Ca and chalcedony geothermometers. These wells have a mean discharge temperature of 31.4 ± 3.1°C and predict a mean subsurface temperature of 47.8 ± 3.4°C. Two wells show an excellent correlation between the Na-K-Ca and quartz geothermometers. One has a discharge temperature of 34°C; temperature of the other well is unknown. These wells, which are located at the southern end of Avra Valley, predict an aquifer temperature of about 76°C (Fig. 2.96).

GEOPHYSICS. The residual Bouguer gravity map of Arizona indicates the presence of two basins beneath Avra Valley, separated by a basement high. Steep gravity gradients along the northeast side of the southern basin and the southwest side of the northern basin (Fig. 2.97) suggest a northwest-trending linear (fault or Silver Bell-Bisbee discontinuity(?) of Titley, 1976) down the length of the valley. This feature coincides with the mercury anomaly identified by Hahman and Allen (1981), and supports the possibility that the mercury anomaly reflects a major basement structure beneath Avra Valley.

TABLE 2.18. Temperatures, depths, and geothermometers for wells in Avra Valley

Location	T_{meas} (°C)	Depth (m)	Grad (°C/km)	T_{chal} (°C)	$T_{Na-K-Ca}$ (°C)	$T_{\alpha-chris}$ (°C)	T_{ave} (°C)
D-11- 8-36aaa*	32	235	46	-	-	-	-
D-11-10- 2cba	24	-	-	57	23	38	31
8ddd	27	-	-	55	41	36	39
15aad	24	-	-	59	28	39	34
22bdd	26	-	-	52	42	34	38
28bad	30	-	-	55	42	36	39
D-11-11- 7ddd	25	-	-	57	32	38	35
D-12- 9- 2 *	53	610	53	-	-	-	-
11 *	52	650	48	-	-	-	-
11 *	44	470	49	-	-	-	-
D-12-10- 3dcd	30	-	-	52	39	34	36
4acd	29	-	-	52	35	34	34
4bdd	36	71	228	57	50	38	54
12ccd	28	-	-	55	36	36	36
20add	27	-	-	56	30	37	33
23ddc	30	-	-	52	35	34	34
33ddd	29	-	-	54	37	35	36
D-12-11- 9acc	24	-	-	52	34	34	34
17acd	-	-	-	45	49	27	47
18cdd	26	-	-	55	38	36	37
20dda	28	-	-	55	44	25	49
D-12-12-19cbb*	35	110	128	63	-	-	-
D-13-10- 5ddd	-	-	-	56	31	37	34
6ddd	31	195	52	-	-	-	-
9ddd	30	-	-	57	33	38	35
15ddd	30	-	-	55	27	36	31
16ddd	31	-	-	54	36	35	35
20cdd	31	155	67	-	-	-	-
22ddd	31	-	-	54	30	35	33
24dcb	29	-	-	55	24	36	30
25acd	31	-	-	56	29	37	33
D-13-11-31ccc*	31	205	52	-	-	-	-
34cdd	-	-	-	47	46	28	46
D-14-10-25caa*	32	218	51	-	-	-	-
D-14-11- 4caa	30	175	53	-	-	-	-
5ccd	30	-	-	55	27	36	31
7bad	31	-	-	55	33	36	34
8ccc	31	-	-	56	25	37	31
33ccc	31	-	-	55	29	36	32
33dcc	30	200	52	-	-	-	-
D-15-10-16dad	-	-	-	48	76	79+	78
23cbc*	31	66	197	50	69	81+	75
D-15-11-11bbb	34	-	-	48	47	30	47
11bbb	42	338	43	-	-	-	-
15bbb	31	610	34	-	-	-	-
15bbb	-	-	-	45	42	27	44

+ = Conductive quartz geothermometer
* = Thermal well
MAT ≃ 21°C

CONCLUSIONS. The geothermal waters in Avra Valley constitute a low-temperature resource. South and southwest of the linear mercury anomaly, 30°C water is fairly ubiquitous at depths of 300 m. The higher geothermometers and the 107 mWm^{-2} heat flow value also occur at the southern end of the valley. North of the mercury anomaly, the geothermal occurence is not well defined, if indeed one exists. The lower gradients and lower surface-discharge temperatures indicate recharge to and shallow circulation in the ground water system.

On the northwestern side of Avra Valley, gradients, heat flow, and one high geothermometer indicate a potential for 50 to 55°C water at 1,000 m. This resource might be used at Silver Bell mine to assist in the copper leaching process. West of Ryan Field, geothermal potential also exists but depth and temperatures are not well defined. This resource, if one exists, might be used at the air field building for space conditioning.

AVRA VALLEY REFERENCES

Allen, T. J., 1981, The subsurface stratigraphy of northern Avra Valley, Pima County, Arizona: M.S. Thesis, Kent State University, 82 p.

Davidson, E. S., 1973, Geohydrology and water resources of the Tucson basin, Arizona: U.S. Geological Survey, Water-Supply Paper, 1939-E, 81 p.

Hahman, Sr, W. R., and Allen, T. J., 1981, Subsurface stratigraphy and geothermal resource potential of the Avra Valley, Pima County, Arizona: Bureau of Geology and Mineral Technology Open-File Report 81-5, 48 p.

Kister, L. R., 1974, Dissolved-solids content of ground water in the Tucson area, Arizona: U.S. Geological Survey Miscellaneous Investigations Series I-844-I, scale 1:250,000.

Lysonski, J. C., Aiken, C. L. V., and Sumner, J. S., 1981, The complete residual Bouguer gravity anomaly map (Tucson AMS sheet): Tucson, Bureau of Geology and Mineral Technology, unpub. map series, 1:250,000 scale.

Oppenheimer, J. M., and Sumner, J. S., 1981, Gravity modeling of the basins in the Basin and Range Province, Arizona: Arizona Geological Society Digest, v. 13, p. 111-115.

Osterkamp, W. R., 1973a, Ground water recharge in the Tucson area, Arizona: U.S. Geological Survey Miscellaneous Investigations Series Map I-844-E, scale 1:250,000.

_____, 1973b, Map showing depth to water in wells in the Tucson area, Arizona: U.S. Geological Survey Miscellaneous Investigations Series Map I-844-D, scale 1:250,000.

Peters, W. C., 1978, Exploration and mining geology: John Wiley and Sons, 696 p.

Roy, R. F., Decker, E. R., Blackwell, D. D. and Birch, F., 1968, Heat flow in the United States: Journal of Geophysical Research, v. 73, p. 5207-5221.

Sass, J. H., Lackenbruch, A. H., Munroe, R. J., Greene, G. W. and Moses, Jr., T. H., 1971, Heat flow in the western United States: Journal of Geophysical Research, v. 76, p. 6376-6413.

Shearer, C. R., 1979. A regional terrestrial heat-flow study in Arizona: Ph.D. dissertation, Socorro, New Mexico Institute of Mining and Technology, 184 p.

Whelen, A., 1979, An appraisal of the geohydrology of Avra Valley, unpublished report, 45 p.

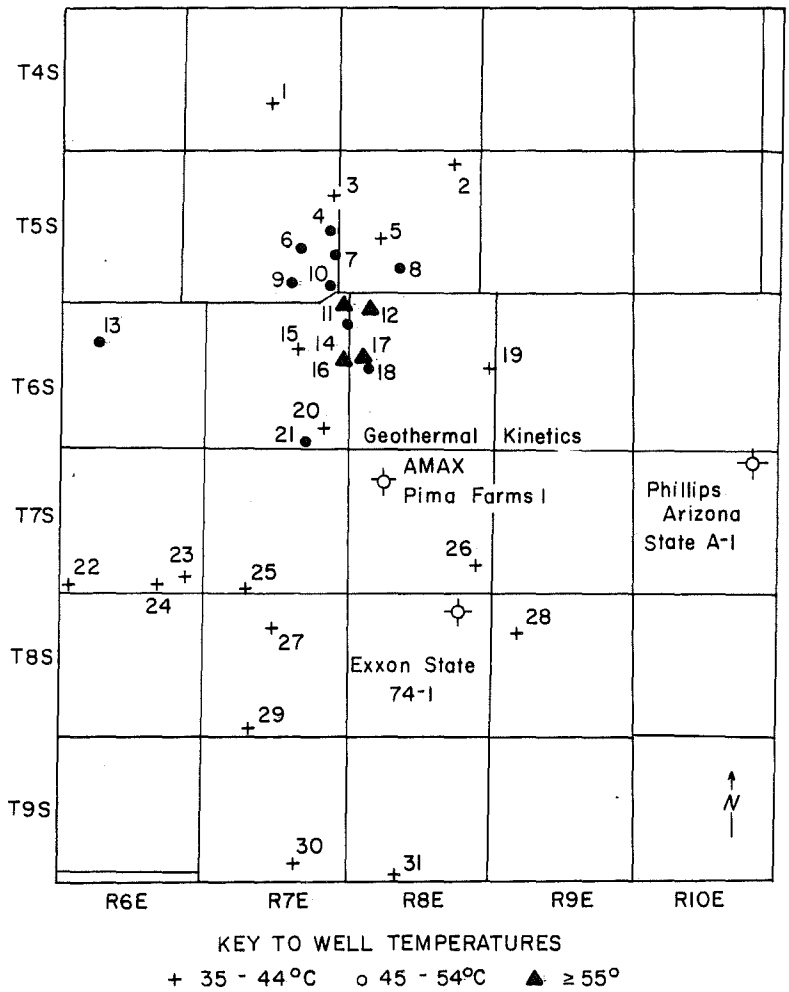

Figure 2.100. Location map of thermal wells (greater than 35°C) and selected deep geothermal and oil and gas exploration tests, Coolidge area

COOLIDGE AREA

INTRODUCTION. More than 20 irrigation wells pump thermal water in the Coolidge, Arizona area and a few of these wells are among the hottest water-producing wells in Arizona (Fig. 2.100; Table 2.19). The occurrence of these 50 to 70°C wells motivated Geothermal Kinetics Systems, Inc. to conduct geothermal exploration, which culminated in 1974 in drilling a deep (2,446 m) test well (Dellechaie, 1975). This well, the Geothermal Kinetics-Amax Exploration No. 1 Pima Farms, produced 82°C water from Pinal Schist in the basement of the Picacho basin. Because no high temperature water suitable for electrical power generation was found by the test, this hole was plugged and abandoned after pump tests. However, it should be noted that with today's higher fossil fuel costs, 82°C water has potential economic use for direct-heat applications.

PHYSIOGRAPHY. The Coolidge area is situated in the Sonoran Desert section of the Basin and Range province. This area overlies the Picacho basin, a nearly flat valley situated between the rugged Picacho Mountains on the southeast and the Sacaton Mountains on the west (Fig. 2.101). The valley floor is drained by McClellan Wash, which flows northward into the Gila River. Several large canals divert water from the Gila River into the Picacho basin for irrigation. In addition to surface-water usage, extensive ground-water development also provides water for irrigation.

GEOLOGY. Paleozoic and Mesozoic rocks are mostly absent from the geologic record in the Coolidge area. This is because post-Laramide and

TABLE 2.19. Thermal wells in the Coolidge area

Well	Location	Temperature °C	Flow Rate L/min	TDS Mg/L	Depth M
1	D-4-7-27BBB	37		714	140
2	D-5-8-2ADA	37		660	
3	D-5-7-12DDD	35		510	306
4	D-5-7-24BD	46	7620	789	469
5	D-5-8-20BOO	37		702	
6	D-5-7-23CO	46			427
7	D-5-7-25ADD	54		9500	591
8	D-5-8-28COO	52		684*	
9	D-5-7-34ACD	42	4808		367
10	D-5-6-36ACC	54		1170	724
11	D-6-7-1AAA	65	3780	1915	914
12	D-6-8-16ADD	72	2271	9120	782
13	D-6-6-8BDD	46			914
14	D-6-7-1DC	49			931
15	D-6-7-10DCD	35		1602	126
16	D-6-7-13ADD	62	5700		914
17	D-6-8-18CDD	61	7500	1101	995
18	D-6-8-18CD	46			989
19	D-6-8-24ADA	37		1494	91
20	D-6-7-35AD	43			789
21	D-6-7-34DD	49	6780	556	774
22	D-7-6-31CCC	40			195
23	D-7-6-35ADD	37		264	146
24	D-7-6-34DDA	35		450	185
25	D-7-7-32-CCD	40		323	466
26	D-7-8-25CC	35			589
27	D-8-7-9ADD	44	946	2440	640
28	D-8-9-7ADD	35		487	420
29	D-8-7-32DDD	36			396
30	D-9-7-34AD	41			610
31	D-9-8-32DDD	37		276	153

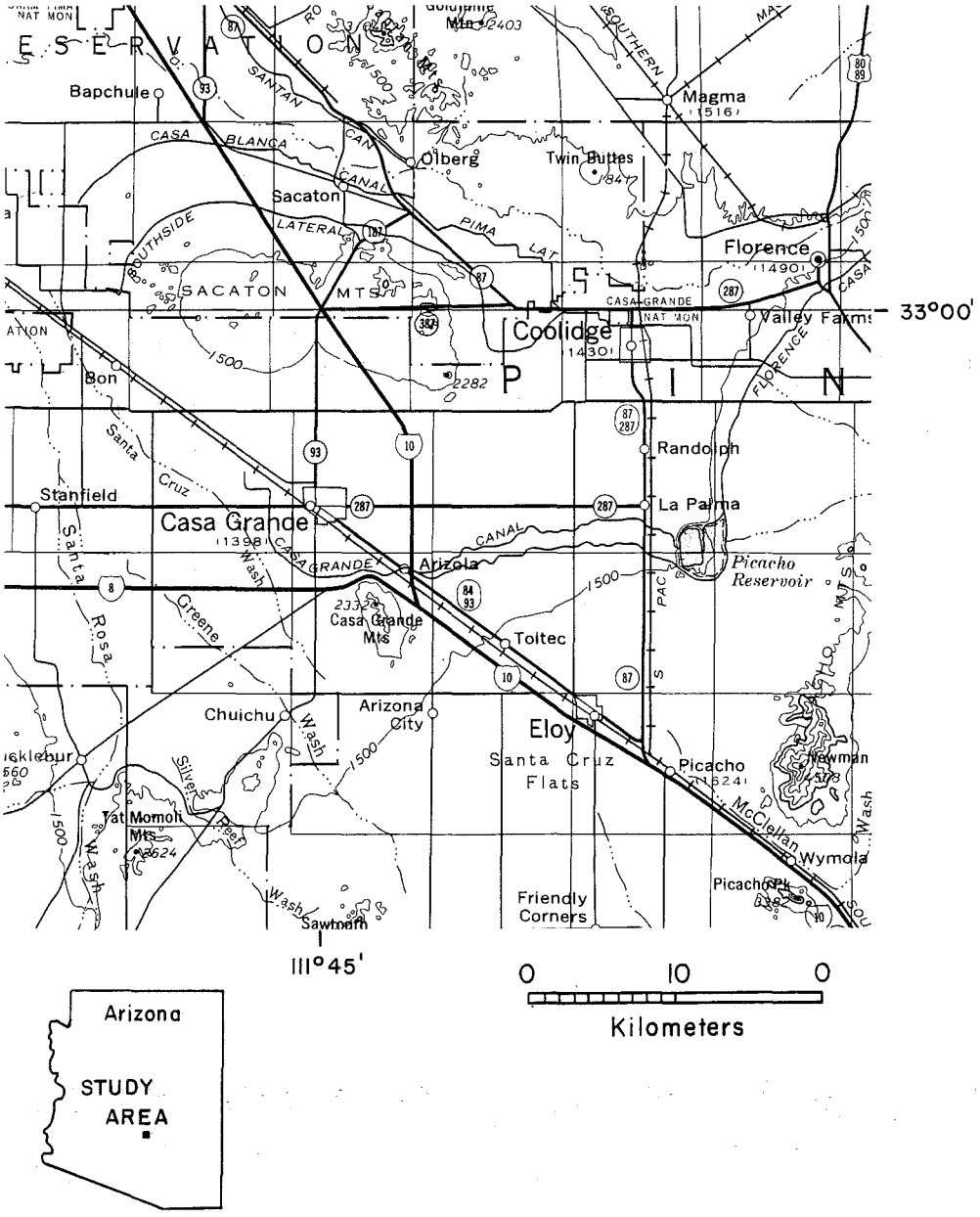

Figure 2.101. Location map of the Coolidge area

probable Mesozoic(?) erosion of the Florence uplift has removed these rocks (Turner, 1962). Pre-Tertiary basement rocks consist of Precambrian Pinal Schist, granite, and diabase, which are intruded by Laramide intermediate to silicic plutons and dikes.

In the Sacaton Mountains, Pinal Schist is invaded by Oracle Granite, while diabase and aplite dikes intrude both the Pinal Schist and the Oracle Granite. Two Laramide plutons intrude the Precambrian rocks and they are associated with copper mineralization. Up to 760 m of Whitetail Conglomerate(?) (Oligocene), composed of steeply dipping gravels with clasts of Oracle Granite and Pinal Schist, is observed at the Sacaton mine on the Sacaton Mountains pediment (Cummings, 1982). Deep drill-hole information indicates that the Sacaton Mountains, at least in the vicinity of the Sacaton mine, are allochthonous. They are deformed by listric normal faults, which merge into a dislocation surface or decollement that overlies Pinal Schist (Cummings, 1982). This faulting post dates the steeply dipping conglomerate.

Two major geologic terranes were mapped by Yeend (1976) in the Picacho Mountains. The northern terrane consists of Precambrian schist and granite to granodiorite, and Tertiary intermediate dikes. The southern Picacho Mountains are formed by a broad north-trending and south-plunging arch of layered granitic gneiss with Tertiary K-Ar dates (Johnson, 1981). These dates record a major thermal disturbance in the Precambrian through Tertiary metamorphic and plutonic rocks.

Immediately south of the main mass of the Picacho Mountains, Picacho Peak stands high above Interstate 10. This peak, a remnant of a pile of trachytic rocks between 22.4 and 20.7 m.y. old, was tilted by listric normal faulting (Shafiqullah and others, 1976).

During 1980, a deep stratigraphic test, the Phillips Petroleum Company Arizona State A-1, was drilled to 5,492 m depth 3 km east of the northern Picacho Mountains. This hole, in section 2, T. 7 S., R. 10 E., drilled through: (1) granite to granodiorite (1.39 m.y. Rb-Sr) at 1,182 to 3,280 m depth; (2) muscovite granite (47 m.y. Rb-Sr) between 3,280 and 3,888 m depth; and (3) into gneiss (25 to 31 m.y. reset K-Ar) from 3,888 to 5,492 m depth (Reif and Robinson, 1981). At 3,658 m in this hole, a zone of chloritic breccia was encountered, which resulted in a "drilling break" (lost circulation?) at 3,675 m. This breccia continued until 3,888 m depth. Reif and Robinson (1981) interpreted a decollement or detachment zone as the cause of the change from breccia to gneiss. This detachment separates unmetamorphosed granitic rocks from a buried metamorphic complex. This morphology is typical of metamorphic core complexes (Davis and Coney, 1979). Seismic profiling near the Arizona State A-1 well in the Picacho basin shows reflective surfaces (detachment?) dipping beneath the basin. The broken nature of the rock along this detachment may allow ground water to circulate to great depth where high temperatures may exist due to the normal geothermal gradient.

Present day physiography of the Coolidge area is the result of late-Tertiary Basin and Range tectonism. The Picacho basin, a graben structure formed by this event, is filled with up to 2.5 km of basin-filling (post mid-Miocene) sediments (Scarborough and Peirce, 1978). These sediments overlie older Miocene volcanic flows and clastic sediments that rest upon crystalline basement. Deep drill holes have encountered thick evaporite strata within the basin-filling stratigraphic sequence. The Geothermal Kinetics-Amax Exploration Pima Farms 1 (section 8, T. 7 S., R. 8 E.)

encountered 442 m of gypsum, anhydrite, and halite between 716 and 1,158 m depth. The upper 180 to 210 m of this sequence contained halite (Peirce, 1981). Halite was also encountered in the Exxon State 74-1 well (section 2, T. 8 S., R. 8 E.) at 652 m depth, while gypsum and anhydrite with clay stringers were encountered between 712 and 2,536 m depth. Miocene volcanic strata and mid-Tertiary clastic sediments underlie the basin-fill sequence and overlie the basement metamorphic complex in the Geothermal Kinetics well and the Exxon well.

Upper-basin fill, penetrated by irrigation wells that are less than 762 m deep, is divided into three major units: an upper sand and gravel unit, a silt and clay unit, and a lower sand and gravel unit (Hardt and others, 1964). The silt and clay unit is 0 to over 600 m thick, and separates the upper and lower sand and gravel units. In the deeper portions of the Picacho basin, the clay and silt overlie thick evaporite sequences that in turn overlie sand and gravel or Miocene volcanic rocks. The lower sand and gravel unit, which is penetrated by deeper irrigation wells, is generally more cemented than the upper sand and gravel unit.

GEOHYDROLOGY. Prior to major ground-water development, ground-water flow was northward and westward toward the Gila River and Casa Grande (Konieczki and English, 1979). As a consequence of long term irrigation pumping, the direction of flow has changed in the southern Picacho basin toward a large water table cone of depression centered near Eloy. Subsidence and ground cracking due to ground-water withdrawal is a major problem in the Eloy area (Laney and others, 1978).

THERMAL WATER. Dellechaie (1975) discussed the thermal irrigation wells in the Coolidge area as part of a report on geochemical studies done

after and during testing of the Pima Farms 1 geothermal test by Geothermal Kinetics Systems and Amax Exploration. Thermal water in the area shows enrichment in sulfate and chloride and a depletion in bicarbonate relative to nonthermal water. In general, thermal water in the Picacho basin has the following cation and anion relationships: (1) $Cl>SO_4>HCO_3$; and (2) Na>Ca>K>Mg. These chemical relationships are compatible with the presence of evaporite minerals at depth within the basin-filling sediments.

Thermal irrigation water in the area ranges from 30°C to 72°C for wells 91 to 914 m deep. Flow rates exceed 5,500 L/min for several of the hotter wells (>45°C). TDS varies widely, between 264 mg/L and 9,120 mg/L, probably as a result of contact by some of these waters with halite and gypsum.

Chemistry of the thermal water reflects the presence of halite and gypsum. Fig. 2.102 is a Piper diagram of water chemistry constructed from analyses of irrigation wells and fluids produced by the Pima Farms 1 test well. Water from the irrigation wells and the test well is sodium chloride. However, differences between the shallower irrigation water and the deeper test water do exist; the irrigation wells have a higher percentage of sulfate and a lower percentage of calcium than the test well.

The Pima Farms 1 test well was pump tested at a rate of approximately 1,100 L/min for 193 hours (Dellechaie, 1975). After 16 hours, both the temperature and fluid chemistry had stabilized and temperatures throughout most of the remaining test were 80 to 82°C (Dellechaie, 1975).

A temperature log of this hole before testing shows a temperature inversion between 1,800 and 2,100 m (Fig. 2.103) (Dellechaie, 1975). Another temperature log made after the hole was cased to 1,800 m and pump tested,

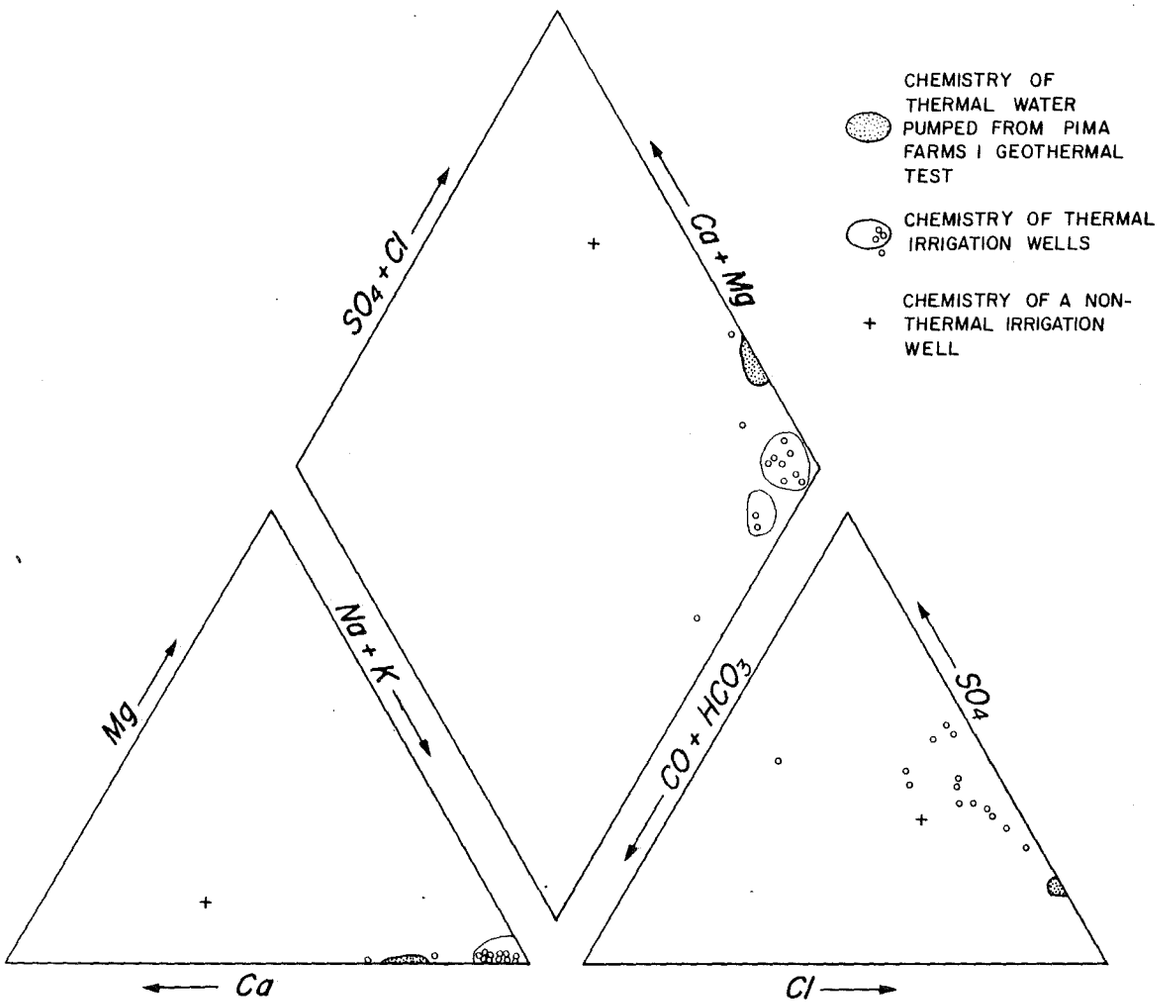

Figure 2.102. Piper diagram showing chemistry of thermal water in the Coolidge area

does not show a temperature anomaly between 1,800 and 2,100 m. During drilling, fluid probably entered a permeable zone at 1,800 to 2,100 m depth and consequently cooled this zone. Later pump tests withdrew the drill fluids and induced formation water flow through this zone, which reheated the rock at 1,800 to 2,100 m depth and removed the thermal disturbance. Water temperatures during the test (80 to 82°C) agree closely with temperatures recorded (83-88°C) after testing the 1,800 to 2,100 m depth interval.

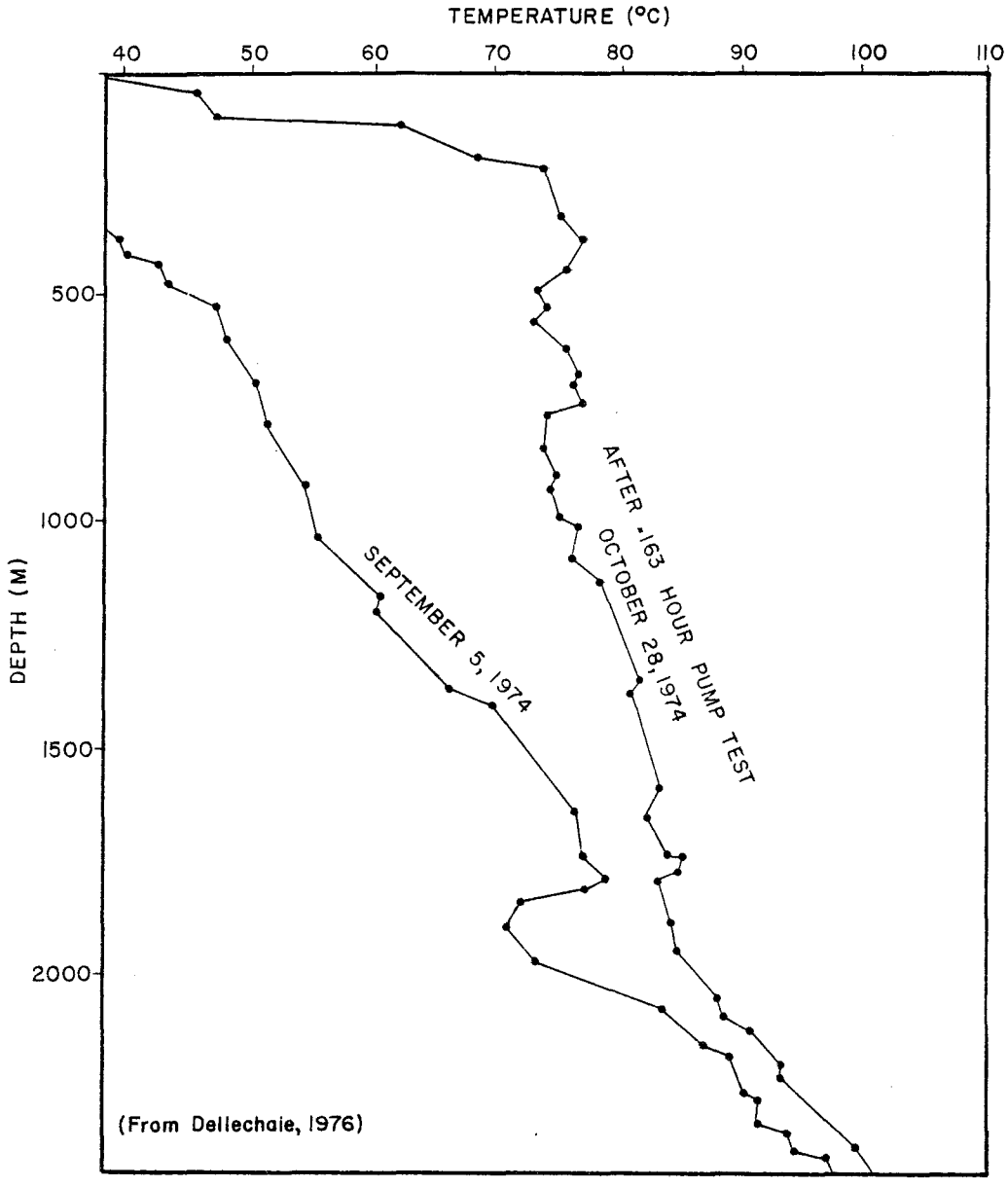

Figure 2.103. Temperature logs of the Geothermal Kinetics-Amax Exploration Pima Farms 1 geothermal test well

The permeable zone at 1,800 to 2,100 m depth in the Pima Farms 1 well may result from important regional structure. This zone is in Precambrian schist; normally schist does not act as an aquifer. However, this permeable zone is immediately below mid-Tertiary sedimentary and Miocene volcanic rocks, which, in the Sacaton Mountains and at Picacho

Peak, are displaced and tilted by listric normal faults that merge into an underlying decollement or detachment fault in Pinal Schist. Because this detachment or decollement may also be present in the Picacho basin, it is reasonable to assume that the permeable zone between 1,800 and 2,100 m depth is caused by a detachment zone and its associated listric faults. The similarity of the stratigraphy below basin fill in the Picacho basin with strata at Picacho Peak and in portions of the Sacaton Mountains argues strongly for this interpretation.

CONCLUSION. Geothermal waters (to 82°C) in the Coolidge area have attractive potential for space heating and cooling, greenhouses, aquaculture, and processing of agricultural products. Geothermal resource development may require reinjection in this area so that the present subsidence and earth cracking problems are not exacerbated. However, geothermal development may help alleviate some ground-water withdrawal problems. Geothermal greenhouses and aquaculture, which employ reinjection and use less water per acre of land than conventional agriculture, have potential to conserve ground water and insure productivity of the land or even increase productivity.

COOLIDGE AREA REFERENCES

Cummings, R. B., 1982, Geology of the Sacaton porphyry copper deposit, Pinal County, Arizona: *in* Titley, S. R., ed., Advances in Geology of the Porphyry Copper Deposits Southweatern North America, The University of Arizona Press, Tucson, Arizona, p. 507-522.

Davis, G. H., and Coney, P. J., 1979, Geological development of the cordilleran metamorphic core complexes: Geology, vol. 7, p. 120-124.

Dellechaie, F., 1975, A hydrochemical study of the south Santa Cruz basin near Coolidge, Arizona: *in* Proceedings Second United Nations Symposium on the Development and Use of Geothermal Resources, U. S. Government Printing Office, vol. 1., p. 339-348.

Hardt, W. F., Cattany, R. E., and Kister, L. R., 1964, Basic ground-water data for western Pinal County, Arizona: Arizona State Land Department Water Resources Report 18, 59 p.

Johnson, G. S., 1981, The geology and geochronology of the northern Picacho Mountains, Pinal County, Arizona: Unpub. M. S. thesis, University of Arizona, 65 p.

Konieczki, A. D. and English, C. S., 1979, Maps showing ground-water conditions in the lower Santa Cruz area, Pinal, Pima, and Maricopa Counties, Arizona - 1977: U. S. Geological Survey Water-Resources Investigation 79-56, Open-File Report.

Laney, R. L., Raymond, R. H., and Winikka, C. C., 1978, Map showing water-level declines, land subsidence, and earth fissures in south-central Arizona: U. S. Geological Survey Water-Resources Investigation 78-83, Open-File Report.

Peirce, H. W., 1981, Major Arizona salt deposits: Arizona Bureau of Geology and Mineral Technology, Fieldnotes, vol. 11, no. 4., p. 1-4.

Reif, D. M. and Robinson, J. P., 1981, Geophysical, geochemical and petrographic data and regional correlation from the Arizona State A-1 well, Pinal County, Arizona: *in* Stone, C. and Jenney, J. P., eds, Arizona Geological Society Digest 13, p. 99-109.

Scarborough, R. B. and Peirce, H. W., 1978, Late Cenozoic basins of Arizona: *in* Callender, J. F., Wilt, J. C. and Clemons, R. E., Land of Cochise, New Mexico Geological Society Twentyninth Field Conference Guidebook, p. 253-260.

Shafiqullah, M., Lynch, D. J., Damon, P. E. and Peirce, H. W., 1976 Geology, geochronology, and geochemistry of the Picacho Peak area, Pinal County, Arizona: *in* Wilt, J. C. and Jenney, J. P., Tectonic Digest, Arizona Geological Society Digest 10, p. 305-324.

Turner, G. L., 1962, The Deming axis, southeastern Arizona, New Mexico, and Trans-Pecos Texas, *in* Weber, R. H. and Peirce, H. W., eds. Mogollon Rim Region, east central Arizona, New Mexico Geological Society Thirteenth Field Conference Guidebook, p. 59-71.

Yeend, W., 1976, Reconnaissance geologic map of the Picacho Mountains, Arizona: U. S. Geological Survey Miscellaneous Field Studies Map MF-778.

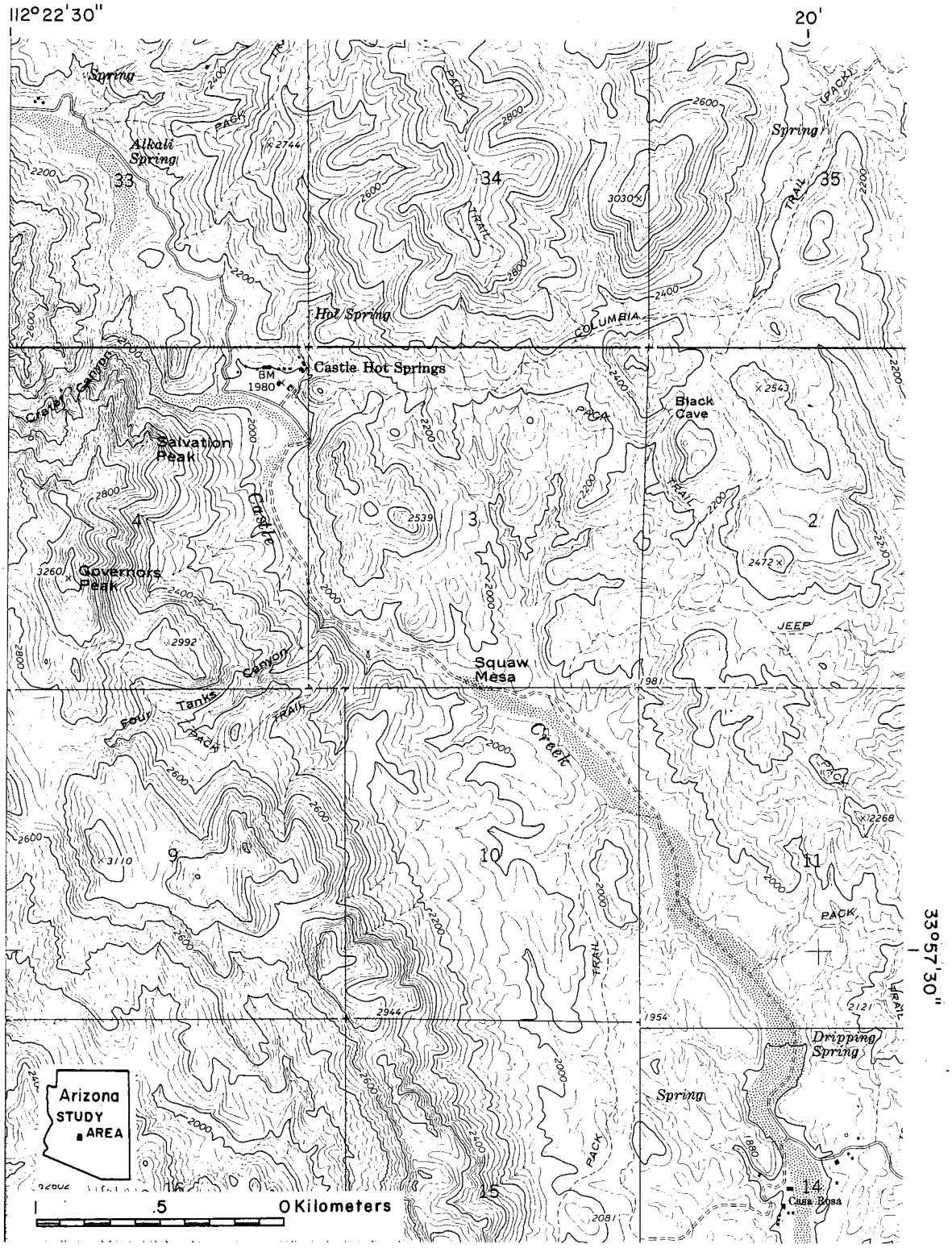

Figure 2.104. Physiographic map of Castle Hot Springs area

CASTLE HOT SPRINGS

INTRODUCTION. Castle Hot Spring, about 80 km northwest of Phoenix, is the site of a once-famous resort of the same name. The property is presently owned by the Arizona State University Foundation, Tempe, and used as a University conference center. During the late 1970s, the Foundation considered using hot water from the inferred geothermal reservoir to heat and cool the conference center buildings. Research into the chemistry, origin, and extent of the hot-spring system was conducted toward that goal (Sheridan and others, 1980; Satkin, 1981), but the idea was eventually abandoned for fear of disturbing the original Castle Hot Spring.

The spring issues 46°C water at a rate of about 1,300 L/min. Results of the preliminary studies indicate a maximum reservoir temperature of about 100°C, and the existence of a more extensive hydrothermal system (>2 km length along a fault zone) than previously recognized.

PHYSIOGRAPHY. Castle Hot Spring is located south of the Bradshaw Mountains, along the north wall of a deep, narrow canyon in the Transition Zone (Fig. 2.104). Topography is rugged; the canyon walls are nearly vertical, and in many places they are separated by little more than the width of Castle Creek. MAT is 21°C, but temperatures during the summer months often exceed twice that.

GEOLOGY. Castle Hot Spring occurs in a northwest-trending graben of Tertiary volcanic rocks displaced into a Precambrian basement complex (Fig. 2.105). The large displacements (300 m) are along northwest-trending

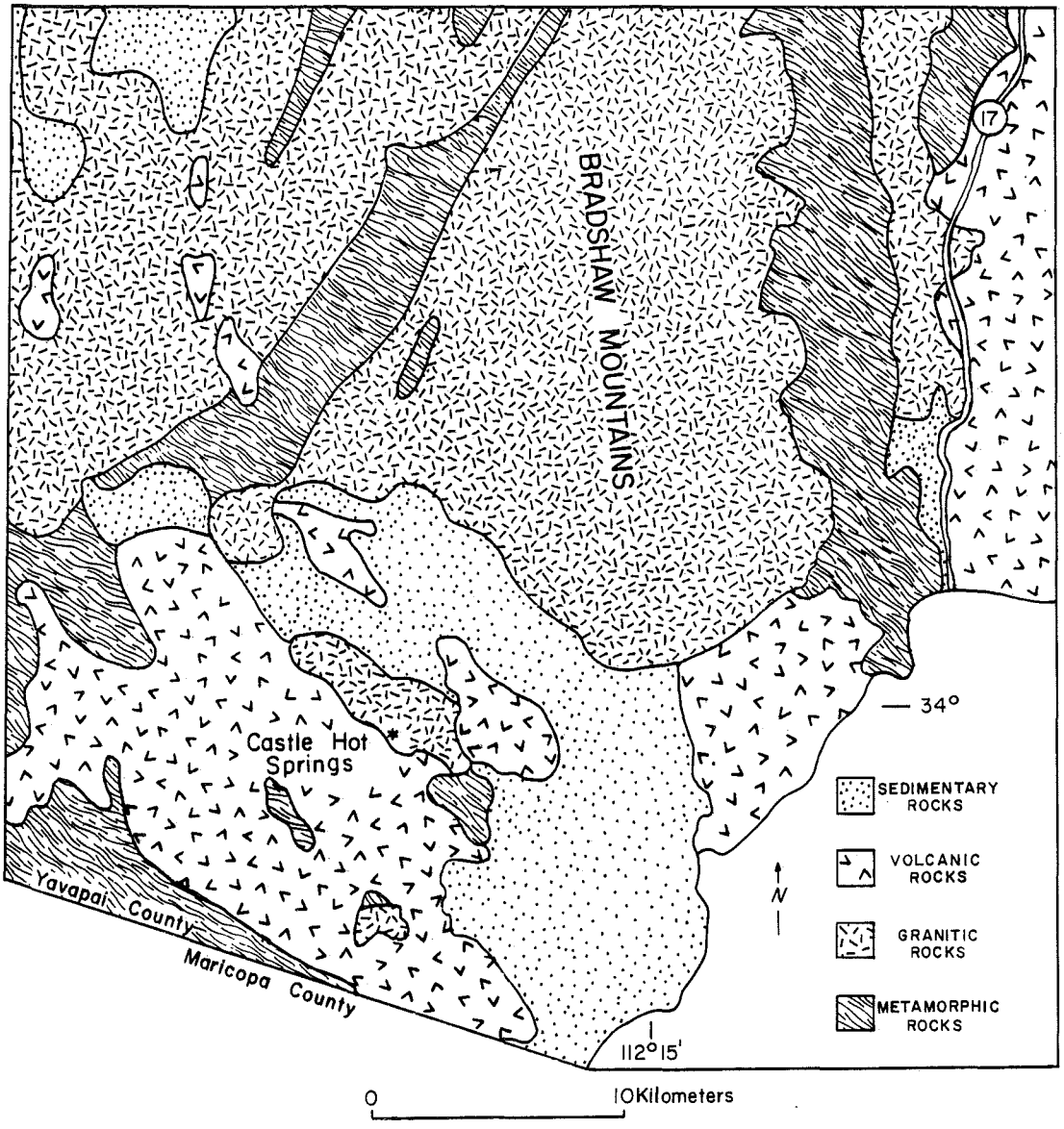

Figure 2.105. Generalized geologic map, Castle Hot Springs area

en echelon faults that placed northeast-dipping volcanic rocks (the downthrown, southwest block) into fault contact with basement rocks (Ward, 1977). The major fault in this system has been called Castle fault by Sheridan and others (1980), who noted that the hot springs emerge from this fault along the northeast margin of the graben.

Terrace deposits 40 to 80 m above Castle Creek indicate filling of the graben with Tertiary-Quaternary gravels. These gravels were later exhumed while the present drainage was being established, but the main spring system remains about 40 m above the present stream level (Sheridan and others, 1980).

Hydrothermal alteration is extensive within the volcanic rocks along the fault contacts. Commonly 5 to 15 percent of phenocrysts and groundmass have been replaced by calcite. Some of the mafic volcanic rocks are stained red as a result of oxidation and hydration of iron-bearing minerals. The intensity of alteration increases to the northwest where large siliceous sinter deposits provide possible evidence of a former high-temperature hydrothermal system. Travertine is being deposited at active hot springs in the Castle Hot Spring area today and is found at the sites of extinct hot springs.

GEOTHERMOMETRY. Satkin sampled the springs and wells in the Castle Hot Spring area between October, 1979 and September 1980. From the samples analyzed (Fig. 2.106). He identified three chemically distinct groups of water. The five samples of thermal water (Group I) emanate from the Castle fault system. They are sodium-chloride-sulfate water with relatively high concentrations of SiO_2, Li, and F, and low Mg. Group II waters are non-thermal and have low TDS. They are characterized by relatively low

concentrations of SiO_2, Li, and F. Group III waters emerge from perennial springs and have much higher TDS than do Group I or II waters. During the same period, Satkin periodically resampled several of the wells and springs, but found no notable changes in water chemistry. From this he concluded that local climate and precipitation have no perceptable effects on chemistry or temperature of the sampled springs or wells, and therefore, probably have no discernable effect on the hot-spring system.

There is excellent agreement between temperatures predicted by the chalcedony and Na-K-Ca geothermometers within each group. The geothermometers indicate a minimum reservoir temperature of about 85°C for Castle Hot Spring and the other thermal waters of Group I. Mixing models predict a maximum reservoir temperature of about 100°C. Group II waters have low estimated temperatures (≈49°C), and Group III waters have predicted temperatures of about 80°C. The Group III waters probably are not a part of the Castle Hot Spring system, based on their distinct water chemistry. They may reflect a separate geothermal resource that warrants additional exploration.

CONCLUSIONS. The heat source for the low-temperature Castle Hot Spring system is most likely heating by deep circulation along normal faults in an area of normal geothermal gradients. The hot water rises along the Castle fault zone where it cools conductively and mixes(?) with shallow cold water, emerging at temperatures somewhat less than 50°C. Development of the resource at the Castle Hot Spring Conference Center appears unlikely. However, because the geothermal system is more extensive than formerly suspected, development farther to the east may be feasible as more people move into that area.

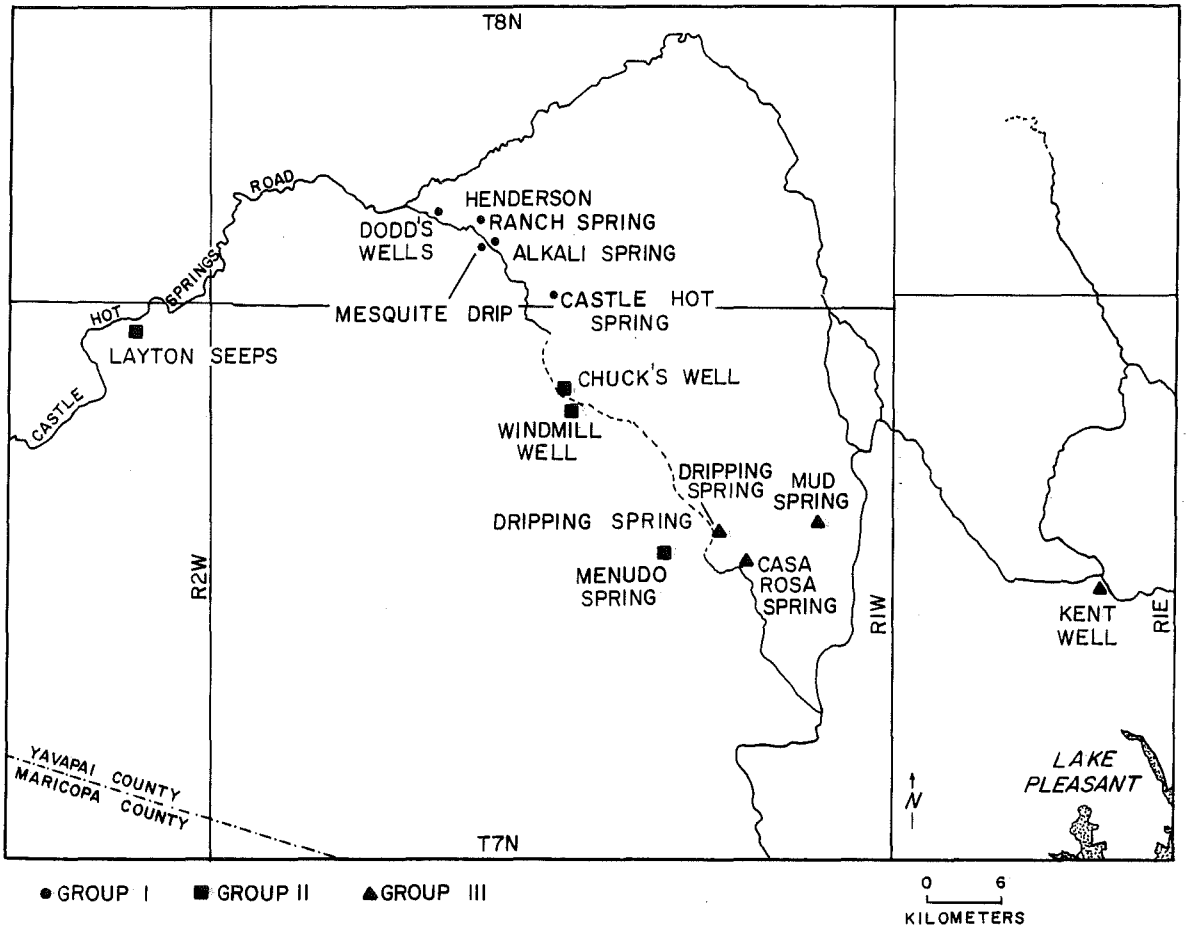

Figure 2.106. Locations of sampled wells and springs, Castle Hot Springs area

Additional exploration along Castle fault and in the area of the Groups III waters is necessary to define the hydrology, extent, age, and volume of these potential geothermal resources.

CASTLE HOT SPRING REFERENCES

Satkin, R. L., 1981, A geothermal resource evaluation of Castle Hot Springs, Arizona: M.S. thesis, Tempe, Arizona State University, 147 p.

Satkin, R. L., Wohletz, K. H., and Sheridan, M. F., 1980, Water geochemistry at Castle Hot Springs, Arizona: Geothermal Resources Council Transactions, v. 4, p. 177-180.

Sheridan, M. F., Satkin, R. L., and Wohletz, K. H., 1980, Final Report: Geothermal resource evaluation at Castle Hot Spring, Arizona: Bureau of Geology and Mineral Technology Open-File Report 80-5, 51 p.

Sheridan, M. F., Wohletz, K. H., Ward, M. B., and Satkin, R. L., 1979, The geologic setting of Castle Hot Springs, Arizona: Geothermal Resources Council Transactions, v. 3, p. 643-645.

Ward, M. B., 1977, The volcanic geology of the Castle Hot Spring area, Yavapai County, Arizona: M.S. thesis, Tempe, Arizona State University, 75 p.

NORTHERN HASSAYAMPA PLAIN

INTRODUCTION. The northern Hassayampa Plain is the site of a shallow well (165 m) that produced 53°C water until abandoned in the late 1970s. Few other wells exist in this area and none are known to be thermal.

The Hassayampa Plain has been the site of very little development or activity. The area was studied in the early 1970s as a possible nuclear power plant site, but was eliminated from consideration. Placer gold mining operations are common and claim stakes are ubiquitous. A few cattle ranches exist in this area. In the northern part of the plain, numerous home-site lots were sold some years ago, in a development called "Whispering Ranch" but no homes have been constructed. The preponderance of the "Whispering Ranch" acreage is on the pediment of the Vulture Mountains where water is scarce. It seems unlikely that extensive development will occur there.

PHYSIOGRAPHY. The northern Hassayampa Plain is in the Sonoran Desert subprovince, about 80 km northwest of Phoenix (Fig. 2.107). It is bounded on the north by the Vulture Mountains and on the southwest by the Belmont Mountains. The intermittent Hassayampa River flows south along the eastern edge of the plain. Elevation of the valley floor is about 625 m in the north, decreasing southward to about 450 m. The MAT is about 20°C. Precipitation is less than 15 cm per year.

GEOLOGY. The Belmont Mountains are a small northwest-trending range of Precambrian igneous and metamorphic rocks, principally granite,

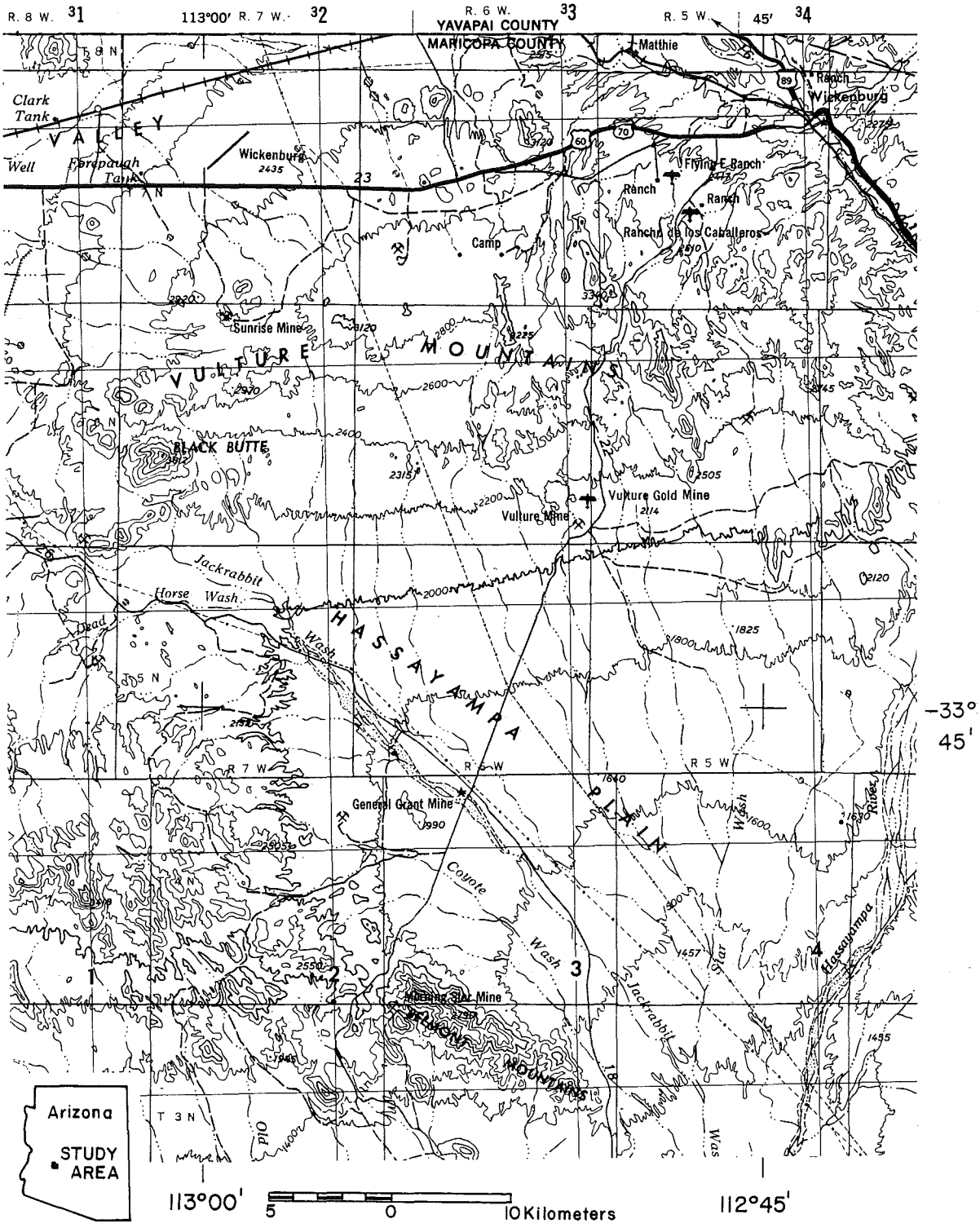

Figure 2.107. Physiographic map of the northern Hassayampa plain

phyllite, and schist. Tertiary volcanic rocks of intermediate composition intrude the southeastern end of the range. Voluminous Tertiary(?) andesites and rhyolites are found northwest of the Belmont Mountains where they unconformably overlie the Precambrian schist and granite. The mountain block is tilted to the southwest. The pediment extends about 1 km basinward from the present range front.

Stone (1979) identified three major structural trends (faults?) that strike northeast, northwest and north-northwest through the area. The first and last trends correlate with regional Laramide and late Tertiary structural features of southern Arizona. The northwest-trending feature is an apparent reflection of the Basin and Range, high-angle normal fault along the Belmont Mountains pediment edge.

GEOHYDROLOGY. Altitude of ground water above mean sea level decreases to the southeast. Shallow bedrock between the Belmont Mountains and the White Tank Mountains to the east appears to form a ground-water divide between the northern and southern Hassayampa Plains. The shallow water-level gradients in the center of the northern plain, compared to steeper gradients closer to the range fronts, indicate a more permeable aquifer beneath the center of the plain.

Depth to water ranges from about 13 m in the Belmont Mountains, where the water is held up by a pediment, to a reported depth of greater than 200 m south of the Vulture Mountains. Recharge to the aquifer is from the contiguous mountain ranges, but the rate of recharge is low owing to low precipitation.

GEOCHEMISTRY. A total of 97 mercury soil samples were collected from the northern Hassayampa Plain. The mean mercury concentration for this

area is 25 ppb. The northwest-trending range-bounding fault is conspicuous from the alignment of samples having mercury contents greater than 25 ppb (Fig. 2.108). The northeast-striking fault is less conspicuous, but apparent nonetheless. Two clusters of relatively high mercury values occur in T. 5 N., R. 7 W. and T. 5 N., R. 5-6 W. The latter cluster is in the same area as the 53°C thermal well.

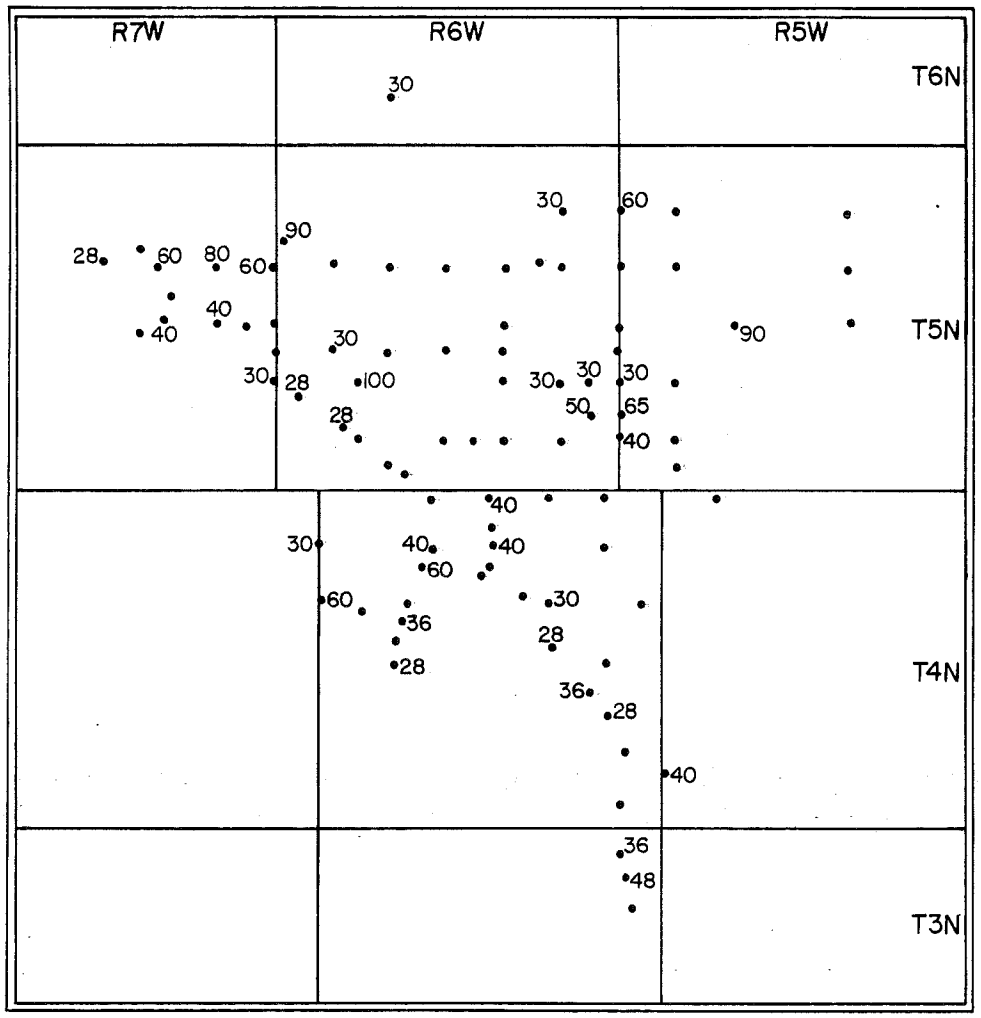

Figure 2.108. Locations of samples collected for mercury-soil survey. Numbers are mercury contents (ppb) greater than 25 ppb.

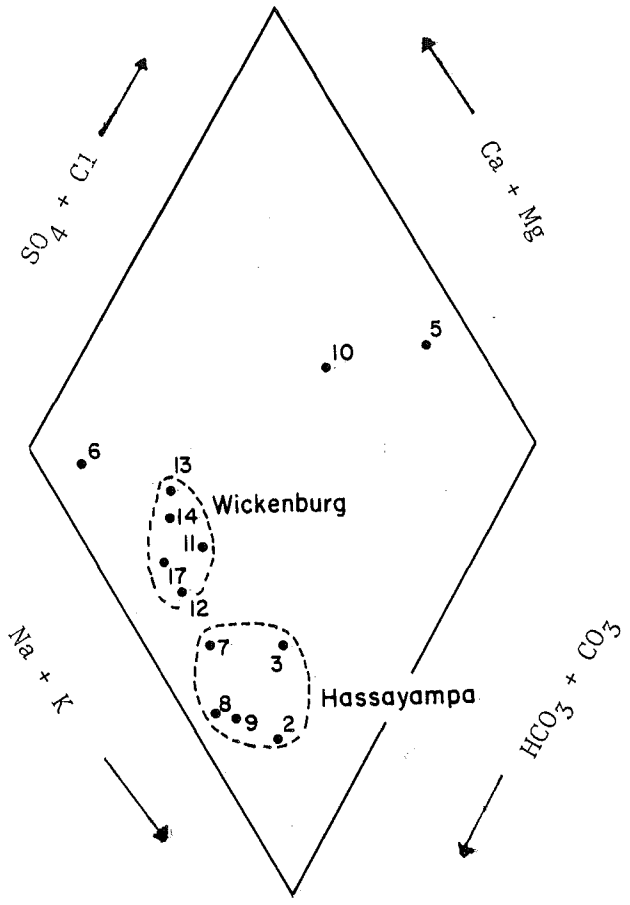

Figure 2.109. Piper diagram showing chemically distinct waters in the northern Hassayampa area

Chemical analyses of water from the northern Hassayampa Plain (nine samples) and from near the town of Wickenburg (eight samples) are distinct between the two groups (Fig. 2.109), indicative of separate source areas. The Wickenburg waters are sodium-calcium bicarbonate type. The Hassayampa waters are sodium-bicarbonate type. Samples 5, 6, and 10 are each distinct in chemical composition, and represent waters from separate sources or waters of mixed origin. Sample 5, from the 53°C thermal well, is sodium-chloride water.

GEOTHERMOMETRY. Minimum aquifer temperatures were estimated using the SiO_2 and Na-K-Ca geothermometers (Table 2.20). Stone (1979) pointed out the following correlations between the Na-K-Ca geothermometer and different silica species used to calculate the SiO_2 geothermometer: quartz and Na-K-Ca for the eastern samples, 1 through 5; α-christobalite and Na-K-Ca for the western samples, 6 through 9; chalcedony and Na-K-Ca for the northern, Wickenburg samples, 10 through 17. The Wickenburg geothermometers predict aquifer temperatures of about 35°C for water in that area. The geothermometers for the northern Hassayampa Plain predict minimum aquifer temperatures of about 70°C for waters in that area.

GEOTHERMAL GRADIENTS. Temperatures were measured in eight wells and Birdwell temperature logs were made available by Fugro, Inc. for three additional wells (Table 2.21). The temperature-depth profiles (Fig. 2.110) show that warm water is rising in wells A, B, and C. These wells also are thermal by definition. The remaining wells have gradients that are in the normal range, and are nonthermal. Isothermal profiles (Fig. 2.111) reveal that the zones of upflow in wells A, B, and C are relatively narrow and discrete(?).

GEOPHYSICS. Two closed aeromagnetic lows are aligned over the northwest-trending Jackrabbit Wash (Sauck and Sumner, 1970) (Fig. 2.112). A second, less-prominent feature is a northeast-trending low-amplitude aeromagnetic anomaly that crosses the more northwesterly closed anomaly. These aeromagnetic features nearly coincide with the northeast and northwest structural trends (faults?) identified by Stone (1979). Low-amplitude aeromagnetic anomalies could result from hydrothermal alteration, or shallow depth (7 to 8 km) to the Curie isotherm (≈525°C) (Sauck, 1972).

TABLE 2.20. Ratios of selected chemical constituents and estimated subsurface temperatures of waters in the northern Hassayampa plain. (Constituents in mg/L; geothermometers in °C. Sample numbers correspond to those in Figure 2.109. See Stone, 1981, for well locations.)

Sample No.*	Measured Temperature °C	Cl/F	Cl/B	Cl/SO_4	Mg/Ca	Mg/Cl	T_{qtz}	T_{chal}	$T_{Na-K-Ca}$
1	28.5	65.6	-	0.81	0.51	0.61	79.4	29.6	-
2	25.0	9.5	128.6	0.10	0.32	0.23	67.1	17.8	54.4
3	-	9.1	32.3	0.15	0.35	0.18	55.3	6.5	53.7
4	25.5	36.2	-	0.51	0.13	0.02	76.6	26.9	-
5	51.0	110.0	-	7.33	0.01	0.002	47.2	-	66.4
6	31.0	48.0	32.4	0.10	0.23	0.55	84.6	34.7	5.0
7	34.0	30.0	26.9	0.13	0.39	0.30	78.0	28.3	41.2
8	25.5	12.0	100.0	0.06	0.26	0.52	94.9	44.7	73.3**
9	28.5	8.4	150.0	0.11	0.40	0.37	68.8	19.4	36.4
10	22.5	147.4	518.5	0.93	0.85	0.39	88.3	38.2	29.9
11	22.0	18.7	215.4	0.10	0.27	0.57	80.8	30.1	34.2
12	27.5	23.0	328.6	0.12	0.44	0.61	94.9	44.7	48.0
13	23.5	40.0	228.6	0.10	0.30	0.72	78.0	28.3	27.1
14	21.0	35.0	200.0	0.09	0.30	0.75	79.4	29.6	28.2
15	-	22.5	-	0.07	0.33	0.89	-	-	-
16	-	37.5	-	0.06	0.29	1.00	-	-	-
17	26.0	9.5	222.2	0.11	-	0.46	58.7	39.3	47.1

Mg correction applied.

TABLE 2.21. Measured geothermal gradients, northern Hassayampa plain, Arizona

Well No.	Location	Total Depth (m)	BH Temp (C^o)	Gradient Interval (m)	Geothermal Gradient ($^oC/Km$)
A	B-5-6-25cab	163	51.6	80 - 163	140.1
B	B-4-6-4aaa	170	40.6	35 - 135	94.8
C	B-5-6-21bbb	160	31.9	30 - 160	87.5
D	B-5-6-10cac	250	30.5	30 - 130 155 - 250	27.7 23.2
E	B-6-5-31bcc	140	26.4	20 - 140	15.6
F*	B-5-5-16bd	95	24.3	5 - 90	33.0
G	B-5-5-22bcc	160	27.8	30 - 160	41.4
H*	B-5-5-21dd	123	32.1	10 - 120	15.0
I*	B-5-5-29bd	105	31.0	15 - 100	44.1
J	B-4-5-5abb	220	28.2	30 - 110 120 - 215	30.7 9.0
K	B-4-5-18dcc	130	25.9	40 - 125	24.8

* Birdwell logs

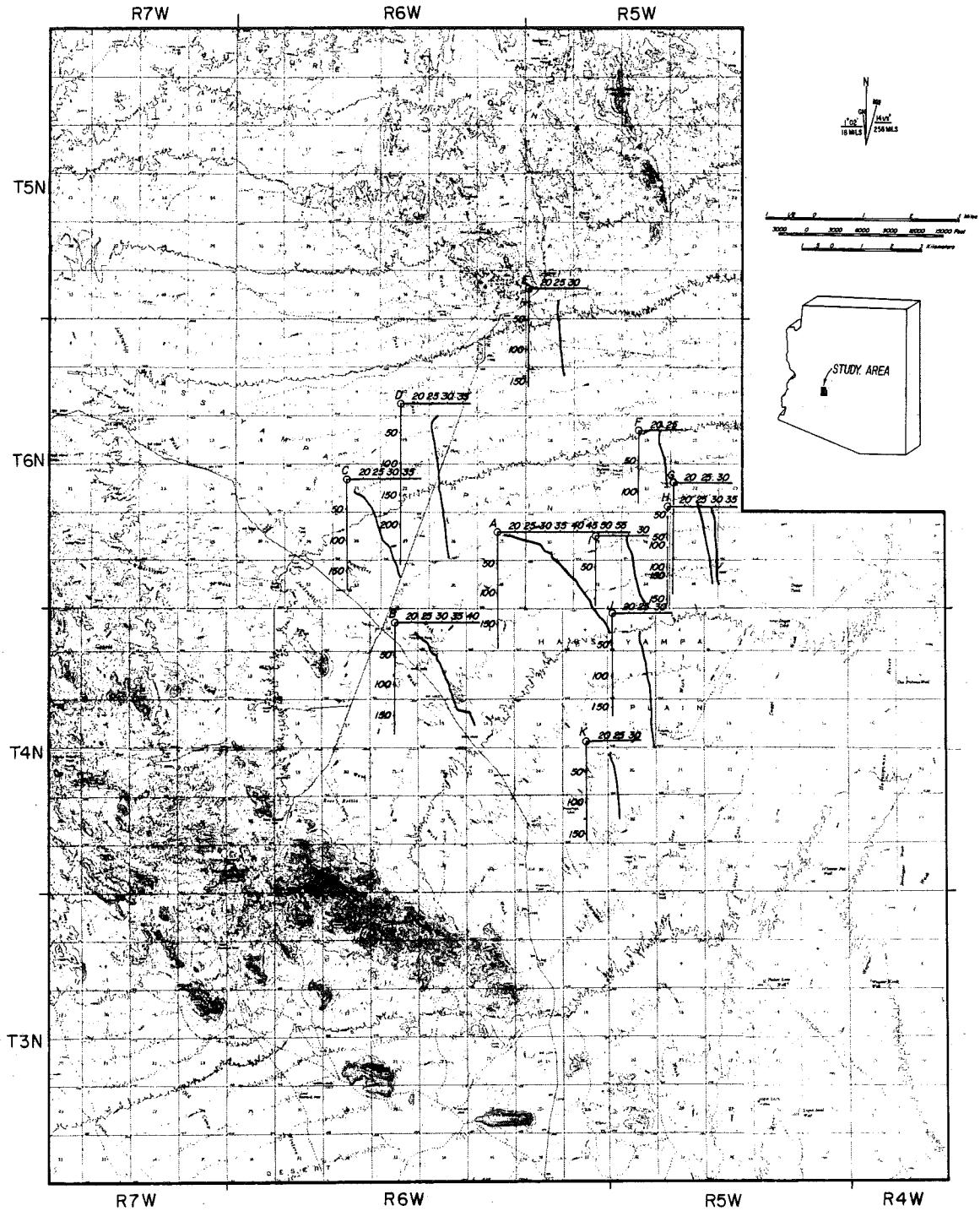

Figure 2.110. Temperature-depth profiles for wells measured on the northern Hassayampa plain. Small circles represent well locations.

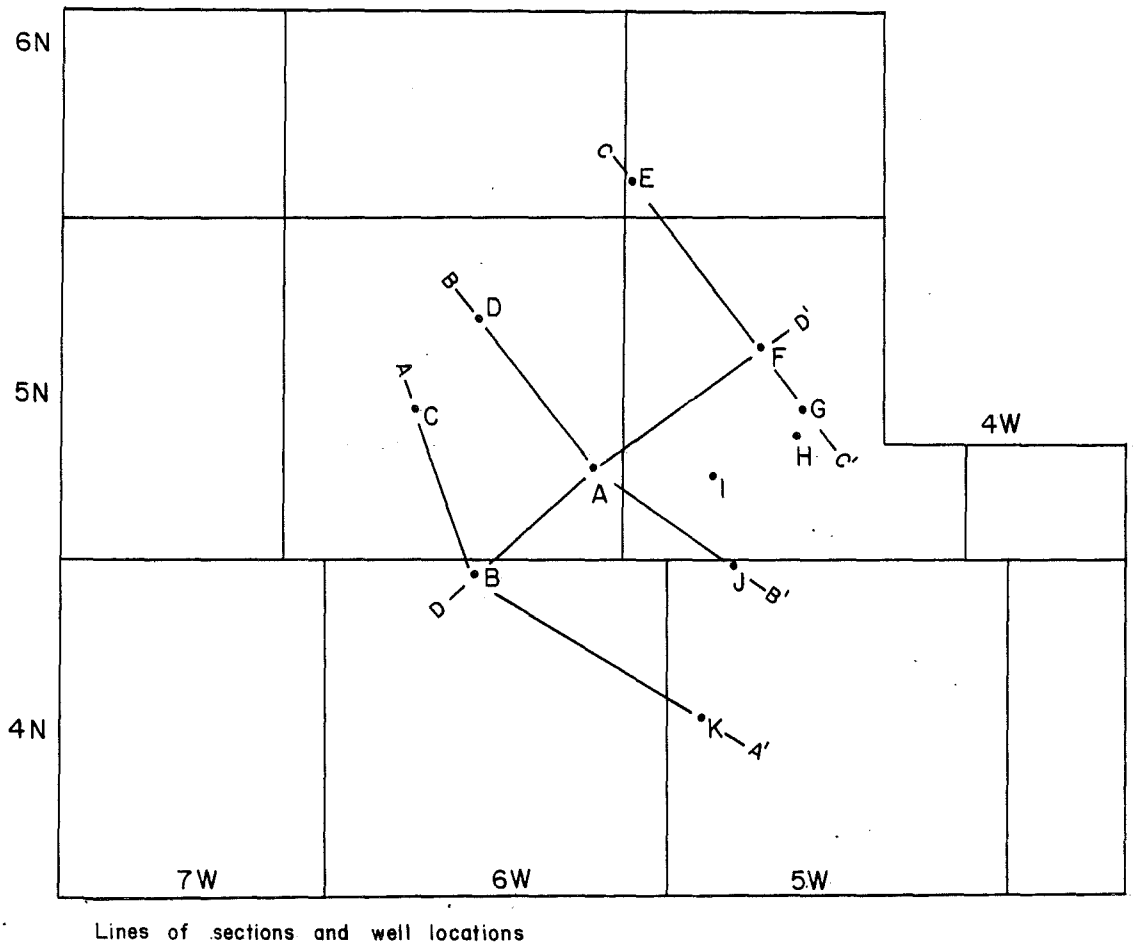

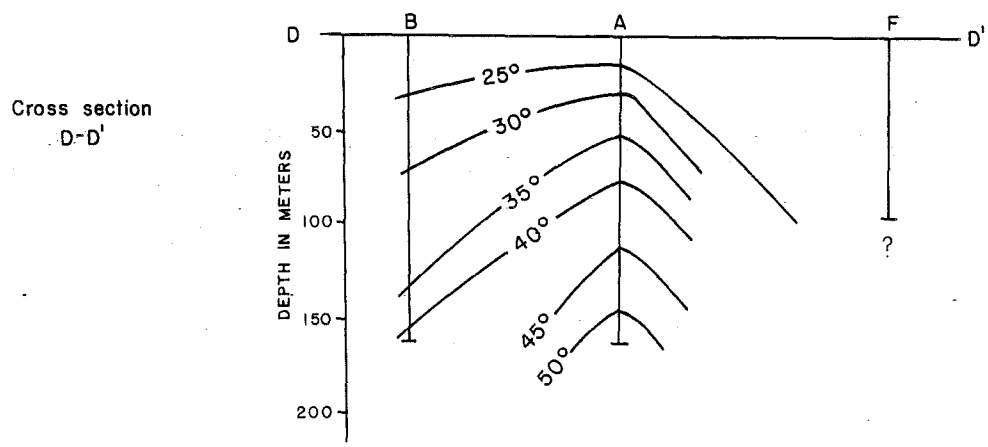

Figure 2.111. Isothermal cross sections, northern Hassayampa plain

Cross section
A-A'

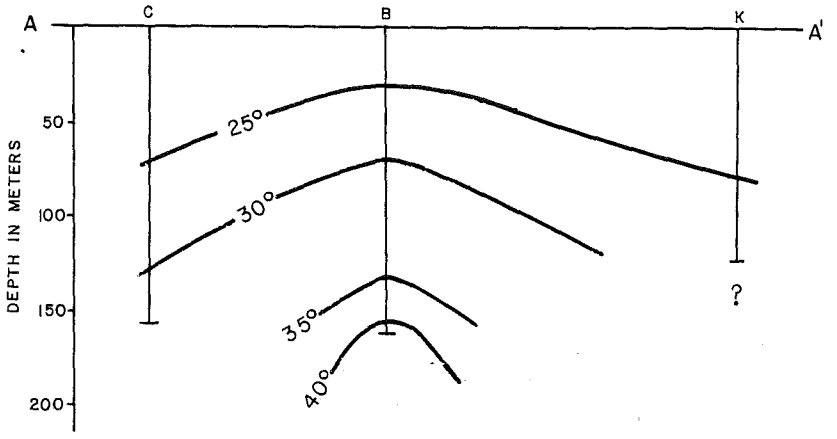

Cross section
B-B'

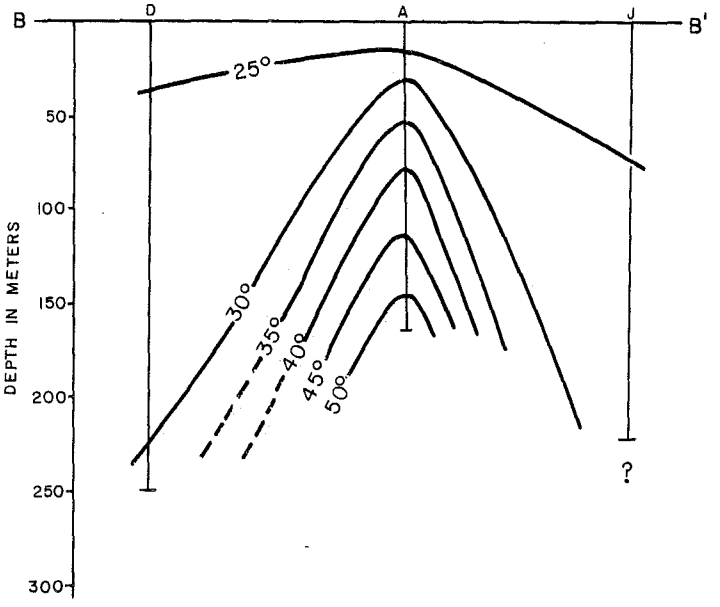

Cross section
C-C'

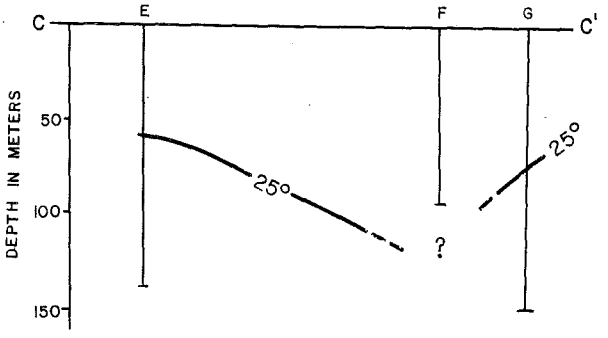

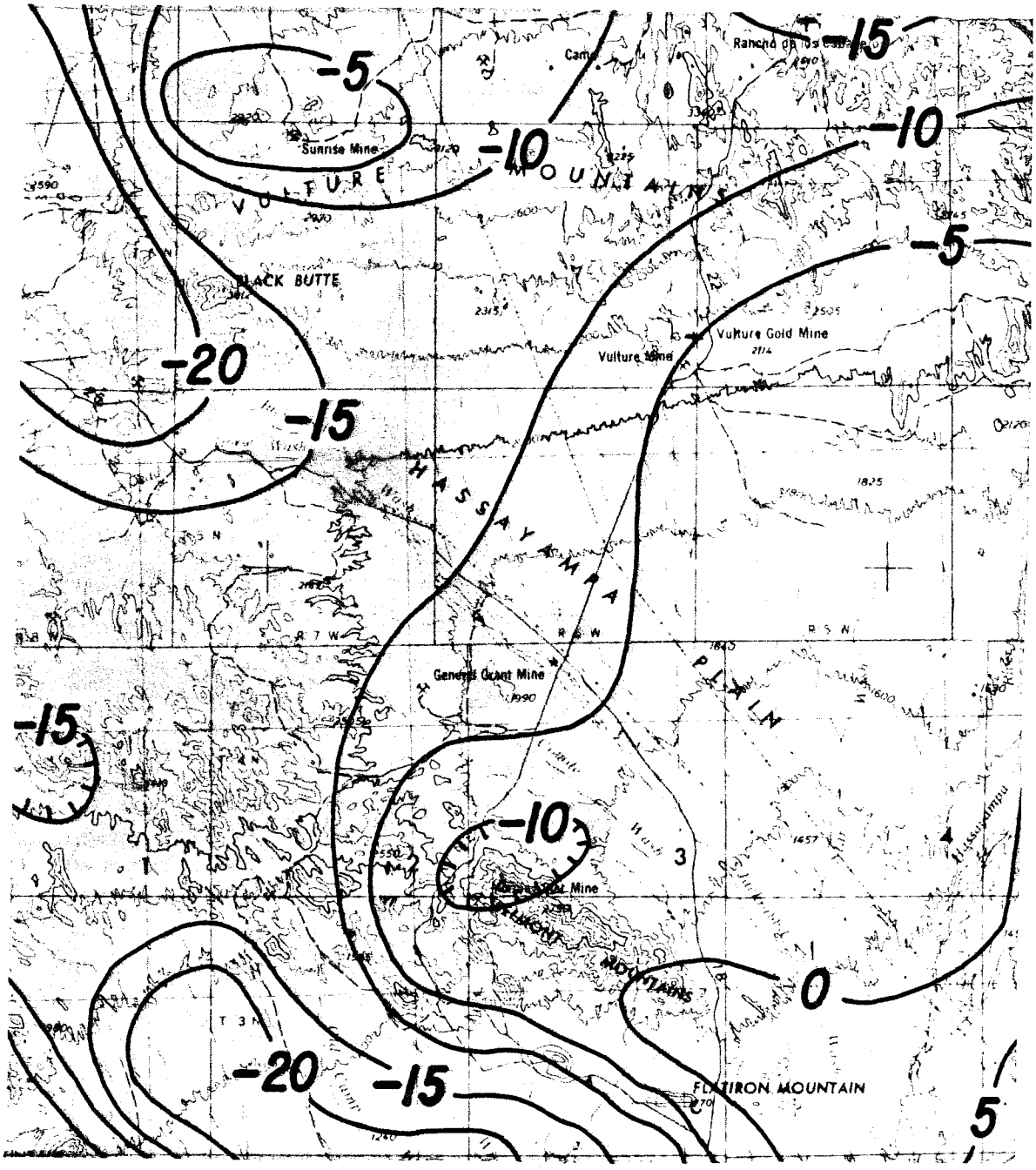

Figure 2.112. Aeromagnetic map of the northern Hassayampa plain. Contour interval is 5 gammas.

A reconnaissance gravity survey (Stone, 1982) (Fig. 2.113) permitted an interpretation of the subsurface structure of this area, and resulted in a better understanding of the geothermal resource. Several features are particularly prominent on the gravity map. (1) The pediment edge along the northeast side of the Belmont Mountains is sinuous rather than linear. This sinuosity suggests that the master fault boundary is segmented and that complex faulting has occurred in the basement, with probable rotation of basement blocks. (2) The deep basin is nearly oval, elongate in a northwest direction. The deepest part of the basin (1,250 m) nearly overlies the northwesternmost closed aeromagnetic low. This coincidence suggests the two features may be a result of the same subsurface structure, such as a thick evaporite deposit or a zone of hydrothermally altered material. (3) Two relatively narrow zones of widely spaced gravity gradients (northwest and northeast trending) reflect shallow bedrock saddles between deeper basins. (4) There is little evidence for a northeast-striking fault through wells A and B as originally proposed by Stone (1979), although a detailed gravity or seismic survey could provide evidence to reverse this conclusion.

Fig. 2.113 shows the location of the thermal-gradient holes with respect to the gravity contours. It is evident that well C (DH-1) is located on the northwest saddle between deeper basins. Higher temperatures in this hole may result from ground water deep in the basin being diverted up and over the bedrock saddle as this water flows southeastward. Wells A and B are located along the western side of the basin, over the northeast and southwest basin-bounding faults, respectively. Based on available

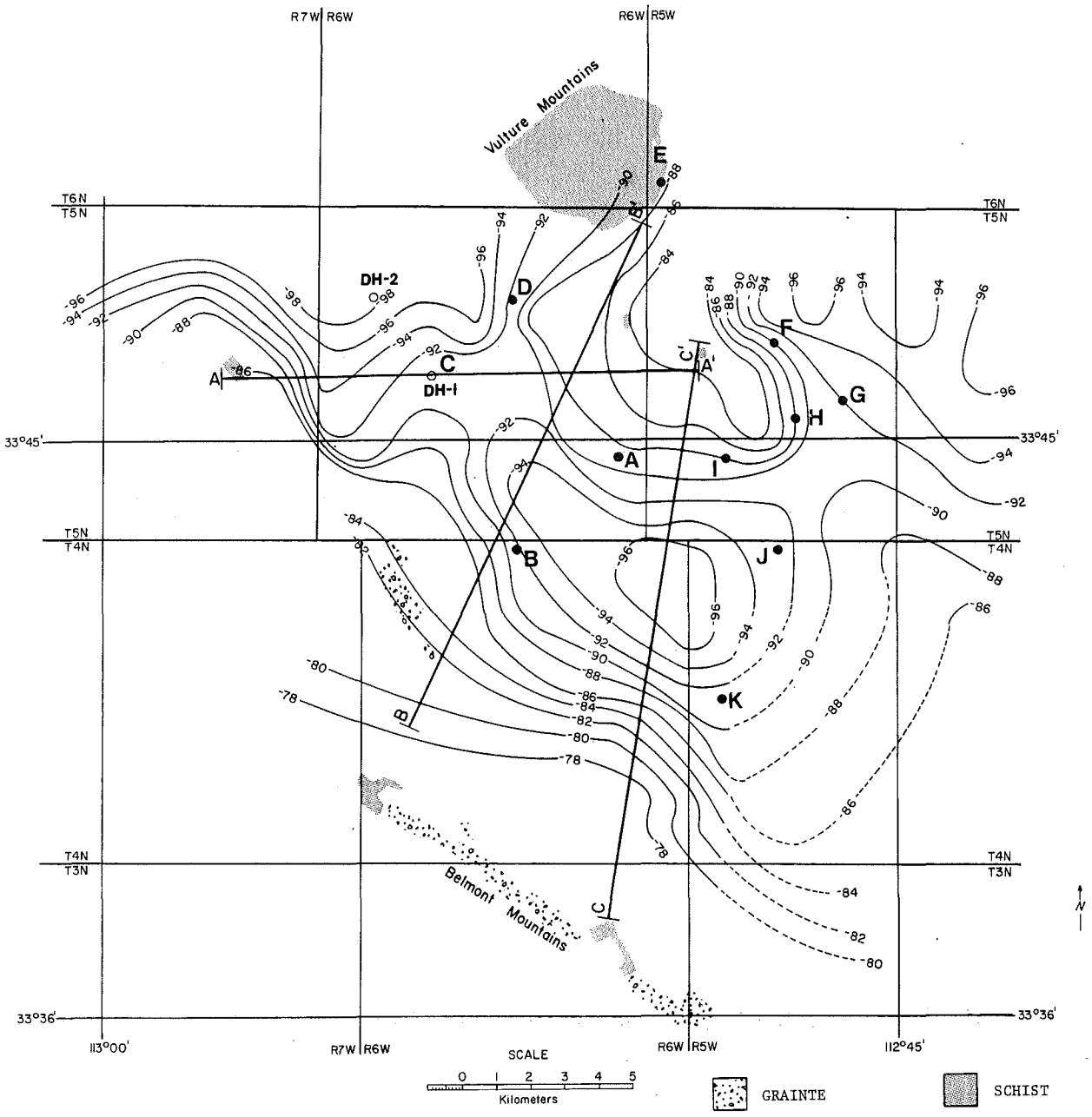

Figure 2.113. Residual Bouguer gravity map of the northern Hassayampa plain. Letters are thermal gradient holes shown in Fig. 2.110. See Stone (1982) for gravity profiles along section lines A-A', B-B' and C-C'.

information, the source area for thermal water in these wells is unknown, but they probably result from forced convection. It appears the wells may derive their water from separate sources. Wells I, J, and K, which also are located along the basin margin, have normal gradients, indicative of little or no vertical water movement along the east and northeast sides of the basin.

CONCLUSIONS. The northern Hassayampa Plain is underlain by a relatively narrow, sediment-filled oval basin that trends northwest. A gravity survey revealed that the southwest margin of the basin is segmented rather than linear, which suggests that the basement blocks are complexly faulted and probably rotated.

Three geothermal gradients (Wells A, B, and C) were earlier inferred to reflect warm water rising from the same area of hydrologic discharge (Stone, 1979). Reinterpretation based on a gravity survey indicates that is not the case. Well C is located above an elevated block and has a high gradient as a result of forced flow of deep warm water up and over the block at a basin hydrologic outlet. Wells A and B are located in separate fault zones, the northeast and southwest, respectively, and are not obviously related.

Meteoric water needs to circulate to depths of only about 1.3 km in a normal-gradient region to achieve the 70°C temperature predicted by the geothermometers. Hydraulic head and lower density allow the heated fluids to rise toward the surface along fault zones. Thermal fluids may exist in a reservoir of fractured rocks comprising the basement of the basin. Overlying, low-heat-conductive basin-fill sediments may confine this water except along major structures.

Alternatively, the thermal fluids may be of such small volume that in most instances they are diluted by shallow cold ground water as they rise into overlying permeable strata. If this is the case, wells A and B may have fortuitously penetrated discrete zones of upwelling, and a geothermal reservoir containing abundant hot water may not exist at greater depth because thermal fluids have not accumulated, due to lack of either sufficient volume of fluid or a suitable reservoir.

The coincidence of a thermal well and a soil mercury anomaly occurring together over a fault zone suggests that a geothermal reservoir may exist at depth. Detailed exploration is warranted in the areas of wells A and B, which may derive fluids from the same reservoir, or may reflect two separate (?) geothermal resources of small areal extent.

NORTHERN HASSAYAMPA PLAIN REFERENCES

Sauck, W. A., and Sumner, J. S., 1971, Residual aeromagnetic map of Arizona: University of Arizona, Tucson, scale 1:1,000,000.

Stone, C., 1982, Geothermal potential of the northern Hassayampa plain, Part II: Bureau of Geology and Mineral Technology Open-File Report 81-25, 38 p.

_____ 1979, Preliminary assessment of the geothermal potential of the northern Hassayampa plain, Maricopa County, Arizona: Bureau of Geology and Mineral Technology Open-File Report 79-17, 42 p.

PAPAGO FARMS

INTRODUCTION. Papago Farms is located in the southwestern part of the Papago Indian Reservation, just north of the international boundary (Fig. 2.114). Climate is semiarid. In most areas on the Reservation, precipitation averages from 12 to 25 cm per year, although twice this amount falls in some of the higher mountains. Mean annual air temperature at Papago Farms is about 20°C. During summer months, temperatures often exceed 45°C.

In 1977, the Papago Indian Tribe renewed farming operations at the site where an earlier farm had been active in the 1950s. By 1981, 980 acres of land were under cultivation. Numerous irrigation wells were drilled in the 1950s for the original operation, and were reserviced for production when the present activity was started up again. Several of these irrigation wells produce large volumes of thermal water (38 to 51°C).

All power at Papago Farms is produced by diesel-powered pumps and generators. Thus, the possibility of using geothermal energy is attractive. The feasibility of such a project is largely dependent on two factors: (1) whether greenhousing, aquaculture, or some other direct-heat application could be incorporated into the overall farm program, and (2) whether small well-head generators, given sufficiently improved technology, could produce electric power from the existing resource.

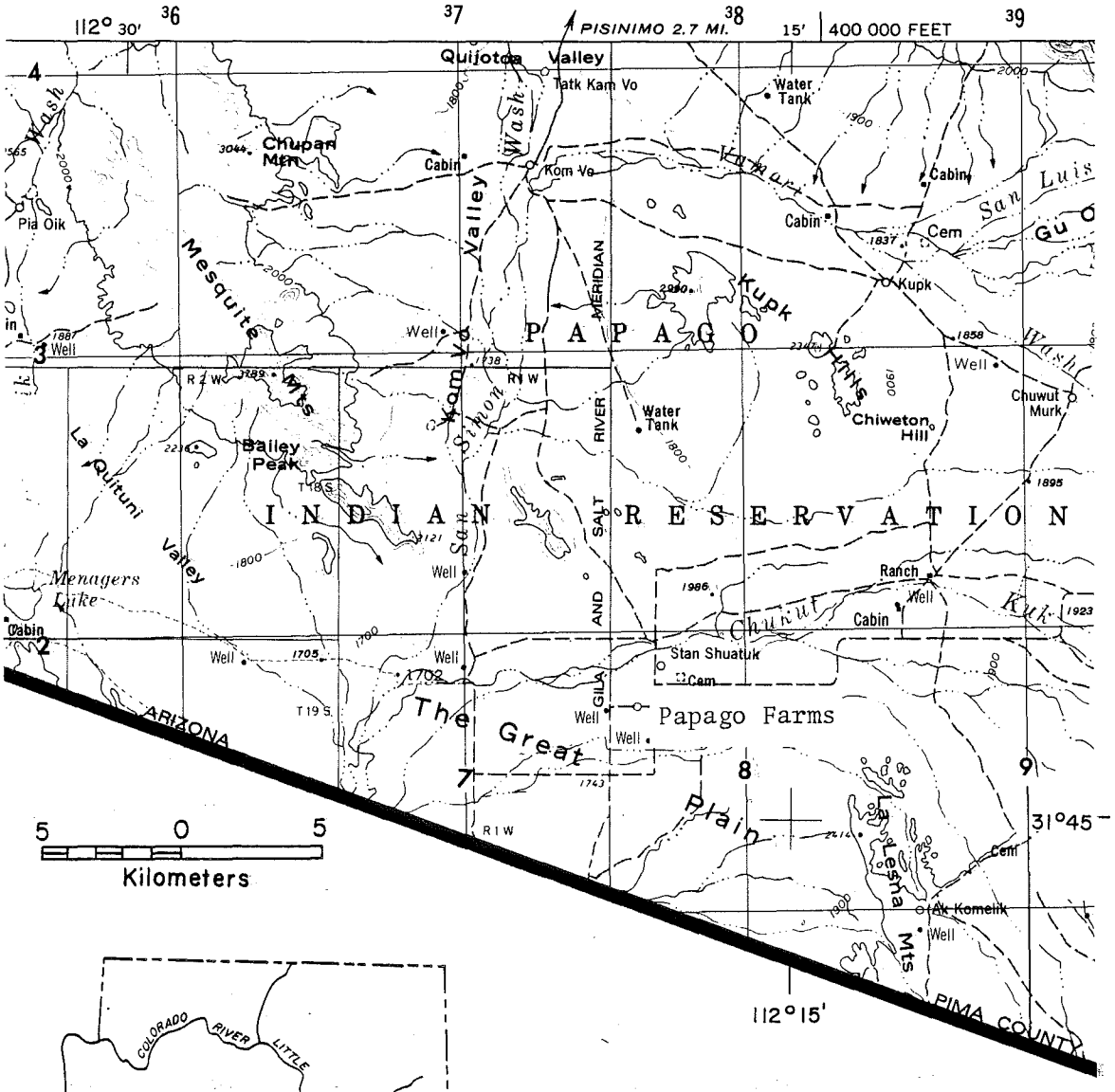

Figure 2.114. Location map of Papago Indian Reservation and Papago Farms

GEOLOGY. Papago Farms is located at the southeast end of the Mesquite Mountains in a broad, nearly flat alluvial valley, the Great Plain (Fig. 2.115). Mountain elevations exceed the general 500-m elevation of the valley floor by at least 150 m, and up to as much as 650 m in the Mesquite Mountains. The Great Plain is at the head of a north-south valley that extends about 40 km into Mexico. The area is underlain by clay, silt, sand, gravel, small amounts of evaporite deposits, and intercalated volcanic rocks. Lakebed and playa deposits are more than 150 m thick near the international boundary and thin to extinction at the margins of the area (Hollett, 1981a). Total thickness of the entire sequence varies from zero along the mountain fronts to 3,000 m south of the farms (Hollett, 1981a).

In Arizona the Great Plain is bounded on the east by the north-striking La Lesna Mountains, a low range of Tertiary volcanic rocks of intermediate composition, which continues south into Mexico. The Kupk Hills are composed of Late Cretaceous-early Tertiary gneiss and comprise the northeastern boundary of the Great Plain. Low, unnamed volcanic hills lie south of the Kupk Hills. The Mesquite Mountains to the northwest are chiefly Tertiary rhyolite, with lesser amounts of Tertiary basalt along the south and east sides of the range. Low mountains of Tertiary volcanic rock occur along the international boundary to the southwest.

Major surface drainage through the Great Plain is the south-flowing San Simon Wash. Chukut Kuk Wash east of the La Lesna Mountains (Fig. 2.115) and Vamori Wash even farther to the east both flow northwest out of

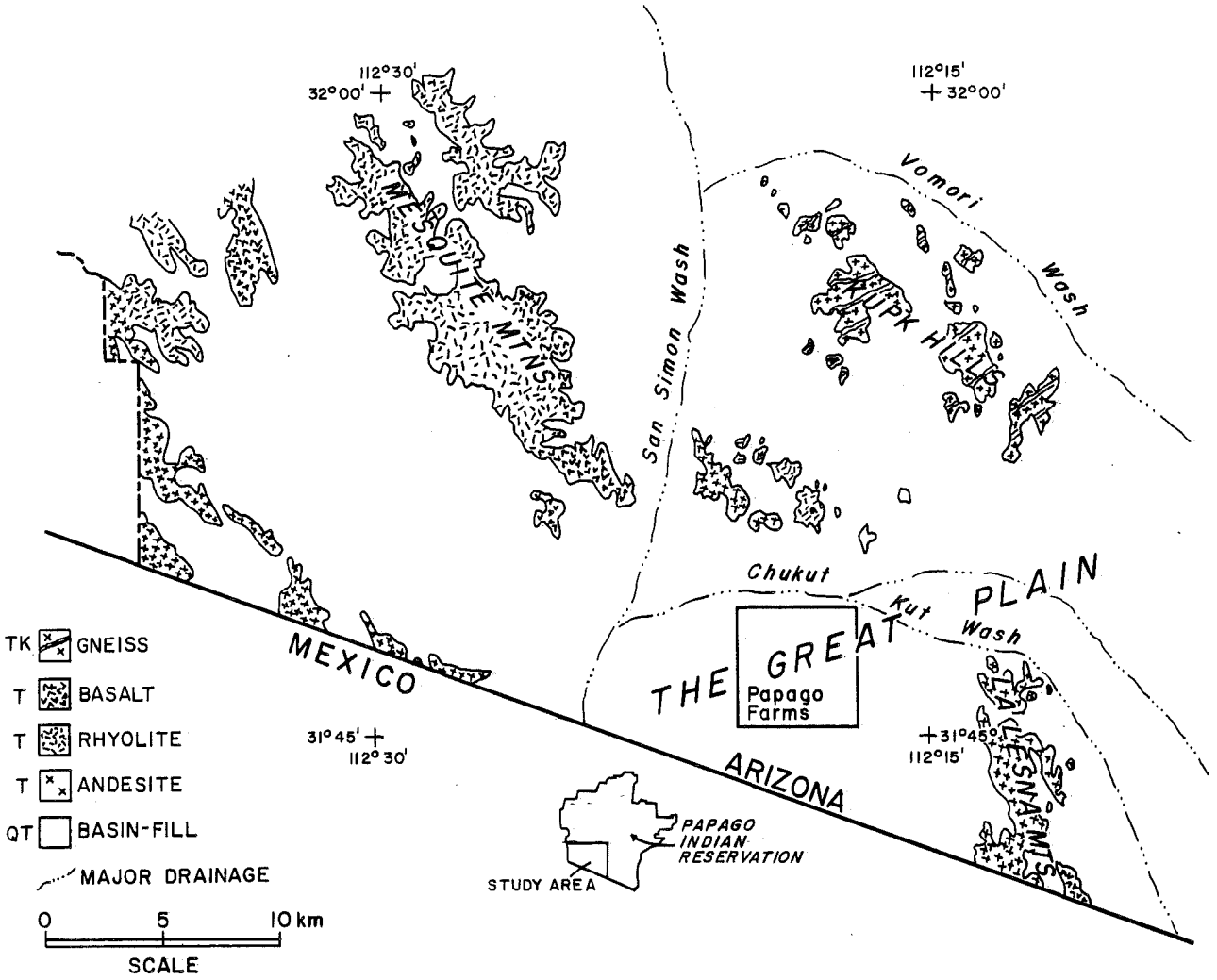

Figure 2.115. Generalized geologic map of Papago Farms area and major surface drainage

Mexico, and then west. Together with numerous smaller washes, they join San Simon Wash north and west of the Great Plain, from which point all surface water flows south back into Mexico.

GEOHYDROLOGY. Ground water in the San Simon Wash area moves largely along the axes of the valleys, generally in the same direction as the surface water. Beneath the Vamori and Chukut Kuk washes, ground water flows northwest towards and around the Kupk Hills (Hollett, 1981b).

North of the Great Plain, these arms of flow join the south-flowing ground water beneath San Simon Wash. Recharge to the ground-water system is derived from precipitation that infiltrates mainly along the mountain fronts. Although ground water is contained in the crystalline and consolidated sedimentary rocks to a small extent, the basin-fill deposits are the main water-bearing unit. Depth to water at Papago Farms is about 60 m.

Quality of water ranges between 180 and 4,900 mg/L TDS. Locally, high levels of arsenic and fluoride pose important water-quality problems in some areas. Southwest of Papago Farms, ground water contains large concentrations of sodium, chloride, bicarbonate, and sulfate. Hollett (1981b) stated that this water may come from evaporite deposits.

GEOCHEMISTRY. Chemical analyses of water from 26 wells from the San Simon Wash area (see Fig. 2.116 for well locations) are given in Table 2.22 (USGS, WRD, Tucson, 1980). Although the chemistry is generally similar for all samples, Stone (1980) identified three groups of ground water, using graphs of various chemical constituents and temperatures (Fig. 2.117). Ground-water characteristics are outlined in Table 2.23.

Group I wells produce mostly nonthermal ($T<31^{o}C$) water; they are located at or near the east side of Papago Farms (Group Ia) and north of the farms (Group Ib). Group I waters have well-head temperatures in the range of 25 to $32^{o}C$, high Cl/F and Mg/Ca ratios, low Na/Ca and Na/K ratios, and generally low (323 ± 37 mg/L) TDS. These waters largely

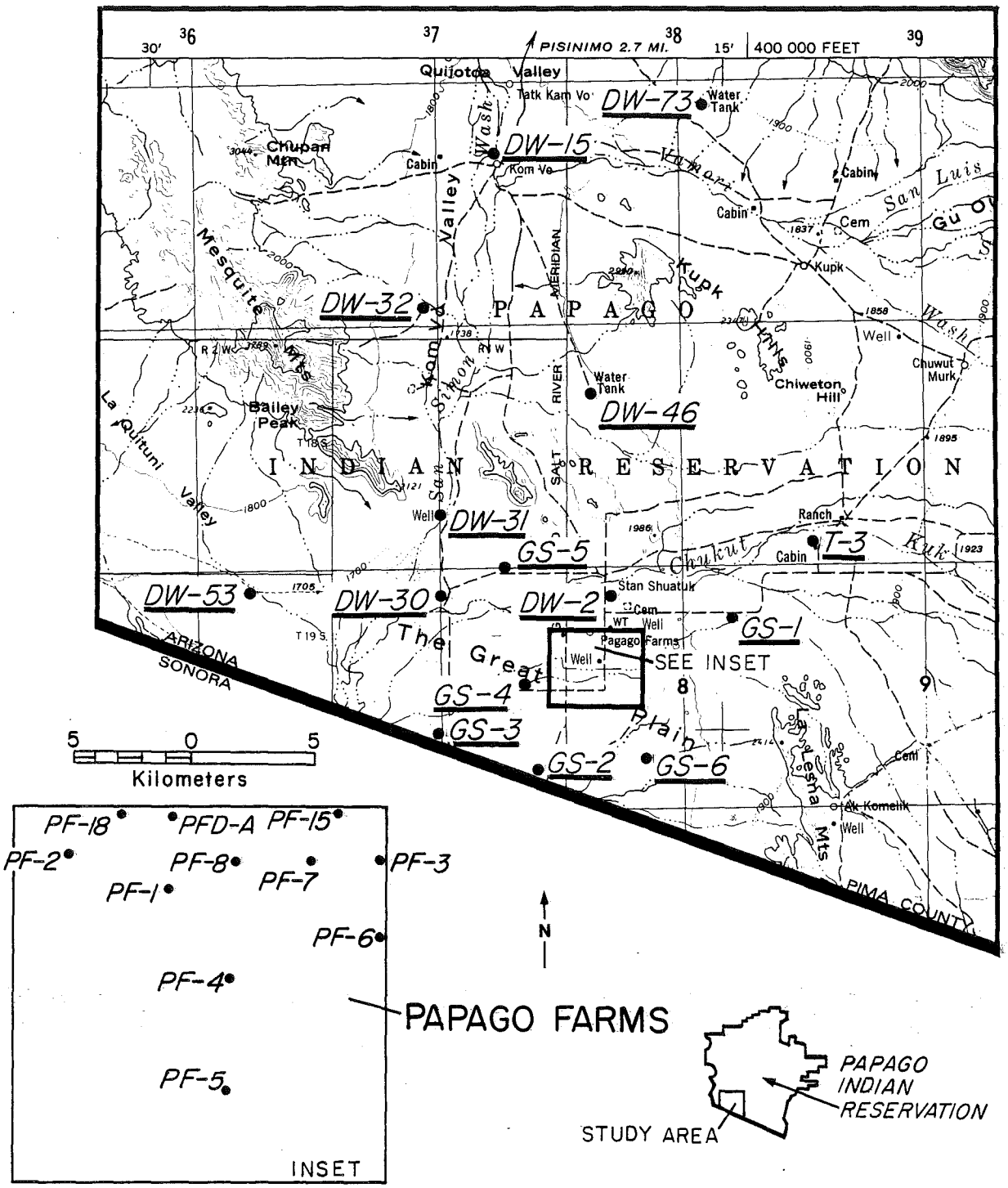

Figure 2.116. Well locations for San Simon Wash area and Papago Farms

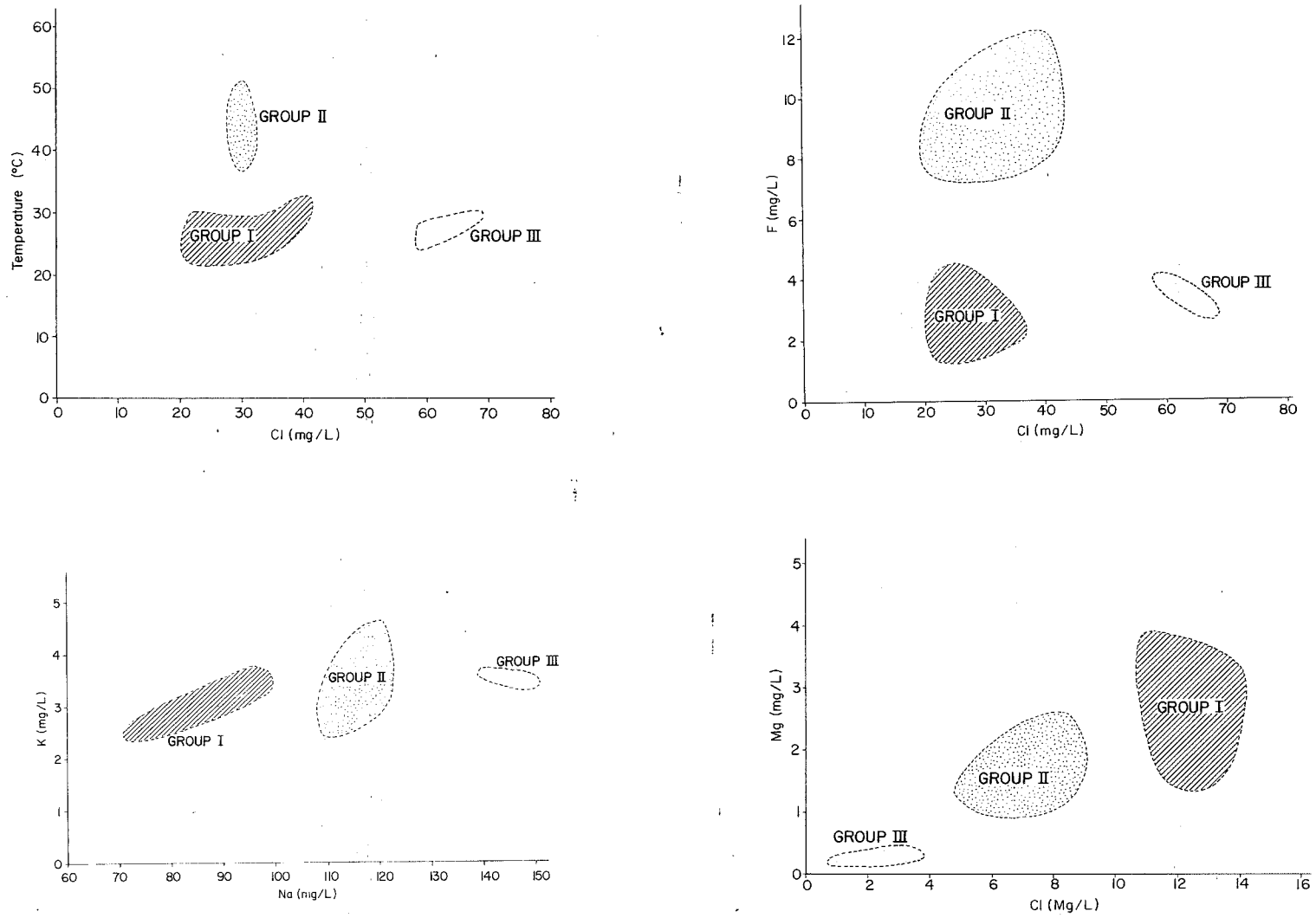

Figure 2.117. Graphs of chemical constituents and temperature showing three distinct groups of ground water for samples listed in Table 2.22

TABLE 2.22. Chemical analyses of ground water, Papago Farms and surrounding areas
(Chemical constituents in milligrams per liter)

Sample No.	Location	pH	Na	K	Ca	Mg	SiO_2	Cl	SO_4	HCO_3	F	B	TDS
*USGS-1	D-19-01 11BBB	7.9	87	3.1	11.0	2.8	41	36	23	190	2.3	0.21	308
USGS-2	C-19-01 36ACC	-	170	0.9	3.2	0.4	27	59	45	270	12.0	0.68	450
USGS-3	C-19-01 28ADC	-	790	2.9	0.8	0.2	18	280	160	1140	54.0	16.0	1885
USGS-4	C-19-01 14DDD	-	150	0.8	1.8	0.3	43	31	24	300	7.9	0.5	409
USGS-5	C-18-01 35CDA	-	120	4.0	8.2	2.5	42	40	33	200	8.3	0.31	377
USGS-6	D-19-01 28CBC	-	110	0.6	13.0	5.9	45	59	37	200	4.0	0.22	375
DW-2	D-19-01 05CBC	7.7	110	3.2	8.1	1.5	37	31	26	220	9.2	0.52	335
PF-1	D-19-01 07DBB	8.0	110	3.2	8.1	1.2	53	31	30	220	11.0	0.32	356
PF-2	C-19-01 12DAA	7.7	110	2.5	6.8	1.1	50	30	30	220	9.3	0.27	348
PF-3	D-19-01 8DAA	-	94	3.3	13.0	2.3	52	26	22	210	4.3	0.24	327
PF-4	C-19-01 18ADA	-	-	-	14.0	3.3	55	40	31	224	12.0	-	390
PF-5	D-19-01 18DDD	7.9	110	2.6	8.8	1.9	38	33	24	210	8.4	0.22	331
PF-6	D-19-01 17AAA	7.9	99	3.4	11.0	3.8	57	23	20	240	7.6	0.24	351
PF-7	D-19-01 08DBB	8.3	120	4.5	7.5	1.8	61	30	30	220	9.4	0.31	374
PF-8	D-19-01 08CBB	-	120	3.1	12.0	1.6	60	30	29	210	8.8	0.75	375
PF-15	D-19-01 08ABD	-	96	3.7	13.0	1.5	53	23	22	220	4.3	0.23	330
PF-18	D-19-01 07BAD	-	-	-	-	-	-	-	-	-	-	-	-
PFD-A	D-19-01 07ABD	8.7	110	2.9	5.0	1.4	31	28	23	-	8.0	0.30	329
DW-30	C-19-01 04DAA	-	140	1.5	3.6	0.3	77	23	23	250	10.0	0.37	353
DW-31	C-18-01 28ABB	7.9	150	3.4	6.8	2.3	32	68	63	200	2.9	0.45	444
DW-53	C-19-02 03ADD	-	1400	11.0	160.0	100.0	35	2100	850	40	1.4	1.40	4880
+Toro-3	D-18-02 31BDA	8.1	72	2.5	13.0	2.9	31	22	18	180	1.6	0.20	258
DW-15	C-17-01 11BCA	7.4	113	3.0	3.4	0.9	28	15	20	222	2.6	0.34	318
DW-32	C-17-01 33BAC	-	-	-	13.0	2.8	30	128	91	170	1.8	-	565
DW-73	D-17-01 03BAA	-	100	2.1	22.0	4.4	32	21	17	220	1.5	0.17	302
DW-46	D-18-01 07ACA	7.4	-	-	17.0	6.4	38	43	45	237	2.0	-	384

* USGS wells in text, maps, and other tables are hereafter referred to by the shorter designation GS.

+ Toro-3 in text, maps, and other tables is hereafter referred to as T-3.

TABLE 2.23. Averaged values for three groups of ground water, Papago Indian Reservation

	GROUP 1 (9)	GROUP 2 (6)	GROUP 3 (6)
TDS (mg/l)	323	353	397
Mg/Ca [1]	0.37	0.32	0.47
Cl/F [1]	5.7	1.7	2.9
Na/K [1]	48	61	298
Temp (°C)	28	43	26
Gradient (°C/km)	37	120	44

[1] atomic ratios

reflect ground water moving west beneath the Great Plain to join the south-flowing water beneath San Simon Wash.

Group II wells cluster slightly west of Group Ia at or near the north end of Papago Farms. These wells produce thermal water with temperatures between 38 and 51°C. The waters have low Cl/F and Mg/Ca ratios and moderate Na/Ca and Na/K ratios relative to Groups I and III. Mean TDS is slightly higher than that of Group I: 353 ± 19 mg/L versus 320 ± 35 mg/L for Group I.

TABLE 2.24. RATIOS OF SELECTED CHEMICAL CONSTITUENTS, CHEMICAL GEOTHERMOMETERS, TOTAL DISSOLVED SOLIDS, TEMPERATURES, WELL DEPTHS, AND GEOTHERMAL GRADIENTS CALCULATED BY METHOD 1 (SEE TEXT) FOR 26 WELLS AT THE PAPAGO FARMS AND SURROUNDING AREAS.

SAMPLE No.	MEAS. T(°C)	DEPTH (M)	GRADIENT (°C/KM)	CL/F[1]	NA/CA[1]	MG/CA[1]	NA/K[1]	T_{SiO_2} (°C)	$T_{Na-K-Ca}$ (°C)	TDS[2]
GROUP IA										
T-3	25	91.5	43.7	7.4	4.8	0.37	48.9	49.5	58.6	258
GS-1	27	153.7	39.0	8.4	6.9	0.42	47.8	62.6	71.8	308
PF-3	28	280.8	24.9	3.2	6.3	0.29	48.7	73.9	71.0	330
PF-6	27	170.7	35.1	1.6	7.8	0.56	49.4	78.6	56.3	327
PF-15	30	91.5	46.9	2.9	6.4	0.18	43.9	74.8	75.5	351
GROUP IB										
DW-15	25	110.0	36.3	3.1	28.9[3]	0.44	64.0[3]	45.1	63.4	318
DW-32	-	97.9	-	38.0[3]	-	0.35	-	48.1	-	565[3]
DW-73	32	-	-	7.5	4.0	0.33	80.6[3]	50.9	46.3	302
DW-46	30	96.6	93.2[3]	11.5	-	0.63	-	58.7	-	384
$\bar{X}$ =	28±2.5		37.6±7.8	5.7±3.5	6.0±1.4	.37±.10	47.7±2.2	60.2±12.9	63.3±10.4	323±37
GROUP II										
DW-2	46	128.0	195.3	1.8	12.0	0.30	58.3	57.4	81.4	335
PF-1	44	218.0	105.5	1.5	12.0	0.25	58.3	74.8	81.4	356
PF-2	38	290.2	58.6	1.7	14.1	0.26	74.7	77.9	76.9	348
PF-7	39	283.5	63.5	1.6	14.1	0.41	45.4	82.1	77.6	374
PF-8	51	193.6	155.0	1.7	8.7	0.22	66.1	81.3	73.3	375
PFD-A	30	120.0	141.7	1.9	19.1	0.48	64.6	49.5	84.5	329
$\bar{X}$ =	43±5.3		119.9±53.9	1.7±.14	13.3±3.4	.32±.10	61.2±9.8	70.5±13.7	79.2±4.0	353±19
GROUP III										
GS-2	25	152.4	26.2	2.6	46.2	0.19	321.3	43.5	65.8	450
GS-3	25	152.4	26.2	2.8	857.5[3]	0.50	463.5	27.3	63.7	1885[3]
GS-4	24	152.4	19.4	0.2	72.4	0.22	310.5	64.5	72.3	409
GS-6	28	153.7	45.5	7.9	7.4	0.75	318.7	66.7	25.9	375
DW-30	26	78.4	63.8	1.2	33.8	0.11	160.3	95.0	77.2	353
DW-53	28	86.9	80.6	800.3[3]	7.6	1.03	216.6	54.9	35.2	4880[3]
$\bar{X}$ =	26±1.7		43.6±24.4	2.9±2.9	33.5±27.5	.47±.36	298.5±104	58.7±23	56.7±21	397±42
MISC.										
GS-5	29	153.7	52.0	2.6	12.7	0.51	50.1	63.4	63.3	377
PF-4	27	290.2	20.6	1.4	22.7	0.35	106.3	64.5	79.4	350
PF-5	27	289.6	20.7	2.1	10.9	0.36	71.3	58.7	81.1	331
DW-31	30	95.1	94.6	12.7	19.2	0.56	74.9	50.9	60.6	444
PF-18	35[4]	105.0	-	-	-	-	-	-	-	-

1. ATOMIC RATIOS
2. MILLIGRAMS PER LITER
3. ANOMALOUS CONCENTRATION, EXCLUDED FROM MEAN-VALUE ESTIMATE
4. TEMPERATURE AT 120 M DEPTH

Group III waters exhibit fewer similarities as a group than do Groups I and II. These waters are nonthermal. They are distinguished by very high Na/K and Na/Ca ratios, both of which exceed Group I ratios by a factor of five or more (Table 2.23). These waters are the most westerly group and their chemistry appears to be strongly influenced by the evaporite deposits mentioned by Hollett (1981b).

GEOTHERMOMETRY. The chalcedony and Na-K-Ca geothermometers were used to estimate minimum aquifer temperatures of ground water at and surrounding Papago Farms (Table 2.24). There is good apparent agreement between the two mean geothermometer values for each group. Also the values are distinctive for each group. For individual wells, agreement between the two geothermometers is excellent for 12 wells (Table 2.25), the four highest values of which are from Group II thermal wells. Not surprisingly, the next two higher values are from Papago Farms wells that are closest to

TABLE 2.25. Geothermometers and measured temperatures for selected wells, Papago Farms and surrounding areas

	TEMPERATURE (^{o}C)			
Well Name	SiO_2	Na-K-Ca	Average*	Measured
PF-7	82-1	77.6	79.9 ± 3.1	39.0
PF-1	74.8	81.4	78.1 ± 4.7	45.0
PF-2	77.9	76.9	77.4 ± 0.7	38.0
PF-8	81.3	73.3	77.3 ± 5.7	51.0
PF-15	74.8	75.5	75.2 ± 0.5	30.0
PF-3	73.9	71.0	72.5 ± 2.1	28.0
GS-1	62.2	71.8	67.0 ± 6.8	27.0
GS-2	64.5	72.3	68.4 ± 5.5	24.0
GS-5	63.4	63.3	63.4 ± 0.1	29.0
DW-31	50.9	60.6	55.8 ± 6.9	30.0
T-3	49.5	58.6	54.1 ± 6.4	25.0
DW-73	50.9	46.3	48.6 ± 3.3	32.0

* Average of T_{SiO^2} and $T_{Na-K-Ca}$

the thermal wells. The geothermometers predict a minimum reservoir temperature of about 80°C.

Mixing of thermal and nonthermal waters may occur at Papago Farms. Water from five thermal wells shows an apparent systematic variation in measured temperature with boron concentration (Fig. 2.118). A temperature of 200°C was predicted from an analysis of PF-7 water. This temperature is unrealistically high, and probably was caused by solution of amorphous silica. PF-7 penetrated a 60-m thick volcanic sequence (Hollett, 1980, personal commun.) which, if it contains a high percent of glass, could explain the excess silica. Mixing models for PF-1, PF-2, and PF-8 waters predicted maximum temperatures of 125°C, 142°C, and 131°C, respectively (Stone, 1980). The general agreement among these temperatures suggests that the maximum probable temperature of the reservoir supplying the hot-water component is about 140°C.

GEOTHERMAL GRADIENTS. Three wells were temperature logged (Fig. 2.119) at the Papago Farms. Warm water is rising in PFD-A, and water is descending in PF-5 and probably in PF-18. It can be inferred from these profiles that PFD-A is located within the geothermal anomaly and PF-5 is situated outside of it. The location of PF-18 with respect to the anomaly is less certain, but it may be on the margin. The gradient measured in PFD-A suggests that the maximum reservoir temperature may be encountered at 1.5 to 2 km depth.

GEOPHYSICS. Based on gravity modeling, Greenes (1980) showed that depth to bedrock beneath the Great Plain increases to the south towards Mexico, and reaches a maximum depth in Arizona of greater than 2,700 m. The basin may be deeper in Mexico. Greenes modeled the Papago Farms

basin as an asymetrical graben with a subsurface bedrock scarp along the eastern pediment edge. He suggested that this scarp, indicated by the strong gravity gradient (Fig. 2.120), is due to faulting. Geochemical evidence, namely the distinct chemical and thermal differences between PF-15, PF-3, and PF-6 Group I water at the eastern edge of Papago Farms, and DW-2 and PF-7 Group II water immediately to the west, suggests a northwest extension of this fault through Papago Farms, between these two sets of wells. The presence of a fault or some other

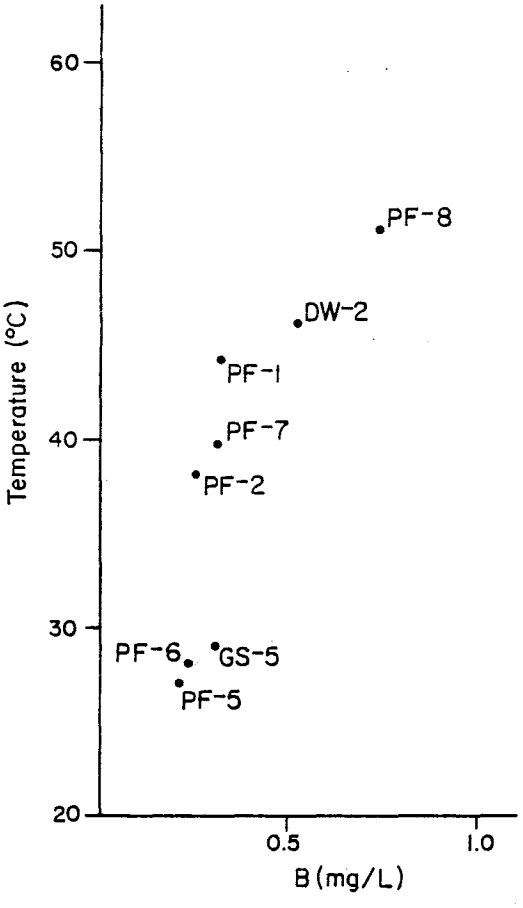

Figure 2.118. Boron (mg/L) versus temperature (^{o}C) for Papago Farms ground water

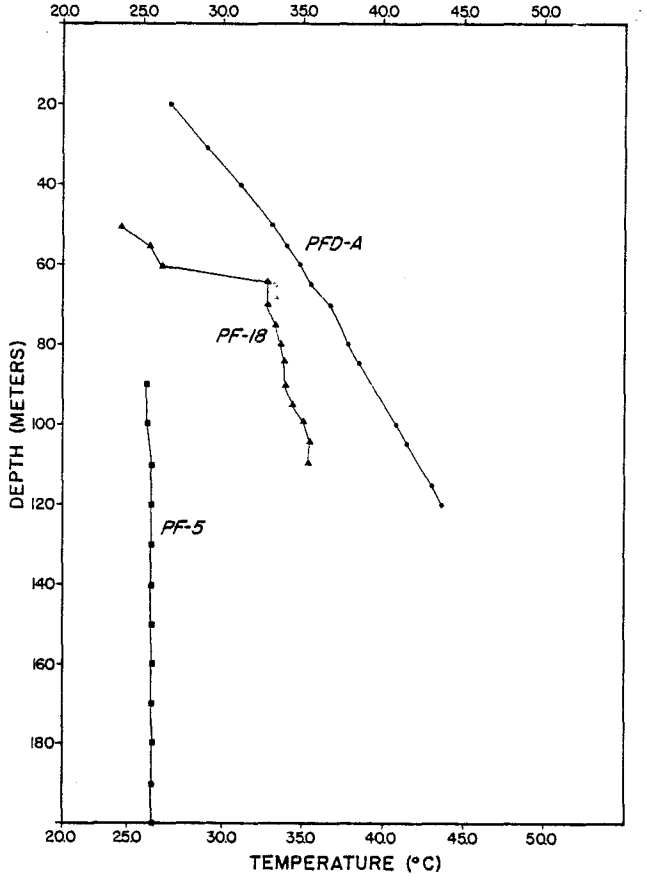

Figure 2.119. Temperature (^{o}C) versus depth (m) for three Papago Farms wells

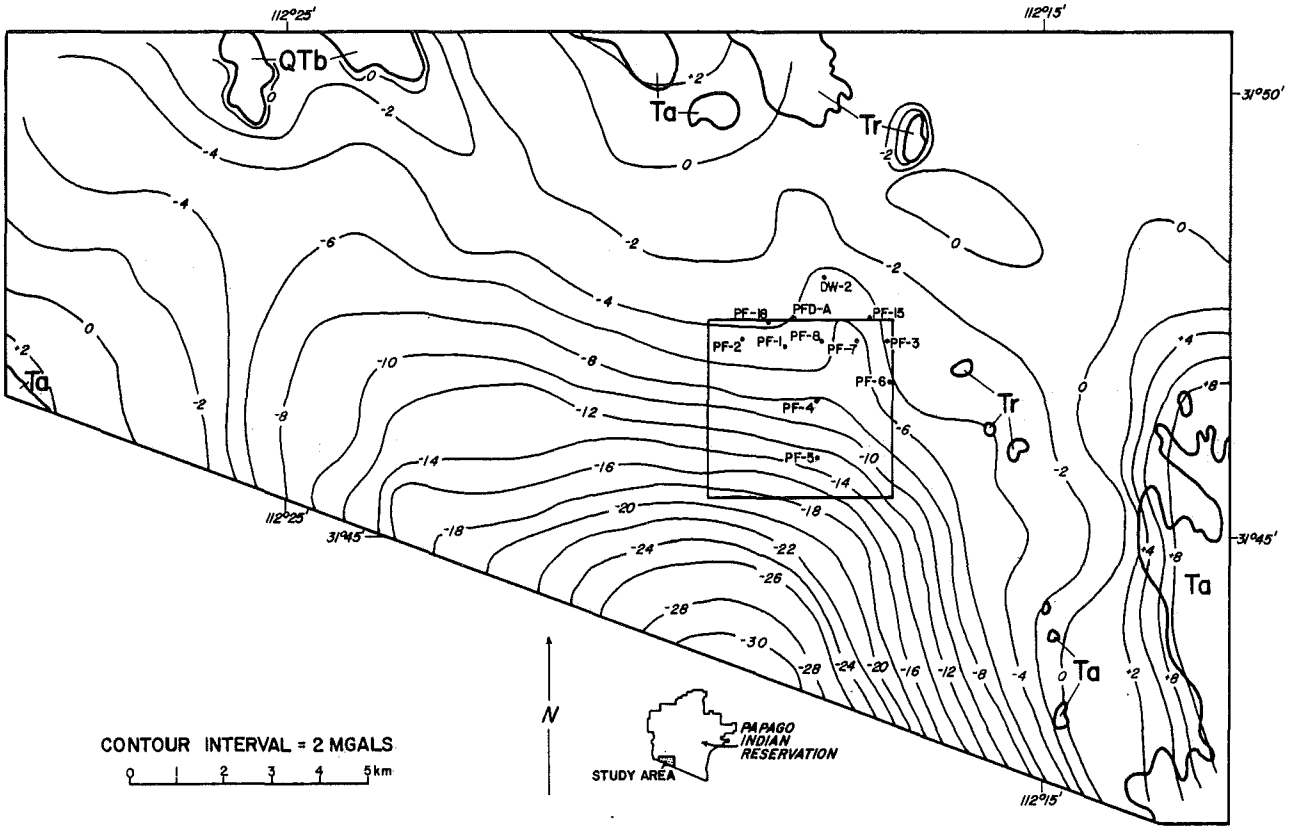

Figure 2.120. Second order residual Bouguer gravity map of Papago Farms and surrounding area (from Greenes, 1980). Square outline is Papago Farms.

structural control between these wells helps explain the observed differences in water chemistry and temperature.

Across the north end of the basin the abruptly steepening gravity gradient suggests the presence of a west-northwest-striking fault zone. Intersection of the two proposed subsurface bedrock faults (Fig. 2.121) could explain (1) the anomalous bulge in the second order residual Bouguer gravity at the north end of the Papago Farms as being the result of hydrothermally cemented (and refractured?) basement rocks and (2) the fact that PF-7, which sits in this bulge, is the hottest well at Papago Farms according to the geothermometers. This postulated fault intersection

suggests that the geothermal fluids are held in a reservoir having fracture permeability.

Stone (1980) suggested that the fault zones are about 1 km wide. The south and west margins of the fault zones are constrained by PF-2, PF-4, and PF-5, which do not penetrate the volcanic sequence penetrated by

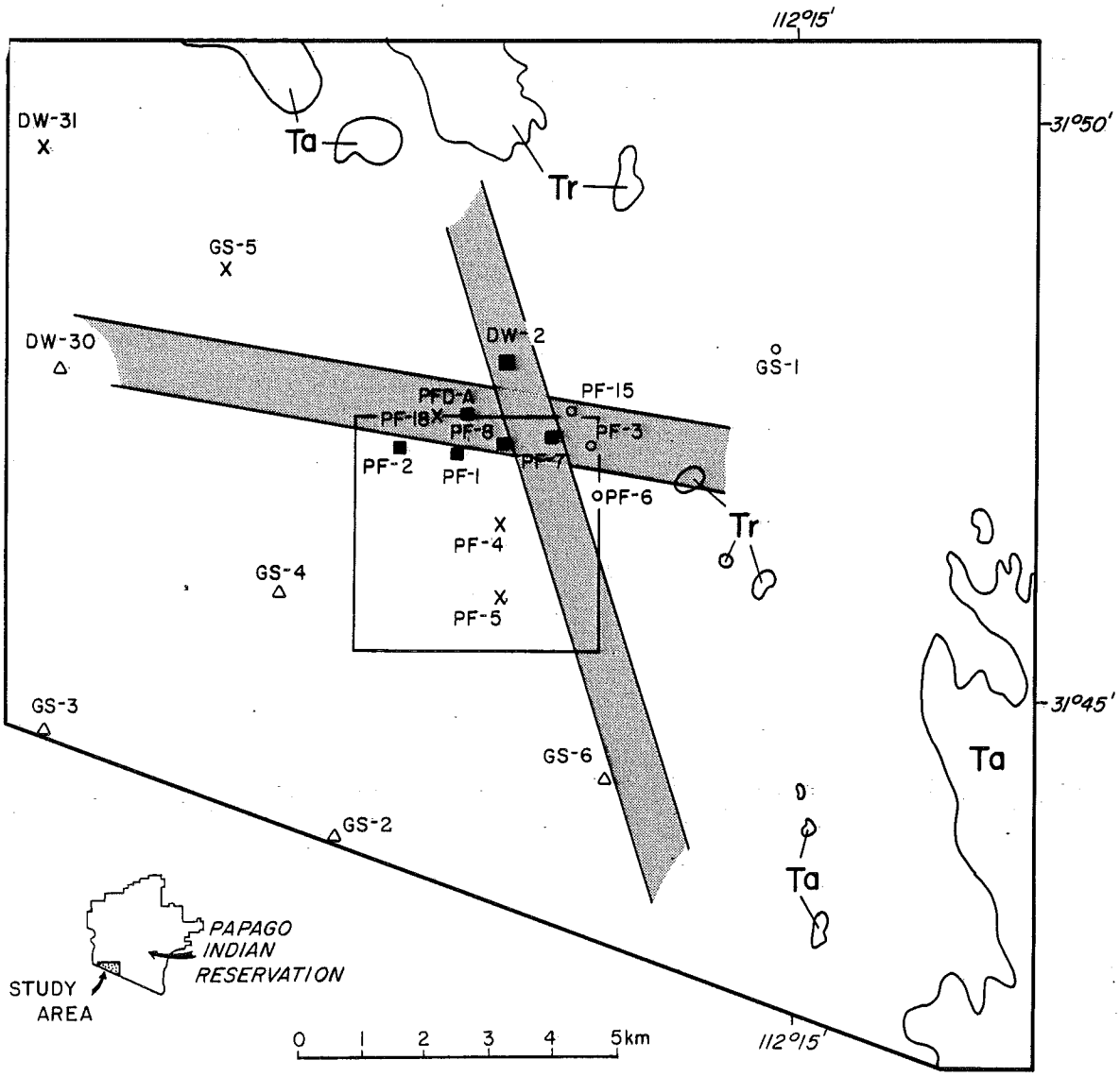

Figure 2.121. Proposed fault zones and fault intersection at Papago Farms (from Stone, 1980)

the other wells (Hollett, 1980, personal commun.). The east margin of the N. 18° W. fault zone is constrained by the thermal and chemical differences between DW-2 and PF-7 water versus PF-3, PF-6, and PF-15 water. The northern boundary of the N. 81° W. fault zone is somewhat arbitrary.

TEMPERATURES. Decreases in ground-water temperatures have been recorded at Papago Farms over a 20-year period (USGS, WATSTORE, 1980). Between about 1958 and 1978 all wells for which data are available show an average temperature decrease of 2.2°C, with declines ranging between 0.5 and 5.0°C for individual wells. A possible explanation is that prolonged irrigation pumping is inducing lateral inflow of large volumes of cold water into the aquifer.

CONCLUSIONS. Water quality from a group of anomalously warm wells at the north end of Papago Farms is chemically homogenous, but distinct from water in neighboring nonthermal wells. Geothermometers and mixing models predict reservoir fluid temperatures in the range of 80 to 140°C.

Geophysical evidence strongly suggests that two fault zones, each about 1 km wide and trending N. 18° W. and N. 81° W., intersect at the northeast corner of Papago Farms, in the area of PF-7. This fault intersection probably has created an area of intensely fractured basement rocks that provides permeability for thermal water flow. Deep circulation of meteoric water is most likely responsible for the heat content of the water. Depth to the geothermal reservoir is uncertain, but may be as shallow as 1.5 to 2 km.

PAPAGO FARMS REFERENCES

Greenes, K. A., 1980, Application of the gravity method to ground-water volume determinations of alluvial basins: M.S. thesis, Tucson, University of Arizona, 28 p.

Hollett, K. J., 1981a, Geohydrology of the Molenitus-Papago Farms area, Papago Indian Reservation, Arizona (abstr.): Geological Society of America Abstracts with Programs, Cordilleran Section, v. 13, no. 2, p. 61.

_____1981b, Maps showing ground-water conditions in the San Simon Wash area, Papago Indian Reservation --- 1979: U.S. Geological Survey Water-Resources Investigations Open-File Report 81-530.

Stone, C., 1980, Preliminary assessment of the geothermal potential at Papago Farms, Papago Indian Reservation, Arizona: Bureau of Geology and Mineral Technology Open-File Report 80-6, 49 p.

SOUTHERN PALOMAS PLAIN

INTRODUCTION. Nearly 50 wells in the southern Palomas Plain have temperatures exceeding 35°C. These wells cluster in three major groups of 10 to 12 wells each and three smaller groups of two to four wells each. Hot springs at Agua Caliente, which are now dry, are associated with one of the smaller well clusters. Many of these same wells have gradients sufficiently high to be called thermal. Average silica and Na-K-Ca geothermometers predict minimum temperatures of 70 ± 20°C. Two areas have geothermometers that predict temperatures of 92 ± 3.3 and 100 ± 3.6°C.

Soil warming using warm irrigation water has been practiced for many years on major grape and citrus ranches in the southern Palomas Plain. The geothermal waters present in this region could also be used for greenhousing, space conditioning and probably aquaculture.

PHYSIOGRAPHY. The Palomas Plain is a broad northwest-trending wedge-shaped valley located about 65 km west of Gila Bend (Fig. 2.122). The valley floor slopes gently to the south-southeast and is dissected to varying degrees by numerous subparallel washes. Elevation changes from about 330 m above sea level in the northwest to 150 m at the southeastern end. The nearby mountain ranges have a maximum relief above the plain of about 325 m. Mean annual temperature is 22°C. Average precipitation is about 13 cm per year.

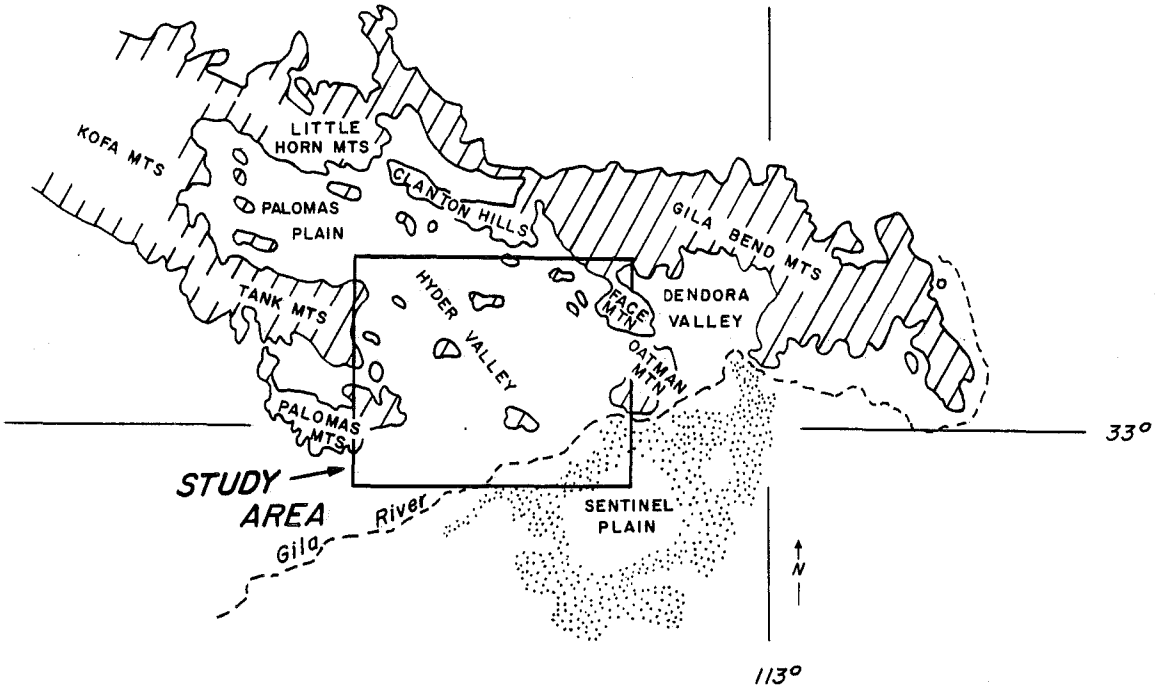

Figure 2.122. Location map of Palomas Plain

GEOLOGY. The Palomas Plain is surrounded by the Tank and Palomas Mountains on the west, the Little Horn Mountains and Clanton Hills to the north, and the Gila Bend Mountains on the east (Fig. 2.123).

The Gila Bend Mountains are composed of Precambrian granite and gneiss on the east and west ends. Late Cretaceous and Tertiary silicic to intermediate composition volcanic rocks overlie these crystalline rocks in most of the central part of the range. Small outcrops of Tertiary limestone, sandstone, and conglomerate are exposed at the southeast end of the Gila Bend Mountains.

The Palomas, Tank, and Little Horn Mountains are composed chiefly of late Cretaceous to mid-Tertiary volcanic flows and tuffs of silicic and intermediate composition. Precambrian(?) granite; Mesozoic rhyolitic to andesitic volcanic rock; Mesozoic schist and gneiss; and small outcrops of

limestone, conglomerate, quartzite, and shale of undetermined age form relatively minor outcrops.

Basalt flows once covered much of the area of the Palomas Plain, but erosion has removed most of this material. Relatively large areas in the eastern and northern mountain range are covered today by remnant basalt flows. Smaller remnants remain in the other mountains. South of the Gila

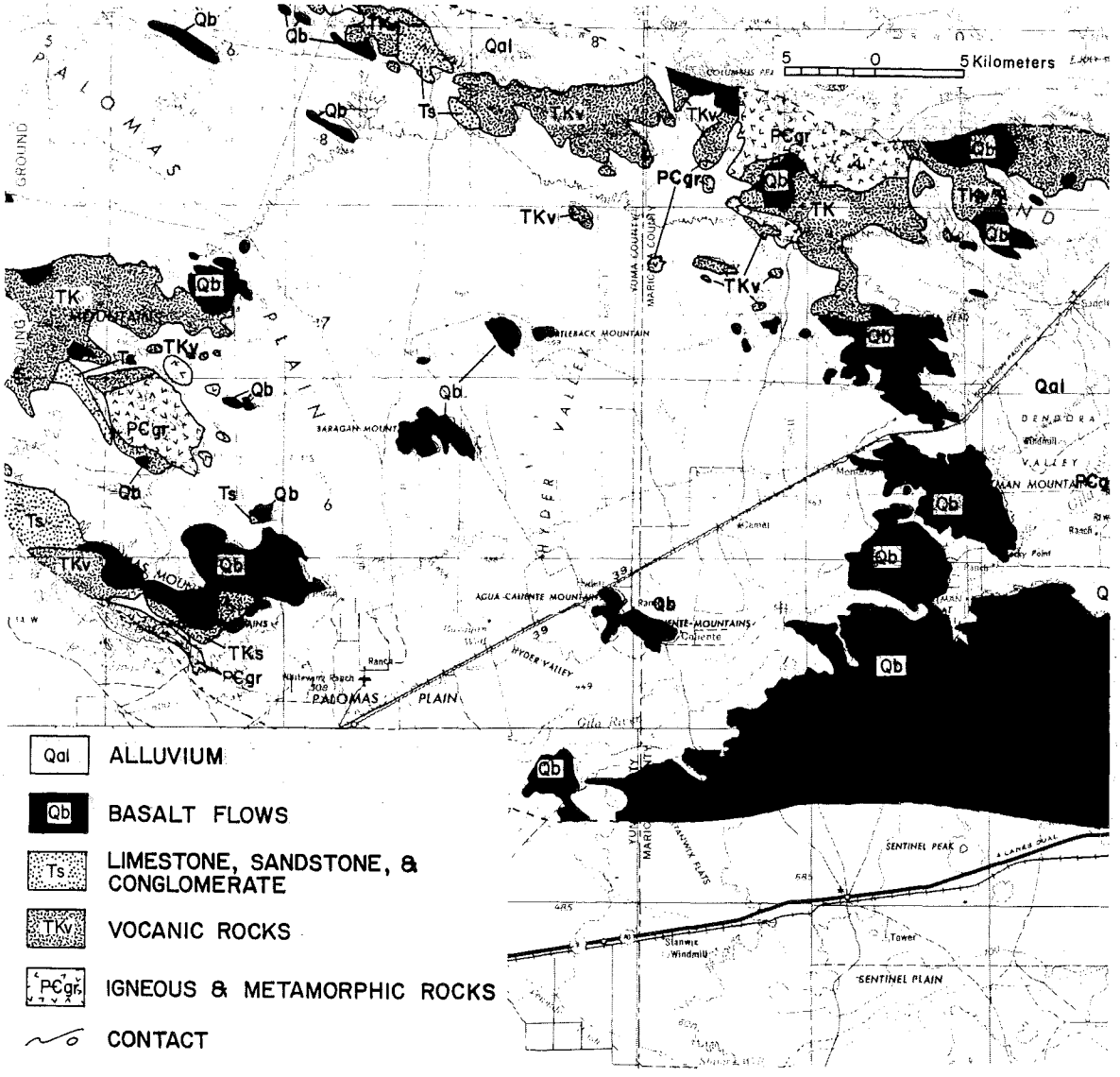

Figure 2.123. General geology of the Palomas Plain area

River, basalts covering the Sentinel volcanic field have K-Ar dates as young as 3.0 ± 0.1 and 1.72 ± 0.46 m.y. (Aldrich and Laughlin, 1981; Shafiqullah and others, 1981).

Alluvial fill beneath the Palomas Plain is similar in character to that in other basins of southern Arizona. Gravel, clay, silt, and sand occur as lenses of varying thickness at various depths (Armstrong and Yost, 1958). Coarse sediments were generally deposited closer to the mountain fronts and finer material toward the center of the valley. Weist (1965) divided the valley-fill deposits into a 60- to 115-m-thick upper unit of mostly sand and gravel, a middle unit consisting of 75 to 230 m of fine-grained material, mainly clay and silt, and a more cemented lower unit composed of coarse sand and gravel. The lower unit varies widely in thickness because the bedrock surface on which it lies is very irregular.

Drillers' logs for only one well (C-5-10-16bbb) show termination in granite (385 m). Well C-5-12-4cdd encountered volcanic sand and tuff at a depth of 240 m. All other drillers' logs penetrate a sequence principally of interbedded sand and clay.

GEOHYDROLOGY. Depth to water beneath the Palomas Plain decreases from about 100 m below land surface along the northern edge of the area to about 10 m along the Gila River. In some places the water is under artesian pressure, probably confined by a thick clay sequence.

A very small amount of underflow into the area comes from the north and southeast. Minor discharge by underflow occurs only along the west edge of the area south of the Palomas Mountains (Weist, 1965).

Dissolved-solids contents range from about 400 to 10,000 ppm, with water along the Gila River having the greatest concentrations. The water is generally sodium-chloride type.

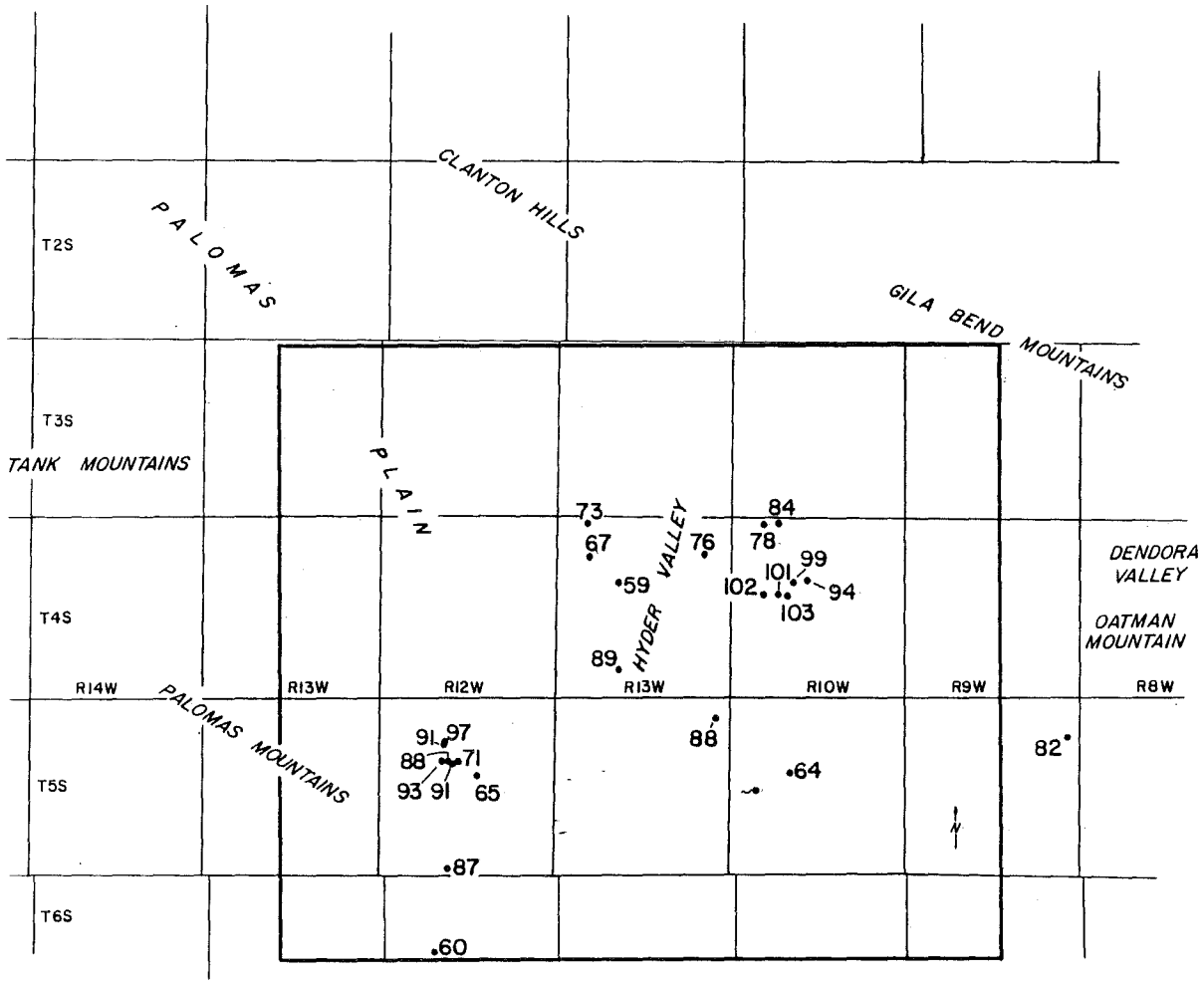

Figure 2.124. Averages of silica and Na-K-Ca geothermometers for the southern Palomas Plain

GEOTHERMOMETRY. Averages of the silica and Na-K-Ca geothermometers, where there is good agreement between temperatures predicted by the two methods, range from about 60 to 103°C (Table 2.26; Fig. 2.124). Generally the higher values are found in two clusters, T. 5 S., R. 12 W., and in the eastern Hyder Valley, T. 4 S., R. 10 W. The geothermometers suggest temperatures of approximately 92 ± 3.3 and 100 ± 3.6°C at these locations, respectively. Average background temperature predicted by the geothermometers is about 70 ± 20°C.

TABLE 2.26. Temperatures, depths, and geothermometers for wells in the southern Palomas Plain

Location	T_{meas} (°C)	Depth (m)	Grad (°C/km)	T_{chal} (°C)	$T_{Na-K-Ca}$ (°C)	T_{qtz} (°C)	T_{ave} (°C)
C-3- 9- 7bcc	27	61	85	51	-	82	-
C-3-10-31bcc	38	-	-	66	127	96	-
C-3-11-34bba	30	-	-	-	-	-	-
C-4- 7-18dda	23	6	200	39	-	70	-
18dd	23	22	60	51	-	82	-
C-4- 8-26ddd	35	59	220	59	-	89	-
27dda	28	31	207	67	-	97	-
31cdd	29	-	-	59	-	89	-
34ddd	26	134	31	-	-	-	-
35bdd	31	83	106	86	-	115	-
35dbb	30	68	122	63	-	94	-
C-4-10- 6bbb*	35	137	95	71	-	101	-
7bbb	34	152	78	-	-	-	-
33bdd	26	195	19	60	-	91	-
6aab*	38	143	111	79	-	108	-
5bbb	34	300	40	51	73	82	78
5abb	36	389	36	48	89	79	84
16abb	32	-	-	59	98	89	94
16bbb	33	-	-	60	106	91	99
17cbb	30	-	-	61	112	92	102
17daa	31	-	-	61	113	92	103
17dbb	30	-	-	61	110	92	101
3daa*	33	138	82	29	-	62	-
C-4-11- 2bbb*	39	162	105	82	-	111	-
5bbb*	39	142	123	72	74	102	73
8bbb*	40	200	90	67	67	97	67
12abb	38	375	42	78	-	107	-
12bbb	35	127	103	71	81	101	76
16bbb	30	152	53	61	57	92	59
21abb	32	419	24	97	-	125	-
33bbb	30	332	24	57	90	88	89
C-5- 9-12aca	25	46	66	54	78	85	82
12acd*	32	186	55	29	46	62	-
12acd*	33	189	57	33	-	62	-
C-5-10- 7cbb	28	47	133	-	-	-	-
16abb	25	23	130	73	-	103	-
16cbc	40	-	-	63	65	94	64
19aa Spring		36	-	-	-	-	-
20dbd	33	-	-	63	-	94	-
28dba	24	32	76	45	-	77	-
C-5-11- 1dcb	32	274	35	56	89	87	88
11cab	37	305	48	66	-	96	-
12cba	31	31	298	-	-	-	-
C-5-12- 4bcb	30	113	68	79	-	109	-
4cbc	30	95	84	68	145	98	-
4bcc	32	152	66	69	153	99	-
4ccc	34	-	-	64	140	95	-
4cdb	35	602	22	69	148	99	-
5aad	31	90	94	68	152	98	-
5abb	32	542	19	69	149	99	-
9bbb	32	171	59	70	149	100	-
9cba	38	503	31	66	97	96	97
9cca	40	489	37	63	87	94	91
15cac	34	145	82	68	61	98	65
16aab	32	191	54	67	74	97	71
16aab	33	122	89	-	-	-	-
16abb	37	-	-	68	80	98	-
16acc	33	282	39	64	-	95	-
16abc	32	-	-	61	90	92	91
16baa*	35	154	35	61	84	92	88
16bbb	37	100	152	-	-	-	-
16bbb	35	139	94	63	91	94	93
21bbb*	34	136	88	69	84	99	-
21bbb	34	187	64	-	-	-	-
21bbd	33	79	143	77	-	106	-
22bbc	34	174	71	74	-	104	-
23acd	28	-	-	62	-	93	-
28aaa	34	218	55	70	-	100	-
35bbb	31	148	58	60	-	91	-
C-6- 9- 9aa	26	56	78	-	-	-	-
32ccb	-	314	-	61	66	92	64
C-6-10- 5bd	23	-	-	-	-	-	-
C-6-12- 3baa	29	244	30	49	-	81	-
7dda	28	494	12	81	59	110	-
17daa	24	63	38	57	63	88	60
17dba	24	53	36	-	-	-	-
18dab	25	24	128	-	-	-	-
18ddd	24	35	68	60	-	91	-

* = Thermal well
MAT = 22°C
Underscored values show best correlation between silica and Na-K-Ca geothermometers used to estimate T_{ave}.

THERMAL REGIME. Three large areas (15 to 23 km^2) each contain 10 to 12 irrigation wells that discharge water having temperatures between 35 and 49°C (Fig. 2.125). Three smaller areas (5 km^2) each contain two to four wells that discharge 38 to 46°C water. One of these smaller groups in T. 5 S., R. 10 W., caused Agua Caliente springs to dry up after the wells were drilled during the 1950s and early 1960s. Temperatures in this cluster are between 36 and 46°C. Geothermometers are in the 75 to 85°C range.

Thermal wells are abundant in the southern Palomas Plain, but most are less than 200 m deep. Figure 2.126 shows thermal and nonthermal wells having depths between 100 and 200 m, and wells having depths greater than 200 m. It can be seen that the majority of thermal wells in T. 5 S., R. 12

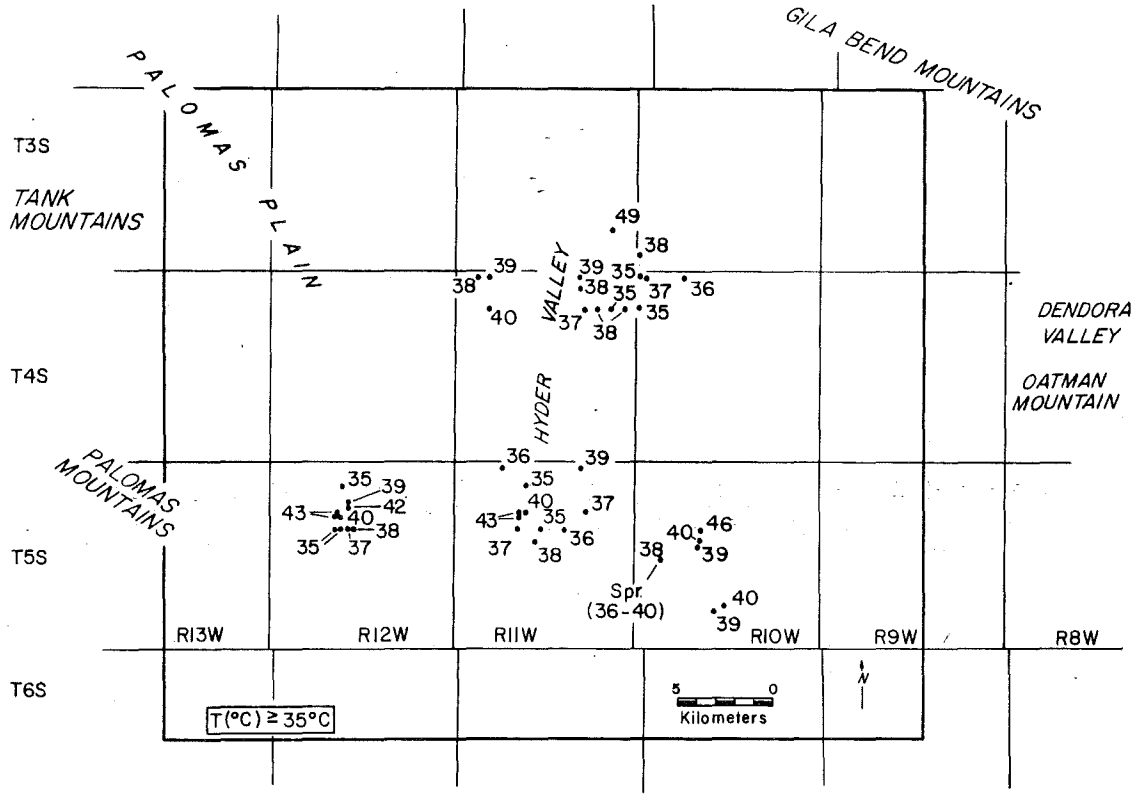

Figure 2.125. Discharge temperatures (greater than 35°C) for wells, southern Palomas Plain

W. are less than 200 m deep, suggesting to us the presence of a very shallow hydrothermal convection system in this area. Well temperatures are 35 to 43°C, and geothermometers predict temperatures of about 90 to 95°C.

A second group of wells having temperatures of 35 to 49°C lies at the nothern end of the Hyder Valley (T. 3-4 S., R. 10-11 W.). Nearly all of these temperatures are from shallow thermal wells. The geothermometers calculated from these waters predict minimum aquifer temperatures in the range of 75 to 85°C. East of this area, in T. 4 S., R. 10 W., shallow non-thermal wells have water chemistry that predicts temperatures of approximately 100 ± 3.6°C. However additional information such as measured temperatures and depths is lacking for these wells.

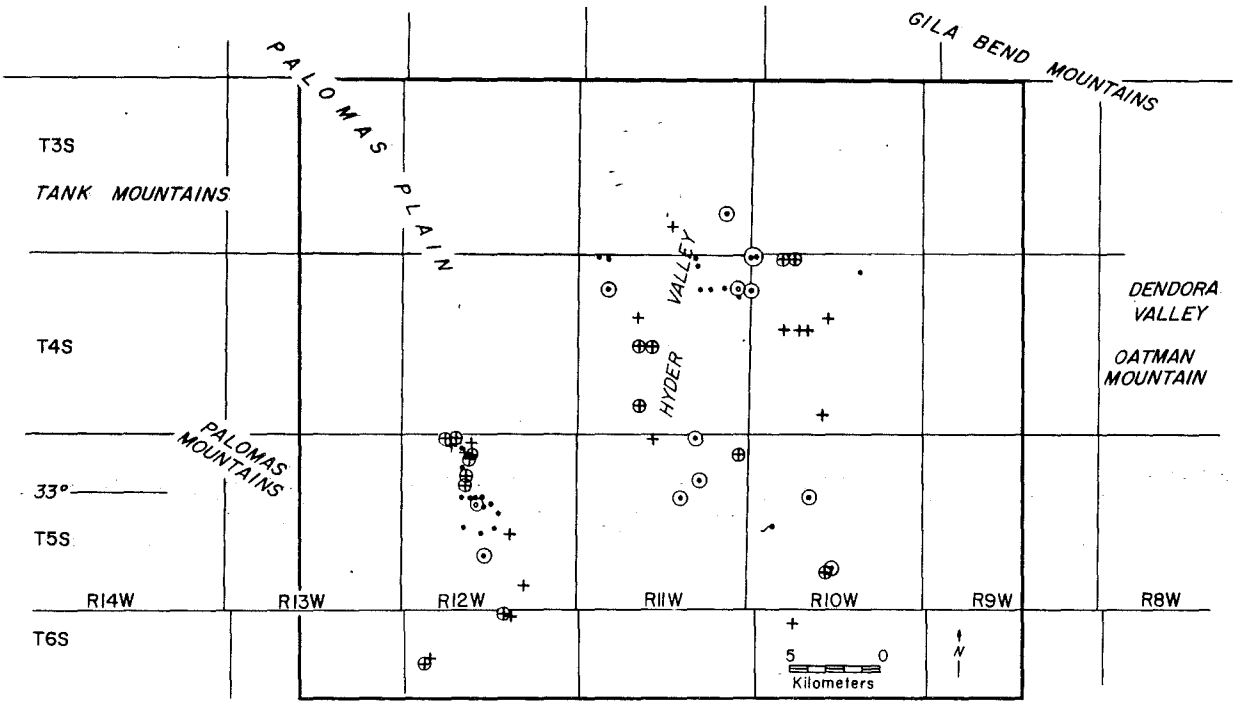

Figure 2.126. Thermal (solid dot) and nonthermal (cross) wells, southern Palomas Plain. Wells greater than 200 m deep have circled symbol.

The third large cluster of 12 wells in T. 5 S., R. 11 W. has water temperatures between 35 to 43°C. Water chemistry is not available for these wells and only five well depths are known. Three of these have estimated gradients exceeding 45°C/km (49.0, 55.7, and 62.5°C/km), which makes them thermal wells.

GEOPHYSICS. The nearest heat flow measurements to the Palomas Plain are 15 to 30 km to the northeast (74-85 and 59 mWm^{-2}) (Sass, 1981, personal commun.; Shearer, 1979), and 20 to 30 km to the south, southwest, and west (all three are 61-73 mWm^{-2}) (Sass, 1981, personal commun.). The 59 mWm^{-2} heat flow (Shearer, 1979) is a C quality (low-reliability) determination. Thus it seems the higher values reflect the regional heat flux of this area. The range of the heat flows surrounding the Palomas Plain are on the low end of normal for the southern Basin and Range province. However, the determinations are at a great enough distance that they do not preclude the possibility of high heat flow in the southern Palomas Plain.

CONCLUSIONS. The coincidence of above-normal well temperatures (to about 50°C), numerous shallow thermal wells, and moderately high geothermometers at discrete locations within the southern Palomas Plain is evidence of several shallow hydrothermal convection systems in this area. Temperatures up to 75°C might be expected at an approximate depth of 1.6 km in some of these areas.

The area is thermally enhanced as a result of lithosphere extension and deep (lower crustal) intrusions (Lachenbruch and Sass, 1978), probably during the late Miocene to Pliocene (Basin and Range disturbance). Locally the geothermal systems may be driven by heat from a cooling intrusion within the crust, a result of repeated and recent extrusions of basaltic

lavas in the Sentinel lava field to the south, or by forced convection of ground water in a high gradient region.

Additional geological and geophysical studies, especially heat flow measurements will aid in understanding and evaluating the geothermal anomalies in the southern Palomas Plain.

SOUTHERN PALOMAS PLAIN REFERENCES

Aldrich, M. J., and Laughlin, A. W., 1981, Age and locations of volcanic centers ≤3.0 m.y. old in Arizona, New Mexico and the Trans-Pecos area of west Texas (modified from Luedke, R. G., and Smith, R. L., 1978): Los Alamos Scientific Laboratory LA-8812-MAP, scale 1:1,000,000.

Armstrong, C. A., and Yost, Jr., C. B., 1958, Geology and ground-water resources of the Palomas plain - Dendora Valley area, Maricopa and Yuma Counties, Arizona: U. S. Geological Survey Water Resources Report No. 4, 49 p.

Lachenbruch, A. H., and Sass, J. H., 1978, Models of an extending lithosphere and heat flow in the Basin and Range province: *in* Smith, R. B., and Eaton, G. P. (eds.) Cenozoic tectonics and regional geophysics in the western Cordilleran: Geological Society of America Memoir 152, p. 209-250.

Shafiqullah, M., Damon, P. E., Lynch, D. J., Reynolds, S. J., Rehrig, W. A., and Raymond, R. H., 1980, K-Ar geochronology and geologic history of southwestern Arizona and adjacent areas: Arizona Geological Society Digest, v. 12, p. 201-260.

Shearer, C. R., 1979, A regional terrestrial heat flow study in Arizona: Ph.D. dissertation, Socorro, New Mexico Institute of Mining and Technology, 184 p.

Weist, Jr., W. G., 1965, Geohydrology of the Dateland-Hyder area, Maricopa and Yuma Counties, Arizona: U. S. Geological Survey Water-Resources Report No. 23, 46 p.

YUMA

INTRODUCTION. Yuma is located in the extreme southwestern corner of Arizona, principally in the Sonoran Desert and partially in the Salton Trough subprovinces (Fig. 2.127). Proximity to the more than 12 identified geothermal anomalies in the Salton Trough in neighboring California and Mexico makes Yuma a favorable exploration target, even though surface thermal features are unknown in this area. Figure 2.128 shows the major political and topographic features of Yuma.

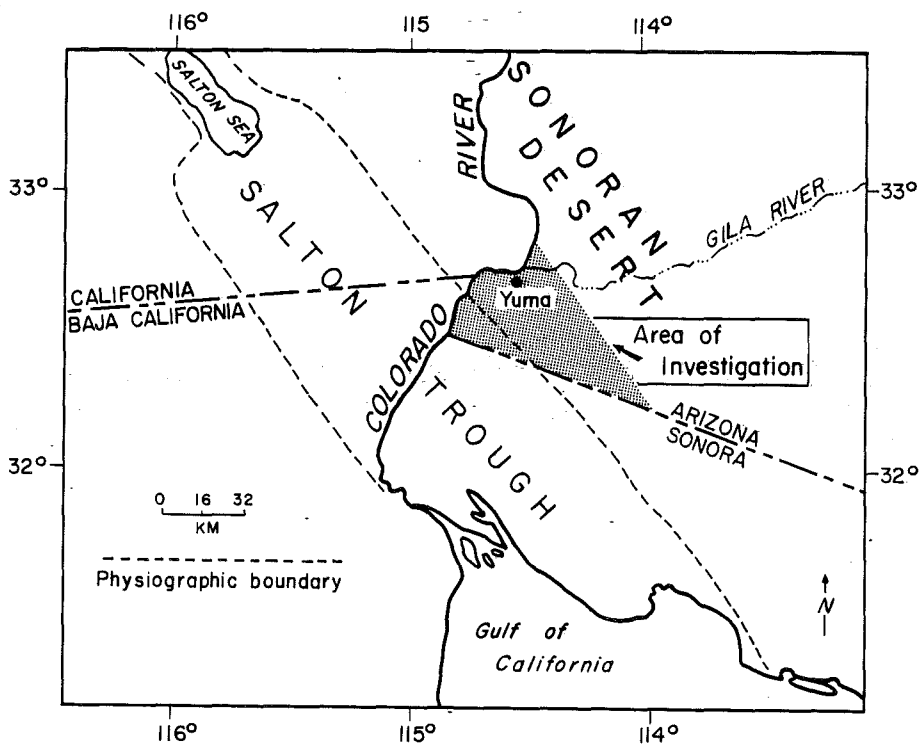

Figure 2.127. Map showing physiographic provinces of southwestern Arizona and the Yuma area of investigation

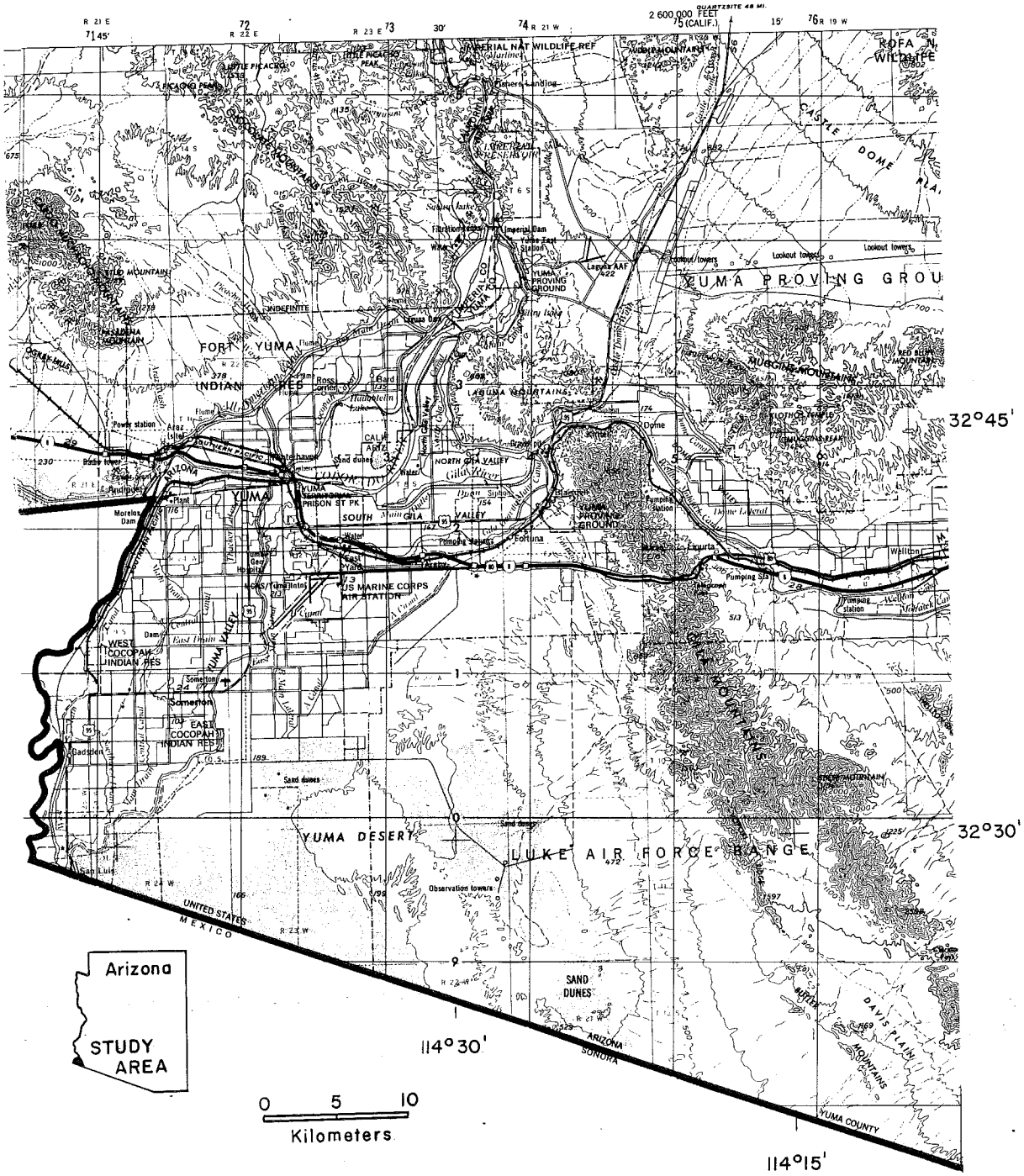

Figure 2.128. Physiographic map of the Yuma area

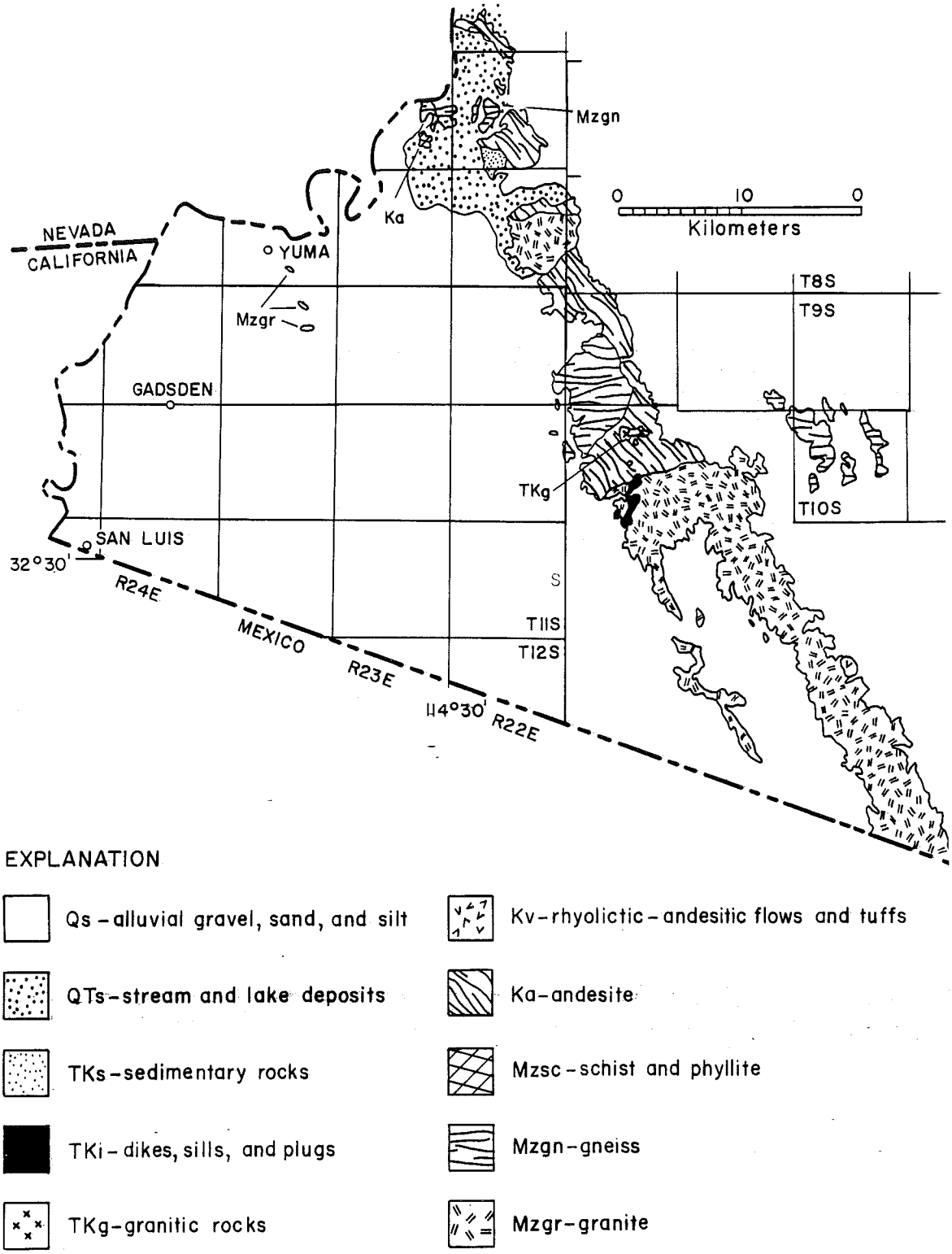

Figure 2.129. Generalized geologic map of the Yuma area

PHYSIOGRAPHY. Yuma is a region of several distinct physiographic or geomorphic subareas. The youngest and most notable features are the Colorado River valley along the California-Arizona border and the Gila River valley north of Yuma. Sand dunes, river terraces and mesas, river valleys, dissected and undissected piedmont slopes, and the surrounding hills and mountains constitute the other major landforms. Elevations vary from greater than 800 m to less than 35 m above mean sea level. Precipitation is about 7.1 cm per year.

GEOLOGY. The principal mountain ranges surrounding Yuma are the Tinajas, Altas, Gila, Butler, and Laguna Mountains in Arizona and the Cargo Muchacho and Chocolate Mountains in California (Fig. 2.129). The Laguna Mountains are principally nonmarine sedimentary rocks of Tertiary age. The Chocolate Mountains are composed of Tertiary volcanic rocks. All other ranges are pre-Tertiary crystalline rocks, chiefly granite, gneiss and schist. The most extensive plutonic rocks have compositions of quartz monzonite and granite. Metamorphic rocks vary from weakly metamorphosed volcanic and sedimentary rocks to strongly metamorphosed schist and gneiss.

Sedimentary rocks began accumulating in early Tertiary in the basins underlying the Yuma region. The stratigraphic units identified by Olmsted and others (1973) are: (1) Tertiary nonmarine sedimentary rocks and associated volcanic rocks, (2) older Tertiary marine sedimentary rocks, (3) the Pliocene Bouse Formation, (4) the Pliocene transition zone (facies), (5) Tertiary and Quaternary conglomerate of the Chocolate Mountains, (6) Pliocene and Pleistocene older alluvium, (7) Quaternary younger alluvium, and (8) Quaternary windblown sand.

The Tertiary nonmarine sedimentary rocks are very coarse grained in many places and are slightly to moderately well indurated. The extent and thickness of these rocks are unknown in many parts of the Yuma area. Volcanism occurred intermittently during the time these nonmarine sedimentary rocks were being deposited. The volcanic sequence is thickest in the Chocolate Mountains and thinner in the Laguna Mountains. Oldest to youngest, the volcanic sequence consists chiefly of andesite, intermediate to silicic pyroclastic rocks, and dark basaltic andesite or basalt. Radiometric dating gives ages of approximately 23 to 26 m.y. for the volcanic rocks.

The older marine sedimentary rocks are moderately well indurated and therefore, like the underlying unit, are probably less permeable and porous than the overlying units. These rocks were not encountered in several test wells below the Bouse Formation, which suggests they are less extensive than the Bouse Formation.

The marine Bouse Formation is the most important of the lower four units because it is the shallowest reliable stratigraphic marker and because it was deposited prior to major strike-slip movement along the San Andreas fault system. The Bouse Formation consists predominantly of clay and silt with interbedded very fine to fine sand. Thickness ranges from zero to 290 m.

Deposition of marine sediments did not cease abruptly. This is indicated by a transition zone (facies), which represents regressive intertonguing of marine and nonmarine strata. This unit is as much as 100 m thick in the southwestern part of the Yuma area, but is missing in

the northeast. These rocks contain abundant clay and silt and some coarser strata, which are slightly to moderately indurated.

Clasts in the conglomerate of the Chocolate Mountains are predominantly ash-flow tuff and welded tuff. These fragments are angular and range in size from granules to boulders. Olmsted and others (1973) inferred from field relations that the older parts of the conglomerate may be equivalent in age to the upper parts of the nonmarine sedimentary rocks, and the younger parts of this unit may be equivalent to the older alluvium.

The older alluvium is Pliocene-Pleistocene. It comprises slightly to moderately indurated fluvial and deltaic sediments deposited chiefly by the Colorado River. Within the Yuma area, the older alluvium is the most widely exposed stratigraphic unit. Thickness ranges up to 760 m in the southwestern part of the area.

The Quaternary younger alluvium is composed entirely of fine-grained Colorado and Gila River deposits, alluvial-fan deposits, and wash and sheet-wash deposits of the most recent major depositional cycle. The windblown sand forms chiefly small dunes in the valleys and sheets of sand on Yuma Mesa.

STRUCTURAL SETTING. Anderson and Silver (1979) recognized that one of the earliest tectonic events to have affected southwestern Arizona was a major left-lateral dislocation of Late Jurassic age, called the Mojave-Sonora megashear. This dislocation zone trends generally northwest from the Sierra Madre Occidental of Sonora, Mexico across the Sonoran, Colorado, and Mojave deserts to the southern Inyo Mountains of California. Anderson and Silver (1979) suggested that as much as 700 to 800 km of offset may

have occurred. The offset disrupted two northeast-trending orogenic and magmatic belts of Precambrian age.

The Laramide orogeny, 40 to 80 m.y.B.P., produced uplift, extensive plutonism and volcanism, and intense compressive deformation. Subsequent tectonic events have been superimposed on the Mojave-Sonora megashear and Laramide structures. The extent to which younger Basin and Range block faulting, mountain uplift, and basin subsidence have affected the Yuma area is unclear, however. Eberly and Stanley (1978) stated that Salton Trough tectonics played a more important role in the Yuma area than did Basin and Range tectonics.

The Salton Trough-Gulf of California system west of Yuma is interpreted as a complex, transitional plate boundary that takes up stress created by two different tectonic regimes: spreading at the East Pacific Rise and transform motion along the San Andreas fault system as the Pacific plate moves northwestward. As a result of continuing motion, the Gulf of California-Salton Trough system is an actively growing rift.

The Salton Trough itself is a deep sediment-filled structural depression created by block faulting followed by subsidence and deltaic deposition from the Colorado River. The trough is the landward extension of the Gulf of California. The present apex of the Colorado River delta forms a low divide between Imperial Valley to the north, in California, and Mexicali Valley to the south, chiefly in Mexico. These two valleys contain the geothermal anomalies that have been identified within the Salton Trough.

The subsurface in the Yuma region comprises several deep basins separated by fault-bounded bedrock highs (Fig. 2.130). Maximum depth to

basement in the Fortuna basin is 4,900 m; in the the San Luis basin, depth to basement is 4,100 m; and in the Yuma trough, it is 1,100 m (Olmsted, 1979, written commun.). The major fault through the area is the

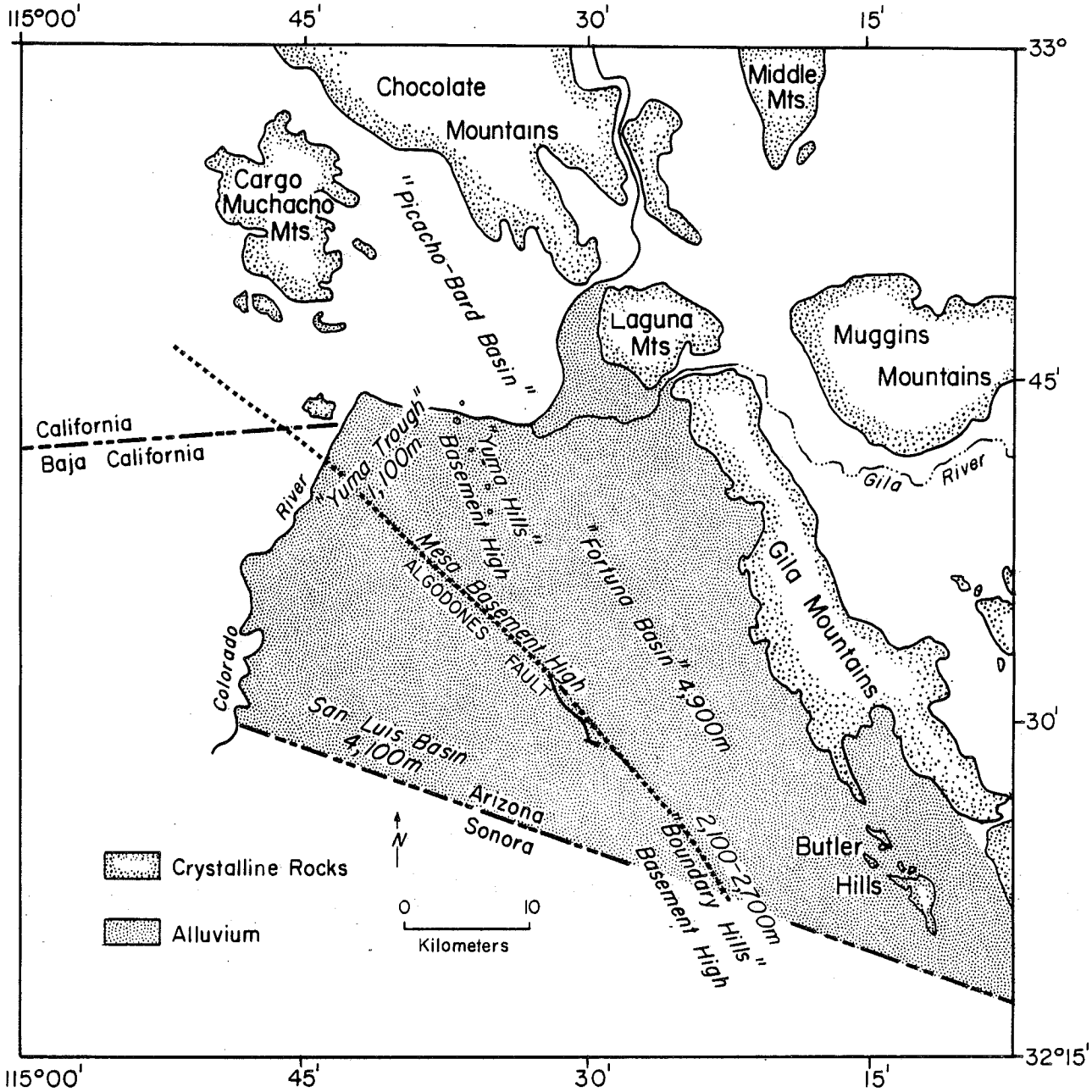

Figure 2.130. Map showing deep basins and bedrock highs, with approximate maximum depths to crystalline rock. Also shown is the Algodones fault.

northwest-trending Algodones fault, inferred to represent the northeast margin of the Salton Trough and to constitute an inactive extension of the San Andreas fault system (Olmsted and others, 1973). Other faults through the Yuma area are shorter en echelon faults that parallel the Algodones fault, and the more north-northwest-trending range-bounding faults of the Laguna, Gila, and Tinajas Altas mountain chain. A number of the subsurface faults were identified by Olmsted and others (1973) through (1) offsets of the Bouse Formation and (2) their observed effect of acting as impermeable ground-water barriers.

GEOHYDROLOGY. The principal source of all shallow ground water and ground-water recharge in the Yuma area is the Colorado River. Smaller sub-areas receive significant recharge from the Gila River. In recent years upstream dams, large-scale pumping from drainage and irrigation wells, and applications of irrigation waters have created a state of flux in the natural hydrologic cycle in this region.

The ground-water reservoir comprises the entire sedimentary section overlying the pre-Tertiary crystalline basement rocks. However, the principal water-bearing units consist almost solely of the older alluvium, younger alluvium, and windblown sand.

The lower four deposits have been called "poorly water-bearing rocks" by Olmsted and others (1973) because they contain either scant quantities of water or water that is highly mineralized. They suggested that the deeper formations may contain some connate water, which has never been flushed out. Electric logs indicate specific conductances up to 15,000 micromhos (approximately equivalent to 9,000 mg/L TDS) from most parts of these lower deposits. In the north-northeast part of Yuma, the abundant

clay and silt of the Bouse Formation form an aquiclude between the underlying nonmarine sedimentary rocks and the overlying deposits that make up the main part of the ground-water reservoir. Electric log data and electrical soundings (Mattick and others, 1973) indicate that the Bouse Formation has a very low average resistivity of 3 ohm-m and the older marine sedimentary rocks have an average resistivity of 8 ohm-m. In general, they interpreted the electrical data in terms of formation coarseness, degree of cementation, and water salinity, and only mentioned the possibility of hot water causing or enhancing the high conductivity of the Bouse.

GEOPHYSICS. Both gravity (Fig. 2.131) and aeromagnetics (Fig. 2.132) of the Yuma area show northwest trends, which are typical of the Basin and Range province and the Salton Trough. Gravity lows generally reflect the deep basins and gravity highs, the near-surface or surface exposures of bedrock. Lineaments (Lepley, 1978) have the same northwest trend that is seen in the gravity, magnetics, and fault traces. Sass and others (1971) published two heat flow measurements in the northern Yuma area, 79.4 and 87.8 mWm^{-2} (Fig. 2.133). Shearer (1979) temperature logged two wells in the southern Yuma area, but was unable to determine the heat flow because drill cuttings were not available. All four thermal gradients (Sass and others, 1971; Shearer, 1979) were measured in deep sediment- filled basins of the same depositional environments. Therefore, we used the thermal conductivities measured by Sass and others (1971) in the northern basin and the gradients measured by Shearer (1979) in the southern Fortuna and San Luis basins to estimate heat flows in the Shearer holes (Table 2.27).

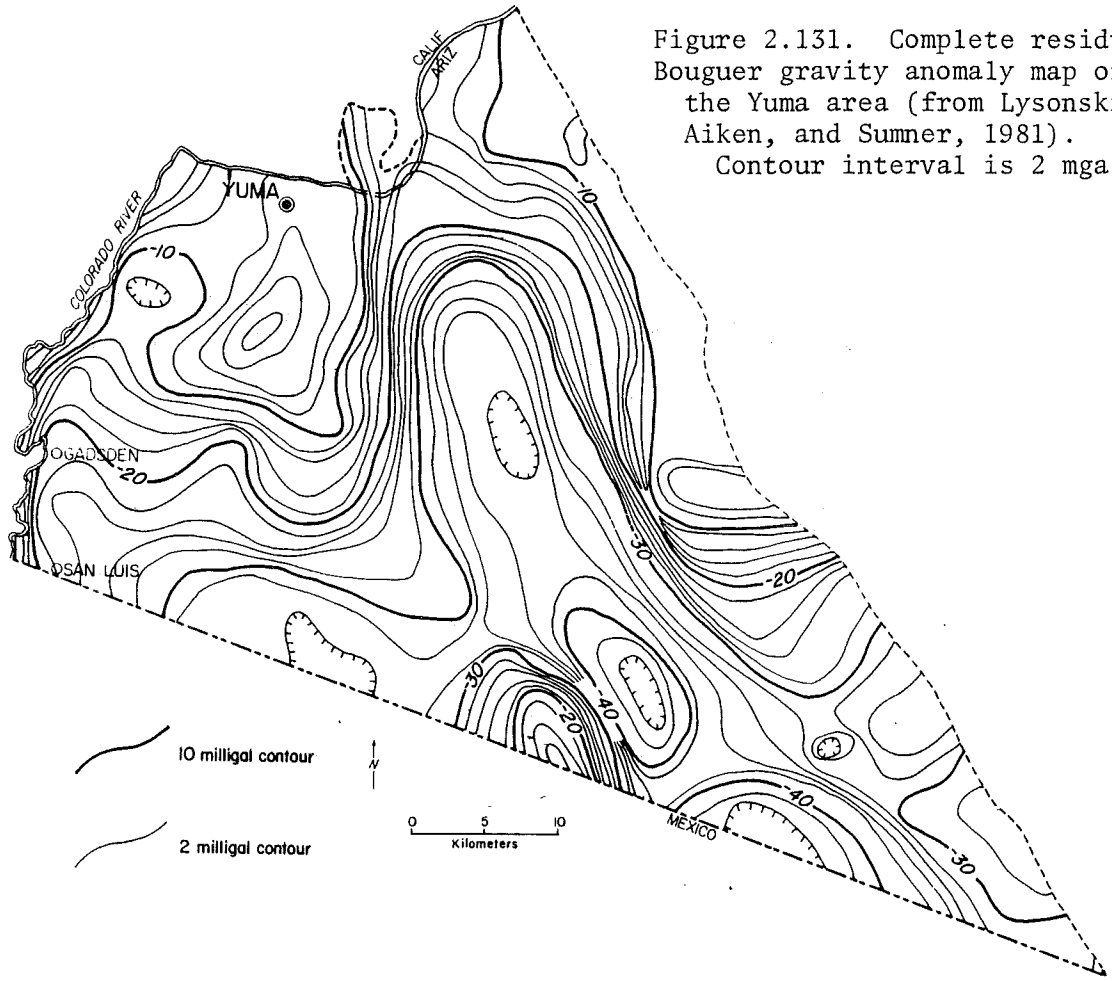

Figure 2.131. Complete residual Bouguer gravity anomaly map of the Yuma area (from Lysonski, Aiken, and Sumner, 1981). Contour interval is 2 mgal.

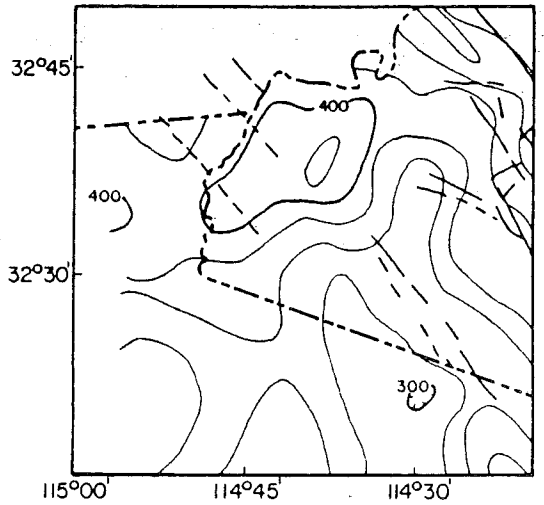

Figure 2.132. Upward-continued composite aeromagnetic map of the Yuma area (from Aiken and others, 1980). Contour interval is 25 gammas. Lineaments from Lepley, 1978.

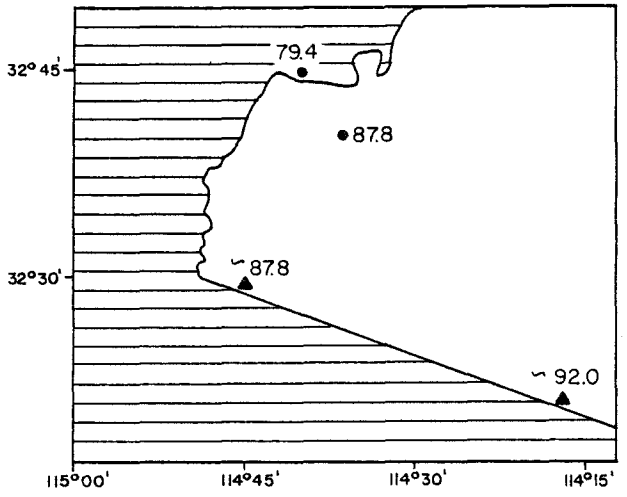

Figure 2.133. Heat flow (mWm^{-2}) in the Yuma area. Circles are measured heat flow (Sass and others, 1971; triangles are estimated heat flow (Stone, 1981).

TABLE 2.27. Heat flow estimates for southern Yuma area

Well Names and Location	Thermal Grad.[1] °C/km	Thermal Cond.[2] W/mk	Heat Flow Range mWm^{-2}
Exxon Federal #1 C-11-24-8ac	39.0	2.09 to 2.34	81.5 to 91.3
CH-28 YM C-13-20-12ab	41.0	2.09 to 2.34	85.7 to 95.9

[1] from Shearer (1979) [2] from Sass and others (1971)

The range of these estimated values compares favorably with the two heat flows published by Sass and others (1971). The data suggest that Yuma is an area of normal Basin and Range heat flow. However, since all of the measurements occur around the periphery of the area, the possibility of a geothermal anomaly occurring in the center is not necessarily precluded.

Olmsted and others (1973) measured water temperatures in the coarse-gravel zone and identified several anomalously warm areas (Fig. 2.134), one of which is in the area of the higher measured heat flow. They ascribed most of the warm anomalies to warm water rising along faults where the faults act as ground-water barriers, but several anomalies they attributed

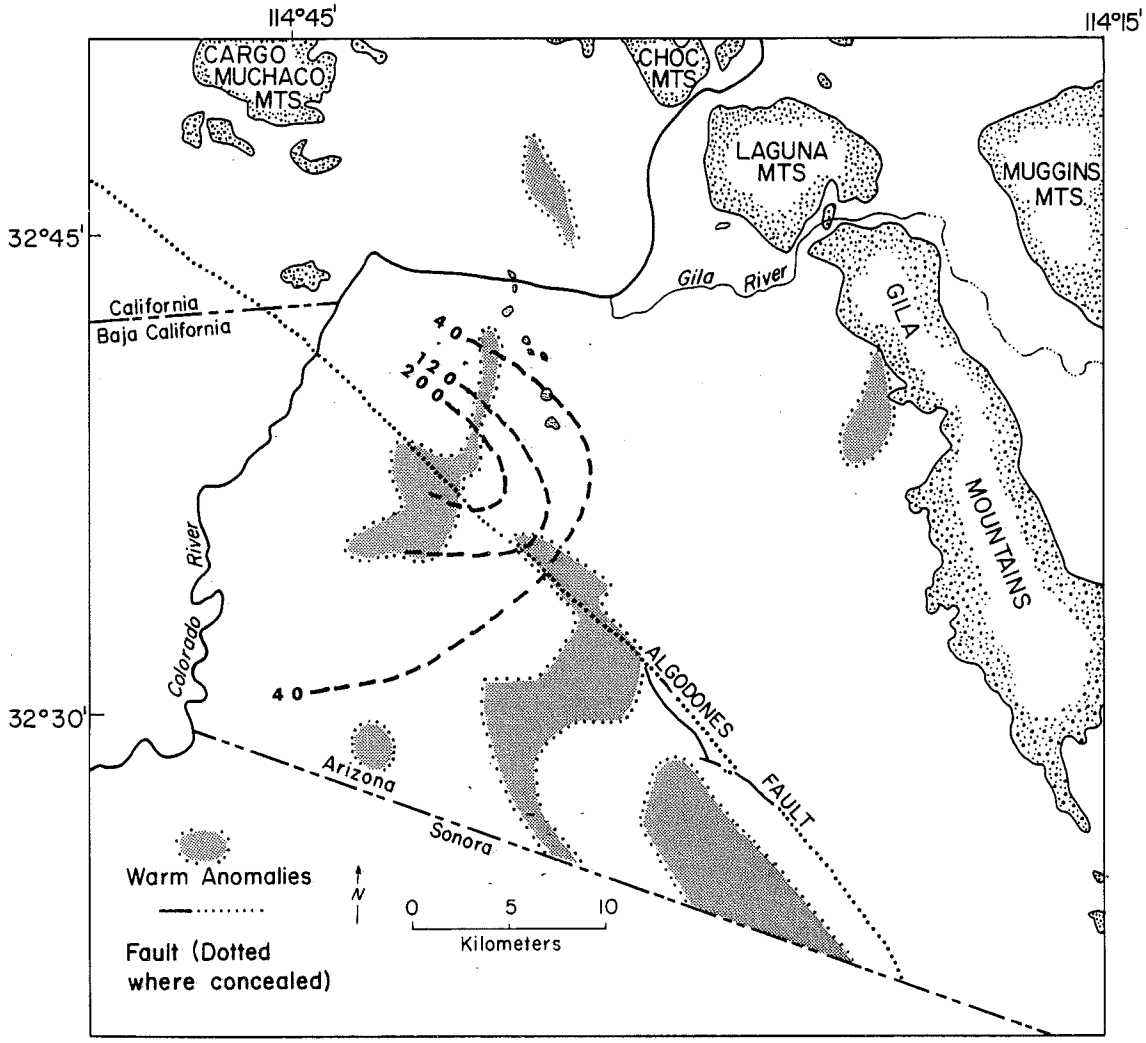

Figure 2.134. Map showing warm-water anomalies of Olmsted and others, 1973 (shaded areas) and geothermal gradient anomaly of Stone, 1981. Contour interval is 80°C/km.

to the effects of alluvium that is less transmissive than alluvium in surrounding areas. These investigators further suggested that some of the warm anomalies may reflect hot zones in pre-Tertiary crystalline rocks. Such areas are good geothermal exploration targets.

Stone (1981) identified a geothermal-gradient anomaly overlying the Mesa basement high (Fig. 2.134) by using linear segments of published

temperature-depth profiles. The gradient anomaly is in the area of a fault-controlled warm anomaly identified by Olmsted and others (1973).

GEOCHEMISTRY. Yuma is a long-standing agricultural community. Large volumes of surface (river) and ground water are applied annually to irrigate crops. Such irrigation has created an artificial ground-water mound that requires pumping from numerous drainage wells to reduce. Pumping has the desired effect of lowering the water table by causing downward leakage of water from the upper, fine-grained zone into the coarse-gravel zone.

One result of such large-scale pumping from wells and heavy applications of irrigation water has been to substantially alter the natural quality of ground water by mixing waters from different sources and of different chemical compositions. The mixing has created in historic times an artificial water chemistry that could effectively mask thermal water leaking from a deep geothermal reservoir. Additional processes that result from irrigation practices also change the chemical composition of ground water. These factors are: (1) concentration by evaporation and evapotranspiration; (2) softening by ion exchange; (3) sulfate reduction; (4) carbonate precipitation; (5) dissolution of salts; and (6) oxidation of dissolved organic substances. Thus the chemical geothermometers have not been useful in detecting thermal water in the Yuma area. This conclusion is exemplified by looking at concentrations of silica in ground water in this area. Silica contents of 153 random samples have a mean value of 27.9 mg/L, with a standard deviation of <u>only</u> ±0.59.

CONCLUSIONS. The Yuma area is a favorable target for geothermal exploration. The area is proximate to and probably actively involved in the Gulf of California-Salton Trough tectonic regime, which has numerous associated geothermal anomalies in neighboring California and Mexico.

It seems likely that as a result of the nearby, active rifting in the Salton-Trough-Gulf of California, the pre-Tertiary basement rocks in the Yuma area may have a high degree of fracture permeability, making them potential geothermal reservoirs.

Zones of anomalously warm water and a geothermal-gradient anomaly along northwest-trending faults suggest the occurrence of hydrothermal systems. Additional study is required in these zones to characterize heat contents and ultimate potential.

Measured and estimated heat flow around the periphery of the Yuma area are normal for the Basin and Range province. The area is large enough, however, that high heat-flow anomalies existing locally within the central region would not be detected by the few measurements that are available.

On the basis of cited evidence, we expect that potential geothermal resources in the Yuma area, when found, will be below the Bouse Formation or in basement rocks and that the fluids are likely to have high TDS.

YUMA REFERENCES

Aiken, C. L. V. Lysonski, J. C., Sumner, J. S., and Hahman, W. R., 1981, A series of 1:250,000 complete residual Bouguer gravity anomaly maps of Arizona: Arizona Geological Society Digest, v. 13, p. 31-37.

Aiken, C. L. V., Wettereuer, R. H., and de la Fuente, M. F., 1980, A merging of aeromagnetic data sets in southwest Arizona and northwest Mexico and analysis of results: Arizona Geological Society Digest, v. 12, p. 31-44.

Anderson, T. A., and Silver, L. T., 1979, The role of the Mojave-Sonora megashear in the tectonic evolution of northern Sonora: *in* Anderson, T. H., and Roldan-Quintana, J., eds., Geology of Northern Sonora, Geological Society of America Guidebook -- Field Trip No. 27, p. 59-68.

Eberly, L. D., and Stanley, T. B., Jr., 1978, Cenozoic stratigraphy and geologic history of southwestern Arizona: Geological Society of America Bulletin, v. 87, p. 921-940.

Lepley, L. K., 1978, Landsat lineament map of Arizona with emphasis on Quaternary fractures, *in* Low Temperature Geothermal Reservoir Site Evaluation in Arizona, Bureau of Geology and Mineral Technology, Tucson, Arizona, p. 63-91.

Lysonski, J. C., Aiken, C. L. V., and Sumner, J. S., 1981, The complete residual Bouguer gravity anomaly map (El Centro AMS sheet): Bureau of Geology and Mineral Technology, unpub. map series, 1:250,000 scale.

Mattick, R. E., Olmsted, F. H., Zohdy, A. A. R., 1973, Geophysical studies in the Yuma area, Arizona and California: U.S. Geological Survey Professional Paper 486-D, 36 p.

Olmsted, F. H., Loeltz, O. J. and Irelan, B., 1973, Geohydrology of the Yuma area, Arizona and California: U.S. Geological Survey Professional Paper 486-H, 227 p.

Sass, J. H., Lachenbruch, A. H., Munroe, R. J., Greene, G. W., and Moses, T. H., Jr., 1971, Heat flow in the Western United States, Journal of Geophysical Research, v. 76, p. 6376-6413.

Shearer, C. R., 1979, A regional terrestrial heat-flow study in Arizona: Ph. D. dissertation, Socorro, New Mexico Institute of Mining and Technology, 184 p.

Stone, C., 1981, A preliminary assessment of the geothermal resource potential of the Yuma area, Arizona: Bureau of Geology and Mineral Technology Open-File Report 81-6, 26 p.

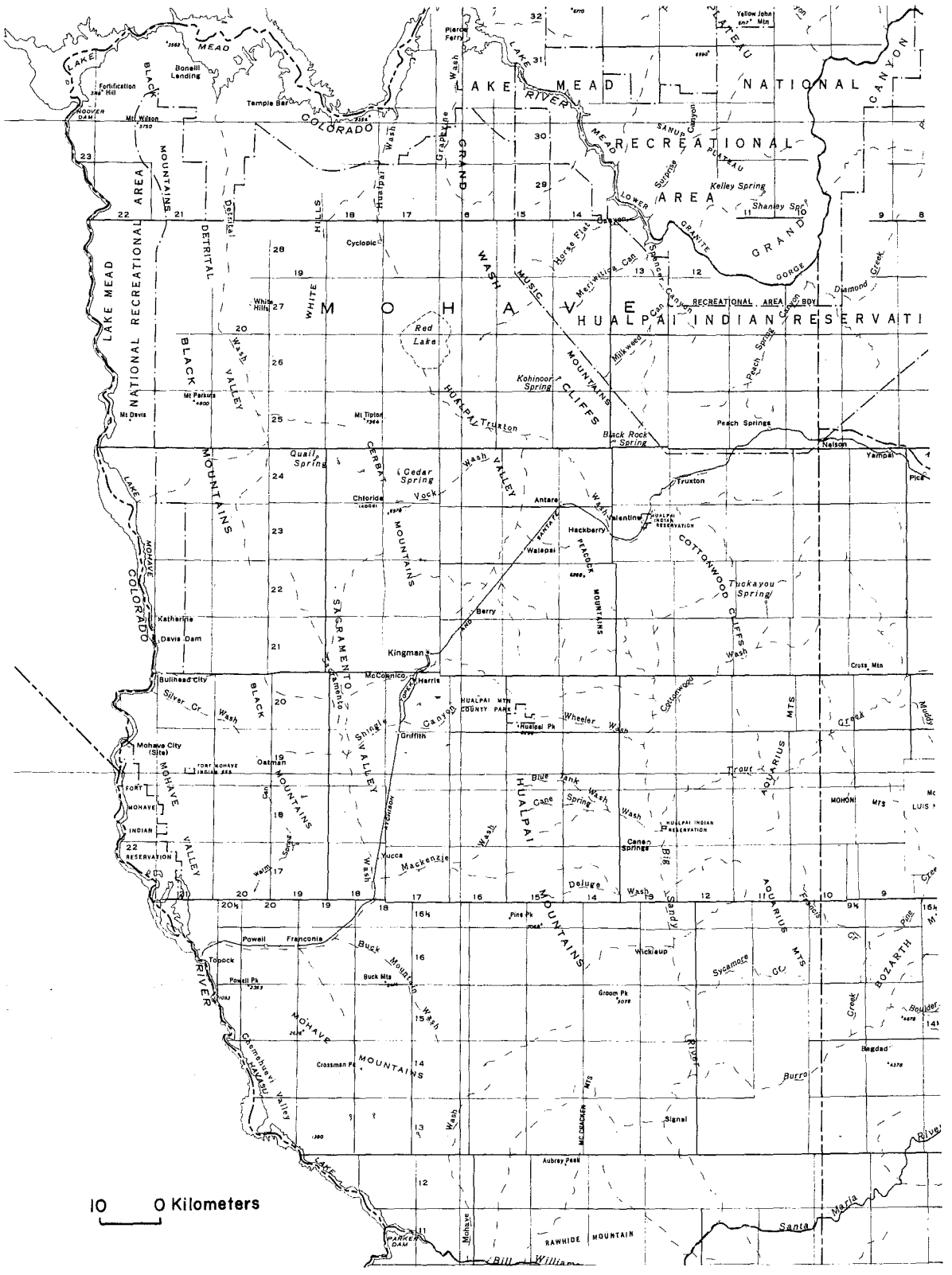

Figure 2.135. Map of Mohave section, Basin and Range province, northwest corner of Arizona

MOHAVE SECTION - BASIN AND RANGE PROVINCE

PHYSIOGRAPHY. The Mohave section (Hayes, 1969) of the Basin and Range province includes that part of Arizona that is north of the Bill Williams and Santa Maria Rivers and west of the Colorado Plateau (Fig. 2.135). The boundary between the Mohave section and the Colorado Plateau is somewhat arbitrary within a transition zone that has characteristics of both areas. Most of this transition zone has a greater affinity to the Basin and Range province than it does to the Plateau because it has incurred Late Cretaceous to early Tertiary and mid-Tertiary volcanism and igneous intrusion as did the Basin and Range province. Near the Colorado River, the Grand Wash Cliffs and Music Mountains separate the Plateau and the Mohave section, while south of Interstate 40, the boundary is traced southeastward around the Aquarius Mountains toward Prescott and the Chino Valley.

In a general, the Mohave section resembles the Mexican Highland section and the Great Basin because their basin-to-range ratios and relief are similar. In fact, Fenneman (1931) placed northwest Arizona in the Great Basin. However, major stratigraphic and tectonic differences exist between the Mohave section and the Great Basin and the Mexican Highland section.

Mountain ranges such as the Cerbat, Hualapai and Black Mountains are between 32 and 112 km long and 8 to 24 km wide; they range mostly between 1,219 and 2,134 m in elevation and have 305 to 1,372 m of relief. Intervening basins such as the Hualapai Valley, Big Sandy Valley, Detrital

Valley, and the Sacramento Valley are between 16 and 24 km wide. Both external and internal drainage is observed in these valleys. Elevations of valley floors range between 610 and 1,219 m, except in western valleys where the through-flowing Colorado River has eroded the surface down to 457 m elevation or less.

GEOLOGY. Prior to mid-Tertiary volcanism and plutonism, the Mohave section was structurally high. It incurred deep erosion, which removed the entire Paleozoic and Mesozoic stratigraphic sequence, except in areas north of the Colorado River. Precambrian basement consists of predominantly Precambrian granitic to granodioritic gneiss, which intrudes high grade metavolcanic rocks (Fig. 2.136). These gneisses, approximately 1,800 m.y. old (Kessler, 1976), comprise the bulk of the Cerbat and Hualapai Mountains and they underlie Tertiary volcanic flows in the Black Mountains and Aquarius Mountains. A few widely scattered granite stocks and batholiths, such as the Lawler Peak Granite at Bagdad and the Hualapai Granite south of Kingman, intrude the gneisses. These granites have large orthoclase phenocrysts and they belong to the 1,400 m.y. Oracle and Ruin Granite suite of southern Arizona. Simple pegmatite dikes and diabase dikes intrude the granite, gneiss, and older metamorphic rocks.

Precambrian rocks in the central Cerbat Mountains (near Chloride) were intruded by Laramide age plutons that are associated with copper mineralization. No Laramide (Late Cretaceous to early Tertiary) volcanic flows are definitely known in this region. The oldest reliably dated volcanic rocks are less than 25 m.y. old and rest nonconformably upon Precambrian basement, Laramide intrusive rocks, or on thin, older Tertiary arkosic sediments.

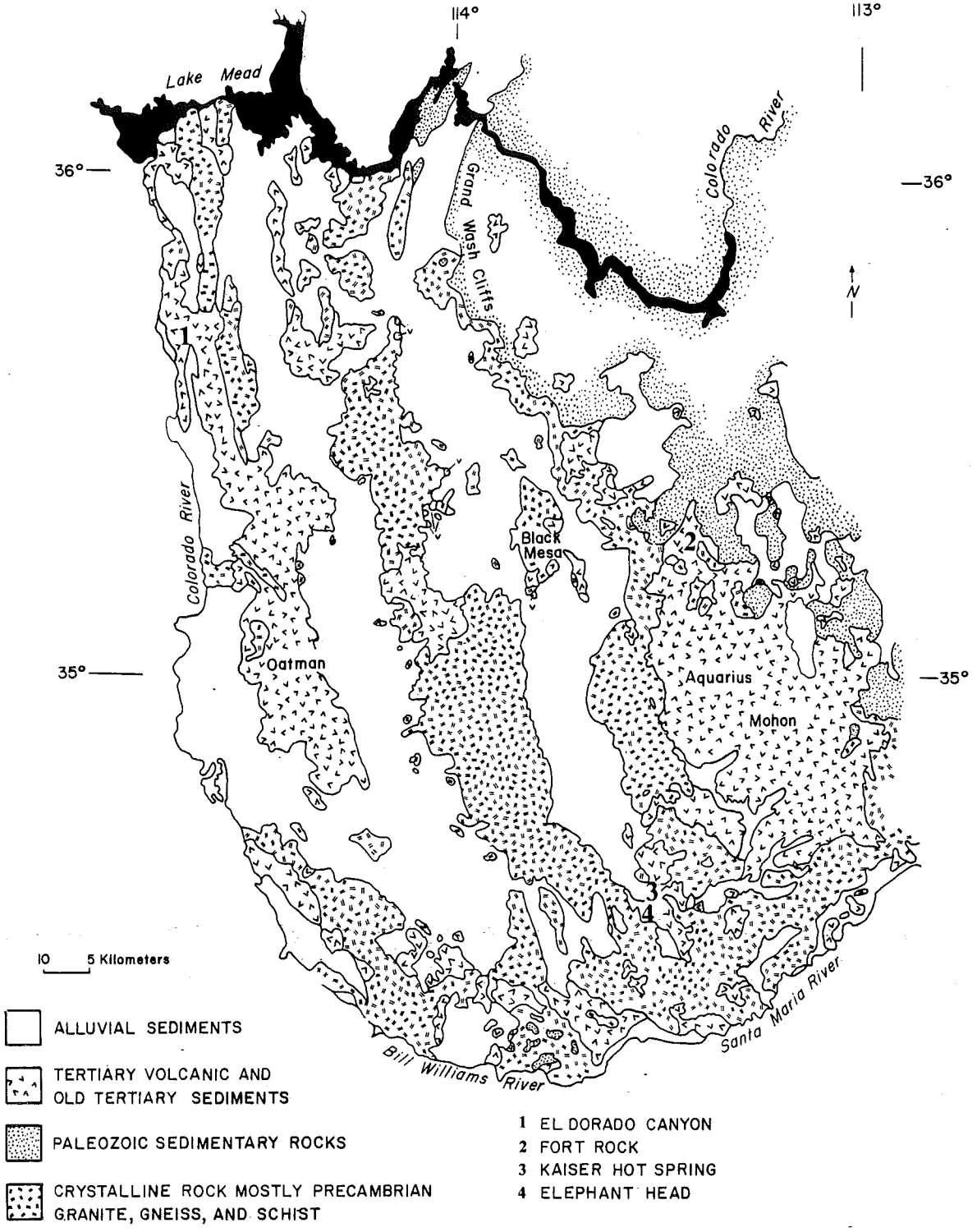

Figure 2.136. Generalized geology of the Mohave section of the Basin and Range province, northwestern Arizona

Even though many ranges expose predominantly Precambrian rocks, mid-to late-Tertiary volcanic rocks probably covered most of the Mohave section prior to Basin and Range faulting. However, intervening basins probably preserve the volcanic rocks beneath basin-filling sediments.

Several distinct eruptive centers were active at various times during the mid to late-Tertiary. They are delineated on the basis of composition and style of eruption, location, and age (Fig. 2.136). The Eldorado (Anderson and others, 1971) and the Oatman (Thorson, 1971) centers are found in the Colorado River-Lake Mead area; the Fort Rock, Black Mesa, Aquarius Mountains, and Mohon Mountains centers (Goff and others, 1979) are found on the eastern margin of the Mohave section. An additional eruptive center, the Kaiser Spring-Elephant Mountain volcanic field occurs south of the Big Sandy Valley (Moyer, 1982).

The Eldorado (19 to 14 m.y.) and the Oatman (>23 to <10 m.y.) volcanic centers are characterized by thick piles (>3 km) of intermediate and silicic rocks, which are intruded by coeval epizonal plutons (Anderson and others, 1971; Thorson, 1971). Volcano-tectonic subsidence and resurgence is indicated by these igneous rocks and interbedded clastic sediments. Older volcanic rocks, intruded by a 22.6 m.y. old stock at Oatman, record the formation of a resurgent cauldron (Thorson, 1971). A distinctive and regionally widespread stratigraphic marker horizon, the Peach Springs Tuff (17 m.y.) may have erupted from another as yet unidentified cauldron in the Eldorado volcanic complex (Young and Brennan, 1974). These thick volcanic piles adjacent to the Colorado River were disrupted and rotated by widespread listric normal faults. Rotated and faulted mid to late-Tertiary volcanic rocks (>14.4 m.y.) are angularly unconformably capped

by scattered untilted basaltic flows (<14.6 m.y.) (Anderson and others, 1971.)

Predominantly basaltic rocks overlie Precambrian rocks on thin arkosic sediments in the transitional zone between the Mohave section and the Colorado Plateau. Until recently, it was not recognized that basaltic volcanism had been accompanied by eruptions of silicic to intermediate rocks.

The Fort Rock volcanic field (24 to 17 m.y.) consists of alkali basalt, latite, and rhyolite, which are overlain by the Peach Springs Tuff (Goff and others, 1979). The Aquarius Mountains volcanic center (18.2 to 17 m.y.) consists of rhyolitic air fall tuff, non-welded ash flows, and rhyolite flows (Goff and others, 1979). The rhyolitic lava flows are confined to the vent area. Black Mesa volcanics, andesite and dacite flows, overlie the Peach Springs Tuff. One of the andesite flows is 13.2 m.y. old (Goff and others, 1979). The Mohon Mountain basalts may be as young as 7 to 8 m.y. (Goff and others, 1979). In the Kaiser Spring-Elephant Mountain area, about 15 km south of the Mohon Mountains area, Shafiqullah and others (1980) reported 8 m.y. ages for basalts in Burro Creek. The Kaiser Spring-Elephant Mountain field has numerous silicic domes, which are partially submerged in a flood of basalt flows (Moyer, 1982). These volcanic rocks mostly overlie Precambrian basement.

Volcanism has continued almost into Quaternary. In the Lake Mead area, the Fortification Basalt (4 to 6 m.y.) is intercalated in the Muddy Creek Formation, a Basin and Range valley-fill sequence.

High angle normal faulting (Basin and Range tectonism) created the present-day first order structure and physiography. Graben structures,

inferred to underlie the valleys are filled with sand and gravel, which were deposited by alluvial fans and with mudstone, gypsum, and halite which were deposited in playa and lacustrine environments. These sediments angularly unconformably overlie either Tertiary volcanic rocks or older alluvial and lacustrine deposits. They sometimes nonconformably rest upon Precambrian rocks. In the Big Sandy Valley, the basin filling Big Sandy Formation, which consists predominantly of lacustrine green and brown mudstone interbedded with zeolitic tuffs, has these relationships with pre-Basin and Range rocks (Sheppard and Gude, 1972; Worley, 1979).

THERMAL REGIME. Seventeen widely scattered heat flow measurements are reported in the Mohave section (Shearer and Reiter, 1981; Sass, personal commun., 1981). With the exception of two measurements on the west side of the Big Sandy Valley and a single value east of Detrital Valley, these heat flow measurements have values typical of the southern Basin and Range province; they vary between 65 and 95 mWm^{-2}. High heat flow values on the west side of the Big Sandy Valley are due to shallow convective systems (Shearer and Reiter, 1981.)

West and Laughlin (1979) used a compilation of regional geophysical data to identify an area that apparently has above-normal crustal temperatures. This area, centered approximately beneath the Aquarius and Mohon Mountains, has no reported heat flow measurements; but it is characterized by an intriguing combination on geophysical anomalies, which suggest high temperatures. A regional residual gravity low, interpreted by Aiken (1976) as either the result of a pluton or elevated crustal temperatures, coincides with a zone of teleseismic P-wave attenuation (Jordan and others, 1965) and a relatively shallow depth (<10km) to the Curie point (about

500°C) (Byerly and Stolt, 1977). Aiken and Ander (1980) reported that magnetotelluric (MT) data indicate a shallow electrically conductive zone beneath the Aquarius Mountains region, which they interpreted as caused by high temperatures at relatively shallow depths in the crust. These geophysical data may indicate a geothermal gradient exceeding 45°C/km in granite.

GEOHYDROLOGY. In general, ground-water flow in this region mimics the topography. Ground water in the Hualapai Valley is 275 m deep near its south end and it is about 80 m deep over the main portion of the valley (Gillespie and Bentley, 1971). Ground-water flow in the Hualapai Valley is northward toward Lake Mead. In the Sacramento Valley, ground-water flow is toward the basin discharge outlet south of Yucca between the Black and Mohave Mountains. The Sacramento Valley water table is less than 90 m deep south of Yucca but it is over 300 m deep at the north end of the valley (Gillespie and Bentley, 1971). Along the south-flowing Big Sandy River in the Big Sandy Valley, ground water is less than 1 m deep, while away from the river at the north end of the valley the water table is 230 m below the surface (Davidson, 1973).

THERMAL WATER. Kaiser Hot Spring, Cofer Hot Spring, and Tom Brown Canyon Warm Spring discharge thermal water in the Big Sandy River drainage area (Fig. 2.137). Kaiser Hot Spring, 37°C, discharges from a 25-m-wide breccia zone striking N. 45° W. The breccia zone is in Precambrian granitic rocks underlying the silicic flows and flow breccias of the Kaiser Spring-Elephant Head volcanic field (Goff, 1979; Moyer, 1982). Kaiser Hot Spring is a sodium bicarbonate water (Fig. 2.137) with high fluoride (7.0 mg/L) and relatively low TDS (Less than 1,000 mg/L) (Goff, 1979).

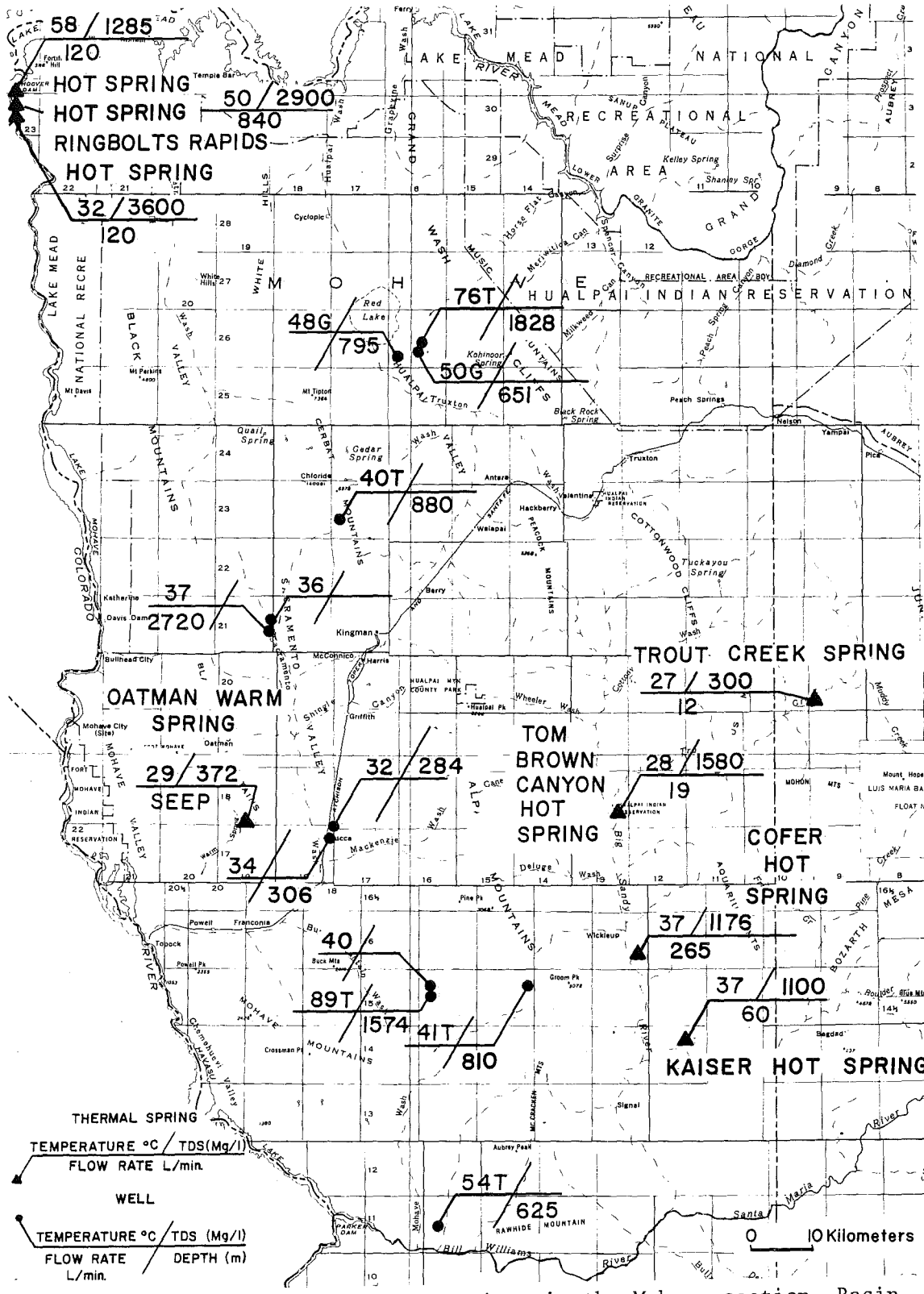

Figure 2.137. Thermal wells and springs in the Mohave section, Basin and Range province, northwestern Arizona

The magnesium-corrected Na-K-Ca geothermometer is 121°C for Kaiser Hot Spring, while the quartz geothermometer is 100°C.

Cofer Hot Springs, 32 to 36°C, discharges from clastic sediments in the Big Sandy Valley southeast of Wikieup. Cofer Hot Spring is a sodium chloride-sulfate water whose TDS is less than 1,200 mg/L (Swanberg and others, 1977; Davidson, 1973). The quartz geothermometer is 110°C for Cofer Hot Spring, while the magnesium-corrected Na-K-Ca geothermometer is 38°C (Swanberg and others, 1977; Goff, 1979).

Tom Brown Canyon Warm Spring (28°C) discharges from clastic sediments on the east side of the Big Sandy Valley. This spring is a sodium chloride water with a TDS of 1,580 mg/L (Swanberg and others, 1977). Both the quartz and magnesium-corrected Na-K-Ca geothermometers predict an 80°C reservoir temperature for the Tom Brown Canyon system (Goff, 1979; Swanberg and others, 1977).

Several thermal wells are reported in the Sacramento Valley. Near Yucca, well B-17-18-12bca discharges 34°C water from a depth of 306 m. Swanberg and others (1977) reported an additional thermal well in T. 17 N., R. 18 W., section 1, which had a temperature of 32°C and a TDS of 284 mg/L. West of Yucca in the Black Mountains, the Oatman Warm Springs seep 29°C water with a TDS of 372 mg/L. South of Yucca on Dutch Flat at the Anderson Ranch, a hot well 395 m deep discharges sodium chloride, 44.5°C, water from basin-filling sediments (Goff, 1979). The quartz and Na-K-Ca geothermometers for this well are 85 and 83°C, respectively.

Duval Corporation has drilled at least five deep wells, greater than 400 m total depth, to supply water for copper mining operations in the Cerbat Mountains (Goff, 1979). Two of these wells in the northern

Sacramento Valley penetrate basin-filling clastic sediments and discharge 36 to 37°C calcium-magnesium bicarbonate water (Goff, 1979).

Bottom hole temperatures of deep test wells in the northern Hualapai Valley north of Kingman have temperatures exceeding 45°C. Well B-26-16-22c, drilled to 1,828 m in the Red Lake salt deposit, has a bottom hole temperature of 76°C (Giardina and Conley, 1978).

McKay (1981) discussed thermal springs, which occur on both sides of the Colorado River in the Black Canyon below Hoover Dam. Most of these springs occur on the west side of the canyon in Nevada; however, three springs were studied on the Arizona side of the canyon. These springs have an estimated composite flow rate of 70 L/sec with individual spring discharges ranging from 2 to 14 L/sec. Temperatures of the springs that are in Arizona range from 32 to 58°C. They have TDS between 1,285 and 3,600 mg/L. Individual springs discharge sodium chloride water from faults and fractures in mid-Tertiary volcanic rocks, which comprise the Black Canyon. Wide variations in chemistry among these springs indicate that mixing of waters from different source areas occurs (McKay, 1981).

CONCLUSIONS. Interpretation of several sets of diverse geophysical data suggests a positive thermal anomaly in the crust in the Aquarius and Mohon Mountains area. While no Quaternary volcanic rocks are known in this area, which might indicate high temperatures or magma at shallow depth in the crust, the Los Alamos National Laboratory has been evaluating the area as a potential hot dry rock (HDR) geothermal site based upon the geophysical inference of high crustal heat. To date, studies by Los Alamos scientists indicate that no high temperature convection systems exist in the Mohave region; rather, several widely scattered low to intermediate

temperature systems (<120°C) occur. These systems are probably the result of forced convective flows of meteoric water to sufficient depth to be heated by the regional geothermal gradient. The chemical quality of these thermal waters is good, making them suitable for direct-heat applications.

Temperature gradients exceeding 37°C/km are possible in the Aquarius-Mohon Mountains region (Goff and others, 1979). Thus, this area may have deep (>4 km) hot dry rock geothermal potential.

Thermal waters in the Black Canyon below Hoover Dam are probably not suitable for development due to the rugged topography and isolation from potential users.

MOHAVE SECTION REFERENCES

Aiken, C. L. V., 1976, Analysis of the gravity anomalies of Arizona: Unpub. Ph.D. thesis, University of Arizona, 147 p.

Aiken, C. L. V. and Ander, M. E., 1980, A regional strategy for geothermal exploration with emphasis on gravity and magnetotellurics: Journal of Volcanology and Geothermal Research, vol. 9., p. 1-27.

Anderson, R. E., Longwell, C. R., Armstrong, R. L., and Marvin, R. F., 1972, Significance of K-Ar ages of Tertiary rocks from the Lake Mead region, Nevada-Arizona: Geological Society of America Bulletin, vol. 83, p. 273-288.

Byerly, P. E. and Stolt, R. H., 1977, An attempt to define the Curie Point isotherm in northern and central Arizona: Geophysics, vol. 42, p. 1394-1400.

Cooley, M. E., 1967, Arizona Highway Geologic Map: Arizona Geological Society, 1:1,000,000 scale.

Davidson, E. S., 1973, Water-resources appraisal of the Big Sandy area, Mohave County, Arizona: Arizona Water Commission Bulletin 6, 40 p.

Fenneman, N. M., 1931, Physiography of Western United States: McGraw-Hill, New York, 534 p.

Giardina, S. Jr., and Conley, J. N., 1978, Thermal gradient anomalies in southern Arizona: Arizona Oil and Gas Conservation Commission Report of Investigation 6, 52 p.

Gillespie, J. B. and Bentley, C. B., 1971, Geohydrology of Hualapai and Sacramento Valleys, Mohave County, Arizona: U. S. Geological Survey Water-Supply Paper 1899-H, 37 p.

Goff, F. E., 1979, "Wet" geothermal potential of the Kingman-Williams region, Arizona: Los Alamos Scientific Laboratory Informal Report LA-7757-MS, 25 p.

Goff, F. E., Arney, B. H., Aiken, C. L. V., West, F. G. and Eddy, A. C., 1979, Preliminary evaluation of the Aquarius Mountains Hot Dry Rock geothermal prospect, Arizona: Geothermal Resources Council Transactions, vol. 3, p. 257-260.

Hayes, P. T., 1969, Geology and topography: *in* Mineral and Water Resources of Arizona, Arizona Bureau of Mines Bulletin 180, p. 35-58.

Jordan, J., Black, R., and Bates, C. C., 1965, Patterns of maximum amplitudes of Pn and P waves over regional and continental areas: Bulletin of Seismological Society of America, vol. 55, p. 693-720.

Kessler, E. J., 1976, Rubidium-Strontium geochronology and trace element geochemistry of Precambrian rocks in the northern Hualapai Mountains, Mohave County, Arizona: Unpub. M. S. thesis, University of Arizona, 73 p.

McKay, W. A., 1981, Hydrogeochemical inventory and analysis of thermal springs in the Black Canyon-Hoover Dam area, Nevada and Arizona: Geothermal Resources Council, Transactions, vol. 5, p. 185-187.

Moyer, T. C., 1982, The volcanic geology of the Kaiser Spring area, S. E. Mohave County, Arizona: Unpub. M. S. thesis, Arizona State University, 220 p.

Shafiqullah, M., Damon, P. E., Lynch, D. J., Reynolds, S. J., Rehrig, W. A., Raymond, R. H., 1980, K-Ar geochronology and geologic history of southwestern Arizona and adjacent areas: *in* Jenney, J. P. and Stone, C., eds., Studies in Western Arizona, Arizona Geological Society Digest 12, p. 201-260.

Shearer, C., and Reiter, M., 1981, Terrestrial heat flow in Arizona: Journal of Geophysical Research, vol. 86, no. B7, p. 6249-6260.

Sheppard, R. A. and Gude, A. J., 1972, Big Sandy Formation near Wikieup, Mohave County, Arizona: U. S. Geological Survey Bulletin 1354-C, 90 p.

Swanberg, C. A., Morgan, P., Stoyer, C. H. and Witcher, J. C., 1977, An appraisal study of the geothermal resources of Arizona and adjacent areas in New Mexico and Utah and their value for desalination and other uses: New Mexico State University, New Mexico Energy Institute Report 6, 76 p.

Thorson, J. P., 1971, Igneous petrology of the Oatman District, Mohave County, Arizona: Unpub. Ph.D. thesis, University of California, Santa Barbara, 189 p.

West, F. G., and Laughlin, A. W., 1979, Aquarius Mountain area, Arizona: a possible HDR prospect: Los Alamos Scientific Laboratory Informal Report LA-7804-MS, 16 p.

Witcher, J. C., Stone, C. and Hahman, W. R. Sr., 1982, Geothermal Resources of Arizona (map): National Geophysical and Solar-Terrestrial Data Center, National Oceanic and Atmospheric Administration, in cooperation with the U. S. Department of Energy and the Arizona Bureau of Geology and Mineral Technology, University of Arizona, scale 1:500,000.

Worley, P. L. H., 1979, Sedimentology and stratigraphy of the Tule Wash area, Mohave County, Arizona: Unpub. M. S. thesis, Arizona State University, 99 p.

Young, R. A., and Brennan, W. J., 1974, Peach Springs Tuff: its bearing on structural evolution of the Colorado Plateau and development of Cenozoic drainage in Mohave County, Arizona: Geological Society of America Bulletin, vol. 85, p. 83-90.

CHAPTER 3

RESIDUAL TEMPERATURE MAP

The Geothermal Group measured temperatures in more than 100 drill holes in Arizona over a four-year period. Most measurements were made in existing water wells and mineral tests, using a thermistor probe with an accuracy of ± 0.001°C. Thirteen holes were drilled solely for the purpose of obtaining gradient or heat flow information. Figure 3.1 shows all the areas where groups of wells were measured. Table 3.1 lists by area all well locations, well names, and the abbreviated well designations, which are used on the temperature-depth profiles. Data tables and profiles for individual areas and wells can be found in Goldstone and Stone (1982).

The idea of making a temperature gradient map of the State of Arizona was rejected because of the obvious errors inherent in comparing gradients over a region as hydrologically and geologically varied as Arizona. Well depths vary from a few tens to several hundred meters. Some thermal gradients are profoundly affected by hydrologic processes, both natural and human induced. Even within a relatively small area having the same conductive heat flow, thermal conductivities may vary laterally to such an extent that gradients can differ by a factor of two or more. Thus, gradient comparisons over a large area are of questionable value. Instead, we constructed a "Residual Temperature Map" (Fig. 3.2) using our temperature measurements and other published and unpublished data (Roy and others, 1968a, 1968b; Sass and others, 1971; Sass, 1979, personal commun.; Shearer, 1979, unpub. Ph.D. disser.).

Figure 3.1. Areas for which measured temperature logs are available

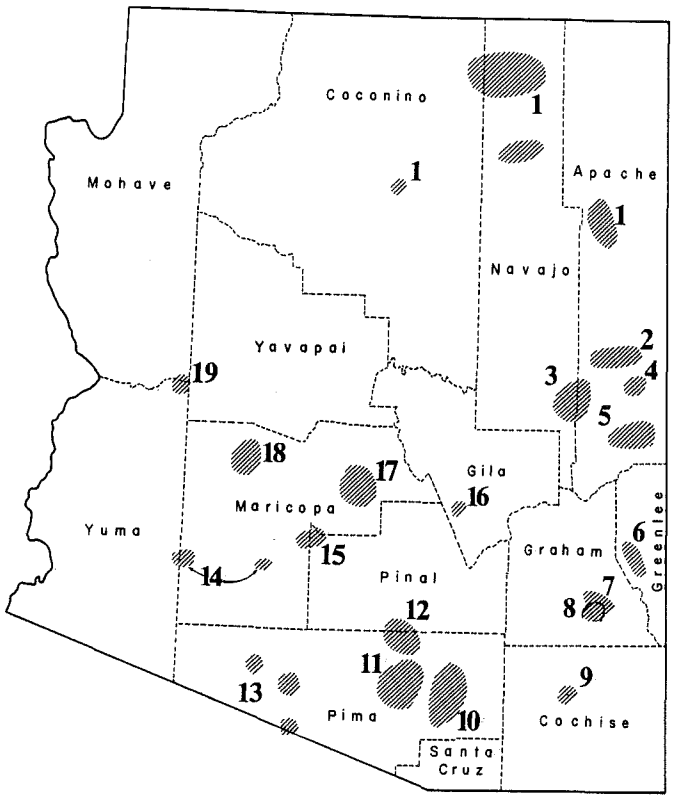

TABLE 3.1. Names of areas shown in Figure 3.1 for which measured temperature logs are available

Area No.	Area Name	Area No.	Area Name
1	Colorado Plateau	11	Avra Valley
2	Concho-St. Johns	12	Silver Bell
3	McNary-Pinetop	13	Papago Indian Reservation
4	Springerville-St. Johns	14	Gila Bend-Hyder
5	Alpine-Springerville	15	Montezuma Castle
6	Clifton	16	Globe-Miami
7 & 8	Safford	17	Scottsdale
9	Willcox	18	Hassayampa
10	Tucson	19	Date Creek

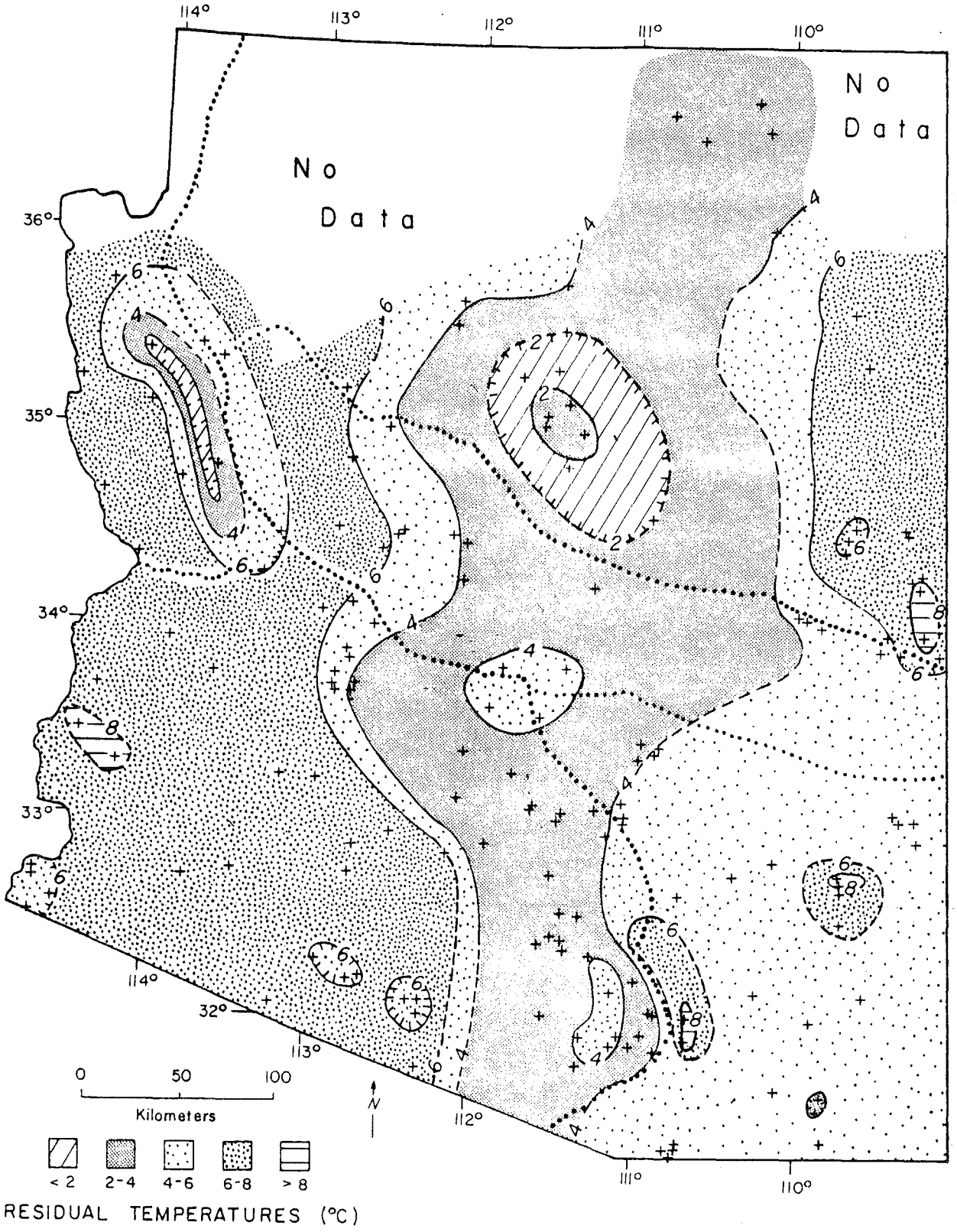

Figure 3.2. Residual temperature map of Arizona. Crosses represent data points.

Figure 3.3. Temperature-depth profile showing excessive ground-water disturbance

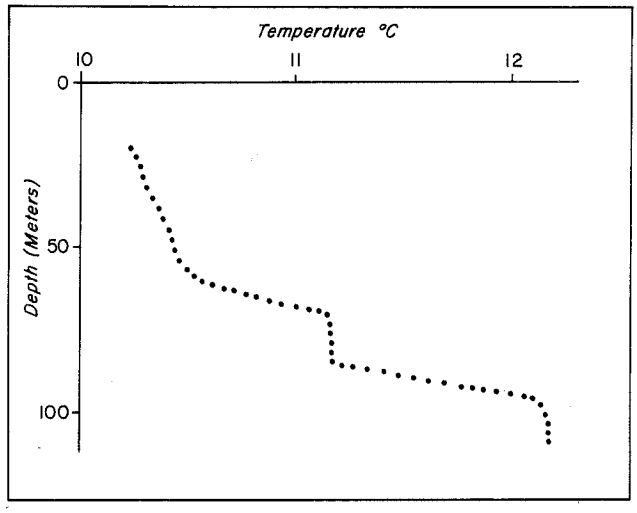

Figure 3.4. Temperature-depth profile showing slight hydrologic disturbance due to ground water moving up the borehole. The temperature predicted by the straight line is 0.3°C less than the measured temperature at 100 m.

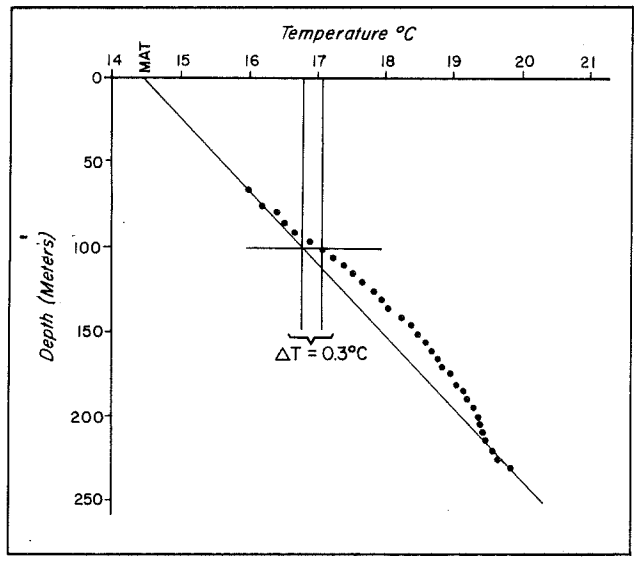

Figure 3.5. Temperature-depth profile showing slight hydrologic disturbance due to ground water moving down the borehole. The temperature predicted by the straight line is 2.2°C greater than the measured temperature at 100 m.

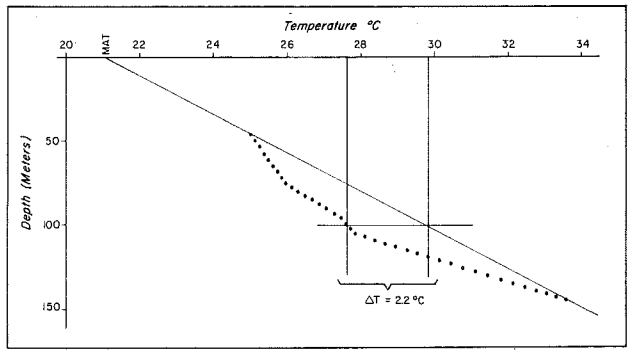

In constructing the Residual Temperature Map, we applied certain interpretive procedures to the data set to help eliminate some of the problems associated with thermal gradients. These procedures are discussed below. While our method was not rigorous, the corrections and adjustments were consistently and carefully applied. In some areas final interpretation was guided by knowledge of local geologic or hydrologic conditions.

The first interpretive procedure was to eliminate all wells that showed excessive ground-water disturbance (Fig. 3.3). An accurate formation temperature at any depth is nearly impossible to ascertain under such highly disturbed conditions. Temperature-depth profiles that showed only slight hydrologic disturbance were fitted by a straight line. If extrapolation of the gradient to the surface approximated the local MAT, the temperature predicted by the straight line rather than the measured temperature at 100 m was used. This procedure increased the temperature for some wells and decreased it for others, depending on whether water was moving down or up the borehole (Figs. 3.4 and 3.5). Temperature corrections made in this way varied between about ±0.5 and 2.0^{o}C.

The second procedure was to select temperatures measured at 100-m depth. Use of this depth avoids seasonal temperature variations that may occur at shallower depths. In addition selection of this depth maximized the number of wells that could be included in the data set because proportionately fewer wells are available with increasingly greater depths. The major drawback of this procedure involves loss of

valuable information from deeper than 100 m. The trade off here is between presenting a standardized map based on a large number of sites and making a possibly invalid comparison between shallow and deep wells.

Third, the local MAT was subtracted from the 100-m temperatures in order to correct somewhat for hole elevation and latitude. Latitude within the state changes by 6 degrees; elevation changes by 2,000 m or more. Except in areas where near-surface heat transfer characteristics (e.g. albedo, thermal inertia) are anomalous, the MAT generally is two or three degrees lower than the less-well-known mean ground surface temperature, which also decreases with increasing elevation and increasing latitude. This correction produced a "number" that could be interpreted as a thermal gradient, but we prefer to avoid that term.

Finally, since rock thermal conductivity, which depends chiefly on mineral content and porosity, has a major effect upon thermal gradient and heat flow, the number thus far derived from temperature measurements in unconsolidated sedimentary rocks could not validly be compared with those derived from temperature measurements in crystalline rocks. A final correction was made to the numbers from sedimentary rocks (Ns) in order to normalize them to those from crystalline rocks (Nc). The correction was $Nc = Ns \times Ks/Kc$, where Ks and Kc are average thermal conductivities for sedimentary and crystalline rocks, respectively. In Arizona, basin-fill sediments have an average conductivity about one half that of crystalline rocks (Sass, 1982, personal commun.), so that our value for Ks/Kc was 0.5. No distinction was made between consolidated and unconsolidated sedimentary rocks as the latter are usually

quite porous in the upper 100 m. The few measurements made in volcanic rocks were corrected in the same manner as the sedimentary numbers. No correction was applied to Colorado Plateau measurements because average measured conductivities for these near-surface sedimentary formations are roughly equivalent to those of crystalline rocks (Bodell and Chapman, 1982; Sass and others, 1982, in prep.).

The resulting map depicts residual temperatures across most of the State of Arizona. Obvious gaps in the data set occur in northwestern Arizona and parts of east-central and northeastern Arizona. In other areas coverage varies from sparse to excellent.

Incorporating the procedures oulined above, our map provides a rough picture of the shallow (≈100 m) conductive thermal regime of Arizona, modified to varying degrees at different locations by both regional and local hydrologic processes. Several prominent features on the map are worth mentioning.

(1) Three residual-temperature zones exhibiting a pronounced north-south trend cut across the major geologic and physiographic province boundaries. The coolest zone is down the center of the state. Western Arizona is warmer than southeastern Arizona.

(2) The thermal transition from cooler to warmer residual temperatures in southeastern Arizona approximates the boundary between the Mexican Highland and the Sonoran Desert subprovinces of the Basin and Range province.

(3) Strong deflections to the southeast occur where the residual-temperature zones cross the Transition Zone.

Other distinctive features include the large, anomalously low "donut" slightly southeast of the San Francisco volcanic field, and the elongate negative anomaly farther west, along the Cerbat and Hualapai Mountains. These areas probably represent zones of high permeability and recharge. The smaller anomalies chiefly in the southern part of the state, are most likely a result of ground-water convection. Numerous other such anomalies must exist in Arizona, but sparse data in many areas preclude their detection at this time.

Superimposing major lineaments and discontinuities on the Residual Temperature Map (Fig. 3.6) allows us to make additional observations. Three small positive anomalies in southeastern Arizona fall along the Morenci lineament. High heat flow and open vertical fracture permeability along this structure could have enabled local hydrothermal convection systems to become established in these areas. A southwestward extension of the Morenci lineament would pass through Papago Farms where a convective geothermal anomaly has been identified by Stone (1980; this volume). The Papago Farms anomaly is not shown on the Residual Temperature Map because wells measured there are too disturbed by ground water to be included. The positive anomaly in east-central Arizona falls along the Jemez lineament.

Two major deflections in the generally north-south residual-temperature zones parallel segments of the northeast-trending Jemez lineament and an extension of the northwest-trending Silverbell-Bisbee discontinuity. The parallelism of these features may be coincidental or it may somehow reflect major crustal inhomogenieties.

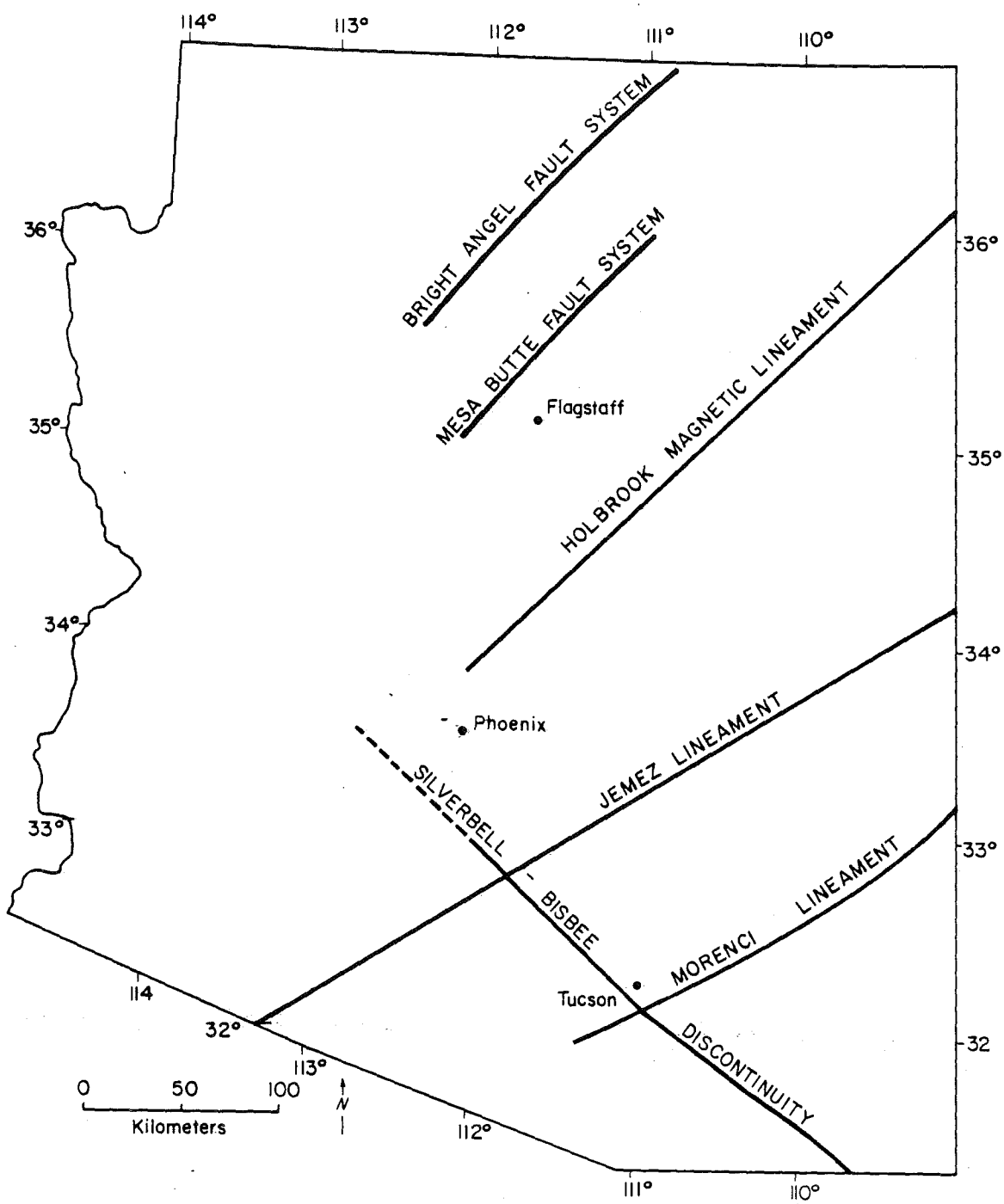

Figure 3.6. Map showing major Arizona lineaments and discontinuities (from Chapin and others, 1978; Titley, 1976)

Historical epicenters (1830 to 1980) and preliminary seismic source regions in Arizona (Fig. 3.7) (DuBois and others, 1981) also correlate well with the Residual Temperature Map. Areas having cool residual temperatures roughly coincide with areas of active historical seismicity, and areas with the warmest residual temperatures approximate seismically quiet zones.

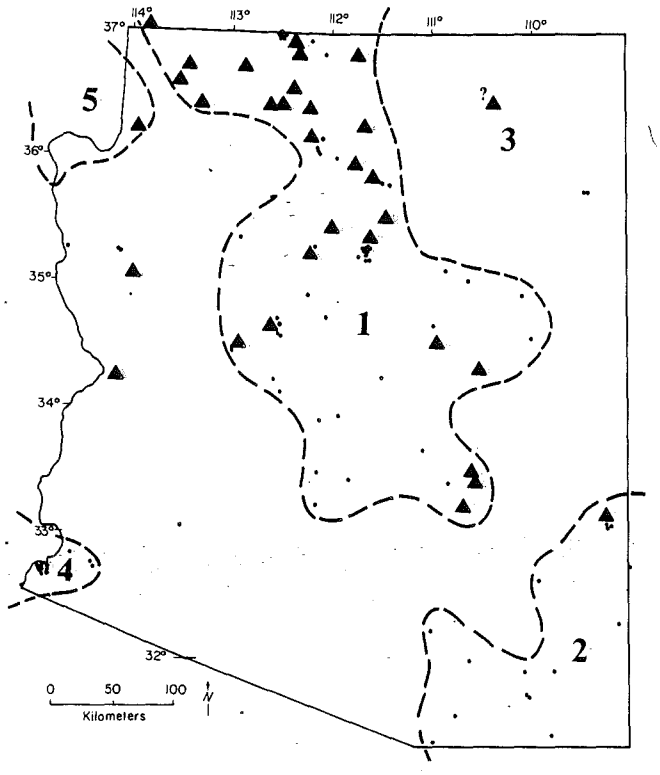

Figure 3.7. Map showing historical earthquake epicenters (1890-1980) and preliminary seismic source regions (from DuBois and others, 1981)

RESIDUAL MAP REFERENCES

Bodell, J. M., and Chapman, D. S., 1982, Heat flow in the north-central Colorado Plateau: Journal of Geophysical Research, v. 87, p. 2869-2884.

Chapin, C. E., Chamberlin, R. M., Osburn, G. R., White, D. W., and Sanford, A. R., 1978, Exploration framework of the Socorro geothermal area, New Mexico, *in* Chapin, C. E., and Elston, W. E. (eds.), Field guide to selected cauldrons and mining districts of the Datil-Mogollon volcanic field, New Mexico: New Mexico Geological Society Special Publication No. 7, p. 115-129.

DuBois, S. M., Sbar, M. L., and Nowak, T. A., 1982, Historical seismicity in Arizona: GPO Sales Program, U. S. Nuclear Regulatory Commission, Washington, D. C., 20555, No. NUREG/CR-2577, RA, 199 p.

Goldstone, L. A., and Stone, C., 1982, Temperature-depth profiles, well-location information, and tabulated temperatures for Arizona wells measured between May, 1979 and March, 1982: Arizona Bureau of Geology and Mineral Technology Open-File Report 82-7, 112 p.

Roy, R. F., Blackwell, D. D., and Birch, F., 1968, Heat generation of plutonic rocks and continental heat-flow provinces: Earth and Planetary Science Letters, v. 5, p. 1-12.

Roy, R. F., Decker, E. R., Blackwell, D. D., and Birch, F., 1968, Heat flow in the United States: Journal of Geophysical Research, v. 73, p. 5207-5221.

Sass, J. H., Lachenbruch, A. H., Monroe, R. J., Greene, G. W., and Moses, T. H., 1971, Heat flow in the western United States: Journal of Geophysical Research, v. 76, p. 6376-6413.

Sass, J. H., Stone, C., and Bills, D. J., 1982, Shallow subsurface temperatures from the Colorado Plateau of northeastern Arizona: U.S. Geological Survey Open-File Report (in prep.).

Shearer, C. R., 1979, A regional terrestrial heat-flow study in Arizona: Ph.D. dissertation, Socorro, New Mexico Institute of Mining and Technology, 184 p.

Titley, S. R., 1976, Evidence for a Mesozoic linear tectonic pattern in southeastern Arizona: Arizona Geological Society Digest, v. 10, p. 71-101.

THERMAL SPRINGS IN ARIZONA

INTRODUCTION. Hot springs have long held man's interest. During cold spells early man probably took advantage of the warmth offered by these springs. Today, hot springs are used to soothe human aches and pains and for relaxation. In a few areas of the world, thermal spring waters are used to heat buildings and greenhouses.

Geologists are very interested in thermal springs. In fact, many early hypotheses about the formation of hydrothermal mineral deposits and the nature of geothermal systems arose from studies of the temperature, chemistry, and geologic setting of hot springs. Today, similar studies continue and are contributing to man's knowledge of the earth and its geothermal resources.

ORIGIN. Thermal springs originate from a combination of special geologic conditions that are basic to any geothermal system. These components must exist and function in concert before a thermal spring system can occur. The special elements are: (1) a heat source; (2) a circulation framework or storage reservoir; (3) a recharge source; and (4) a discharge mechanism. The most basic element is the heat source because it alone separates thermal springs from all others.

Natural conductive flow of heat from the earth's mantle and radiogenic heat produced in the crust are the major heat sources for Arizona thermal springs. Igneous heat (heat from hot rocks or magma) sources are important in many areas such as Yellowstone National Park and the

Cascade Range of the Pacific Northwest, but such sources have not been identified in Arizona.

Ground water in Arizona acquires its anomalous temperature by circulating to great depths in accordance with the normal regional temperature gradient. Deeply circulating water gathers and transports heat, a process called convection. Convection can result from buoyant (internally induced) water flow, caused by a vertical differential in water density. This system is known as free convection and is commonly associated with very high temperature gradients and good permeabilities. Thermal springs associated with predominantly free convection frequently have an igneous heat source.

Convection can also be caused by pressure that is externally induced, called forced convection. Forced convection can occur where the water table in a ground-water recharge zone is significantly higher than the water table in the discharge area. Flow is forced by maintaining hydraulic pressure through continual addition of water to the recharge end of the system. The depth of flow is controlled by hydraulic pressure and the permeability, morphology, and dimensions of the circulation system.

Two types or models of circulation systems are commonly used to describe forced convection geothermal systems. The simplest system is called a pipe model (Donaldson, 1982; Lowell, 1975). In this case a synclinal fold of high permeability strata or a U-shaped arrangement of linked fractures in a fault plane provides a deep-reaching conduit, which connects a recharge area at higher elevation with a discharge area at lower elevation (Fig. 3.8). Flow is induced both by

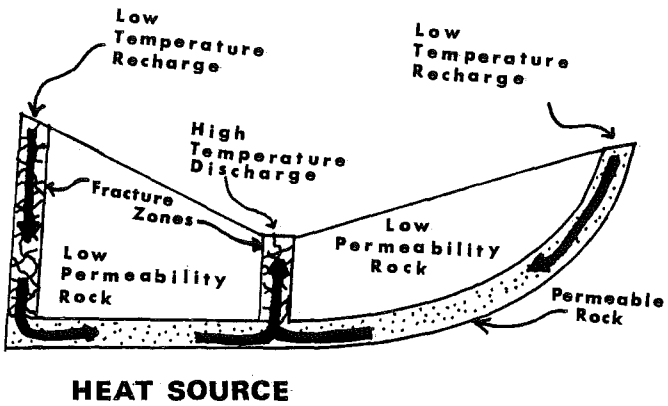

Figure 3.8. Pipe model for forced convection thermal spring system

hydraulic pressure and by density contrasts (buoyancy) between denser cold water in the recharge limb and less dense hot water in the discharge conduit.

The other forced convection system occurs in a porous medium in a regional ground-water flow system. Domenico and Palciauskas (1973) modeled the temperature perturbation resulting from a simple regional ground-water flow system in a basin with homogeneous geology (Fig. 3.9). Their studies illustrate that forced convection arising from regional ground-water flow is capable of creating significant geothermal anomalies, even when rock permeability is low.

Freeze and Witherspoon (1966, 1967, 1968) and Toth (1962) mathematically modeled the affects of topography and geologic heterogeniety on a regional ground-water flow system. Toth (1962) showed that a flow system in a basin with hilly topography becomes complex because local and intermediate flow systems are superimposed on the regional system (Fig. 2.140). He assumed that the water table mimics topography in his model. Freeze and Witherspoon (1967) showed that flow patterns become almost rectilinear where rocks with high-permeability contrasts exist. Highly

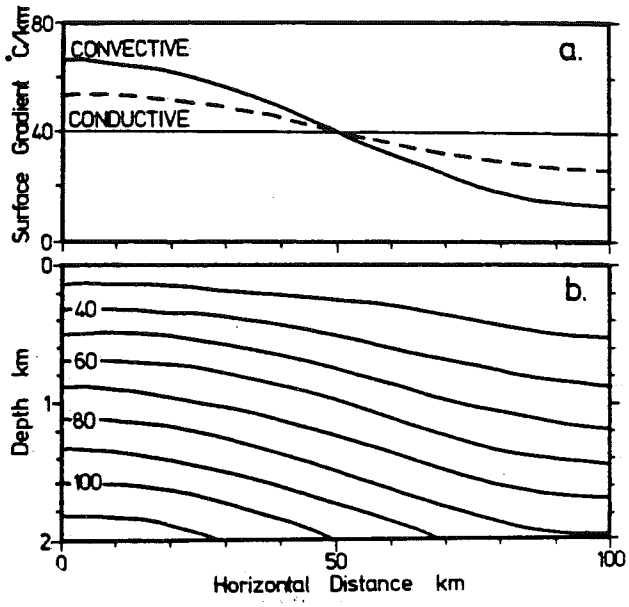

Figure 3.9. Diagram showing thermal disturbance from a regional ground-water flow system in a basin 100 km long, with a hydraulic conductivity of 200 millidarcies, and a hydraulic gradient of 0.1 percent. The analytical approach of Domenico and Palciauskas was used to construct this model. Part (a) shows temperature gradient. A 40°C/km is a normal undisturbed conductive gradient. The convective gradient line shows the affect of regional flow on the temperature gradient. Part (b) shows temperature distribution. Isotherms are in °C. (From Morgan and others, 1981.)

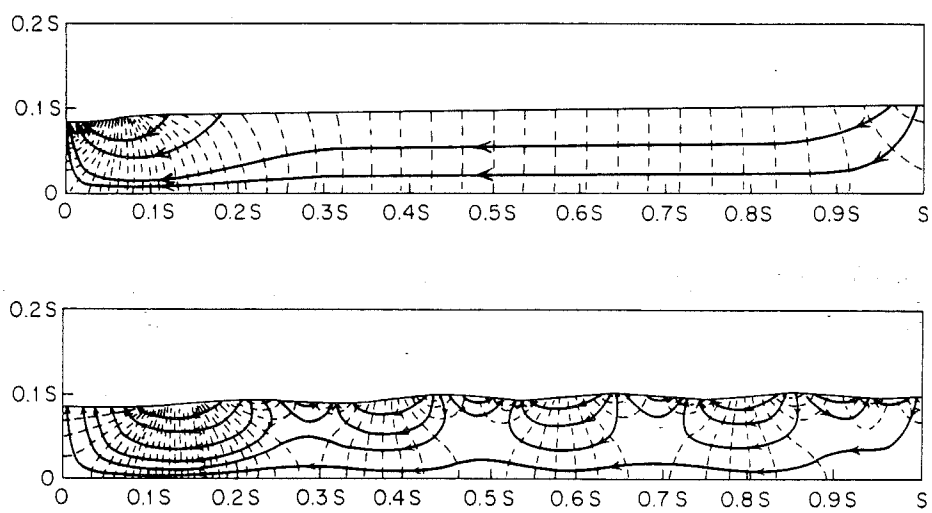

Figure 3.10. Diagram showing the effects of topography on regional ground water flow patterns. Lateral and vertical dimensions are ratios of regional flow-system lengths. (From Freeze and Witherspoon, 1967.)

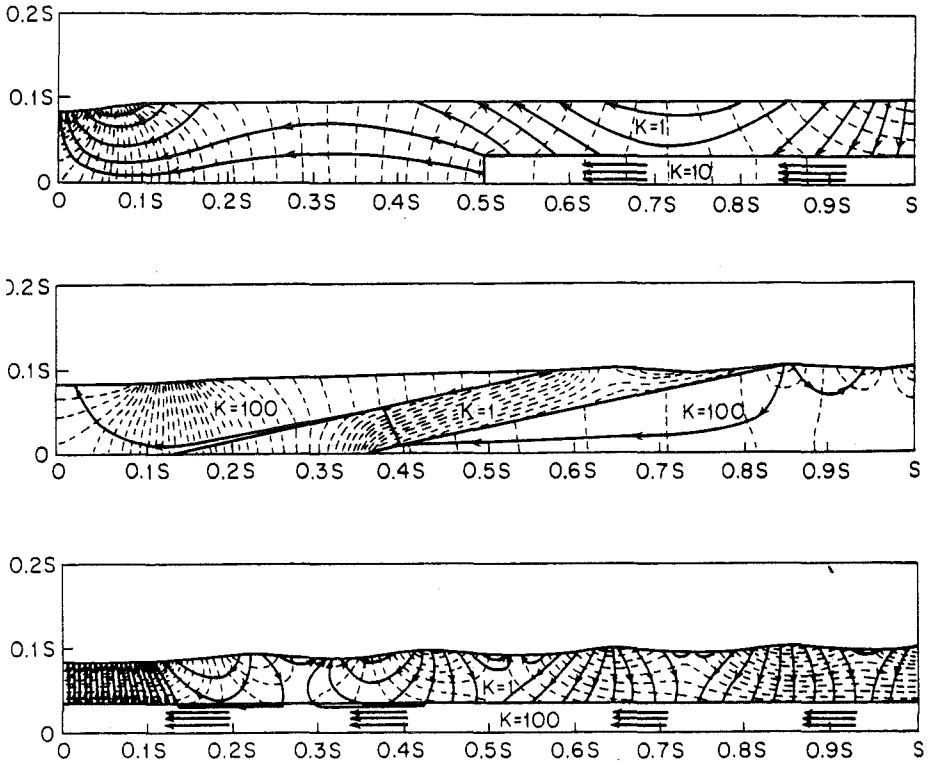

Figure 3.11. Diagrams showing the influence of geology and regional ground-water patterns. K is hydraulic permeability (units unspecified). Dimensions are ratios of regional flow-system lengths. (From Freeze and Witherspoon, 1967.)

permeable rocks have horizontal flow, while low permeability rocks have vertical flow (Fig. 3.11). Geologic heterogeneity and resulting contrasts in permeability and topographic (water table) variations within a regional flow system can profoundly affect the volume of water transmitted and the flow rate along a particular flow path.

Temperatures of thermal springs resulting from forced convection are controlled not only by the depth of water flow and the regional temperature gradient; their temperatures are also regulated by the water flow rate. Turcotte and Schubert (1982) showed that a particular moderate flow rate through the pipe-model system maximizes the spring temperature, which is

about one-half the wall-rock temperature at the base of the system. Where water flow rate is very low, water flowing up the discharge limb of the system loses heat to the wall rocks; when this water reaches the surface it is only slightly warmer than when it entered the system. With very rapid flow, there is less heat transfer, the water at the base of the system being heated only slightly, and the spring discharge temperature is again only moderately warmer than when it entered the system.

REGIONAL SETTING. Figure 3.12 shows Arizona thermal spring. Their numbers refer to numbered springs in Table 3.2. On a regional scale, Arizona thermal springs are controlled by ambiguous crustal inhomogeneity and structure (Fig. 3.13), represented by aeromagnetic linears. They occur where topographic relief is greatest, and most often in areas with relatively large exposures of crystalline basement rocks. Thirty-five out of 45 Arizona thermal springs lie in a 120-km wide, northwest-trending belt that straddles central Arizona just south of the Colorado Plateau. Most of this belt, which includes Kingman, Prescott, Globe, Safford, and Morenci, coincides with the Transition Zone, a region that has characteristics of both the Colorado Plateau and the Basin and Range province. However, this zone has some unique properties of its own, such as ubiquitous exposures of Precambrian basement rocks, large deep canyons, and generally rugged, high-relief topography. Most of the northern boundary of the Transition Zone is formed by the south-facing Mogollon Rim escarpment, which is as much as 700 m high.

Two thermal springs in southwest Arizona formerly existed near the northeast-trending Gila trough. These springs are now dry, probably as a result of ground-water development. Six thermal springs occur east

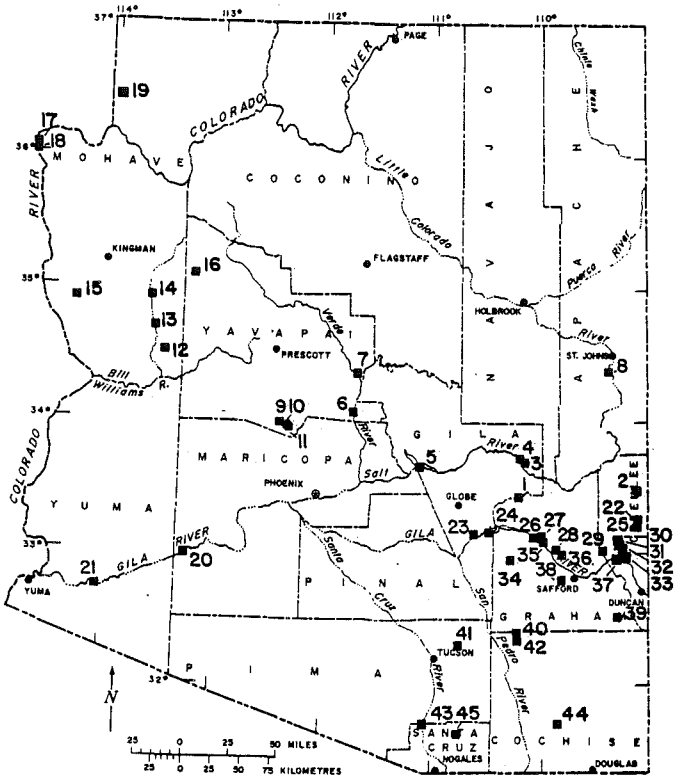

Figure 3.12. Locations of Arizona thermal springs. Numbers refer to numbers in Table 3.2.

of longitude 111°W. in southeastern Arizona in the Mexican Highland section of the Basin and Range province. Only four thermal springs occur near Quaternary volcanic fields (Fig. 3.14), but none of these volcanic fields contain silicic rocks. In fact, the distribution pattern of thermal springs and young volcanic rocks shows little overlap. Therefore, we have ruled out an igneous heat source for these springs. Thermal springs do coincide with most areas showing Quaternary faulting and historical earthquakes (Fig. 3.14). The major exception is the Flagstaff area and the Kaibab Plateau-Grand Canyon region.

The residual aeromagnetic map of Arizona with major geophysical lineaments (defined by bold lines) is shows in Figure 3.13. Dots represent thermal springs, from which it can be seen that only one out

TABLE 3.2. Thermal springs of Arizona

#	NAME	LOCATION	T°C	T-MAT°C
1	Warm Spring	A-1-20-12AC*	29.4	14.4
2	Hanna Creek Hot Springs	A-1-31-29AD	55.5	42.5
3	Warm Spring	A-4½-20-36CB*	24.4	10.4
4	White River Salt Spring	A-4½-20-35AD*	28.3	13.3
5	Roosevelt Dam Hot Spring	A-4-12-19DDB	48.0	28.0
6	Hot Spring	A-9-6-26AB*	36.6	17.6
7	Verde Hot Springs	A-11-6-3B	41.0	23.0
8	Salado Spring	A-12-28-17DCA	21.7	11.7
9	Henderson Ranch Spring	B-8-1-33BAC	30.3	11.3
10	Alkalai Spring	B-8-1-33DB	31.2	12.2
11	Castle Hot Springs	B-8-1-34CC	54.7	35.7
12	Kaiser Hot Spring	B-14-12-10AD	37.0	19.0
13	Cofer Hot Spring	B-16-13-25CAD	37.0	18.0
14	Warm Spring	B-18-13-25DB	28.3	10.3
15	Warm Spring	B-18-19-33DC	29.2	10.2
16	Spring	B-20-9-30CC	27.0	14.0
17	Hot Spring	B-30-23-15CBD	32.0	12.0
18	Hot Spring	B-30-23-26BBC	30.0	10.0
19	Pakoon Spring	B-35-16-24BD	28.0	10.0
20	Agua Caliente Spring	C-5-10-19AA	40.0	18.0
21	Radium Hot Spring	C-8-18-12CC	60.0	38.0
22	Spring	D-2-31-35ABB*	25.6	10.6
23	Mescal Warm Spring	D-3-17-20CBC	29.1	14.0
24	Coolidge Dam Hot Spring	D-3-18-17DC	36.6	18.6
25	Miguel Raton Spring	D-3-31-3ADC	26.7	11.7
26	Spring	D-4-23-21AA	27.2	10.2
27	Spring	D-4-23-21AD	31.5	14.5
28	Tom Niece Spring	D-4-23-22BD	28.3	11.3
29	Eagle Creek Hot Spring	D-4-28-35ABB	42.5	25.5
30	Clifton Hot Spring	D-4-30-18CCD	70.0	53.0
31	Clifton Hot Spring	D-4-30-18CDC	50.0	33.0
32	Clifton Hot Spring	D-40-30-19CAA	33.0	16.0
33	Clifton Hot Spring	D-4-30-30DBC	38.0	21.0
34	Warm Spring	D-5-19-23BDD	26.0	11.0
35	Indian Hot Springs	D-5-24-17AD	48.8	30.8
36	Spring	D-5-24-16CB	33.0	16.0
37	Gillard Hot Spring	D-5-29-27AAD	84.0	67.0
38	Spring	D-7-24-13DC	29.4	12.4
39	Spring	D-10-29-23DD	26.1	10.1
40	Spring	D-12-21-31CA	32.5	17.5
41	Agua Caliente Spring	D-13-16-20CDD	32.0	12.0
42	Hookers Hot Spring	D-13-21-6AAC	52.0	37.0
43	Agua Caliente Spring	D-20-13-13BA	27.0	11.0
44	Antelope Spring	D-20-24-21DC	25.5	10.5
45	Monkey Spring	D-21-16-3C	28.3	13.3

*Unsurveyed

of 15 of these hot springs is located farther than 30 km from the geophysical lineaments. The single exception, Hookers Hot Spring, lies astride the Morenci lineament. The apparent association of hot-spring activity with aeromagnetic linears is probably not coincidental. These aeromagnetic anomalies probably represent ancient, deep-seated crustal structures that allow deep flow of ground water. The west-northwest

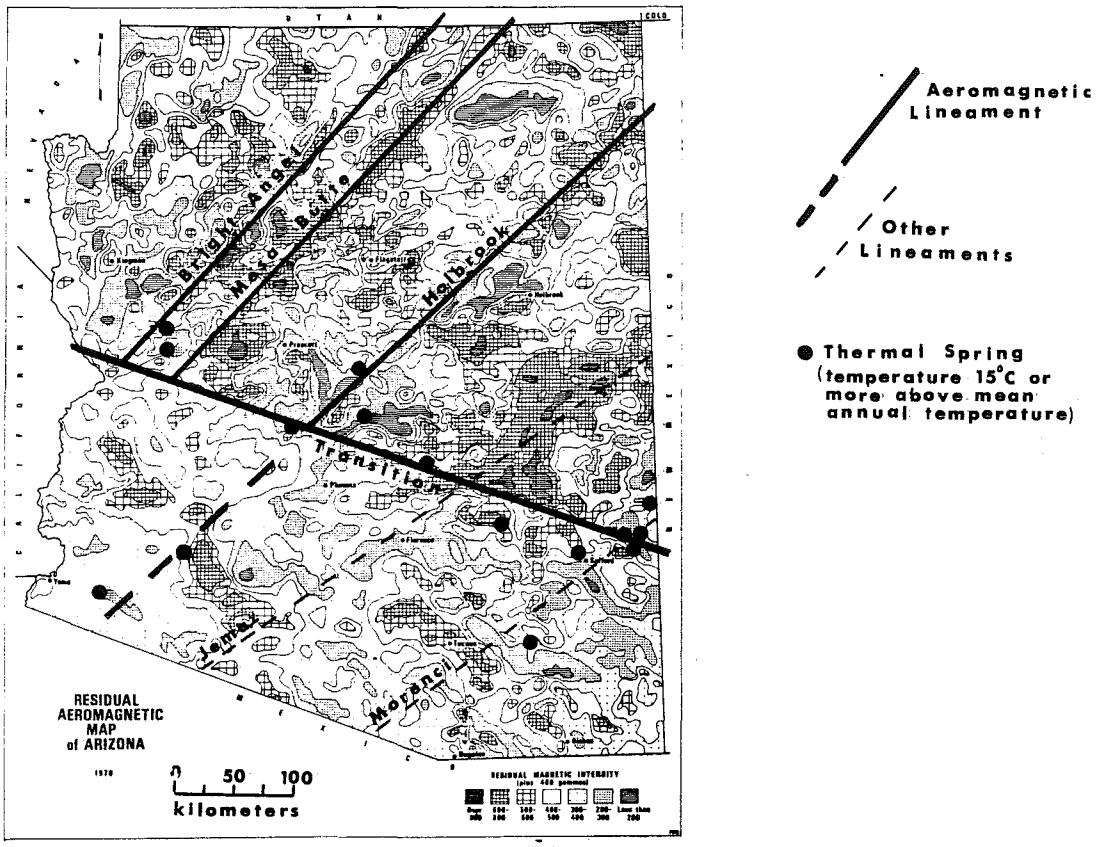

Figure 3.13. Residual aeromagnetic map of Arizona showing major lineaments (From Sauck and Sumner, 1974)

and northeast directions of the linears are common Precambrian and Mesozoic structural and intrusive orientations.

LOCAL SETTINGS. Arizona thermal springs in the Transition Zone and Mexican Highland section nearly always occur on or immediately adjacent to large faults and they tend to occur where surface drainage basins become constricted. The existence of thermal springs within a few 100 m downstream from man-made dams in Arizona is dramatic evidence of this basin-constriction phenomenon. These dams were built at drainage constrictions. Thermal springs occur below Hoover Dam, Roosevelt Dam, and Coolidge Dam. Note, however, that not all drainage constrictions have thermal springs.

Thermal springs in Arizona also occur on structures that are transverse to regional surface drainage, as well as on or immediately adjacent to streams and rivers. Indian Hot Springs near Safford is an exception. Indian Hot Springs is leakage from an artesian aquifer (see section titled Gila Valley from Safford to Indian Hot Springs, this volume).

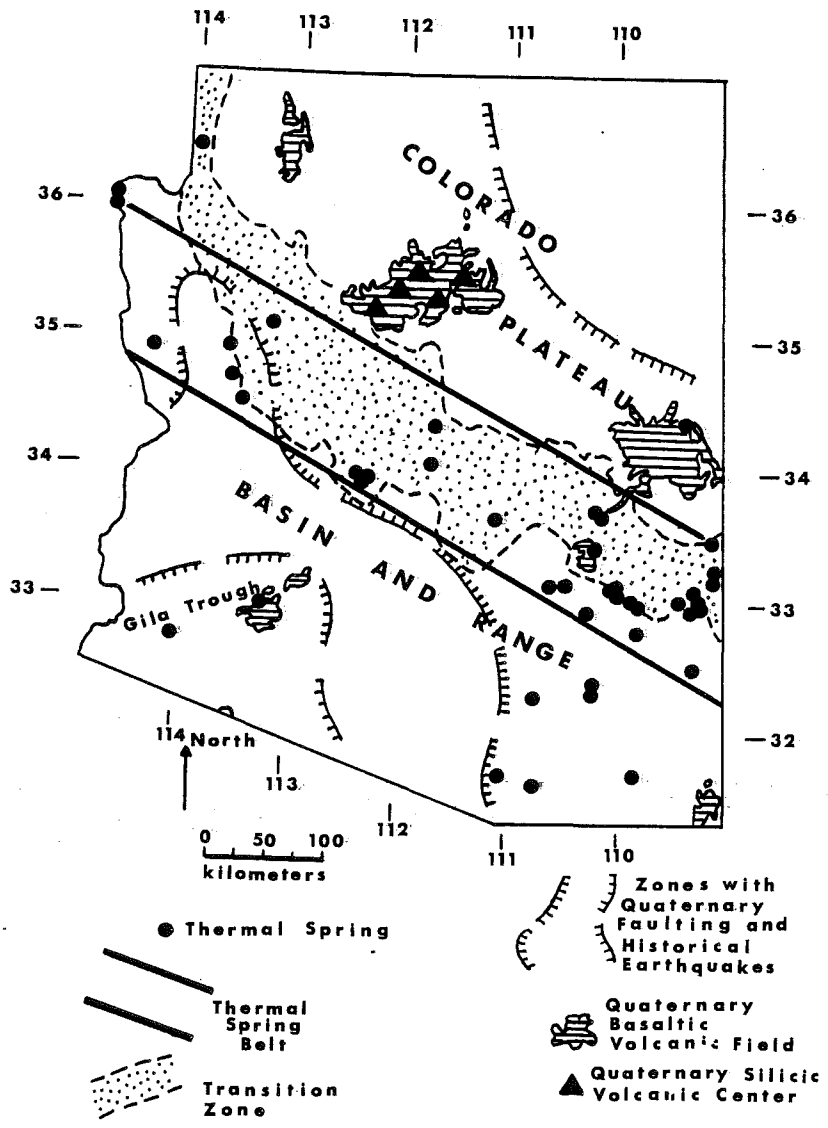

Figure 3.14. Relationship of thermal springs to Quaternary volcanism, faulting, and historical earthquakes

THERMAL SPRINGS IN ARIZONA REFERENCES

Domenico, P.A., and Palciauskas, V.V., 1973, Theoretical analysis of forced convective heat transfer in regional ground-water flow: Geological Society of American Bulletin, v. 84, p. 3803-3814.

Donaldson, I. G., 1982, Heat and mass circulation in geothermal systems, Wetherill, G. W., Albee, A. L., Stehli. F. G., eds., Annual Review of Earth and Planetary Sciences: Annual Reviews, Inc., v. 10, p. 377-395.

Freeze, R. A., and Witherspoon, P. A., 1966, Theoretical analysis of regional ground-water flow; 1. analytical and numerical solutions to the mathematical model: Water Resources Research, v. 2, p. 641-656.

Freeze, R. A., and Witherspoon, . A., 1967, Theoretical analysis of regional ground-water flow; 2. effect of water-table configuration and subsurface permeability variation: Water Resources Research, v. 3, p. 623-624.

Freeze, R. A., and Witherspoon, P. A., 1968, Theoretical analysis of regional ground-water flow; 3. quantitative interpretations: Water Resources Research, v. 4, p. 581-590.

Lowell, R. P., 1975, Circulation in fractures, hot springs, and convective heat transport on mid-ocean ridge crests: Royal Astronomical Society Journal, v. 40, p. 351-365.

Morgan, P., Harder, V., Swanberg, C. A., and Daggett, P. H., 1981, A convection model for Rio Grande rift geothermal resources: Transactions, Geothermal Resources Council, v. 5, p. 193-196.

Sauck, W. A. and Sumner, J. S., 1970, Residual aeromagnetic map of Arizona: Department of Geosciences, The University of Arizona.

Toth, J., 1962, A theory of groundwater motion in small drainage basins in central Alberta: Journal of Geophysical Research, v. 67, p. 4375-4387.

Turcotte, D. L. and Schubert, G., 1982, Geodynamics, application of continum physics to geological problems: New York, John Wiley and Sons, 450 p.

Waring, G. A., 1965, Thermal springs of the United States and other countries of the world--a summary: U. S. Geological Survey Professional Paper 492, 383 p.

Witcher, J. C., 1981, Thermal springs of Arizona: Fieldnotes, State of Arizona Bureau of Geology and Mineral Technology, v. 11, no. 2, p. 1-4.

CHAPTER 4

EXPLORATION METHODS

INTRODUCTION. Numerous exploration methods exist that aid in the search for and evaluation of geothermal energy resources. Time, money, and geologic setting dictate which methods are used in a given exploration program. In this chapter we discuss the exploration methods used in Arizona, the data obtained by these methods, their merits, and the relative cost in dollars and time required for each technique. A discussion of all exploration methods currently used in geothermal work can be found in Ward and others (1981) and Lumb (1981).

LITERATURE SEARCH. The initial phase in any exploration program is to search out all work that already has been done in an area of interest. Geologic mapping and geochemical and geophysical surveys that have been published are reasonably easy to locate. Additional valuable information can be culled from unpublished sources. Well logs and water chemical analyses are on file with the U. S. Geological Survey, Water Resources Division, the Arizona Department of Water Resources and various city water departments. Utilities that have developed well fields to supply water to coal-fired power plants also have useful stratigraphic, aquifer, and water-quality data. Unpublished masters' theses and Ph.D. dissertations from both in-state and out-of-state universities often contain useful geologic, geophysical, and geochemical information. It is helpful to contact members of the state and federal geological surveys who are conducting on-going exploration in the state. Finally, private companies

engaged in mineral or petroleum exploration have a considerable amount of confidential information. Occasionally such information is no longer important to them and will be released upon request.

After compiling available information it must be evaluated in terms of reliability and usefulness to the project. If the quality of the data is questionable, they must be checked against other data sets. Otherwise, questionable data probably should be rejected. Following a careful evaluation, an exploration program is devised that will generate the maximum, most useful information possible within time and budget constraints.

GRAVITY. A gravity survey does not identify or define a geothermal resource, per se. Rather it is an exploration technique that defines subsurface structures by measuring differences in rock density. In the Basin and Range province, geothermal systems occur in the sediments or volcanic rocks that fill the basins in the crystalline rocks underlying the basin-filling material, or within the master faults bounding the basins. Therefore, accurately defining the boundaries, size and depth to basement of a given basis is essential. A detailed gravity survey will also aid in identifying bedrock ridges within the basin, fault traces, and fault widths.

Exact locations and elevations are necessary to conduct an accurate gravity survey. If this information is available, the field work for a gravity survey is relatively straightforward. One person can drive or walk from station to station, stopping at each to record latitude, longitude, elevation, and the dial reading on the gravity meter. After the entire area has been surveyed, the data are corrected by computer, and

gravity values are plotted on a map. Computer programs also exist to generate three-dimensional models and two-dimensional cross-sectional profiles across an area. In a basin with adequate road access, about 12 to 15 gravity measurements can be made in a day. Thus at mile spacings, an area about 60 mi^2 can be surveyed by one person in a week.

If accurate elevations and locations are not known through detailed topographic maps, it is necessary to run survey lines to obtain this information. In this case at least two people are required for the field work, and the time required to complete the gravity study is nearly doubled.

The area in which we ran a gravity survey in Arizona had inadequate gravity coverage prior to our work (see northern Hassayampa area, this volume). The time and manpower spent on this study provided invaluable information on understanding the basin structure and thus on evaluating the hydrothermal system situated therein.

SOIL SAMPLING. Soil sampling consists of collecting several grams of undisturbed soil from a depth of 8 to 12 inches below the surface. Soil is most commonly analyzed for mercury content because mercury is a highly volatile element associated with numerous known geothermal systems. Although instruments exist for analyzing mercury in the field, we placed our samples in plastic "zip-loc" bags and sent them to a commercial laboratory for analysis. The cost in 1979 was $3.50 per sample for preparation and analysis.

Our mercury soil surveys identified both geothermal anomalies and major tectonic structures (see Safford, northern Hassayampa, and Avra

Valley area reports, this volume). One person can easily collect 10 to 20 or more soil samples in a day. Thus, at mile spacings an area about 50 to 100 mi^2 can be sampled by one person in about one week. For the manpower and cost required to conduct a mercury soil survey, the information gained is helpful in initially identifying the location of range-bounding faults and the possible presence and size of a geothermal anomaly. Such a survey is preliminary and requires more sophisticated follow-up exploration work.

WELL LOGGING. Measuring temperatures is the single most direct method of confirming the presence of a geothermal anomaly. Temperatures can be measured of water issuing naturally from springs, seeps, and artesian wells; water being pumped from irrigation and domestic wells; and water or air at depth in boreholes. This latter technique is called well logging, and is accomplished by lowering a thermistor, mounted on the end of a lightweight cable, into a borehole and reading the thermistor resistance at discrete intervals, usually every five meters. Resistance values are converted into temperatures for each reading by using tables constructed from thermistor-temperature calibration curves. Temperatures are accurate to $\pm$ 0.01 C.

The resultant temperature-depth profiles yield much valuable information. They can indicate zones of warm or cold water entering or exiting a borehole and whether water is rising, descending, or moving laterally in a formation. If ground-water movement is not excessive a geothermal gradient can be estimated. In any case, the bottom-hole temperature is the most reliable value if sufficient time has elapsed after drilling. When a number of bottom-hole temperatures are available from wells in the same

area and with nearly the same depths, the bottom-hole temperatures can be used to construct an isothermal map that can aid in targeting a geothermal anomaly.

Temperature-depth profiles are best used in conjunction with lithologic information from the same or nearby boreholes. The identification of important lithologic strata from these logs, such as clay, evaporite, or volcanic deposits, significantly increase the value of temperature-depth profiles and their interpretation.

Over a five year period we measured temperatures in over 100 domestic and irrigation water wells and mineral test holes. Most of the temperature-depth profiles from this work indicated ground water moving in the borehole or in the formation. The gradients, therefore, could not be extrapolated with accuracy to depths greater than those measured. The other information derived from well logging, however, is well worth the time and money spent acquiring it. One person can log between five and eight hundred-meter-deep holes in one day, if distances between sites is not great and if the boreholes are not greatly disturbed by ground-water movement. A portable temperature-logging system with 600 m of cable cost about $4,000 in 1980.

HEAT-FLOW DRILLING. If time and budget permit, heat-flow measurements provide the most valuable and reliable information, short of deep test holes, for confirming and targeting a geothermal anomaly.

Thermal gradients, used alone, can give misleading results because gradients will vary in a borehole due to penetrating rocks of different thermal conductivities. Gradients also differ between boreholes for the same reason. Thus, when comparing thermal gradients between boreholes or

different segments in the same borehole, it is sometimes difficult to distinguish between effects due to variable heat flux and effects due to differing rock thermal conductivity. Heat-flow measurements help obviate this problem because heat flow is a product of the thermal gradient and the thermal conductivity.

The most reliable heat-flow measurements generally come from holes drilled into unfractured crystalline rock solely for that purpose. In such holes, the chances of ground water movement are minimal. Coring can provide rock samples large enough for reliable thermal conductivity measurements. Good heat-flow measurements can be made in boreholes drilled into most rock types, so long as gradients are not disturbed by ground water and rock samples (including drill cuttings) are available for measurement. Less reliable heat flows can sometimes be estimated from measurements made in boreholes showing slight ground-water disturbance.

Heat-flow holes are small bores, usually four to five cm in diameter and 50 to 100 m deep. The holes are cased with pile that is plugged at the bottom and then filled with water. Conventionally, thermal conductivity is measured in the laboratory. After the thermal effects due to drilling have dissipated, temperatures are measured in the borehole. An exception to the conventional technique is the in situ heat-flow determinations being made in unconsolidated sediments during pauses in the drilling operations, by the U.S. Geological Survey (Sass and others, 1979), a technique still in the experimental stages.

We drilled heat-flow holes in the Springerville-Alpine area (five holes), Clifton (one hole), and the Safford area (seven holes) (Stone, 1980;

Witcher and Stone, 1981; Witcher, 1982). (See also those area reports, this volume).

The Clifton heat-flow determination was useful, but it is difficult to characterize an anomaly with a single or even several measurements.

The results derived from the heat-flow drilling at Springerville-Alpine were less than satisfactory. Three of the five holes were drilled into basalt lava flows, which produced copious amounts of water. The holes were terminated in volcanic rocks rather than in the unknown underlying formations, as a result of which valuable stratigraphic information was lost and the three holes were useless for heat-flow determinations. The other two holes were drilled in sedimentary roack and yielded good data. This project was not cost effective. Had the drilling contract been given to a company experienced in drilling in basaltic volcanic rocks, the drilling difficulties may have been resolved and knowledge of the heat flow and stratigraphy of the Springerville-Alpine area would have been greatly increased.

The information gained from the three heat-flow drilling programs was most useful in the Safford area. Seven shallow holes (30 m deep) were drilled in the area of an identified mercury anomaly. While the holes were exceptionally shallow and sediment porosity was estimated rather than measured, the relative heat-flow values determined from this study confirmed and further targeted the geothermal anomaly. This program cost $20,000 in 1981 and was cost-effective.

RESISTIVITY SURVEYS. An electrical resistivity survey maps lateral and vertical variations in the ability of the earth to retard an electri-

cal current. Resistivity is influenced by rock type and porosity, the presence of water, steam, or gas ground-water salinity, and temperature. Extremely low resistivities (< 3 ohm meter) are commonly associated with clay, very high porosity, brines and high temperatures (>150 C), or any combination of these factors. Resistivity surveys are frequently used in geothermal exploration because they are capable of detecting heat and porous zones. However, geologic interpretation of a survey is frequently difficult and ambiguous without knowledge of other geologic and geophysical information. Therefore, it is better to delay until later in an exploration program. If conducted resistivity surveying during initial stages of a program it is probably best to interpret results in terms of subsurface structure and lithology, rather than geothermal parameters. The value and cost effectiveness of a resistivity survey may vary depending upon the geologic setting.

Direct current (D.C.) Schlumberger and dipole-dipole surveys have been used in exploration for geothermal resources in Arizona. These surveys differed mainly in the type of colinear electrode array used. The Schlumberger survey uses two moveable current electrodes situated on the ends of the array and two stationary potential electrodes near the array center; the dipole-dipole array uses two current electrodes placed at one end of the array and two potential electrodes at the other end. Greater depth measurement using either array is accomplished by increasing the spacing between current and potential electrodes. During surveys the voltage difference between the current and potential electrodes is determined at various electrode spacings. This voltate difference is used to calculate apparent earth resistivity.

Schlumberger surveys were conducted in the Springerville area (Young, 1979; Young, 1980) and in the Safford area (Phoenix Geophysics, 1979). In the Springerville area, the Schlumberger array was employed in two different ways: (1) the electrode spacing remained unchanged from site to site; and (2) the array electrode spacing was expanded at each survey site. By expanding electrode spacings, a depth "sounding" of resistivity is produced, which is interpretable in terms of vertically layered earth resistivity. The non-expanded array is used to map lateral changes in average apparent resistivity down to the maximum depth penetration of the array. Interpretation of the Springerville Schlumberger surveys are ambiguous due to a lack of subsurface structure and lithology information. Resistivity changes in this area may relate to ground-water quality, lithology, or geothermal systems.

Two types of resistivity surveys were run in the Safford basin. A single Schlumberger survey site was occupied at Safford in order to obtain a sounding of vertical resistivity variations and to compliment the dipole-dipole survey. Dipole-dipole resistivity profiling (100 line miles) was accomplished in the basin using a 2,000-foot (608 m) electrode separation. Dipoles were spread a maximum of five electrode spacings at each survey site during profiling. This resistivity data provided information on lithology of basin-fill sediments and ground water. Areas underlain by saline groundwater and salty or gypsiferous sediment had very low resistivities (<3 Ohm-meter).

Resistivity surveys are apparently most useful initially for reconnaissance mapping of subsurface lithology where drill hole data are

sparse. Resistivity data are best used and interpreted in later stages of exploration when additional and independent geologic and geophysical information is available.

SEISMIC SURVEYS. Swarms of shallow microearthquakes (between magnitude -2 and 4) are often observed in geothermal areas; however, they are not observed in all geothermal areas, nor are they restricted to geothermal areas alone. Seismic surveys to detect microearthquakes are conducted with arrays of five to fifteen small, high gain, portable seismometers with one-Hertz vertical-component geophones. These surveys attempt to locate the zones of greatest seismicity often near active faults where many high-temperature geothermal systems are localized. However, due to a significant lithologic or structural inhomogenity, which is frequently associated with geothermal areas, good hypocenter locations may be difficult to obtain.

During the summer of 1978, between 12 and 19 sensitive portable seismometers were operated for two weeks total time in the San Bernardino Valley, the Clifton-Morenci region, and the Springerville region (Sbar, 1979; Natali and Sbar, 1982). The University of Arizona, New Mexico State University, and the University of Texas at El Paso worked together on these surveys in order to place a maximum number of seismometers in the field. The NMSU and UTEP groups were under contract with Los Alamos Scientific Laboratory to investigate potential geothermal areas in the Aquarious Mountains - Prescott region and in the St. Johns areas of Arizona. Seismometers were spaced between 10 and 15 km apart in the San Bernardino Valley and in the Clifton-Morenci area, and 20 km apart in

the Springerville area. The seismic equipment had gains of one to six million at 10 Hertz, which is ideal for measuring microearthquakes with frequencies between 1 and 20 Hertz. Sbar (1979) estimated that a magnitude 0 seismic event was the threshold of detection for these networks, and that a station operating at a gain of 2.5 million should detect a magnitude 0 event at a distance of 10 km.

The only microearthquake recorded during the study was in the San Bernardino Valley just north of the international boundary with Mexico. The Springerville and Clifton-Morenci areas were aseismic during the survey, but the two-week monitoring period may have been too short.

Microearthquakes frequently occur in sporadic swarms in Arizona that are most probably related to regional tectonic stress than to geothermal processes (Sbar, 1979; Natalie and Sbar, 1982). For example, identical two-week seismic surveys recorded microearthquakes in the Prescott area and in the San Bernardino Valley, Sonora, Mexico where recent faulting and historical earthquakes with magnitude greater than 5 have occurred.

Numerous and frequent mine blasts were recorded during these surveys. By using these mine blasts, a reversed seismic refraction study of deep crystal structure was made between Globe, Arizona and Tyrone, New Mexico (Gish and other, 1981). This study included areas with geothermal potential at Safford and Clifton-Morenci. Interpretation of the data implies enhanced regional heat flow favorable for geothermal resources in the Morenci region.

Microearthquake surveys are not a cost effective method of exploring for geothermal resources in Arzona. Only regional heat flow and tec-

tonic stress information is interpretable from such studies in this state. However, seismic reflection surveys such as the ones currently used in oil and gas exploration may be cost effective in deep geothermal reservoir identification. However, to date no geothermal exploration programs are believed to have used reflection seismic surveys in Arizona.

WATER CHEMISTRY. Ground-water chemistry is a common geothermal exploration tool. The reason is rather straightforward. Dissolved constituents in ground water and geothermal water are a result of aquifer residence time rock-water interaction, and temperature. Additional factors such as mixing water from different geologic environments or movement of ground water through different kinds of rock are important, too. Thus, water emerging at the surface from a well or spring carries with it a chemical imprint that may indicate subsurface temperature, lithology, recharge source, and flow path.

We used spring and well water chemistry in nearly every Arizona study area. We routinely calculated silica and cation geothermometers on nonthermal and geothermal water. Chemical geothermometry can accurately predict subsurface temperatures, provided basic geologic assumptions are satisfied. Literature describing the use, interpretation, and physical base of aqueous chemical geothermometers is found in Fournier and Truesdell (1973), Fournier and Rowe (1966), Fournier and Potter (1979), and Fournier (1977).

Major factors adversely influencing the use and interpretation of geothermometers in Arizona include the non-temperature dependent solution of silica by water rich in dissolved carbon dioxide. This condition causes acid breakdown of silicate minerals such as feldspar in basin-fill

sediment, with release of excess silica into the ground water. Where evaporite minerals occur in basin-fill sediments, the Na-Ka-Ca geothermometer may be unreliable because of the non-temperature dependent addition of excess Ca to ground water. We found that mixing of geothermal water and nonthermal water was indicated when Li, B, and Na contents from several closely spaced wells or springs showed a linear relationship to dissolved chloride contents. Also low ratios of Na/K or Mg/Cl can be used as qualitative indicators of geothermal potential.

A Piper diagram showing milliequivalent percent of major cations and anions is useful to interpret water flow paths and aquifer lithology. Millequivalent ratios of chloride plus sulfate versus bicarbonate is often useful in southern Arizona waters to qualitatively determine aquifer residence time, recharge source, and to map ground-water flow directions. In general, higher ratios indicate older water or water that has had contact with evaporite minerals; low ratios tend to indicate young, recharge water.

Sampling, analyzing, and interpreting ground-water chemistry is very cost effective. An analysis for Na, K, Ca, Mg Cl, SO_4, HCO_3, F, B, Li, and silica cost less than $80 in 1981. Additional costs for water geochemistry surveys include salaries and field expenses.

GEOLOGIC MAPPING. Geologic mapping is an indispensible aid for interpreting structural features and geophysical and temperature-gradient information. Reconnaissance mapping was used to ground truth features observed in aerial photographs or described in the literature and to determine the quality and usefulness of existing geologic maps. For example, reconnaissance mapping in the Safford basin confirmed the existence

of young fault scarps that were inferred from aerial photographs (see area reports, this volume) Wichter, 1981). Also, reconnaissance mapping in the Clifton area determined that available published maps had insufficient structural detail for geologic interpretation at the Clifton Hot Springs. In order to remedy this, detailed mapping at 1:24,000 scale was done at Clifton, which provided the needed structural information (Cunningham, 1981). The cost of geologic mapping at Clifton was approximately $500 per square mile. Geologic mapping ranks high in terms of cost-effective exploration because it provides a basis to evaluate and interpret all other data gathered during exploration.

GEOHYDROLOGIC DATA. Geohydrologic information obtained during a literature search or while drilling temperature-gradient holes is one of the most valuable data sets in geothermal exploration. We found that particular attention should be given to the number of aquifers, geologic control of aquifers, water quality, aquifer hydraulic tests, and water-table information. These data are available in substantial detail for many areas of Arizona.

EXPLORATION METHODS REFERENCES

Cunningham, J. E., 1981, Preliminary detailed geologic map and cross-section of the Clifton Hot Springs and San Francisco River area: State of Arizona Bureau of Geology and Mineral Technology Open-File Report 81-22, scale 1:24,000.

Fournier, R. O., 1977, Chemical geothermometers and mixing models for geothermal systems: Geothermics, v. 5, p. 41-40.

Fournier, R. O., and Potter, R. W., 1979, Magnesium correction to the Na-K-Ca chemical geothermometer: Geochimica et Cosmochimica Acta, v. 43, p. 1543-1550.

Fournier, R. O., and Rowe, J. J., 1966, Estimation of underground temperatures from silica content of water from hot springs and wet steam wells: American Journal of Science, v. 264, p. 685-697.

Fournier, R. O., and Truesdell, A. H., 1973, An empirical Na-K-Ca geothermometer for natural waters: Geochimica et Cosmochimica Acta, v. 37, p. 1255-1275.

Gish, D. M., Keller, G. R., and Sbar, M. L., 1981, A refraction study of deep crustal structure in the Basin and Range-Colorado Plateau of eastern Arizona: Journal of Geophysical Research, v. 86, no. 37, p. 6029-6038.

Lumb, J. T., 1981, Prospecting for geothermal resources, *in* Rybach, L., and Muffler, L. J. P., eds., Geothermal Systems - principles and case histories: New York, John Wiley and Sons, Ltd, p. 77-108.

Natali, S. G. and Sbar, M. L., 1982, Seismicity in the epicentral region of the 1887 northeastern Sonoran earthquake, Mexico: Bulletin of Seismological Society of America, v. 72, no. 1, p. 181-196.

Phoenix Geophysics Inc., 1979, Report on the reconnaissance resistivity and VLF-EM surveys of the Safford valley area, Graham County, Arizona: State of Arizona Bureau of Geology and Mineral Technology Open-File Report 81-22, 10 fig., 15 plates, 14 p.

Sbar, M. L., 1979, Analysis of short-term microearthquake activity related to potential geothermal areas in Arizona: State of Arizona Bureau of Geology and Mineral Technology Open-File Report 80-1c, 11 p.

Stone, C., 1980, Springerville geothermal project-geology, geochemistry, geophysics -- Final Report: State of Arizona Bureau of Geology and Mineral Technology Open-File Report 80-4, 23 p.

Ward, S. H., Ross, H. P., and Nielson, D. L., 1981, Exploration strategy for high-temperature hydrothermal systems in the Basin and Range province: American Association of Petroleum Geologists Bulletin, v.65, no. 1 p. 86-102.

Witcher, J. C., 1981, Geothermal resource potential of the Safford-San Simon basin: State of Arizona Bureau of Geology and Mineral Technology Open-File Report 81-26, 131 p.

Witcher, J. C., 1982, Exploration for geothermal energy in Arizona Basin and Range -- a summary of results and interpretation of heat flow and geochemistry studies in Safford basin, Arizona: State of Arizona Bureau of Geology and Mineral Technology Open-File Report 82-5, 51 p.

Witcher, J. C., and Stone, C., 1981, Thermal regime of the Clifton-Morenci area, Arizona (abstr.): Geological Society of America Abstracts with Programs, Cordilleran Section, v. 13, no. 2, p. 114.

Young, C. T., 1979, Geoelectrical studies near Springerville, Arizona: Transactions, Geothermal Resources Council, v. 3, p. 805-808.

Young, C. T., 1980, Geothermal reconnaissance on the Fort Apache Indian Reservation using electrical methods: Transactions, Geothermal Resources Council, v. 4, p.269-272.

APPENDICES

CONVERSION FACTORS AND TABLES

Mass	1 kilogram (kg) = 2,205 pound (lb) 1 ton (short) = 2,000 lb
Length	1 meter (m) = 3.281 feet (ft) 1 ft = 0.3048 m 1 inch (in) = 2.54 centimeters (cm) 1 kilometer (km) = 0.6214 mile (mi) 1 mi = 1.609 km
Area	1 km^2 = 0.3861 mi^2 1 mi^2 = 640 acres = 1 section
Volume	1 liter (L) = 0.2642 gallon (gal) 1 gal = 3.785 L 1 barrel (bbl) = 42 U.S. gal 1 km^3 = 0.2399 mi^3 1 mi^3 = 4.1684 km^3 1 mcf = 1000 ft^3
Temperature	degrees Celsius (^oC) = 5/9 (degrees Fahrenheit - 32) ^oF = (degrees Celsius x 9/5) + 32) degrees Kelvin (^oK) = ^oC + 273.15
Temperature Gradient	10^oC/km = 0.55^oF/100 ft 1^oF/100 ft = 18.23^oC/km
Energy	1 calorie (cal) = 3.9665 x 10^{-3} British thermal unit (Btu) 1 Btu = 252.1 cal 1 quad = 1 x 10^{15} Btu 1 joule (J) = 0.239 cal
Power	1 watt (W) = 0.239 cal/sec 1 cal/s = 4.184 W 1 W = 1 J/sec 1 Btu = 0.2930 W 1 W = 3.413 Btu
Heat Flow	1 heat flow unit (HFU) = 1 x 10^{-6} cal/cm^2 sec 1 thermal conductivity unit (TCU) = 1 x 10^{-3} cal/cm sec ^oC 1 heat generation unit (HGU) = 1 x 10^{-13} cal/cm^3 sec 1 HFU = 41 84 mW/m^2 1 TCU = 0.4184 W/mK 1 HGU = 0.4184 μW/m^3

Other Energy Conversions

Fuel Unit	Millions of Btu's	Barrels of Oil Equivalents
1 bbl domestic crude oil	5.6	1.0
1 mcf dry natural gas	1.02	0.1823
1 bbl residential fuel oil	6.287	1.1227
1 ton western sub-bituminous coal	18.0	3.2143
1 quad	1 x 10^9	178 x 10^5
1 ton of refrigeration	0.288	0.0514

Pressure: 10^5 pascal (Pa) = 1 bar
1 bar = 14.50 lb/in^2 = 1 atmosphere

CONVERSION FACTORS AND TABLES

Prefixes

10^{-6} = Micro (μ)
10^{-3} = Milli (m)
10^{-2} = Centi (c)
10^{-3} = Kilo (K)
10^{-6} = Mega (M)
10^{-9} = Gila (G)

Temperature Table

°F	°C	°F	°C	°F	°C	°F	°C
41	5	131	55	221	105	311	155
50	10	140	60	230	110	320	160
59	15	149	65	239	115	329	165
68	20	158	70	248	120	338	170
77	25	167	75	257	125	347	175
86	30	176	80	266	130	356	180
95	35	185	85	275	135	365	185
104	40	194	90	284	140	374	190
113	45	203	95	293	145	383	195
122	50	212	100	302	150	392	200

Properties of Water

Density = 1 g/cm^3 = 62.43 lb/ft^3 = 8.345 lb/gal
Specific Heat = 1 cal/g°C = 1 btu/lb°F

Well Depth Table

Feet	Meters	Feet	Meters	Feet	Meters
5	1.52	900	274.32	2100	640.08
10	3.05	1000	304.80	2200	670.56
25	7.62	1100	335.28	2300	701.04
50	15.24	1200	365.76	2400	731.52
100	30.48	1300	396.24	2500	762.00
200	60.96	1400	426.72	3000	914.40
300	91.44	1500	457.20	4000	1219.20
400	121.92	1600	487.68	5000	1524.00
500	152.40	1700	518.16	6000	1828.80
600	182.88	1800	548.64	7000	2133.60
700	213.36	1900	579.12	8000	2438.40
800	243.84	2000	609.60	9000	2743.20

Flow Rate Table

1 ft^3/sec = 28.31 Liters/sec (L/s) = 448.8 Gallons/Minute (gpm)

(gpm)	(L/s)	gpm	L/sec	gpm	L/sec
5	0.32	300	18.92	2500	157.70
10	0.63	400	25.23	3000	189.24
25	1.58	500	31.54	3500	220.78
50	3.15	1000	63.08	4000	252.32
100	6.31	1500	94.62		
200	12.62	2000	126.16		